# TRABAJO DE FIN DE MÁSTER

---

## "Fenómeno de Bombeo en Compresores Centrífugos Aplicados a la Automoción"

---

**Realizado por: D. Ricardo Lang**
**Dirigido por: Dr. José Galindo Lucas**

**Valencia, 21 de junio de 2010**

---

## Máster en Motores de Combustión Interna Alternativos

DEPARTAMENTO DE MÁQUINAS Y MOTORES TÉRMICOS

# Contenido

**Resumen** .......... 2

**Summary** .......... 2

**Introducción** .......... 2

**Objetivos** .......... 4

**Planteamiento y Metodología** .......... 4

**Conclusión** .......... 5

**Documentos Aportados** .......... 5

**Combination of CFD and experimental techniques to investigate the flow in centrifugal compressors near the surge line** .......... 8

**Analysis of different turbocharger surge situations in automotive engines** .......... 15

**On-Engine Measurement of Turbocharger Surge Limit** .......... 23

**Analyse et mesure des phénomènes de pompage entrée compresseur. Parte 1** .......... 39

**Analyse et mesure des phénomènes de pompage entrée compresseur. Parte 2** .......... 103

**Surge analysis and prediction in transient. Parte 1** .......... 134

**Surge analysis and prediction in transient. Parte 2** .......... 216

## Resumen

El presente Trabajo de Fin de Máster exhibe los estudios realizados acerca del bombeo en el conjunto compresor centrífugo y motor alternativo. El estudio ha sido efectuado mediante simulación numérica tridimensional, unidimensional y cerodimensional además de la correspondiente validación en laboratorio de ensayos. Se han realizado diferentes propuestas de modelización para el cálculo CFD de manera de aproximarse lo más posible a la configuración real del compresor y sus accesorios de acoplamiento al motor alternativo, sin extender excesivamente el tiempo de cálculo de las simulaciones.

## Summary

This master thesis presents the results from the study of surge phenomena in centrifugal compressors as part of the turbocharging assembly on internal combustion engines (ICE). The study was accomplished by using 0, 1 and 3-dimensional simulation tools whose results were compared with test data from an experiment performed in several combustion engines, finding good agreement between calculated data and measured ones. During the 3D calculation were applied several models in order to find the real conditions for compressor and its coupling elements to the ICE without extending the calculation time during simulations.


## Introducción

Los turbocompresores han sido utilizados por años como un medio efectivo para aumentar la potencia de los motores de combustión interna alternativos, especialmente en los motores diesel. Actualmente en el sector de la automoción está ampliamente extendida esta técnica. Sin embargo, en los últimos años ha habido una tendencia a la disminución del tamaño de las plantas motrices (conocida como “downsizing”en inglés). Esto implica desarrollar motores de menor desplazamiento volumétrico para las mismas demandas de potencia, y además, cada vez más estrictos requerimientos de polución y consumo de combustible. El “downsizing”ha llevado al turbocompresor a sus límites, puesto que se requiere una mayor presión de carga para mantener la potencia erogada por los motores más pequeños. Además, buscando mejoras en la conducción automovilística se requieren altos torques a las más bajas velocidades de motor posibles. De manera que estos requerimientos hacen que el compresor sea sometido a severas condiciones de trabajo, puesto que debe comprimir bajos gastos de aire a alta relación

de compresión.
El compresor centrífugo provee energía al fluido de trabajo aumentando su presión, usando como principio de funcionamiento las fuerzas centrípetas (centrífuga aparente) generadas por su rotor. El rotor del compresor tiene álabes con un ángulo de diseño determinado de manera que puedan encausar el flujo en el canal de impulsión lo más eficientemente posible. Al igual que en un perfil alar, el ángulo de ataque que tengan los álabes respecto de la dirección de circulación del fluido será fundamental al objetivo de tener una distribución de presiones adecuada alrededor de los mismos. Pero como es razonable pensar, debido a que el compresor debe trabajar en un amplio rango de velocidades de flujo, porque así lo demanda el gasto de aire requerido por el motor alternativo, el ángulo de ataque que se tenga en los álabes no será siempre el óptimo para una correcta distribución de presiones en los mismos. De manera que para una determinada relación de presiones demandada, una disminución del gasto trasegado incurre en un aumento del ángulo de ataque del flujo respecto de los álabes, llegando a un punto crítico donde la capa limite sobre los perfiles se desprenderá y ya no será posible lograr el incremento de presiones deseado, a menos que se corrijan los factores que han causado el desprendimiento. Cabe mencionar que la incapacidad del compresor de proveer el incremento de presiones demandado por causa del desprendimiento de la capa límite, no es el fenómeno de bombeo en sí, aunque si está íntimamente relacionado. Generalmente se lo conoce como "rotating stall"o desprendimiento rotativo (en español), y se caracteriza por empezar como un evento localizado, es decir, no en todo el ojo del rodete del compresor, y que se desplaza en la dirección de rotación del rotor pero a una velocidad menor. Sin embrago, a medida que aumenta el incremento de presión de demanda o disminuye el gasto trasegado, el desprendimiento se generalizará, con lo cual la máquina ya no cumplirá con su función.
Al vincular el compresor centrífugo al motor alternativo, se genera un volumen detrás del primero, es decir, del compresor. El volumen lo integran los accesorios de conexión, tanto a la entrada como a la salida del compresor y además, el mismo volumen desplazado por el motor alternativo. Este volumen global exhibirá ciertas características aero-acústicas, que interactuarán con el desempeño del compresor centrífugo. Específicamente, cuando las condiciones de operación sean las que llevan al desprendimiento rotativo (rotating stall), se contará con un volumen determinado detrás del compresor a una cierta presión que él mismo no será capaz de sostener. De manera que el flujo cambia de sentido en busca del equilibrio hasta que el compresor recupere nuevamente su capacidad operativa. Una vez dada la recuperación, el compresor vuelve a cargar el volumen, pero si las condiciones de presión y gasto siguen siendo tales que propendan al des-

prendimiento, se dará un nuevo ciclo de descarga; y así sucesivamente. A este ciclo de carga y descarga se lo denomina “fenómeno de bombeo”.
La investigación a lo largo de los años ha determinado que diferentes geometrías tanto a la entrada como a la salida del compresor centrifugo, modificarán el umbral del comienzo del bombeo. Sin embargo, experimentalmente es muy complicado, tecnológicamente hablando, poder medir la evolución del flujo en el compresor, la voluta, accesorios, etc., razón por la cual es difícil conocer los mecanismos que gobiernan el bombeo. Además, como el patrón de flujo en el compresor es altamente tridimensional, siempre a presentado inconvenientes para la modelización. Sin embargo, a estas alturas del desarrollo informático se cuentan con herramientas de cálculo fluido-dinámico tridimensional como es el caso del CFD, capaces de realizar simulaciones y la posterior visualización de patrones de flujos de diversos dispositivos.

## Objetivos

Usando estas herramientas informáticas, se pretende visualizar el patrón de flujo dentro del compresor centrífugo y sus geometrías solidarias en operación normal del mismo, poco antes, durante y despúes del bombeo. Además se prueban diversas geometrías a la entrada y a la salida del compresor con el objetivo de ver como modifican el patrón de flujo del conjunto. Dado que hay geometrías más favorables que otras, ver el desarrollo del patrón de flujo en cada una sería particularmente útil para poder justificar su desempeño.

## Planteamiento y Metodología

Debido a que lo propuesto es relativamente novedoso, la estrategia metodológica seguida para conseguir los objetivos planteados ha ido adaptándose a medida que se fueron teniendo resultados y adquiriendo experiencia. En primeras instancias se realizó el mayado de un modelo CAD de compresor con una cantidad de celdas adecuadas a nuestro criterio y capacidades de cálculo de las estaciones informáticas. A medida que se fue ganando experiencia, se corrigieron la maya y ciertos parámetros y criterios de cálculo de manera de que la simulación se hiciera estable. Una vez logrado lo dicho, se fueron creando diferentes geometrías 3-dimesionales para colocarlas a la entrada del compresor además de una geometría 0-dimensional a la salida del mismo, siempre con el objetivo de que la simulación sea lo más realista posible.
Paralelamente se han realizado una importante cantidad de ensayos en la-

boratorio persiguiendo la validación de los resultados obtenidos mediante la simulación computacional. También se ha desarrollado una técnica experimental para medir la línea de bombeo en condiciones próximas a las de operación real.

## Conclusión

Finalmente, se puede decir como conclusión que los resultados de las simulaciones han sido aceptables. Como se podrá apreciar en el artículo adjunto "Combination of CFD and experimental techniques to investigate the flow in centrifugal compressors near the surge line", los modelos fueron evolucionando de manera de obtener resultados cada vez más acertados respecto de los ensayos de laboratorio. Sin embargo, también fueron haciéndose más evidentes ciertos detalles de modelado a mejorar, como ser la densidad de maya o zonas de alto número de Mach, que actúan en detrimento de los resultados obtenidos. Para finalizar en términos de modelización, se puede decir que el modelo unidimensional también ha demostrado muy buena respuesta ante lo complejo de la predicción del fenómeno ("Analysis of different turbocharger surge situations in automotive engines"). Como conclusión se ve que, en coherencia con los objetivos centrales del trabajo, las simulaciones han permitido tener una idea más acabada de los factores envueltos en el fenómeno bombeo del compresor centrífugo y las formas en las que se puede mejorar la operación del mismo.
Respecto a la técnica desarrollada para medir la línea de bombeo en banco motor ("On-Engine Measurement of Turbocharger Surge Limit "), se puede concluir que demuestra un desempeño más fiable que la técnica tradicional de medición de prestaciones del turbo-grupo en banco de ensayos de flujo continuo.

## Documentos Aportados

A continuación se adjuntan los siguientes documentos resultados de la investigación, en su correspondiente formato de presentación:

- Artículo en SAE 2008: "Combination of CFD and experimental techniques to investigate the flow in centrifugal compressors near the surge line". Presenta los resultados de los primeros trabajos de simulación numérica CFD sobre el compresor centrífugo. Son expuestos detalles sobre el tipo de mayado utilizado, las condiciones de contorno y cálculo seleccionadas.

- Artículo en SIA 2010: "Analysis of different turbocharger surge situations in automotive engines". Presenta los resultados de una modelización unidimensional del compresor centrífugo y sus accesorios periféricos.

- Artículo en Experimental Techniques: "On-Engine Measurement of Turbocharger Surge Limit". Presenta los resultados del desarrollo de la técnica experimental de medición de la línea de bombeo en banco motor.

- Reporte técnico: "Analyse et mesure des phénomènes de pompage entrée compresseur". Se presenta en dos apartados exponiendo los resultados obtenidos del cálculo 3D realizado con diferentes geometrías a la entrada del compresor centrífugo en condiciones de operación cercanas a bombeo. Además, se exhiben los resultados de trabajos experimentales de validación y los realizados para extender la medición de las prestaciones del compresor más allá del límite de bombeo con objetivos de simulación numérica.

- Reporte técnico: "Surge analysis and prediction in transient". Se presenta en dos partes exponiendo los resultados de las validaciones experimentales de las simulaciones del bombeo; además las estrategias de cálculo y los resultados de las simulaciones 1 y 3-dimensional del bombeo del compresor centrífugo en régimen transitorio.

2008-01-0300

# COMBINATION OF CFD AND EXPERIMENTAL TECHNIQUES TO INVESTIGATE THE FLOW IN CENTRIFUGAL COMPRESSORS NEAR THE SURGE LINE

**Margot X., Gil A., Tiseira A., Lang R.**
CMT- Motores Térmicos
Universidad Politécnica de Valencia, Spain



## ABSTRACT

Surge phenomenon is becoming a limitation of the low end torque for downsized turbocharged Diesel engines. The stable operation of centrifugal compressors is limited at low flow rates because of the occurrence of surge. In the present work a CFD analysis of the flow inside automotive centrifugal compressors near the surge line is carried out. For this purpose, the actual geometry of a compressor –including its inducer, rotor, diffuser and volute– has been modelled with a CFD code. Initially, steady calculations have been performed to have a first approximation of the flow characteristics inside the compressor. In these calculations, a source term is imposed in the momentum equations to simulate the movement of the rotor and its effects on the air when it passes through it. In order to get a better understanding about the phenomena that occur inside the compressor when surge starts, the same compressor has been calculated for different cases with the same rotor speed and different mass flow rates. The geometry of the inlet duct has also been varied.

Some calculations in transient conditions, including moving meshes (rotor) have then been performed for very low mass flow rates in order to simulate in more realistic conditions the beginning of stall that leads to surge.

CFD results have been compared with experimental results and good agreement has been found for the compressor map points calculated. Hence, a complete 3D analysis can be performed to help to understand the stalled flow and the surge phenomenon.

## INTRODUCTION

Over the last decades turbocharging has been increasingly used in internal combustion engines and is nowadays included in most Diesel engines. An automotive turbocharger usually consists of a centripetal turbine that drives a centrifugal compressor mounted on the same shaft.

Obviously, it is necessary to select appropriately the turbocharger, as it is a key component that affects engine efficiency and performance. Hence, it is essential to avoid working points (choke and surge) that could lead to total breakage of the turbocharger system. Different active control systems can be used to stabilize the compressor in surge zones, and reduce the oscillations. Gravdahl et al. [1, 2] use drive torque actuation to extend the stable operating zone of the compressor. Another control method is the use of a throttle placed after the plenum installed downstream of the compressor [3, 4] in the test rig.

In the case of centrifugal compressors it is known that unsteady behavior occurs when the air mass flow through the compressor is lower than the critical value. This unstable phenomenon is denoted as surge, and corresponds to a periodic return of the compressed fluid through the compressor into its inlet. Surge causes a significant drop in all compressor parameters and mechanical deterioration (blades, shaft, i.e.).

Nowadays, most of the researchers and manufacturers use 1D computer codes [1, 6] to simulate a match between the turbocharger and the engine. The characterization of turbochargers is experimentally made by manufacturers, and the data are transferred to engine manufacturers or researchers by means of maps. However, test conditions may be sometimes quite far from real engine conditions [7], which may cause a mismatch that could seriously affect the accuracy of the models. Furthermore, in the maps provided by manufacturers, the stable operation zone is delimited by the 'surge line', but there are no objective criteria that allow locating this zone and the mechanism that causes the surge phenomenon is not well documented.

Some researchers have developed turbocharger test benches [8, 9] capable of reproducing with real exhaust gases flow conditions quite close to the real engine conditions. These installations are capable of detecting surge using an objective criterion based on the frequency domain of the instantaneous downstream pressure measurement [8]. When surge appears, the pressure spectrum shows higher low frequency contents than in stable operation.

Another approach for gaining insight into the flow inside the turbocharger is the application of three-dimensional calculation codes, which are able to solve the governing flow equations. When applied to internal combustion engines, the so-called CFD codes [10] have to address specific problems linked to the flow unsteadiness, high Reynolds numbers involved, and the complex variable geometry of the solid boundaries. However, these problems have been partially solved in recent years as result of the significant improvement in power and speed of modern computers, and in the ability of the CFD codes to solve complex flows.

Some calculations of the flow in turbochargers have been previously presented. Krain [11] carried out one of the first CAD studies to obtain optimized blade profiles for the rotor of centrifugal compressors. Wang [12] has also widely contributed to the use of 3D-CFD tools to design this component of the system. More recently, Larosiliere et al [13] and Koutmoutsos et al [14] have studied the variation in the flow structure between the rotor blades when the mass flow rate decreases, but also the interaction between the rotor blades and the diffuser vanes. Engeda et al. [15] used CFD to perform a parametric study on the chord-length of the vanes and optimize the geometry of the diffuser vanes. Pan et al. [16] performed 3D calculations to analyze the influence of the volute geometry on the operation of the diffuser vanes, and therefore on the efficiency of the compressor. Finally, Dickmann et al. [17] performed unsteady calculations on a simplified geometry –without the volute– near the surge line, and analyzed the response in frequency domain of the calculations. They also carried out some FEM calculations of the surface of the rotor blades to investigate their displacement when the pressure field near the surge line is imposed on the surface of the blades. Schmidtmann et al. [18] performed 2D calculations with their own code for a throttled compressor, and they analyzed the instabilities –rotating stall and the surge phenomena– that appear when the compressor is throttled.

In this work CFD calculations of a complete real compressor geometry are presented. The approach followed may be divided in two parts: steady calculations in the stable operation zone of the compressor, and unsteady calculations near the surge line. Steady calculations are not capable to reproduce the flow in surge conditions, but are useful to obtain a virtual map in the stable zone, and also to obtain the initial conditions for unsteady calculations near the surge line. Unsteady calculations have also been performed by reducing the mass flow rate to levels near surge. The 3-D solution highlights certain phenomena related to surge, and allows observing the flow inside the domain in this situation and detecting instability –rotating stall- cells upstream of the inducer that lead to surge.

## METHODOLOGY

The work is centered on the CFD calculations of the complete real compressor geometry. The first stage consists in reproducing the map of the compressor for a given rotation speed in the stable operating zone by means of steady calculations. When the compressor is close to surge conditions, the steady models are not capable of providing converged solutions because of the unsteadiness of the surge phenomenon. Therefore, unsteady calculations are required to reproduce the instability processes –rotating stall and the surge phenomena– that appear in the compressor when the mass flow rate is reduced to critical values.

The calculations have been validated with the experimental data of the compressor map, as obtained by the measurements in the turbocharger test bench described below.

It is worth mentioning that calculations have been performed at a rotation speed of 150 000 rpm (150 krpm) because this point presents significant instabilities for a wide range of air mass flow before the surge line.

## EXPERIMENTAL SET UP

The test bench for the characterization of turbochargers is based on a heavy-duty diesel engine (see Table 1), which is used as a hot, and pulsating mass flow generator. The engine is devoid of its original turbocharger, and boosted with an additional screw compressor (see Table 2) in order to ensure the necessary air mass flow, and to generate the required turbine inlet conditions.

| Characteristics of the internal combustion engine | |
|---|---|
| Number of cylinders | 1-6 |
| Swept volume (l) | 9.84 |
| Compression ratio | 17.8:1 |
| Engine speed (rpm) | 800-2000 |
| Maximum power | 257kW |
| Number of valves per cylinder | 2 |
| Fuel injection pump | In-line |

Table 1. Engine characteristics.

| Characteristics of the screw compressor | |
|---|---|
| Air mass flow rate (kg/s) | 0.27-0.61 |
| Compression ratio (bar) | 1.5-4 |
| Operation shaft speed (rpm) | 1800-3600 |
| Shaft power (kW) | 30-130 (25) |
| Air outlet maximum temperature (ºC) | 130 |

Table 2. Screw compressor characteristics.

An electromagnetic brake is installed between the engine and the screw compressor (see Figure 1) in order to absorb the spare power of the engine, and therefore, control the rotating speed of the system. Also a gear-box is present to adapt the rotating speed of both machines, see Figure 1. In addition, a settling tank with an electronically controlled discharge valve is needed between the screw compressor and the engine in order to purge the intake system when the compressor supplies too much air mass flow rate for a given rotation speed, as shown in the scheme of Figure 1.

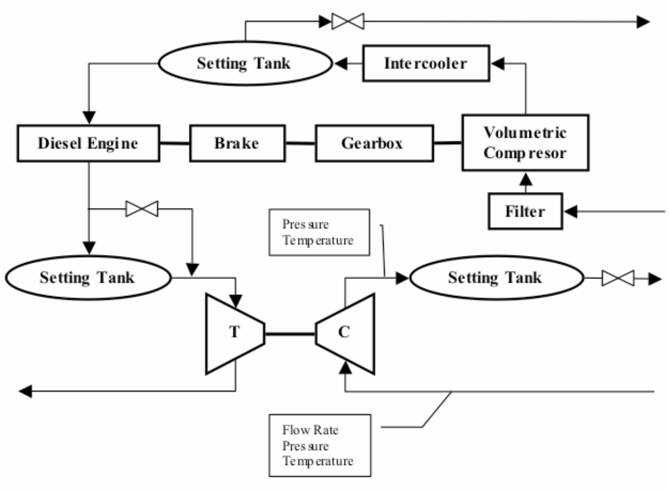


Figure 1. Basic installation turbocharger test bench diagram.

It is worth mentioning that as the radial turbine is directly fed with the exhaust gases from the engine manifold, it is possible to modify the number of cylinders discharging into the turbine in order to adapt the gas flow rate to different type of turbines. To achieve this, a set of valves has been installed in the exhaust manifold. Furthermore, if the measurements of the turbocharger are performed in steady conditions, a settling tank that reduces the pulses of the gas flow can be installed between the exhaust manifold and the turbine inlet, see Figure 1.

*Criterion used for experimental surge limit location*

As commented above, compressor surge is a key factor that limits the boosting capacity of the turbocharger at low engine speeds. A clear definition of the surge area will allow a correct performance and efficiency of the engine and will avoid possible breakage of the turbocharger system.

Historically, turbocharger compressor surge has been associated with certain instabilities of the measured variables, noise effects or by significant gas temperature rise at the compressor inlet. During these experiments, the operator has to decide when the surge has started, on the basis of the measured variables. But this is a subjective procedure, and it does not allow automating turbochargers testing.

The significant variations of the compressor measured variables (pressure, air mass flow, and rotating speed) that are encountered when surge appears can be used to objectively locate the phenomenon. An algorithm based on the frequency –discrete-time Fourier series [19, Proakis]– analysis permits to determine the unstable behavior. The most sensitive variable to surge is the pressure downstream of the compressor. When there is surge, the pressure spectrum shows higher low frequency contents than in stable operation. The main frequency peak can be located between 5 and 15 Hz, depending on the downstream compressor size in the installation arrangement, and the amplitude peak depends on the operating conditions.

## CFD MODEL AND SIMULATION

A finite volume commercial program has been used to solve the discretized Navier-Stokes equations. The standard k-$\varepsilon$ turbulence model for high Reynolds numbers with wall functions is used for closure. The program is based on the pressure-correction method [20] and uses SIMPLE algorithm for the steady calculations, and the non-iterative PISO algorithm [10] for the unsteady cases. The first order upwind differencing scheme is used for the momentum, energy and turbulence equations.

The geometry includes the cone intake duct, the rotor, the diffuser, and the volute, see Figure 2. Since the computational domain is very complex, composed by four zones with different topologies and requirements, each zone is meshed separately, and connected by means of arbitrary interfaces that connect common faces of adjacent zones. Figure 3 shows the differenced sub-domains that form the grid, with a hexahedral semi-structured mesh, except in the volute. In this element, the junction of the smaller section with the exit has to be meshed by means of a tetrahedral mesh.

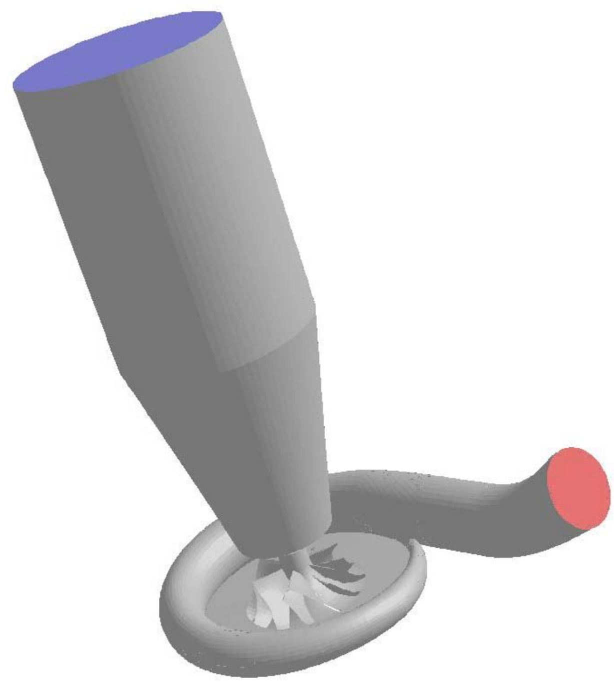

Figure 2. CFD domain and boundary conditions.

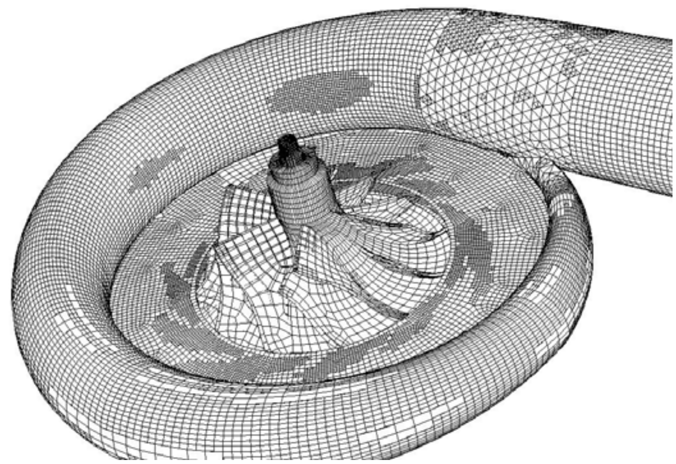

Figure 3. Mesh and successive refinements.

A mass flow rate boundary condition has been applied at the inlet, with average values for total inlet temperature and turbulence parameters. The exit boundary condition is at constant static pressure.

A source term is included in the momentum equations to take into account the rotor motion effects [10] in the steady calculations. Successive calculations have been performed for a given rotor speed –150 000 rev/min–, by reducing the inlet mass flow rate from a point close to choke to a point close to surge. Near surge, the steady calculations diverge due to the unsteadiness [17] of the phenomena. However, the solutions of the steady calculations have been used as initial conditions for the transient calculations. The operating point close to surge is achieved by traveling along the speed line, from a stable operation point to the smaller mass flow rates that produce instabilities. A moving mesh is required for the transient calculations: the sub-domain corresponding to the moving zones –rotor–, is configured in the model with the corresponding rotating motion, and joined with the rest of the system by means of sliding arbitrary interfaces [10]. In the transient calculation the inlet boundary condition varies in time: the mass flow rate reduces linearly to levels that lead to surge, see Figure 4.

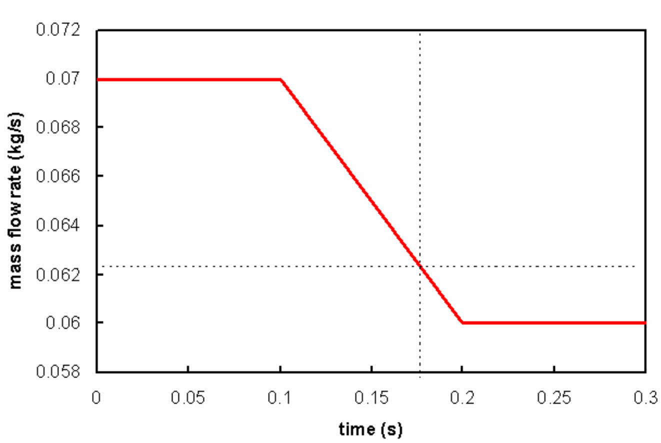


Figure 4. Variable inlet boundary condtion for unsteady calculations.

A semi-automatic adaptive mesh refinement procedure [10] has been applied in order to obtain a mesh-independent solution. The procedure consists in detecting zones with high velocity gradients, and performing successive refinements, until the solution does not change and the number of cells remains constant, as shown in Figure 5.

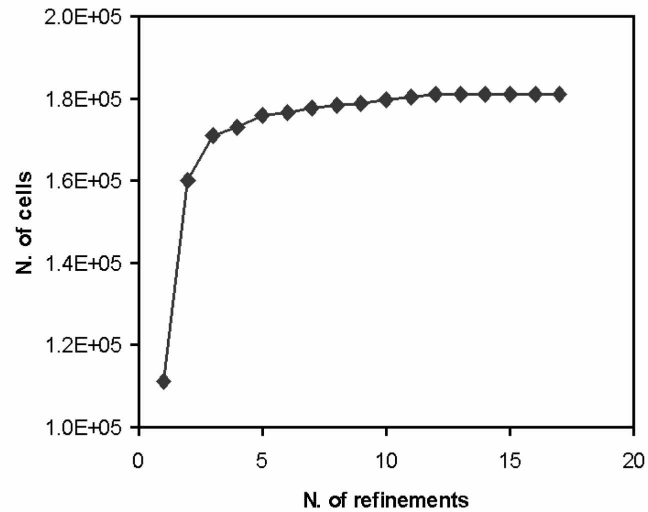


Figure 5. Number of cells of each successive refinement.

## RESULTS

First the compressor was characterized in the turbocharger test bench described above, in order to obtain the compressor map, see iso-regime lines from 50 krpm to 190 krpm in Figure 6. The surge line is obtained by means of the FFT analysis of the signals measured in the compressor. On one hand, a thermo-couple is installed in the compressor shroud immediately upstream of the inducer in order to detect the temperature gradients when reverse flow appears. On the other hand, the instantaneous pressures upstream and downstream of the compressor are measured, since these are the most significant variables to detect surge. In this way, the surge line is objectively defined, as presented in Figure 6.

Figure 6 also represents the 150 krpm iso-regime line obtained with the CFD steady calculations in the stable operation zone, obtained by changing the mass flow rate in the inlet boundary condition of the model. Both the experimental and CFD results show good agreement for points in the whole range of mass flow rates, from high to unstable points near surge. Near choke calculations yield higher pressure ratios than experiments. This can be explained by the fact that in this working area the flow is transonic, and the solver used in this study is not well adapted to this type of flows [10]. Different pressure-velocity coupling and discretization schemes [10] would be necessary if choke were to be studied in detail, which is beyond the scope of this study.

The last stable steady calculated point –0,07 kg/s– is immediately on the right of the surge line. The pressure ratio prediction in this point agrees well with the experimental results (P2c/P1c = 2.241, Δ% ≈ 0,4%, see also Figure 7). Mass flow rates lower than this lead to instabilities and divergence in the calculations and no results can be obtained with the steady calculations.

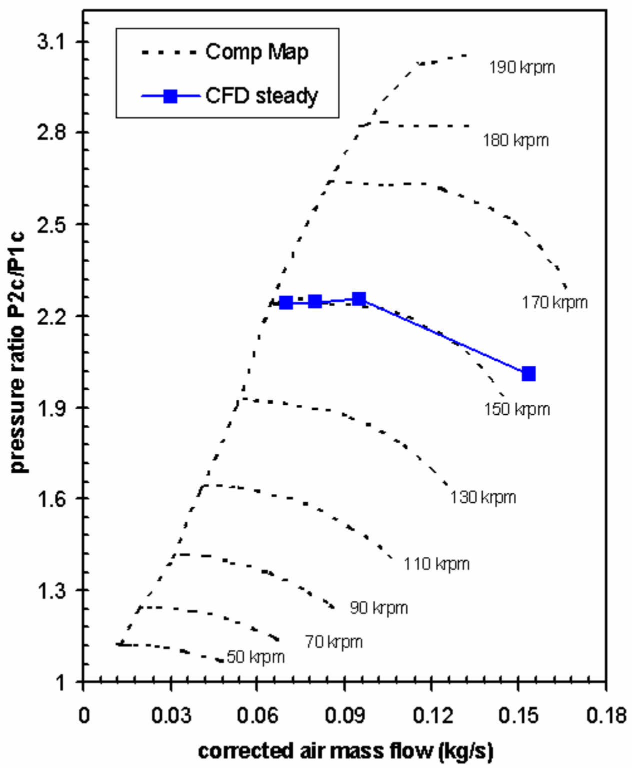

Figure 6. Compressor Map and modeled steady line at 150 krpm

From this point –0,07 kg/s–, unsteady calculations are required in order to get closer to the surge line. As explained in the previous section, unsteady calculations with variable inlet boundary conditions (see Figure 4) have been performed in order to get closer to the surge line.

Figure 7 shows a zoom of the compressor map for 150 krpm, near the surge line. In this figure the CFD results obtained by means of the transient calculations are also represented by a continuous line. The computed pressure ratio presents an incipient unstable behavior in the proximity of the surge line, with increasing oscillations for corrected mass flow rates lower than 0,066 kg/s. It seems that the model captures the flow behavior just before the origin of the surge phenomenon.

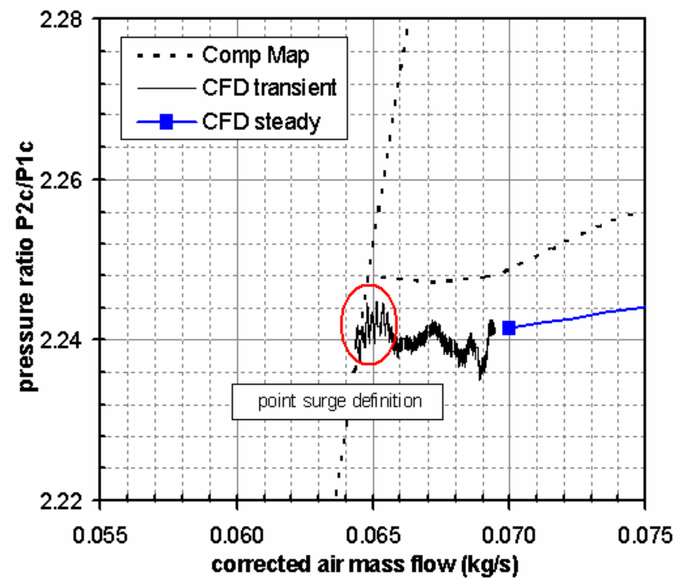

Figure 7. Compressor map near the surge zone and transient results.

Figures 8 and 9 show the static pressure –relative to atmospheric pressure– and the axial velocity respectively, in a cross section immediately upstream of the inducer impellers, for a steady calculation in the stable operating zone. Figures 10 and 11 represent the same variables and in the same section, but for an instant corresponding to the unstable behavior commented above, when surge is starting. Both the contours of the stable and unstable operating zones are in the same scale to make their interpretation easier. Negative axial velocity in these cases means that air is flowing normally, from the inlet to the compressor diffuser. On the contrary, positive velocities –light colors– point out to zones with reverse flow.

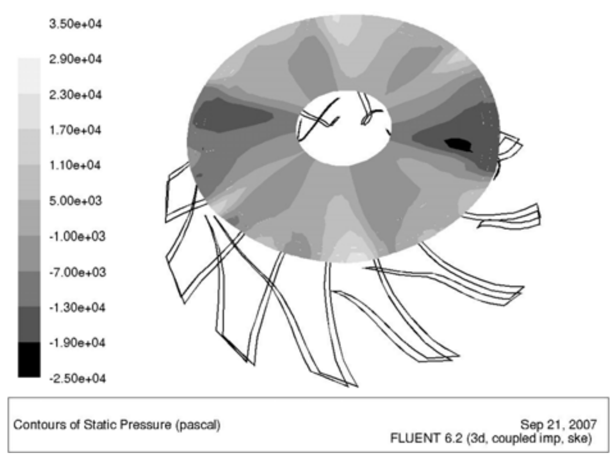

Figure 8. Pressure contours upstream of the inducer. Steady calculation. Stable operating point (0,10 kg/s).

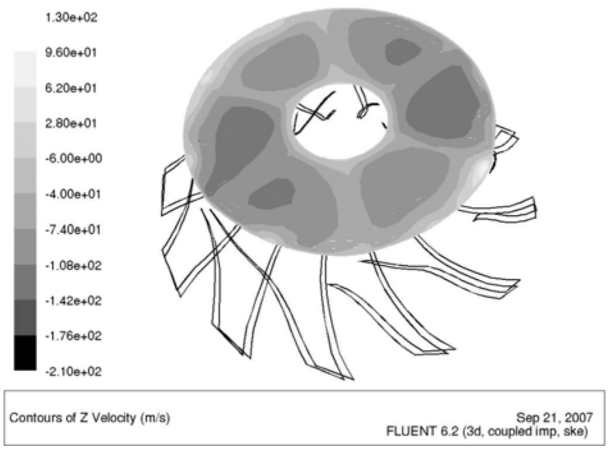


Figure 9. Axial Velocity contours upstream of the inducer. Steady calculation. Stable operating point (0,10 kg/s).

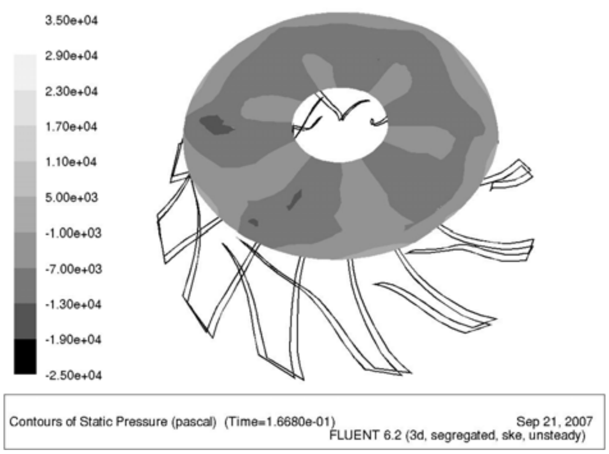


Figure 10. Pressure contours upstream of the inducer. Transient calculation. Operating point near surge.

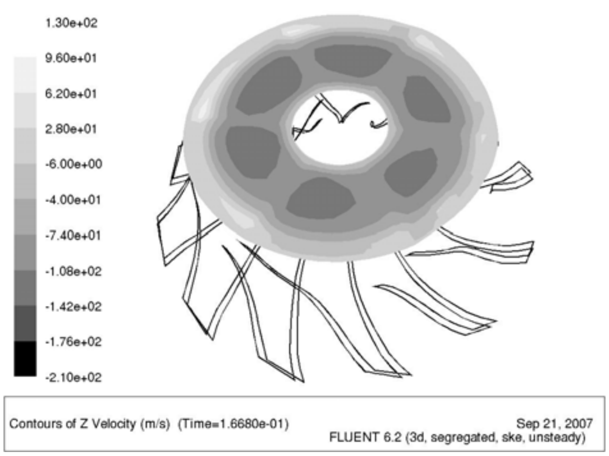


Figure 11. Axial Velocity contours upstream of the inducer. Transient calculation. Operating point near surge.

The steady selected point is inside the stable operating zone of the compressor, but pressure contours in Figure 8 show two instability zones (with lower pressure levels) that lead to reverse flow in the periphery of the impellers placed immediately downstream of these cells (see positive axial velocities in Figure 9). The circumferential position of the instability cells can be directly related to the geometry of the volute in the minimum and maximum area junction (volute passage). At low flow rates, circumferential pressure distortion is detected around the volute passage [21], as shown in Figure 12. The distortion is transmitted back to the impeller inlet and causes the instability cells, as commented above.

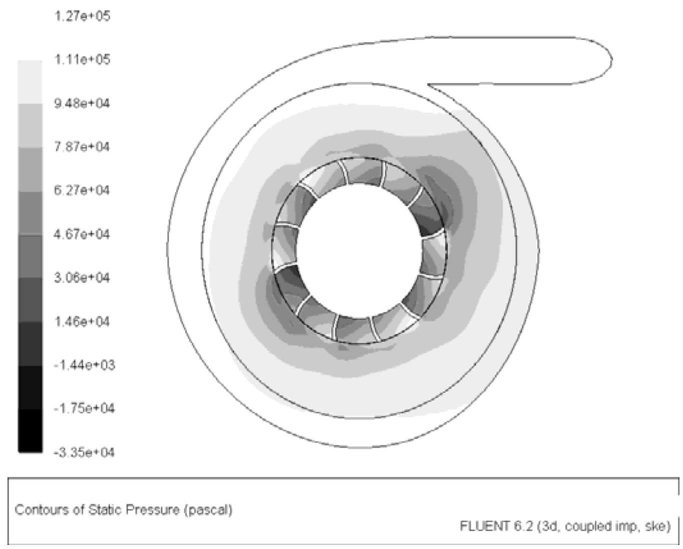


Figure 12. Pressure contours in the volute. Steady calculation. Stable operating point (0,10 kg/s)

The instability cells grow as the mass flow rate decreases to levels near to those producing surge. As commented above, Figure 10 shows the static pressure in an unstable point near surge. It is clear that now the instability cells –low pressure, dark gray– fill the whole section. These instability cells can be assigned to the so-called rotating stall phenomenon, which is precursor of surge.

Furthermore, for a given rotation speed, when the mass flow rate decreases, the velocity in the periphery is clearly dominated by the tangential component, so the fluid cannot flow up trough the rotor. Moreover, inside the rotor there is an unfavorable pressure gradient –lower pressure upstream– that makes that effect more significant. Consequently, zones with positive velocity –reverse flow in the periphery, light colors in Figure 11– can be detected for this working point.

## SUMMARY AND CONCLUSIONS

A combined methodology that includes CFD calculations and experiments has been successfully applied in order to study the behavior of centrifugal compressors working near the surge line.

Steady and transient CFD calculations have been performed on a 3D domain that reproduces the real geometry of the compressor to obtain a virtual map for a given compressor rotation speed of 150 krpm. The election of this speed is justified because this point presents significant instabilities for a wide range of air mass flows before the surge line.

The steady calculations allow reproducing with accuracy the compressor map in its stable operation zone. Near the surge line, the calculation diverges below a critical mass flow rate, due to the transient nature of the surge phenomenon. Therefore, unsteady calculations are necessary to reproduce the instability processes –rotating stall and the surge phenomena– that appear in the compressor when the mass flow rate is reduced to these critical values. The instability is detected in the compressor CFD map because higher oscillations in the pressure ratio are detected nearer the surge line.

Also analysis of the internal 3D flow has been performed in order to get a better understanding of the compressor behavior. Although the visualized steady point is inside the normal operating zone of the compressor, pressure contours show two instability zones –lower pressure levels– that lead to back flow in the periphery of sections immediately upstream of the rotor. These instability cells grow – low pressure zones fill the whole section– as the mass flow rate decreases to levels near to those producing surge, and recirculation is more evident.

## REFERENCES


1. Gravdahl J. T., Egeland O., Vatland S. O. "*Drive torque actuation in active surge control of centrifugal compressors*". Automatica 38 (2002) 1881-1893.
2. Gravdahl J. T., Egeland O., Vatland S. O. "*Active surge control of centrifugal compressors using drive torque*". Proc. of the 40th IEEE Conf. on Decision and Control. Orlando, Florida USA (2001).
3. Blanchini F., Giannatasio P. "*Adaptative control of compressor surge instability*". Automatica 38 (2002) 1373-1380.
4. Belta C., Gu G., Sparks A., Banda S. "*Rotating stall control for axial flow compressors*". Automatica 37 (2001) 921-931.
5. Watson N. "*Transient performance simulation and analysis of turbocharged diesel engines*". SAE Paper 810338, 1981.
6. Payri F., Benajes J., Galindo J., Serrano J. R. "*Modelling of turbocharged diesel engines in transient operation. Part 2: wave action models for calculating the transient operation in high speed direct diesel engine*". Proc. Inst. Mech. Eng. Part D 216 (2002) pp. 479-493.
7. Luján J. M., Galindo J., Serrano J. R. "*Efficiency characterization of centripetal turbines under pulsating flow conditions*". 2001 SAE Trans. – J. Engines 110 (3) (2002) 233-239.
8. Galindo J., Serrano J.R., Guardiola C., Cervelló C. "*Surge limit definition in a specific te st bench for the characterization of automotive turbochargers*". Exp. Therm. Fluid. Sci. 30 (2006) 449-462.
9. Luján J.M., Bermúdez V., Serrano J. R., Cervelló C. "*Test bench for turbocharger groups characterization*". SAE Paper 2002-01-0163. (2002).
10. Fluent 6 User's Guide. Fluent Inc, 2001.
11. Krain H. "*A CAD Method for Centrifugal Compressor Impellers*". ASME, J. of Eng. for Gas Turbine and Power, April 1984, Vol. 106 pp. 482-488.
12. Wang X.F., Xi G., Wang Z.H. "*Aerodynamic optimization design of centrifugal compressor's impeller with Kriging model*". Proc. of the Inst. Mech. Eng., Part A: J. Power and Energy Vol. 220 Nº6, pp. 589-597, 2006.
13. Larosiliere L. M., Skoch G.J., Prahst P.S., "*Aerodynamic Synthesis of a Centrifugal Impeller Using CFD and Measurements*". NASA Technical Memorandum 107515, AIAA-97-2878, 1997.
14. Koumoutsos A., Tourlidakis A., Elder R.L., "*Computional Studies of Unsteady Flows in a Centrifugal Compressor Stage*". Proc. of the Inst. Mech. Eng., part A: Journal of Power and Energy 2000, Vol. 214 pp. 611-633.
15. Engeda A., "*Experimental and Numerical Investigation of the Performance of a 240 kW Centrifugal Compressor with Different Diffusers*" ELSERVIER Exp. Therm. Fluid Sci. (28) 2003, pp. 55-72.
16. Pan D., Whitfield A., Wilson M., "*Design Considerations for the Volutes of Centrifugal Fans and Compressors*", IMechE, part C: Journal of Mechanical Engineering Science 1999, Vol. 213 pp. 401-410.
17. Dickmann H-P., Wimmel T. S., Szwedowicz J. "*Unsteady flow in a turbocharger centrifugal compressor: Three-Dimensional computational fluid dynamics simulation and numerical and experimental analysis of impeller blade vibration*". J. of turbomachinery (2006), Vol. 128, pp. 455-465.
18. Schmidtmann O., Anders J. M. "*Route to surge for a throttled compressor – a numerical study*". J. Fluids and Structures (2001) 15, 1105, 1121.
19. Proakis J. G., Manolakis D.G. "*Digital signal processing*". Chapter 5. Prentice Hall Inc. Upper Saddle River, New Jersey, 1996.
20. Versteeg HK., Malalasekera W. "*An introduction to computational fluid dynamics. The finite volume method*". LongMan Scientific &Technical, 1995.
21. Pan D., Whitfield A., Wilson M. "*Design considerations for the volutes of centrifugal fans and compressors*". IMechE, part C: Journal of Mechanical Engineering Science 1999, Vol. 213 pp. 401-410, 1999.

# Analysis of Different Turbocharger Surge Situations in Automotive Engines

F. Payri, J. Galindo, F.J. Arnau, R. Lang

CMT-Motores Térmicos. Universidad Politécnica de Valencia. Cno. Vera s/n. 46022. Valencia. Spain

**Abstract**: In the trend of downsizing automotive petrol and diesel engines there are limitations related to the engine dynamic behaviour at low speeds. One of the reasons for this is surge inception in compressor turbochargers when they work at high compression ratio and low flow. Compressor surge leads to detectable noise, loss of performance and the reduction of compressor life. Surge is rare at steady engine running conditions but it can be more frequent in certain engine transients like decelerations and at sudden load decrease.

In the proposed paper, the different engine situations where surge is more likely to happen are analyzed. A model able to simulate surge inception and development is described. The model is used to model surge inception in different engine conditions: steady, deceleration at full load and sudden pedal release.

**Keywords**: Turbocharging, unsteady flow, stall, surge, modelling, compressor.

### 1. Introduction

Turbocharging automotive internal combustion engines has allowed in the last decades for an improvement in performance. In the last years a clear trend of downsizing has appeared consisting in reducing the engine displacement while maintaining the rated power output. This means that for the same vehicle weight and speed the engine load is higher and therefore both fuel consumption and emissions are reduced. This goes well in line with the objective of lowering $CO_2$ generation.

Downsizing has several positive effects but makes the design of the boosting system more complicated. In order to have the same effective power with a smaller engine the boosting pressure has to be increased accordingly to the displacement reduction. This is particularly difficult to achieve at low engine speed penalising the low end torque and driveability. First, the turbine has to be small enough to run properly with low gas flow. Second, the increase of compression ratio at low flows is limited by the surge instability. This explains how compressor surge in automotive turbochargers has become a frequent topic in the last years.

Surge phenomenon is known for decades as an instability problem concerning not only the compressor but also its piping system. In a centrifugal compressor at constant rotating speed when the flow is reduced from the design value, compressor performance is worsened because of higher incident losses in the inducer. This may be seen in the reduction of isentropic efficiency. If the flow is reduced further, the flow is stalled in certain parts of the compressor. When stall appears the performance loss is even more relevant and compression ratio may decrease as air flow is reduced. Stall is a flow situation that can be shown as an instability phenomenon but it cannot be confused with surge. Stall instability has usually higher frequency than surge. Besides, stall is a compressor phenomenon, while surge involves the compression circuit.

When the compressor is coupled to a piping system with a flow controller at the compressor outlet circuit: a counter-pressure valve in a gas-stand, the intake valves in an engine or the turbine in a gas turbine; the set compressor-circuit may become instable. If the controlling valve is partially closed, the pressure of the compressed air between compressor and valve will increase. As the increase in outlet pressure is seen by the compressor, the mass flow is reduced. If the flow is reduced further to the surge limit, the compressor cannot maintain a so high compression ratio and suddenly the flow is inversed. In this new situation, the compressed air in the volume between compressor and valve escapes through the valve and also through the compressor and subsequently the pressure will decay. Below a given value in the compression ratio the compressor recovers and the flow is inversed again to the normal way. This will lead to a pressure recovery in the reservoir. Surge pulsations are related to the filling and emptying of the volume between compressor and valve.

In this paper, an analysis of different engines situations where surge can appear. This analysis includes the experimental methods to measure and detect surge; a compressor model able to represent the most relevant phenomena and some guidelines on how to reduce the risk of surge in different driving conditions.

The paper is structured as follows. First, the different facilities and experimental techniques used to study surge are presented in section 2. Next section presents the theoretical basis of an unsteady non-dimensional compressor model able to predict surge. Section 4 presents the methodology proposed to detect surge. Section 5 presents some results of surge in different transient conditions. Section 6 presents the modelling results. Finally, main conclusions are drawn.

## 2. Experimental setup

The most common facility used to measure turbocharger performance is the steady gas-stand. In this facility, a steady flow is produced to blow the turbocharger turbine. In the compressor side, a simple circuit including a filter, the intake pipe, the compressor, the outlet pipe, a reservoir and finally a controlling valve that sets the compressor operating point. This is presented in Figure 1.

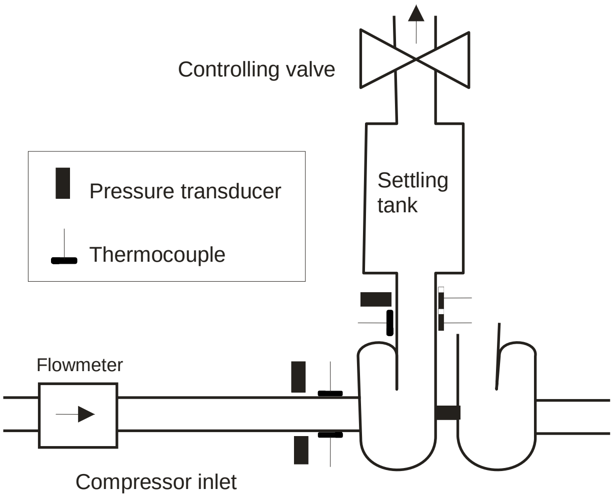


Figure 1: Usual compressor circuit in gas-stand testing.

In order to measure the compressor performace within the surge zone a different resistant circuit can be used. The controlling valve is installed at the compressor outlet reducing as possible the volume between compressor and valve. This reduces the amplitude and increases the frequency of pressure pulsations when operating in surge.

This allows for measuring an extended map (Figure 3) where the isospeed lines are drawn beyond the surge line.

Even though the gas-stand is commonly used to define surge line, tests on engine test bench are normally required to confirm the surge limit. The reason is that surge limit in gas-stand can be different to the one that is finally found in the actual engine for several reasons. It is known that the geometry of the compressor inlet duct has an important on stall development and thus on surge limit [1]. In addition, stall development can also be affected by pressure oscillations produced by engine breathing [2].

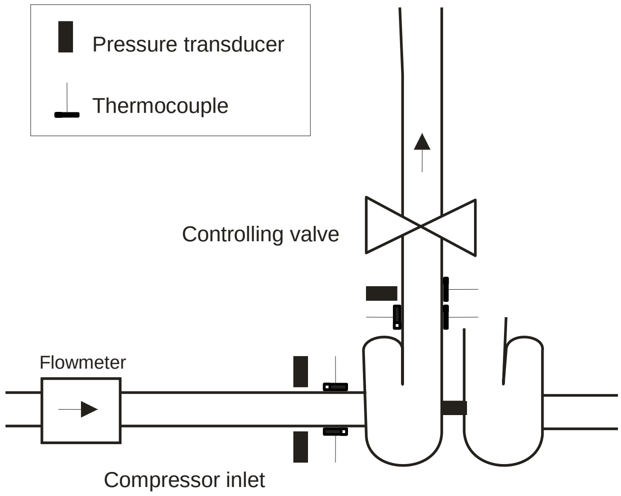


Figure 2: Compressor circuit with close-coupled valve to measure extended map.

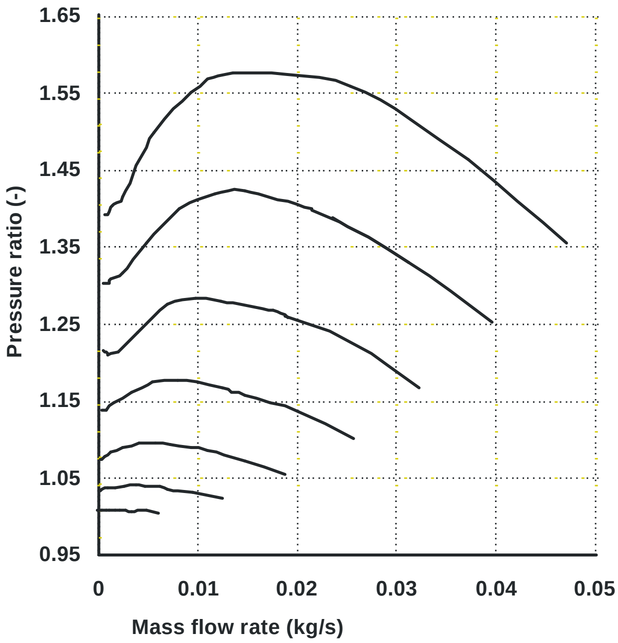


Figure 3: Extended compressor measured map with isospeed lines within the surge zone.

There are different ways for measuring surge limit on engine. The difficulty is that in an engine the compressor, the engine and the turbine work with the same flow. This limits the operating conditions that can be achieved in the compressor. A systematic way to measure surge line on the engine is to perform steady tests at constant speed and increasing boosting pressure. In order to increase turbine energy the fuel mass has to be chosen to have a minimum air-to-fuel ratio value. Figure 4 presents some results of steady engine tests at different boosting pressure and engine speed plotted in a compressor map.

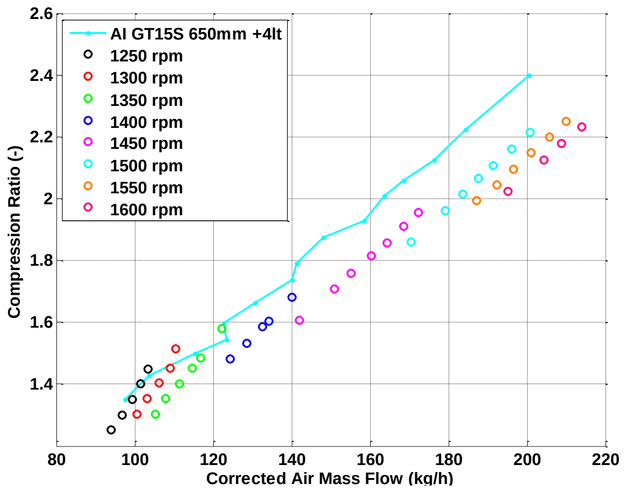


Figure 4: Compressor map with steady tests at constant speed and increasing boosting pressure.

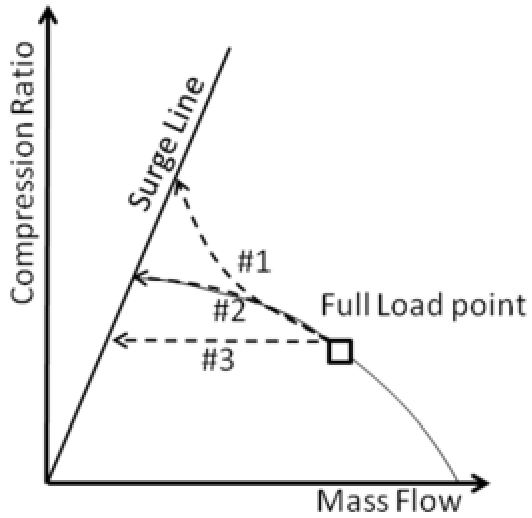


Figure 5: Air injection technique trajectories in the compressor map according to the turbine control: #1 turbine at fixed position, #2 controlling compressor speed, #3 controlling boosting pressure.

However this technique may have some limitations. On one hand, if the turbine is too big it will not produce enough work to increase the compressor compression ratio to attain surge limit. On the other hand, when the turbine is big there are les chances to go into surge. As a consequence, with this technique only a part of the surge line can be measured. Another problem is that sometimes constant engine speed lines in the compressor map are parallel to surge line. This makes more difficult to detect surge as it is discussed below.

A different technique to measure the surge line on the engine test bench is to inject air in the intake line between the compressor and the engine. Since the engine is a volumetric machine the engine flow is a function of the engine speed and intake density. When the air is injected the compressor air flow is reduced so that the total is that aspirated in the engine. As the compressor flow is reduced the operating point approaches to surge line. If the turbine has a variable geometry mechanism, there are different possibilities to control the turbine while the air injection is progressively increased. The first is to keep constant position and then the energy at the exhaust will be constant during the process. The second is to control the turbine position to keep constant intake manifold pressure. This can be done using the engine controls. The third option is to control the turbine in order to keep constant the (corrected) compressor speed. To do this is necessary to have the compressor speed signal and to use it in a closed loop control using an external control device. Figure 5 shows these three control options plotted as trajectories on the compressor map from a steady full load point towards the surge line.

There are several advantages of the air injection technique. First, the complete surge line can be measured. Since the intake air is increased with the amount injected it is possible to attain a broad range of compressor speeds. The compressor operating point is not limited by the turbine exhaust energy. Other benefit with the air injection technique is that the operating point trajectory is perpendicular to the surge line, therefore, the transition from stable operation to surge is well defined. Figure 6 (top) shows the air mass flow measured at the compressor inlet in a test with air injection. The bottom plot shows the same variable but going into surge by increasing boosting pressure in the engine at constant speed. It can be seen that in the top plot (air injection) surge appears suddenly between second 23 and 24. In this moment low frequency pulsations appear in the signal indicating the development of surge cycles. It is worth to note that even though the registered air mass flow is always above 60 kg/h, these pulsations correspond to deep surge, meaning that the flow in the compressor is reversed following the process explained in section 1. The reason why these backflows are not registered in the flow sensor is that the sensor is located more than 1 meter upstream and there the flow pulsations are partially damped.

In the bottom part of Figure 6 shows that when increasing boosting pressure towards surge line, surge cycles does not appear as abruptly than in the air injection test. As the compression ratio is increased come isolated surge cycles may appear (at seconds 23, 25 and 27) but the compressor recovers itself. In this case it is difficult to state where surge limit is located.

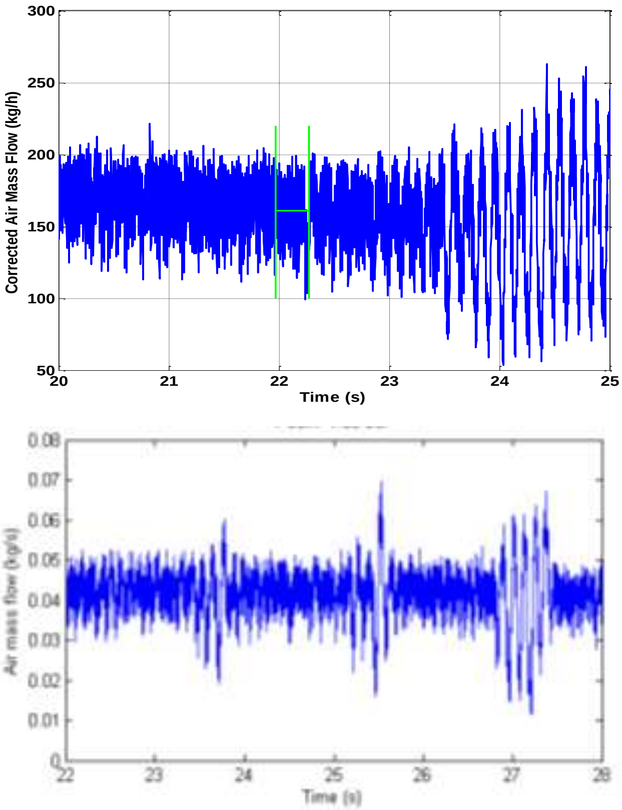


Figure 6: Evolution of air mass flow in surge tests: (top) air injection technique, (bottom) increasing boosting pressure at constant engine speed.

### 3. Surge detection technique

One of the toughest issues when trying to measure surge limit is the way to decide when the compressor is under surge. Surge is known to be an unstable running condition that can be heard and also can be registered with air mass flow or dynamic pressure sensors as it has been shown in Figure 6. However, pulsating operation can be found in the compressor mounted on the engine or even in the steady gas-stand out of surge zone. What characterizes better the surge unstable cycles is first, their frequency that is related to the natural frequency of the circuit between the compressor and the controlling valve, because during surge cycles this volume fills and empties. Surge cycles frequency is usually around 5-15 Hz for automotive turbochargers due to the volume of the outlet duct, intercooler and intake manifold. Second, the amplitude is related to the trajectories in the compressor map at nearly constant compressor speed from the maximum compression ratio close to the surge limit to the minimum value at zero flow. For instance in Figure 3 at maximum speed the maximum compression ratio is about 1.57 and the minimum value is around 1.39. Therefore, the pressure pulsations will be around 1.57-1.39 = 0.18 since the inlet pressure is about 1 bar then the amplitude is about 180 mbar.

The proposed way to detect surge is to look at the amplitude of the signals (air mass flow, compressor inlet/outlet pressure ...) in the frequency range between 5-15 Hz [3]. To do this the signals have to be processed by a Fourier Transform into the frequency domain. In this work, the signals have been treated in Matlab (© Mathworks). Figure 8 shows the spectrograms obtained with Matlab functions for the signals presented in Figure 6.

In the figure the darker points have higher amplitude at the corresponding frequency read in the y-axis. In the top plot the air injection procedure is presented. As the time goes the air injection flow is increased and this drives the compressor to surge in second 23. In this moment high amplitude contents appear around 8 Hz. The appearance of surge cycles is abrupt and easy to detect. The surge limit corresponding point can be processed averaging the measured variables some seconds before surge.

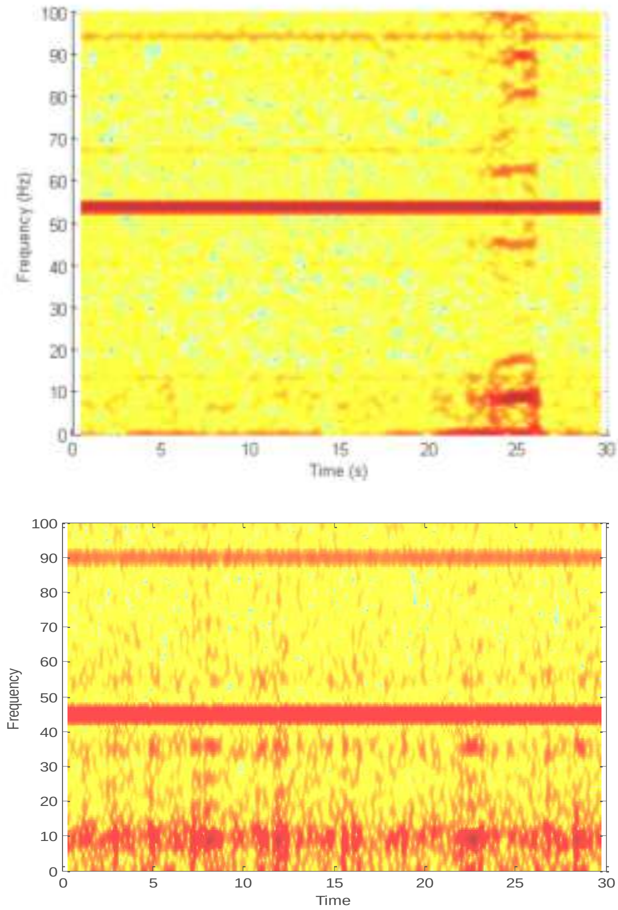


Figure 7: Spectrograms of compressor outlet pressure in Figure 6: (top) air injection technique, (bottom) increasing boosting pressure at constant engine speed.

Bottom plot in Figure 7 shows the spectrogram of air mass flow signal shown in Figure 6. This test has been conducted increasing the boosting pressure progressively at constant engine speed. Since the trajectory of the process is nearly parallel to the surge line as presented in Figure 4, surge does not appear suddenly but some surge cycles may appear isolated during stable operation. As the compressor operating point approaches to surge the surge pulsations become more frequents and its amplitude increases. But it is not easy to estate when surge has appeared.

In order to have an objective criterion to determine if the compressor is in surge or not, a procedure has been developed. The compressor is lead to deep surge at different rotating speeds. The amplitude of surge cycles is obtained in the low frequency range (5-15 Hz). A limit of low frequency amplitude is set as a percentage of that in deep surge. When this threshold is exceeded then it is considered to be in surge.

### 4. Compressor model

Some authors have proposed compressors models able to simulate surge unstable behavior. The first one was proposed by Greitzer in 1976 [1]. Basically, the model consisted in a filling-and-emptying model of the reservoir between the compressor and the controlling valve and the flow characteristics of compressor and valve. The unsteady part of the model was achieved introducing a first order delay in the calculation of the compressor compression ratio to the steady value interpolated in the compressor map. Though this model was proposed to axial compressors since it is based on the compressor map information, it was also used for radial compressors by other authors [5][6].

In this paper, a model based on the Greitzer's model has been used [7]. The model is implemented in a complete engine one-dimensional gas-dynamic model. The compressor node is non-dimensional connecting the inlet and outlet ducts that are calculated as 1D. In the compressor node the conservation equations are imposed as follows. The continuity equation imposes the conservation of mass.

$$\rho_i u_i S_i = \rho_o u_o S_o \qquad [1]$$

Where $\rho$ is density, $u$ is speed and $s$ is duct cross section. Subindex $i$ stands for input and $o$ for output.

The momentum conservation equation is imposed using the calculated pressure increase in the compressor due to the wheel effect. As proposed by Greitzer, an extended compressor map as the one presented in Figure 3 is used. Also, the steady compression ratio interpolated in the map is not used directly but with a delay as shown in Eq (2). The time delay is calculated as the time that a fluid particle takes to go through the compressor (Eq. 3).

$$\frac{d\pi}{dt} = \frac{\pi - \pi_{map}}{\tau} \qquad [2]$$

$$\tau = \frac{L}{\bar{u}} \qquad [3]$$

where $\pi$ is the total-to-total compression ratio, t is time, $\tau$ is the time delay and subindex ***map*** stands for steady value interpolated in the map. $L$ is the compressor equivalent length and $\bar{u}$ is mean velocity in the compressor.

Finally, the third conservation equation is the energy equation that allows the calculation of the temperature increase according to the actual compressor work (Eq.4). For inverse flow the hypothesis made is that the flow is isothermal.

$$T_{o0} = T_{i0} + \frac{\pi^{\frac{\gamma-1}{\gamma}} - 1}{\eta} \qquad [4]$$

where $T$ is temperature, $\eta$ is compressor isentropic efficiency, $\gamma$ is the ratio of specific heats and subindex **0** stands for stagnation conditions.

In order to connect with the pipes the Method of Characteristics is used. The compatibility equation is imposed at both duct ends. Also, in the incoming duct entropy is imposed as an input in the compressor node.

These 6 equations allow for the calculation of thermodynamic properties (pressure, temperature and mass flow) at the pipes ends. This model is intrinsically transient so there is no need to modify it for engine transient operation.

### 5. Experimental results

Different transient tests have been also carried out to quantify the effect of surge in different driving conditions. The most risky engine situations appear when the engine air mass flow is reduced suddenly. Two different situations have been tested starting from full load and low-medium speed: reducing suddenly engine speed at constant load and reducing suddenly engine load at constant engine speed. Figure 8 presents the trajectories of these transient tests on an engine map and on the compressor map.

The first situation is sudden pedal release from full load operation at low speed. This can be related to a driving situation in which a loaded vehicle is climbing and suddenly the driver release the accelerator pedal. In this case, effective torque falls instantaneously but engine speed decreases at a rate depending on vehicle inertia, road inclination and other. Due to the accumulation effect in the intake line between the compressor and the engine, the air mass flow in the compressor falls faster than compression ratio leading instantaneously the compressor to surge. Once compression ratio and turbocharger speed are reduced the compressor re-enters in the stable operation.

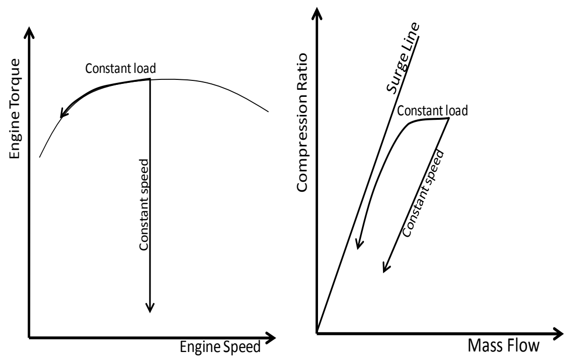


Figure 8: Transient analysed in the paper plotted on the engine (left) and compressor maps (right).

Figure 9 shows that surge cycles during pedal release transients may be observed in most compressor related variables. It is more perceptible in the air mass flow signal, but also compressor outlet pressure has big oscillations due to surge.

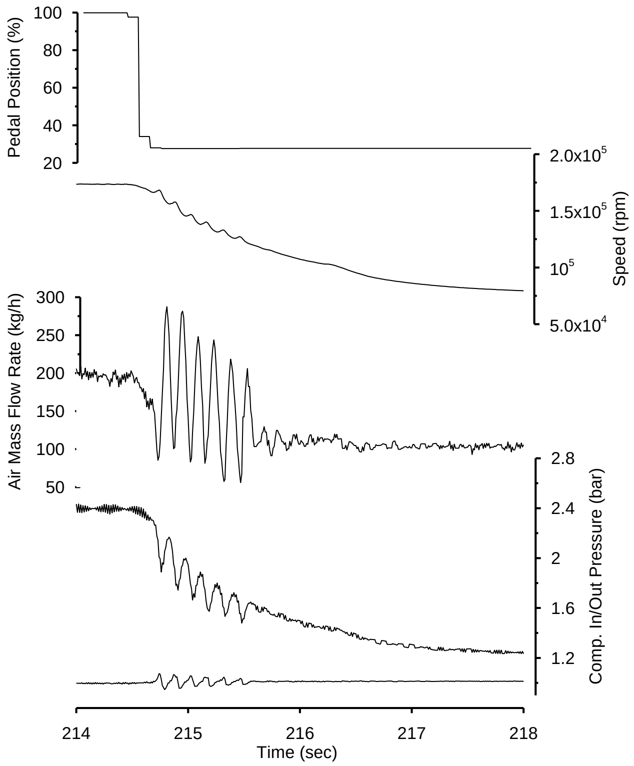


Figure 9: Measured variables during a pedal release transient with some surge cycles.

Surge cycles are less noticeable in speed and inlet pressure signals. In this type of transient, the entry in surge is abrupt and so easy to detect and to reproduce.

The trajectory in the compressor map is rather normal to the surge line as it is shown in Figure 10. It has to be said again that the air mass flow oscillations measured in the flow meter at a certain distance from the compressor are underestimated. Air mass flow in the compressor actually oscillates between negative and positive values. Although air mass flow cannot be measured properly during surge cycles, it can be at the start of the transient and later when the compressor becomes again stable. Figure 10 shows good agreement between steady surge line and the points at the beginning and at the end of surge cycles.

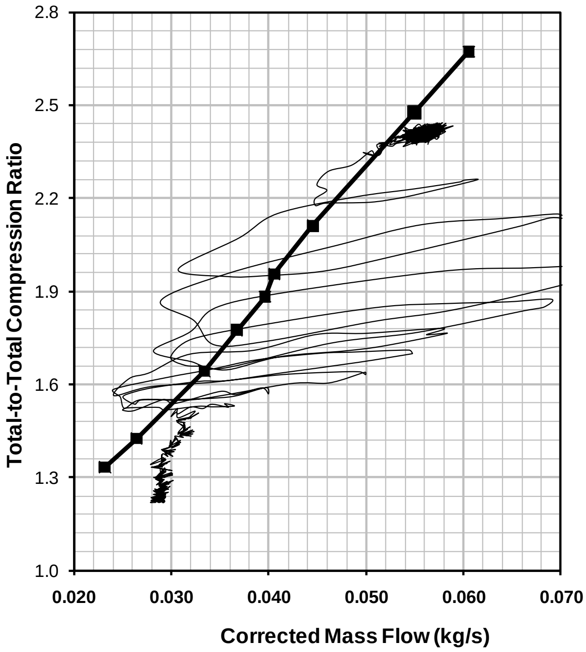


Figure 10: Trajectory of a sudden pedal release plotted on the steady compressor map.

The second situation where the compressor can enter into surge starts in the same operating point. The engine is at full load and low-medium speed so that the compressor is operating by the surge line as already presented in Figure 8. The engine speed is then reduced while maintaining full load.

The occurrence of surge is related to the rate of speed decrease. If this transient is slow, the compressor will follow the steady full load curve and there would not be surge. But, if the deceleration is quick enough the compressor may enter in surge.

Figure 11 shows the evolution of compressor outlet pressure, engine speed and turbine command from 2000 to 1200 rpm in 10 seconds. It can be seen that at the end of the transient test several surge cycles appear.

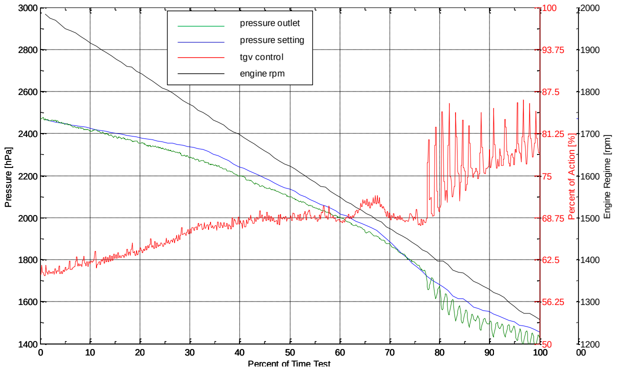


Figure 11: Evolution of compressor outlet pressure (green line) during the transient test

Figure 12 presents the amplitude of the signal in the low frequency range. A peak at the end of the transient reveals surge oscillations.

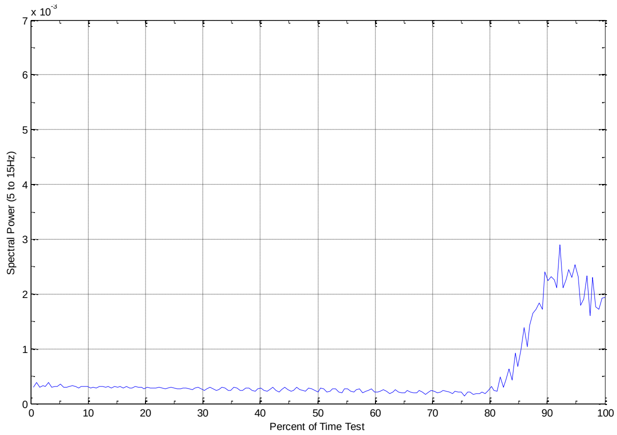


Figure 12: Amplitude at low frequency 5-15 Hz during the transient test.

Figure 13 plots the transient on the compressor map showing surge at rotating speeds below 120 krpm. The positive side is that in this transient surge appears at low rotating speeds and therefore the pressure pulsations amplitude is lower than at higher speeds.

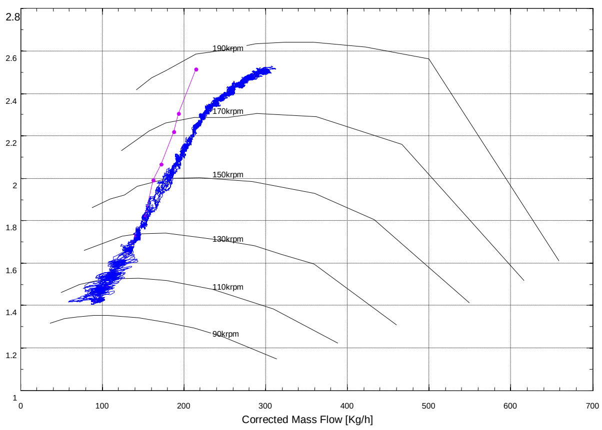


Figure 13. Evolution of compressor operating point plotted on the steady compressor map.

## 6. Model prediction

The model presented in section 4 has been used to simulate both transient tests presented above. For a good prediction of surge it is important not only to have an unsteady model as the one presented; but also that the engine model is able to predict the decrease in turbocharger speed and boosting pressure. The pressure reduction can be accounted as a discharge process in the volume of the intake line as a function of the mass flows at the compressor and at the engine and the rate of decrease of turbine work.

Figure 14 shows the results of the compressor model in the sudden pedal release shown in Figure 9. The model predicts surge pulsations of about the same amplitude and frequency than the measured pulsations. It seems that the model predicts more surge cycles than the tests.

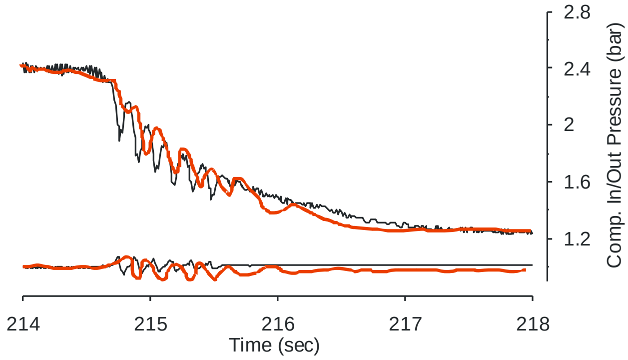


Figure 14: Modelled (red) vs measured (black) compressor inlet and outlet pressure during a sudden pedal release.

Figure 15 shows the same comparison for a sudden deceleration from 2000 to 1250 rpm at full load as that presented in Figure 11. This situation is harder to simulate because the transient trajectory moves parallel to surge line as presented in Figure 13. Small errors in the prediction of compressor air mass flow can modify the prediction of the moment when surge starts. However, again the agreement amplitude and frequency of surge pulsations is quite good. Also, the number of surge cycles is well estimated.

These results show the potential in the use of the Greitzer-type surge models to predict surge cycles in this kind of engine transients. Somehow, the calculation of surge during transients is easier than steady operation where other factors like pressure pulsations during the cycle have more influence. During the transients the compressor operating point is controlled by the sudden variations in air mass flow or compression ratio.

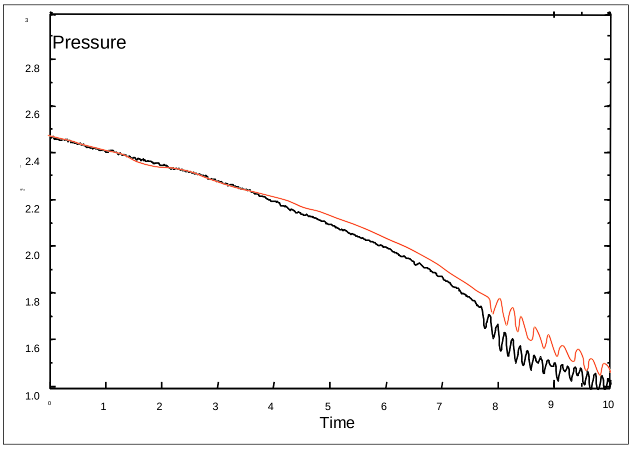


Figure 15: Modelled (red) vs measured (black) compressor outlet pressure during a sudden deceleration at full load.

## 7. Conclusion

This paper presents an experimental and modelling of surge phenomenon in automotive turbochargers. In the paper some experimental techniques have been presented to analyse surge in steady or transient operation. In particular, a method to detect surge is proposed based in the analysis of measured signals in the frequency domain.

Two different driving situations where the risk of surge is more likely are analysed: sudden pedal release from full load and fast deceleration at full load. It has been showed that the surge occurrence is dependent on the rate of decrease in speed/load.

A model able to deal with surge instabilities has been presented. This model is based on the steady information of an extended compressor map and a delay imposed in the calculation of the compressor operating point. The model proves to be a good tool to predict surge in the described transient tests. The combination of tests and predictive models is the best strategy to analyse complex fluid phenomena like surge.

## 8. Acknowledgement


The authors acknowledge the contribution of Raúl Luján to the tests presented in this paper. They also thank Mr. Lahjaily and Mr. Giménes from Renault S.A.S. France for their support.

The work has been partially supported by Spain's Ministerio de Ciencia through project TRA2007-65433.

R.Lang is indebted to Generalidad Valenciana through grant GRISOLIA/2008/009


## 9. References


[1] Galindo J., Serrano, J.R., Margot X., Tiseira A., Schorn N., Kindl H.: "Potential of flow pre-whirl at the compressor inlet of automotive engine turbochargers to enlarge surge margin and overcome packaging limitations", International Journal of Heat and Fluid Flow, Vol. 28, 3, 2007.

[2] Galindo, J., Guardiola, C., Climent, H. Tiseira, A.: "On the Effect of Pressure Pulsations on Surge Margin of Small Centrifugal Compressors for Automotive Engines", Experimental Thermal and Fluid Science, Vol. 33, 8, 2009.

[3] Galindo J., Serrano, J.R., Guardiola, C., Cervelló, C.: "Surge Limit Definition in a Specific Test Bench for the Characterization of Automotive Turbochargers with Pulsating and Continuous Flow", Experimental Thermal and Fluid Science, Vol. 30, 5, 2006.

[4] Greitzer, E.M.: "Surge and Rotating Stall in Axial Flow Compressors Part II: Experimental Results and Comparison with Theory", ASME Journal of Engineering for Power, Vol.98, 1976.

[5] Fink, D.A., Cumpsty, N.A., Greitzer, E.M.: "Surge Dynamics in Free Spool Centrifugal Compressor System", ASME Journal of Turbomachinery, Vol.114, 1992.

[6] Theotokatos, G., Kyrtatos, N.P.: "Diesel Engine Transient Operation with Turbocharger Compressor Surging", SAE Paper 2001-01-1241, 2001.

[7] Galindo, J., Serrano, J.R., Climent, H., Tiseira, A.: "Experiments and modelling of surge in small centrifugal compressor for automotive engines", Experimental Thermal and Fluid Science Vol. 32, 3, 2008.

Experimental TECHNIQUES SEM
A Publication for the Practicing Engineer

# ON-ENGINE MEASUREMENT OF TURBOCHARGER SURGE LIMIT

| | |
|---|---|
| Journal: | *Experimental Techniques* |
| Manuscript ID: | Draft |
| Manuscript Type: | Technical Article |
| Date Submitted by the Author: | n/a |
| Complete List of Authors: | Galindo, José; Universidad Politécnica de Valencia, CMT-Motores Térmicos<br>Tiseira, Andrés; Universidad Politécnica de Valenci, CMT-Motores Térmicos<br>Arnau, Francisco; Universidad Politécnica de Valenci, CMT-Motores Térmicos<br>Lang, Ricardo; Universidad Politécnica de Valenci, CMT-Motores Térmicos |
| Keywords: | Fluid Mechanics |
| Topic : | Sensors and Instrumentation |
| | |

# ON-ENGINE MEASUREMENT OF TURBOCHARGER SURGE LIMIT

J. Galindo, A. Tiseira, F.J. Arnau, R. Lang

CMT-Motores Térmicos. Universidad Politécnica de Valencia.

P.O. Box 22012. Spain E46071. galindo@mot.upv.es +34963879656

## ABSTRACT

In this paper a new experimental technique is presented to measure the turbocharger surge limit in a regular engine test bench. It is known that the surge margin on engine tests may be very different to that obtained in a steady flow gas-stand. In particular, surge is very dependent on the flow pattern produced by the compressor inlet duct and also on the piping upstream and downstream the compressor. The technique is based in the injection of pressurized air into the intake manifold. In the paper this technique is compared to other ways of measuring the compressor map on engine. Some results with different compressor arrangements are presented and discussed. Finally, this technique allows for measuring not only the actual surge line but also the complete compressor performance map.

## INTRODUCTION

Turbocharging is a strategy used for years to increase the internal combustion engine power output. The trend in the last period has been the downsized engine that has similar or even better performance with a lower displacement capacity. Further advantages are obtained with downsizing concerning engine efficiency and pollutant emissions. On the other hand, some drawbacks have to be regarded as well. Since performance is maintained in these downsized engines the maximum air flow is kept almost unchanged. However, to maintain effective torque with lower cylinders displacement, compression ratio in the turbocharger has to be increased proportionally. This is difficult at low engine speed. All this has made the boosting system the key factor in the development of downsized petrol and diesel engines.

The development of automotive engine boosting systems is based on the use of compressor and turbine maps usually supplied by its manufacturer and obtained in tests facilities called gas-stands [1]. In these gas-stands the turbochargers are blown by a steady hot compressed air flow [2][1]. In the compressor side a simple straight duct is usually employed at the compressor inlet, and a big reservoir and a controlling valve at the compressor outlet. The steady compressor map is then obtained closing the valve from an open position progressively until the compressor begins to surge; the turbine flow is set so that the turbocharger speed is kept constant.

Surge phenomenon is known for decades as an instability that appears in centrifugal and axial compressors when they work at low mass flow rate for a given pressure ratio or shaft speed [3]. This results in pressure oscillations that are noisy and can be very destructive in some operating conditions. It is worth to remember that surge is a phenomenon depending not only on the compressor but also on its piping circuit [4]. The surge instability is produced by the coupling between the declining performance of the compressor when air mass flow is reduced and the resistant circuit characteristics [3]. When the compressor flow is reduced from the design point, some stalled flow appears either in the diffuser or in the impeller due to the inadequate design in that operating condition. When the flow is further reduced, these recirculation flows go towards the impeller inlet producing an unstable fluctuating flow that rotates with the wheel movement. This is known as rotating stall [6]. Depending on the compressor speed, this stalled flow can obstruct some of the vanes in the compressor wheel leading to a reduction of the compressor performance in terms of compression ratio and efficiency. This is reflected in a change of the slope of iso-speed lines in the compressor map. The increase of the lines slope combined with the characteristics of the resistant circuit determines the resulting stability operation point [7]. At a given flow rate, the compressor operating point becomes unstable and the compressor begins to surge. Surge leads typically to a low frequency fluctuating flow where the compressor running point goes from the stable operation point to negative flows. This results in pressure oscillations that depending on their amplitude can destroy the compressor quite fast [8].

The problem for automotive engine developer is that the surge line obtained in steady flow bench and with a simple piping around the compressor may differ from the surge limit when the same compressor is tested on the engine test bench [9]. There are several reasons for this different behavior. First, compressor inlet duct is usually different to a straight one. Or it may be modified during the engine development project. Even, there can be different compressor entries for the same engine installed in different vehicles. This can modify impressively the surge limit for better or for worse [10]. Second, the pulsating flow induced by the aspirations of the cylinders has been proved to modify the occurrence of the instability leading to surge. Minimum air mass flow at a given compressor speed may be reduced up to 15% when increasing pressure pulsations amplitude at 200 mbar [11].

The objective of the paper is to propose an experimental procedure to measure the compressor surge limit in actual engine conditions and furthermore using a regular engine test bench. With this method the compressor surge can be characterized with the actual engine conditions concerning the inlet ducting geometry and intake line acoustics. Therefore a more realistic surge limit can be obtained.

Next section presents the description of the facility and the measurement procedure. Then some results are presented to show the benefits of the proposal methodology. Last section states the conclusions of this paper.

## DESCRIPTION OF THE EXPERIMENTAL SET-UP

In this work, two facilities are used. The first is a regular gas-stand where the turbocharger compressor map is measured in steady controlled conditions [2]. Figure 1 depicts the gas-stand setup that includes a hot gas steady flow generated in our case by an 11-liter diesel engine. The compressor takes the room air through an air filter and a flow meter, and impels it to a reservoir of about 10 liters and then through a controlled valve the air goes to the atmosphere. Even though this facility has been modified to produce pressure pulses at the turbine and the compressor [11], in this case steady flow in both turbomachines has been imposed.

The second facility used in this work is a regular engine test bench in which the engine speed is controlled with an asynchronous dynamometer. The engine has to be instrumented to measure at least air mass flow and compressor inlet and outlet pressure. Modern automotive engines are usually instrumented with a hot plate anemometer between the air filter and the compressor, and absolute pressure piezorresistive gauges at the filter outlet and at the intercooler outlet. With these sensors it is possible to obtain the performance map of the compressor where some pressure losses in the piping and intercooler are included.

It is not easy to lead an automotive turbocharger mounted on the engine into surge. First, the engine full load is limited among other criteria by surge occurrence. Second, air flow and compression ratio cannot be freely modified since they are linked to the volumetric pump that is the engine. Consequently, when the boosting pressure is increased the mass flow rate increases as well. The only way to make the turbocharger on an engine running properly is during transient tests, e.g. releasing the accelerator pedal suddenly at full load and low engine speed. These tests are not suitable to measure the surge line because it is hard to determine in transient the flow conditions just before entering into surge and then to locate these points on the compressor map.

There are different ways to make independent the compressor and engine flows having their pros and cons. The first is to make a bleeding of the air coming from the turbocharger to the atmosphere so that the compressor air mass flow is different (higher) than that of the engine. The problem is that it is usually impossible to go to surge because the air flow in the compressor is maintained. A second method is to open the intake manifold to the atmosphere. In this procedure a valve is needed downstream the compressor to control the turbocharger compression ratio. For this purpose, the intake throttle in both petrol and diesel engine can be used. The flaw in this technique is that the engine becomes naturally aspirated and the turbine flow and work is reduced. This limits the energy available and only compressor operating points below a given speed can be measured. Besides, with this method the engine is not connected to the compressor and therefore pressure pulsations generated by cylinder aspirations are not accounted for.

The method proposed in this paper is to inject compressed air into the intake manifold so that the engine air flow will be the addition of the injected plus the compressor air flows. Since the air mass aspirated by the engine is depending on the intake manifold density, the more the injected air, the more reduced is the compressor air mass. Compared to the previous method, it has the advantages that the actual intake line is assessed and then the real intake line acoustics is considered. Also, since the air injection system supplies the air the compressor does not, the engine operating point is stable even when the compressor begins to surge. This is important because the turbine is fed steadily and it can blow at very high compressor speeds allowing for measuring the whole compressor map including its surge line. Figure 2 shows a sketch of the system. It includes besides the engine a source of compressed air, the line to the engine and as close to the engine as possible a controlling valve.

The source of compressed air has to fulfill two requirements. The air pressure has to be above the engine boosting pressure and the available flow has to be enough to reduce the compressor flow from full load steady points to surge. The needed flow of pressurized air is related to the distance between the surge line to be measured and the engine full load curve. This can be visualized in the compressor map as the distance between points A and B marked in Figure 3. Hopefully, a simple compressed air supply available in many testing facilities is usually enough to cover these requirements. The compressed air line and the controlling valve have to have an effective section suitable to inject the maximum flow needed. The requirements for the controlling valve besides the maximum section are that the proportionality of the opening section has to be good to control low air flows and it has to be controlled externally to the testing cell. Also, it is recommended that the valve is mounted as close to the intake manifold as possible, but the location where the air is injected into the intake manifold is unimportant. This can be done with a simple manual valve or a controlled one. In current diesel or petrol engines, it is possible to use the EGR valve as controlling valve closing the EGR line in the exhaust manifold. Using the EGR valve has several advantages: first it is usually mounted in the cold side of the EGR valve close to the intake manifold; second, its proportionality is usually very good; and third, it can be controlled changing the air mass flow maps in the ECU (Electronic Control Unit).

The evolution that the compressor will follow when the amount of air injected is increased depends on the control of the turbine.

- If a variable geometry or waste-gated turbine is set to a constant position, the process will be nearly at constant turbine power and the turbocharger speeds up slowly as the compressor mass flow is reduced. This is marked as #1 in Figure 4. To do this is necessary to put manual control in the ECU turbine controller.
- If it is controlled to hold constant boosting pressure the process will be at constant compressor ratio reducing slightly the turbocharger speed. This is the actual control strategy for the turbine in automotive engines, so that it is the natural strategy is the ECU is left as it is (mark #3 in Figure 4).
- If the test cell has the possibility to control externally the turbine or waste-gate position, it may set to maintain constant corrected turbocharger speed so that the usual compressor map at given compressor speed may be obtained (mark #2 in Figure 4).

The testing procedure is as follows. The engine operating point is set to full load and low speed. If possible, it is good to approach to surge closing further the turbine. Care must be taken with maximum in-cylinder pressure limit value. Then, the measurement recording is switched on and the air injection valve is progressively open reducing the air flow through the compressor. This opening process has to be as slow as possible to get an even evolution of flow variables in the moment before going into surge. Surge may be detected in different ways such as noise, temperature increase at the compressor inlet or increase in the oscillations amplitude in air mass flow or inlet or outlet pressure sensors. This can be visualized in an oscilloscope during the tests. The whole transient process is registered with the high and low frequency acquisition systems. To detect surge a sampling rate of 100 Hz is high enough. The type of signals measured is presented in Figure 5. It can be seen that the evolution going from stable to surge operation is smooth and it is clear when the instability develops so that the last stable operating point can be obtained by averaging the dynamic signals just before surge develops. This is marked as red line in Figure 5. This procedure is repeated for different compressor compression ratios or speeds and the whole surge line can be measured.

# RESULTS AND DISCUSSION

A first result of the air injection technique as a means to measure the actual on-engine surge line is presented in Figure 6. It is plotted there the compressor map measured in a regular gas-stand with a straight inlet duct. In this map it is represented the full load operating points of a 2.2 liter automotive diesel engine. It is worth to remark that the full load curve goes into the surge zone as predicted by the steady map. The air injection technique allows for measuring on the engine test bench a different surge line with the same compressor entry geometry. This is marked in Figure 6 as green dots. Using the air injection technique it is possible to reach values of compression ratio as high as 3. Most important, air injection technique allows for measuring different compressor inlet geometries. In Figure 6 a bended duct at the compressor inlet surge line is presented (pink squares). This results show how a well designed entry may enlarge surge margin allowing for an increase of engine low end torque.

A second result in a different engine is presented in Figure 7. Several compressor inlet geometries have been tested in a 1.6 liter automotive diesel engine. In this case, surge line measured on the gas-stand with a straight pipe in the compressor inlet (thin continuous line) does not differ to much from that measured on engine with the air injection technique at low speed (thick green line with triangles). But the agreement is worse at high speed. Other compressor inlet geometries have been measured on engine as well. The bended pipe with an elbow at the compressor inlet (thick pink line with dots) does not produce in this particular case much increase in surge margin. Compared to previous engine result it has to be said that the bend radius in this case is larger and then the effect of the elbow is lower. A tapered pipe with an angle of 19º at the compressor inlet (thick blue line with squares) leads to higher surge margin compared to the straight pipe case. Finally, the best among all the geometries tested was a cylindrical plenum of 1 liter volume installed at the compressor entry (thick red line with diamonds).

In Figure 7 it is plotted a dashed line indicating the loci of engine operating points at constant speed. The intersection of the engine line with the different surge lines show the potential increase in compression ratio/mass flow with each compressor inlet geometry. The figure shows that the gas-stand test would predict a compression ratio value of 1.5, while the on-engine tests with the straight and bended pipe should predict 1.6, the tapered pipe 1.7 and finally, the plenum more than 1.9. This clearly shows the importance of a good estimate on surge margin on engine low end torque prediction.

The air injection technique to measure surge line has many advantages. First, surge line is measured in real engine conditions. Pressure pulsations are very similar to those of the engine. It is true that the air injection modifies slightly the acoustics of the entire intake line, but if the controlling valve is located as close as possible to the intake manifold, the change in acoustics would be low. In this way, to use the EGR valve as controlling valve is a good option.

A second advantage of the air injection methodology is that surge points may be measured at relatively high compressions ratios as proven above. Since the engine air intake is maintained during the test, energy release from combustion and turbine work, also are. With other ways to lead the compressor to surge, the reduction in air mass flow is translated in less turbine power and so less compression ratio at a given engine speed can be reached.

A third benefit of the proposed methodology is that the transient process from stable to unstable operation is really smooth in a quasi steady manner as it can be seen in Figure 5. As already mentioned this eases the accurate determination of the surge line. Even once the compressor is in surge all the engine parameters can be maintained because the loss of compressor performance due to surge is compensated by the air injection system. In other methods, once the compressor becomes unstable, the decrease in air mass flow may enter the engine into the smoke limiter control reducing the injected fuel. This makes the engine torque to be reduced. Next, depending on the control of the test bench low frequency cycles may appear where the compressor enters in surge, the engine speed increases, then the compressor becomes stable again, the engine speed decreases and so forth.

# CONCLUSIONS

A procedure to measure a compressor map and more precisely its surge limit on the engine test bench has been presented. This technique allows for measuring the surge limit in actual engine conditions accounting for the effect of the compressor inlet geometry and the entire line acoustics. The procedure consists in inject compressed air into the intake manifold reducing progressively the air mass flow through the compressor. This procedure allows to lead the compressor to surge in a very smooth test so that the last stable point can be accurately measured. Depending on the controls in the turbine side slightly different trajectories can be followed on the compressor map.

The air injection technique has been used to measure surge lines with two different engines with different compressor inlet geometries and compared to the surge line measured in a steady gas-stand. The results show that the proposed methodology leads to more realistic results in terms of surge margin and allows for comparing different geometries.

The proposed technique has several benefits. It accounts for actual engine conditions including the effect of the compressor entry geometry and engine intake line acoustics. Second, the complete compressor surge line can be measured up to high speed. And finally, the tests is carried out in transient but it is a sequence of quasi-static conditions and the compressor goes into surge in a smooth manner.

## ACKNOWLEDGMENTS

This work has been funded by Spain's Ministerio de Ciencia y Tecnología through project TRA2007-65433. The authors acknowledge R. Luján for his valuable contribution to the tests. Ricardo Lang is indebted to the Generalidad Valenciana through grant GRISOLIA/2008/009.

## REFERENCES

[1] Hajilouy-Benisi, A., Rad, M. and Shahhosseini, M.R., "Empirical assessment of the performance characteristics in turbocharger turbine and compressor", *Experimental Techniques*, **34**: 54-67 (2010). doi:10.1111/j.1747-1567.2009.00542.x

[2] Galindo, J., Serrano, J.R., Guardiola, C. and Cervelló, C., "Surge limit definition in a specific test bench for the characterization of automotive turbochargers", *Experimental Thermal and Fluid Science*, **30**: 449-462 (2006).

[3] Oakes, W.C., Lawless, P.B., Fagan, J.R. and Fleeter, S., "High-speed centrifugal compressor surge initiation characterization", *Journal of Propulsion and Power*, **18**: 1012-1018 (2002).

[4] Galindo, J., Serrano, J.R., Climent, H. and Tiseira, A., "Experiments and modelling of surge in small centrifugal compressor for automotive engines", *Experimental Thermal and Fluid Science*, **32:** 818-826 (2008).

[5] Fink, D.A., Cumpsty, N.A. and Greitzer, E.M., "Surge dynamics in a free-spool centrifugal compressor system", *Journal of Turbomachinery*, **114**: 321-332 (1992).

[6] Greitzer, E.M., "Surge and rotating stall in axial flow compressors - 2. Experimental results and comparison with theory", *J Eng Power Trans ASME*, **98A**: 199-217 (1976).

[7] Gravdahl, J.T. and Egeland, O., "Centrifugal compressor surge and speed control", *IEEE Transactions on Control Systems Technology*, **7**: 567-579 (1999).

[8] Kurz, R. and White, R.C., "Surge avoidance in gas compression systems", *Journal of Turbomachinery*, **126**: 501-506 (2004).

[9] Engeda, A., Kim, Y., Aungier, R. and Direnzi, G., "The Inlet Flow Structure of a Centrifugal Compressor Stage and Its Influence on the Compressor Performance", *Journal of Fluids Engineering, Transactions of the ASME*, **125**: 779-785 (2003).

[10] Galindo, J., Serrano, J.R., Margot, X., Tiseira, A., Schorn, N. and Kindl, H., "Potential of flow pre-whirl at the compressor inlet of automotive engine turbochargers to enlarge surge margin and overcome packaging limitations", *International Journal of Heat and Fluid Flow*, **28**: 374-387 (2007).

[11] Galindo, J., Climent, H., Guardiola, C. and Tiseira, A., "On the effect of pulsating flow on surge margin of small centrifugal compressors for automotive engines", *Experimental Thermal and Fluid Science*, **33**: 1163-1171 (2009).

[12] Payri, F., Galindo, J., Climent, H. and Guardiola, C., "Measurement of the oil consumption of an automotive turbocharger", *Experimental Techniques*, **29**: 25-27 (2005).

## LIST OF FIGURE CAPTIONS

Figure 1. Layout of the gas-stand.

Figure 2: Engine layout with the air injection system.

Figure 3. Compressor map measured on a regular gas-stand, engine full load and surge limit points (triangles) measured by air injection technique.

Figure 4. Trajectories of different air injection tests with different turbine control strategies.

Figure 5. Evolution of some measured signals during the air injection test.

Figure 6. Compressor map with gas-stand surge line (continuous black line), on-engine with a straight pipe (green dots), on-engine with a bended pipe (pink squares).

Figure 7. Surge lines measured with air injection technique corresponding to different compressor entry geometries.

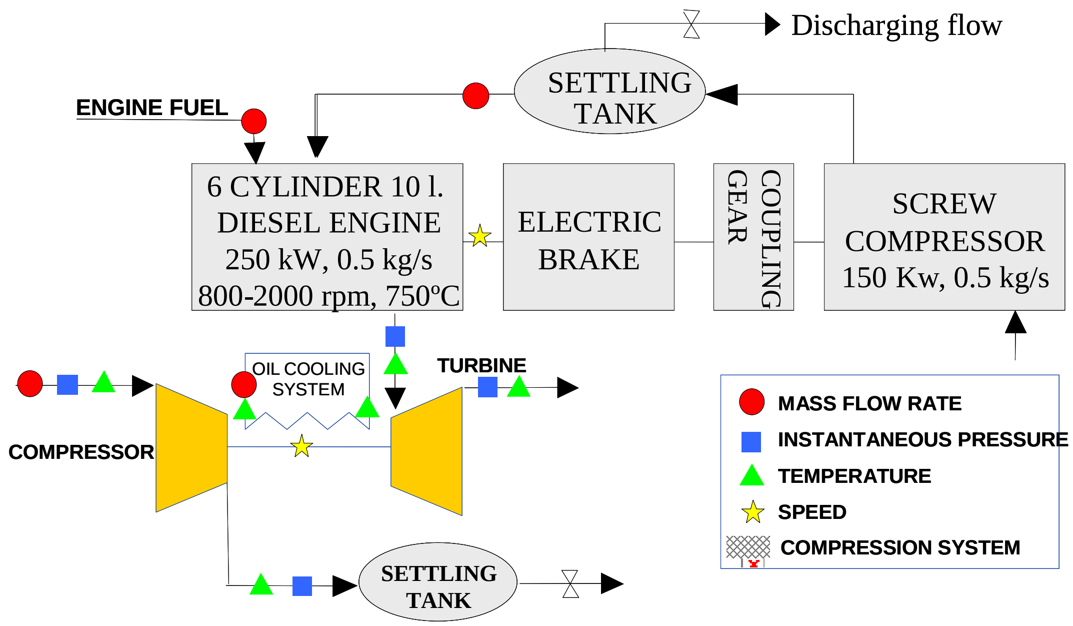


Figure 1. Layout of the gas-stand.

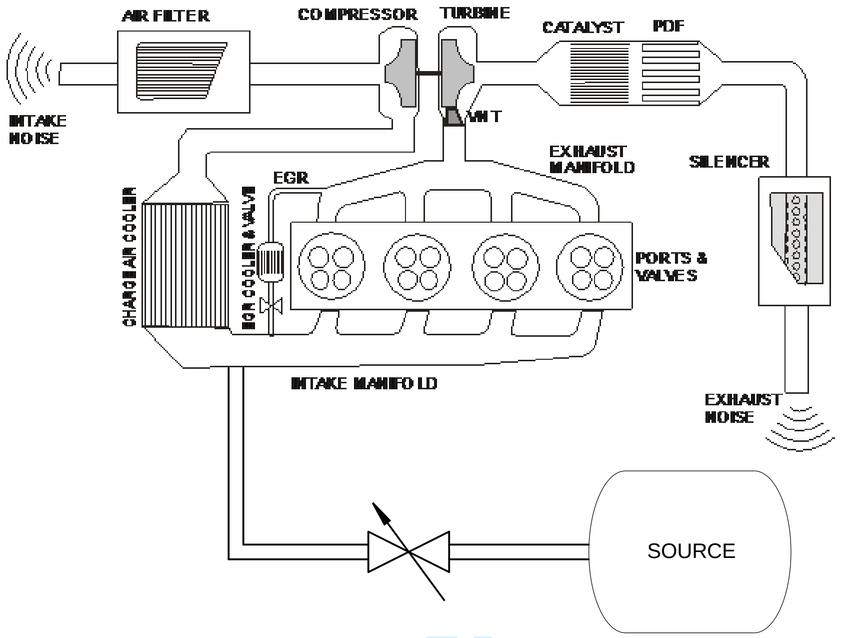


Figure 2: Engine layout with the air injection system.

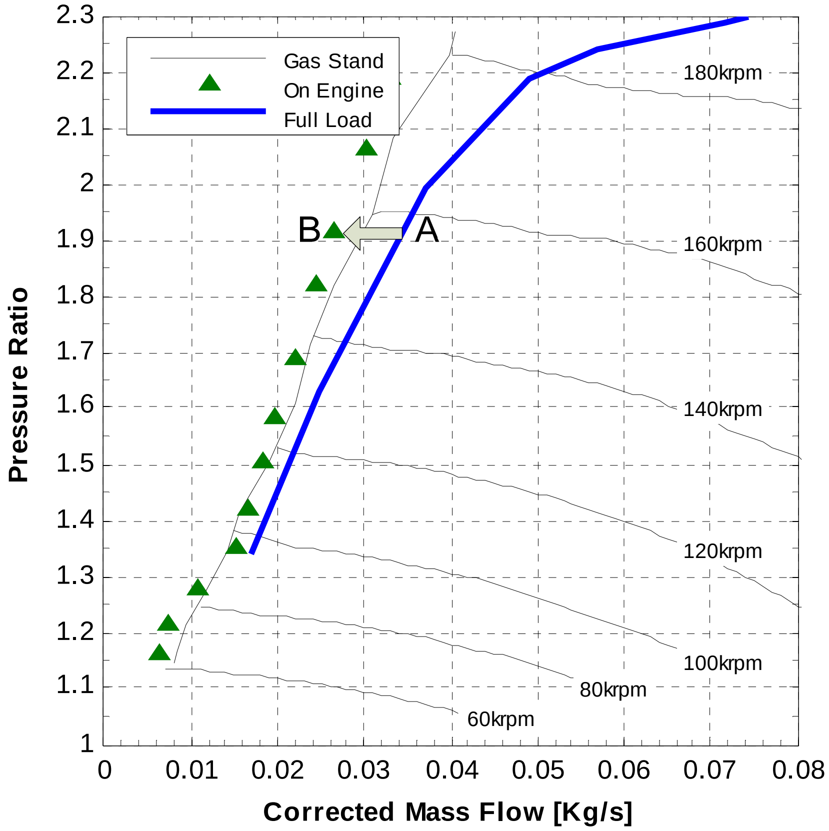


Figure 3. Compressor map measured on a regular gas-stand, engine full load and surge limit points (triangles) measured by air injection technique.

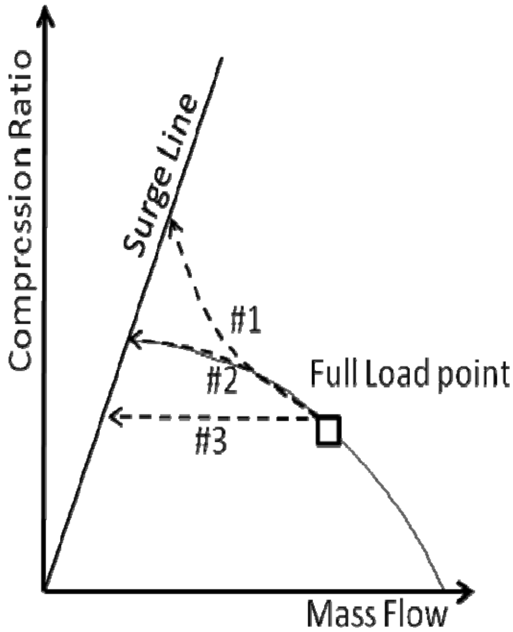


Figure 4. Trajectories of different air injection tests with different turbine control strategies.

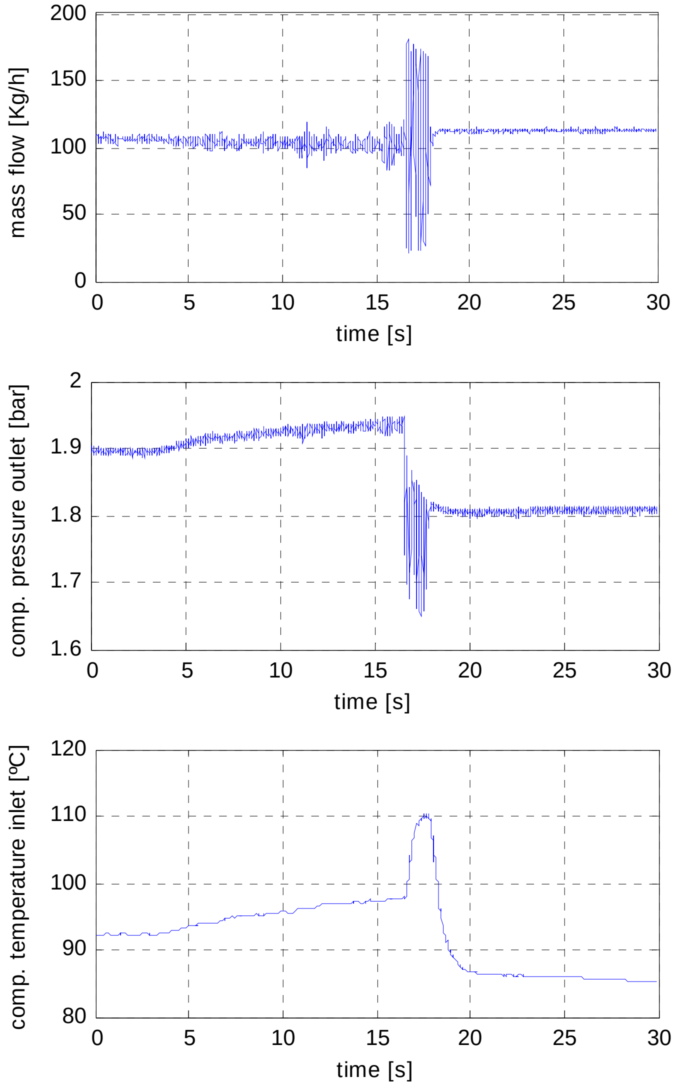


Figure 5. Evolution of some measured signals during the air injection test.

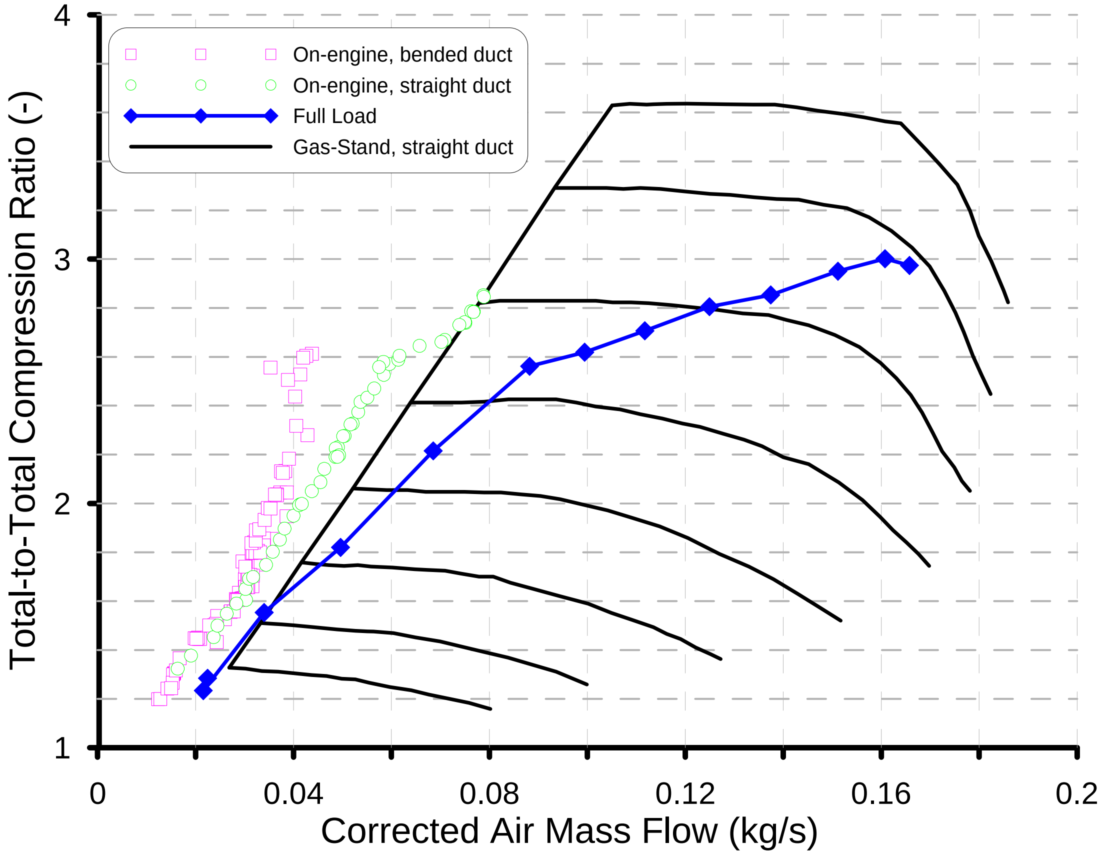


Figure 6. Compressor map with gas-stand surge line (continuous black line), on-engine with a straight pipe (green dots), on-engine with a bended pipe (pink squares).

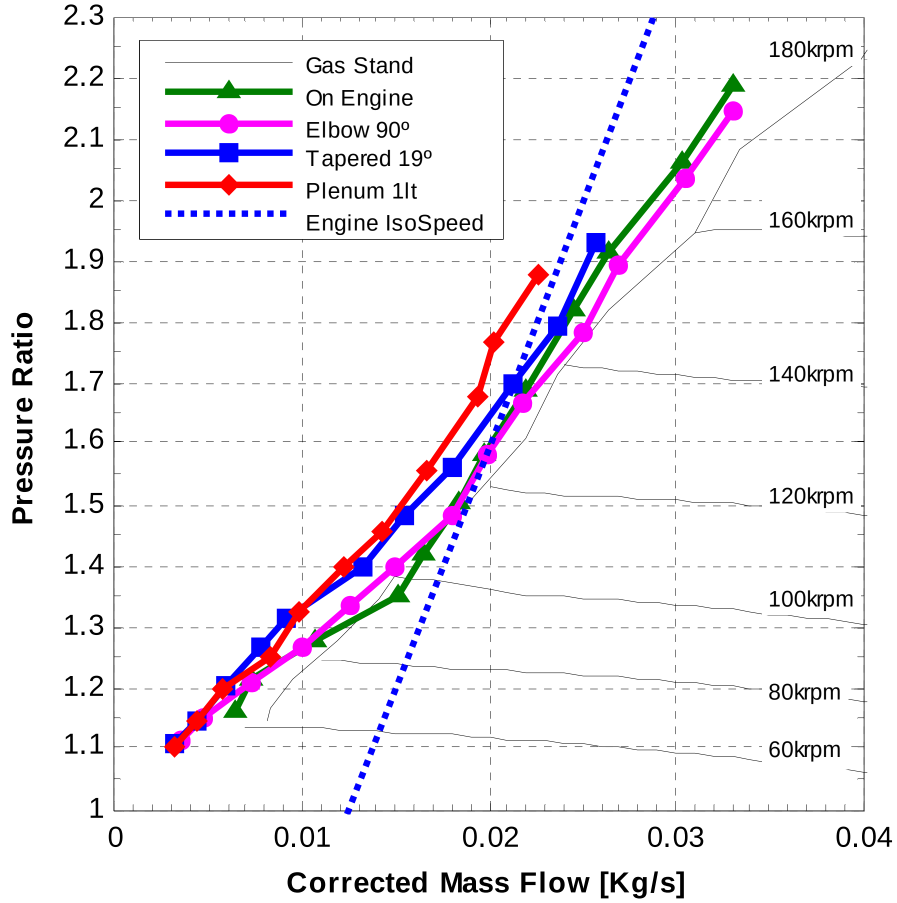


Figure 7. Surge lines measured with air injection technique corresponding to different compressor entry geometries.

# PROJET POMPAGE CMT

*"Analyse et mesure des phénomènes de pompage entrée compresseur"*

# CONTENTS

1. **Gas-stand tests**
2. **Engine tests**
3. **CFD calculations**

UNIVERSIDAD POLITECNICA DE VALENCIA

motores térmicos

# GAS-STAND RESULTS: EXTENDED MAP

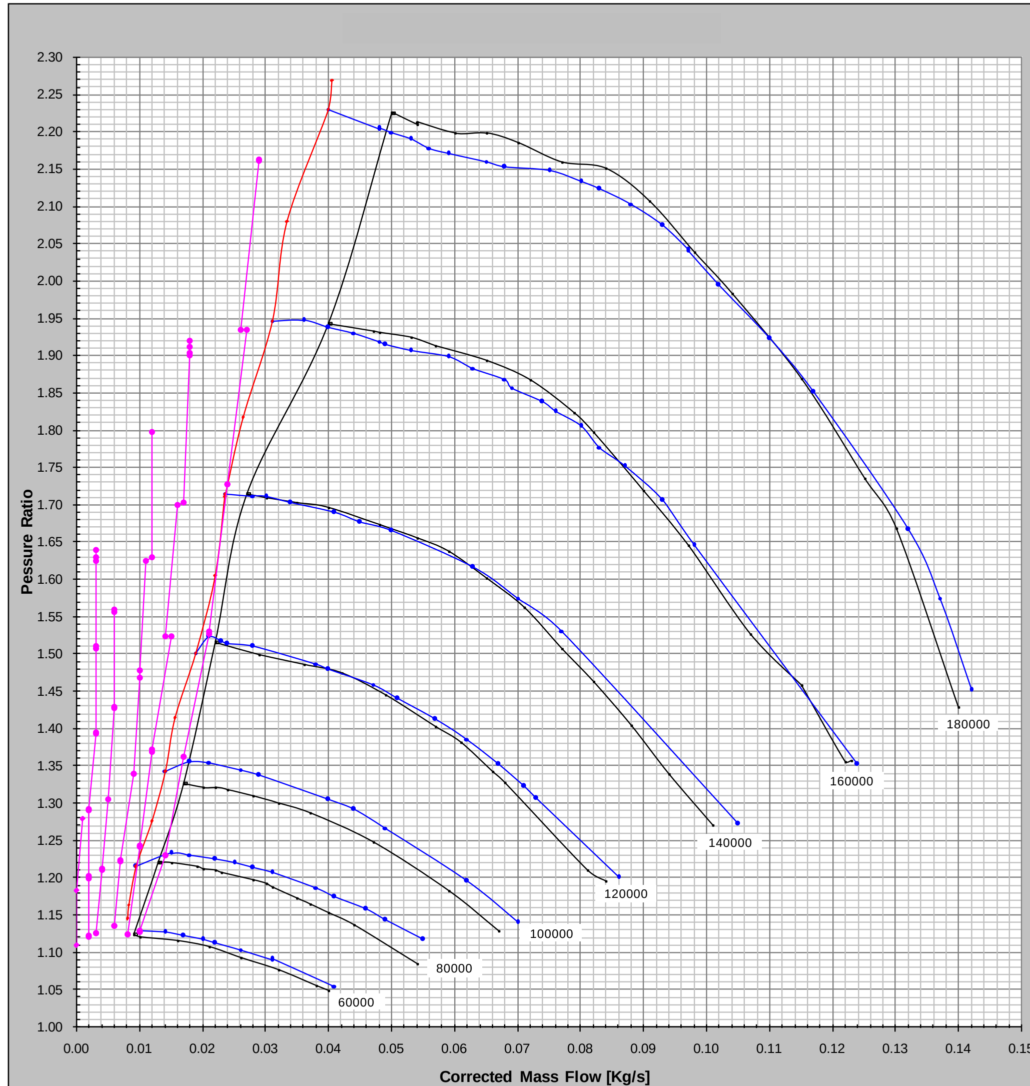


First unit

Second Unit

2nd Unit Surge line

2nd Unit Surge zone measured with close coupled orifices

# GAS-STAND RESULTS: EXTENDED MAP

Extended Map
Surge Line

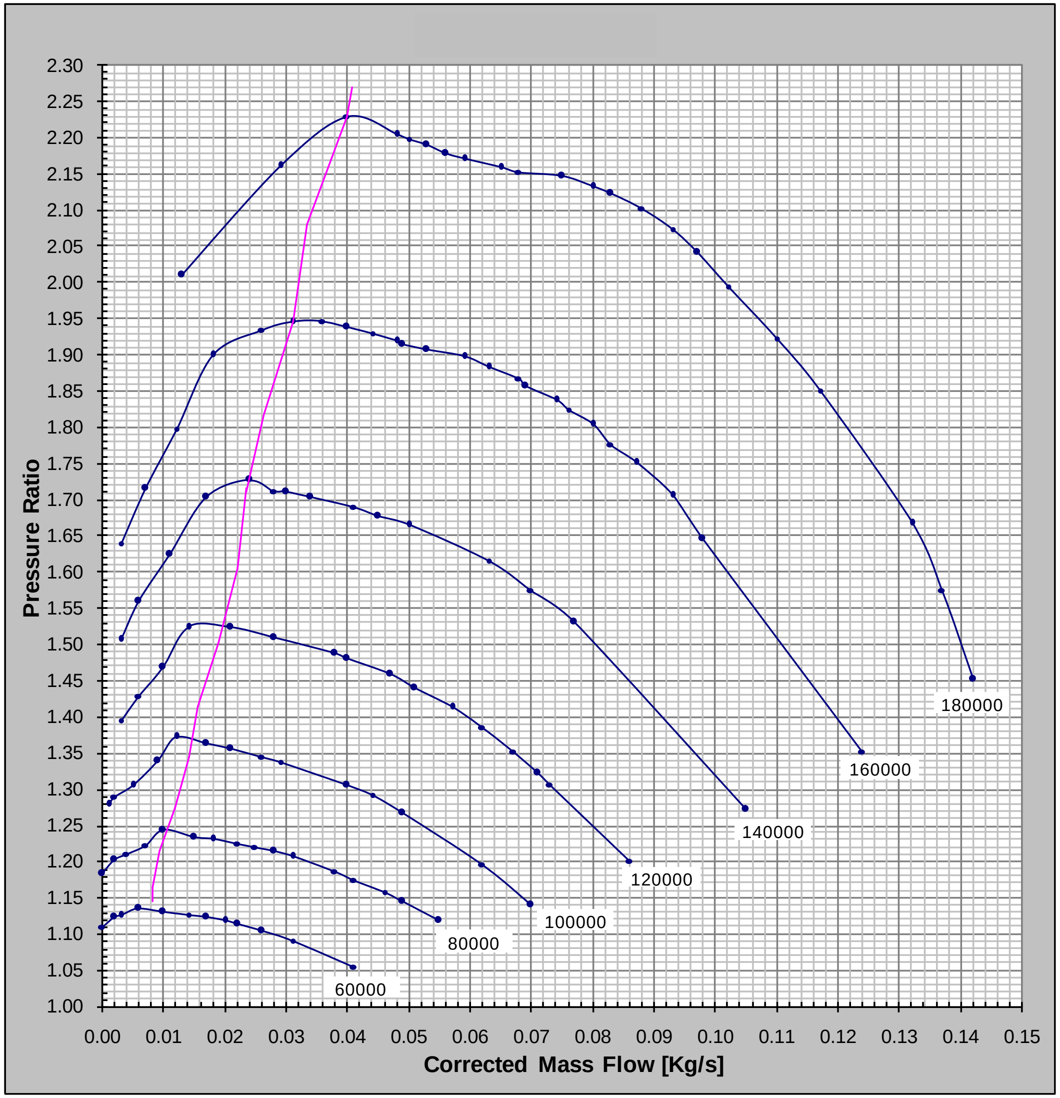

# ENGINE TESTS

**PROCEDURES TO GO TO SURGE**

1. **Closing intake throttle with the engine running as naturally aspirated**
2. **Injecting compressed air within the intake manifold**

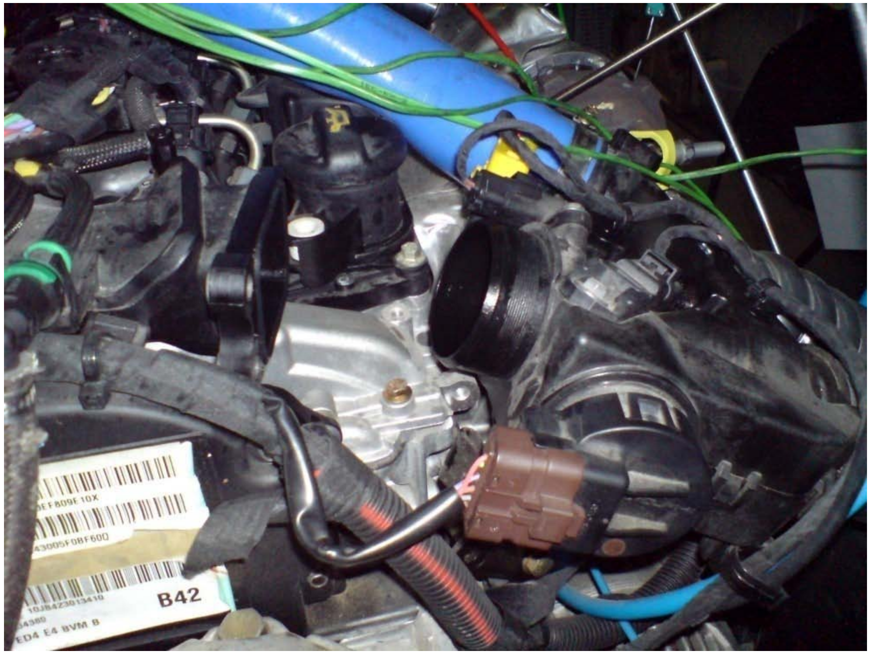

# ENGINE TESTS

| GEOMETRY | Throttle | Air Injection |
|---|---|---|
| Straight Pipe | 2 | 3 |
| Elbow 90º | 2 | 2 |
| Reservoir 5 l. | 1 | 3 |
| Elbow 90º + Res. 5 l. | 1 | 2 |
| Straitght pipe (30 cm) + Res. 5 l. | 1 | 2 |
| Tapered pipe + Res. 5 l. | 1 | 2 |
| Reservoir 1 l. | - | 3 |
| Flow deflector 20 mm | - | 4 |
| Flow deflector 25 mm | - | 1 |
| Flow deflector 28 mm | - | 1 |

# Straight Inlet Duct

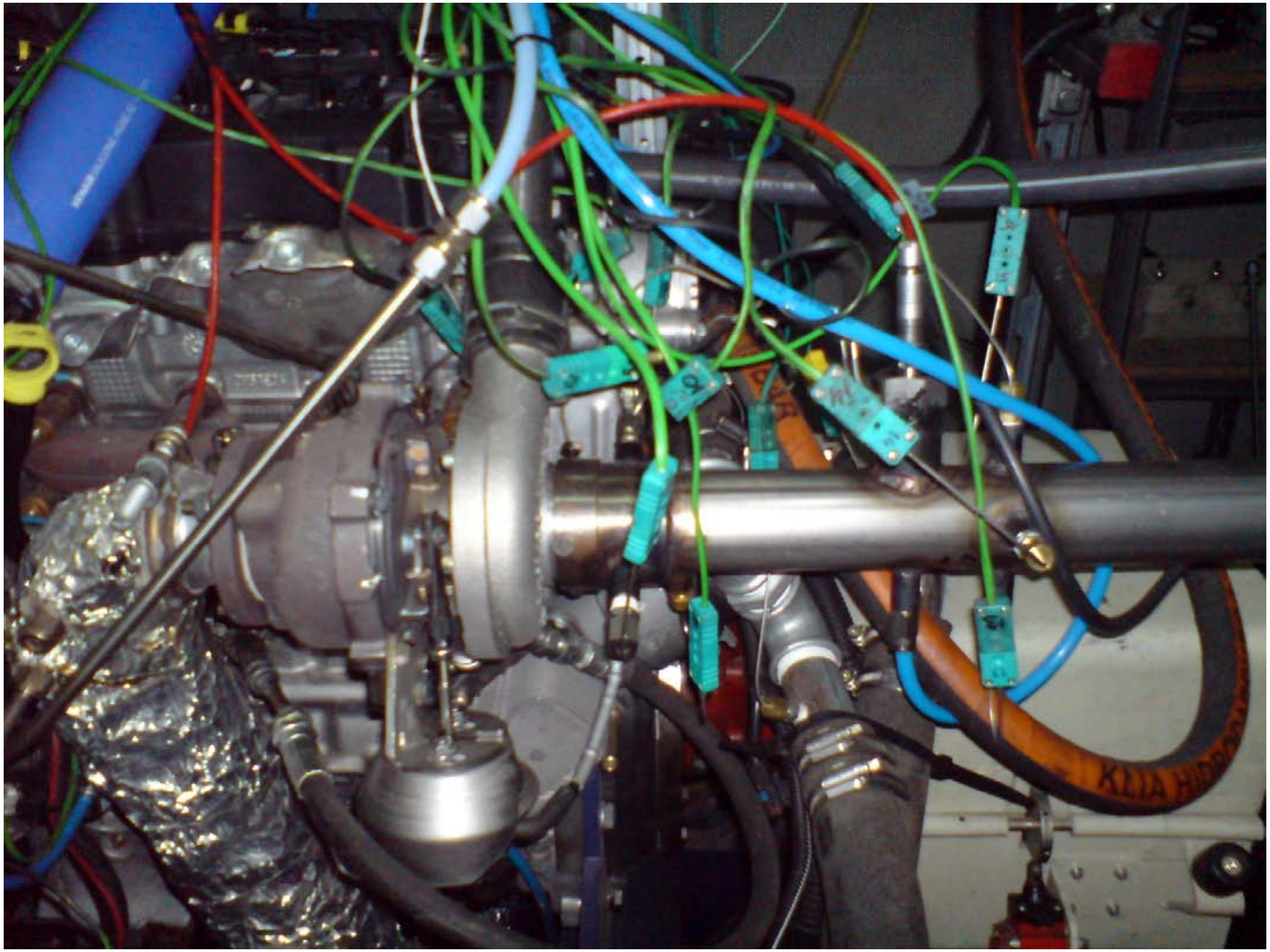

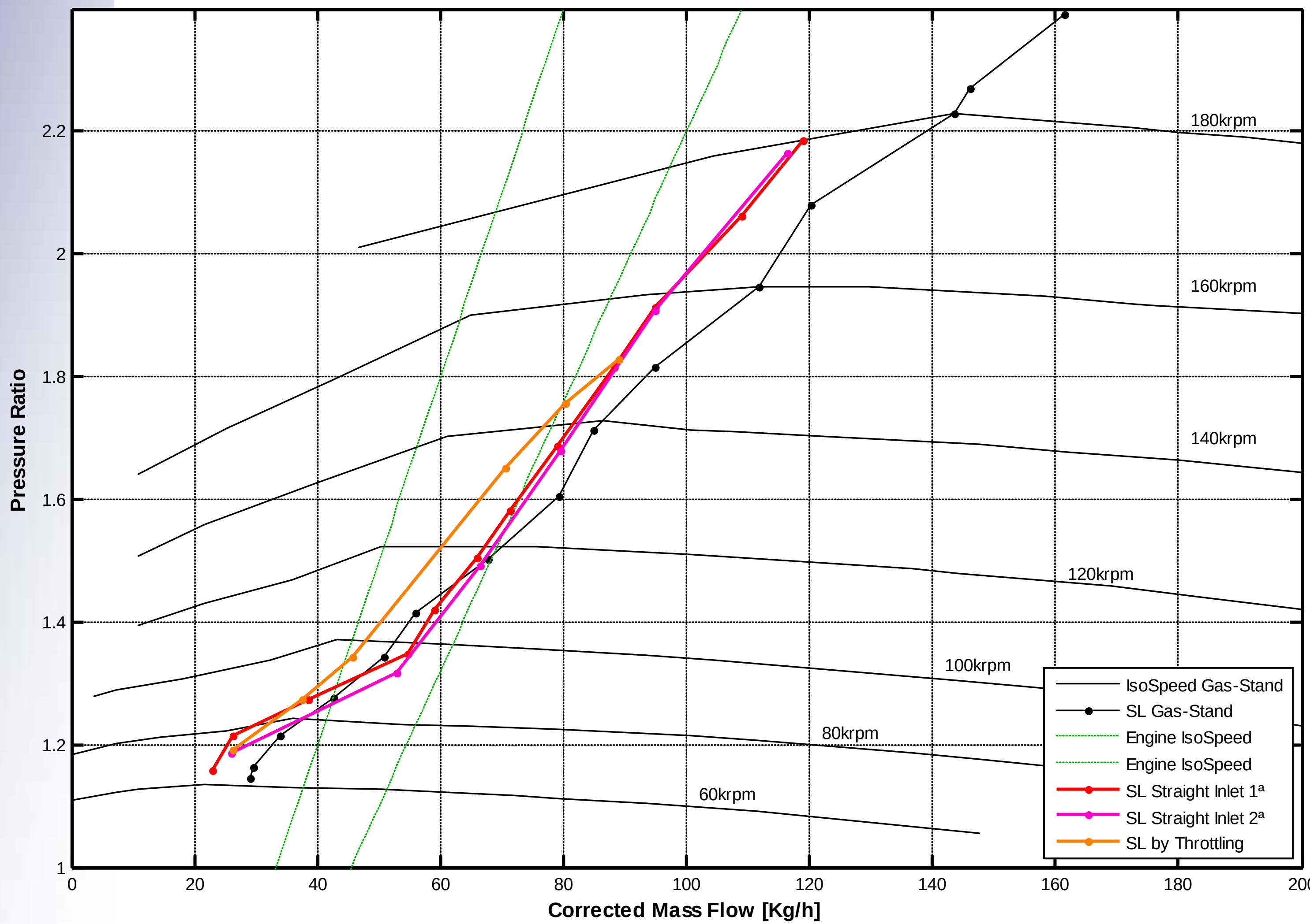
Pressure Ratio
Corrected Mass Flow [Kg/h]
1
1.2
1.4
1.6
1.8
2
2.2
0
20
40
60
80
100
120
140
160
180
200
180krpm
160krpm
140krpm
120krpm
100krpm
80krpm
60krpm
IsoSpeed Gas-Stand
SL Gas-Stand
Engine IsoSpeed
Engine IsoSpeed
SL Straight Inlet 1ª
SL Straight Inlet 2ª
SL by Throttling

# ENGINE TESTS: STRAIGHT DUCT

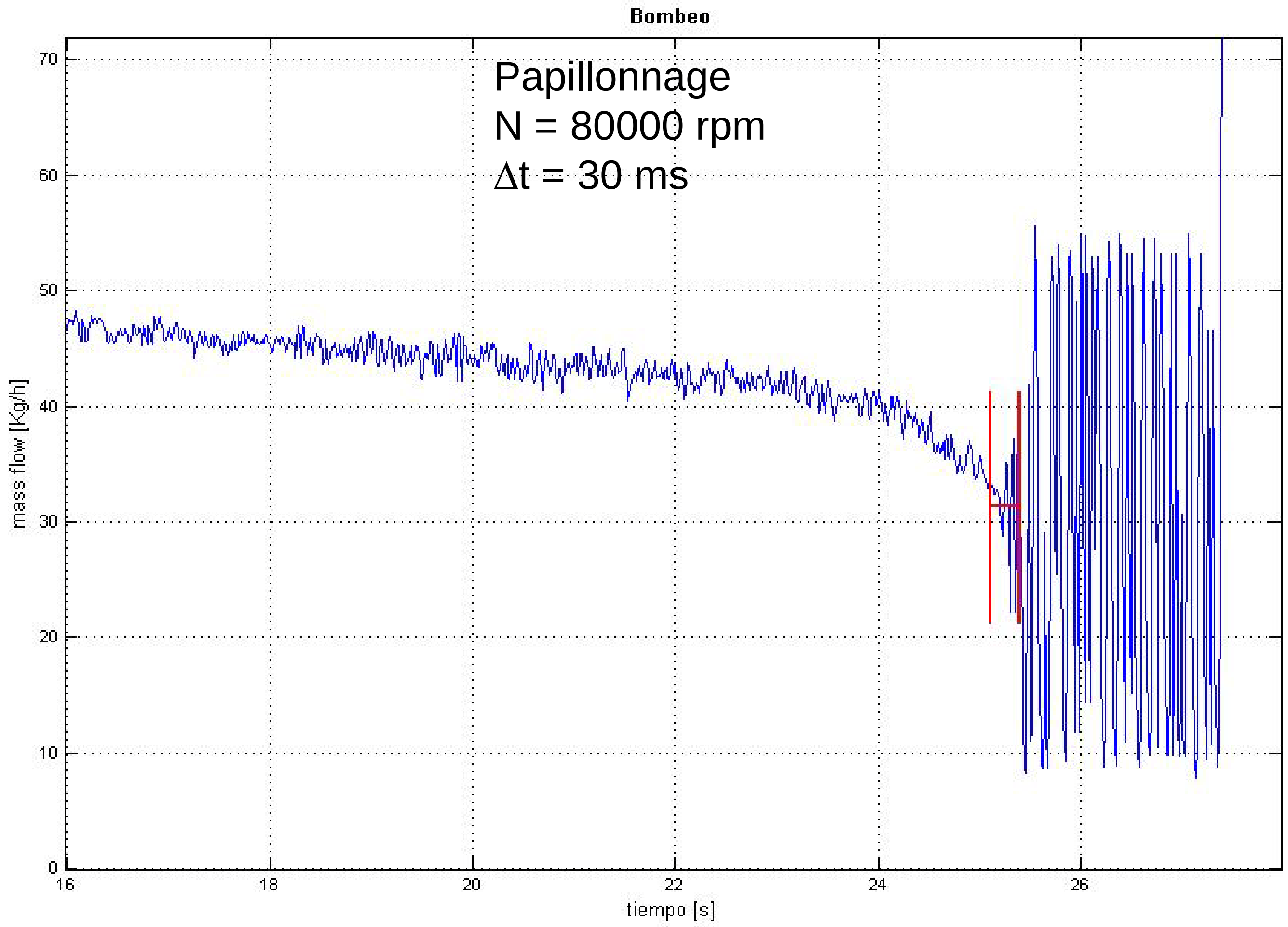

# ENGINE TESTS: STRAIGHT DUCT

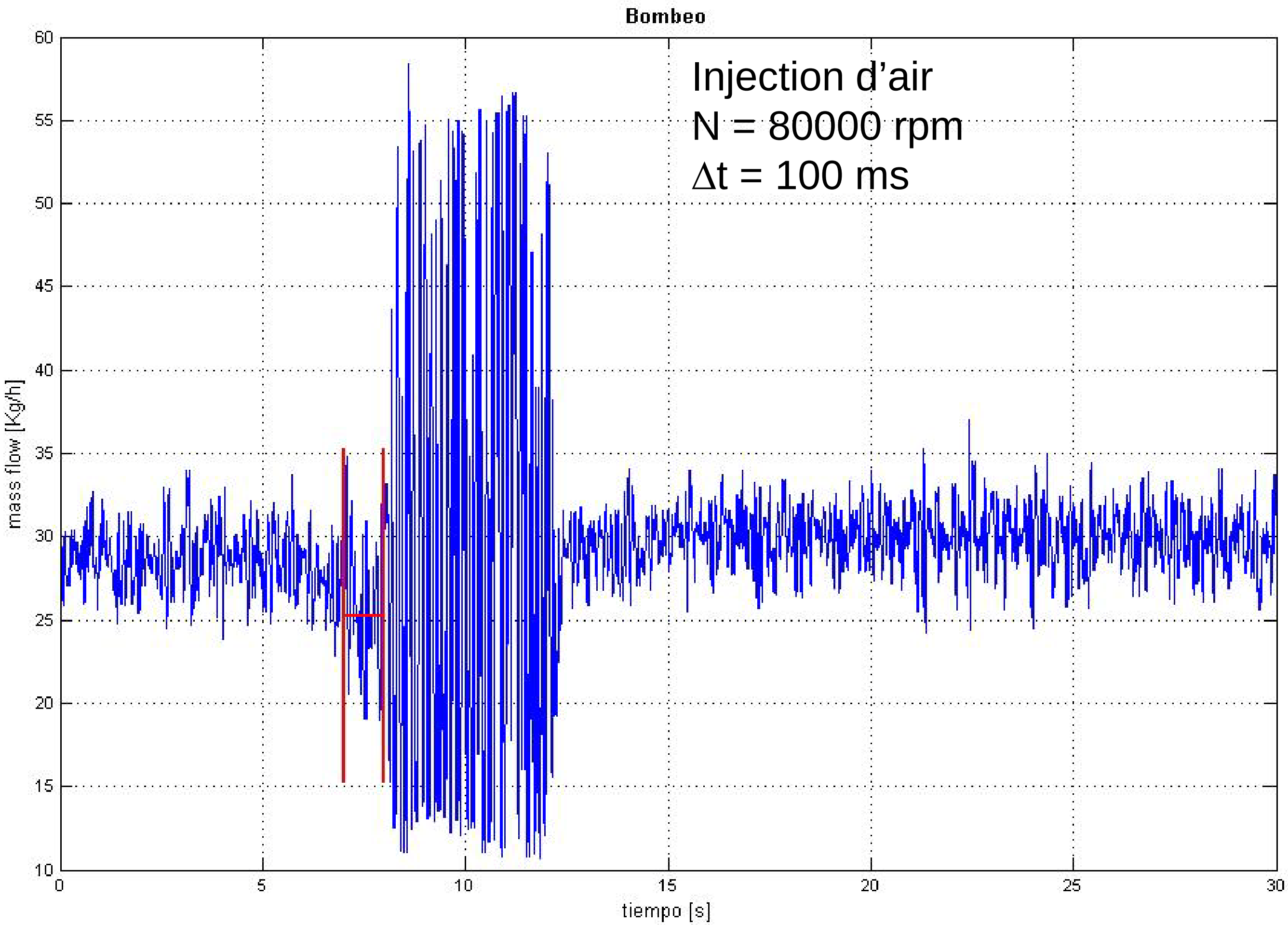

# ENGINE TESTS: STRAIGHT DUCT

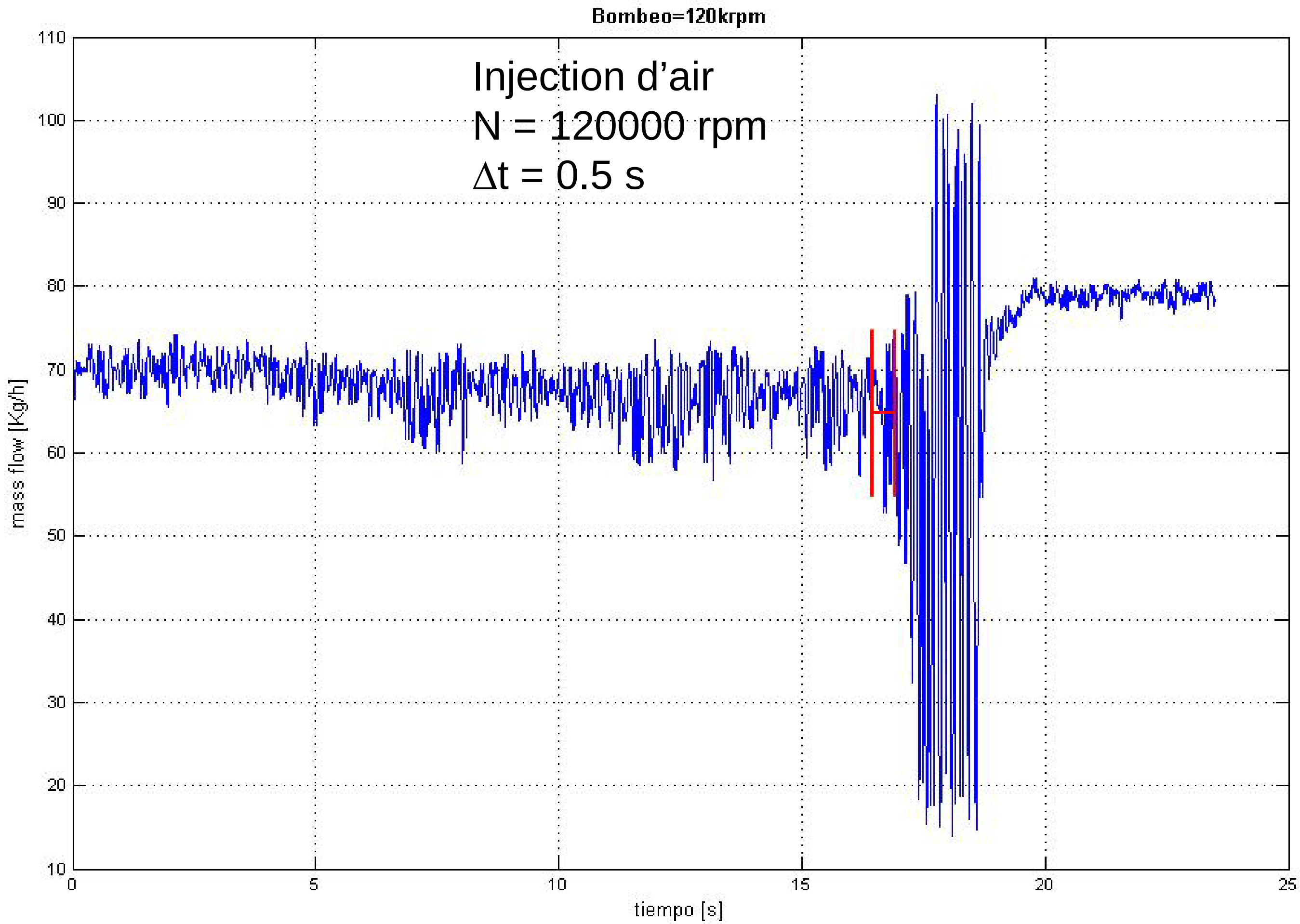

# ENGINE TESTS: STRAIGHT DUCT

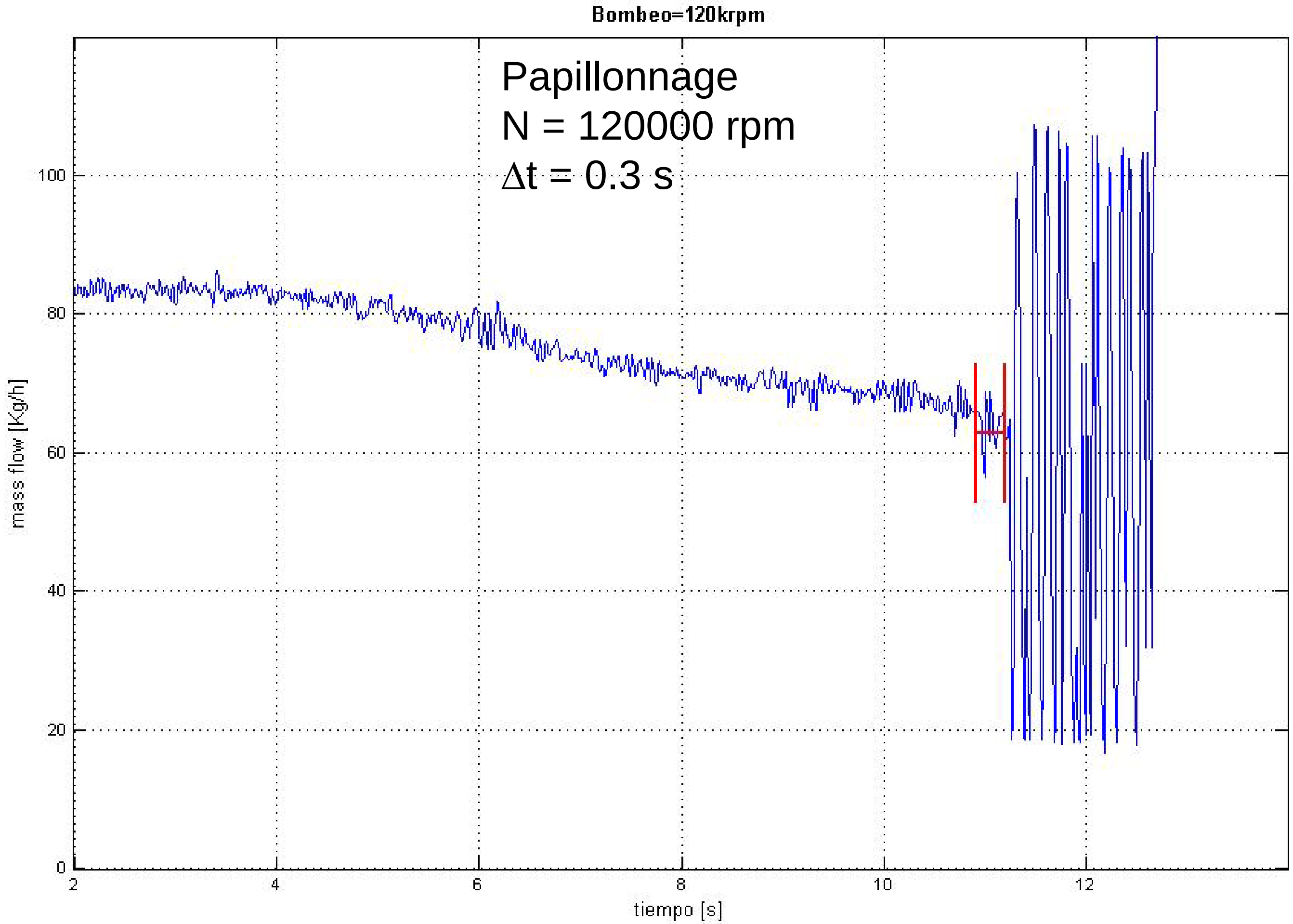

# ENGINE TESTS: Straight Duct

## FIRST CONCLUSIONS

- **The surge line measured on engine is different to that measured on gas-stand**
- **The injection air method is easier to control and more repetitive. The throttle closes even if the command is set constant.**
- **The throttling method leads to different surge line than air injection.**
- **With throttling is difficult to measure at high compressor speed**

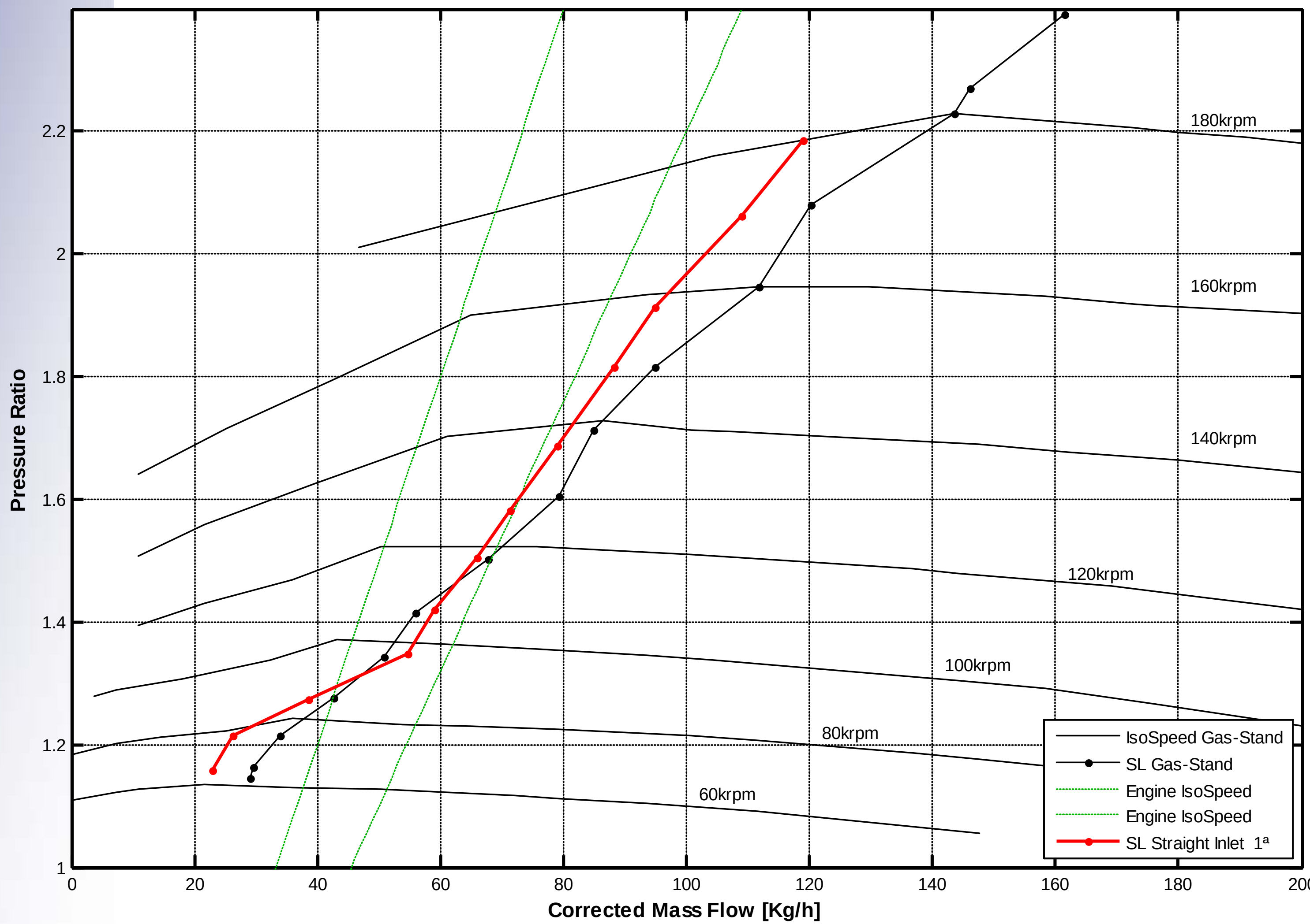
Pressure Ratio
Corrected Mass Flow [Kg/h]
180krpm
160krpm
140krpm
120krpm
100krpm
80krpm
60krpm
IsoSpeed Gas-Stand
SL Gas-Stand
Engine IsoSpeed
Engine IsoSpeed
SL Straight Inlet 1ª
0
20
40
60
80
100
120
140
160
180
200
1
1.2
1.4
1.6
1.8
2
2.2

# COMPRESSOR INLET GEOMETRIES
## Elbow 90º

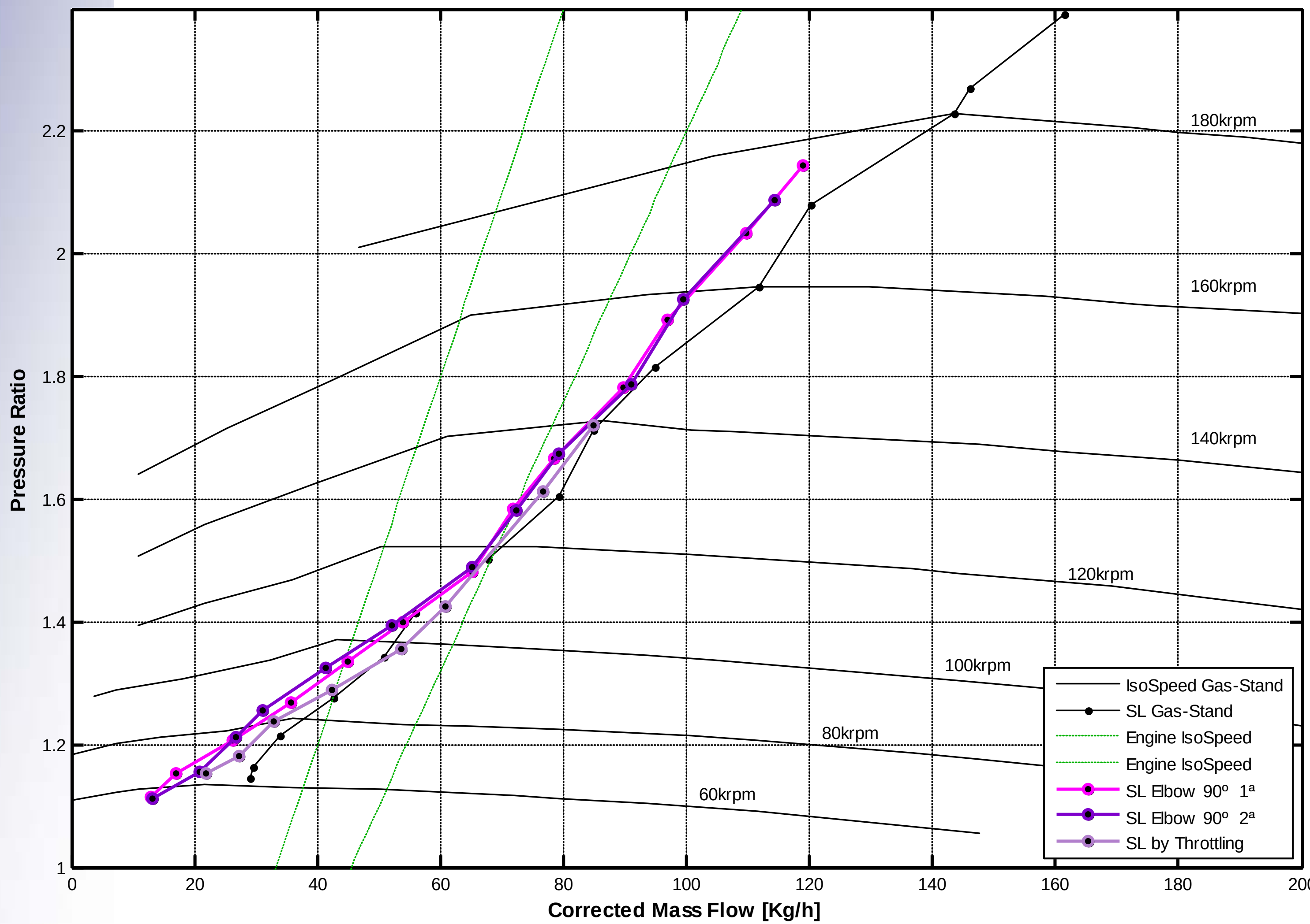
Pressure Ratio
Corrected Mass Flow [Kg/h]
180krpm
160krpm
140krpm
120krpm
100krpm
80krpm
60krpm
IsoSpeed Gas-Stand
SL Gas-Stand
Engine IsoSpeed
Engine IsoSpeed
SL Elbow 90º 1ª
SL Elbow 90º 2ª
SL by Throttling
0
20
40
60
80
100
120
140
160
180
200
1
1.2
1.4
1.6
1.8
2
2.2

# COMPRESSOR INLET GEOMETRIES
# Elbow 90º

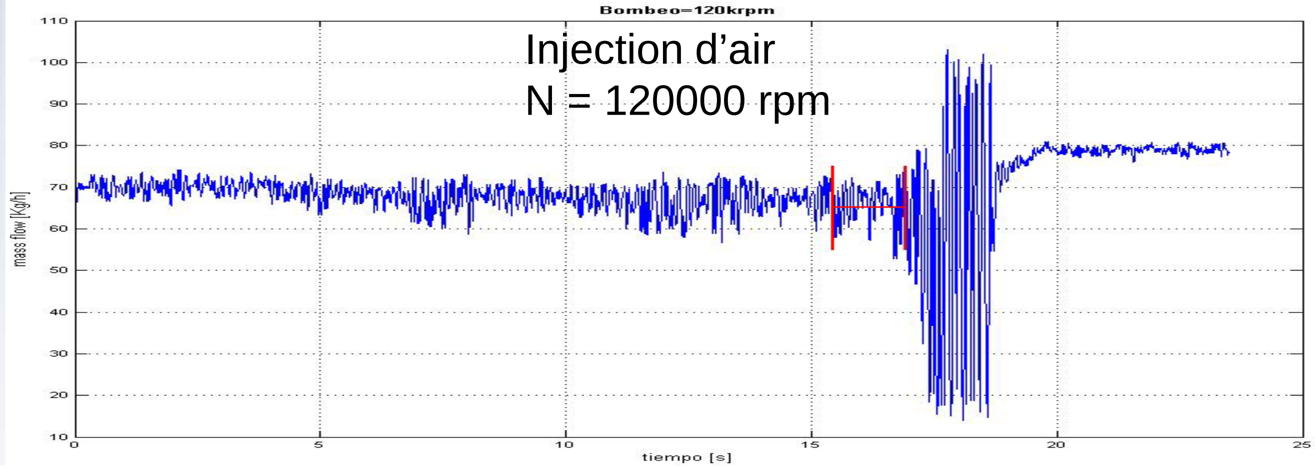


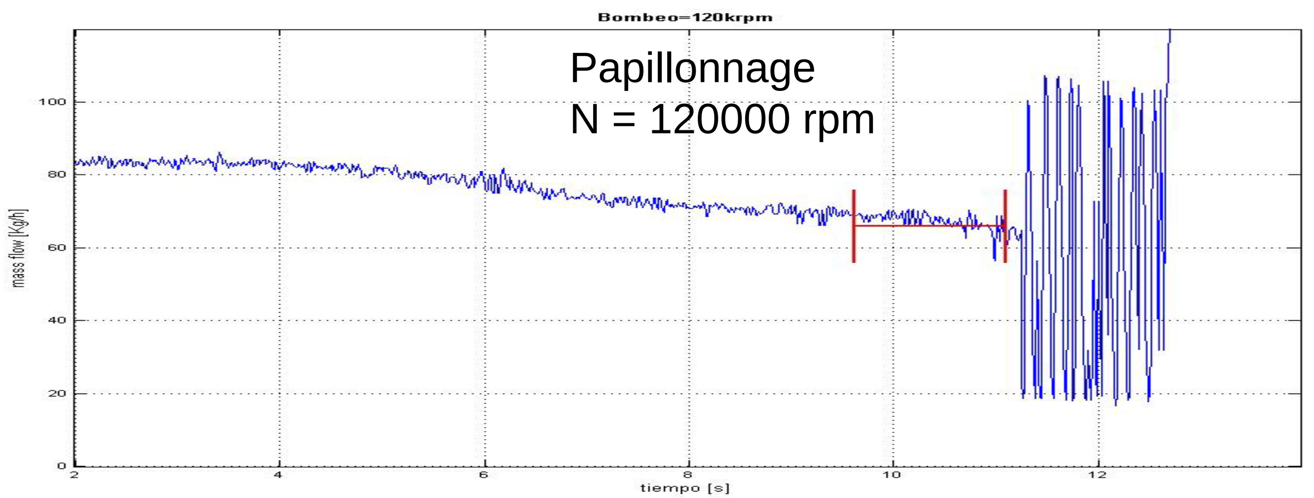

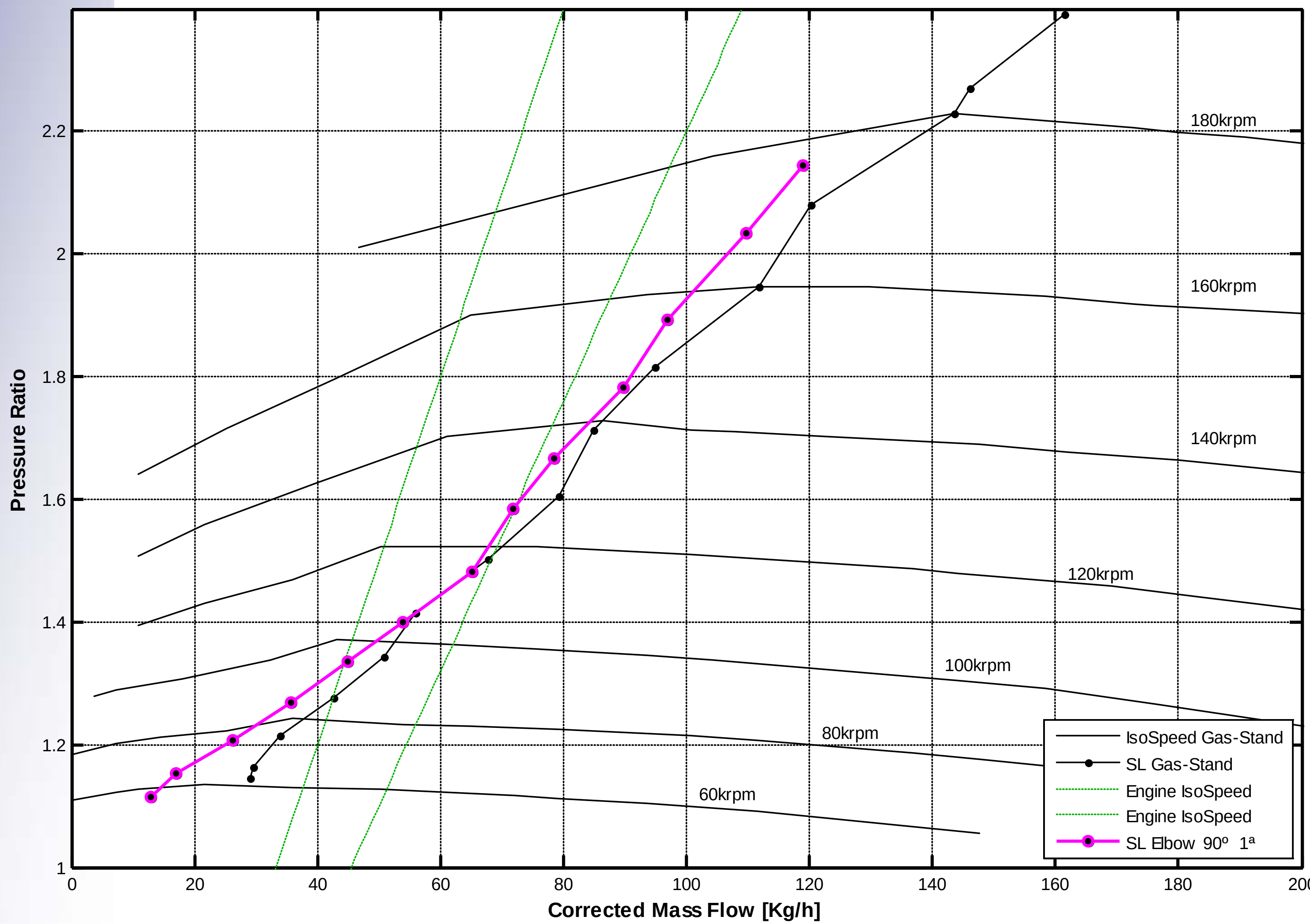
180krpm
160krpm
140krpm
120krpm
100krpm
80krpm
60krpm
IsoSpeed Gas-Stand
SL Gas-Stand
Engine IsoSpeed
Engine IsoSpeed
SL Elbow 90º 1ª
Pressure Ratio
Corrected Mass Flow [Kg/h]

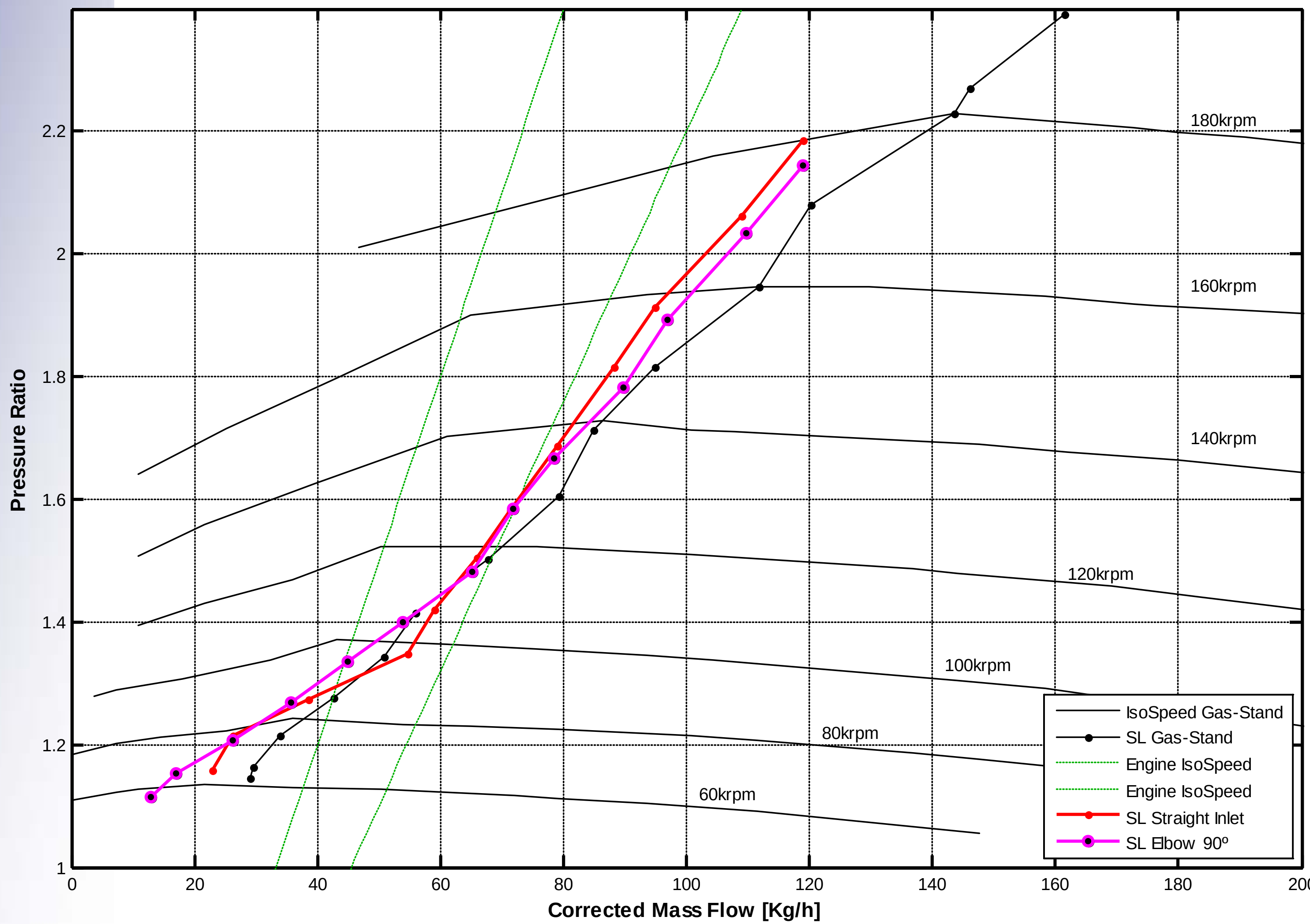
Pressure Ratio
Corrected Mass Flow [Kg/h]
2.2
2
1.8
1.6
1.4
1.2
1
0
20
40
60
80
100
120
140
160
180
200
180krpm
160krpm
140krpm
120krpm
100krpm
80krpm
60krpm
IsoSpeed Gas-Stand
SL Gas-Stand
Engine IsoSpeed
Engine IsoSpeed
SL Straight Inlet
SL Elbow 90º

# ENGINE TESTS: Elbow 90º

## FIRST CONCLUSIONS

- **There is not much difference between the 90º elbow and the straight duct.**
- **Again, the injection air method is more easily to control and more repetitive. The throttle closes even if the command is set constant.**
- **The injection air method shows better surge limit for the elbow at low speed and worse at high speed (this agrees with our experience)**
- **The throttling method does not show anything because the repetitiveness is of the order of the difference**

# Volume 500cm³

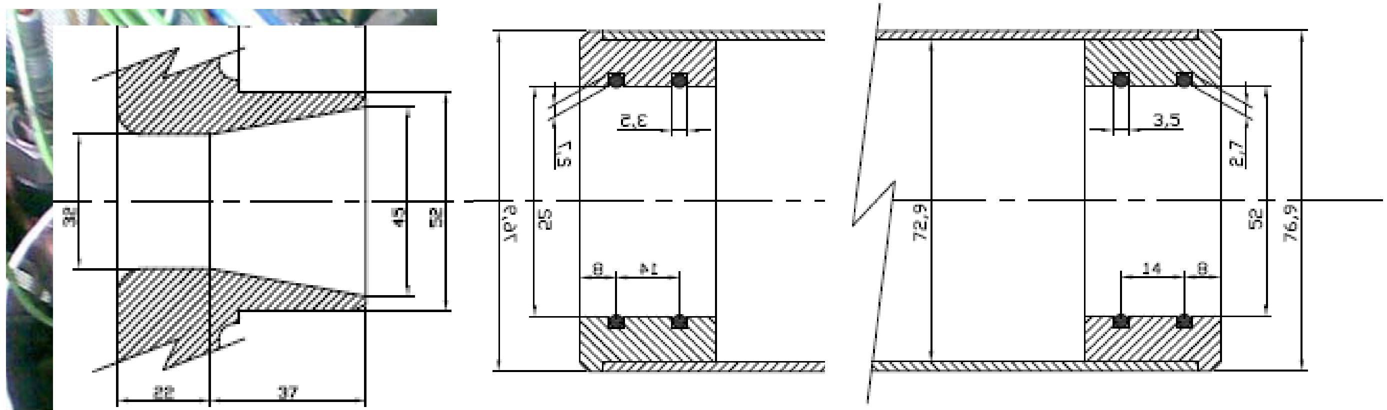


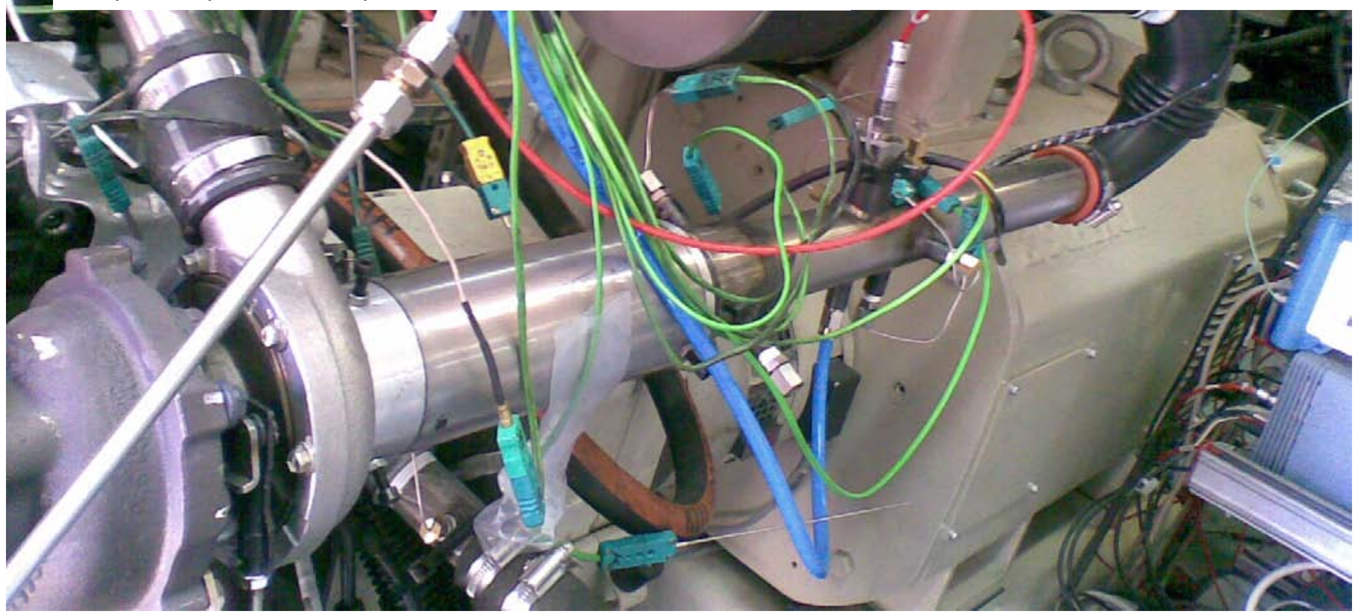

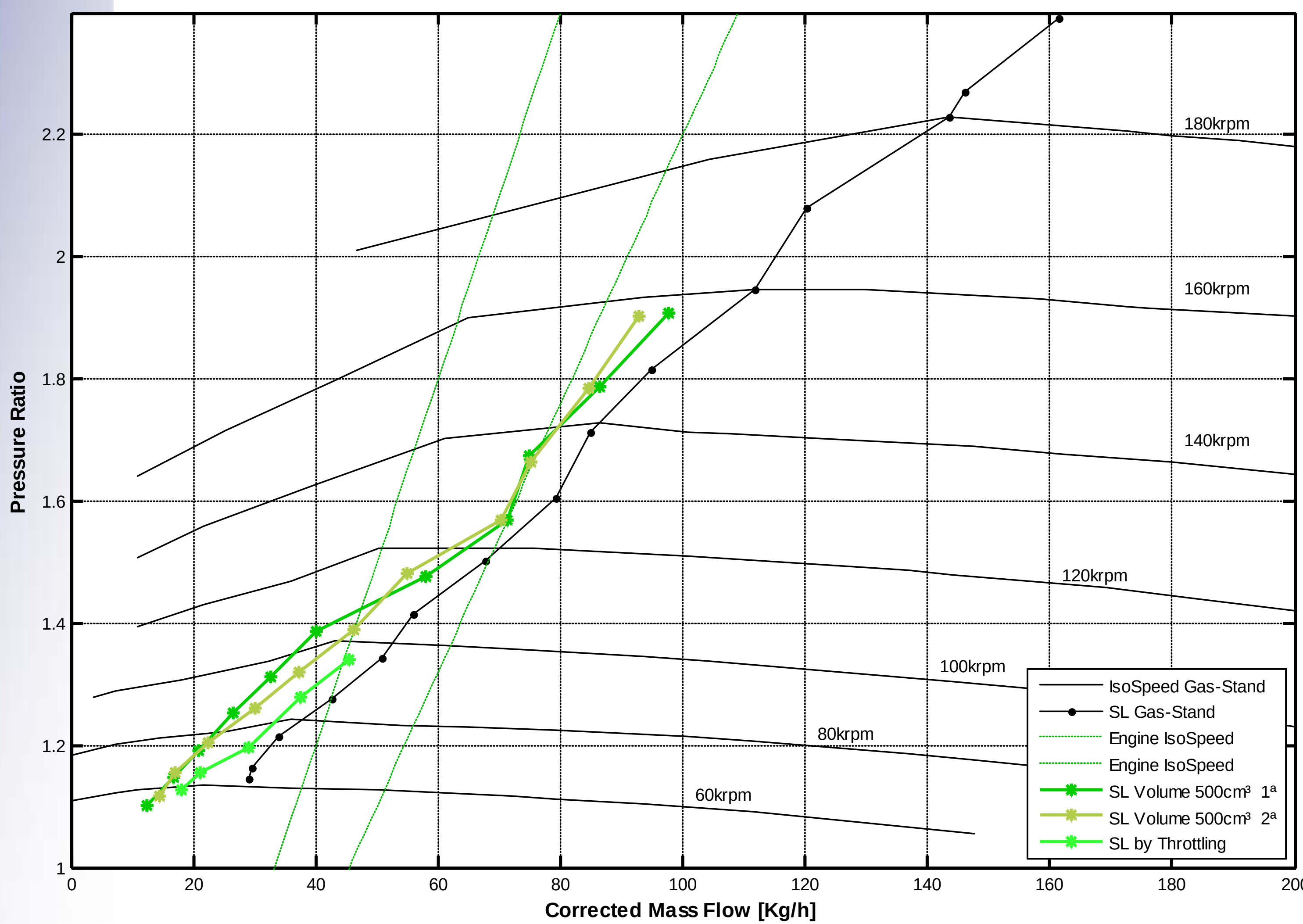
Pressure Ratio
Corrected Mass Flow [Kg/h]
180krpm
160krpm
140krpm
120krpm
100krpm
80krpm
60krpm
IsoSpeed Gas-Stand
SL Gas-Stand
Engine IsoSpeed
Engine IsoSpeed
SL Volume 500cm³ 1ª
SL Volume 500cm³ 2ª
SL by Throttling

# Volume 500cm³

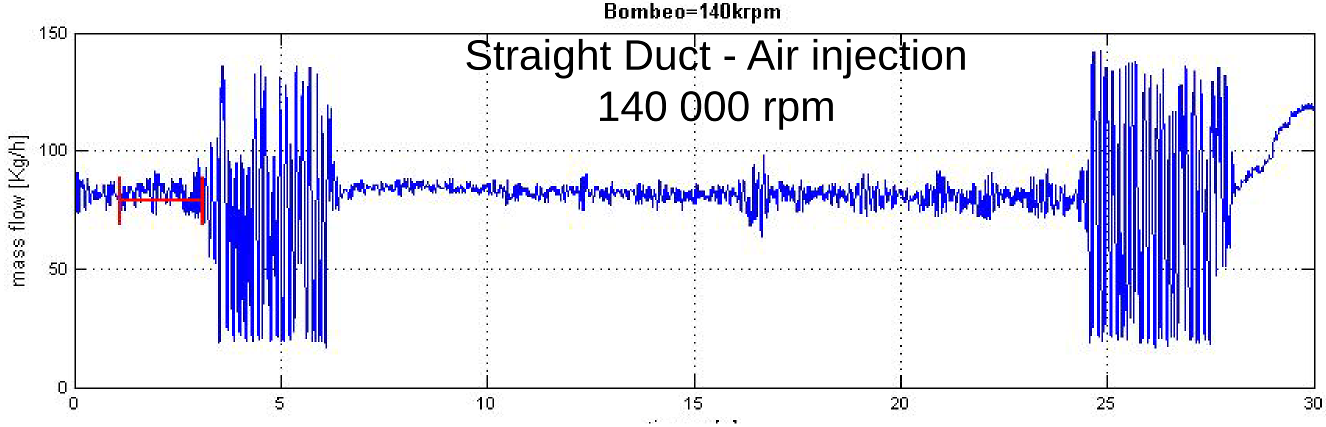


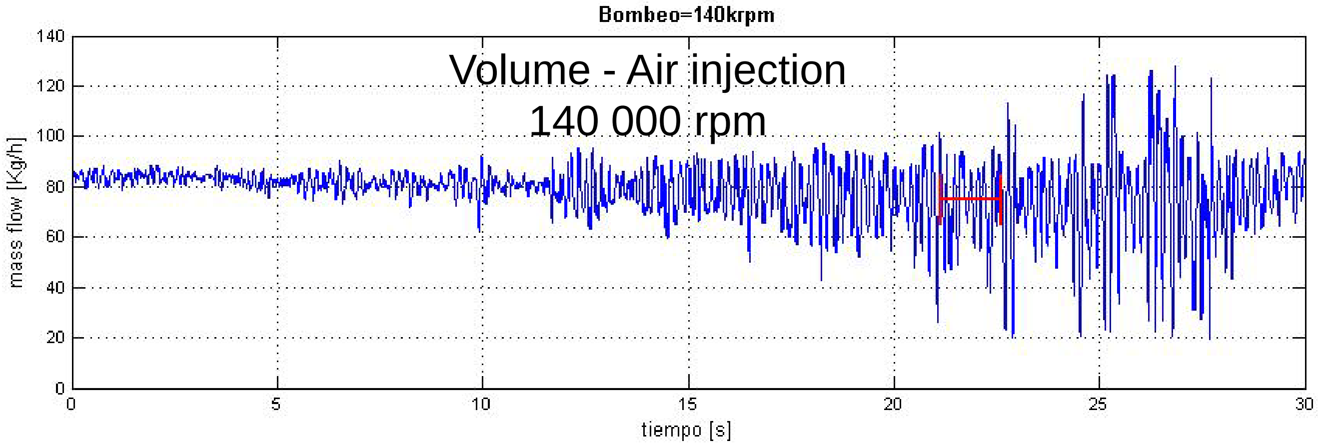

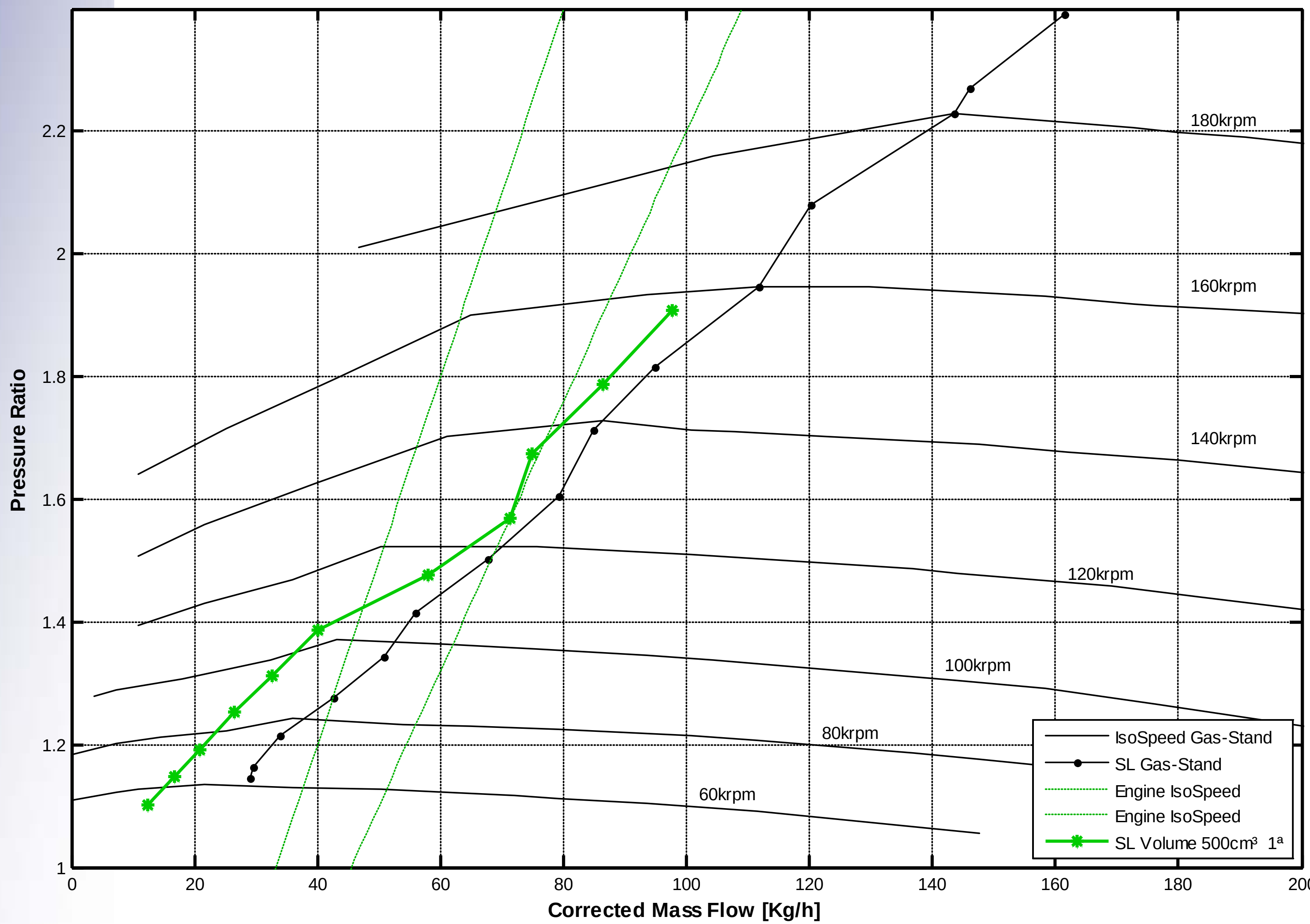

Pressure Ratio
Corrected Mass Flow [Kg/h]
180krpm
160krpm
140krpm
120krpm
100krpm
80krpm
60krpm
IsoSpeed Gas-Stand
SL Gas-Stand
Engine IsoSpeed
Engine IsoSpeed
SL Volume 500cm³ 1ª

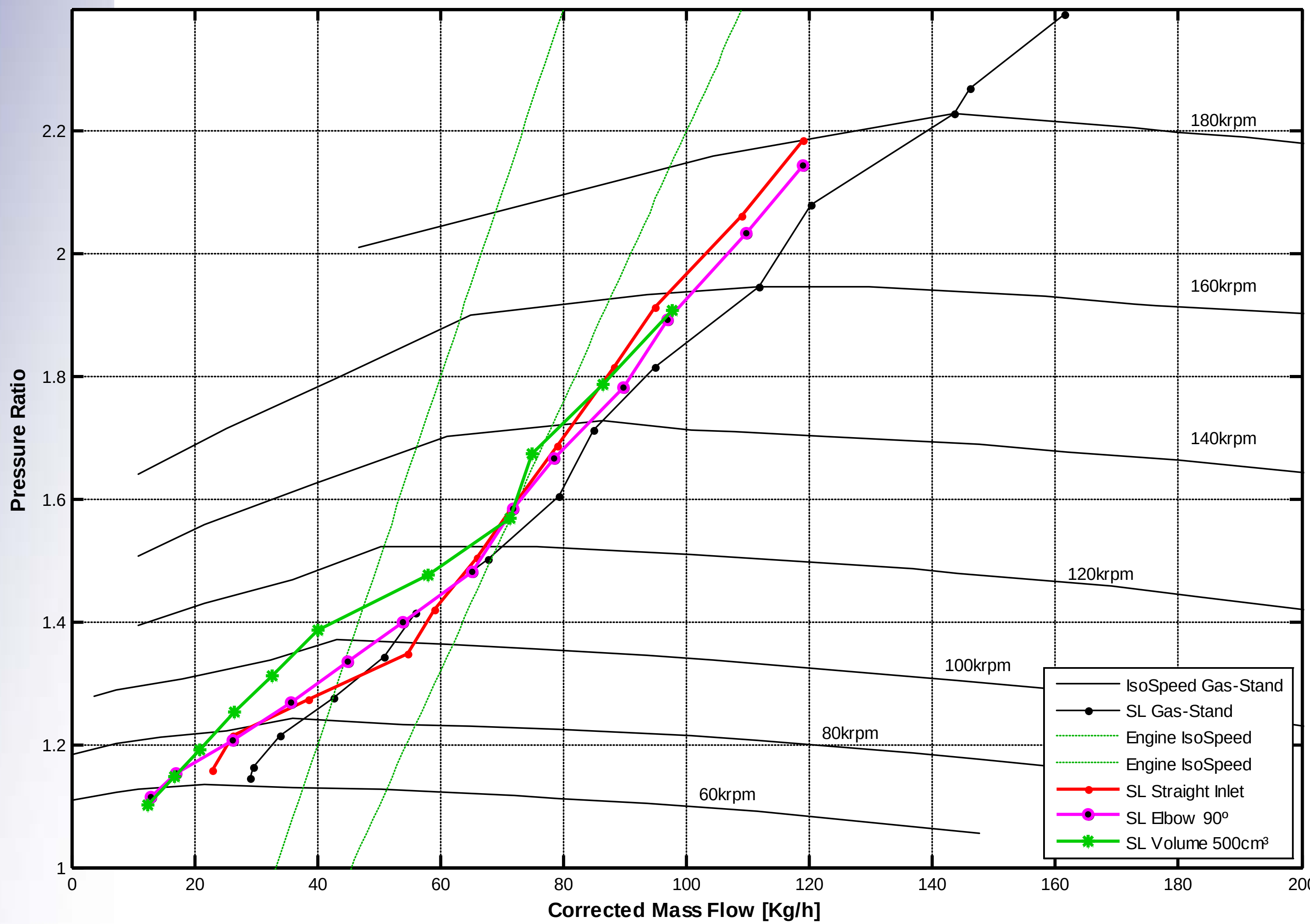
Pressure Ratio
Corrected Mass Flow [Kg/h]
180krpm
160krpm
140krpm
120krpm
100krpm
80krpm
60krpm
IsoSpeed Gas-Stand
SL Gas-Stand
Engine IsoSpeed
Engine IsoSpeed
SL Straight Inlet
SL Elbow 90º
SL Volume 500cm³

# ENGINE TESTS: Intake Volume

## FIRST CONCLUSIONS

- **It shows an improvement on surge margin at low speed (20 kg/h at 100 krpm)**
- **The noise when arriving to surge is different to that of previous tests (straight duct and elbow)**
- **The surge inception is not as sharp as before and it is possible to return to stable operation.**
- **Is that an aerodynamic effect? (modification of flow at compressor inlet)**
  - *Put further the volume from the compressor*

# Elbow 90º and volume 500cm³

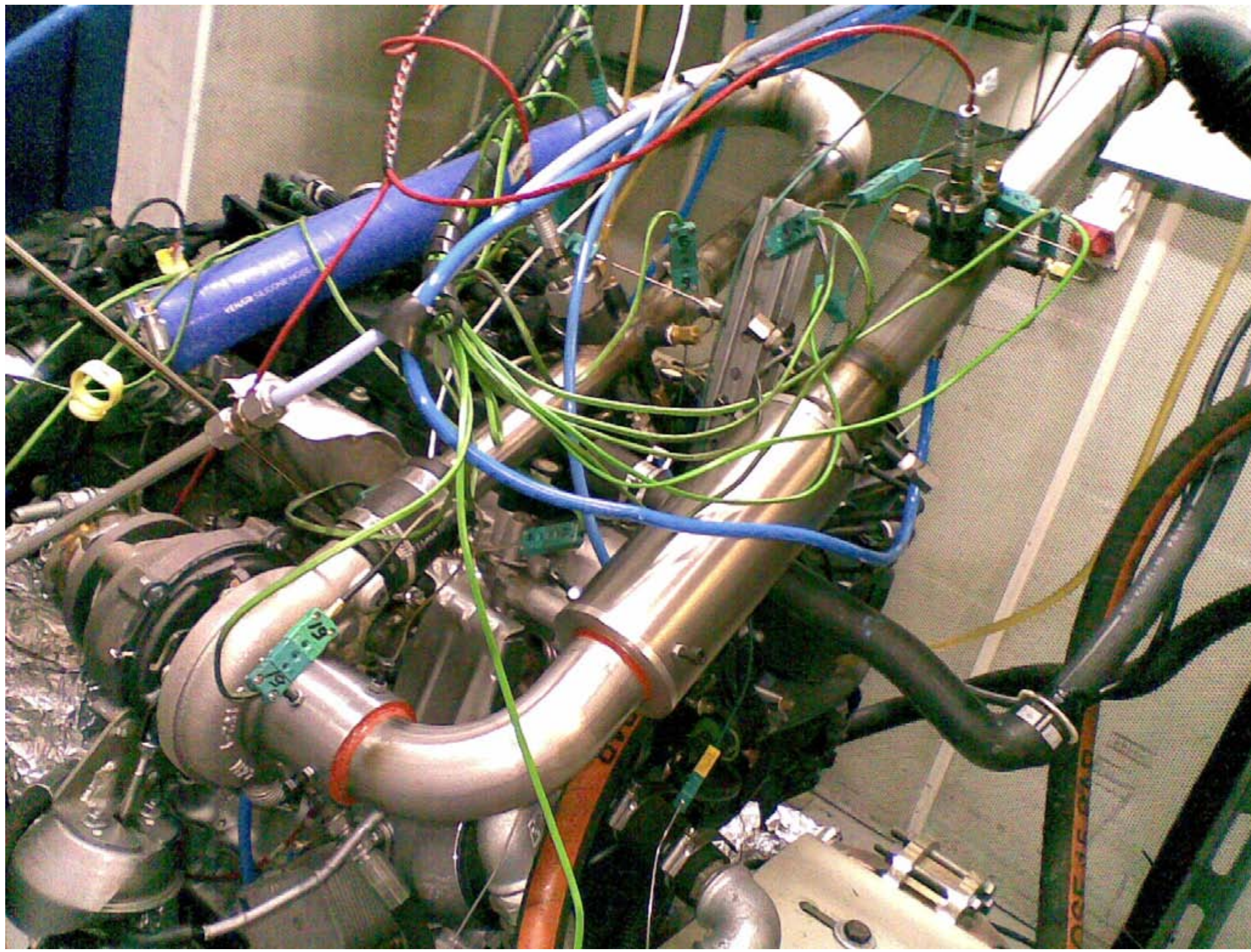

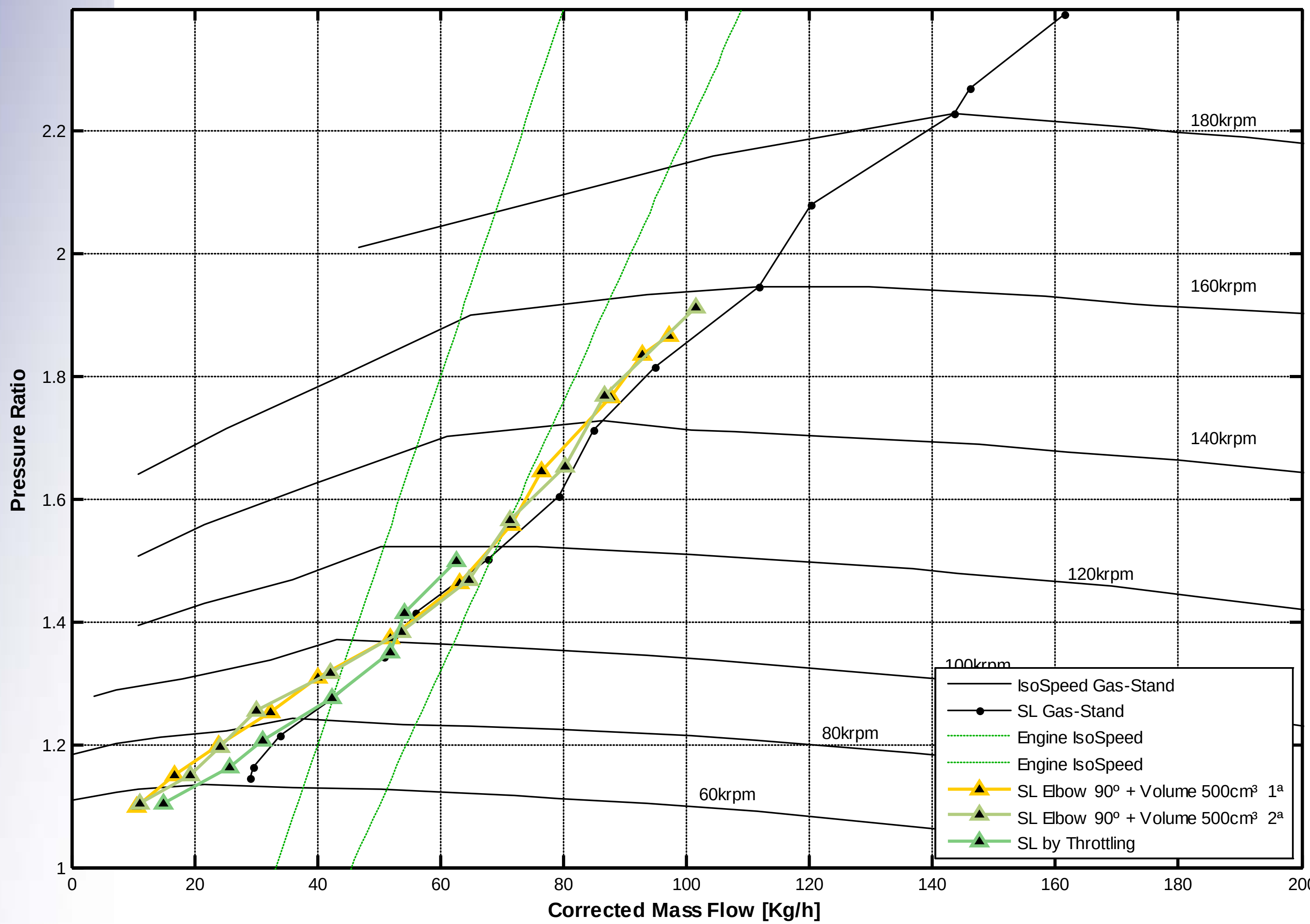
Pressure Ratio
Corrected Mass Flow [Kg/h]
180krpm
160krpm
140krpm
120krpm
100krpm
80krpm
60krpm
IsoSpeed Gas-Stand
SL Gas-Stand
Engine IsoSpeed
Engine IsoSpeed
SL Elbow 90º + Volume 500cm³ 1ª
SL Elbow 90º + Volume 500cm³ 2ª
SL by Throttling

# Elbow 90º and volume 500cm³

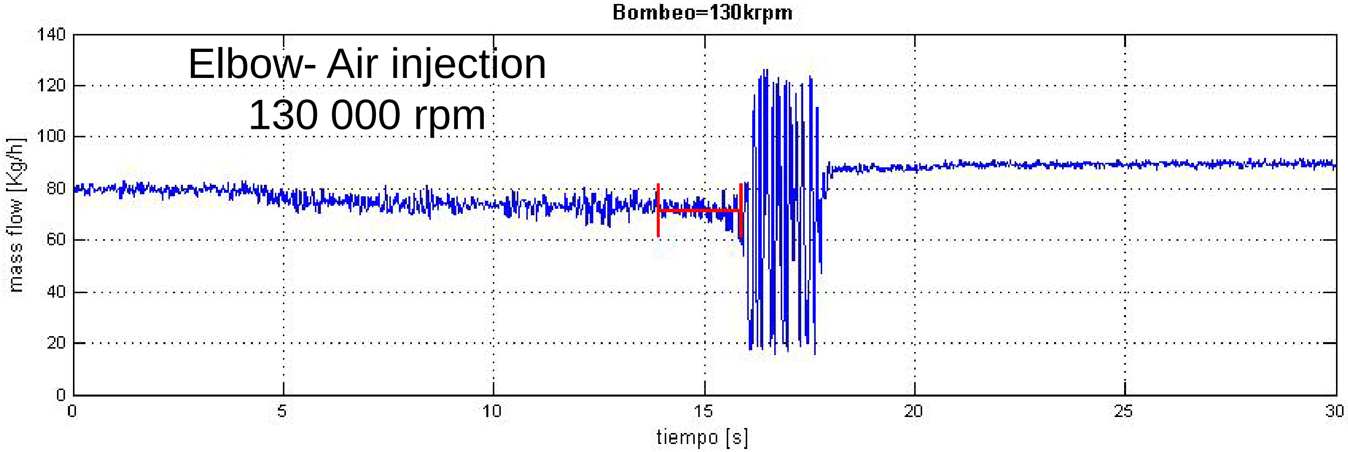


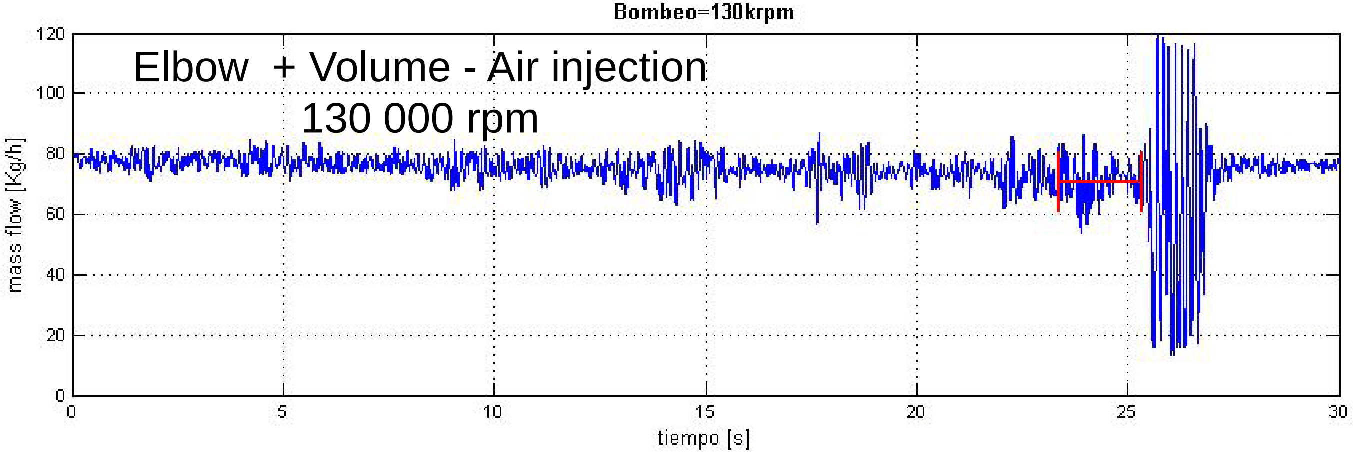

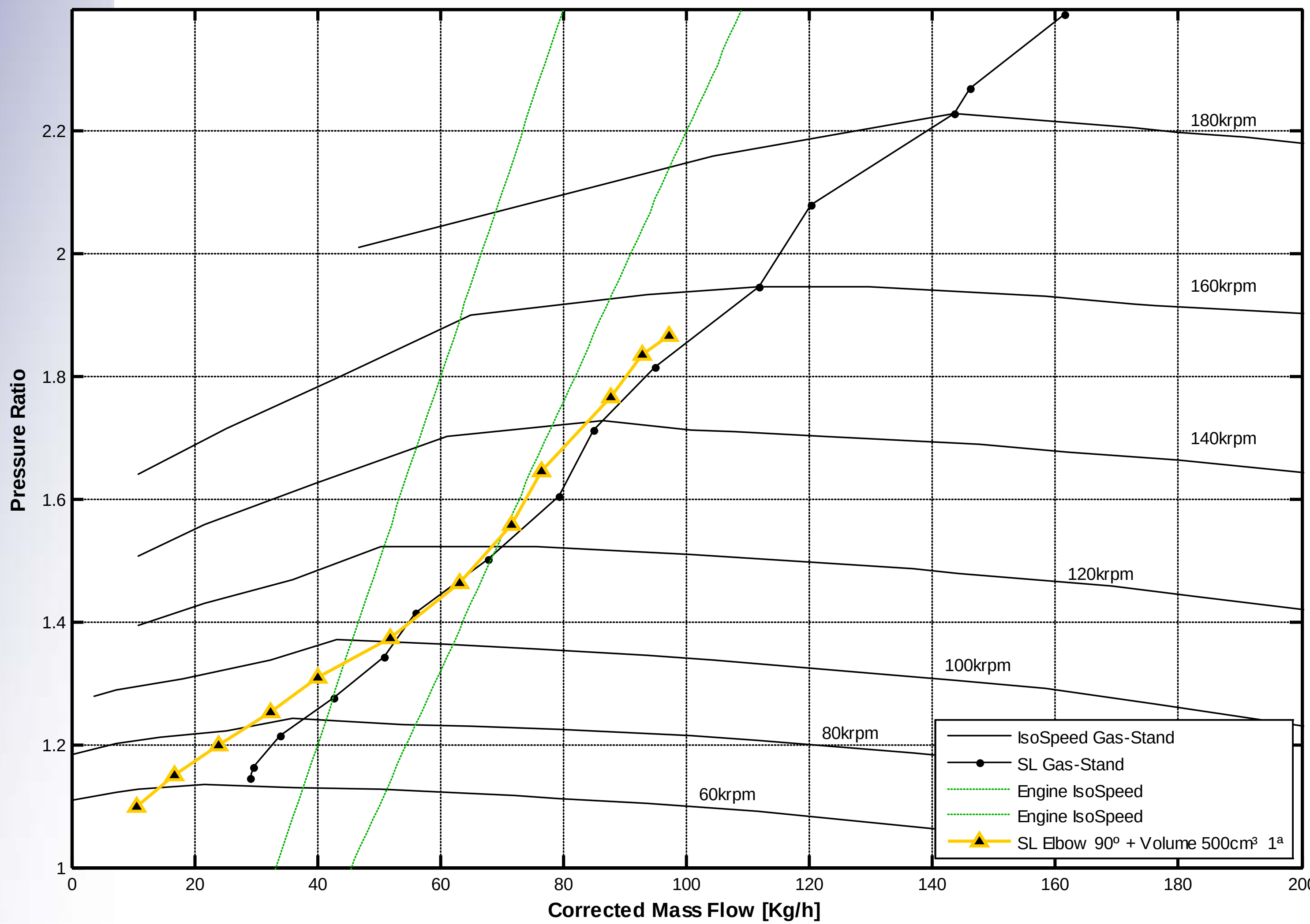
Pressure Ratio
Corrected Mass Flow [Kg/h]
180krpm
160krpm
140krpm
120krpm
100krpm
80krpm
60krpm
IsoSpeed Gas-Stand
SL Gas-Stand
Engine IsoSpeed
Engine IsoSpeed
SL Elbow 90º + Volume 500cm³ 1ª
2.2
2
1.8
1.6
1.4
1.2
1
0
20
40
60
80
100
120
140
160
180
200

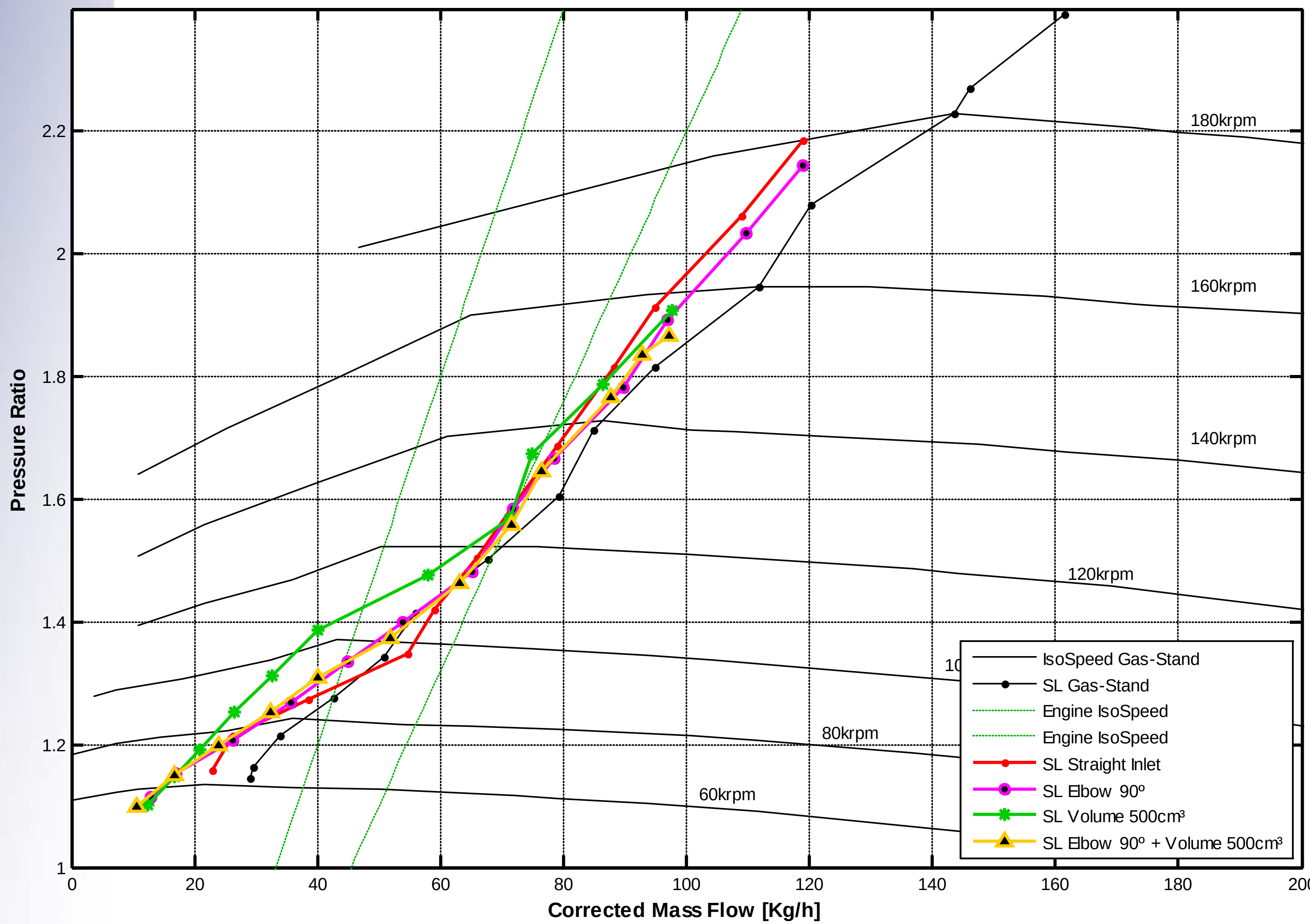
Pressure Ratio
Corrected Mass Flow [Kg/h]
180krpm
160krpm
140krpm
120krpm
80krpm
60krpm
IsoSpeed Gas-Stand
SL Gas-Stand
Engine IsoSpeed
Engine IsoSpeed
SL Straight Inlet
SL Elbow 90º
SL Volume 500cm³
SL Elbow 90º + Volume 500cm³

# ENGINE TESTS: Elbow 90º + Intake Volume

## FIRST CONCLUSIONS

- **All the improvement shown in the intake volume case disappears when the elbow is installed.**
- **The different noise and more stable situation also changes to the previous situation.**
- **The Elbow + Volume behaves just like an elbow. The volume has not influence.**
- **The volume has to be close to the compressor inlet to lead to a positive effect.**

# 30cm Straight Inlet and Volume 500cm³

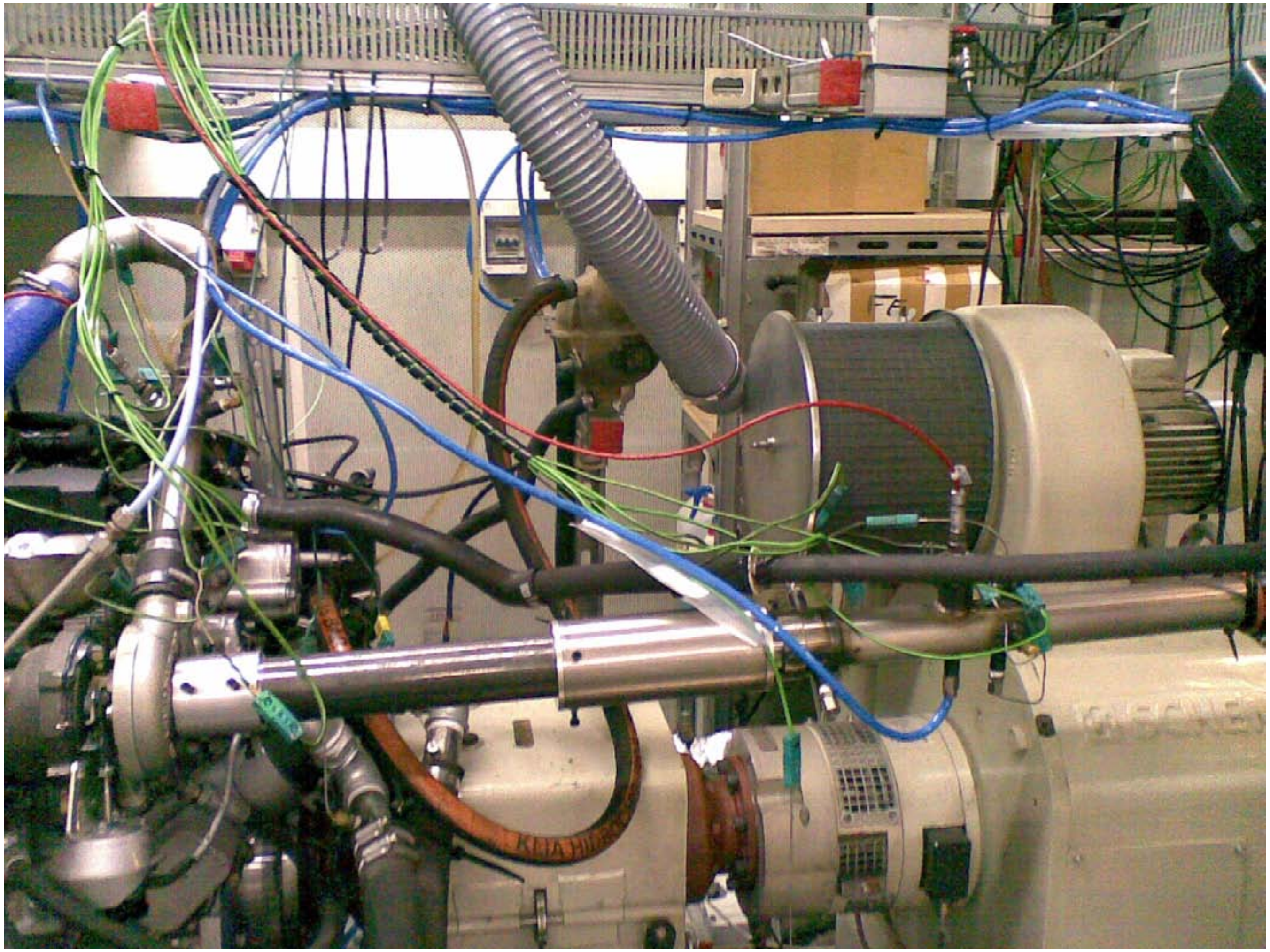

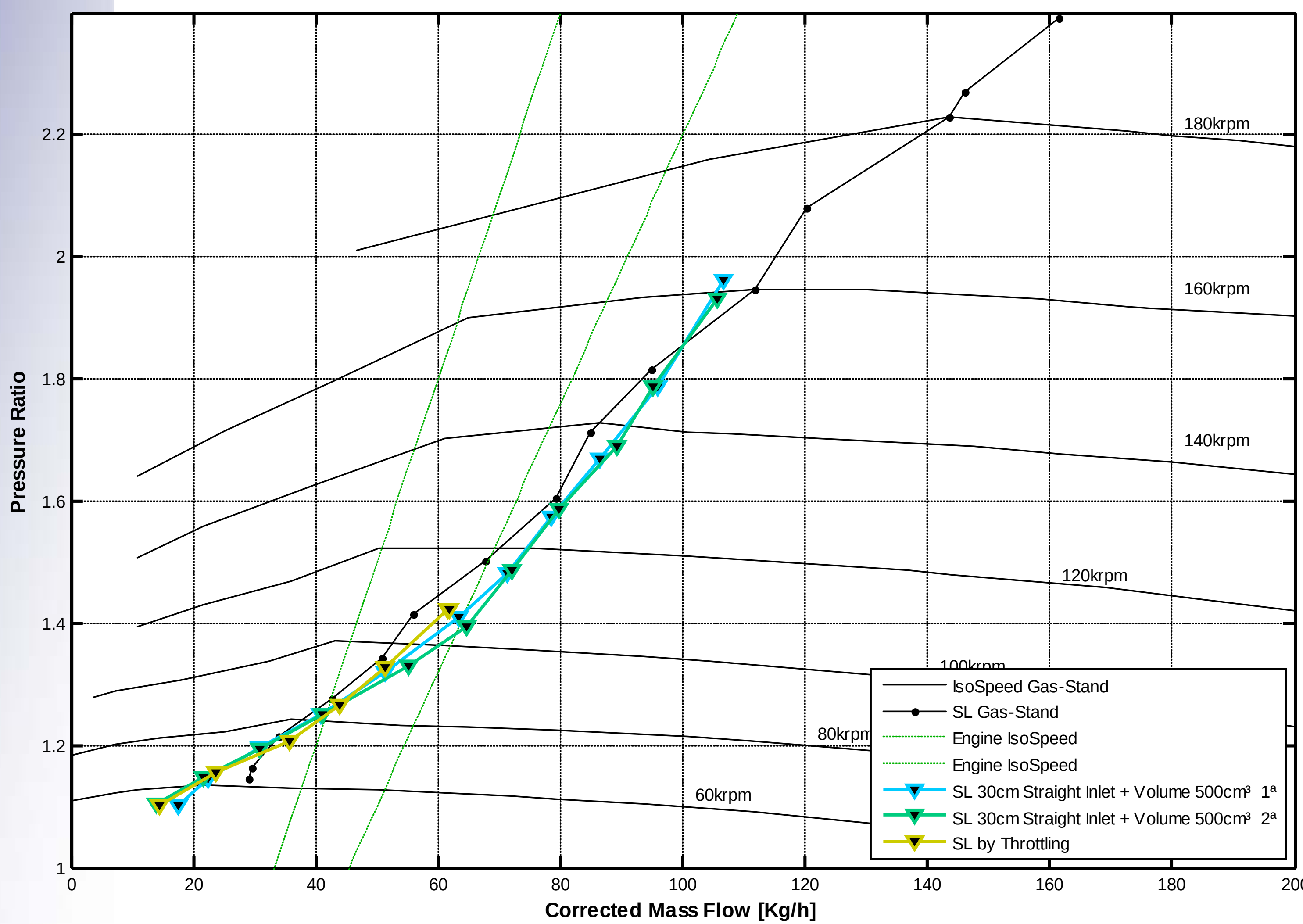
Pressure Ratio
Corrected Mass Flow [Kg/h]
180krpm
160krpm
140krpm
120krpm
100krpm
80krpm
60krpm
IsoSpeed Gas-Stand
SL Gas-Stand
Engine IsoSpeed
Engine IsoSpeed
SL 30cm Straight Inlet + Volume 500cm³ 1ª
SL 30cm Straight Inlet + Volume 500cm³ 2ª
SL by Throttling

# Straight duct (30 cm) and volume 500cm³

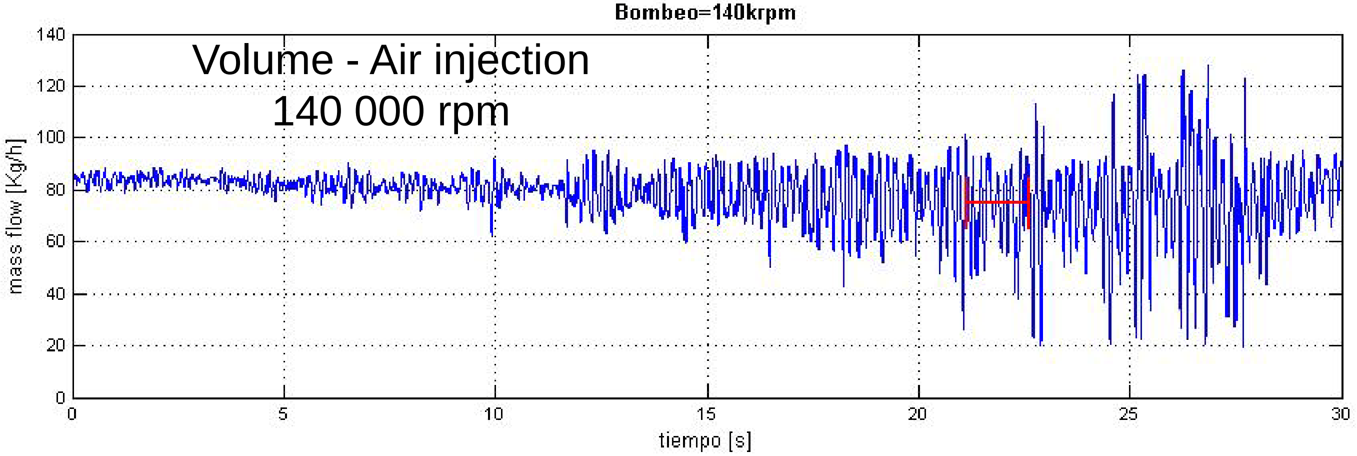


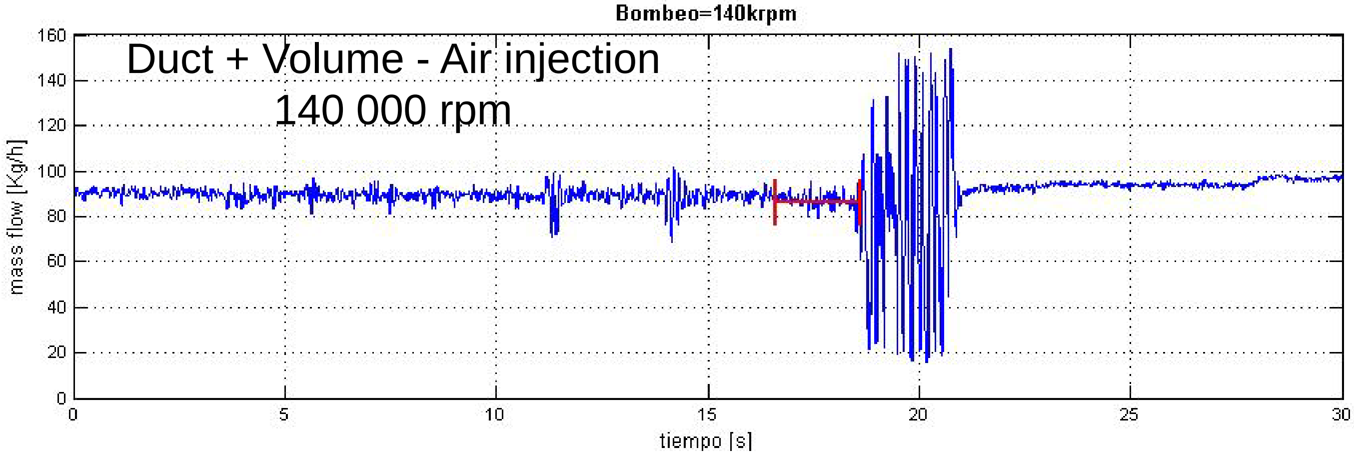

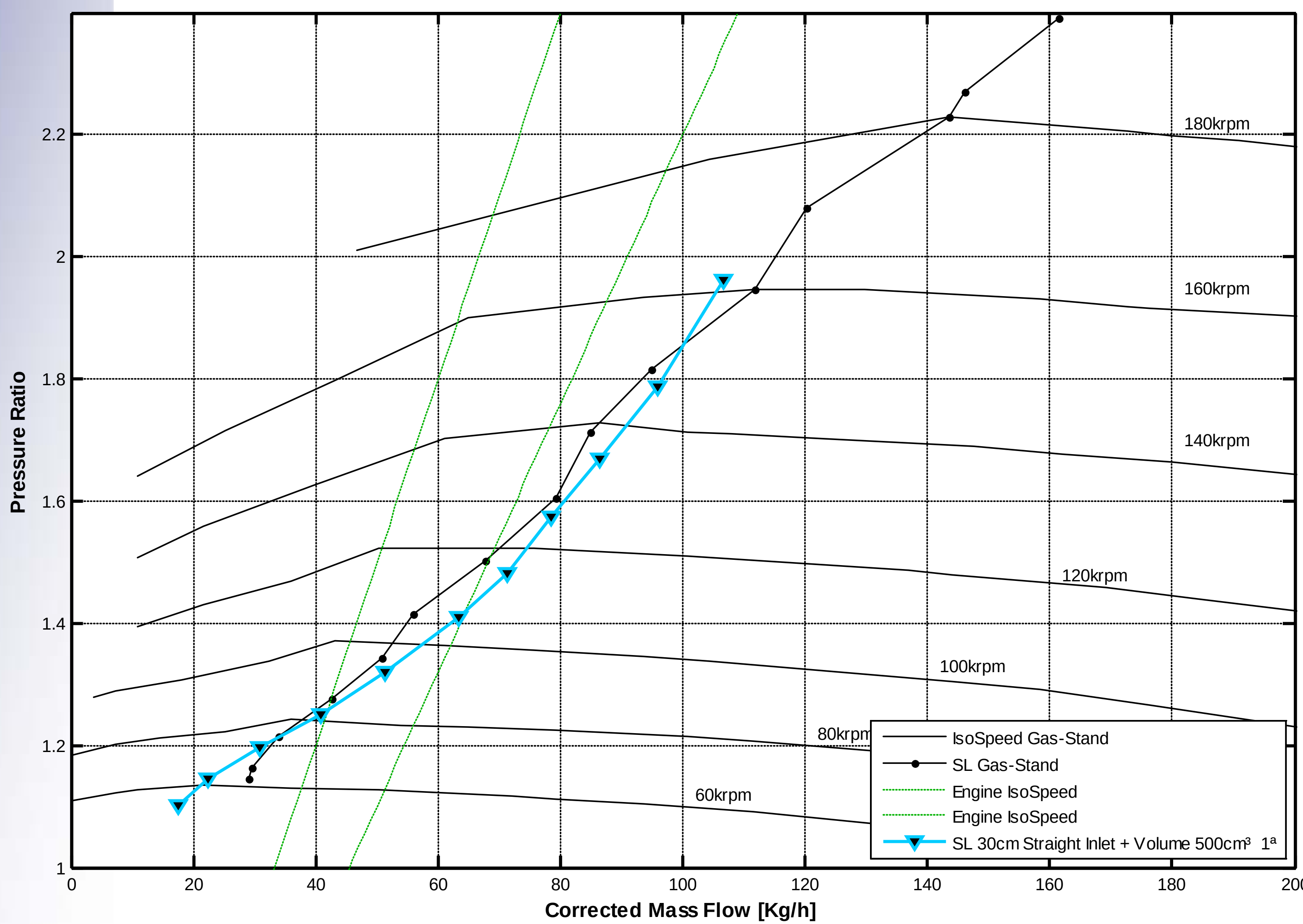
Pressure Ratio
Corrected Mass Flow [Kg/h]
180krpm
160krpm
140krpm
120krpm
100krpm
80krpm
60krpm
IsoSpeed Gas-Stand
SL Gas-Stand
Engine IsoSpeed
Engine IsoSpeed
SL 30cm Straight Inlet + Volume 500cm³ 1ª
0
20
40
60
80
100
120
140
160
180
200
1
1.2
1.4
1.6
1.8
2
2.2

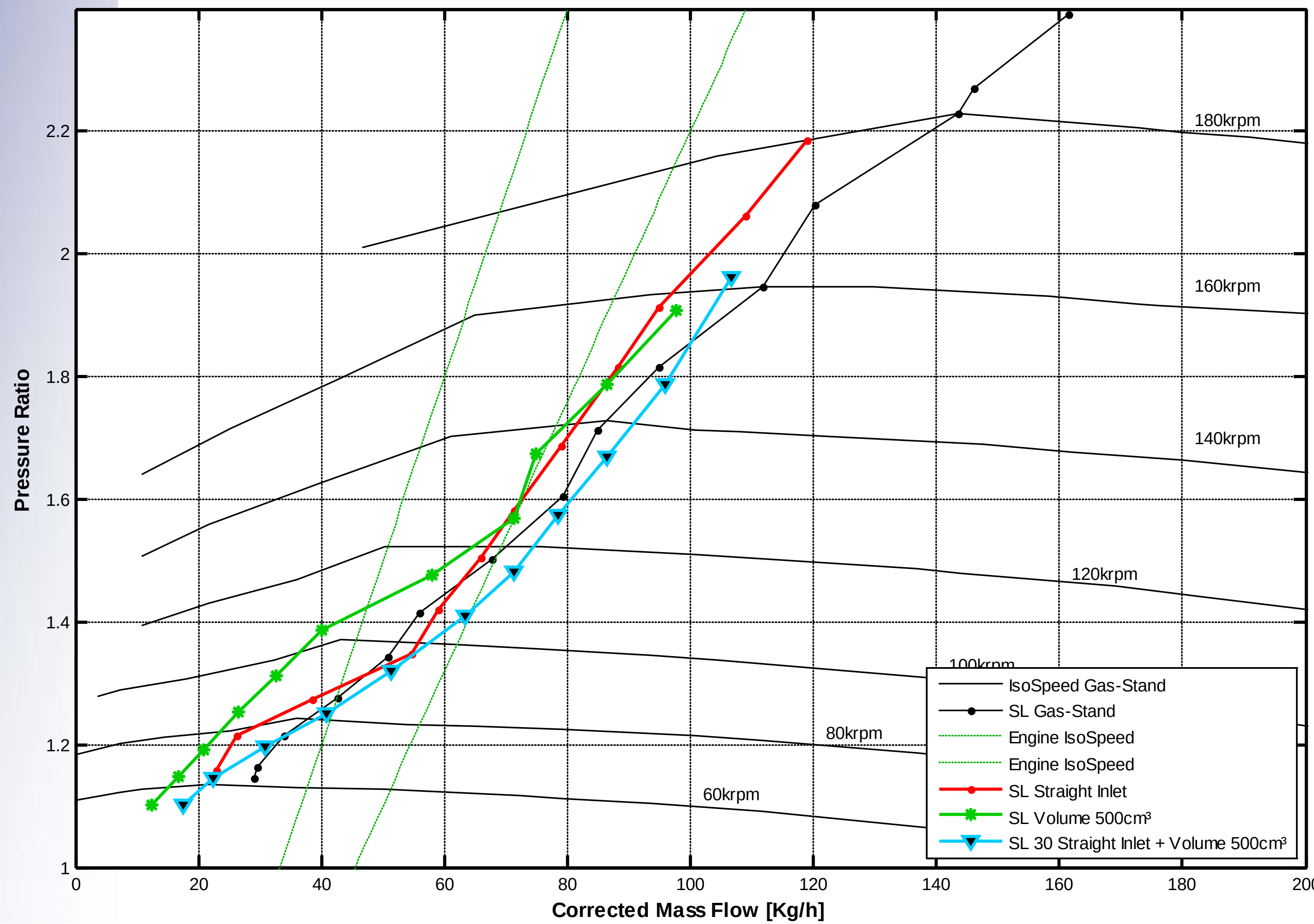
Pressure Ratio
Corrected Mass Flow [Kg/h]
180krpm
160krpm
140krpm
120krpm
100krpm
80krpm
60krpm
IsoSpeed Gas-Stand
SL Gas-Stand
Engine IsoSpeed
Engine IsoSpeed
SL Straight Inlet
SL Volume 500cm³
SL 30 Straight Inlet + Volume 500cm³

# ENGINE TESTS: Duct (30 cm) + Intake Volume

## FIRST CONCLUSIONS

- **When the volume is far away from the compressor inlet the surge margin is very worsened. The results are even worse than the straight duct line.**
- **The worse surge margin can not be justified by the volume pressure losses since they are negligible.**
- **The noise and the more stable behavior is modified when the volume is far from the compressor.**

# Tapered duct 19º + Volume 0.5 l.

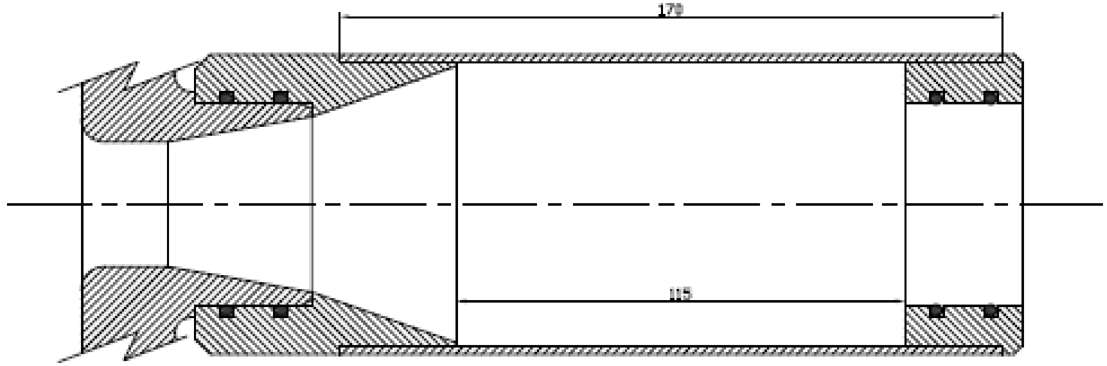


# Tapered duct 19º + Volume 0.5 l.

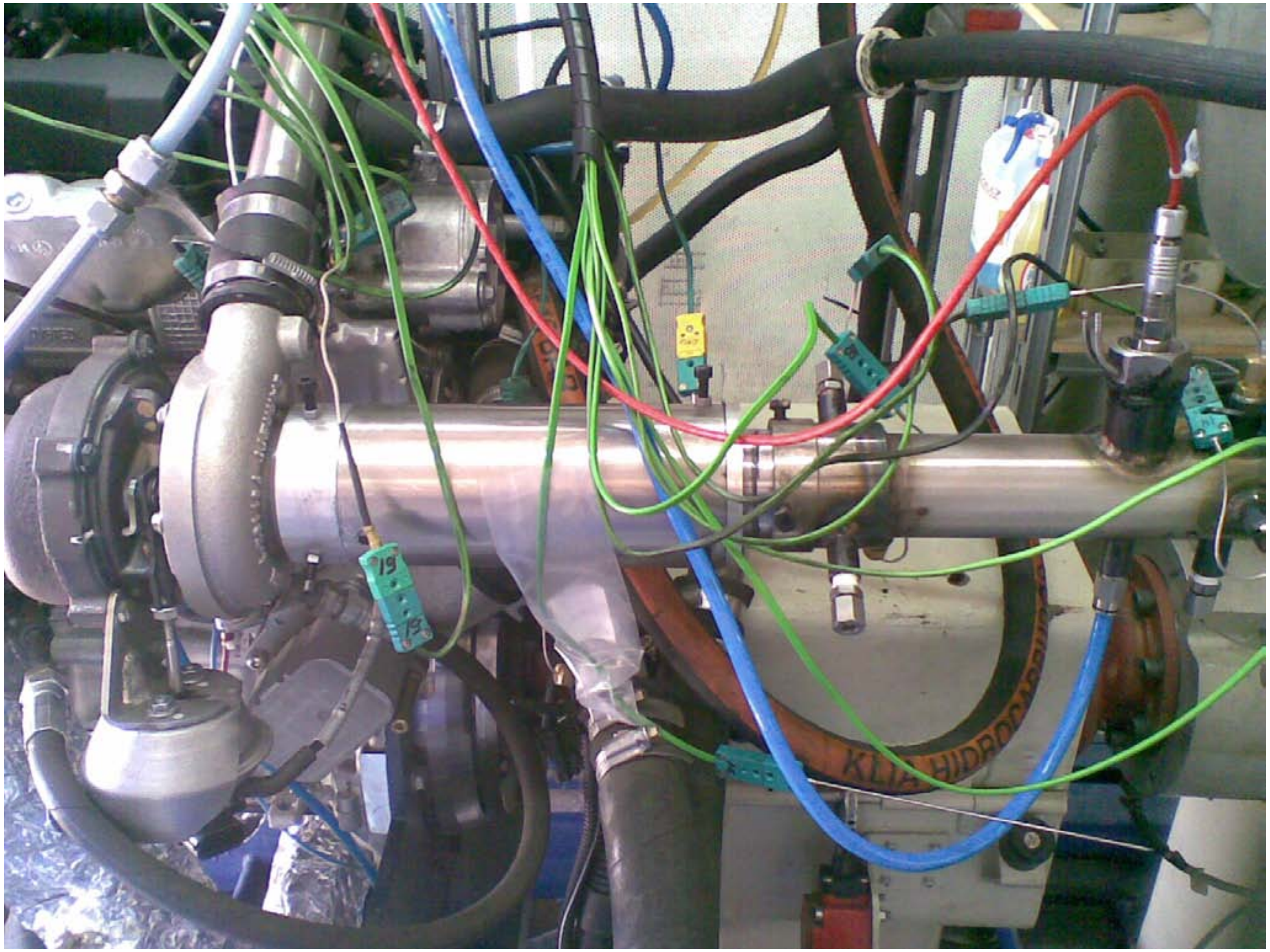

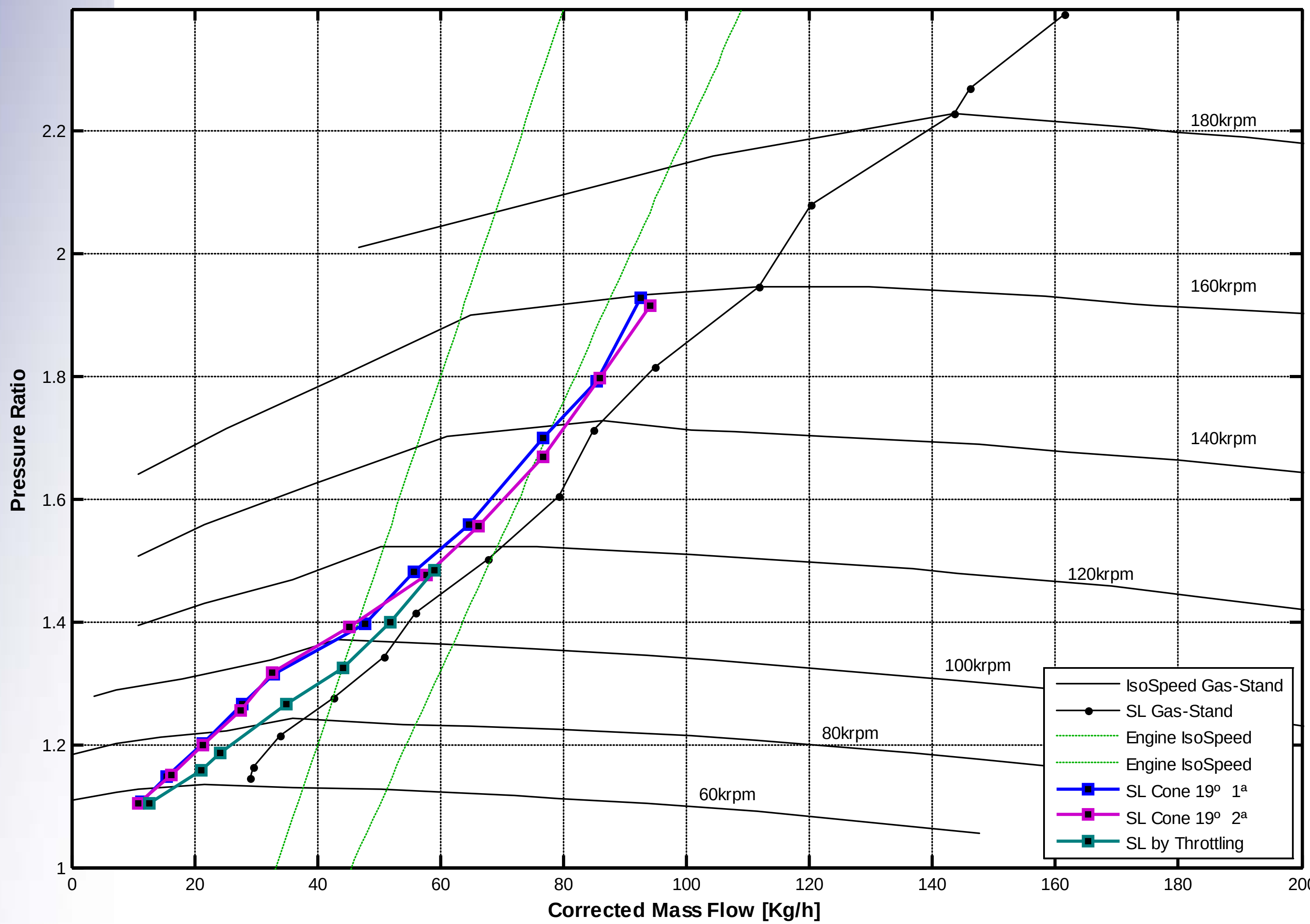
Pressure Ratio
Corrected Mass Flow [Kg/h]
1
1.2
1.4
1.6
1.8
2
2.2
0
20
40
60
80
100
120
140
160
180
200
180krpm
160krpm
140krpm
120krpm
100krpm
80krpm
60krpm
IsoSpeed Gas-Stand
SL Gas-Stand
Engine IsoSpeed
Engine IsoSpeed
SL Cone 19º 1ª
SL Cone 19º 2ª
SL by Throttling

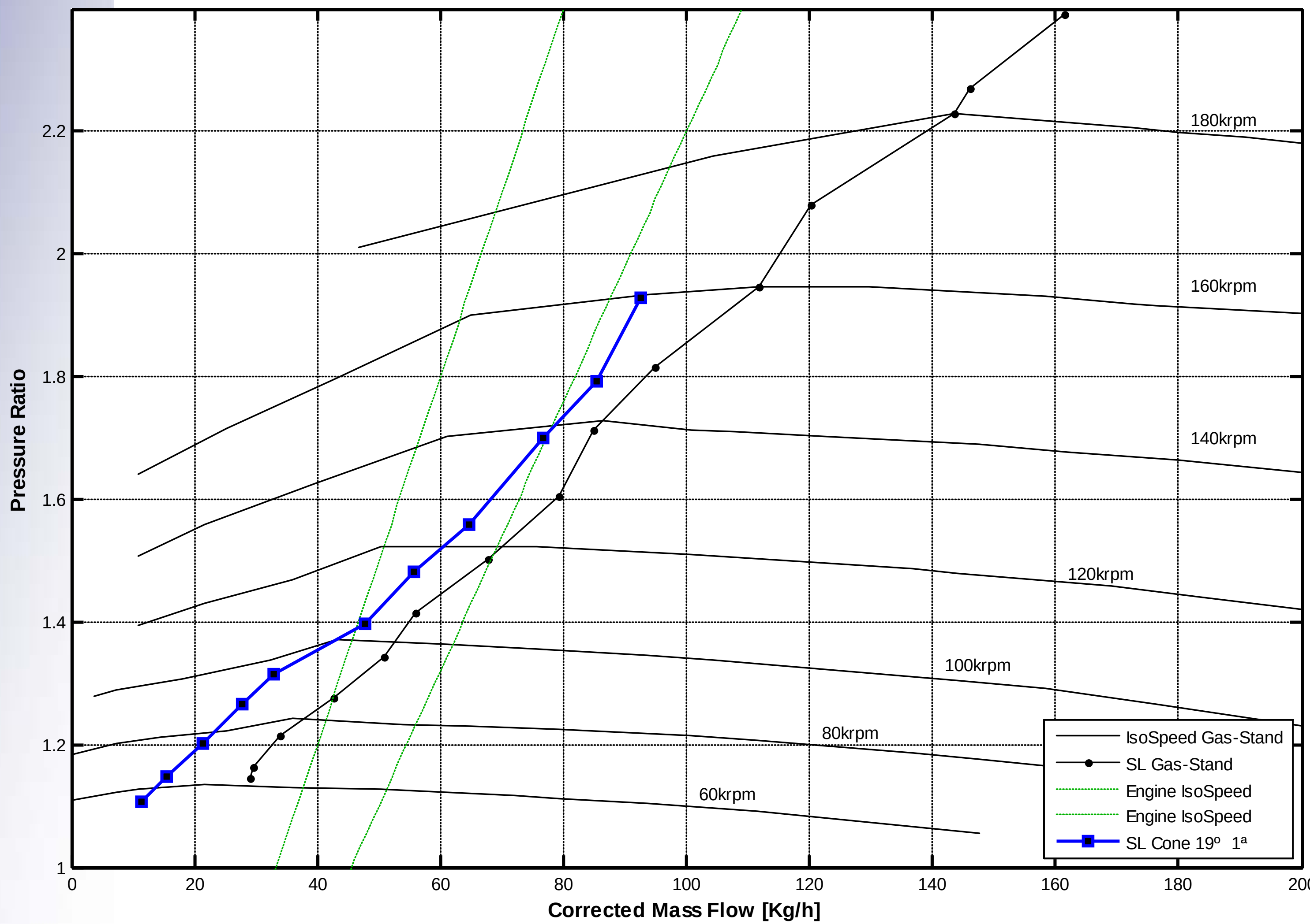
Pressure Ratio
Corrected Mass Flow [Kg/h]
180krpm
160krpm
140krpm
120krpm
100krpm
80krpm
60krpm
IsoSpeed Gas-Stand
SL Gas-Stand
Engine IsoSpeed
Engine IsoSpeed
SL Cone 19º 1ª

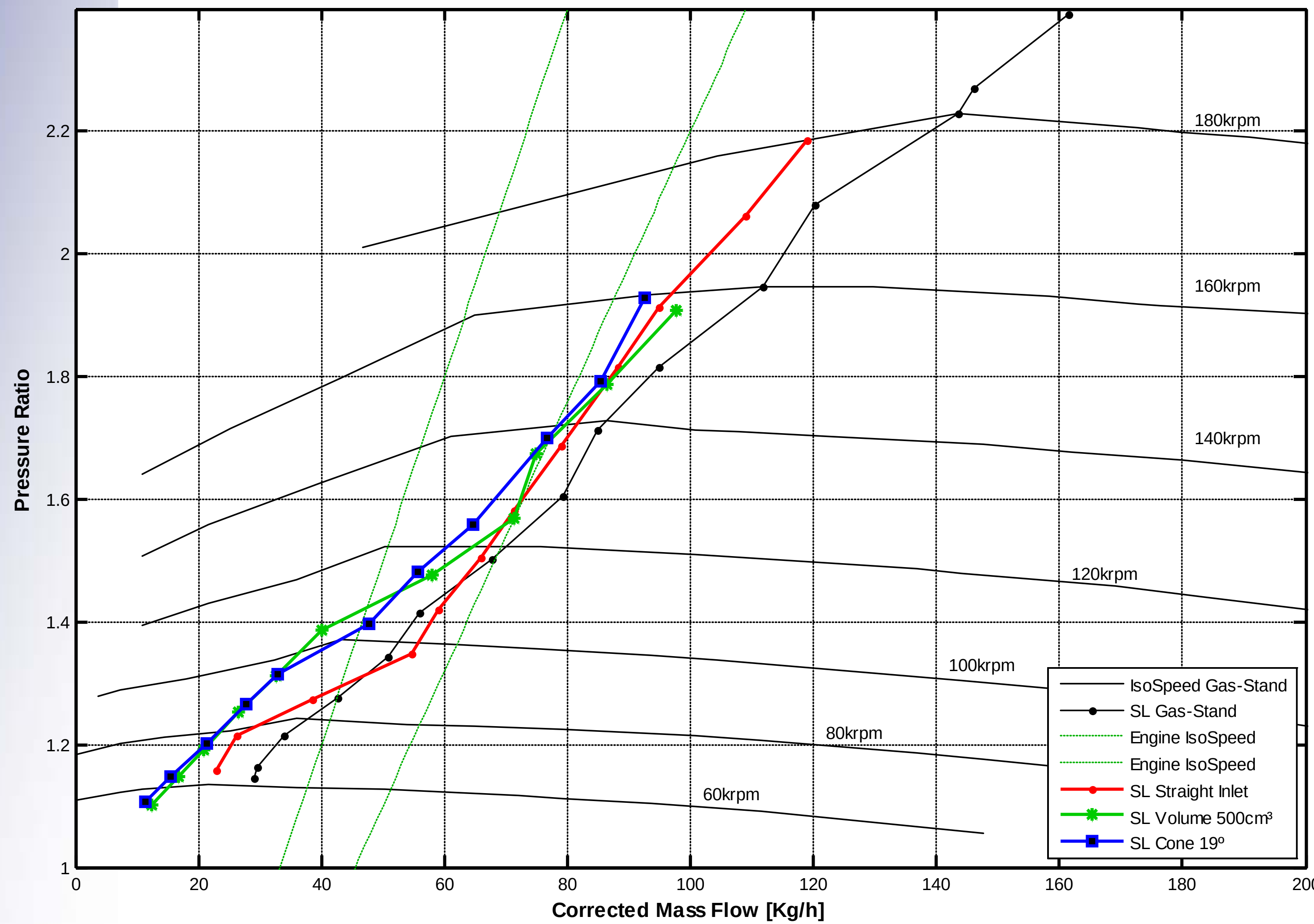
Pressure Ratio
Corrected Mass Flow [Kg/h]
1
1.2
1.4
1.6
1.8
2
2.2
0
20
40
60
80
100
120
140
160
180
200
180krpm
160krpm
140krpm
120krpm
100krpm
80krpm
60krpm
IsoSpeed Gas-Stand
SL Gas-Stand
Engine IsoSpeed
Engine IsoSpeed
SL Straight Inlet
SL Volume 500cm³
SL Cone 19º

# ENGINE TESTS: Tapered duct + Volume 0.5 l.

## FIRST CONCLUSIONS

- **The results are close similar to those of the volume 0.5 l. But it is expected to have less pressure loss at high mass flow rate (full power point)**
- **Slightly increase in compression ratio can be noticed compared to volume 0.5 l.**
- **The dynamics of surge are similar to that of the volume 0.5 l.**

# Volume 1000cm³

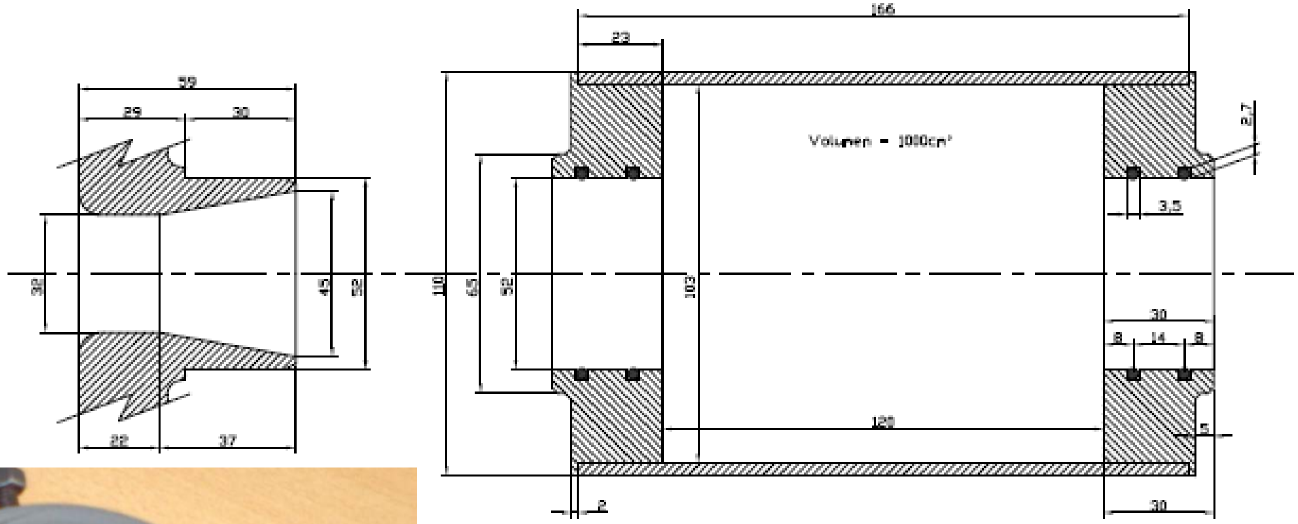


# Volume 1000cm³

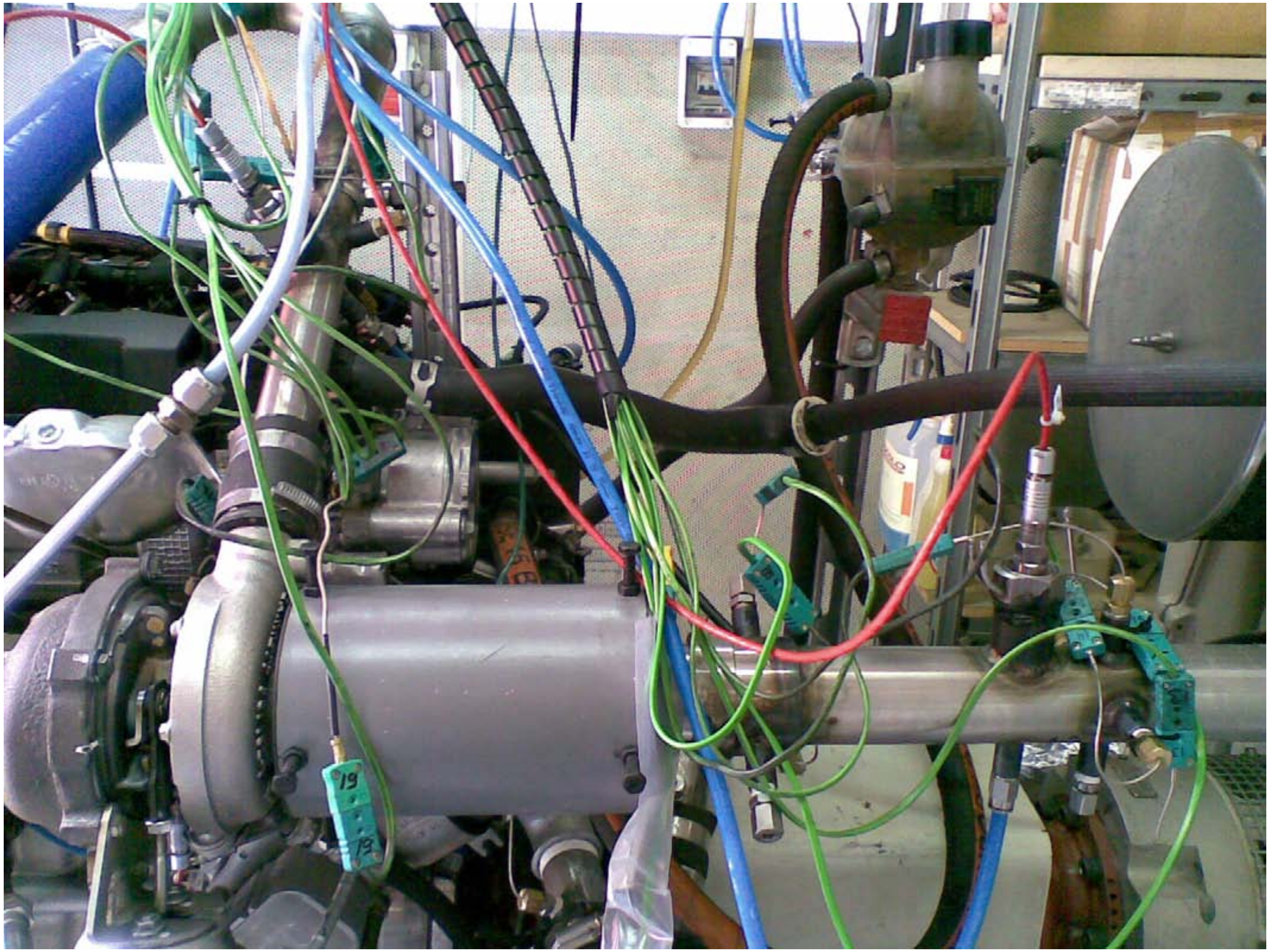

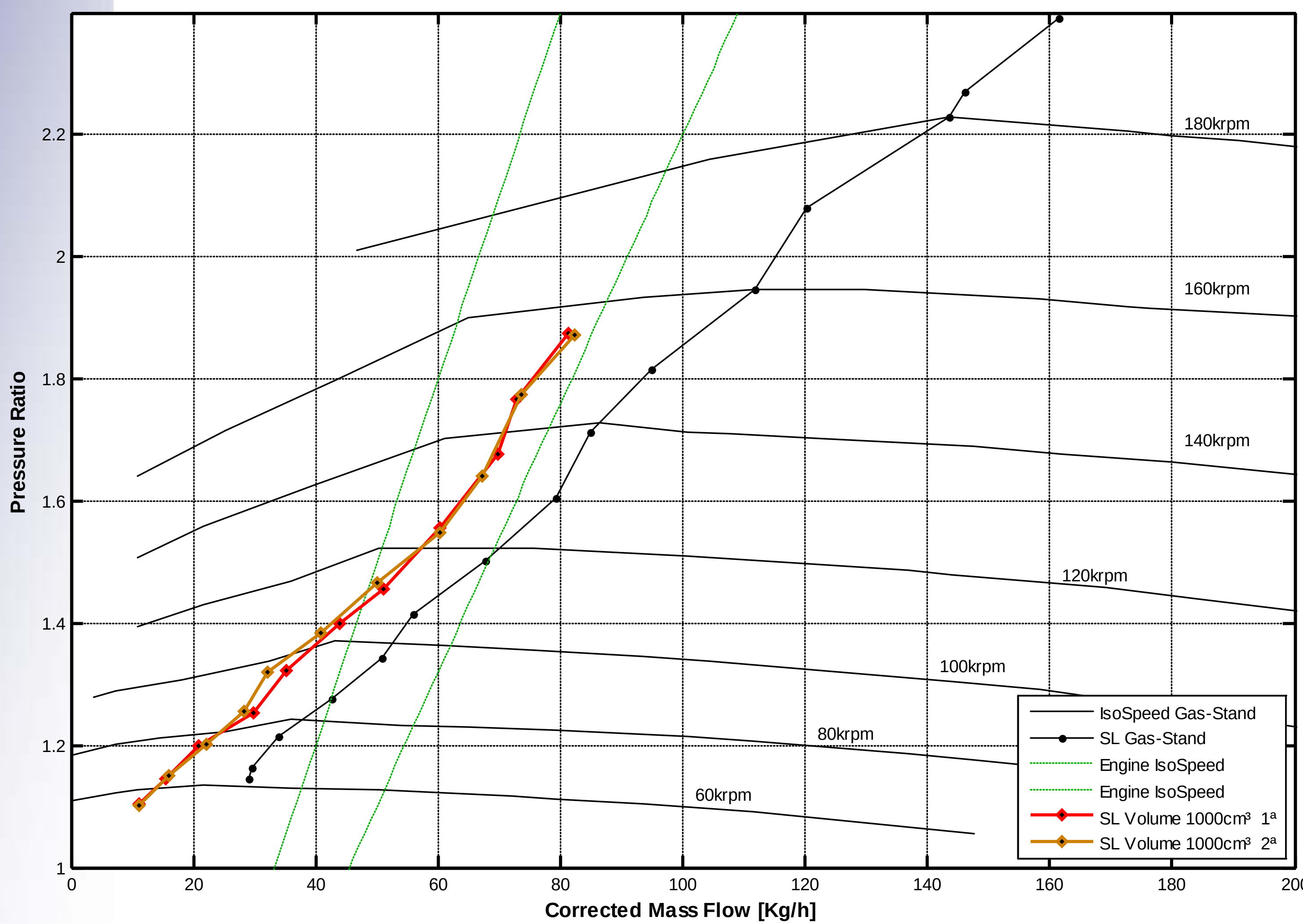

Pressure Ratio
Corrected Mass Flow [Kg/h]
180krpm
160krpm
140krpm
120krpm
100krpm
80krpm
60krpm
IsoSpeed Gas-Stand
SL Gas-Stand
Engine IsoSpeed
Engine IsoSpeed
SL Volume 1000cm³ 1ª
SL Volume 1000cm³ 2ª

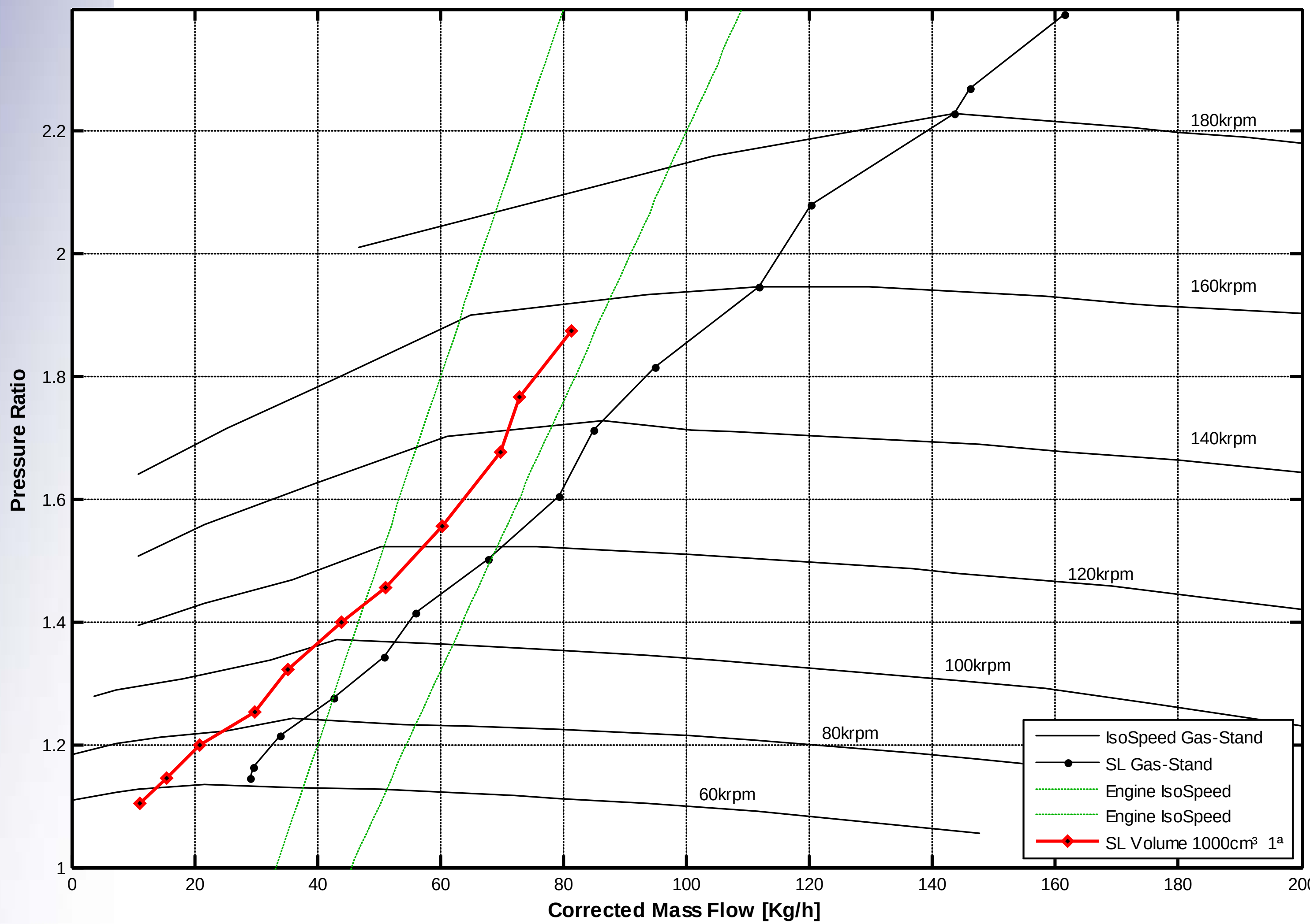

Pressure Ratio
Corrected Mass Flow [Kg/h]
1
1.2
1.4
1.6
1.8
2
2.2
0
20
40
60
80
100
120
140
160
180
200
180krpm
160krpm
140krpm
120krpm
100krpm
80krpm
60krpm
IsoSpeed Gas-Stand
SL Gas-Stand
Engine IsoSpeed
Engine IsoSpeed
SL Volume 1000cm³ 1ª

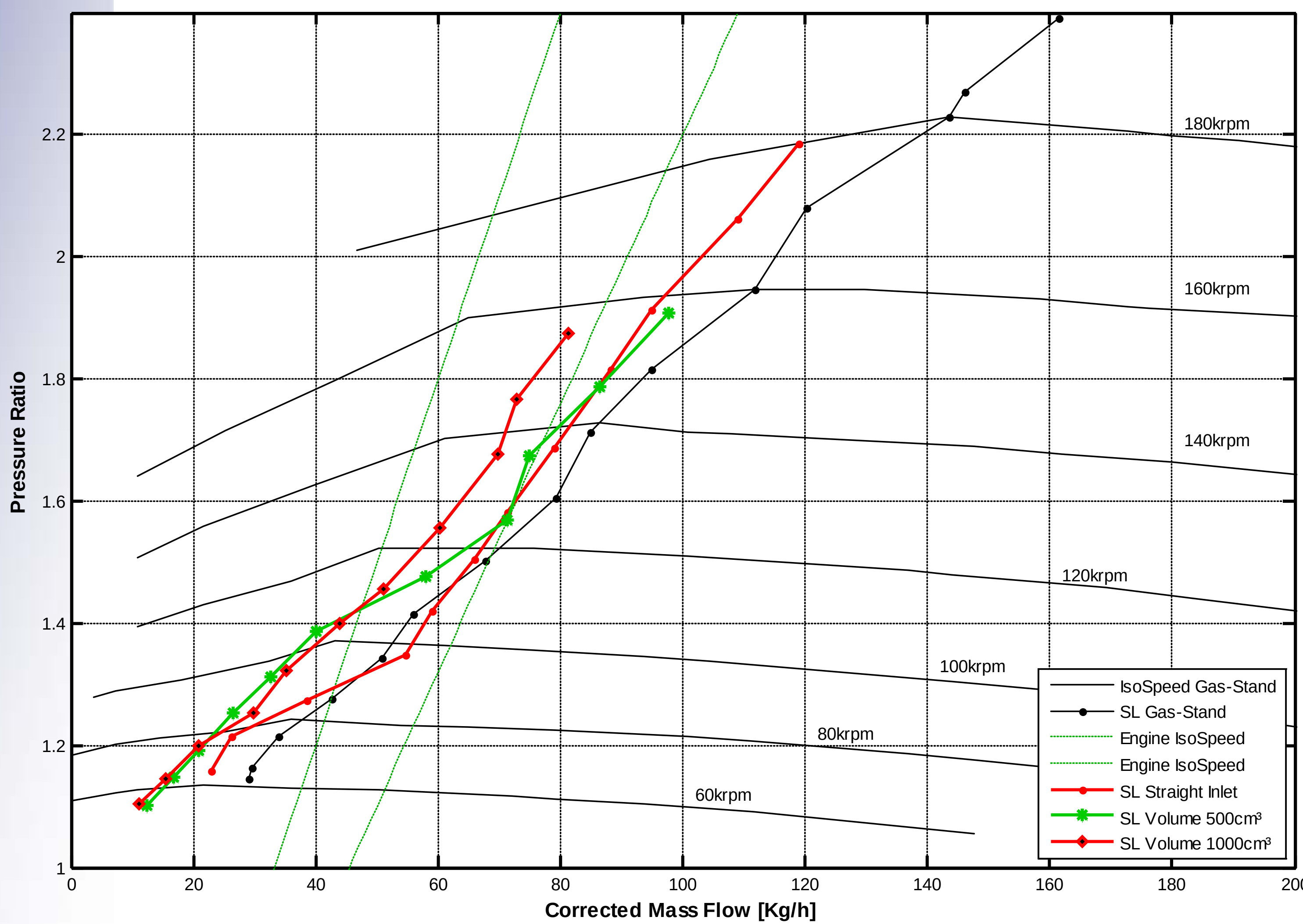
Pressure Ratio
Corrected Mass Flow [Kg/h]
1
1.2
1.4
1.6
1.8
2
2.2
0
20
40
60
80
100
120
140
160
180
200
180krpm
160krpm
140krpm
120krpm
100krpm
80krpm
60krpm
IsoSpeed Gas-Stand
SL Gas-Stand
Engine IsoSpeed
Engine IsoSpeed
SL Straight Inlet
SL Volume 500cm³
SL Volume 1000cm³

# ENGINE TESTS: Intake Volume 1 liter

## FIRST CONCLUSIONS

- **It shows an improvement on surge margin at low speed and at high speed (around 15 kg/h)**
- **Compared to the smaller volume it improves at high compressor speed**

# Flow deflector: 20mm ø y at 3mm from wheel

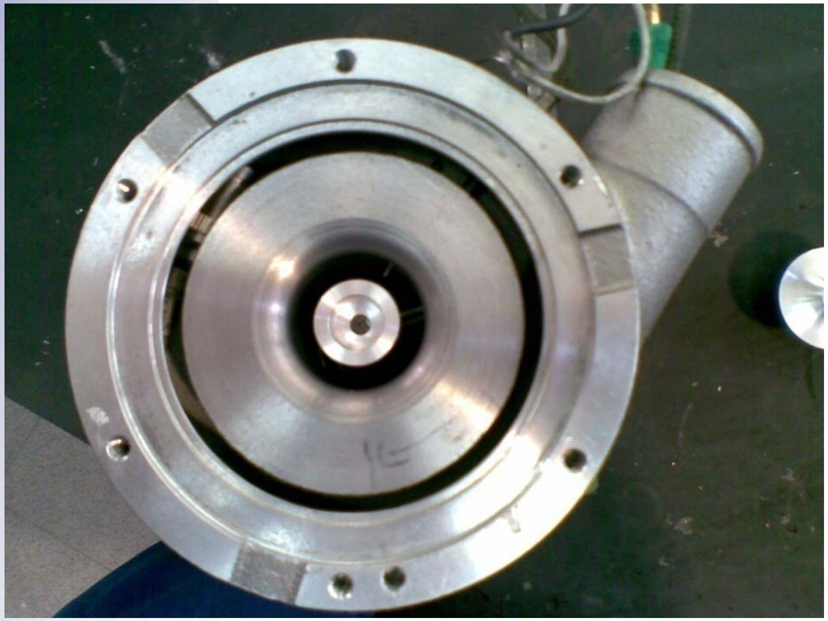

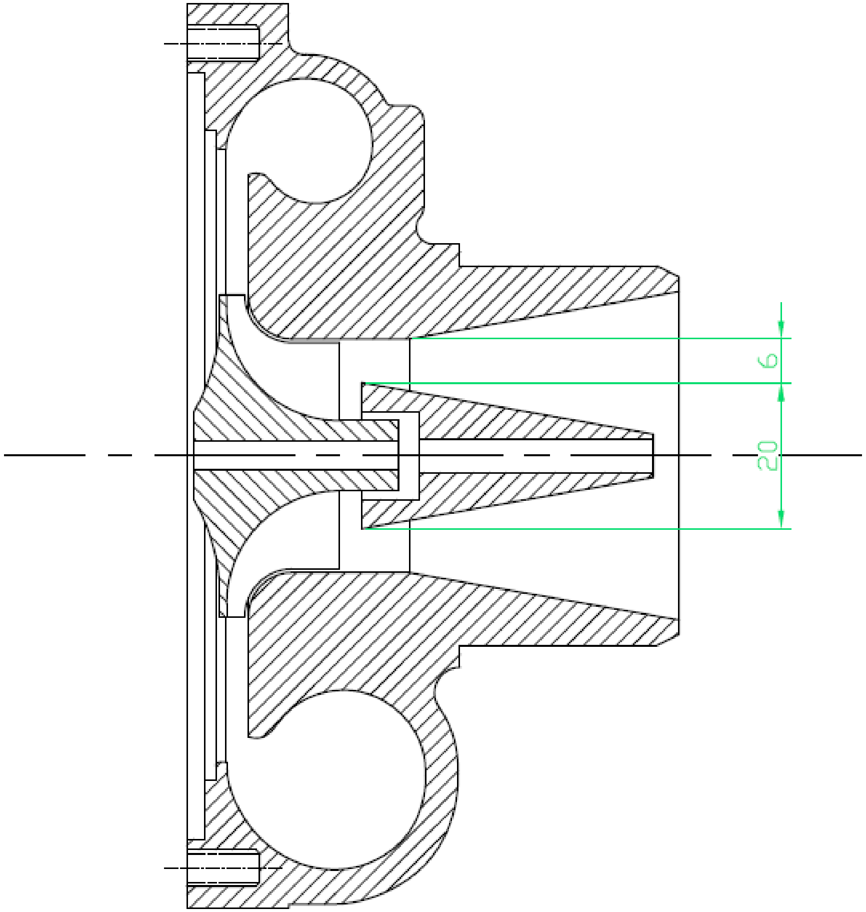

# Aerodinamics bodies comparation

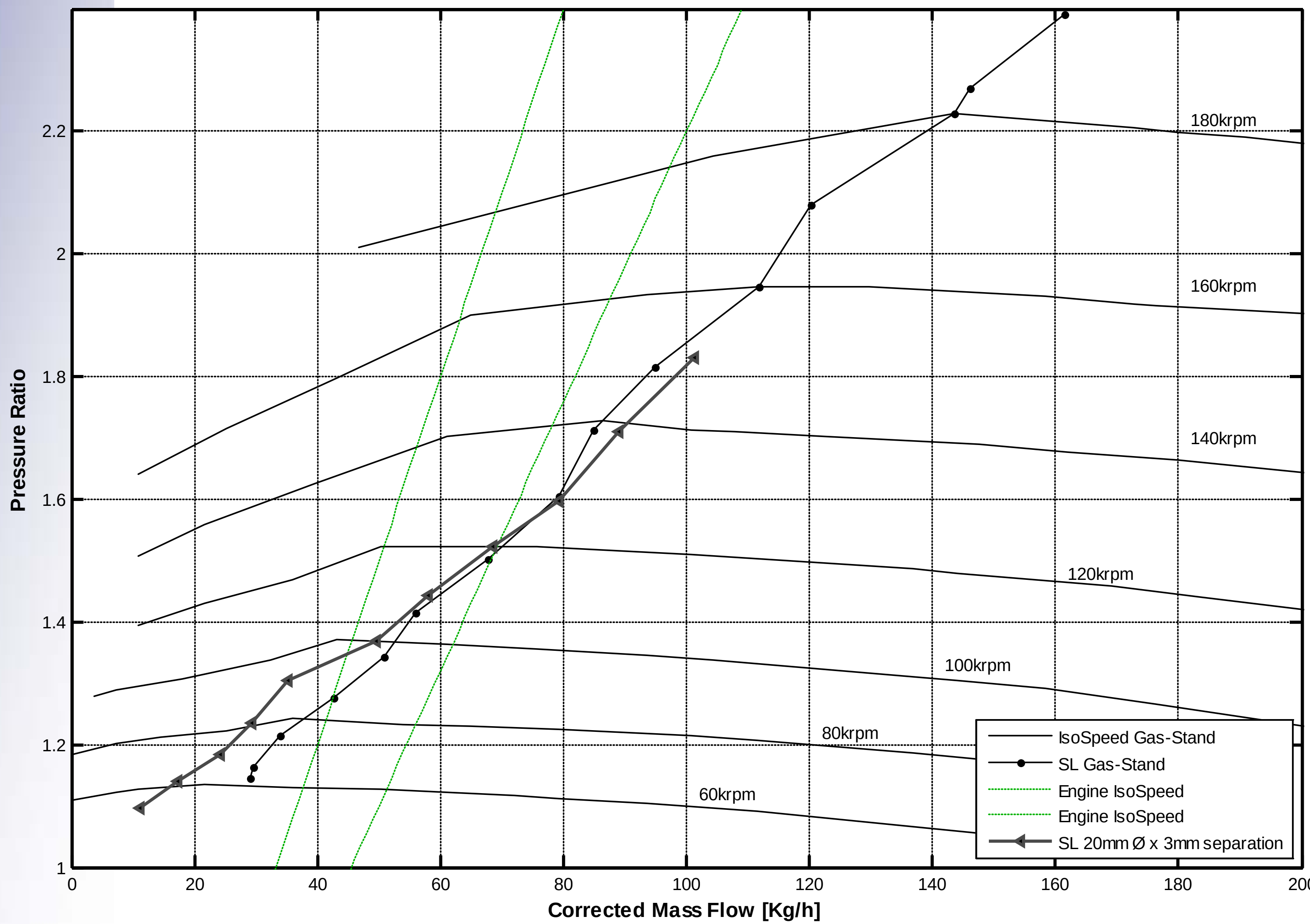
Pressure Ratio
Corrected Mass Flow [Kg/h]
180krpm
160krpm
140krpm
120krpm
100krpm
80krpm
60krpm
IsoSpeed Gas-Stand
SL Gas-Stand
Engine IsoSpeed
Engine IsoSpeed
SL 20mm Ø x 3mm separation
1
1.2
1.4
1.6
1.8
2
2.2
0
20
40
60
80
100
120
140
160
180
200

# Flow deflector: 20mm ø y 1mm separation

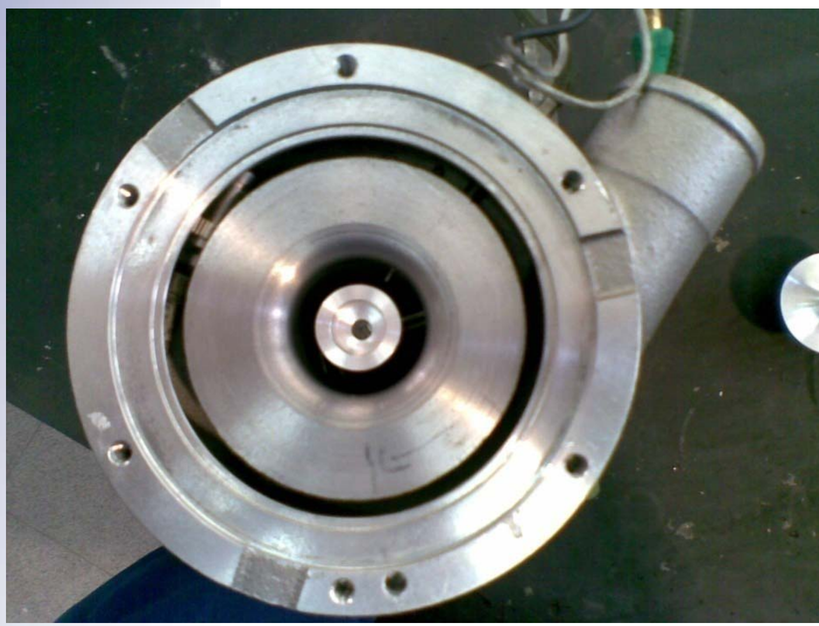

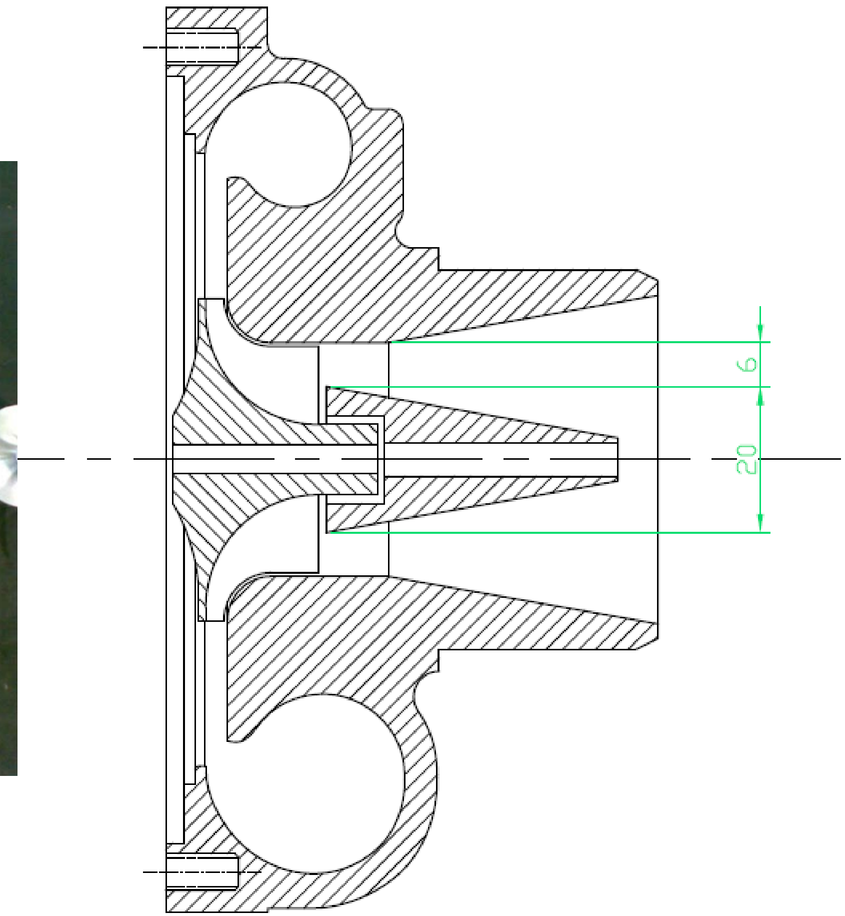

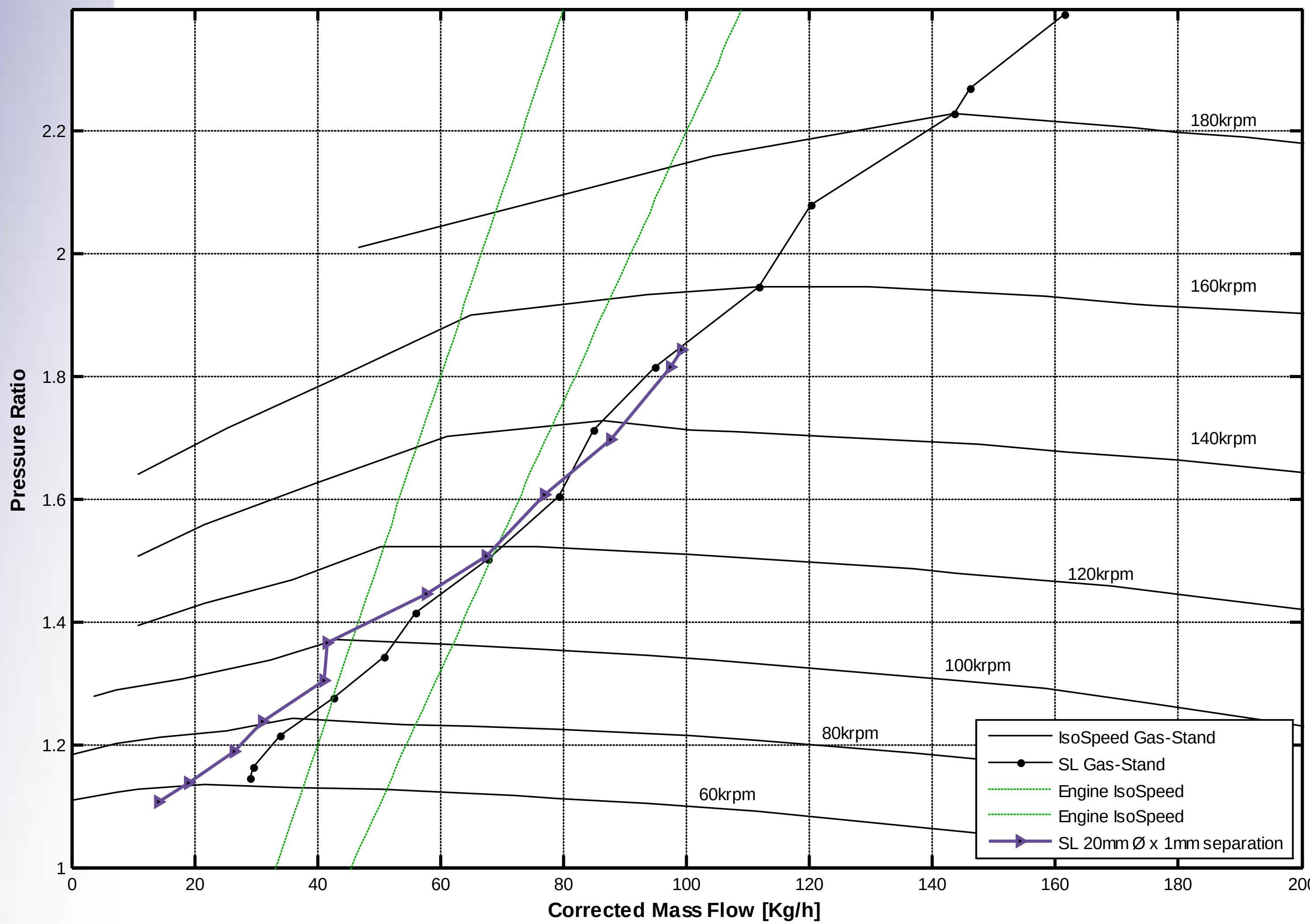
Pressure Ratio
Corrected Mass Flow [Kg/h]
1
1.2
1.4
1.6
1.8
2
2.2
0
20
40
60
80
100
120
140
160
180
200
180krpm
160krpm
140krpm
120krpm
100krpm
80krpm
60krpm
IsoSpeed Gas-Stand
SL Gas-Stand
Engine IsoSpeed
Engine IsoSpeed
SL 20mm Ø x 1mm separation

# Aerodinamic body: 28mm ø y 1mm separation

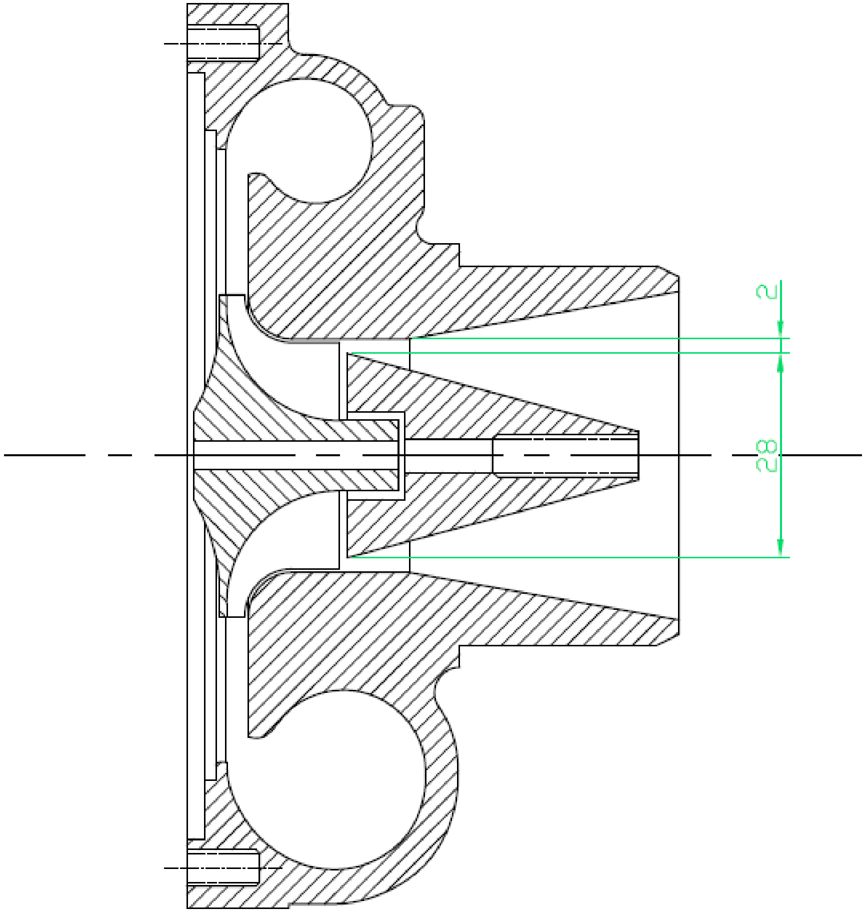

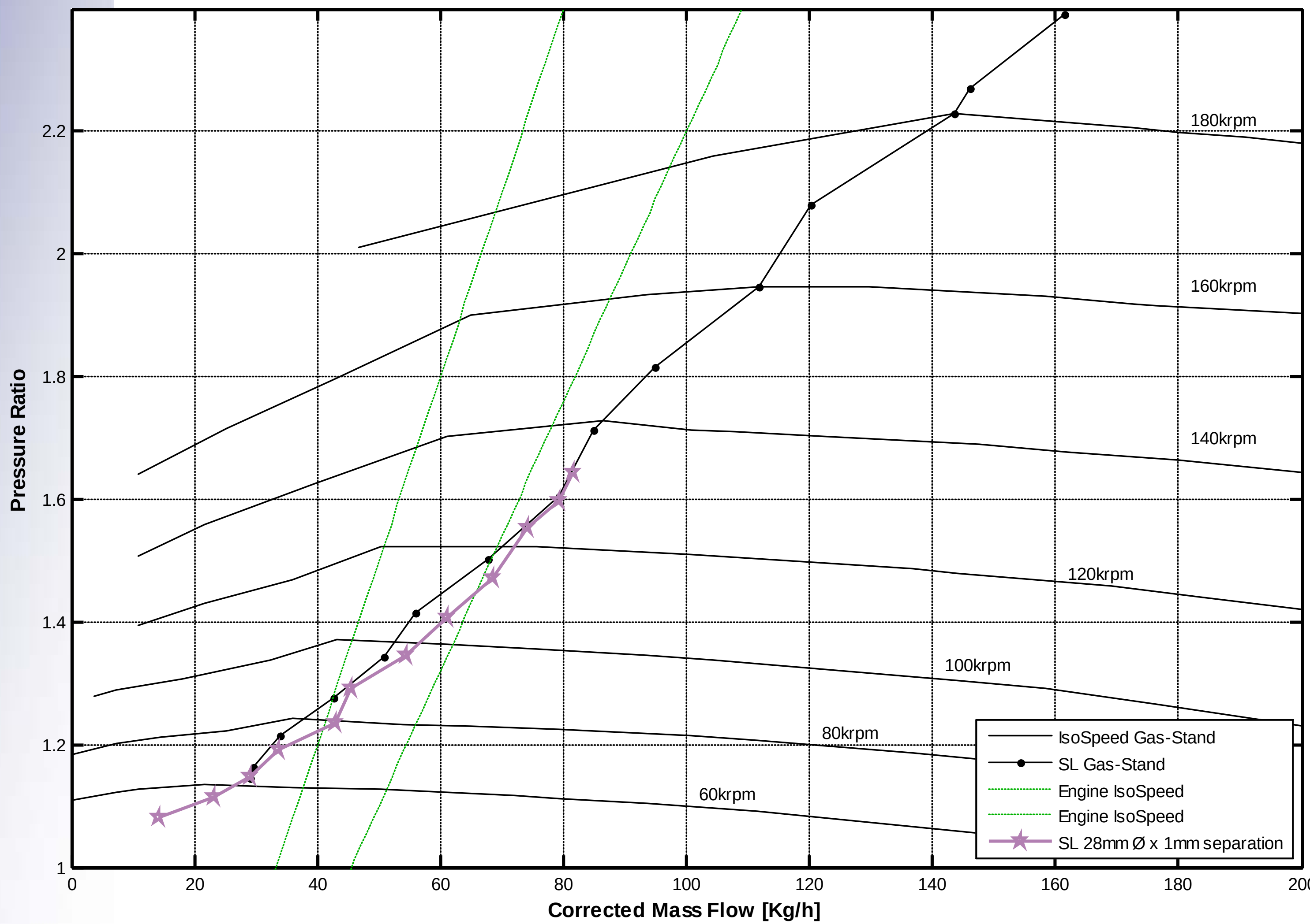
Pressure Ratio
Corrected Mass Flow [Kg/h]
1
1.2
1.4
1.6
1.8
2
2.2
0
20
40
60
80
100
120
140
160
180
200
180krpm
160krpm
140krpm
120krpm
100krpm
80krpm
60krpm
IsoSpeed Gas-Stand
SL Gas-Stand
Engine IsoSpeed
Engine IsoSpeed
SL 28mm Ø x 1mm separation

# Aerodinamic body: 25mm ø y 1mm separation

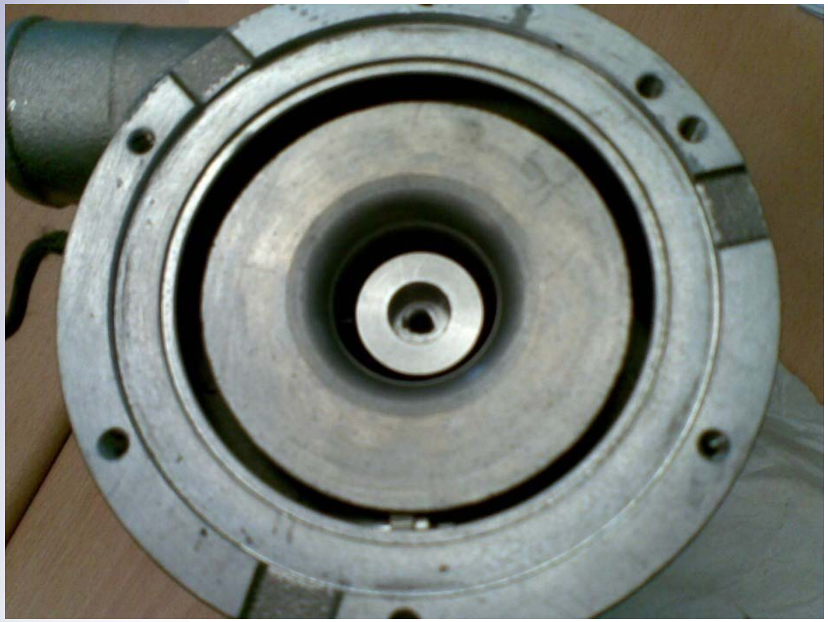

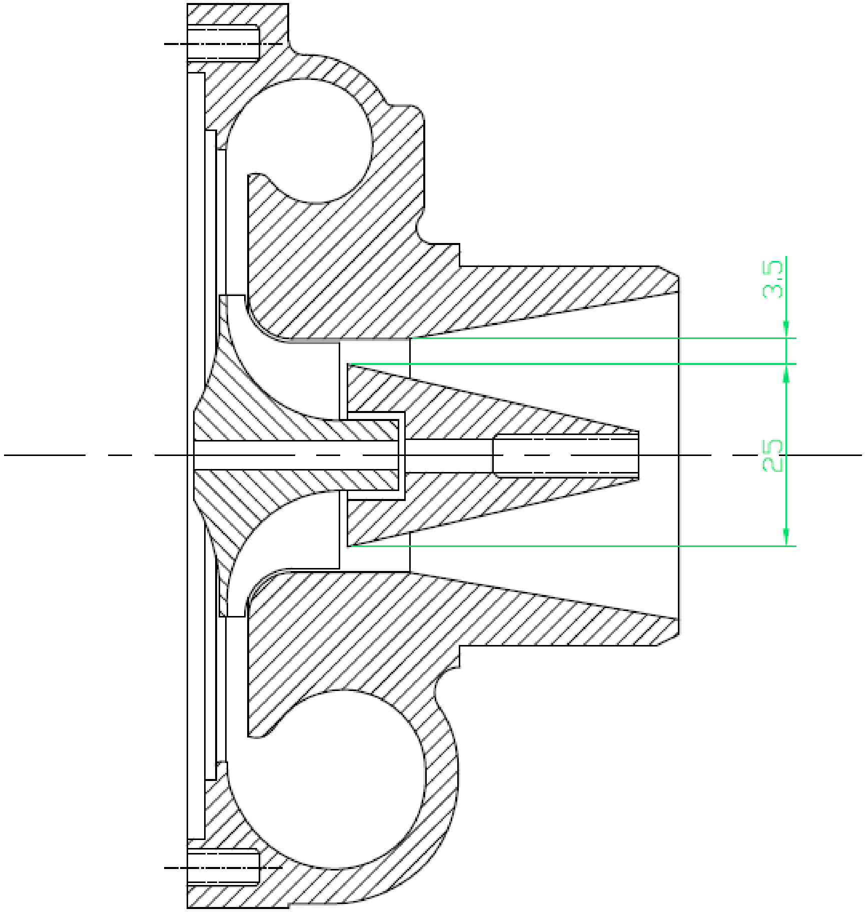

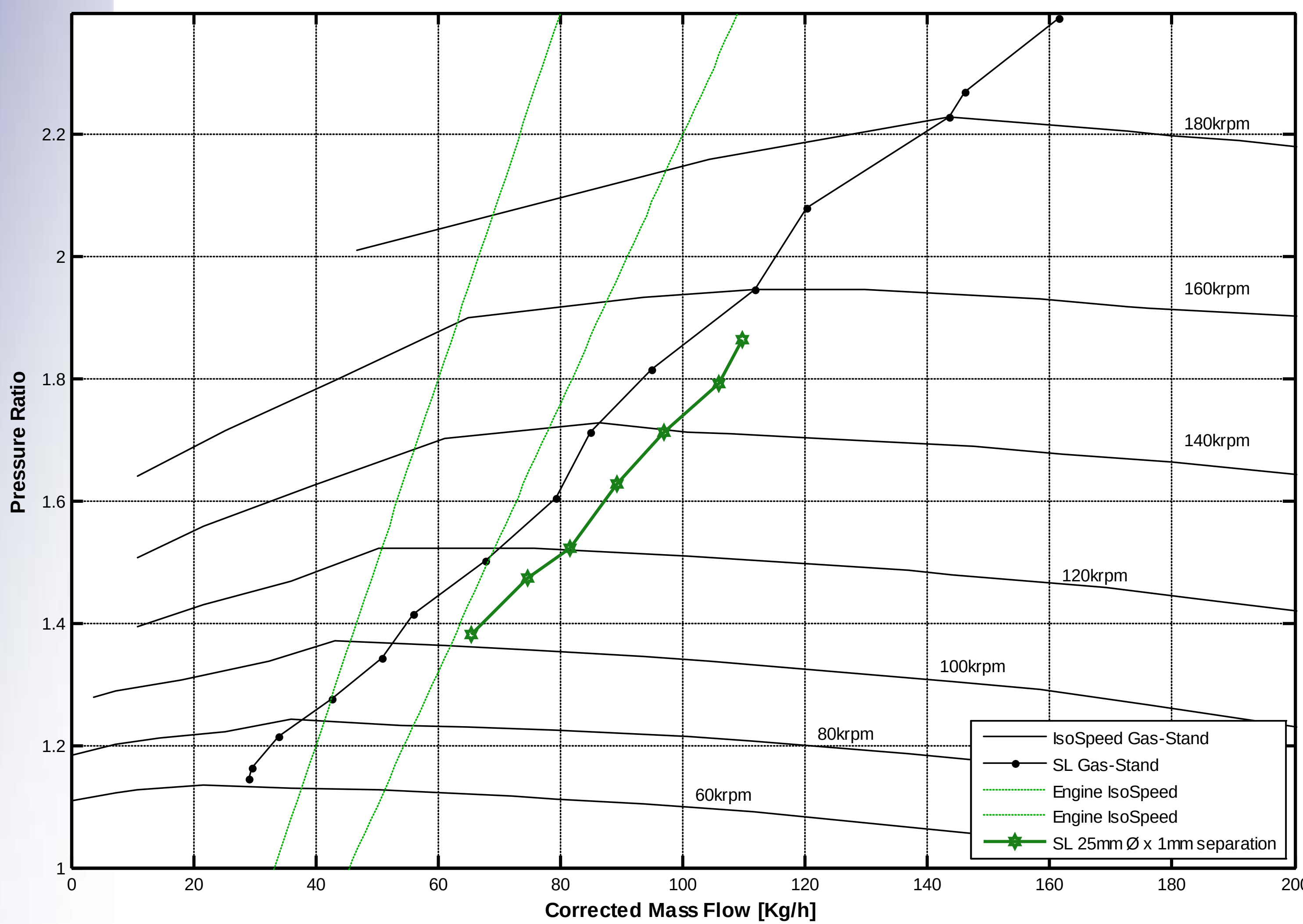
Pressure Ratio
Corrected Mass Flow [Kg/h]
180krpm
160krpm
140krpm
120krpm
100krpm
80krpm
60krpm
IsoSpeed Gas-Stand
SL Gas-Stand
Engine IsoSpeed
Engine IsoSpeed
SL 25mm Ø x 1mm separation

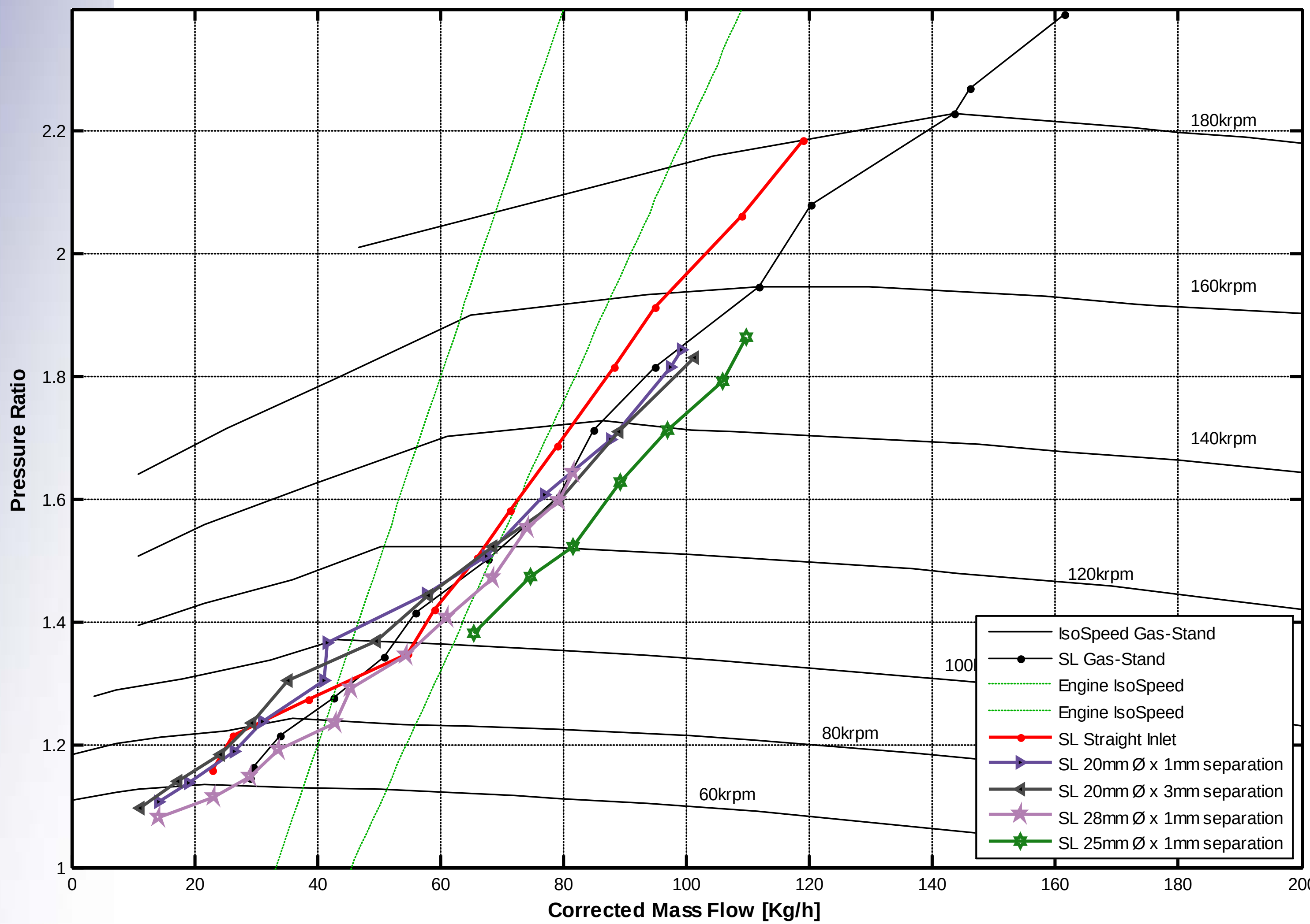

Pressure Ratio
Corrected Mass Flow [Kg/h]
180krpm
160krpm
140krpm
120krpm
100k
80krpm
60krpm
IsoSpeed Gas-Stand
SL Gas-Stand
Engine IsoSpeed
Engine IsoSpeed
SL Straight Inlet
SL 20mm Ø x 1mm separation
SL 20mm Ø x 3mm separation
SL 28mm Ø x 1mm separation
SL 25mm Ø x 1mm separation

# ENGINE TESTS: Flow Deflectors

## FIRST CONCLUSIONS

- They improve marginally only at low-medium compressor speed
- If the outer diameter is to big the pressure loss is so high that all the map is lowered in compression ratio

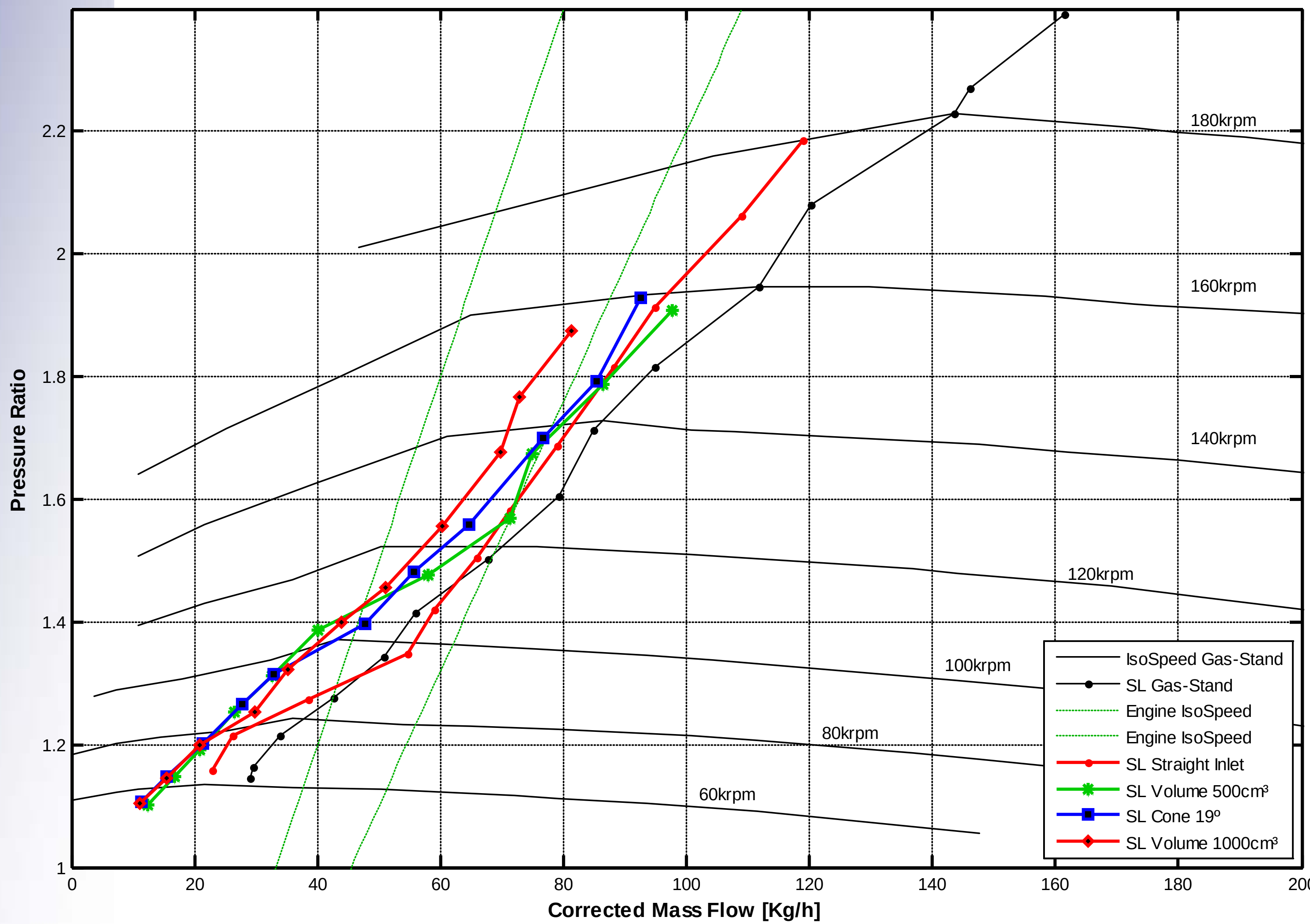

Pressure Ratio
Corrected Mass Flow [Kg/h]
1
1.2
1.4
1.6
1.8
2
2.2
0
20
40
60
80
100
120
140
160
180
200
180krpm
160krpm
140krpm
120krpm
100krpm
80krpm
60krpm
IsoSpeed Gas-Stand
SL Gas-Stand
Engine IsoSpeed
Engine IsoSpeed
SL Straight Inlet
SL Volume 500cm³
SL Cone 19º
SL Volume 1000cm³

# SUMMARY

- **METHODOLOGY: The air injection leads to more repetitive, stable and smooth surge inception. Surge line measured throttling is different to that of air injection.**
- **GEOMETRY:**
  - **On engine straight inlet line has increased surge line than gas-stand**
  - **The elbow improves slightly surge margin at low speeds (as in our experience)**
  - **The 0.5 l. volume increases significantly surge margin at low speed and changes the dynamics of surge. When the volume is moved away, by an elbow or by a duct, all the benefit is lost. A tapered entry to the compressor may improve slightly the surge line.**
  - **A  bigger volume (1 liter) improves in the whole speed range**
  - **The flow defectors do not improve surge margin**

DESIGN CRITERION: Volume 1 l. + tapered ducts at its inlet and outlet to reduce pressure losses

# PROJET POMPAGE CMT

*"Analyse et mesure des phénomènes de pompage entrée compresseur"*

# CFD COMPRESSOR SIMULATION NEAR SURGE

- **Methodology**
- **CFD domain**
- **Mesh**
- **Results**
  - **Steady**
  - **Transient**
- **Geometries:**
  - **Straight Pipe**
  - **Elbow**
  - **Volume 0.5 l.**

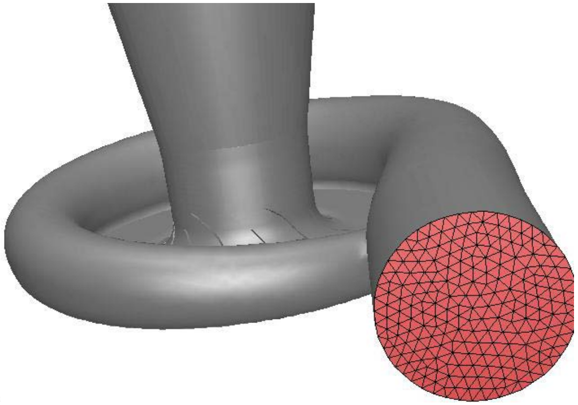

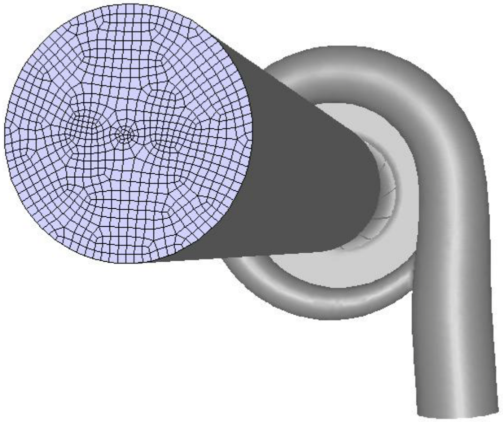

# METHODOLOGY

- CFD calculations on real compressor geometry.
- Steady state calculations for stable operation zone in the compressor map.
- Transient calculations with variable boundary conditions near surge line.

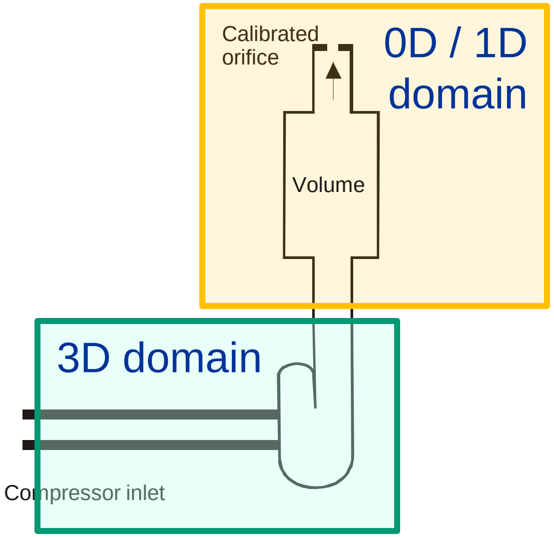

# CFD DOMAIN

- CFD domain includes the real geometry of all the components of the compressor:
  - Inlet cone duct
  - Rotor
  - Diffuser
  - Volute
  - Outlet duct

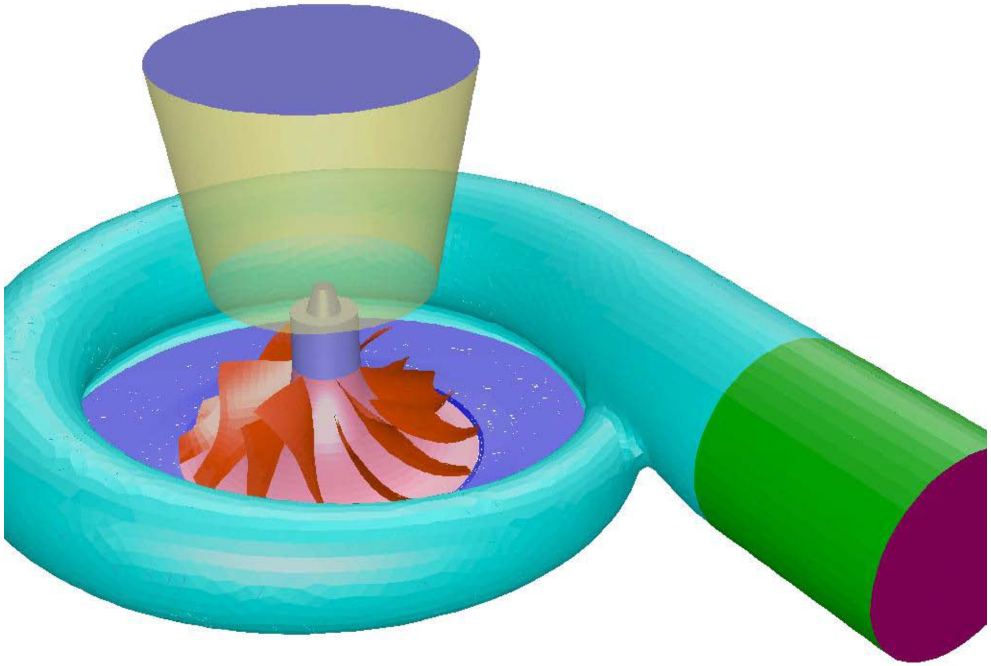

# MESH

- Hybrid HEX / TET mesh.
- Semi-structured mesh for ducts and rotor
- Hex-core mesh for difusser and volute
- Arbitrary interfaces between inlet / rotor and rotor / diffuser
- Semi-automatic adaptative refinement based on velocity gradients

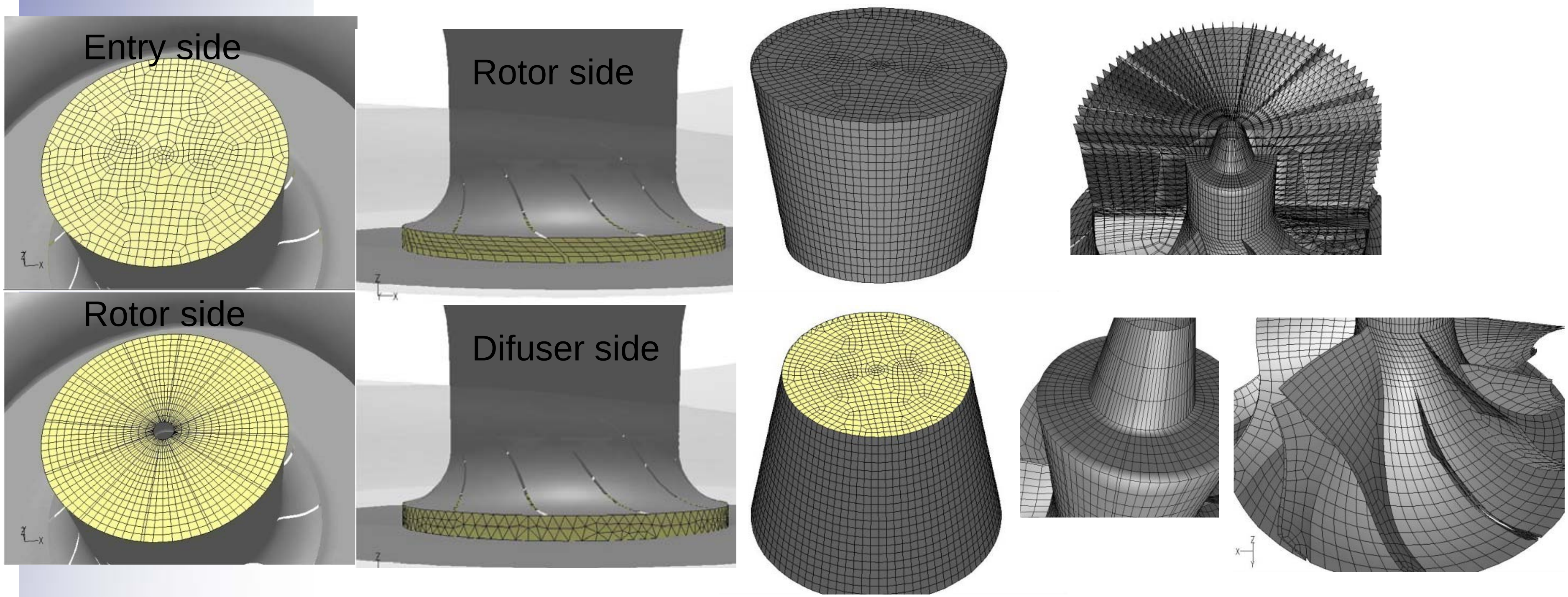

# MESH

- Hybrid HEX / TET mesh.
- Semi-structured mesh for ducts and rotor
- Hex-core mesh for difusser and volute
- Arbitrary interfaces between inlet / rotor and rotor / diffuser
- Semi-automatic adaptative refinement based on velocity gradients

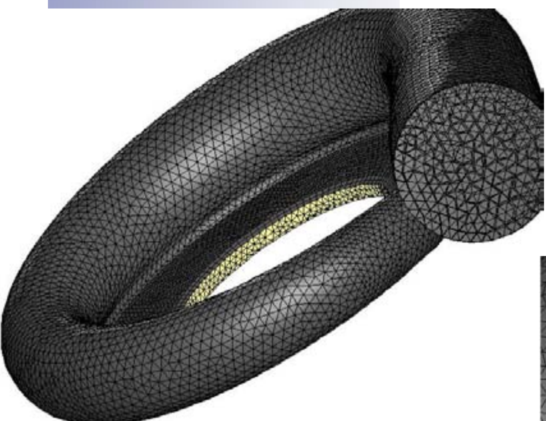

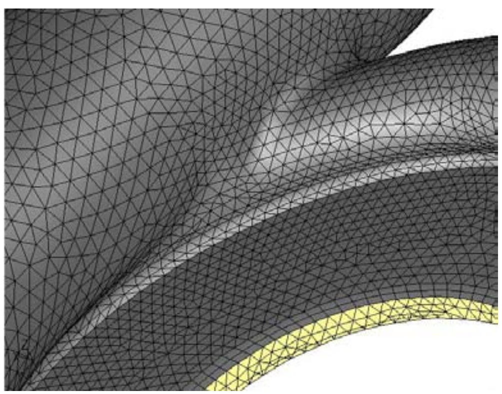

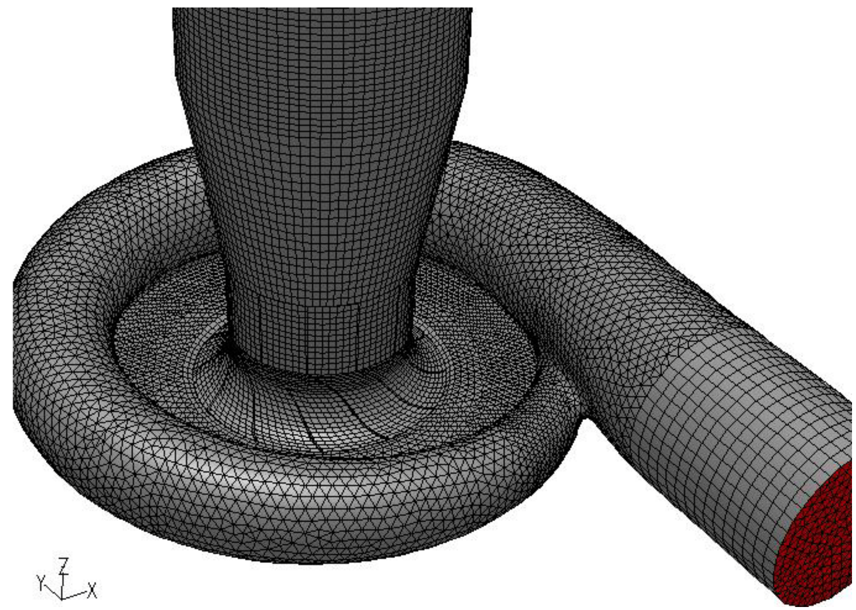

# MESH

- Hybrid HEX / TET mesh.
- Semi-structured mesh for ducts and rotor
- Hex-core mesh for difusser and volute
- Arbitrary interfaces between inlet / rotor and rotor / diffuser
- Semi-automatic adaptative refinement based on velocity gradients

## Mesh independence

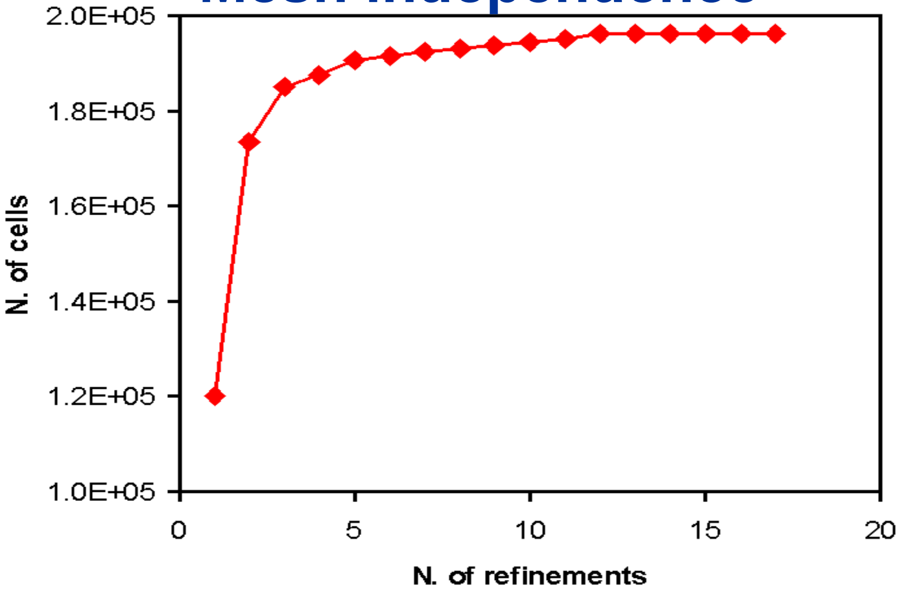

# TURBULENCE MODELLING

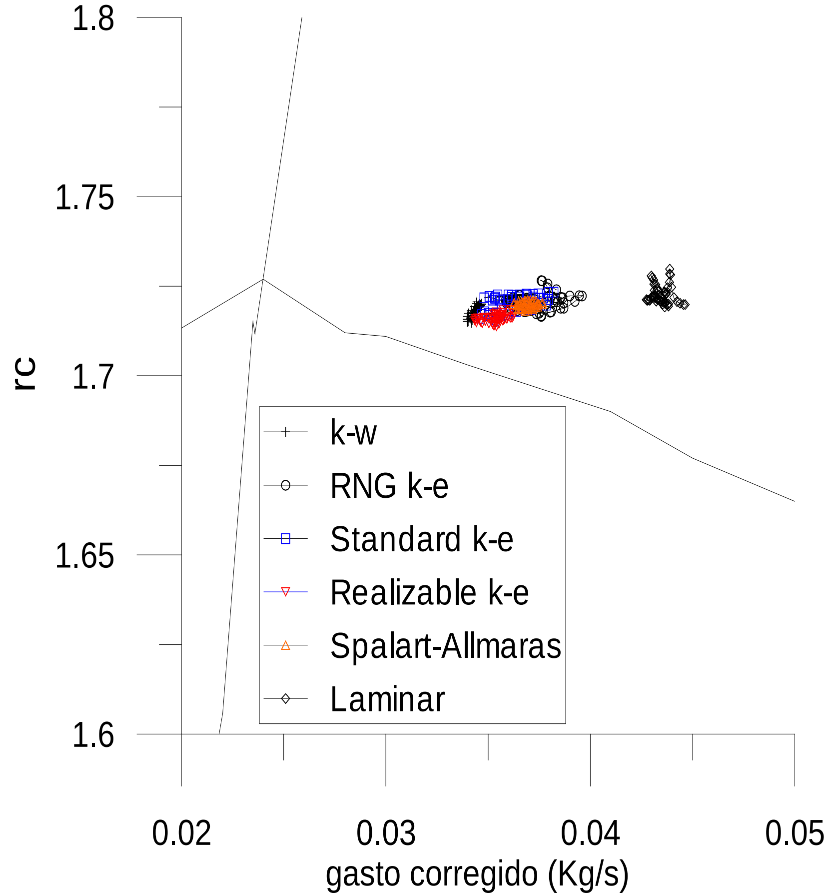

# PARALELLISATION

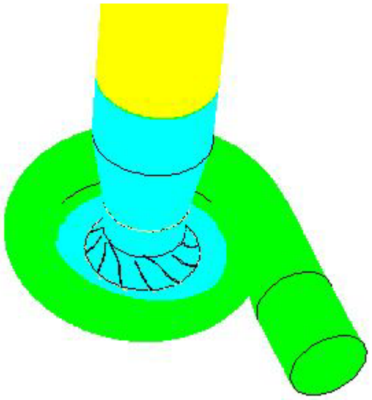

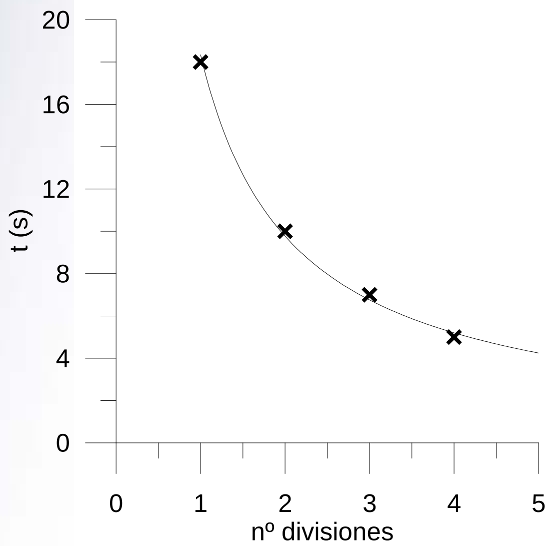


| domains | Cells | Transfer faces | t (s) |
|---|---|---|---|
| 1 | 283050 | 0 | 18 s/subit |
| 2 | 141455 | 850 | 10 s/subit |
| | 141595 | 850 | |
| 3 | 94564 | 810 | 7 s/subit |
| | 94086 | 1701 | |
| | 94400 | 891 | |
| 4 | 71903 | 1774 | 5 s/subit |
| | 76720 | 814 | |
| | 67202 | 1912 | |
| | 67225 | 952 | |

# RESULTS

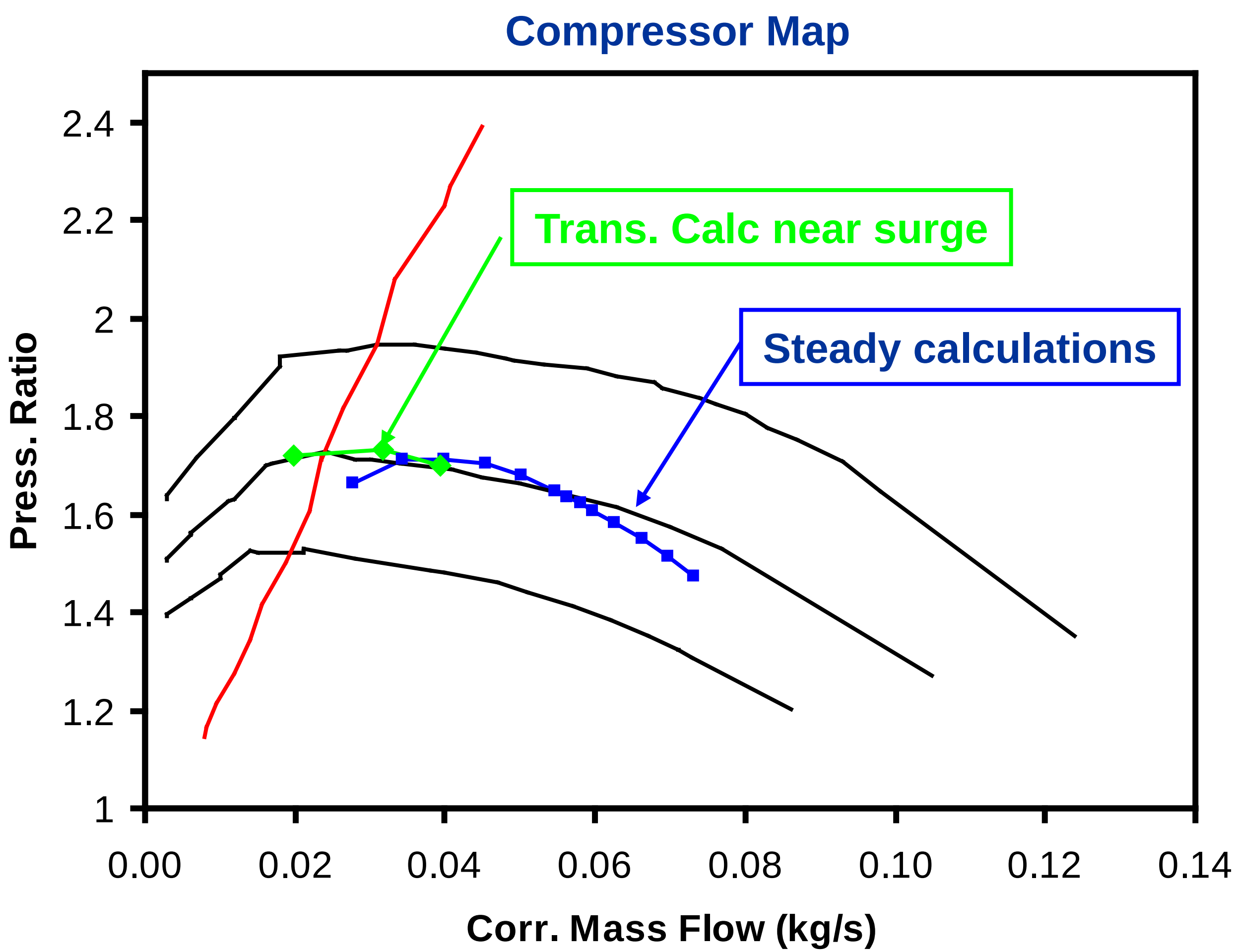
Compressor Map
Trans. Calc near surge
Steady calculations
Press. Ratio
2.4
2.2
2
1.8
1.6
1.4
1.2
1
0.00
0.02
0.04
0.06
0.08
0.10
0.12
0.14
Corr. Mass Flow (kg/s)

# RESULTS

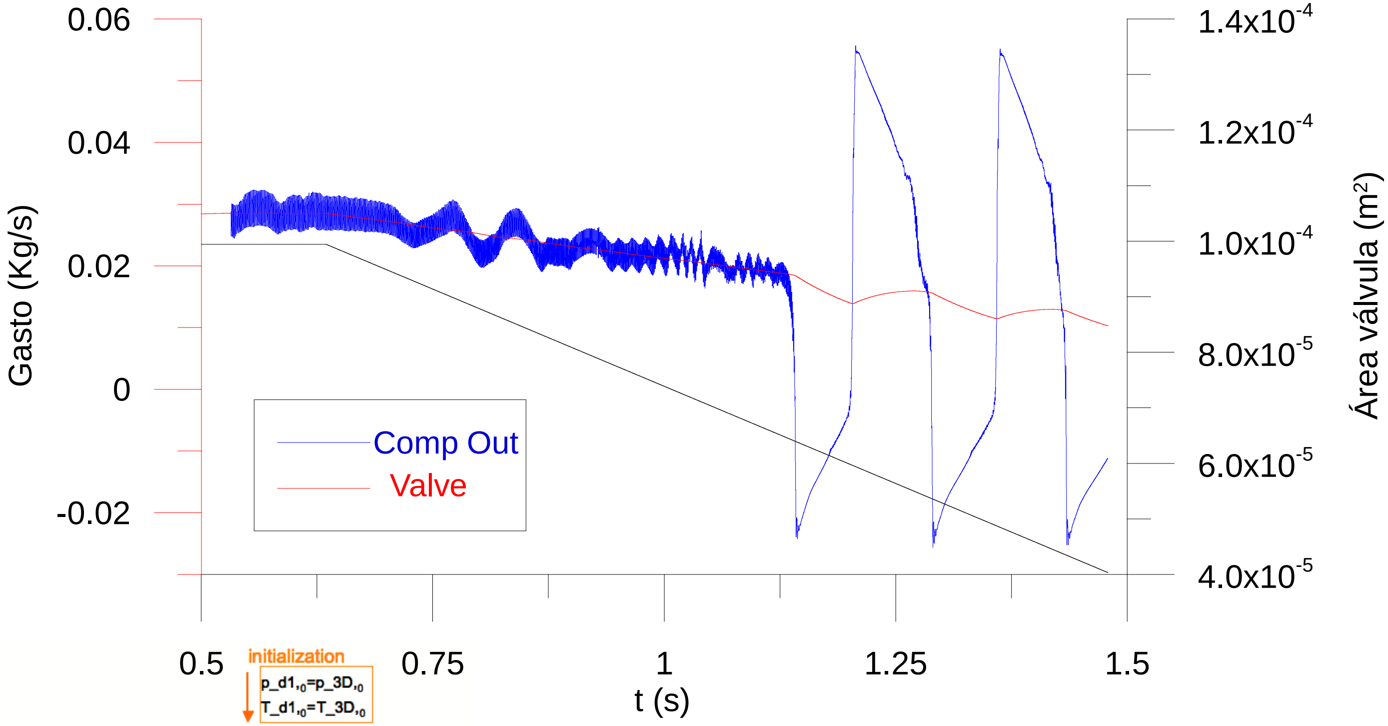
0.06
0.04
0.02
0
-0.02
Gasto (Kg/s)
1.4x10-4
1.2x10-4
1.0x10-4
8.0x10-5
6.0x10-5
4.0x10-5
Área válvula (m2)
Comp Out
Valve
0.5
0.75
1
1.25
1.5
t (s)

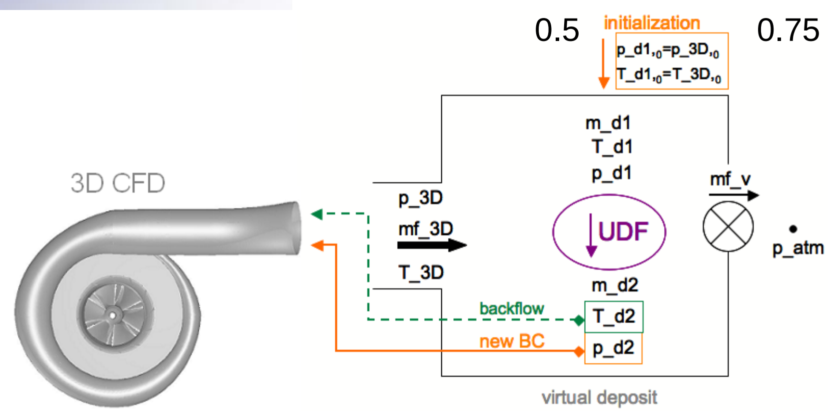
initialization
p_d1,0=p_3D,0
T_d1,0=T_3D,0
m_d1
T_d1
p_d1
mf_v
3D CFD
p_3D
mf_3D
T_3D
UDF
p_atm
m_d2
backflow
T_d2
new BC
p_d2
virtual deposit

# RESULTS

First surge cycle

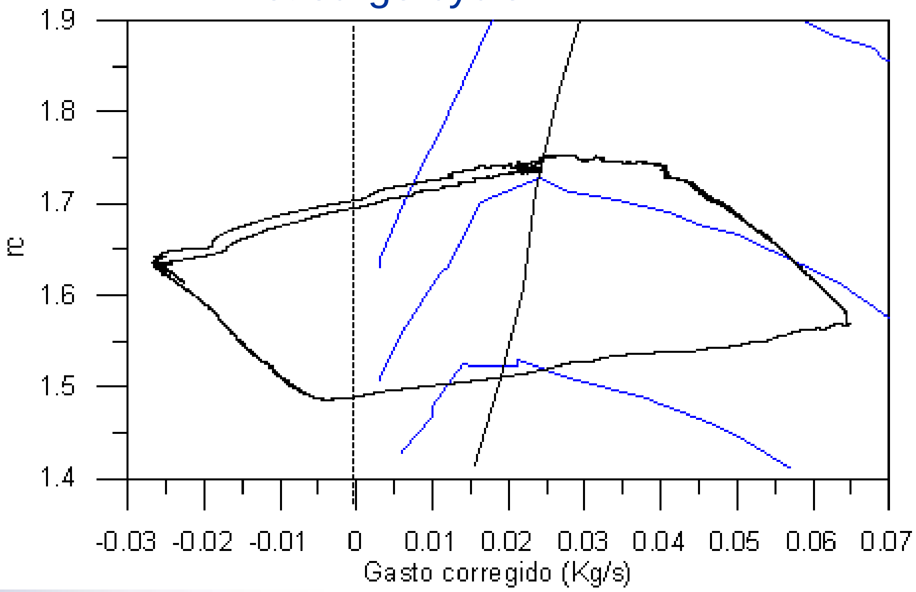


First & second surge cycle

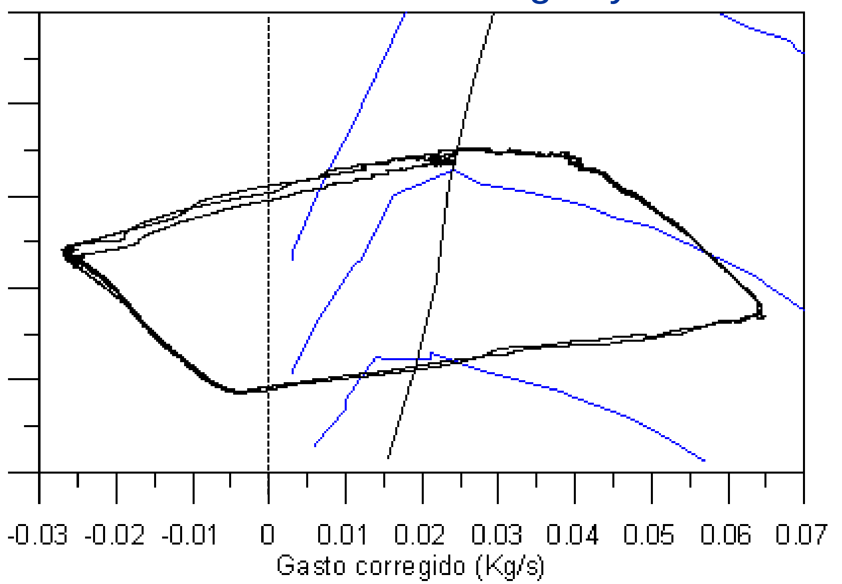

# RESULTS

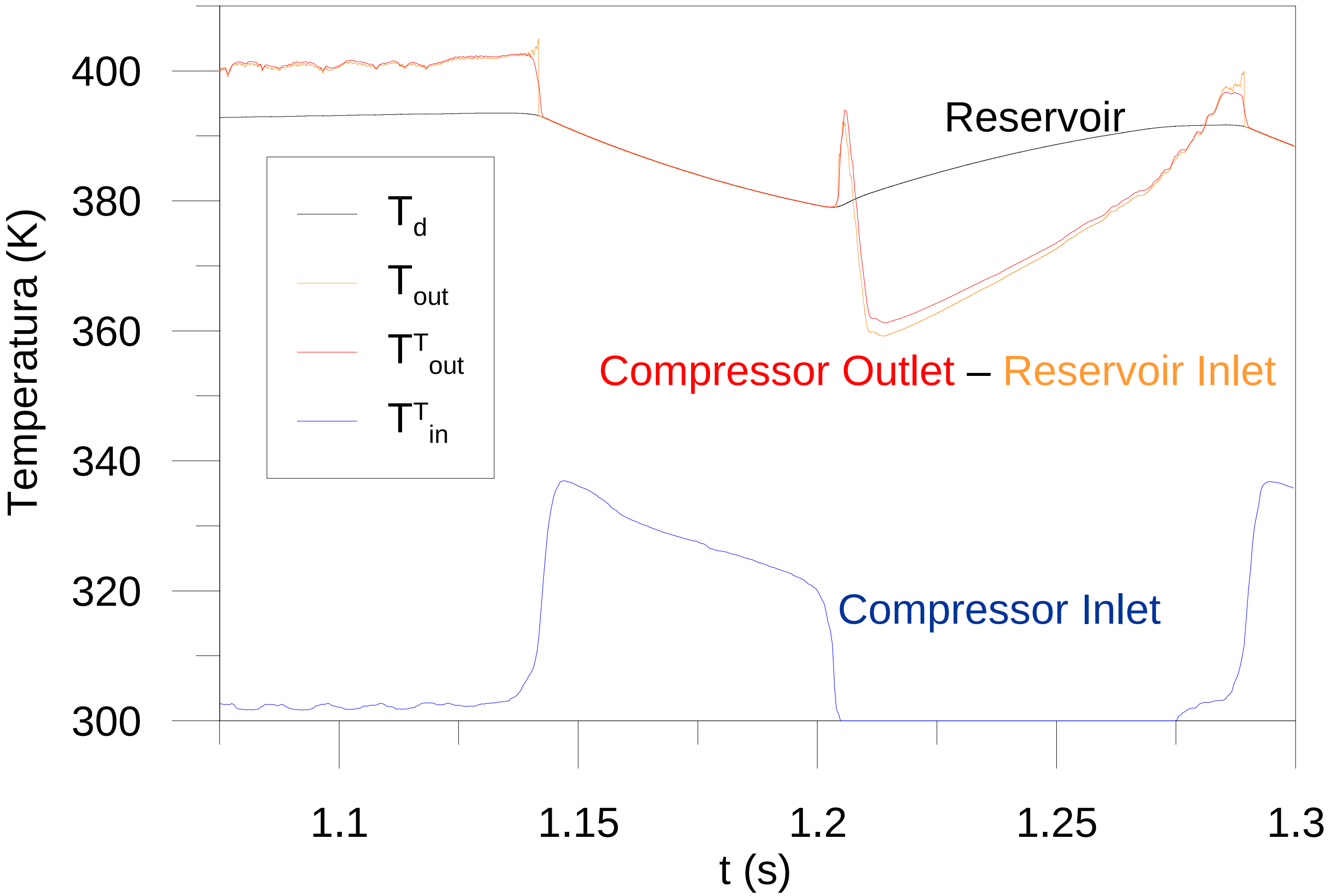
Temperatura (K)
400
380
360
340
320
300
1.1
1.15
1.2
1.25
1.3
t (s)
$T_d$
$T_{out}$
$T^T_{out}$
$T^T_{in}$
Reservoir
Compressor Outlet – Reservoir Inlet
Compressor Inlet

# RESULTS


Axial velocity
1.00e+02
9.00e+01
8.00e+01
7.00e+01
6.00e+01
5.00e+01
4.00e+01
3.00e+01
2.00e+01
1.00e+01
0.00e+00
-1.00e+01
-2.00e+01
-3.00e+01
-4.00e+01
-5.00e+01
-6.00e+01
-7.00e+01
-8.00e+01
-9.00e+01
-1.00e+02

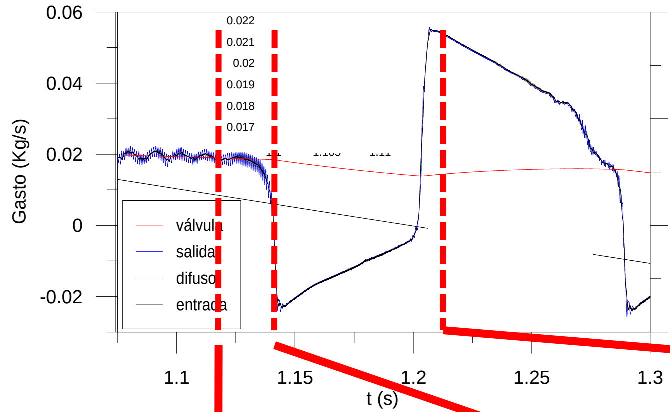
0.06
0.04
0.02
0
-0.02
Gasto (Kg/s)
1.1
1.15
1.2
1.25
1.3
t (s)
0.022
0.021
0.02
0.019
0.018
0.017
válvula
salida
difuso
entrada

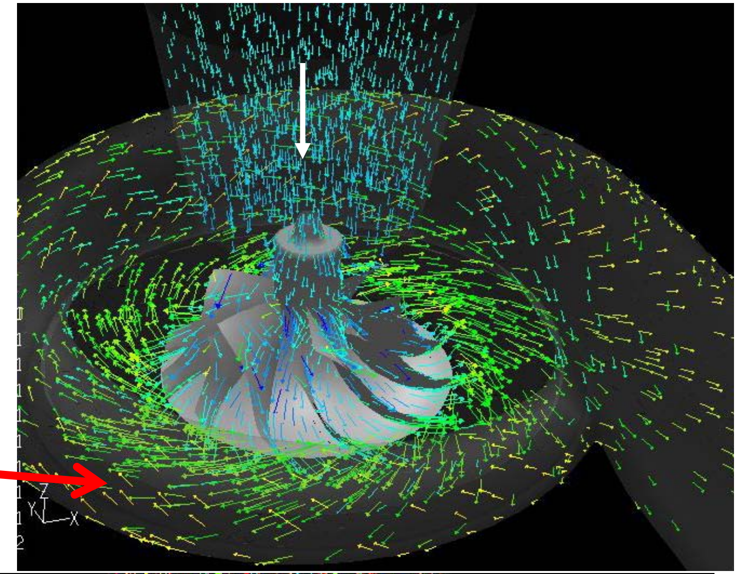

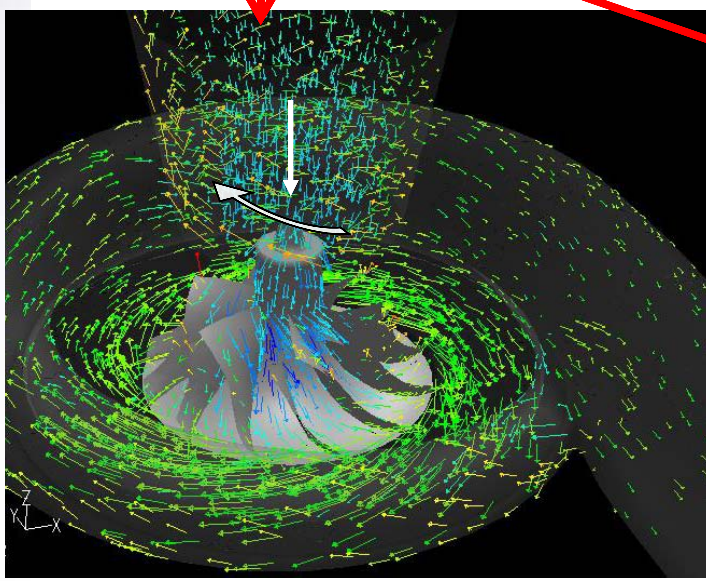

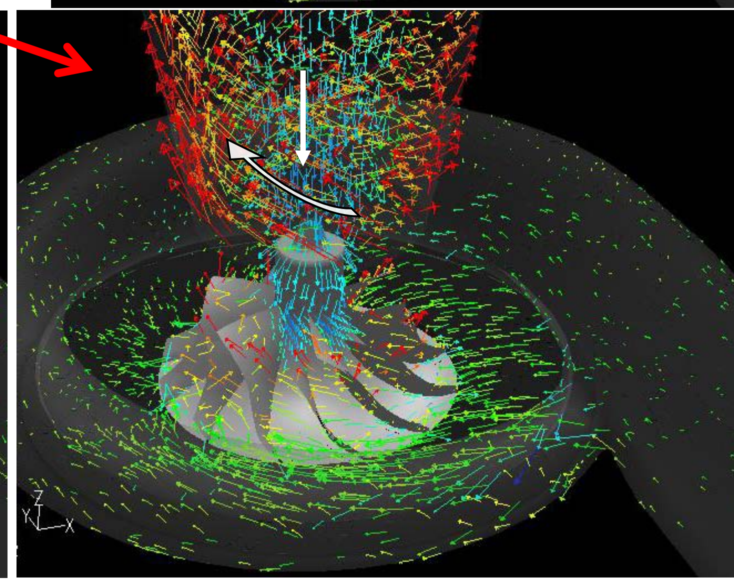

UNIVERSIDAD POLITECNICA DE VALENCIA

motores térmicos

# RESULTS

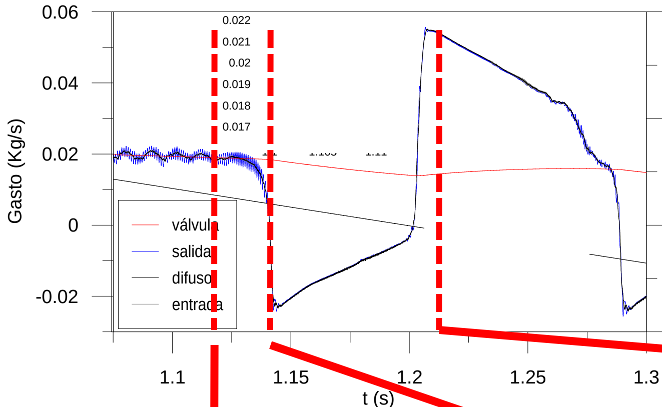


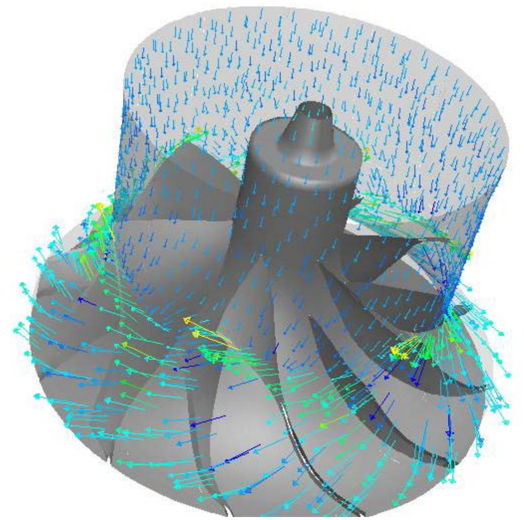

Axial velocity

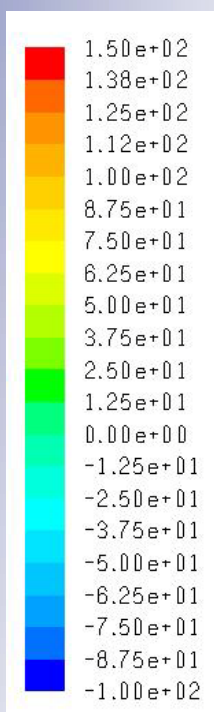


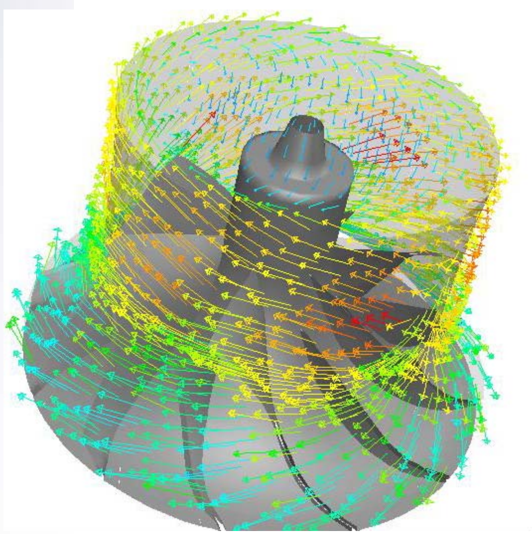

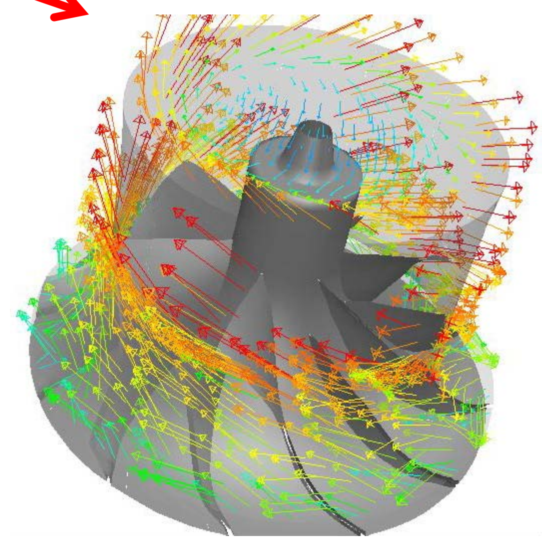

# RESULTS

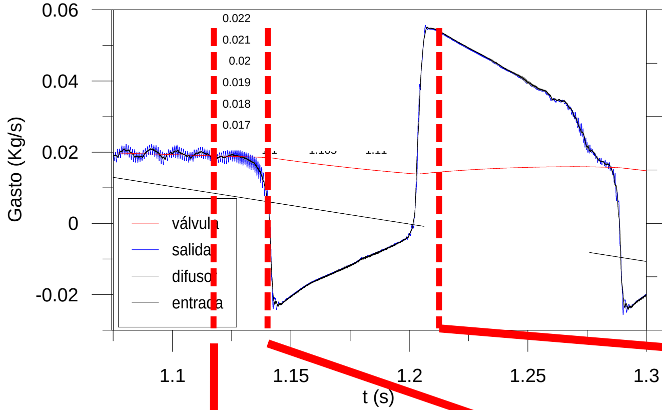


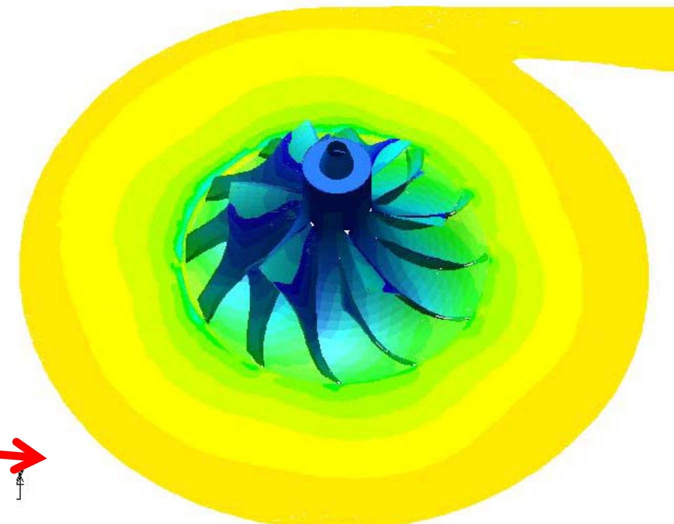

## Static Pressure

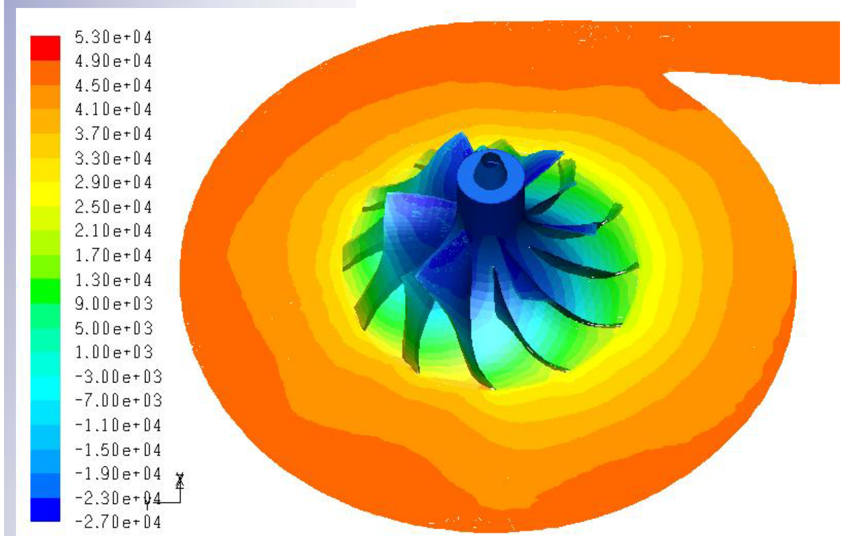


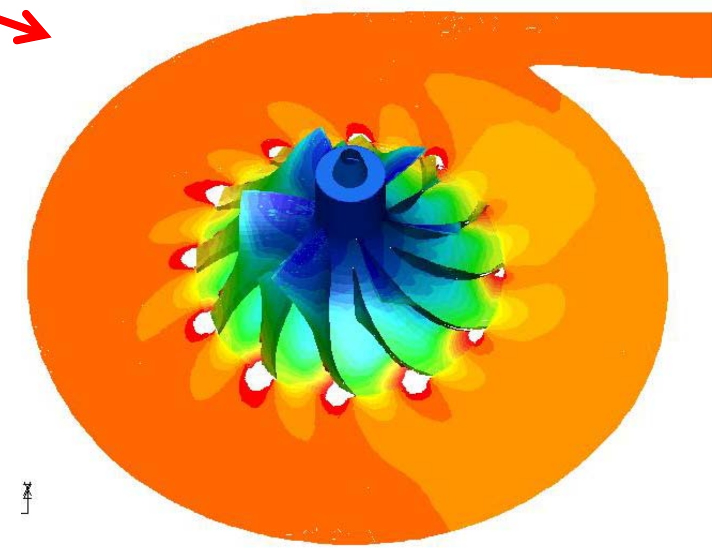

# RESULTS

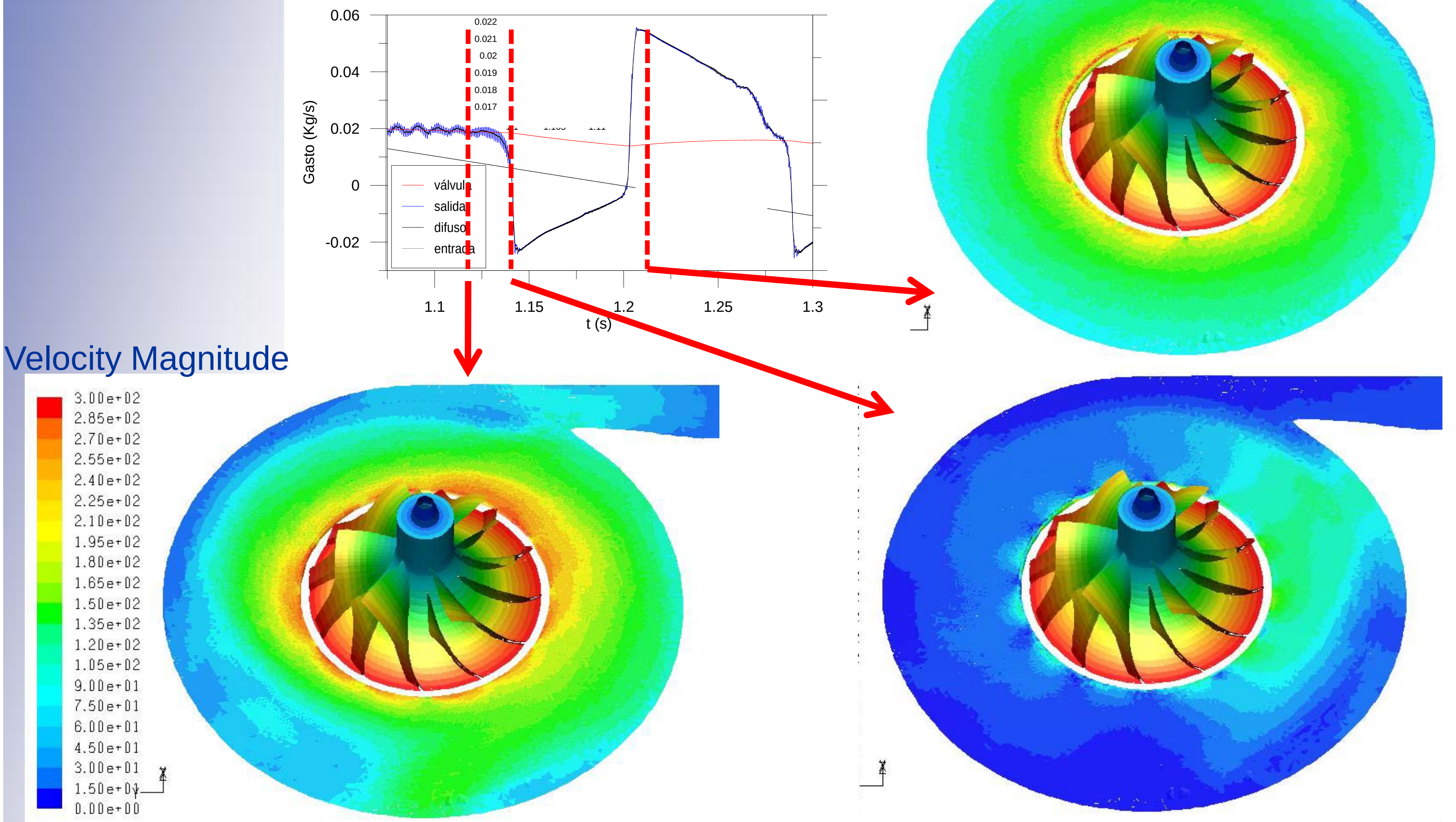
Velocity Magnitude
0.06
0.04
0.02
0
-0.02
Gasto (Kg/s)
0.022
0.021
0.02
0.019
0.018
0.017
válvula
salida
difuso
entrada
1.1
1.15
1.2
1.25
1.3
t (s)
3.00e+02
2.85e+02
2.70e+02
2.55e+02
2.40e+02
2.25e+02
2.10e+02
1.95e+02
1.80e+02
1.65e+02
1.50e+02
1.35e+02
1.20e+02
1.05e+02
9.00e+01
7.50e+01
6.00e+01
4.50e+01
3.00e+01
1.50e+01
0.00e+00

# RESULTS

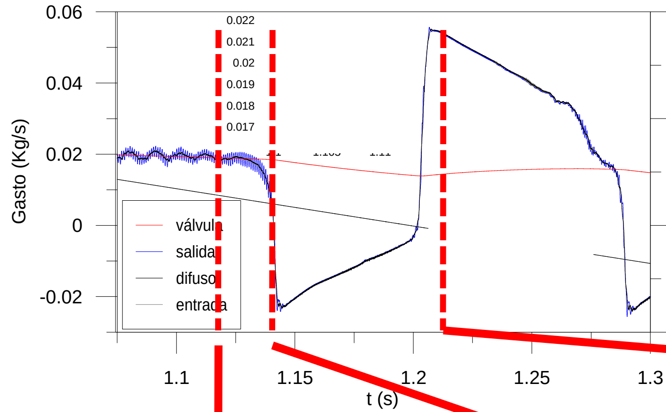


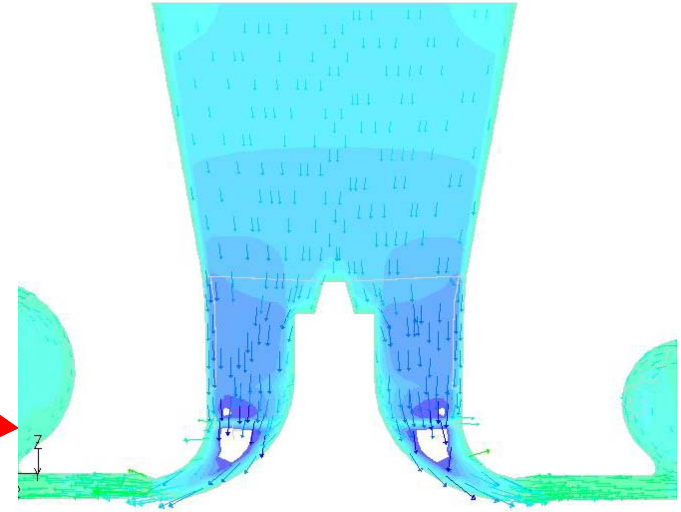

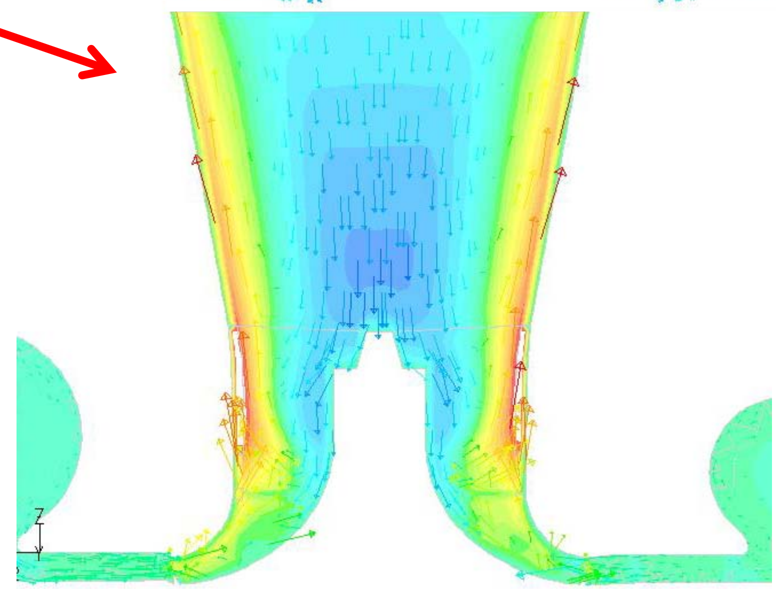

Axial Velocity

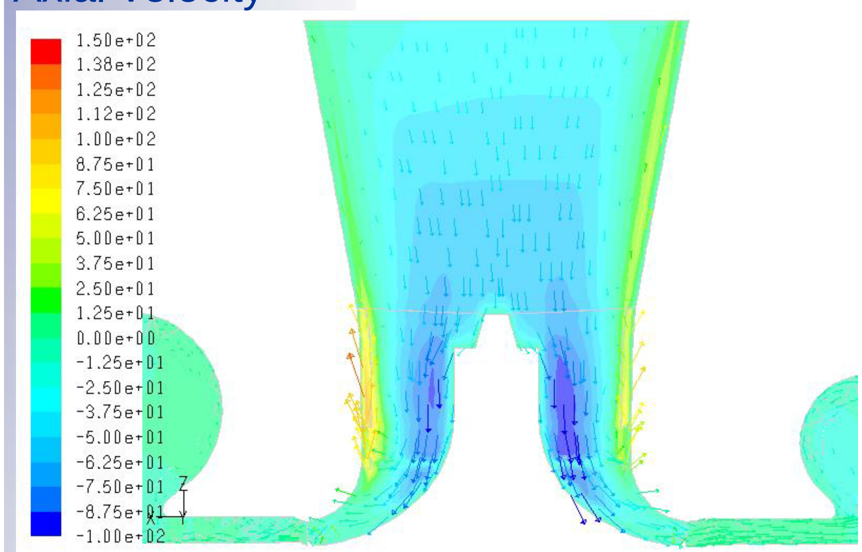

# RESULTS

Temperature

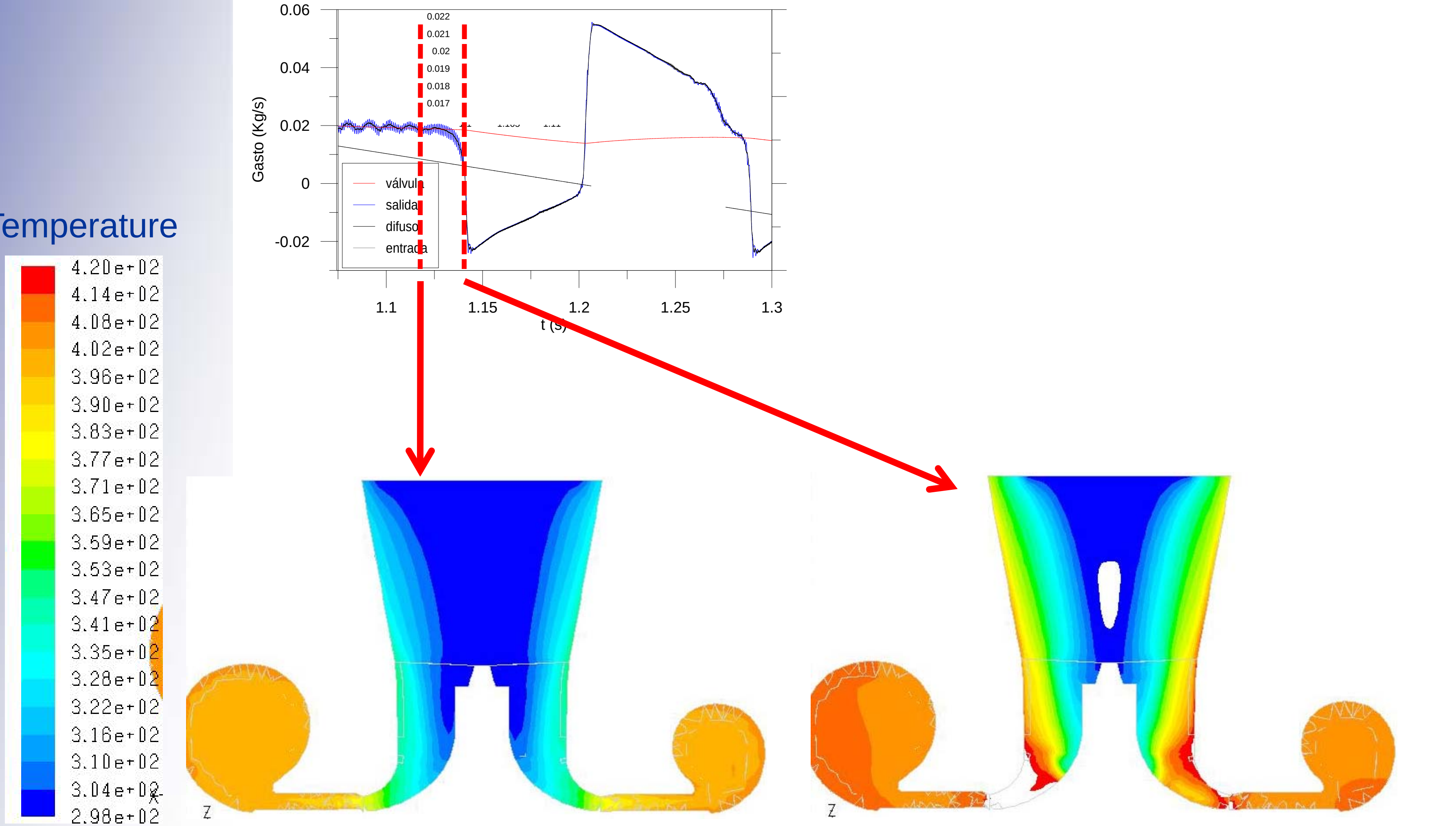

# GEOMETRY ANALYSIS

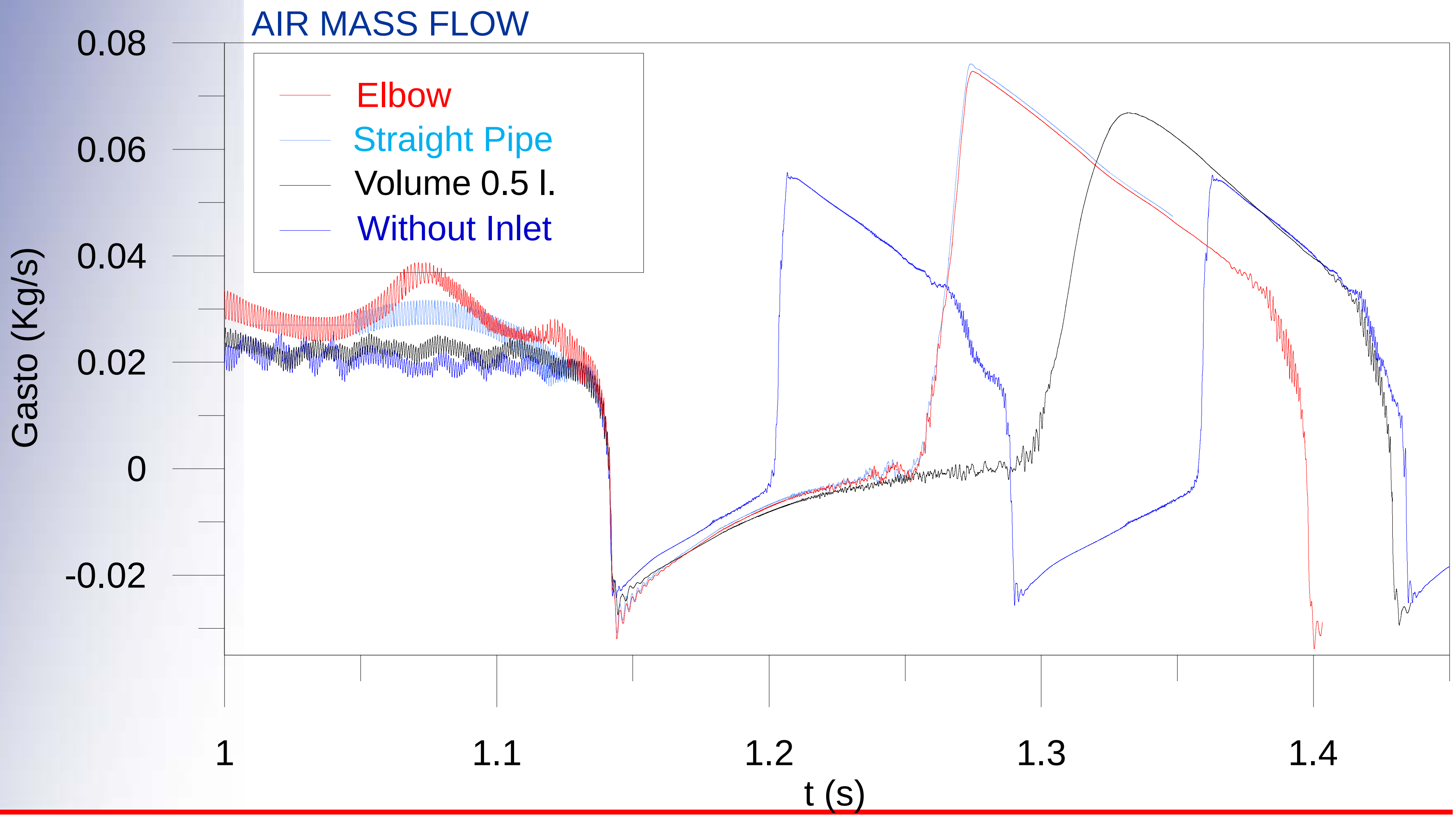

# GEOMETRY ANALYSIS

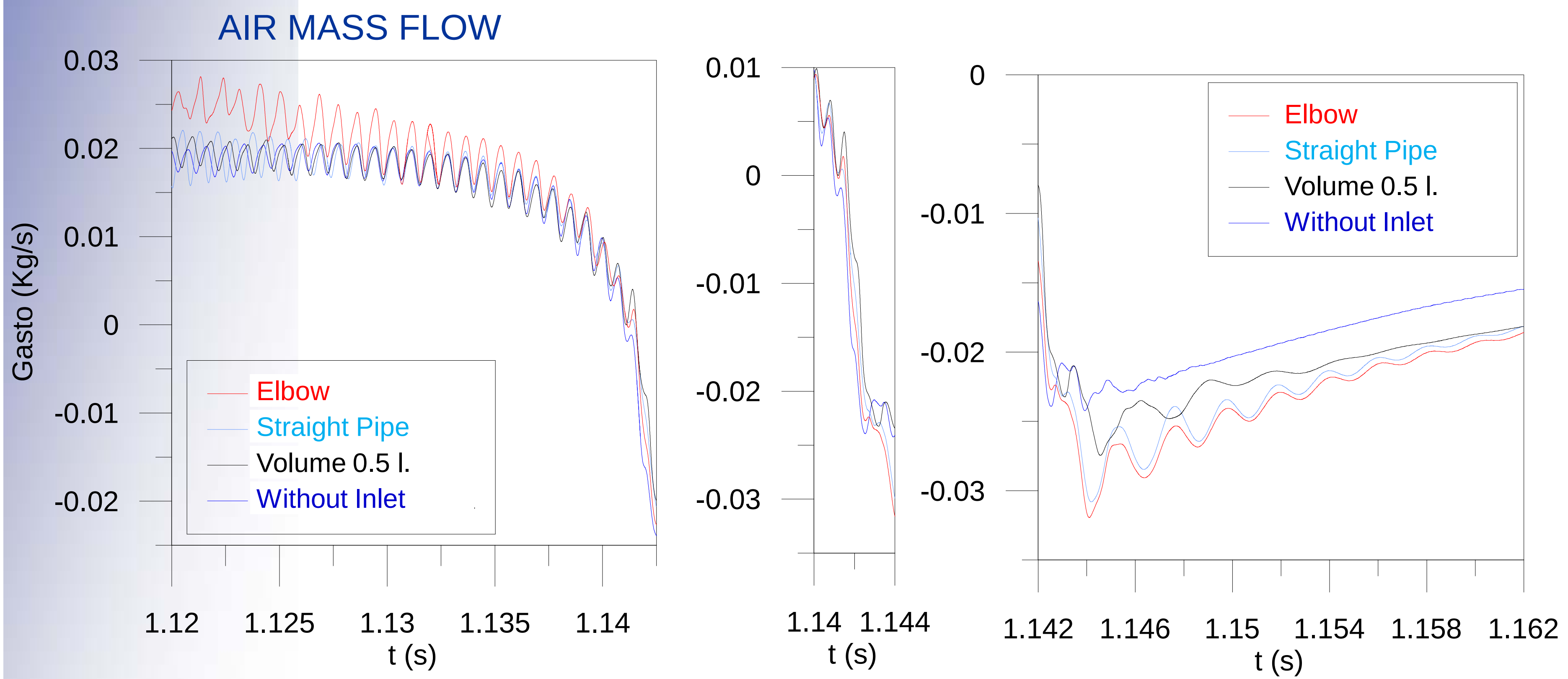

# GEOMETRY ANALYSIS

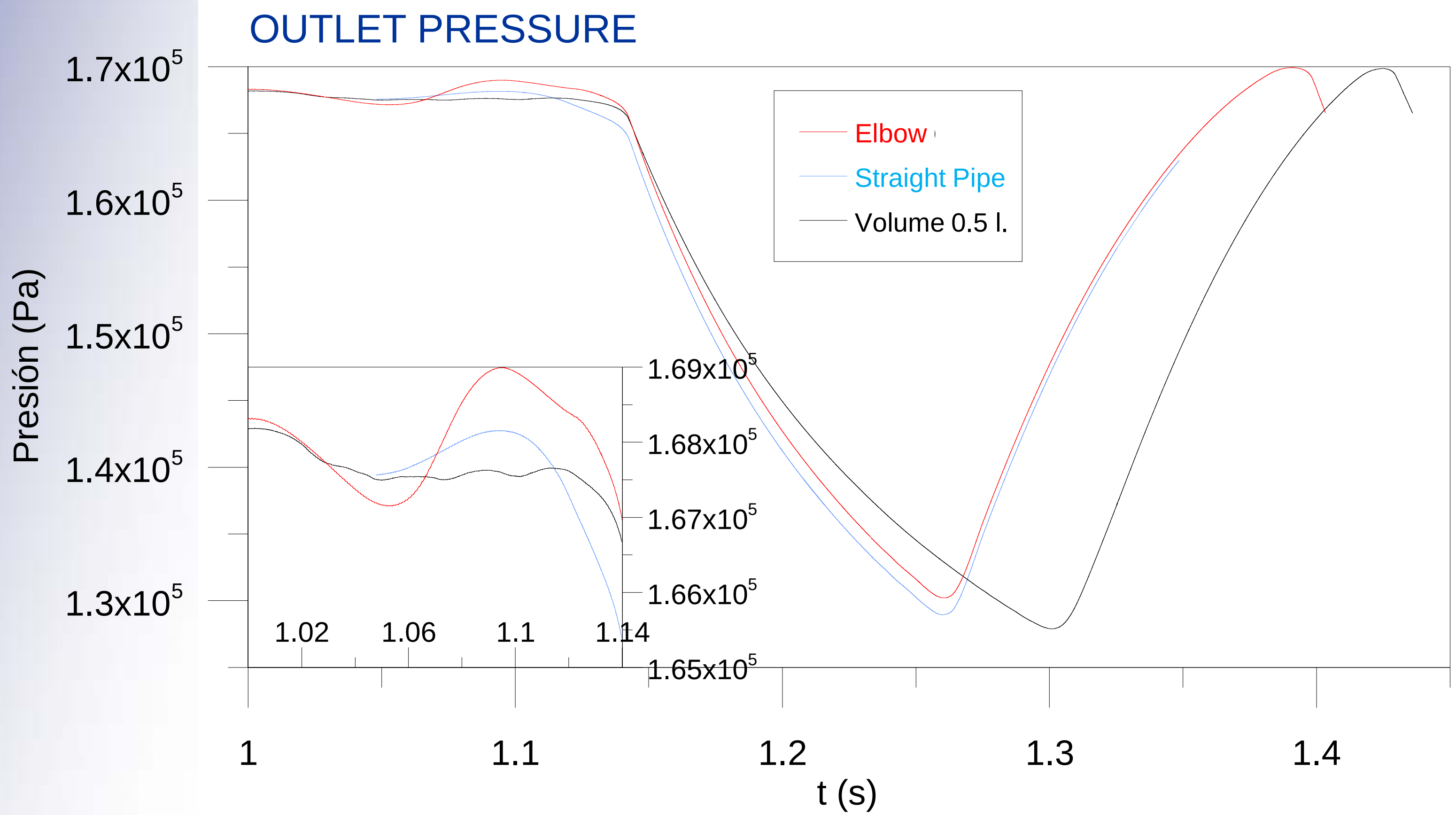

# GEOMETRY ANALYSIS

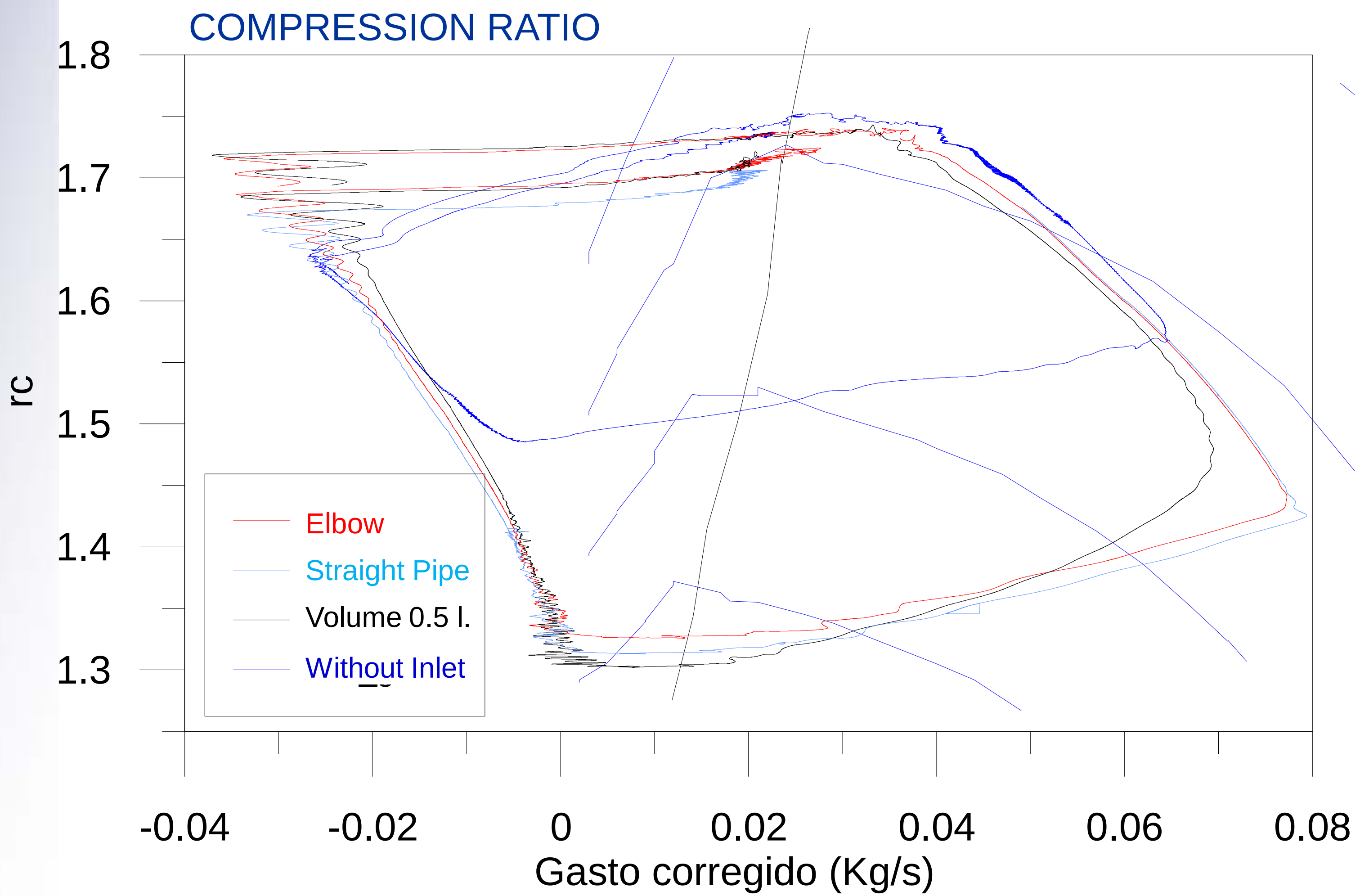

# GEOMETRY ANALYSIS

Axial velocity

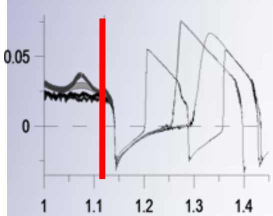


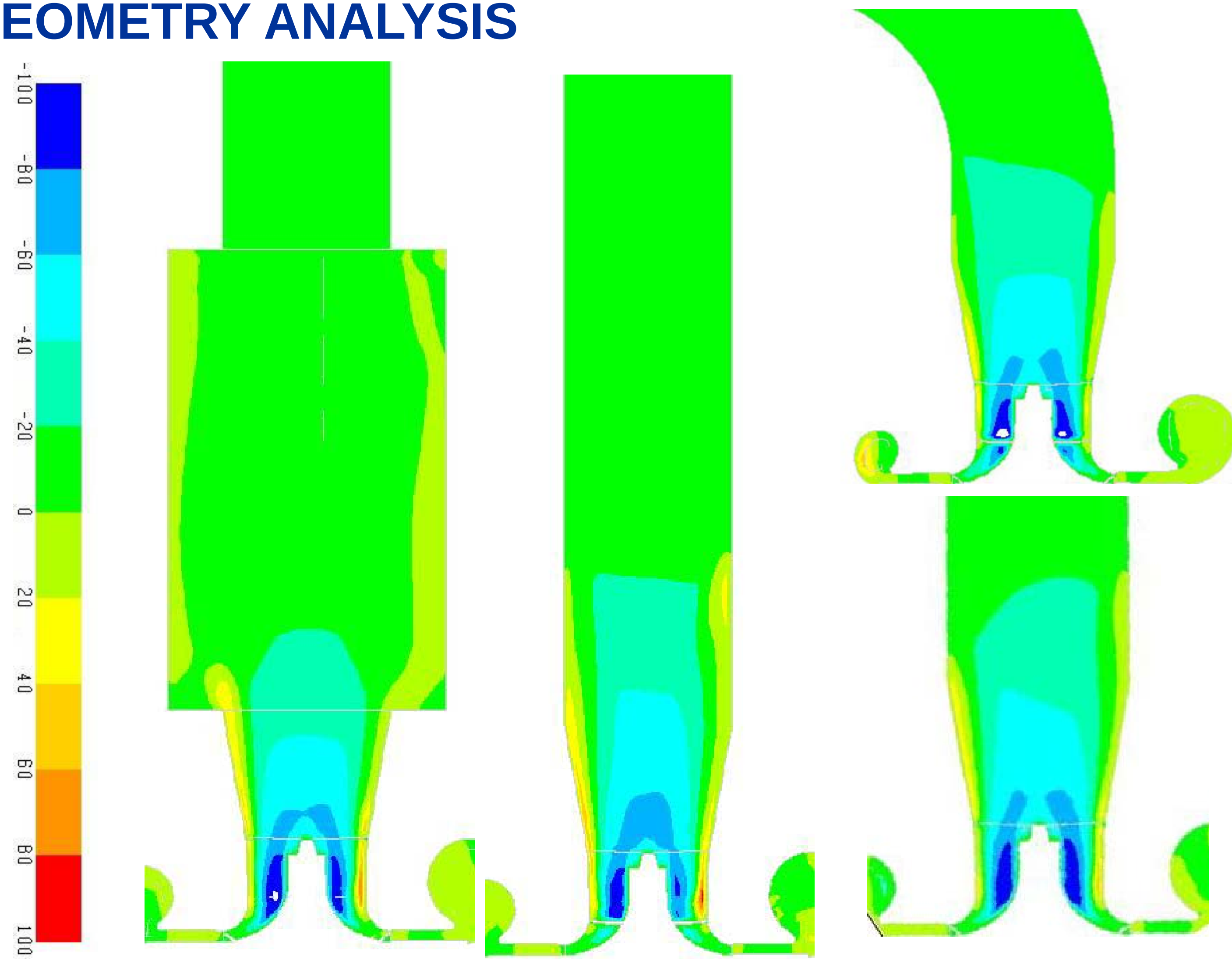

# GEOMETRY ANALYSIS

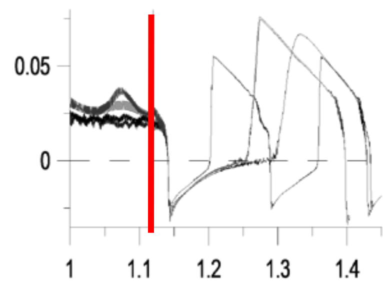


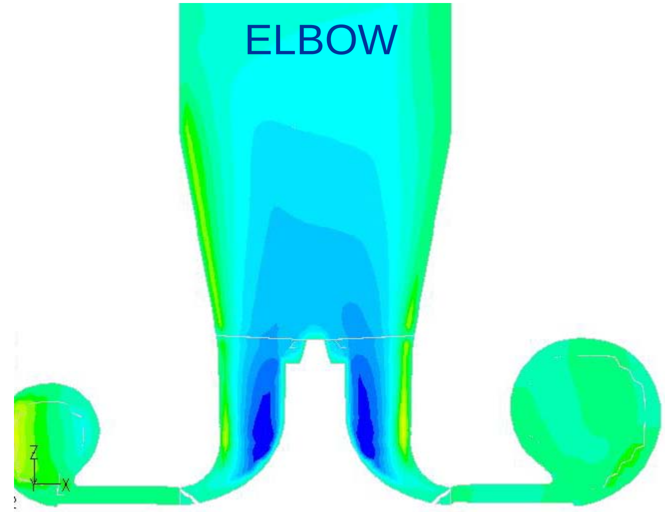


Axial velocity

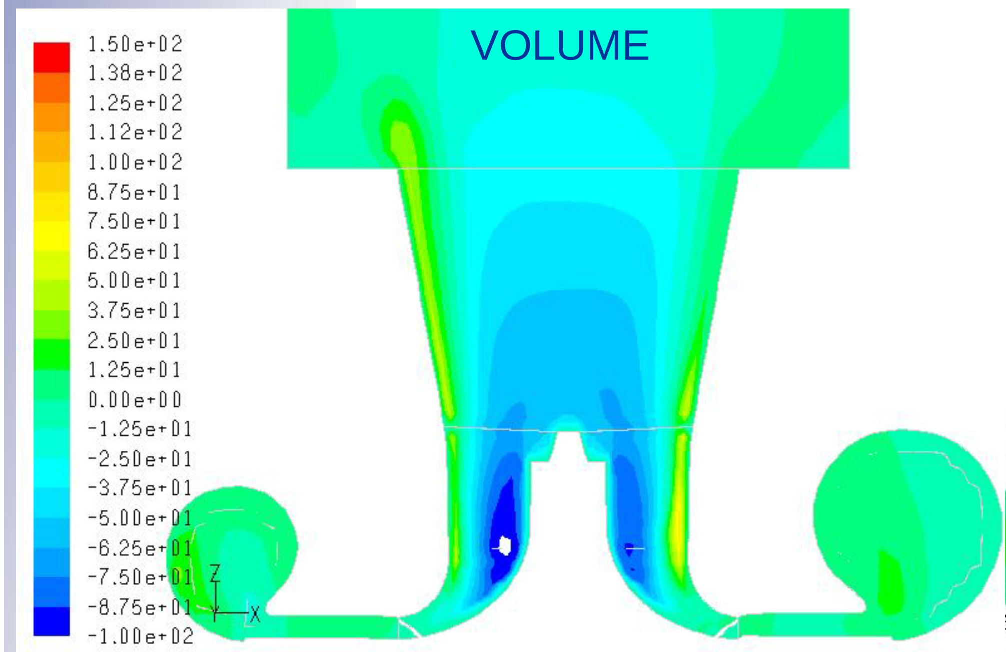


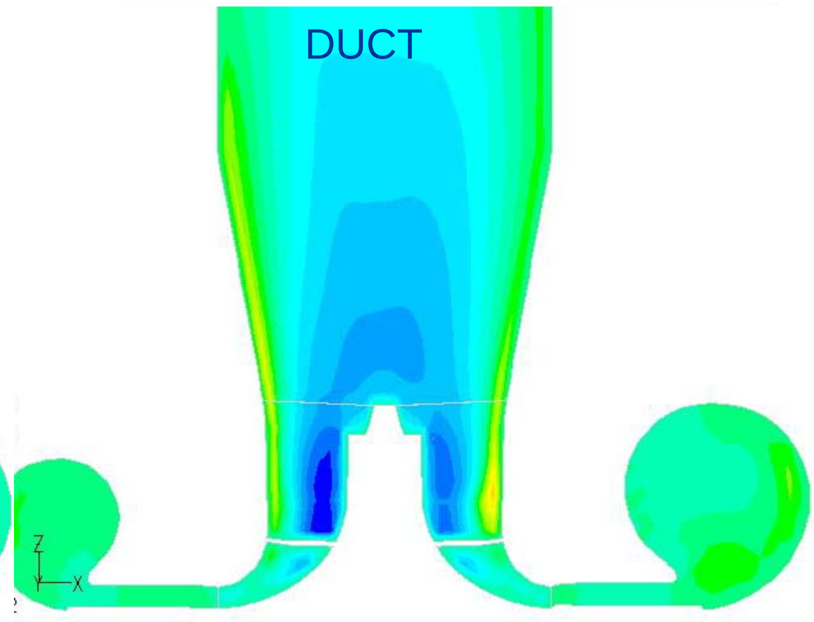

# GEOMETRY ANALYSIS

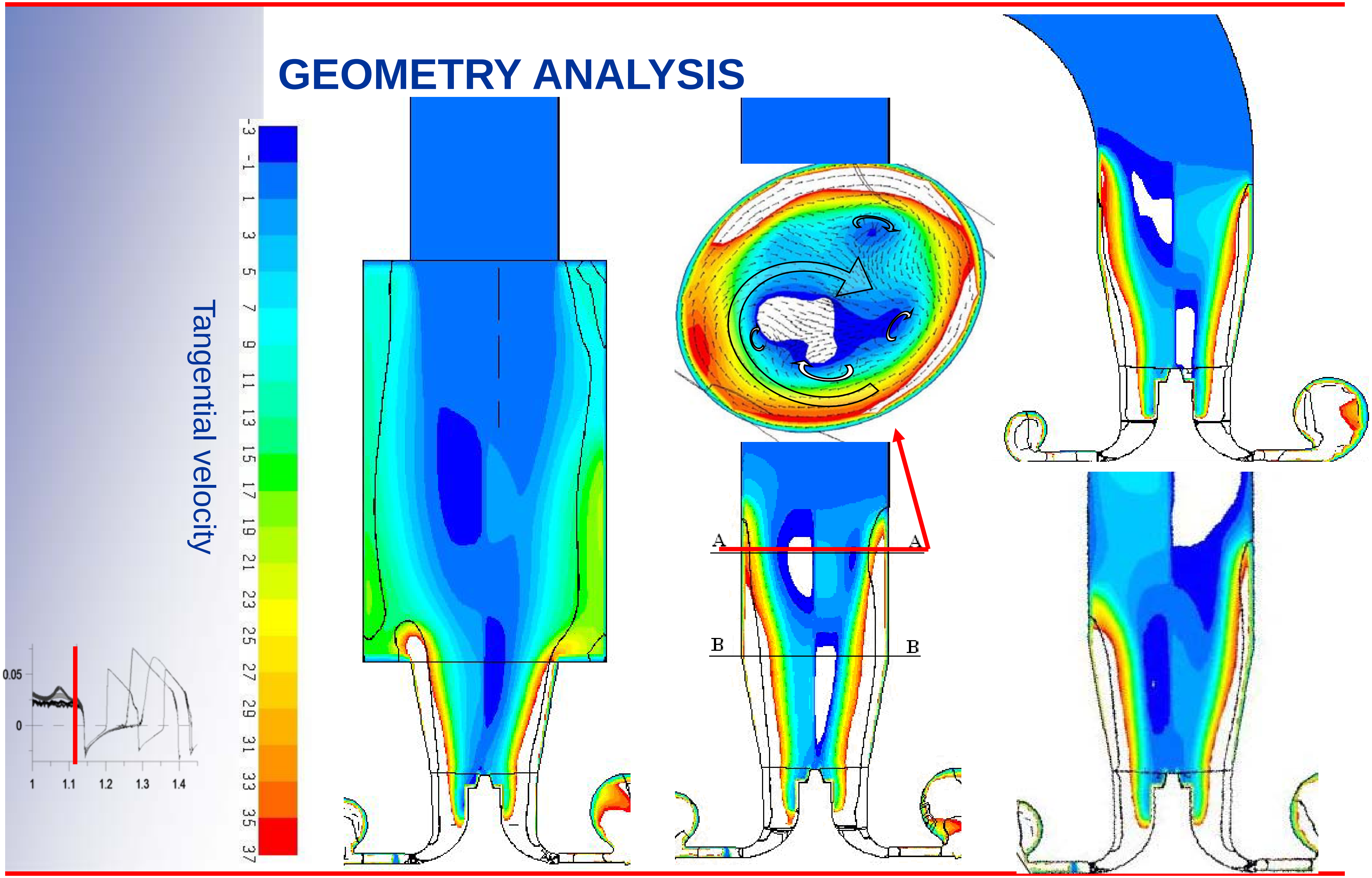

# GEOMETRY ANALYSIS

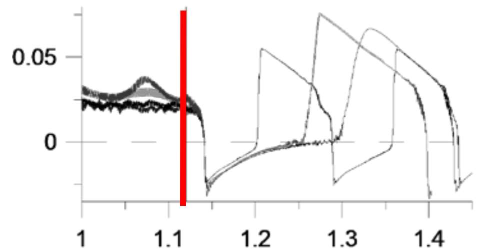


ELBOW

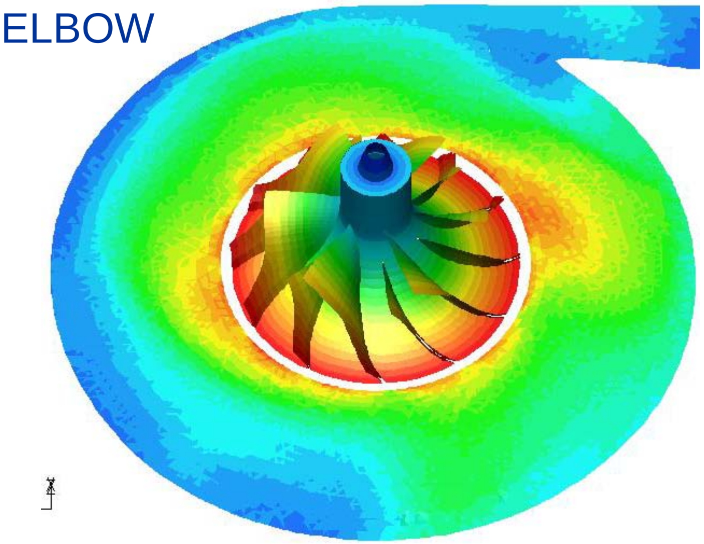

Velocity Magnitude

VOLUME

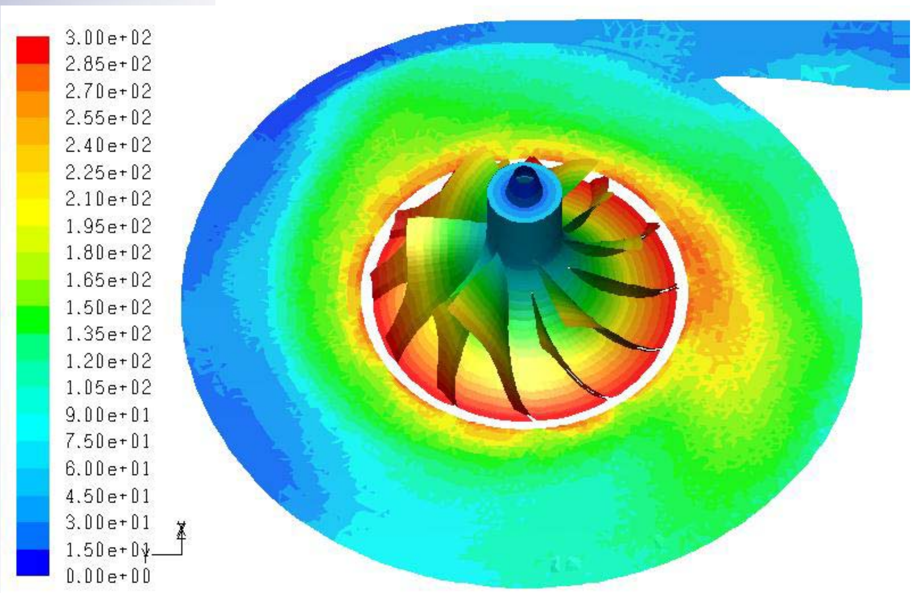


DUCT

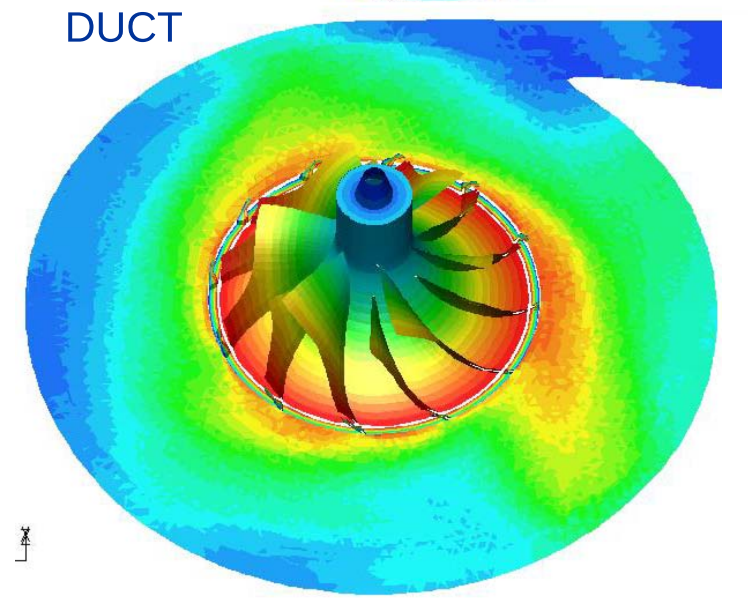

# GEOMETRY ANALYSIS

Static Pressure

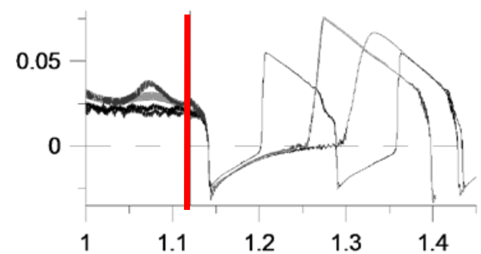


ELBOW

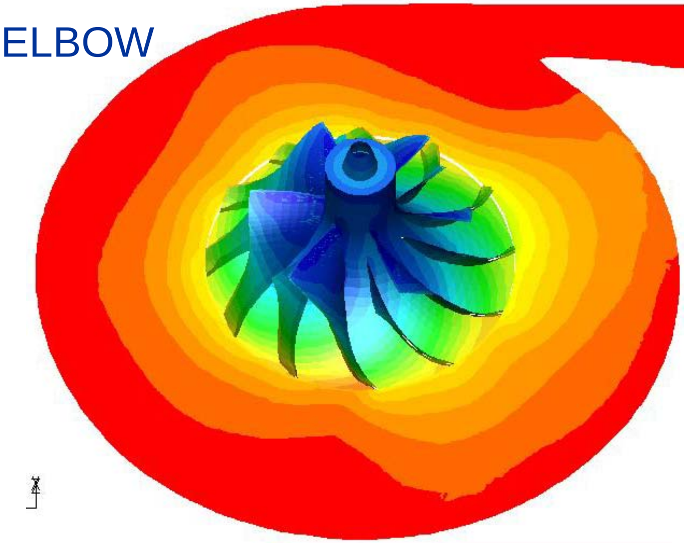

VOLUME

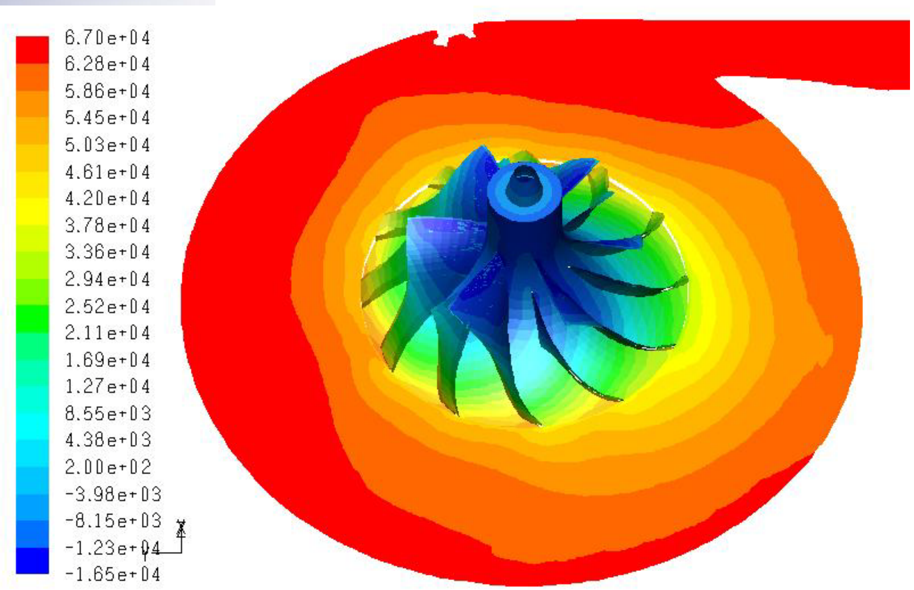


DUCT

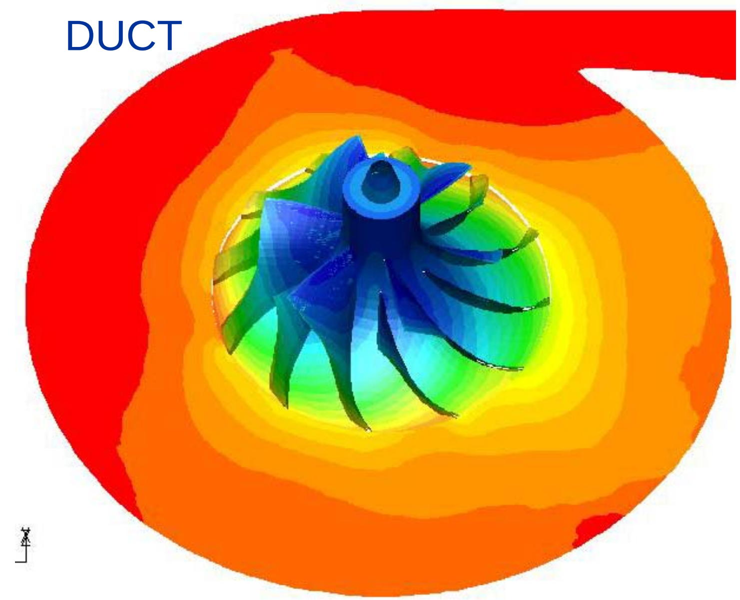

# GEOMETRY ANALYSIS

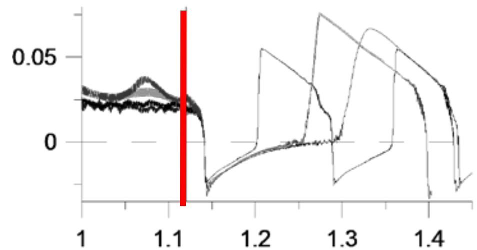


ELBOW

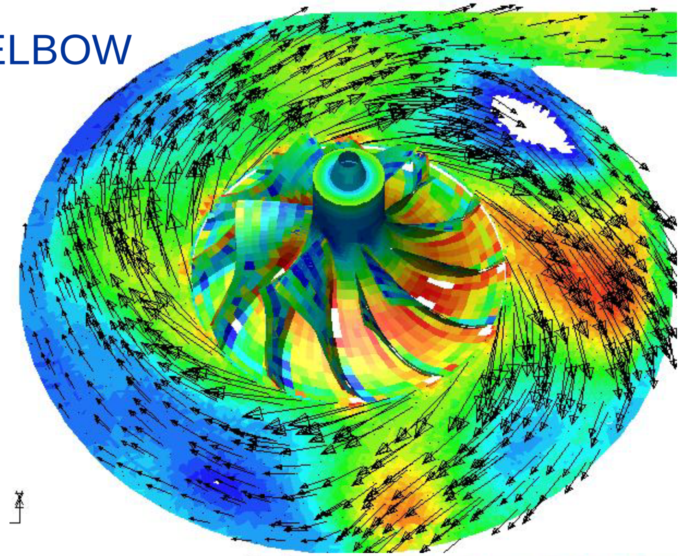

Radial Velocity

VOLUME

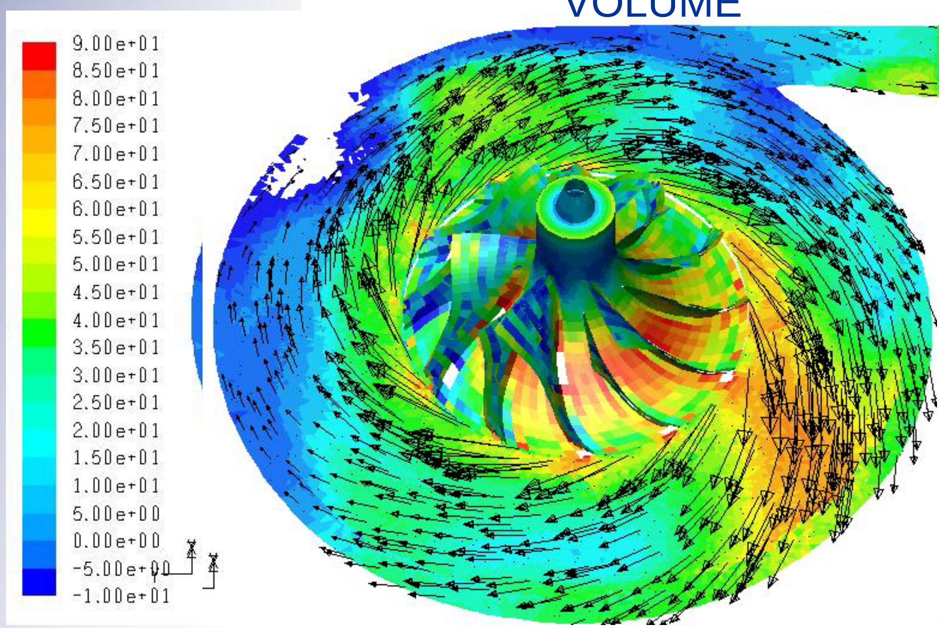


DUCT

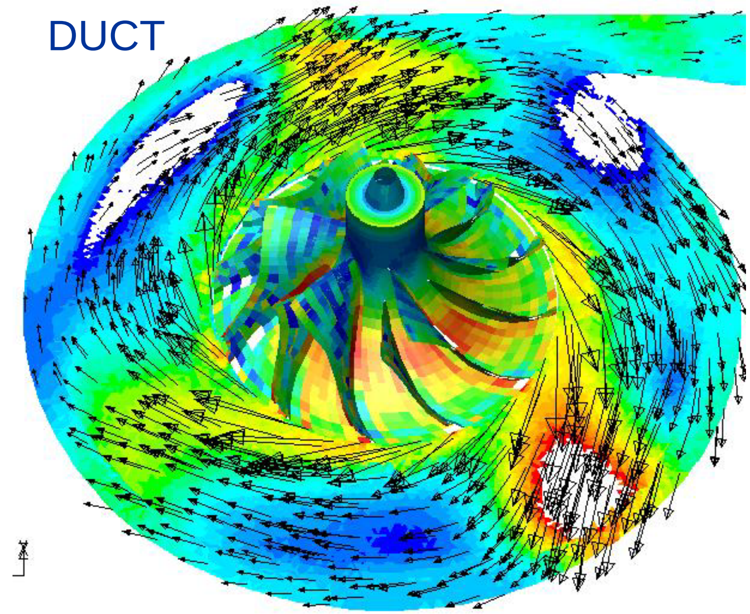

# GEOMETRY ANALYSIS

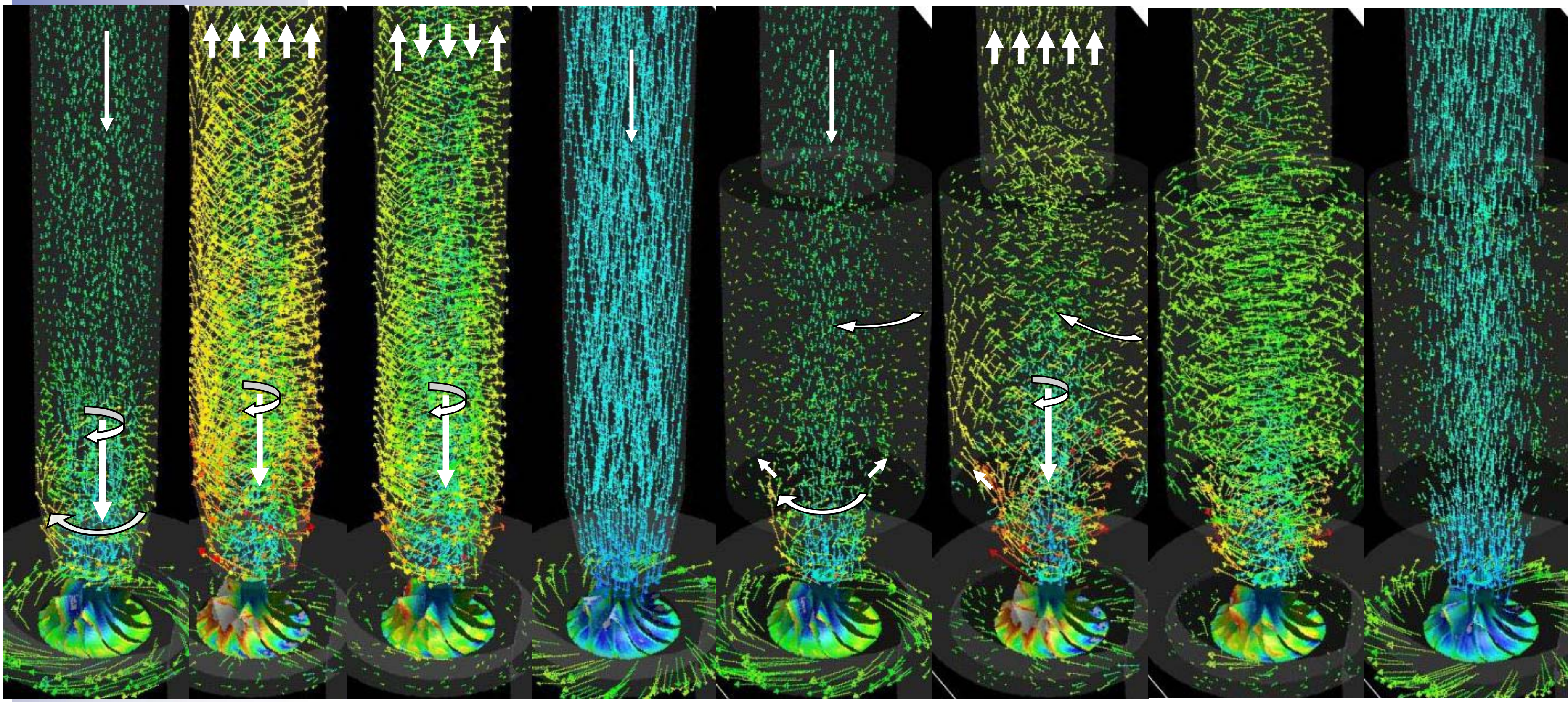

t = 1.12 s | ($\dot{m}$ $_{neg}$ max) | $\dot{m}$ = -0.0035 Kg/s | ($\dot{m}$ $_{pos}$ max) | t = 1.12 s | ($\dot{m}$ $_{neg}$ max) | $\dot{m}$ = -0.0035 Kg/s | ($\dot{m}$ $_{pos}$ max)

## Summary

- The calculation of the surge cycle leads to quite correct mean values
- The mesh is too coarse to lead to correct local velocity fields. However, it give an insight on how the inlet geometry may affect the flow at the wheel inlet

GEOMETRY ANALYSIS

- Quantitatively, it is difficult to predict surge margin for each geometry ↔ Longer calculations are needed with a finer mesh
- Qualitatively, CFD calculations may show why the volume upstream may improve surge margin: *the swirling hot backflow is directed towards the outer diameter and the interaction with the inlet flow is lower*
- However, a finer mesh would lead to a more accurate velocity field

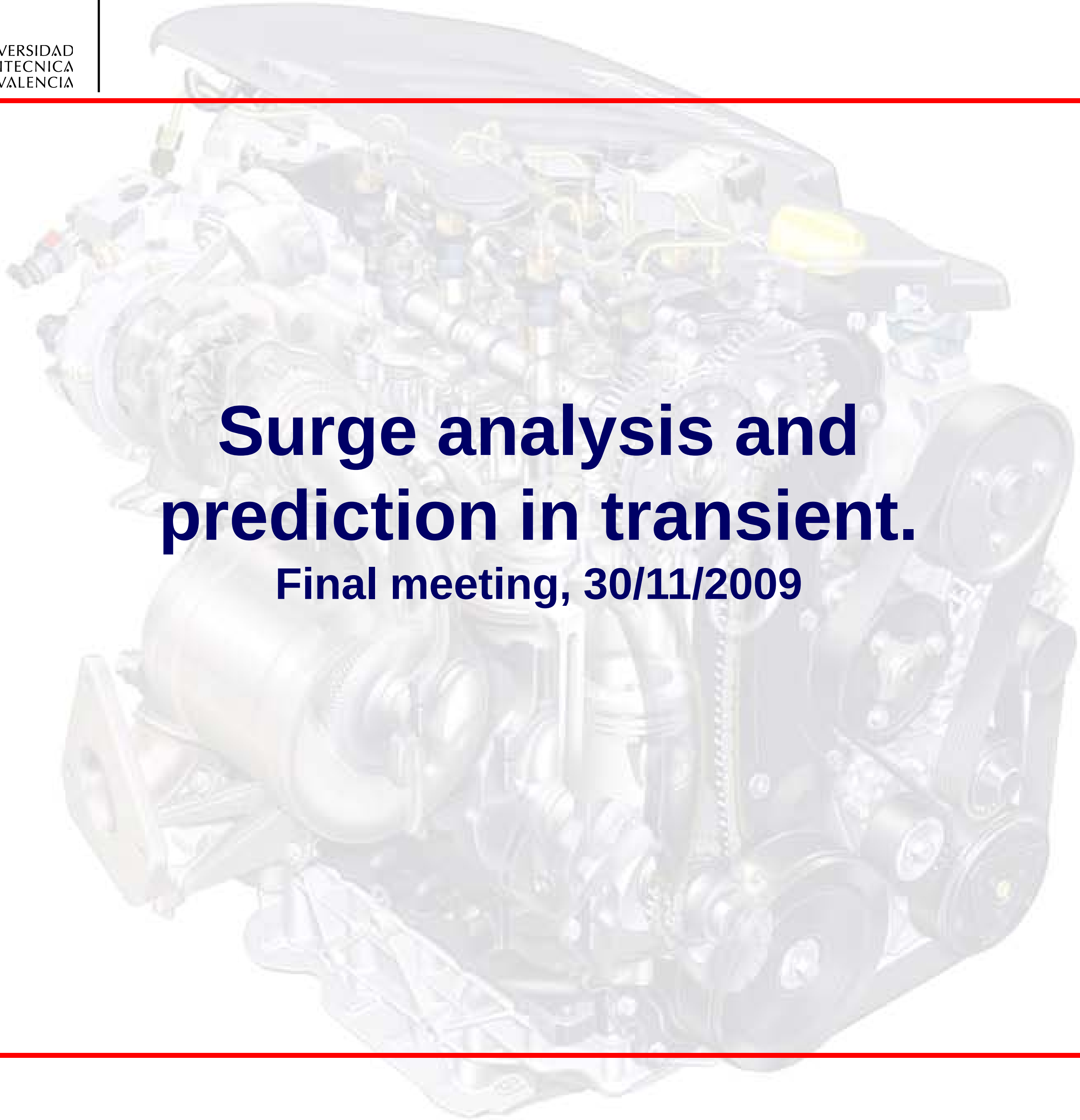

# Surge analysis and prediction in transient.

**Final meeting, 30/11/2009**

# Contents

- Introduction
  - Background and objectives
- Experimental procedure
  - Steady tests
  - Transient tests
- Experimental Results
- Modeling
- Discussion

# Introduction: Background

- In a previous project a non-steady compressor model was proposed able to predict surge under steady and pulsating conditions
- An experimental test study in a pulsating gas stand showed that pulsating flow may increase the steady surge margin

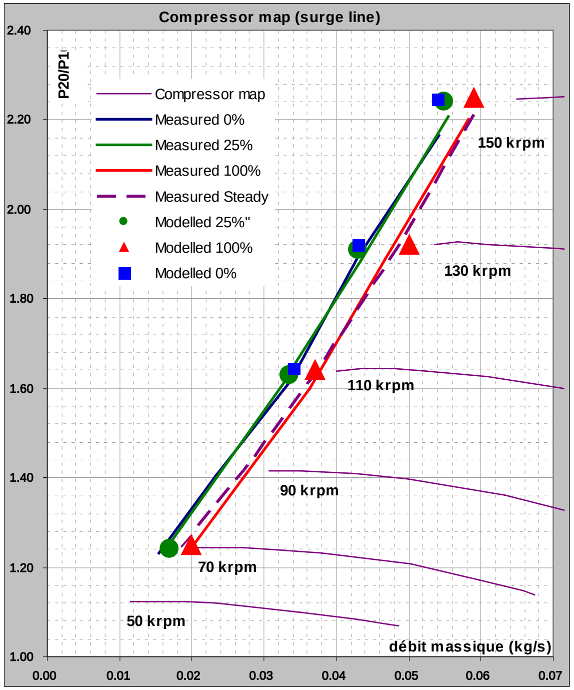


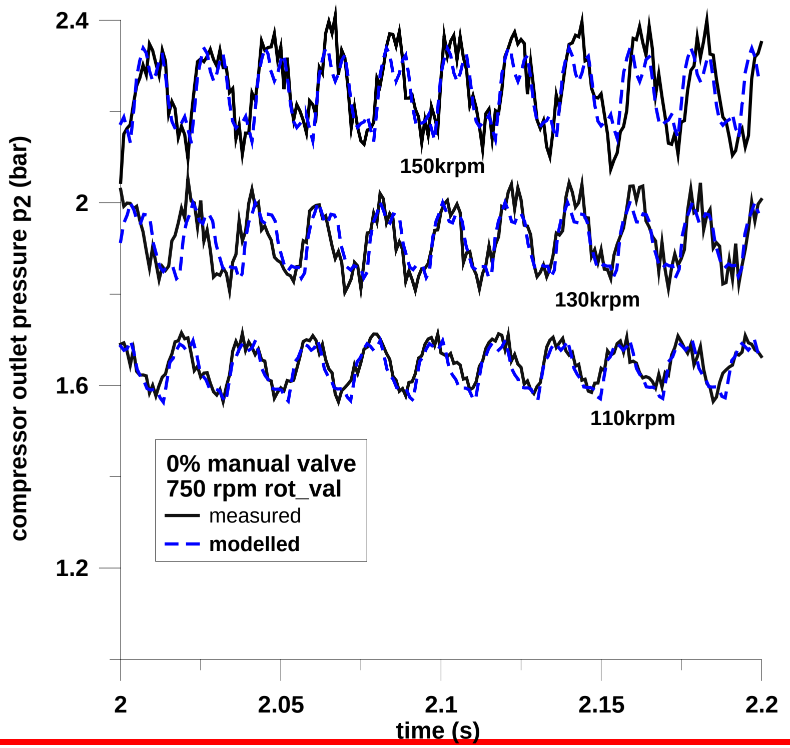

# Introduction: Objectives

- To analyze the physical phenomena which govern the surge during transient operating. Particularly, the reasons making the surge appear in transient even when the steady conditions are not favorable to surge.
- To determine whether a surge is possible in transient conditions without its installation and propagation.
- To model the surge phenomenon during engine accelerations or decelerations with 1D code with identifying the main variables of importance in the code.
- To find out strategies and technical solutions to avoid transient surge.
- To implement the modeling into GT-Power which is the 1D code used by (enterprise) for gas exchange simulations.

# Introduction: Work Plan

- Experimental
  - Characterization of components in **test flow rig**
  - Extended compressor maps measurement in **gas-stand**.
  - Develop **methodology** to detect/quantify surge
  - **Engine tests** with different upstream/downstream compressor geometries in **steady** and **transient**.
- Modelling
  - To calibrate the model
  - To use the user function to model the tests campaigns
  - To develop a User Function in GT with the compressor model
  - Transfer to (enterprise)

# Experimental Procedure

## o Engine Test Bench

- Steady Tests
    - Increase $p_{\mathrm{boost}}$ at constant engine speed, AFR, $p_{\mathrm{cyl\ max}}$, $T_{\mathrm{intake}}$
- Transient Tests
    - Load step from bmep=2 bar up to FL at constant engine speed, $T_{\mathrm{intake}}$

## o Gas-Stand

- Steady Tests

# Experimental Procedure

- Air Injection Technique

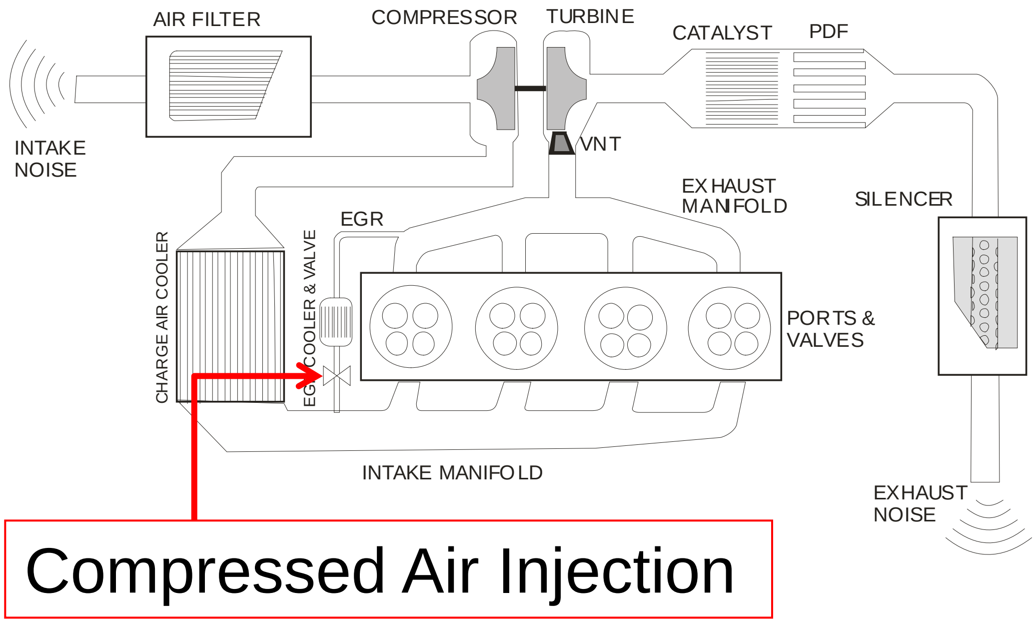


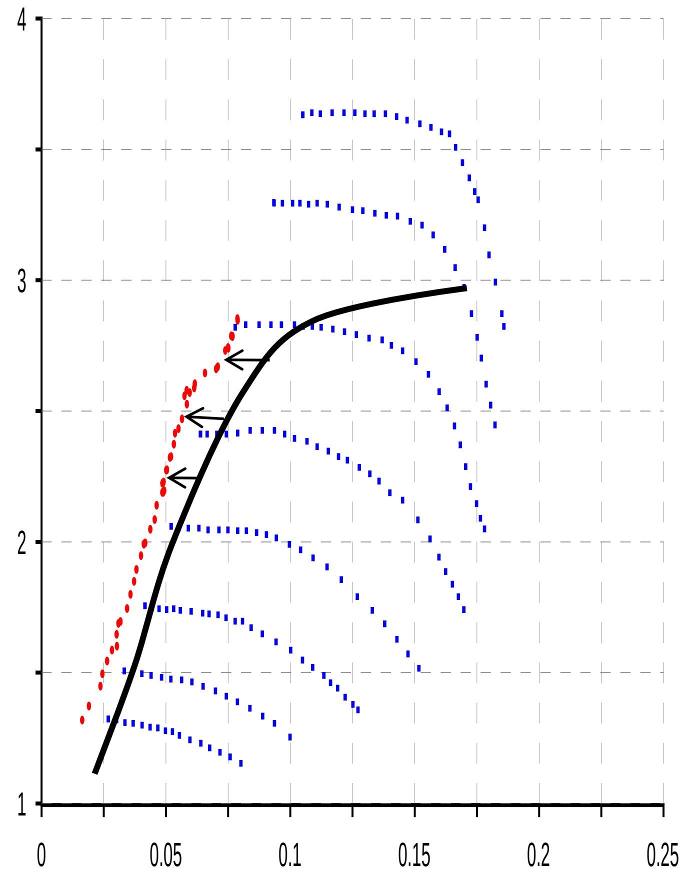

# Experimental Procedure

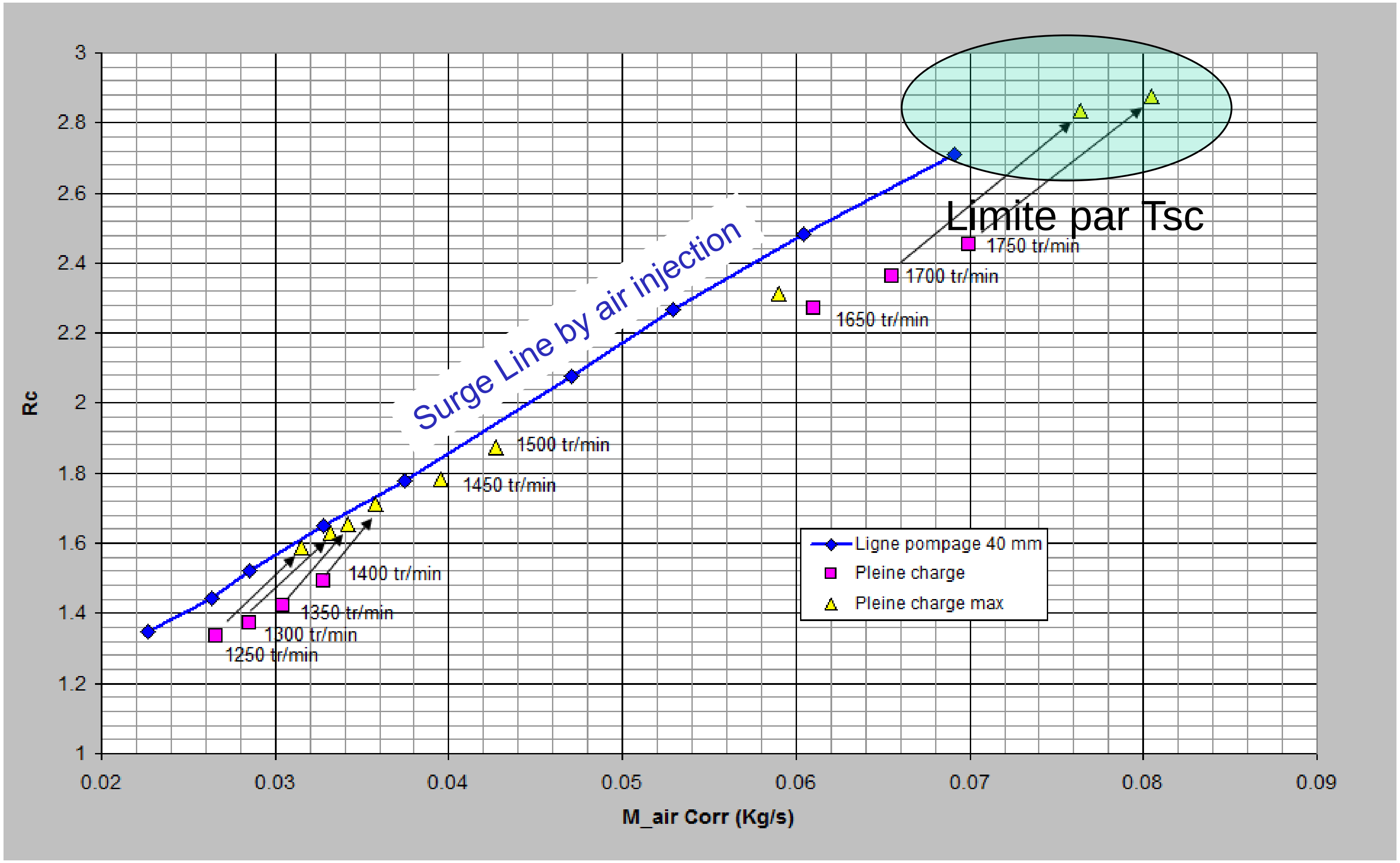

# Experimental Procedure: Effect $T_{intake}$

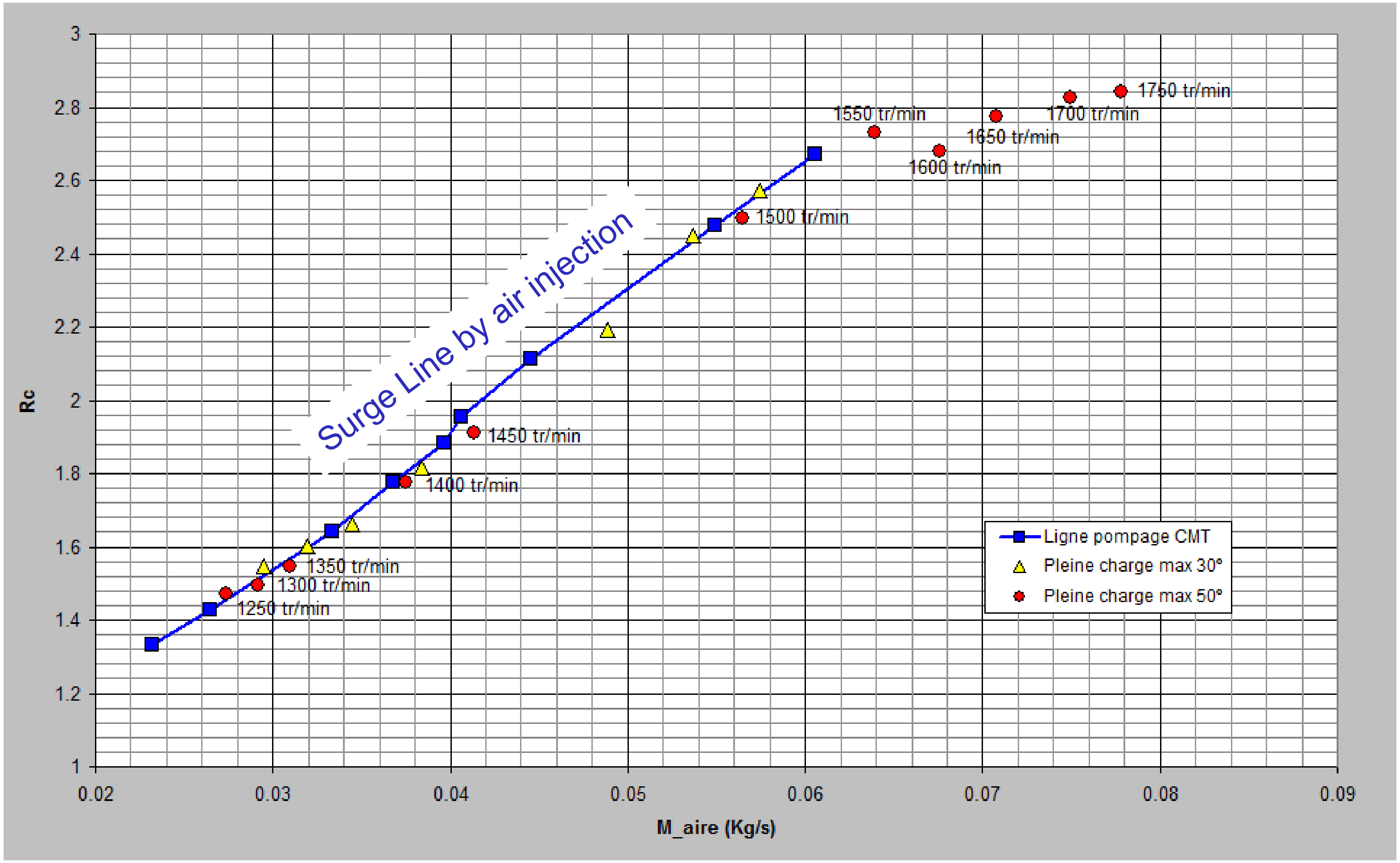

# Experimental Procedure: Effect $T_{intake}$

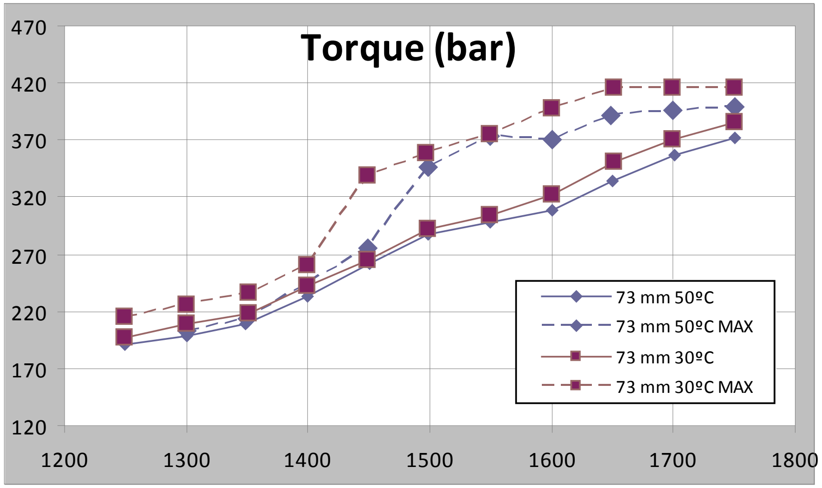


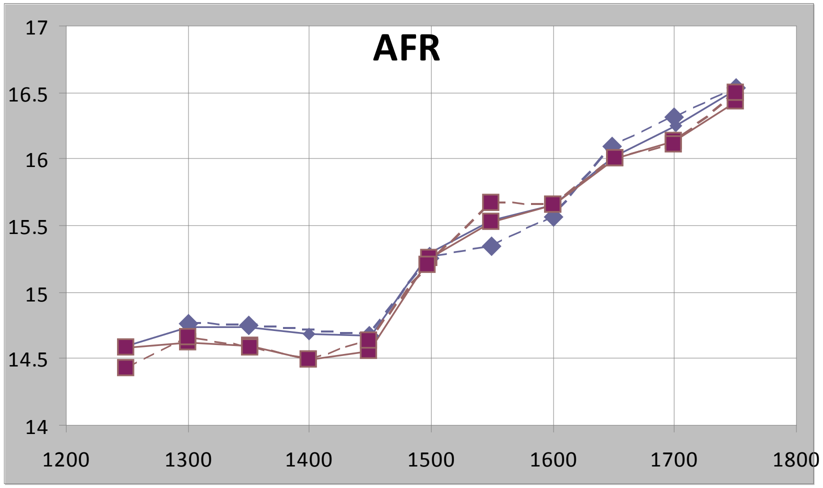


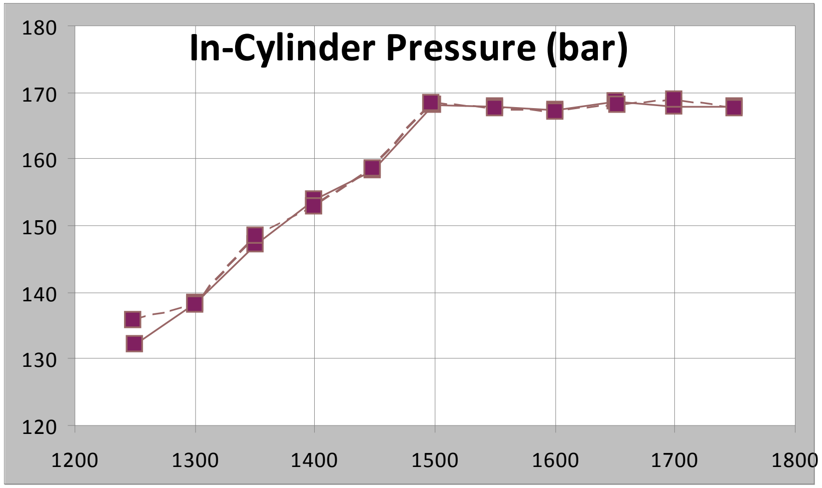


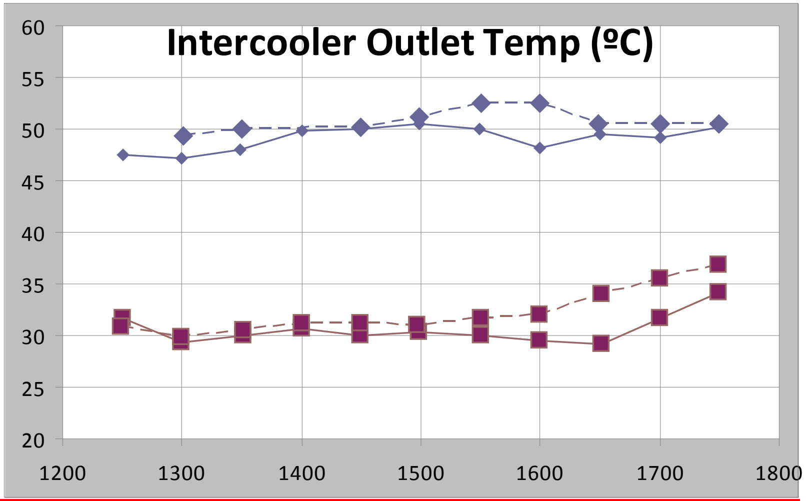

# ❑ Experimental Procedure: Effect $T_{intake}$

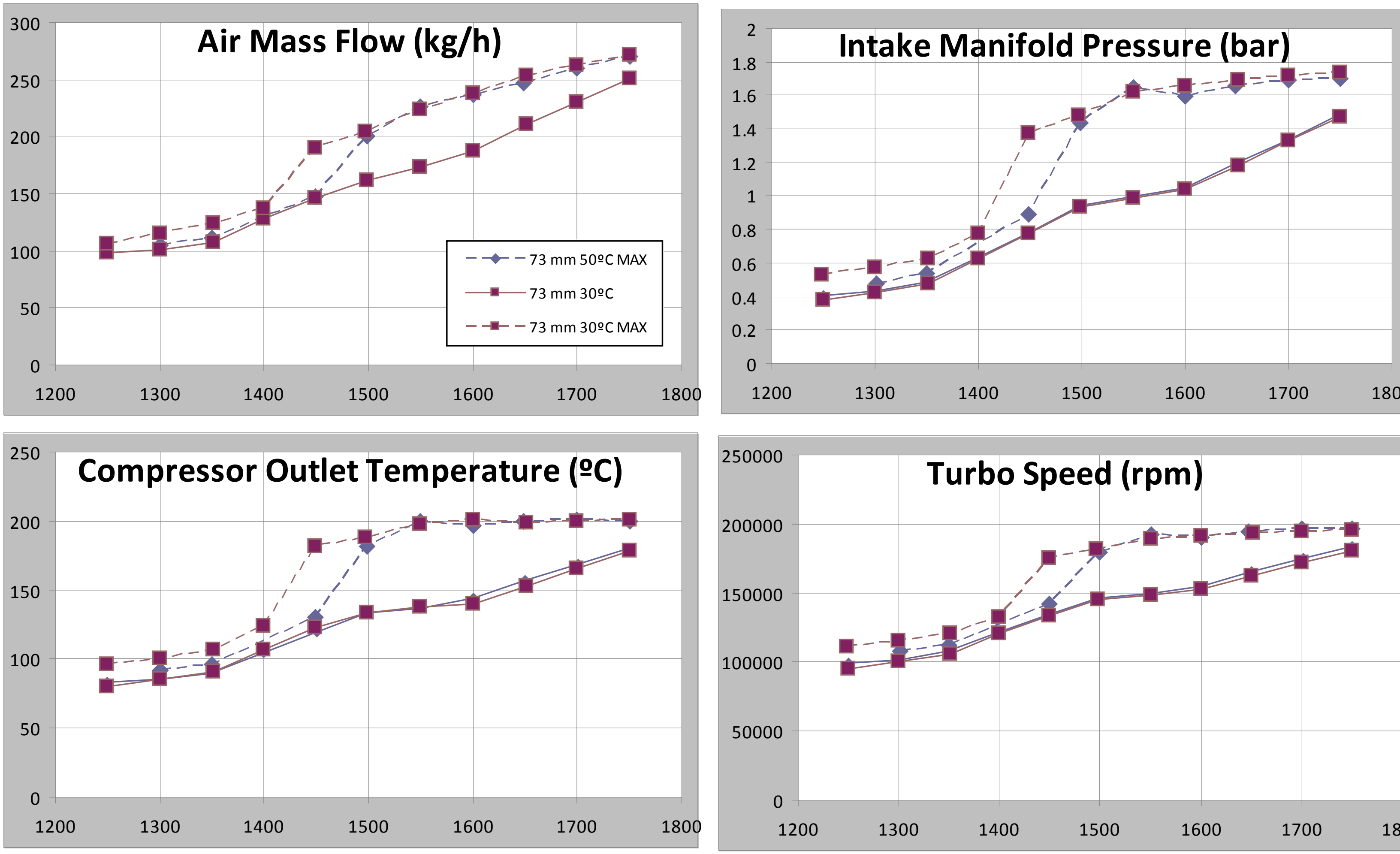

# Results volume 70 mm: Transient Tests

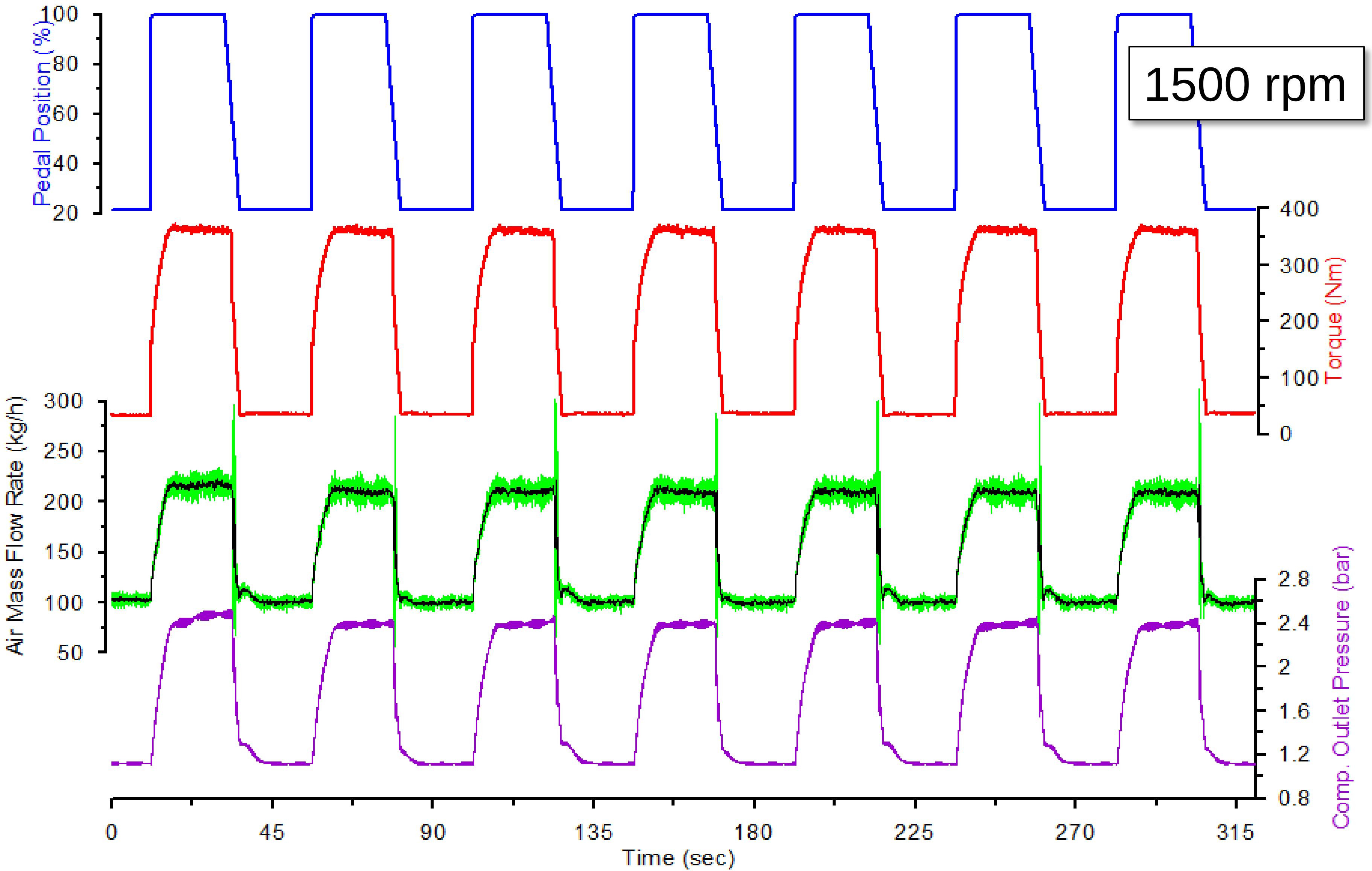

# Results volume 70 mm: Transient Tests

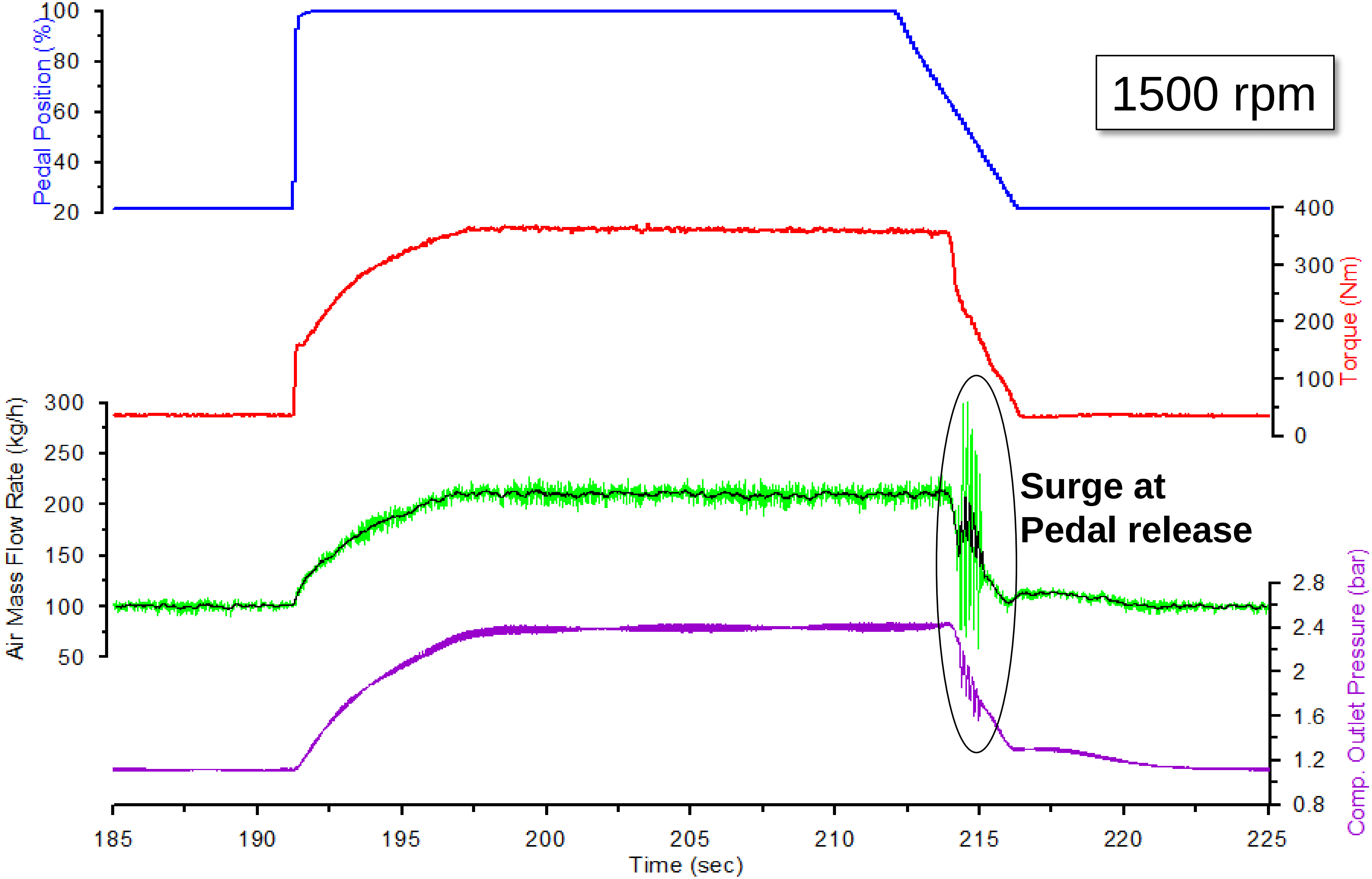

# Results volume 70 mm: Transient Tests

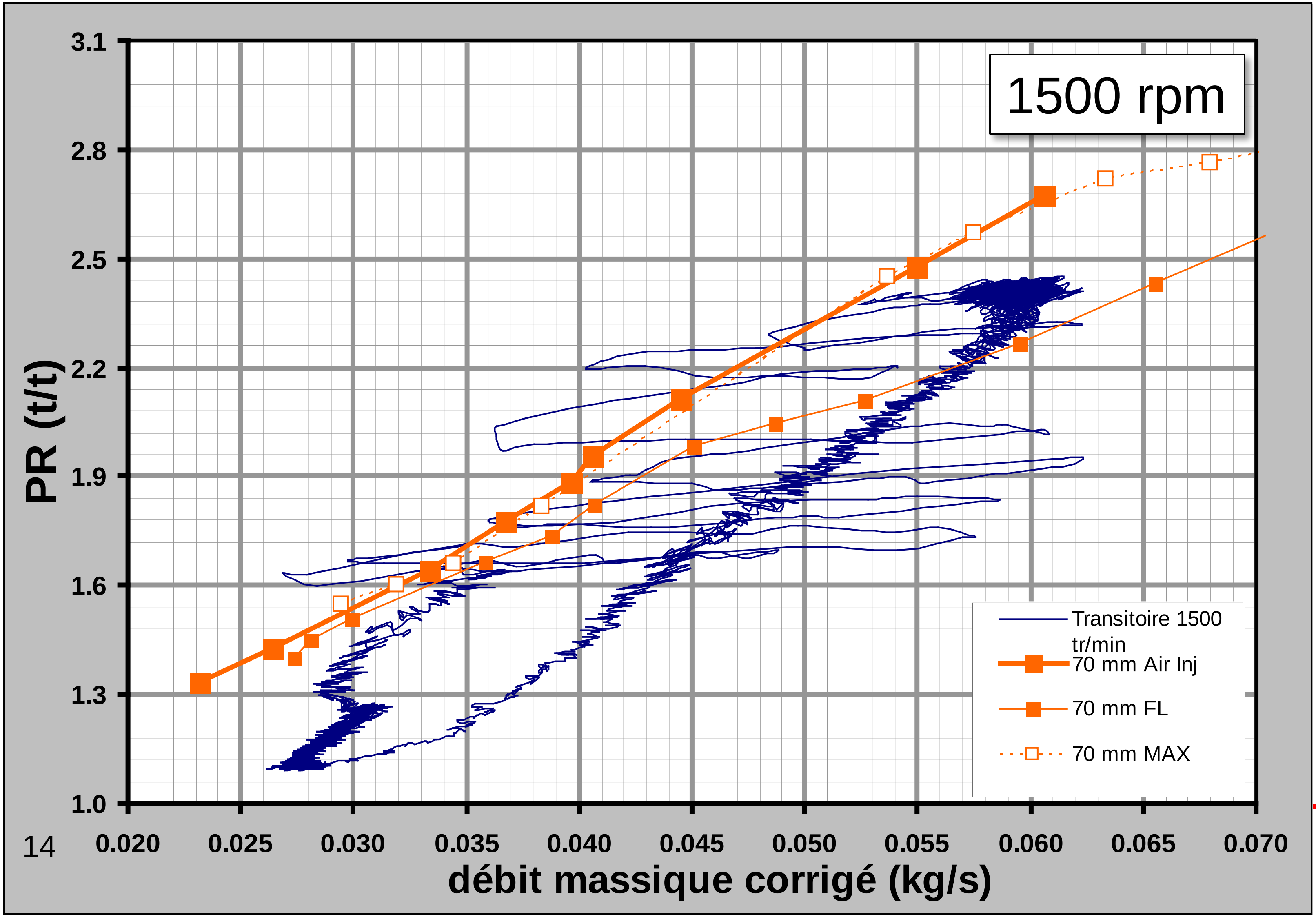

# Experimental procedure: Conclusions

- **Air Injection** method leads to similar results that regular engine tests closing the turbine at iso-AFR and iso- pcyl max.
- Surge line plotted in the compressor map is not affected by **intake temperature**. But, obviously has influence on engine torque.
- There is not risk of surge in sudden load **transient** tests at steady speed. The more risky situation is the pedal release (even more with engine deceleration)
- **Steady surge line** fits well to the transient surge loops at pedal release

# Contents


- Introduction
  - Background, Objectives, Methodology
- Experimental procedure
- Volume before compressor
- Resonator before compressor
- Discussion
- Conclusion

# Volume before compressor: Experimental Matrix

| *count* | *NAME* | *Volume* | *Step Position* | *Cavity position* | *Radius* |
|---|---|---|---|---|---|
| 1 | BASE-A | | | | |
| 2 | SERVol1 | Vol1 | X1 | NEAR COMPRESSOR | WO radius |
| 3 | SERVol2 | Vol2 | | | |
| 4 | SERVol3 | Vol3 | | | |
| 5 | SERVol4 | Vol4 | | | |
| 6 | SERVol5 | Vol5 | | | |
| 7 | SERVol6 | Vol6 | | | |
| 8 | SERVol7 | Vol7 | | | |

| *Count* | *NAME* | *Volume* | *Step Position* | *Cavity position* | *Radius* |
|---|---|---|---|---|---|
| counted | SERVol-OPT | volOPT | X1 | NEAR COMPRESSOR | WO radius |
| 9 | SERVolOPT+50 | volOPT | X=1+50mm | NEAR COMPRESSOR | WO radius |
| 10 | SERVolOPT-50 | volOPT | X=-50mm | | |

| *Count* | *NAME* | *Volume* | *Step Position* | *Cavity position* | *Radius* |
|---|---|---|---|---|---|
| counted | SERVol-Pos-OPT | VolOPT | posOPT. | NEAR COMPRESSOR | WO radius |
| 11 | SERvol-Pos-OPT-r05 | | | | Radius = 5mm |
| 12 | SERvol-Pos-OPT-r10 | | | | Radius = 10mm |
| 13 | SERvol-Pos-OPT-cone | | | | Conical junction between the duct and the cavity |

| *Count* | *NAME* | *Volume* | *Step Position* | *Cavity position* | *Radius* |
|---|---|---|---|---|---|
| counted | SERVol-Pos-R-OPT | volOPT | posOPT. | Near Compressor | r-opt |
| 14 | SERvol-Pos-R-OPT-FAA | | | Near the Air Filter | |
| 15 | SERvol-Pos-R-OPT-MID | | | In the middle | |

# ❑ Volume before compressor

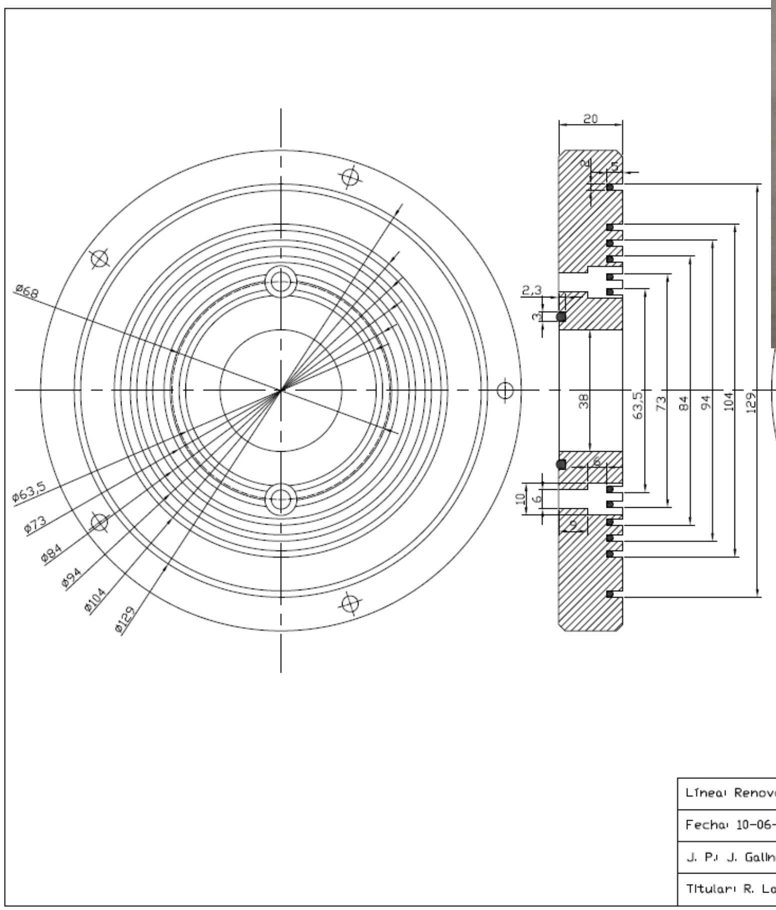


# ❑ Volume Before Compressor

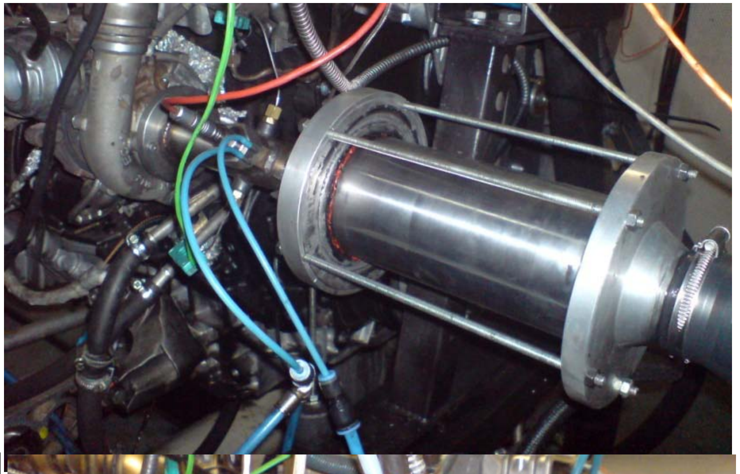

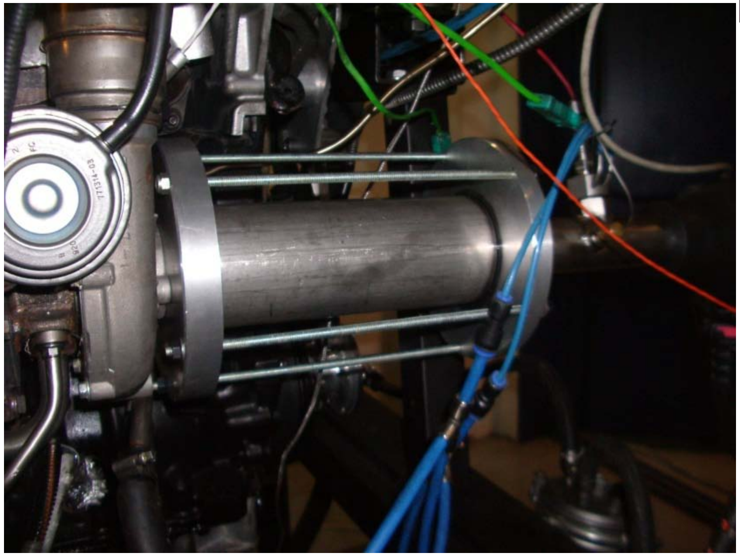

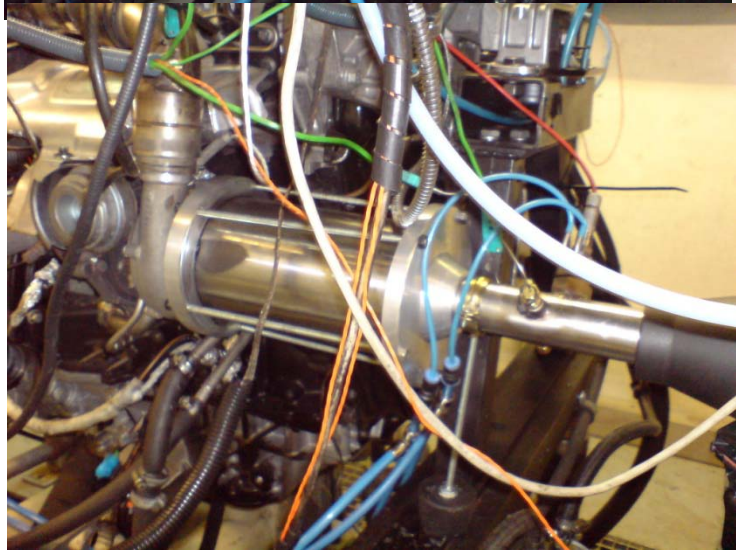

# ❑ Volume Before Compressor: Volume Effect

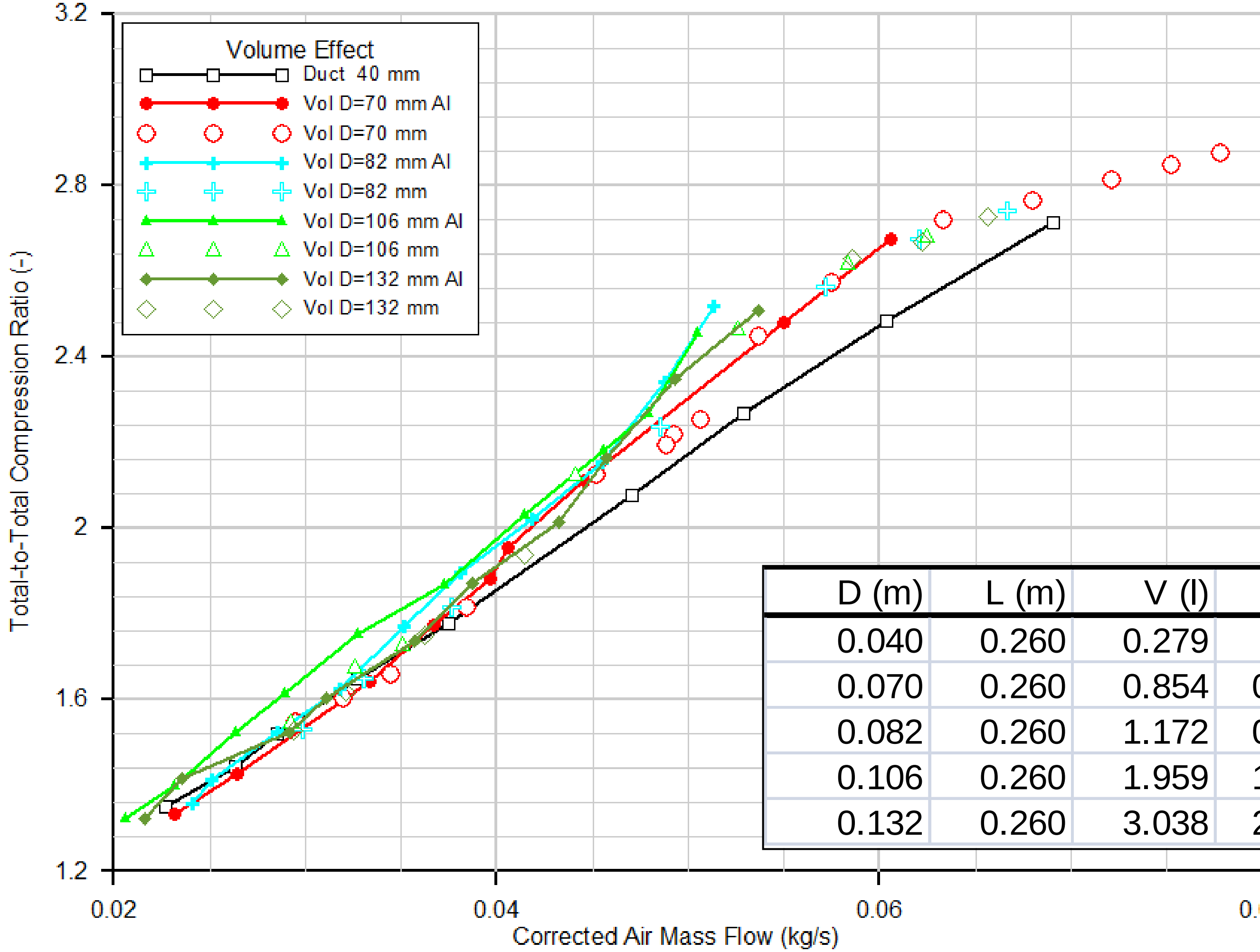


| D (m) | L (m) | V (l) | ΔV(l) | DV(%) |
|---|---|---|---|---|
| 0.040 | 0.260 | 0.279 | | |
| 0.070 | 0.260 | 0.854 | 0.575 | 206% |
| 0.082 | 0.260 | 1.172 | 0.893 | 320% |
| 0.106 | 0.260 | 1.959 | 1.680 | 602% |
| 0.132 | 0.260 | 3.038 | 2.759 | 989% |

# Volume Before Compressor:Volume Effect

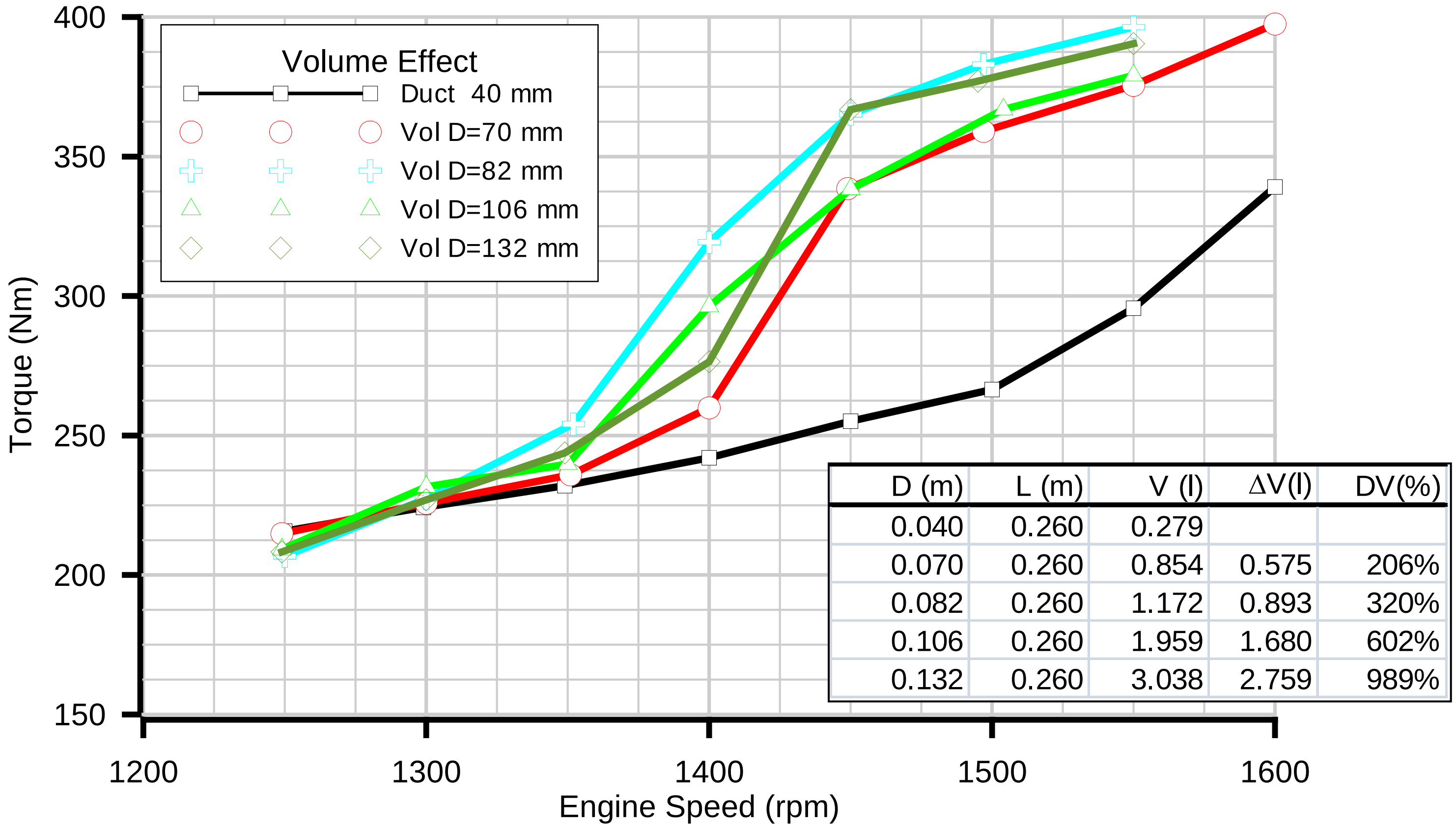


| D (m) | L (m) | V (l) | ΔV(l) | DV(%) |
|---|---|---|---|---|
| 0.040 | 0.260 | 0.279 | | |
| 0.070 | 0.260 | 0.854 | 0.575 | 206% |
| 0.082 | 0.260 | 1.172 | 0.893 | 320% |
| 0.106 | 0.260 | 1.959 | 1.680 | 602% |
| 0.132 | 0.260 | 3.038 | 2.759 | 989% |

# Volume Before Compressor:Volume Effect

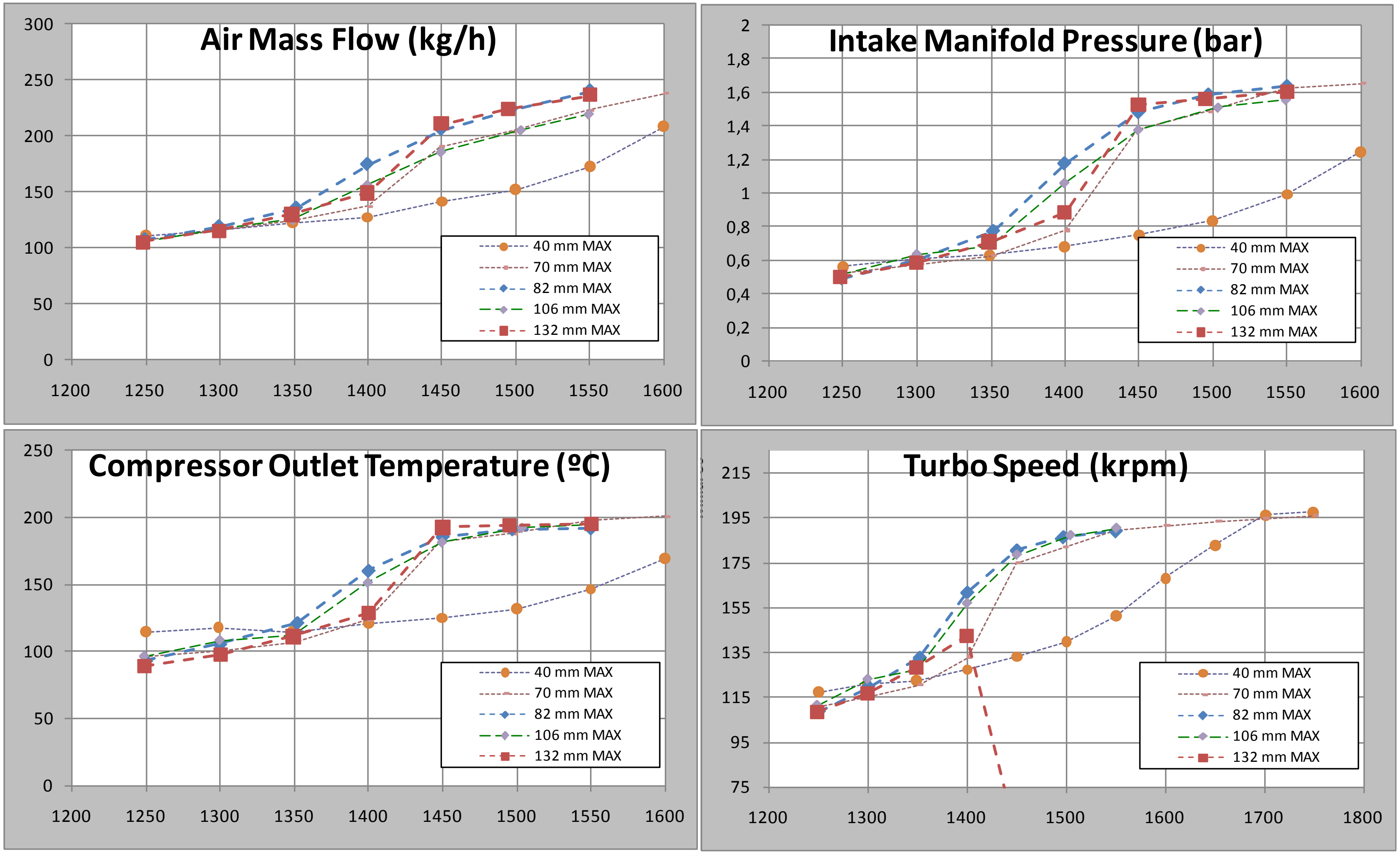

# ❑ Volume Before Compressor: Position Effect

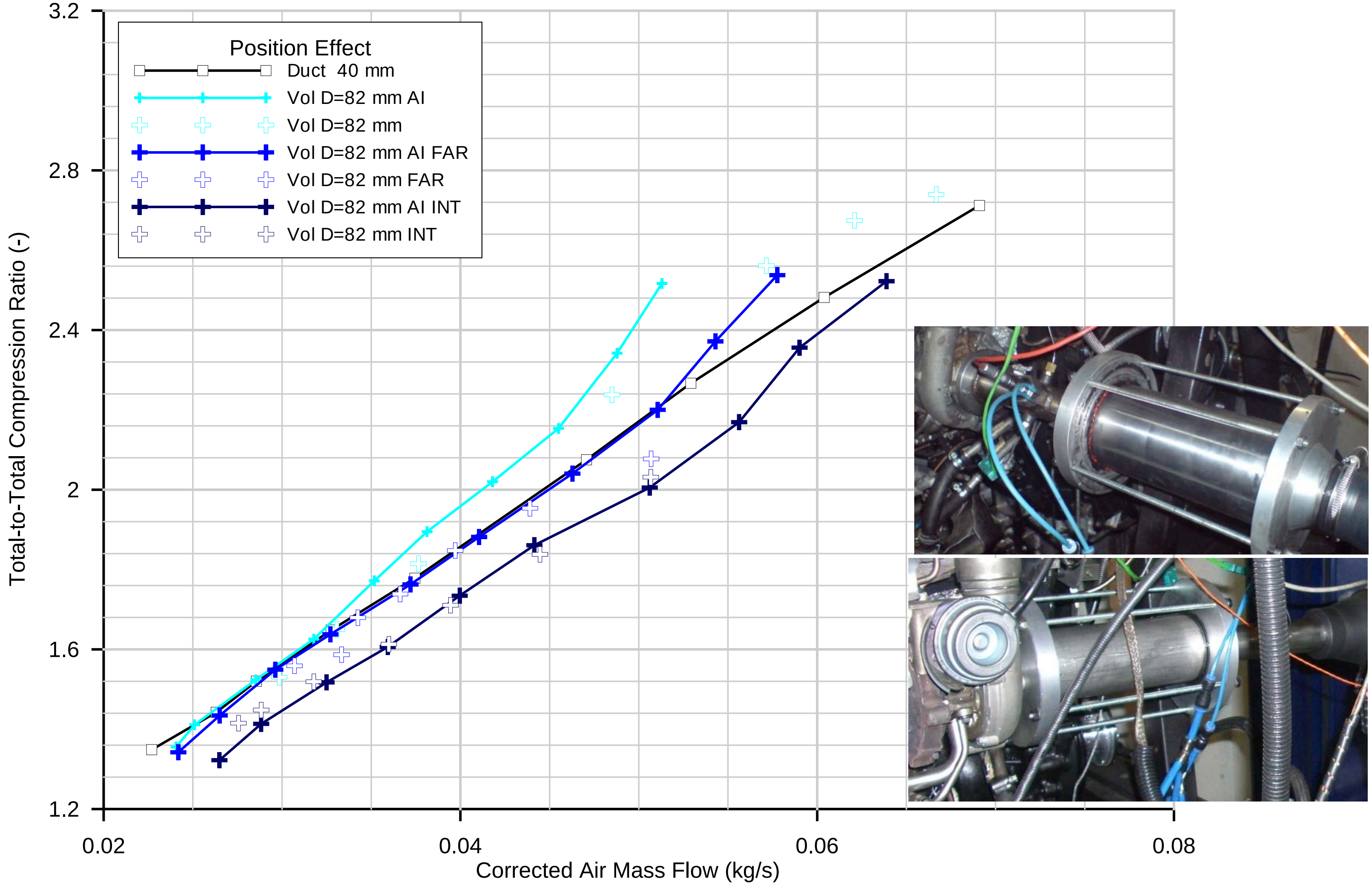

# Volume Before Compressor: Position Effect

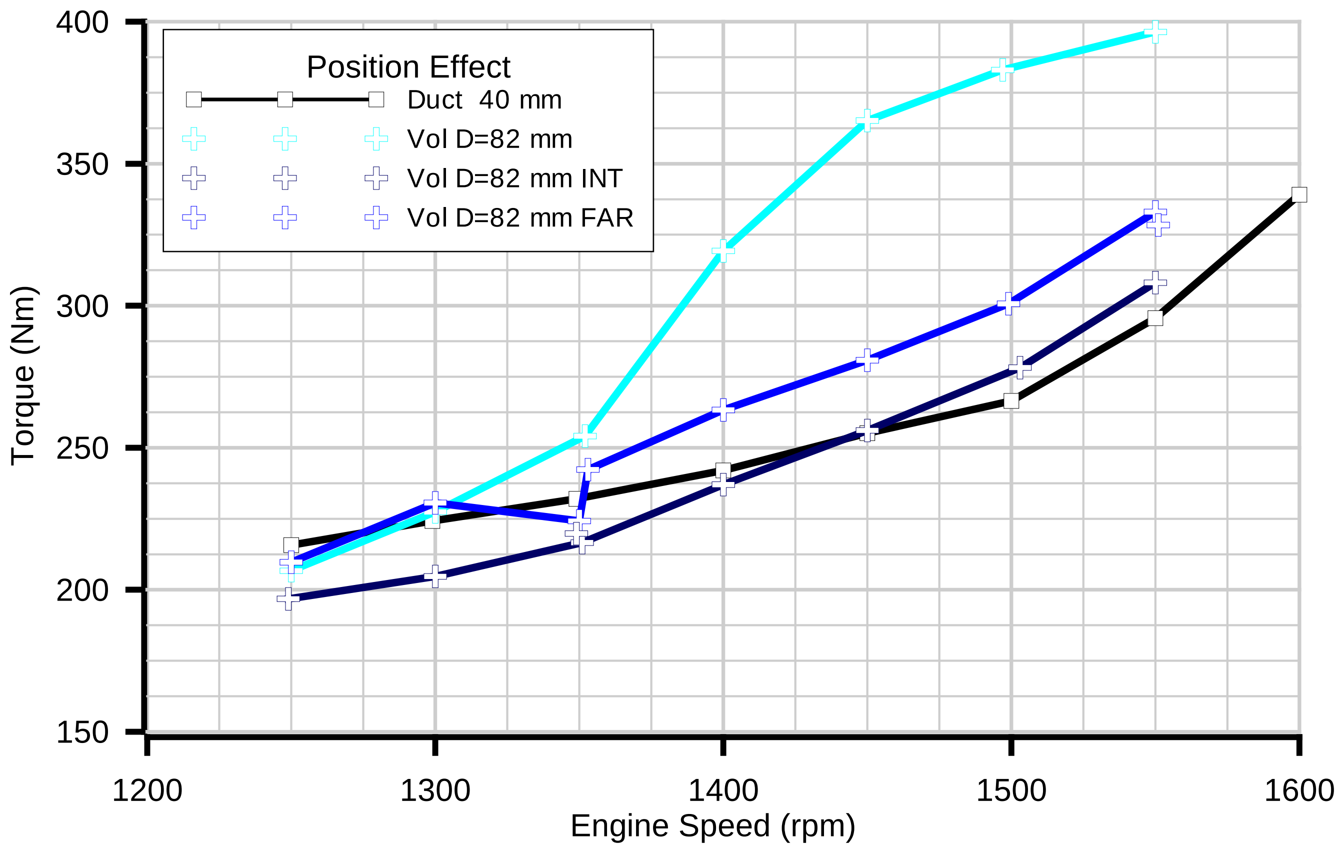

# Diameter effect: Isovolume

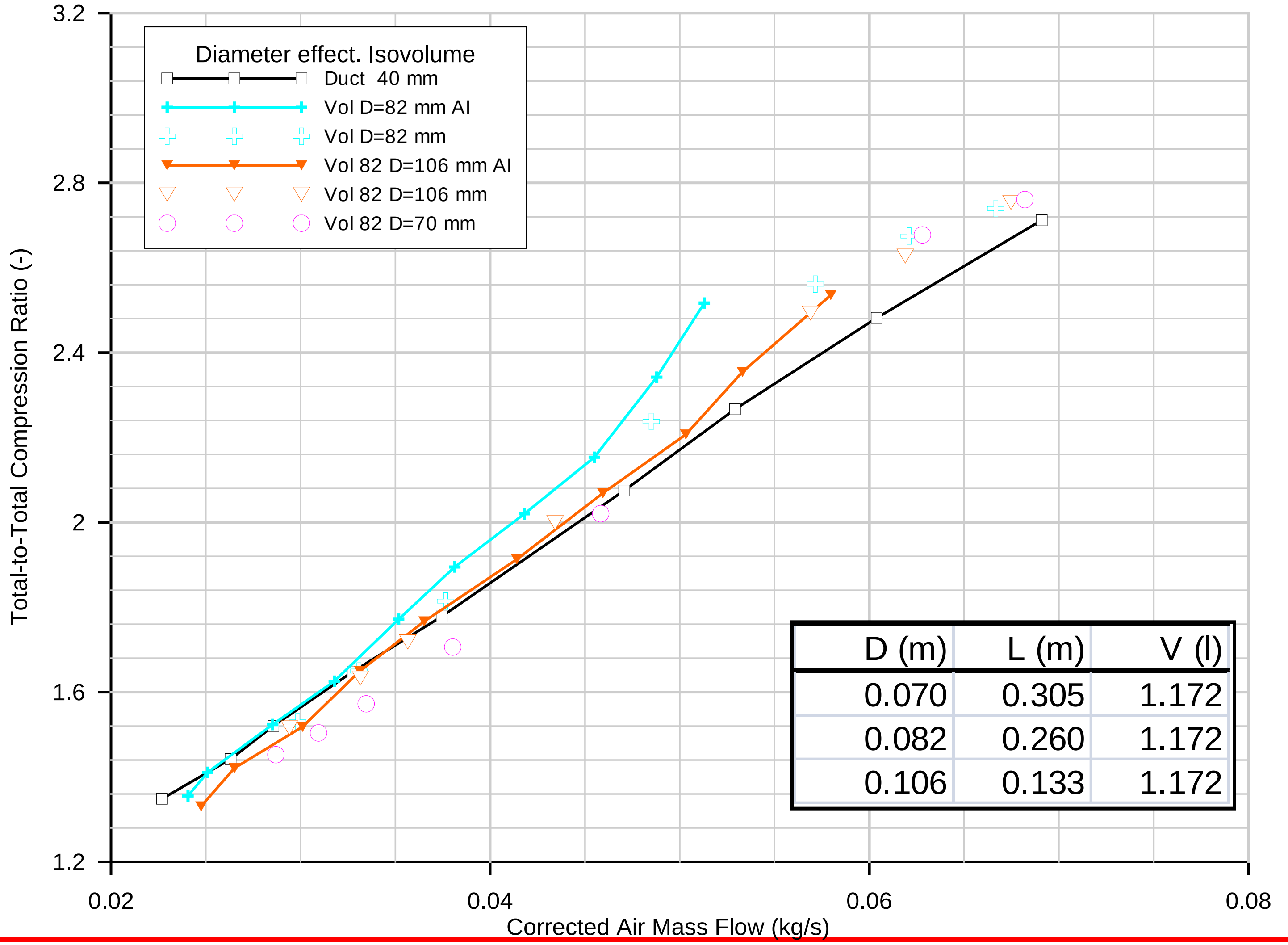


| D (m) | L (m) | V (l) |
|---|---|---|
| 0.070 | 0.305 | 1.172 |
| 0.082 | 0.260 | 1.172 |
| 0.106 | 0.133 | 1.172 |

# Volume Before Compressor:Diameter Effect. Isovolume

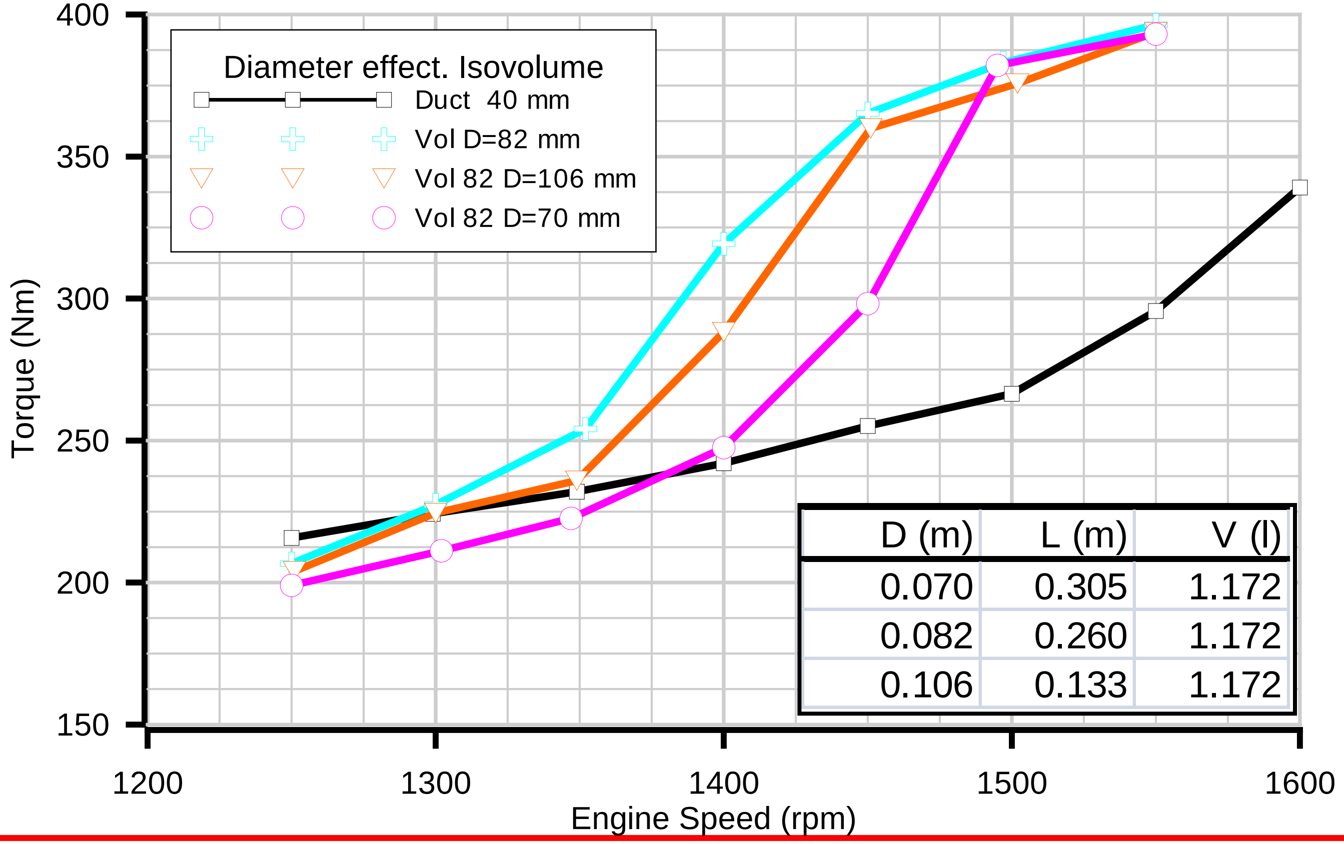


| D (m) | L (m) | V (l) |
|---|---|---|
| 0.070 | 0.305 | 1.172 |
| 0.082 | 0.260 | 1.172 |
| 0.106 | 0.133 | 1.172 |

# Volume Before Compressor: Radii Effect

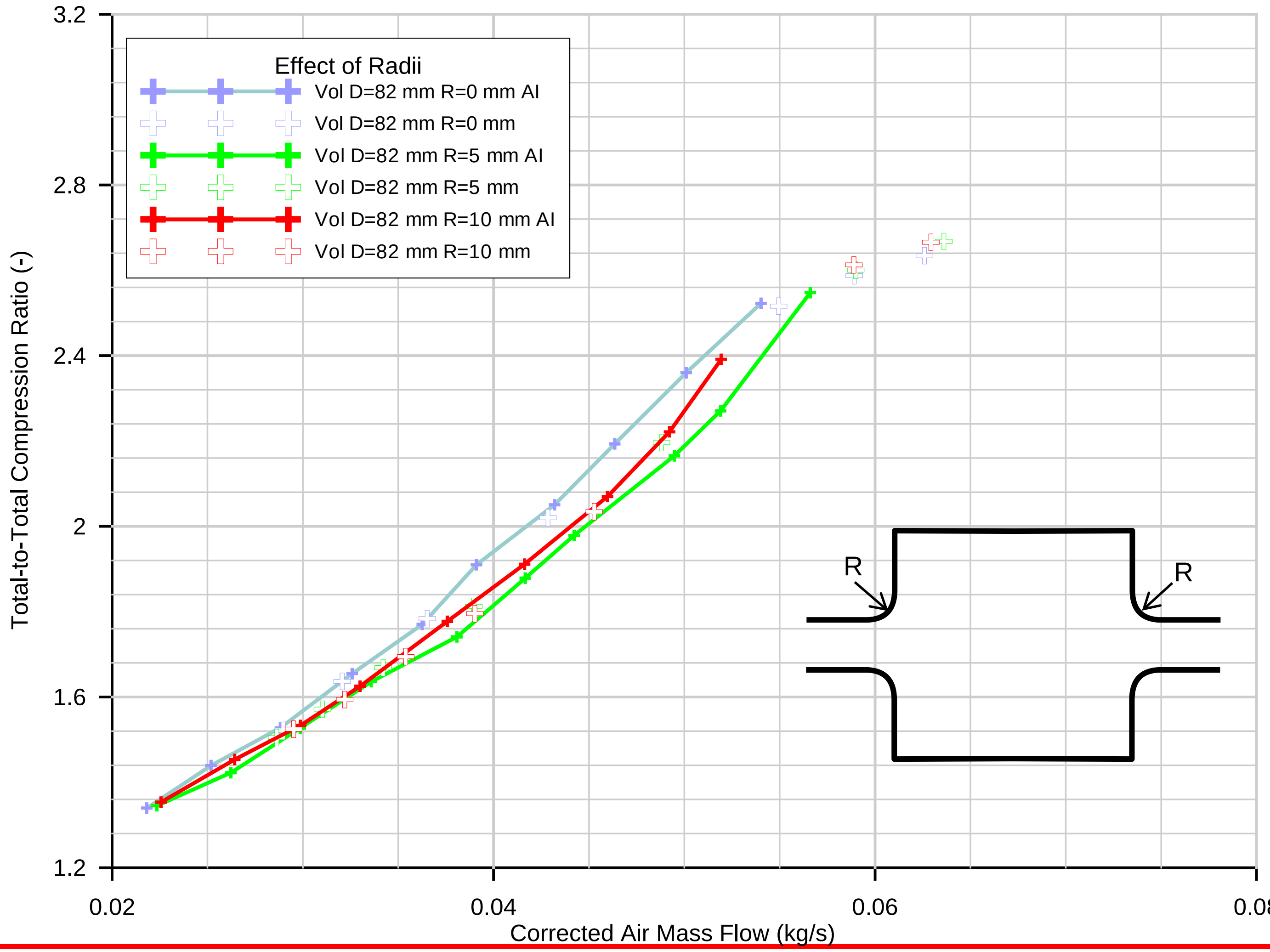

# Volume Before Compressor: Radii Effect

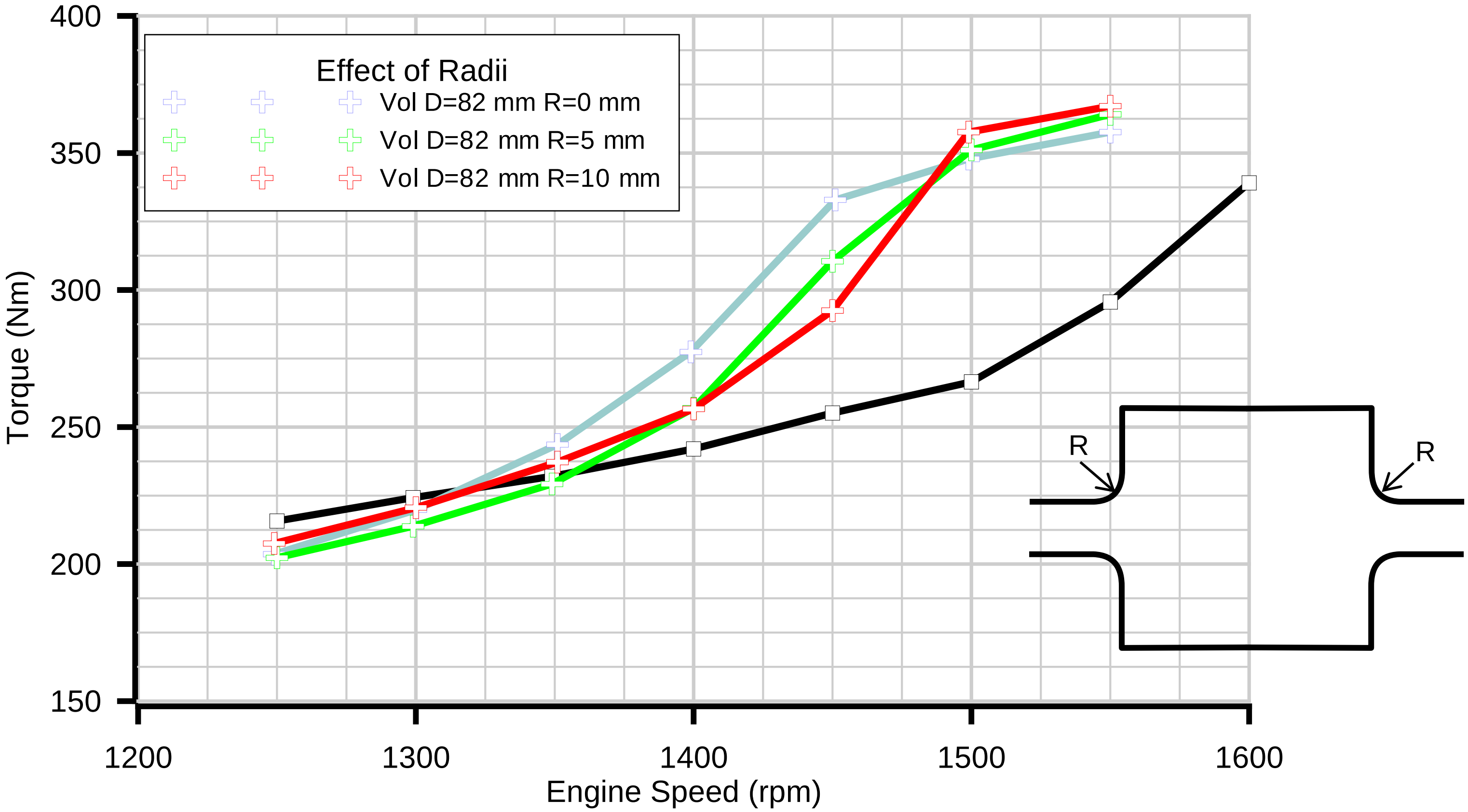

# Volumes engine Tests: Conclusions

## Concerning the dimensions of the volume:

- o The volume corresponding to D= 82 mm leads to the best results
- o The diameter of 82 mm seems to be the best
- o To introduce rounded entry does not improve surge

## Concerning the position of the volume:

- The volume has to be as **close** as possible to the compressor

# Gas-Stand Tests: volume

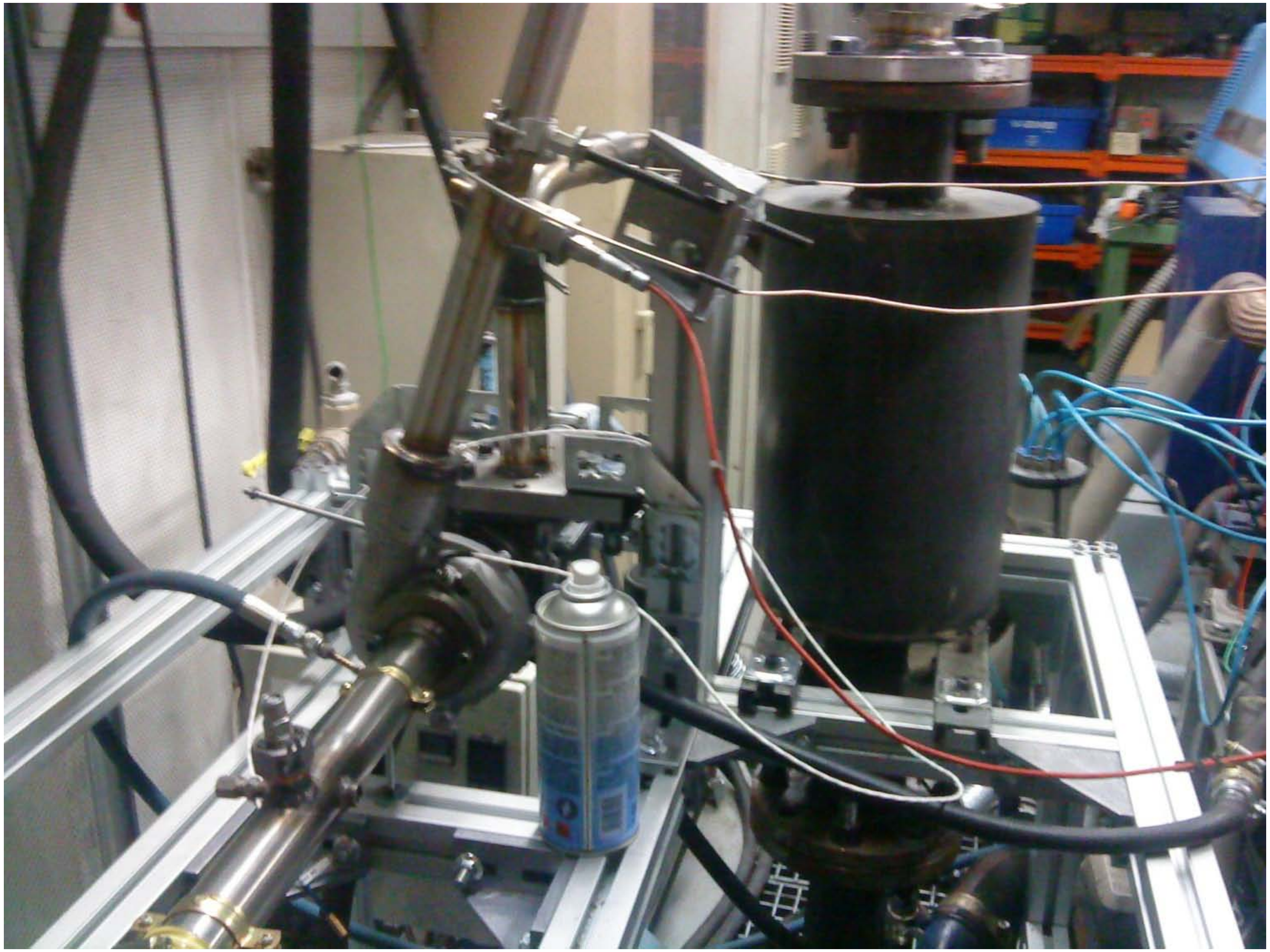

# Gas-Stand Tests: Volume effect

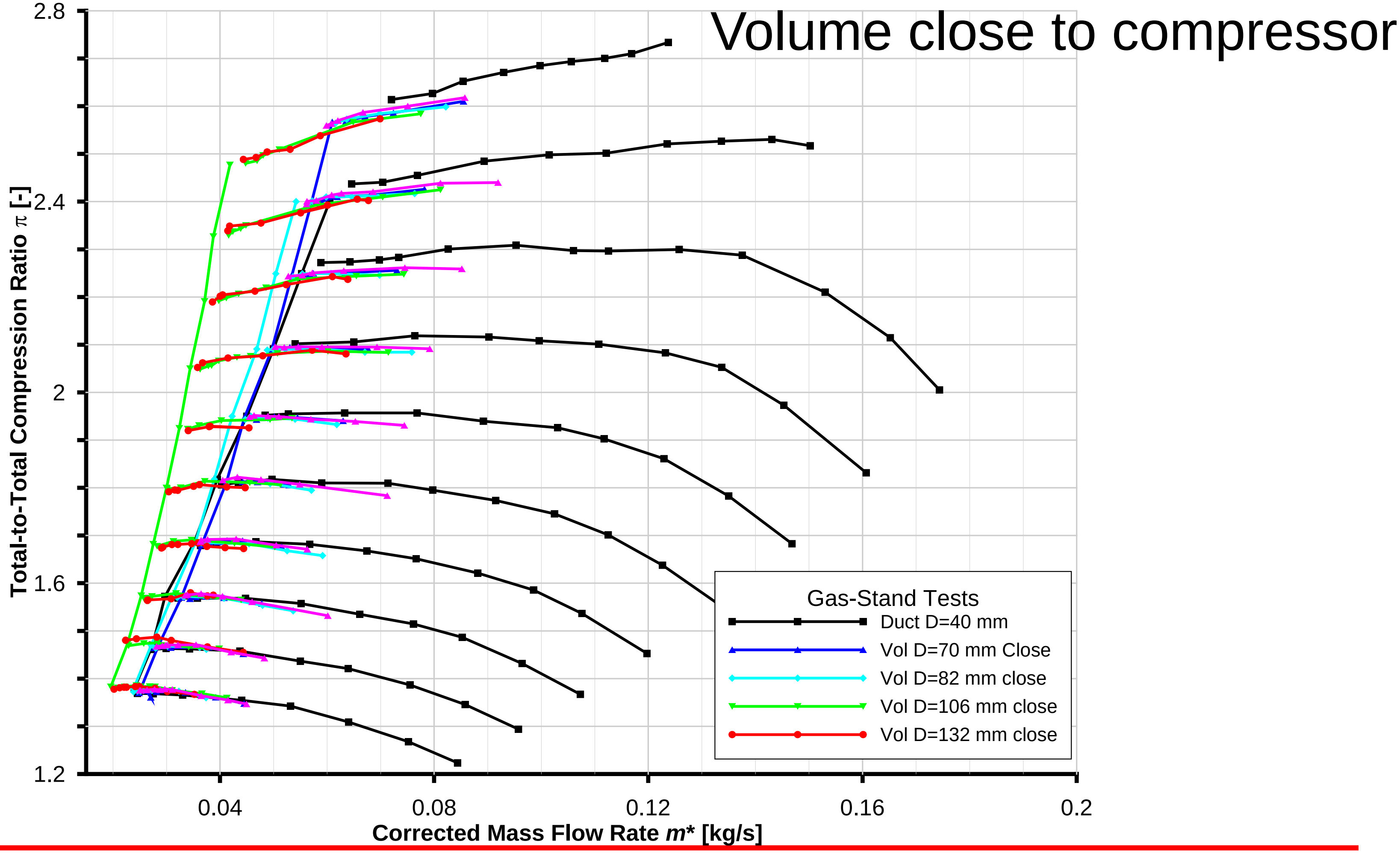

# Gas-Stand Tests: Volume effect

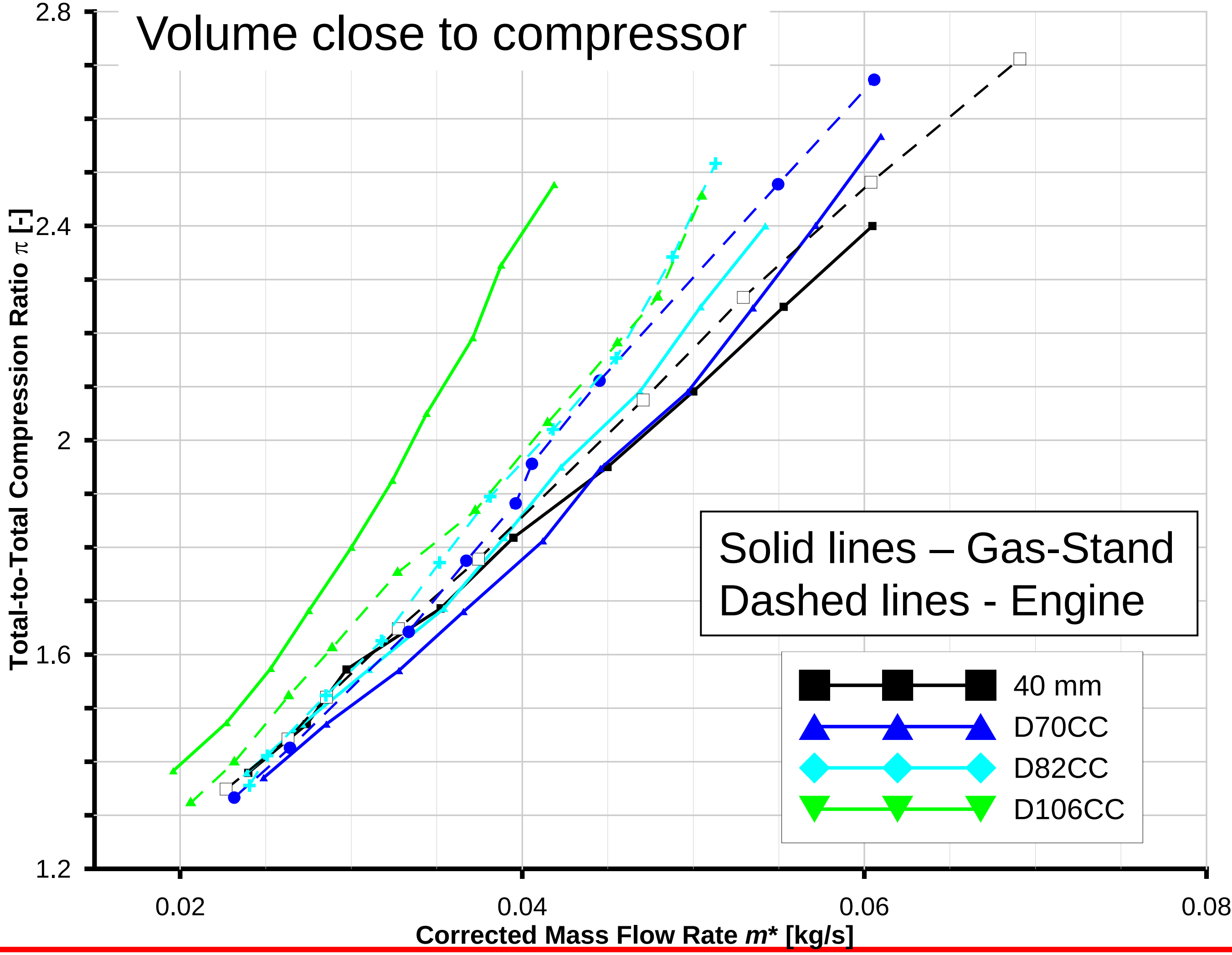

# Gas-Stand Tests: Volume effect

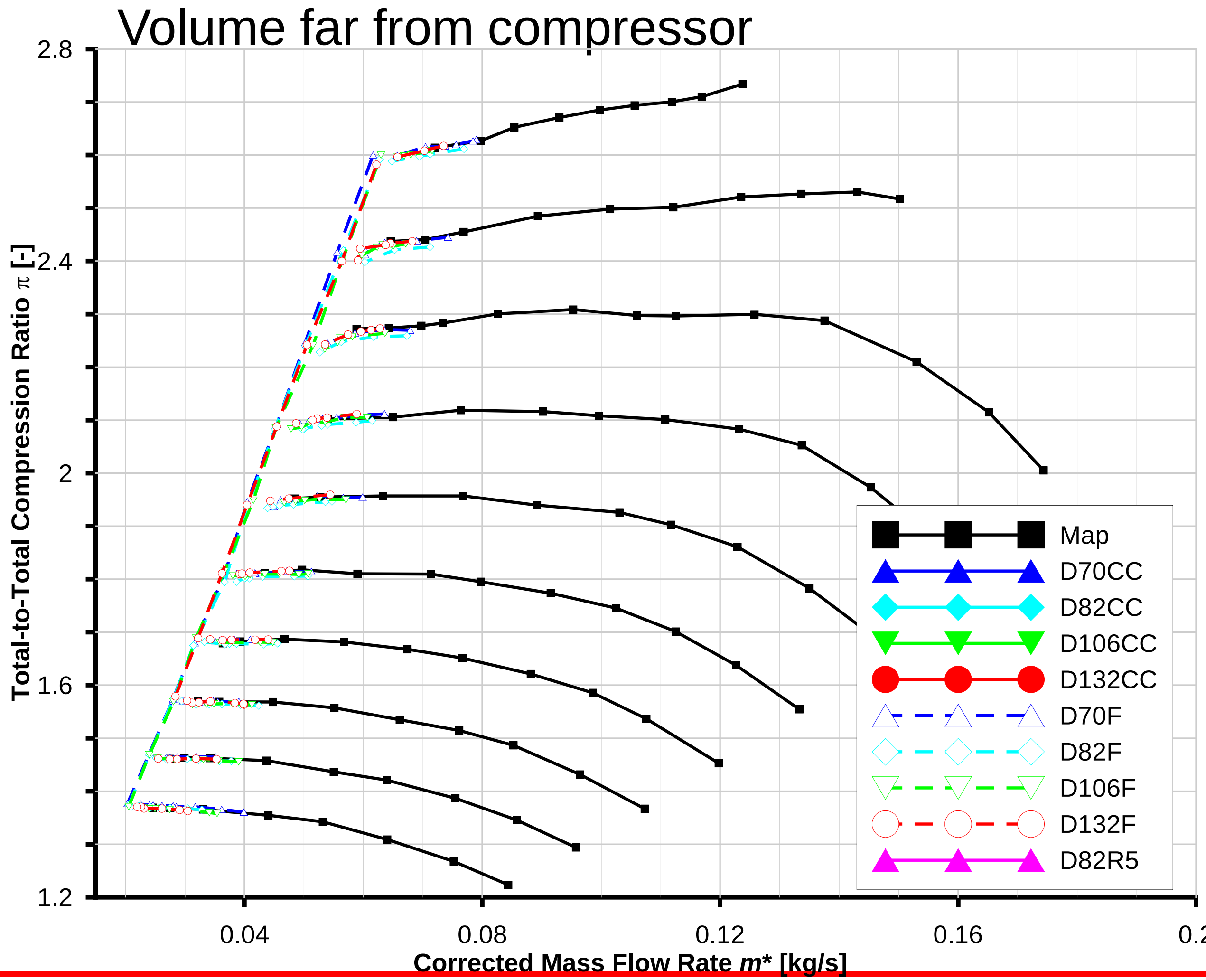

# Gas-Stand Tests: Volume effect

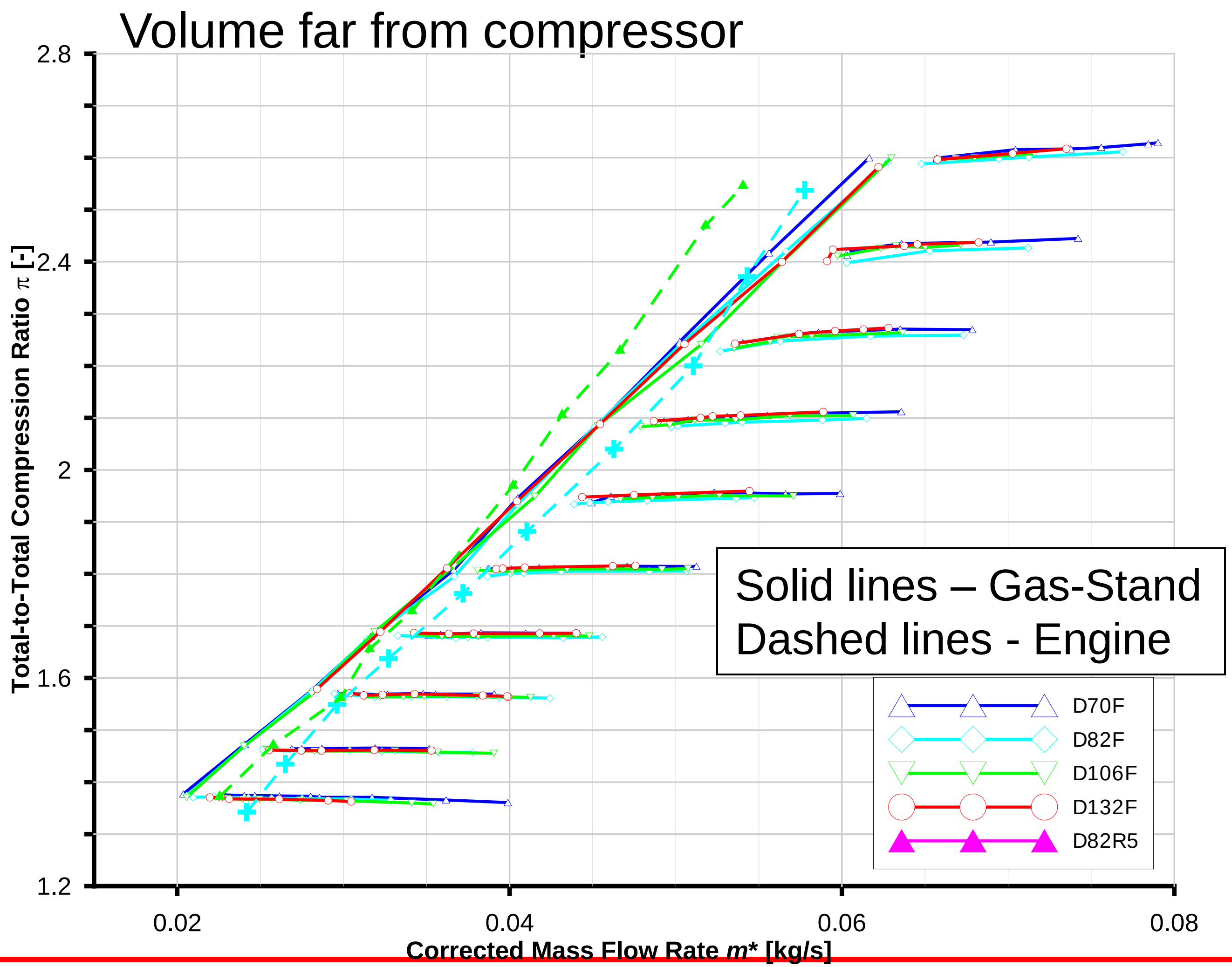

# Gas-Stand Tests: Volume effect

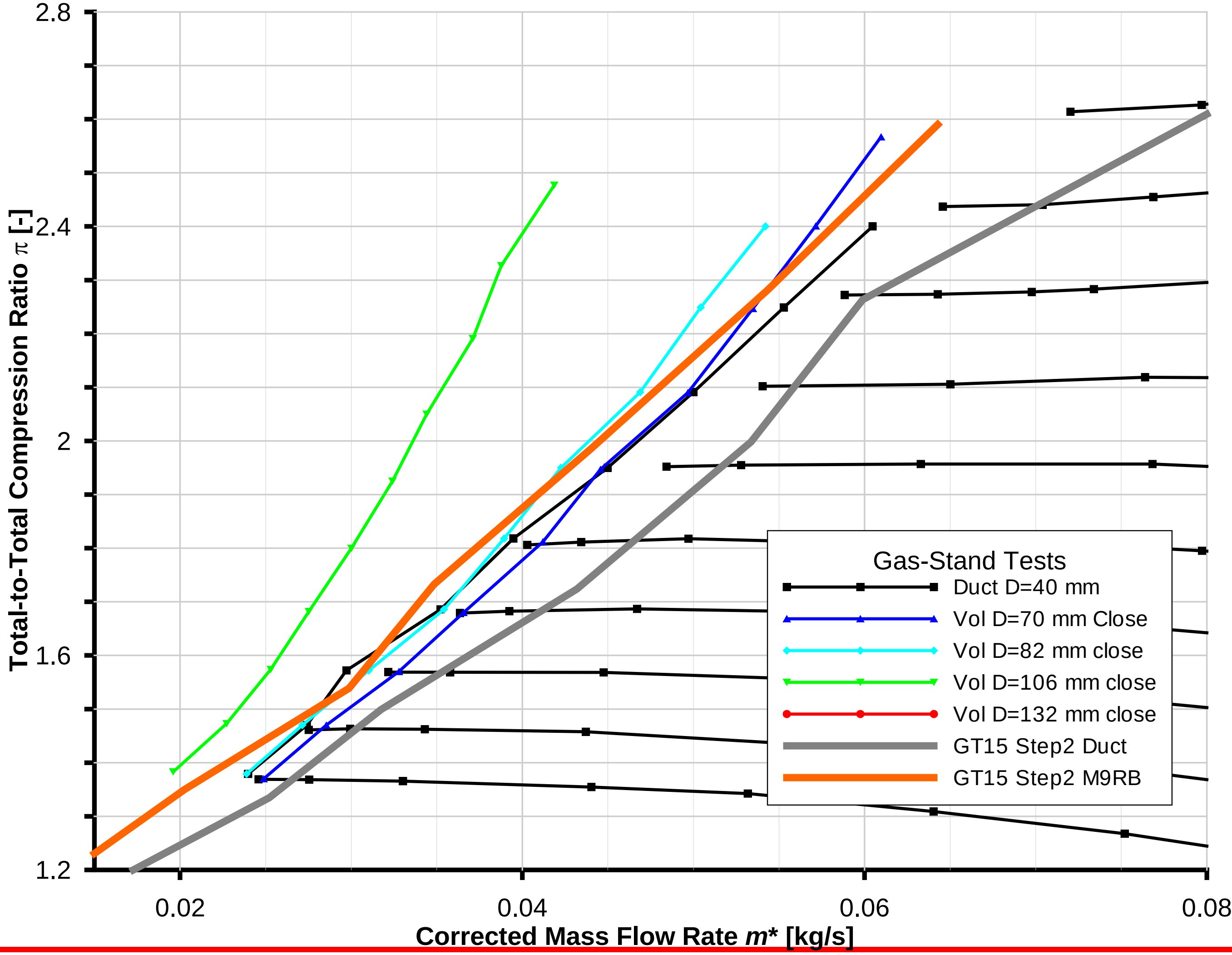

# Conclusions Volume before Compressor

Gas Stand tests:

- The bigger the volume the more increased surge margin (different from engine results)
- The influence of the volume on surge margin is much more important in gas-stand tests than in engine tests
- When the volume is far from the compressor its influence is avoided. This means that in steady flow the volume has only **Aerodynamic Effects** on compressor surge. This is of course the same case on the engine

# CFD calculations

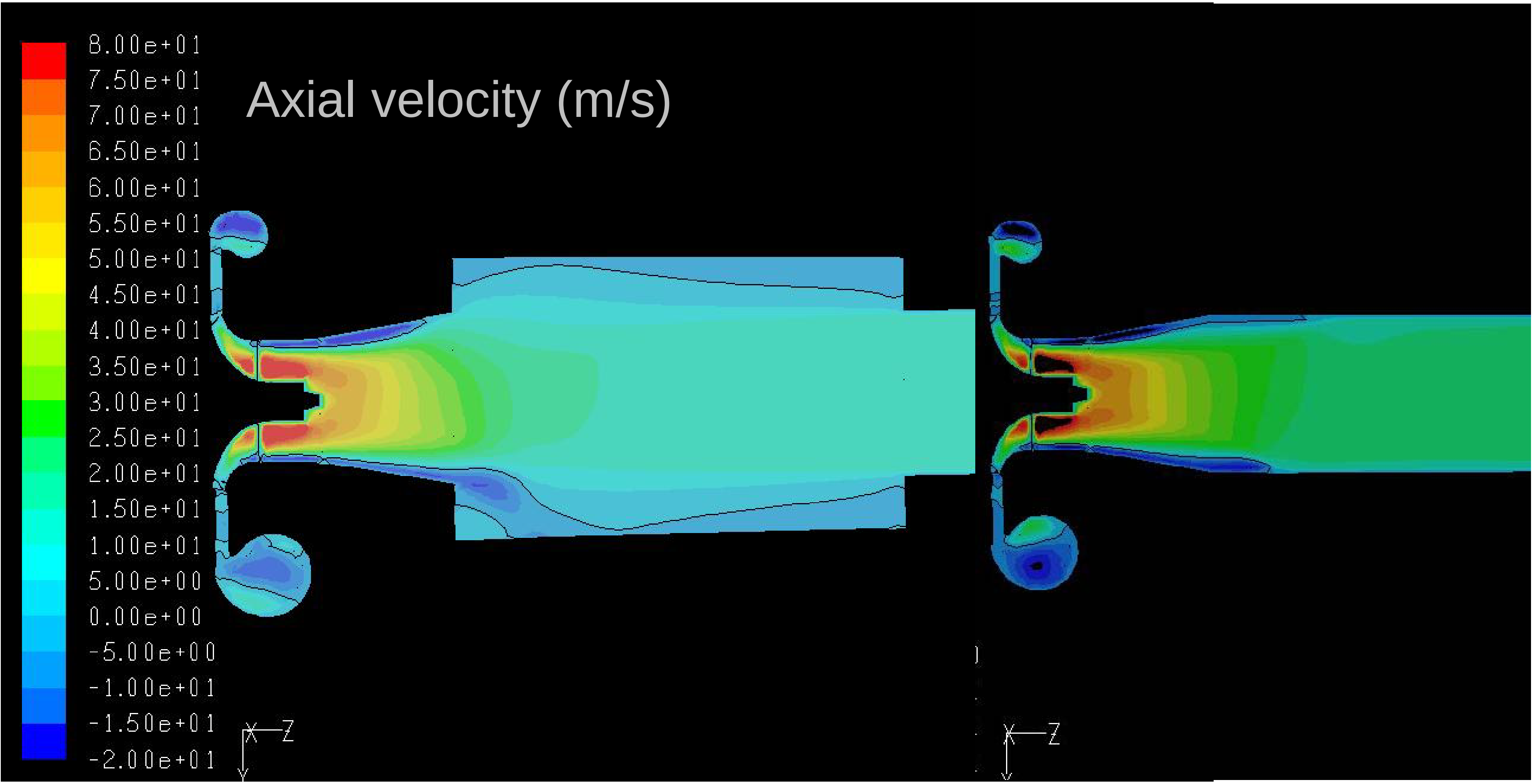

# CFD calculations

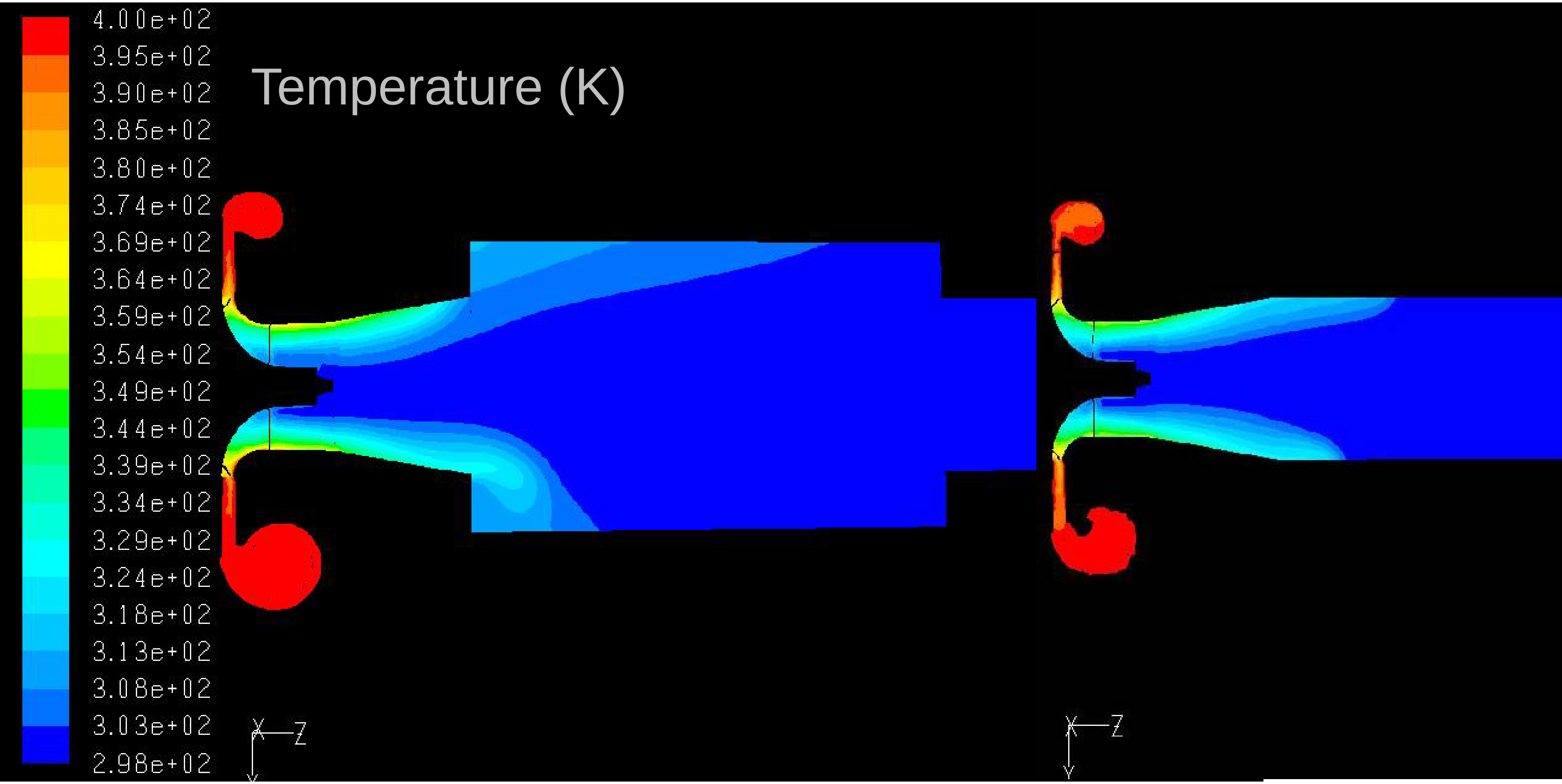

# Contents

- Introduction
  - Background, Objectives, Methodology
- Experimental procedure
- Volume before compressor
- Resonator before compressor
  - Low Frequency resonator (≈10 Hz)
  - High Frequency resonator (≈50 Hz)
- Discussion
- Conclusions

# Low frequency resonator tests

| | | | | |
|---|---|---|---|---|
| Volume (L) | 3 | 3 | 3 | 3 |
| **Length (mm)** | **780** | **499** | **347** | **222** |
| Diameter (mm) | 8 | 8 | 8 | 8 |
| Section (mm²) | 50 | 50 | 50 | 50 |
| **Frequency (Hz)** | **8** | **10** | **12** | **15** |

| | | | | | |
|---|---|---|---|---|---|
| **Volume (L)** | **1.0** | **1.5** | **2.0** | **2.5** | **3.0** |
| **Length (mm)** | **1040** | **693** | **520** | **416** | **347** |
| Diameter (mm) | 8 | 8 | 8 | 8 | 8 |
| Section (mm²) | 50 | 50 | 50 | 50 | 50 |
| Frequency (Hz) | 12 | 12 | 12 | 12 | 12 |

| | | | | |
|---|---|---|---|---|
| Volume (L) | 2 | 2 | 2 | 2 |
| **Length (mm)** | **293** | **520** | **813** | **1170** |
| **Diameter (mm)** | **6** | **8** | **10** | **12** |
| Section (mm²) | 28 | 50 | 79 | 113 |
| Frequency (Hz) | 12 | 12 | 12 | 12 |

# Essais resonateur

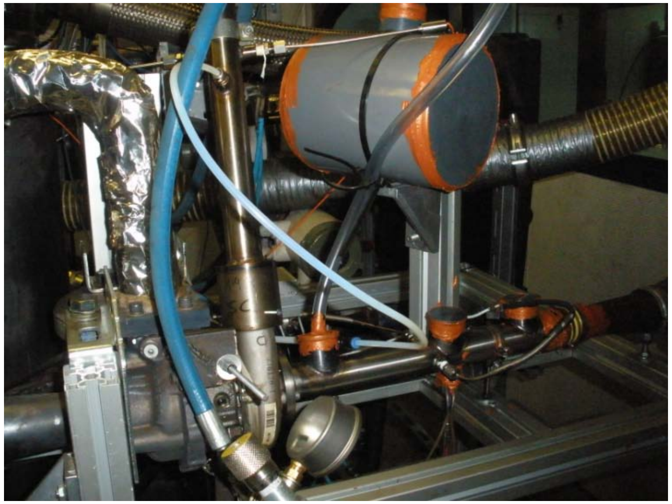

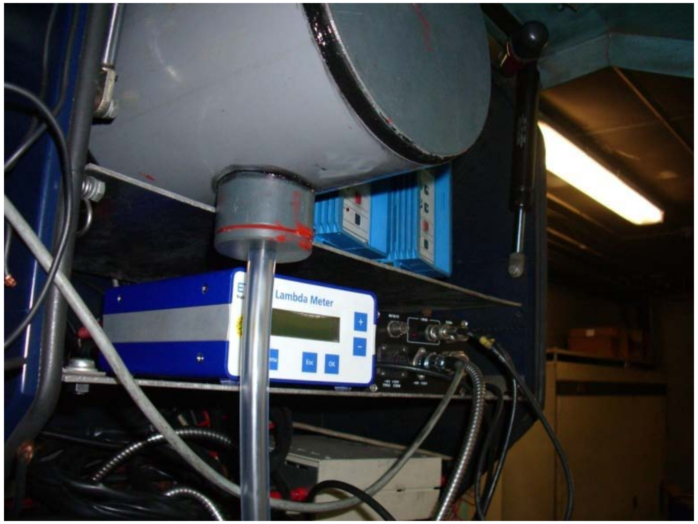


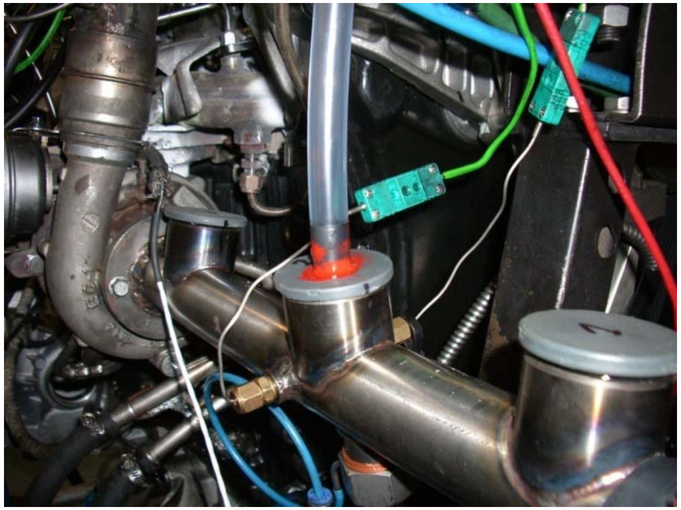

# LF resonator: length effect

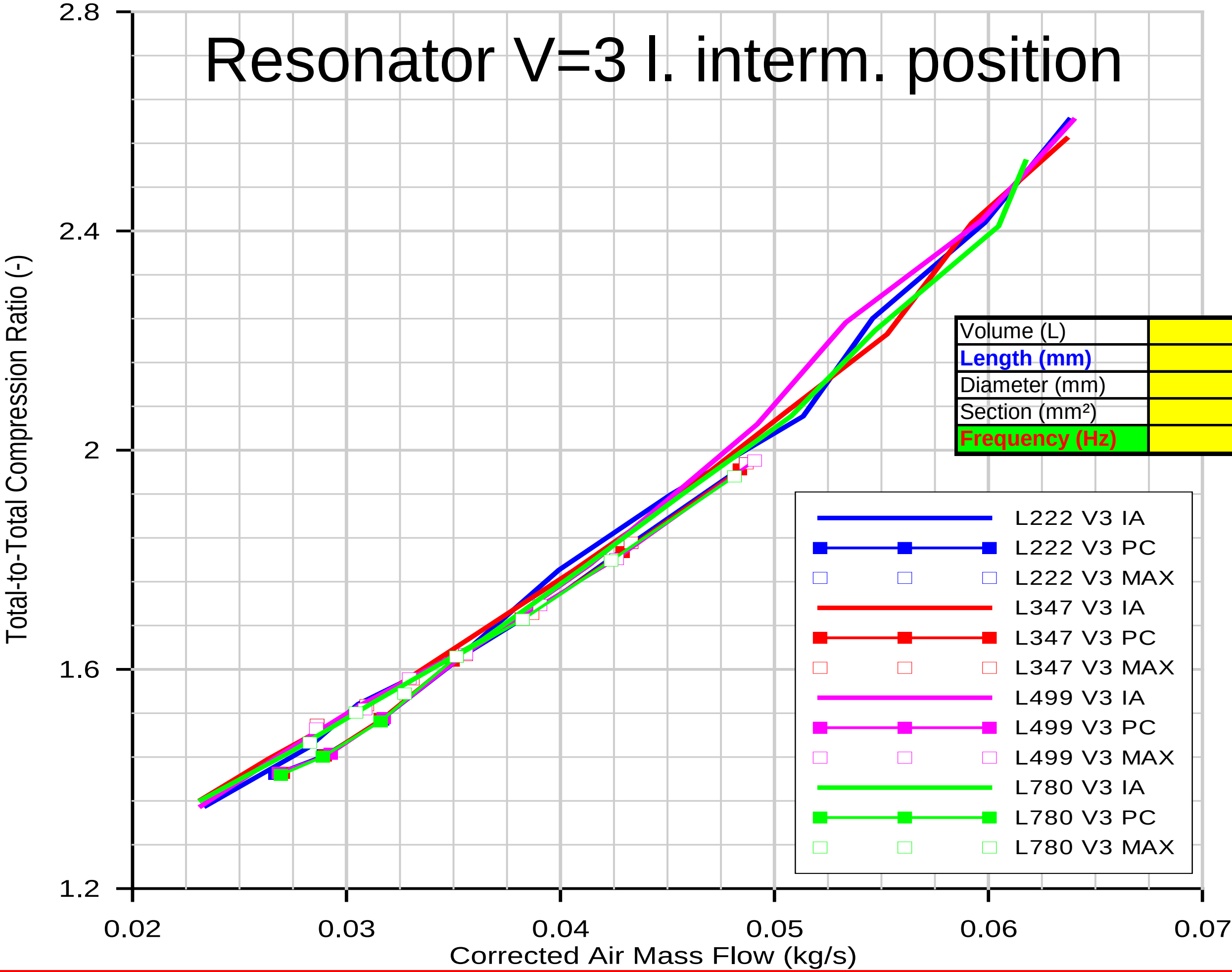


| | | | | |
|---|---|---|---|---|
| Volume (L) | 3 | 3 | 3 | 3 |
| **Length (mm)** | **780** | **499** | **347** | **222** |
| Diameter (mm) | 8 | 8 | 8 | 8 |
| Section (mm²) | 50 | 50 | 50 | 50 |
| **Frequency (Hz)** | **8** | **10** | **12** | **15** |

# LF resonator: length effect

Resonator V=3 l. interm. position

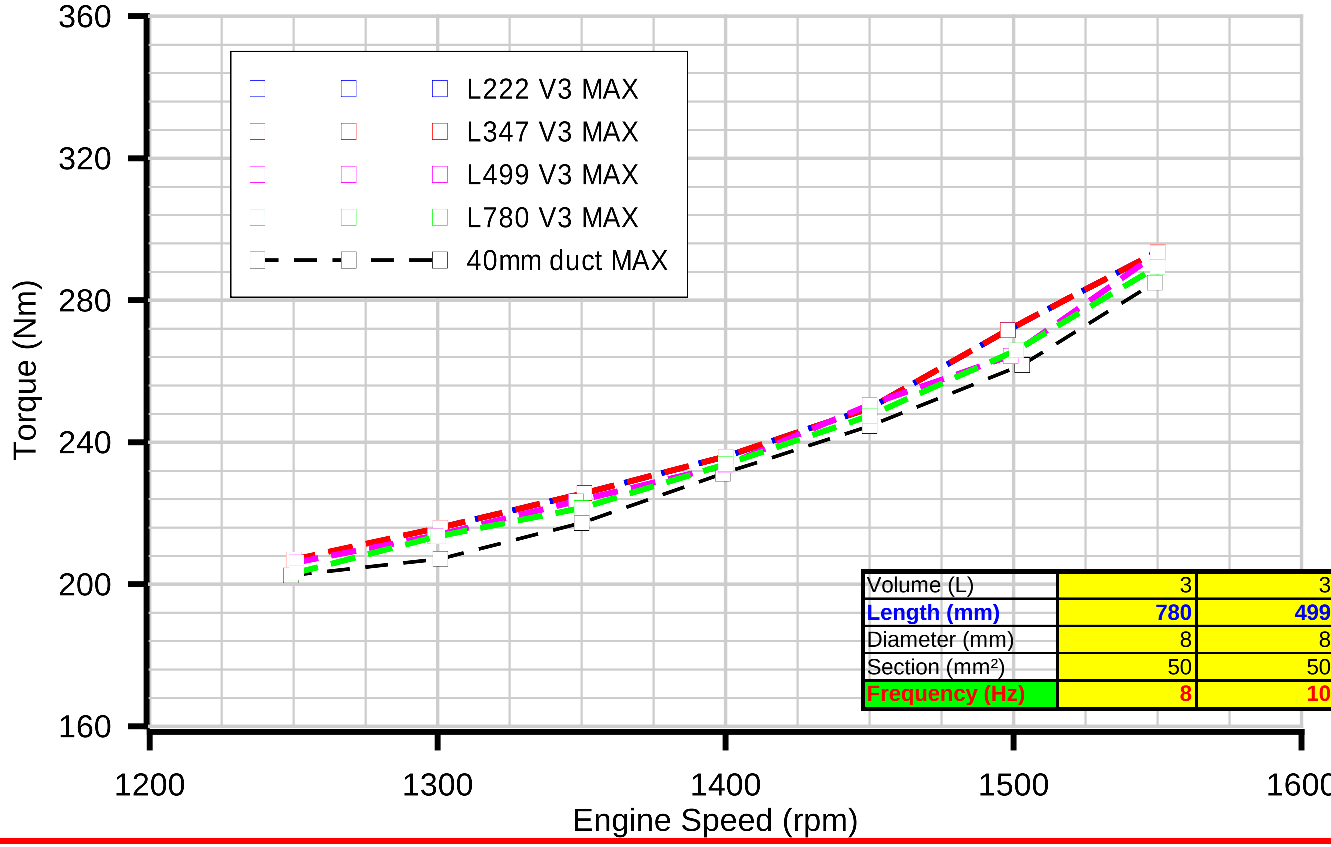


| | | | | |
|---|---|---|---|---|
| Volume (L) | 3 | 3 | 3 | 3 |
| **Length (mm)** | **780** | **499** | **347** | **222** |
| Diameter (mm) | 8 | 8 | 8 | 8 |
| Section (mm²) | 50 | 50 | 50 | 50 |
| **Frequency (Hz)** | **8** | **10** | **12** | **15** |

# ❑LF resonator: length effect

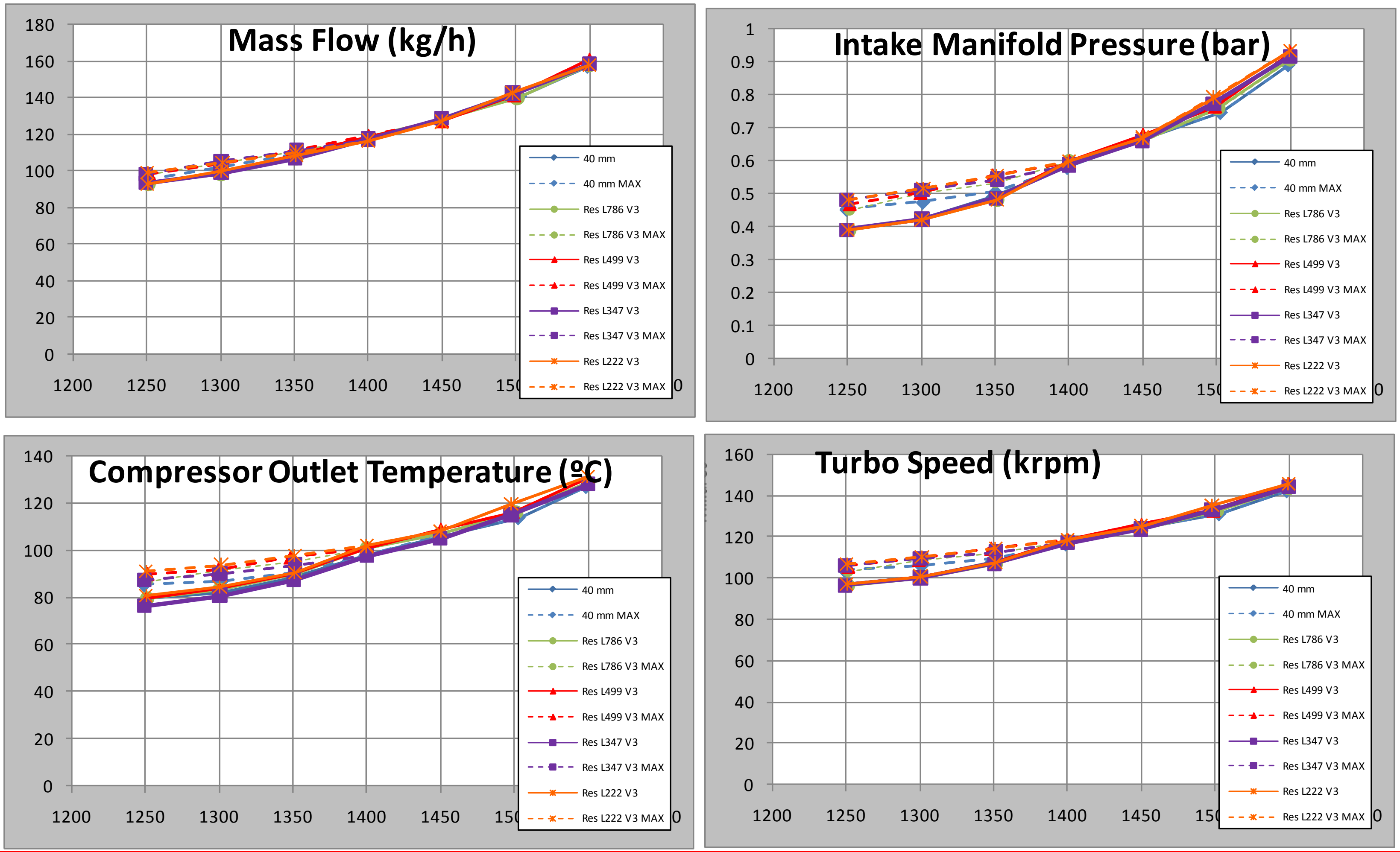


Resonator V=3 l. interm. position

# ❑LF resonator: volume effect

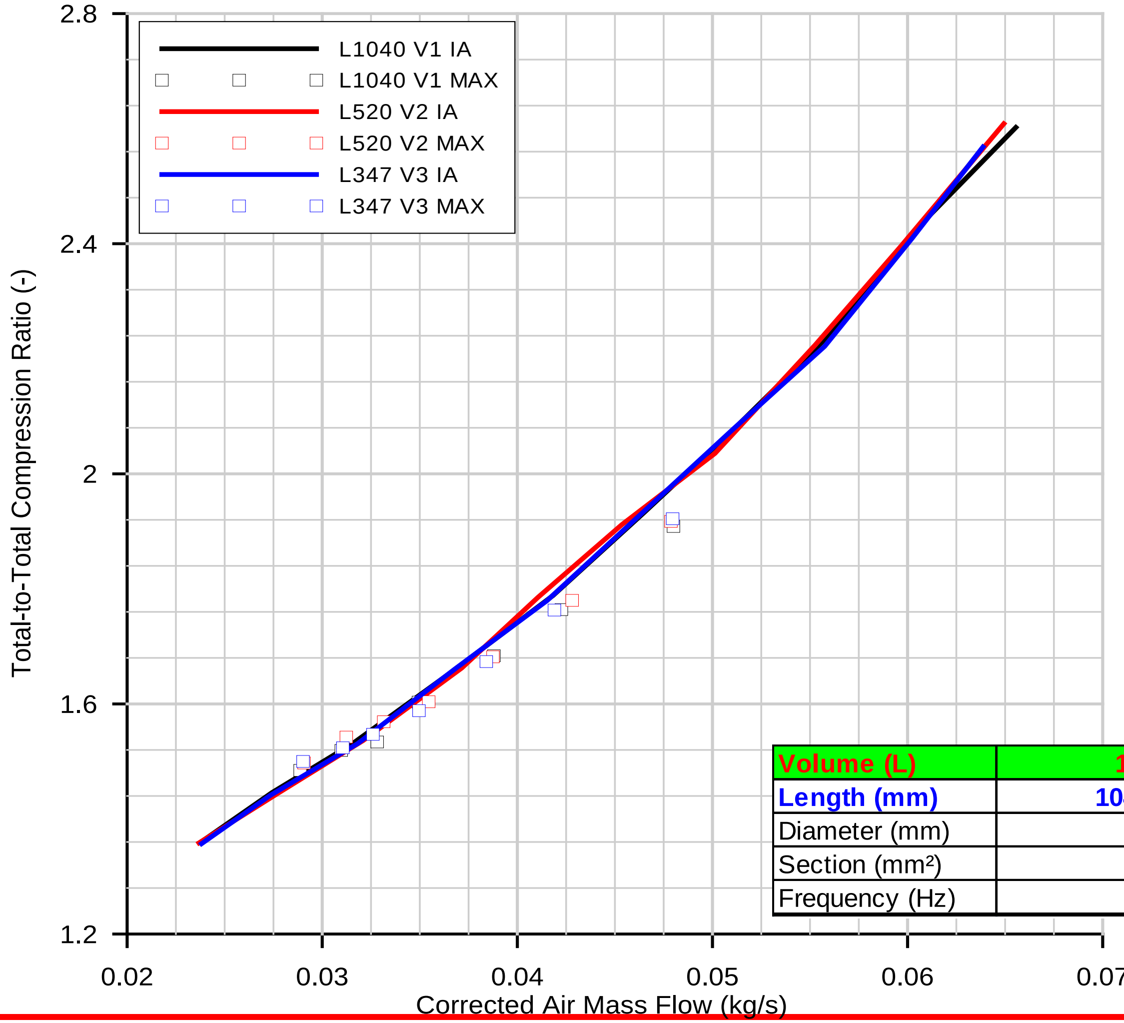


| Volume (L) | 1.0 | 2.0 | 3.0 |
|---|---|---|---|
| Length (mm) | 1040 | 520 | 347 |
| Diameter (mm) | 8 | 8 | 8 |
| Section (mm²) | 50 | 50 | 50 |
| Frequency (Hz) | 12 | 12 | 12 |

# LF resonator: volume effect

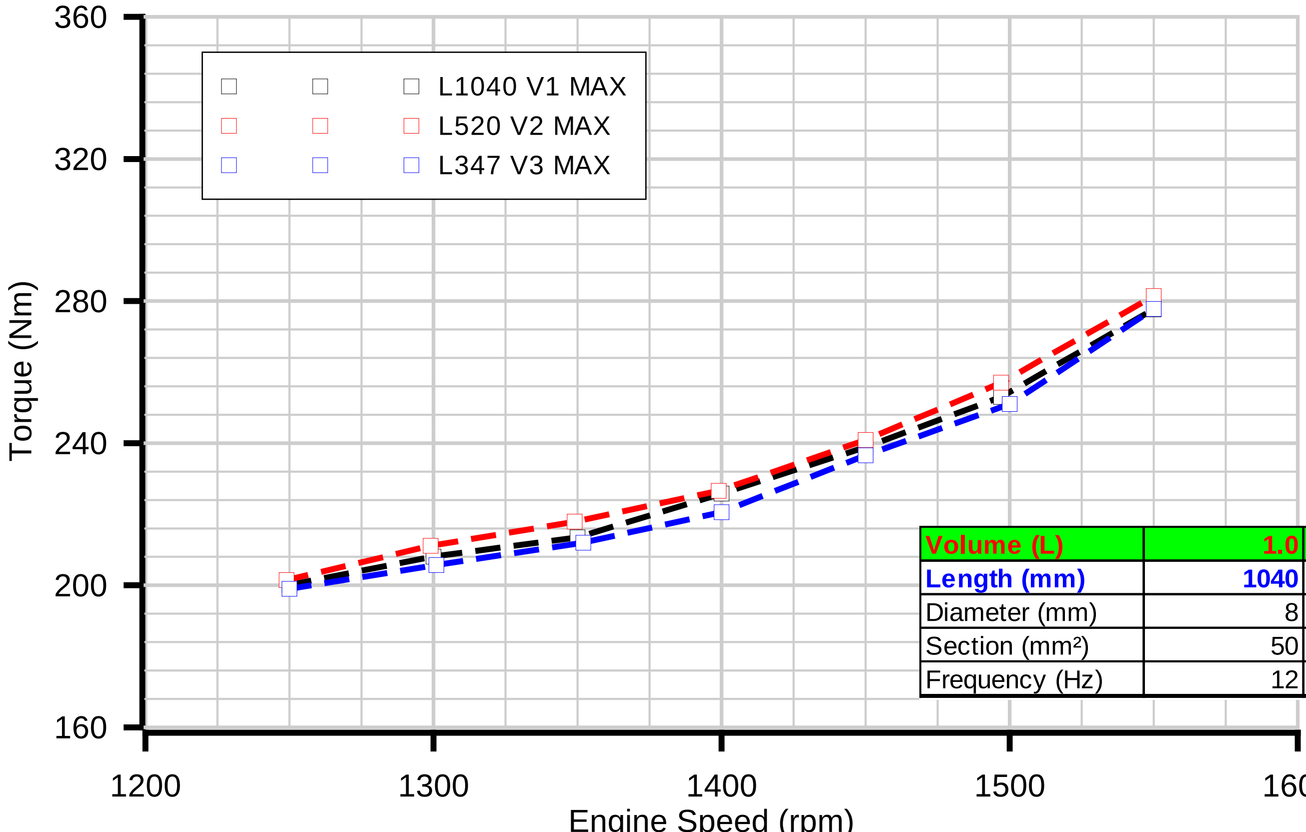


| Volume (L) | 1.0 | 2.0 | 3.0 |
|---|---|---|---|
| **Length (mm)** | **1040** | **520** | **347** |
| Diameter (mm) | 8 | 8 | 8 |
| Section (mm²) | 50 | 50 | 50 |
| Frequency (Hz) | 12 | 12 | 12 |

# ❑LF resonator: Diameter effect

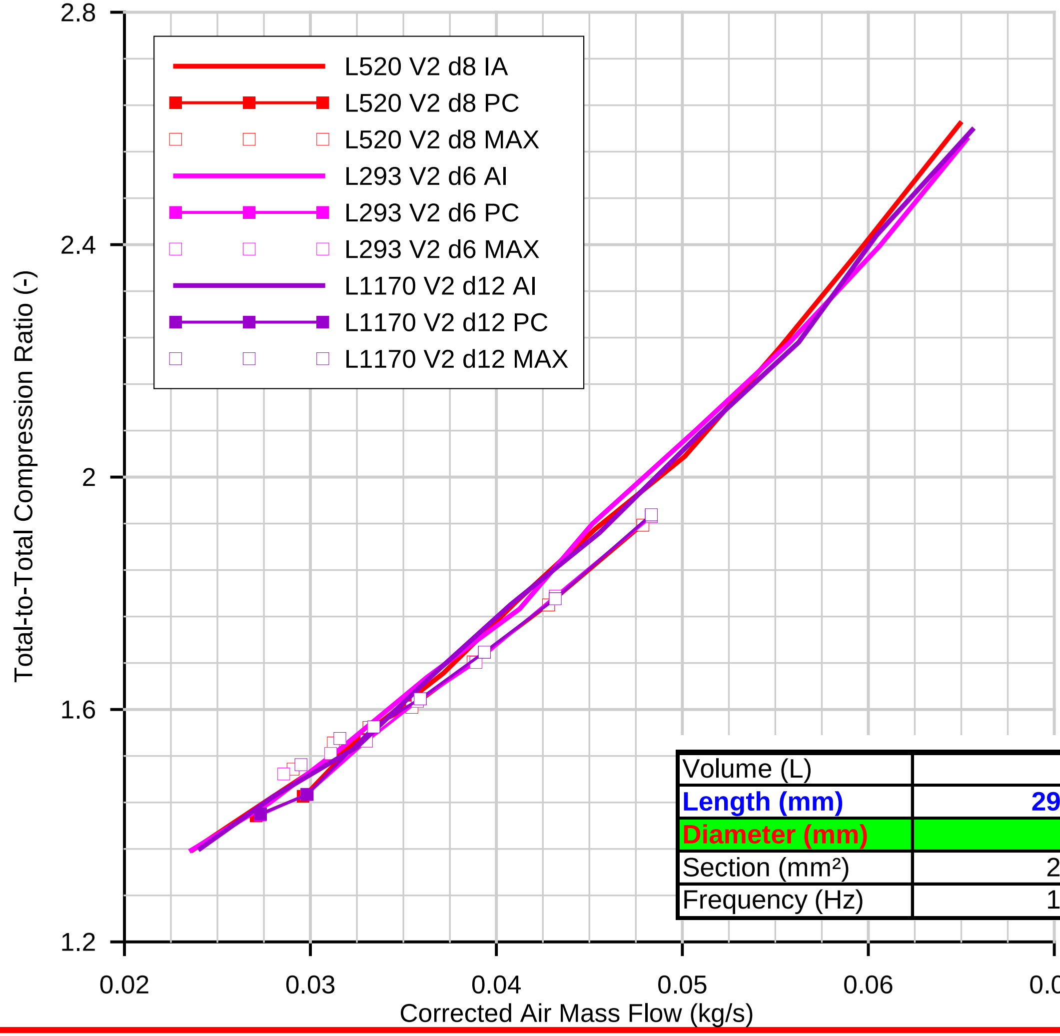


| | | | | |
|---|---|---|---|---|
| Volume (L) | 2 | 2 | 2 | 2 |
| **Length (mm)** | **293** | **520** | **813** | **1170** |
| **Diameter (mm)** | **6** | **8** | **10** | **12** |
| Section (mm²) | 28 | 50 | 79 | 113 |
| Frequency (Hz) | 12 | 12 | 12 | 12 |

# LF resonator: Diameter effect

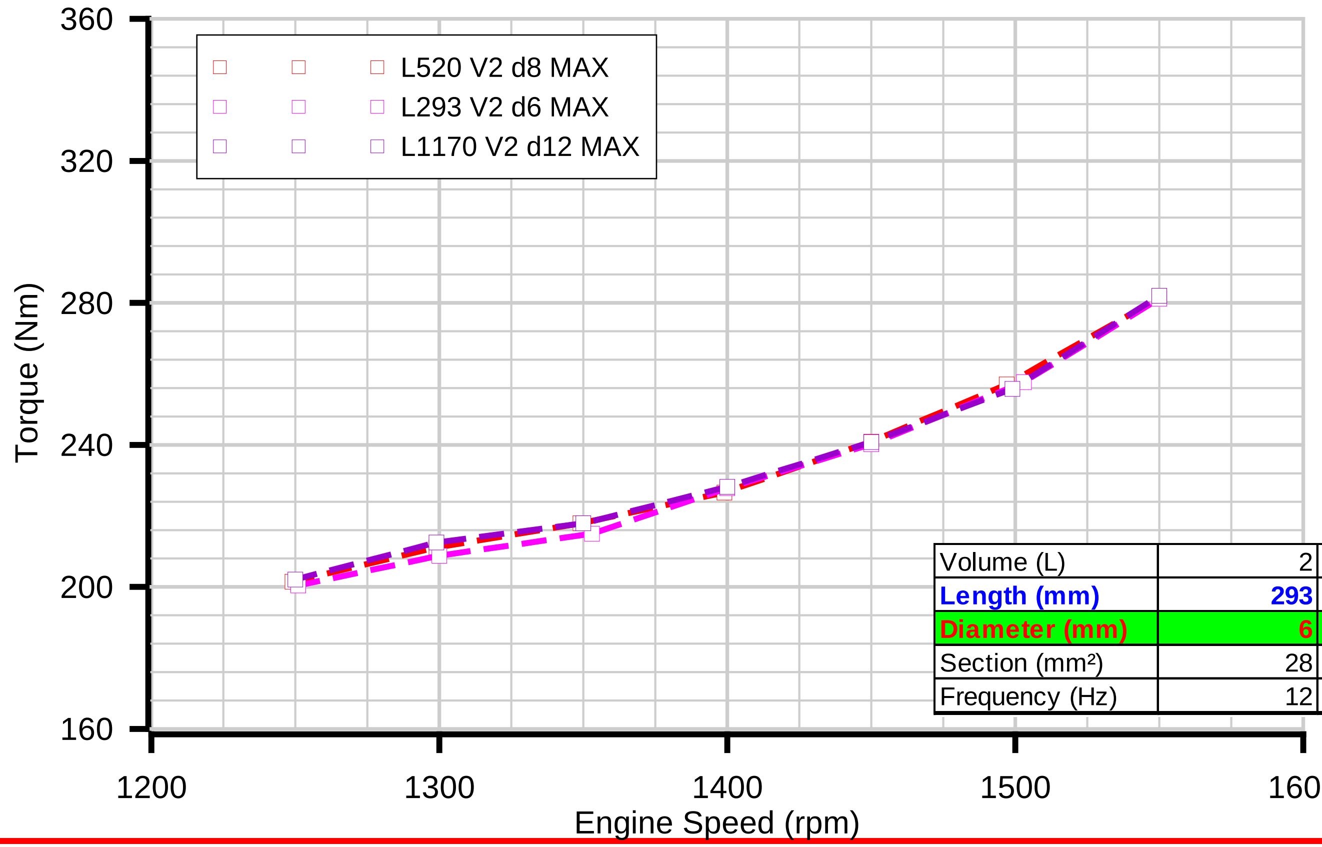


| | | | |
|---|---|---|---|
| Volume (L) | 2 | 2 | 2 |
| **Length (mm)** | **293** | **520** | **1170** |
| **Diameter (mm)** | **6** | **8** | **12** |
| Section (mm²) | 28 | 50 | 113 |
| Frequency (Hz) | 12 | 12 | 12 |

# LF resonator: Position effect

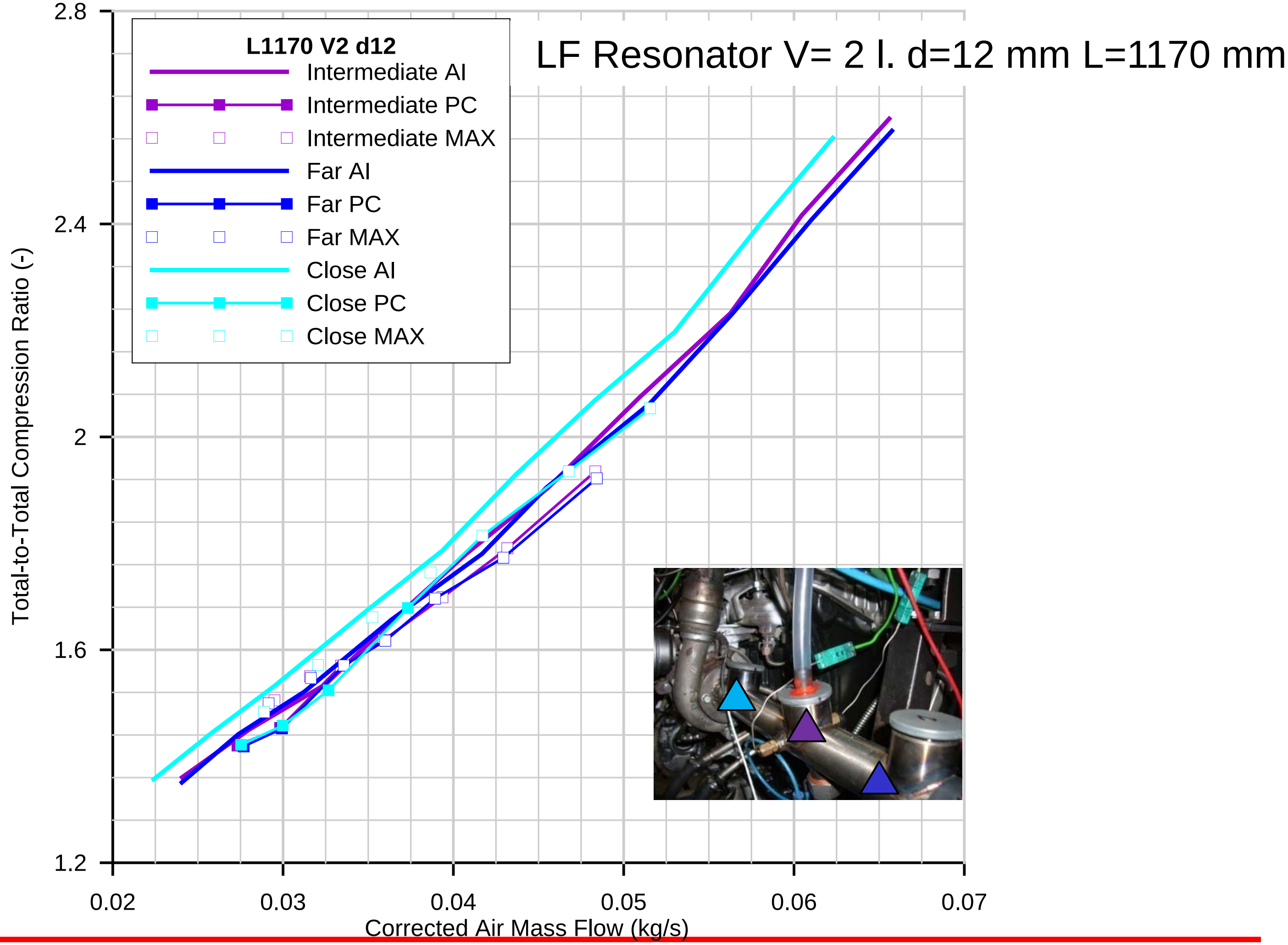

# LF resonator: Position effect

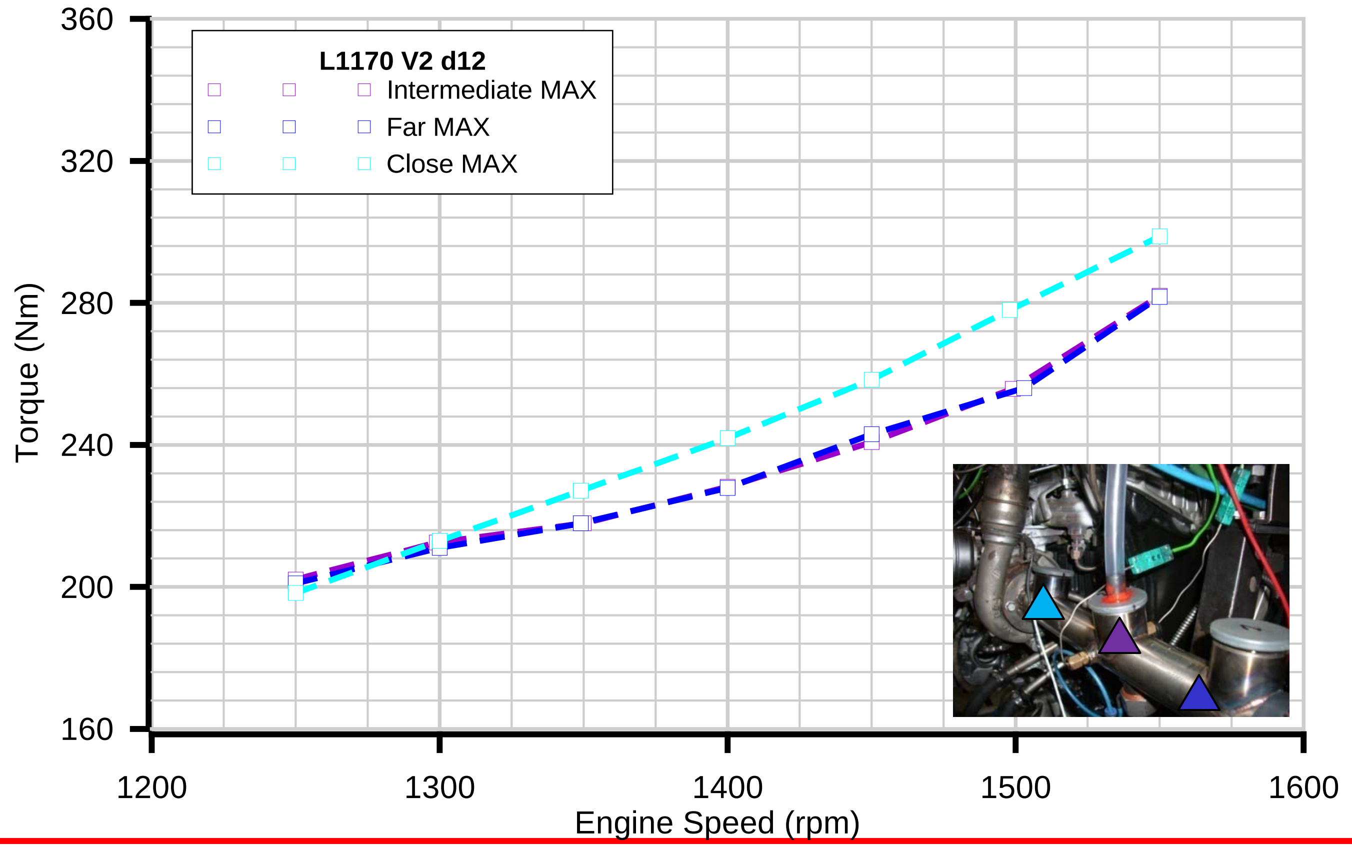

# LF resonator: Diameter effect

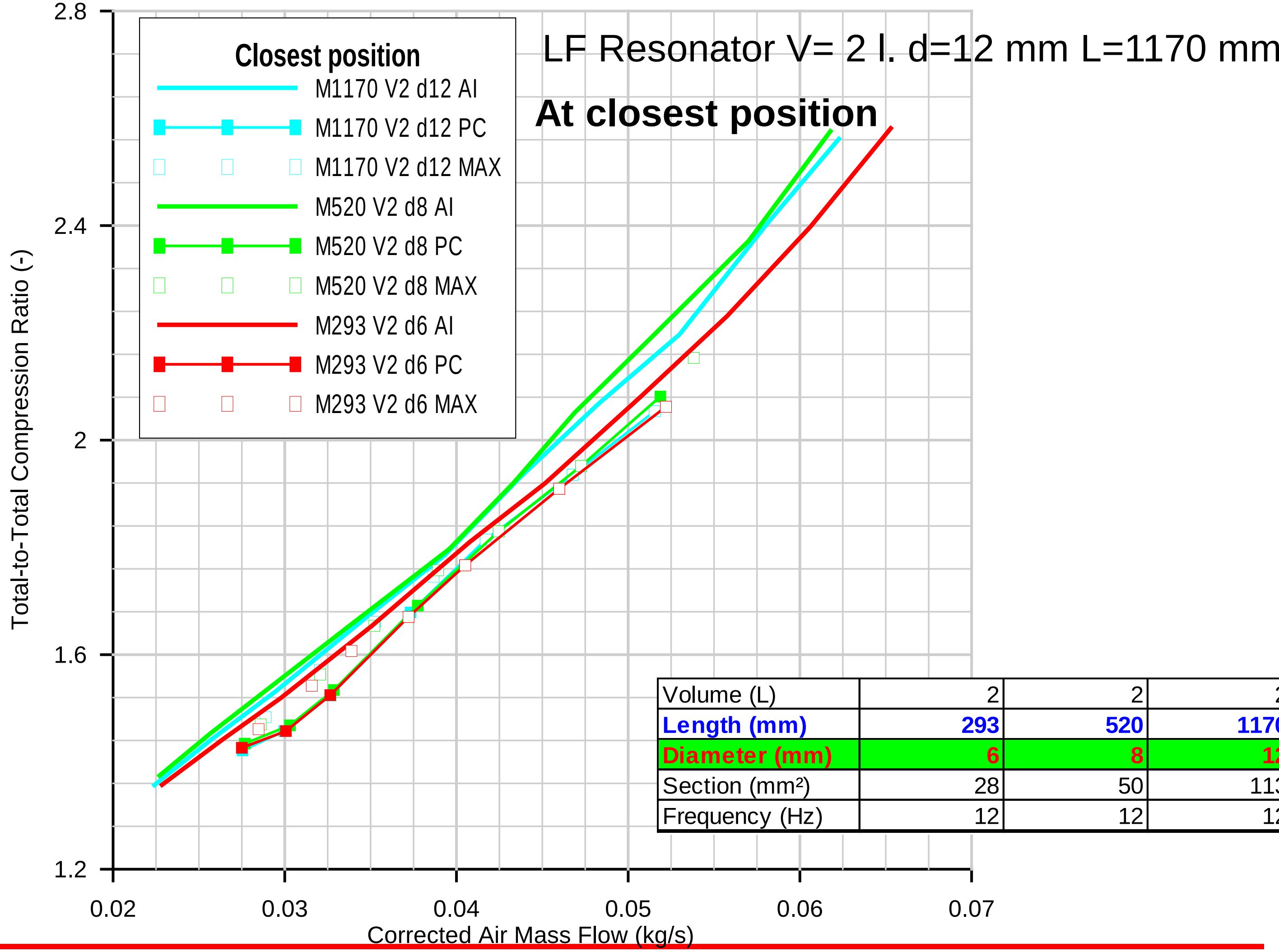


| Volume (L) | 2 | 2 | 2 |
|---|---|---|---|
| **Length (mm)** | **293** | **520** | **1170** |
| **Diameter (mm)** | **6** | **8** | **12** |
| Section (mm²) | 28 | 50 | 113 |
| Frequency (Hz) | 12 | 12 | 12 |

# LF resonator: Diameter effect

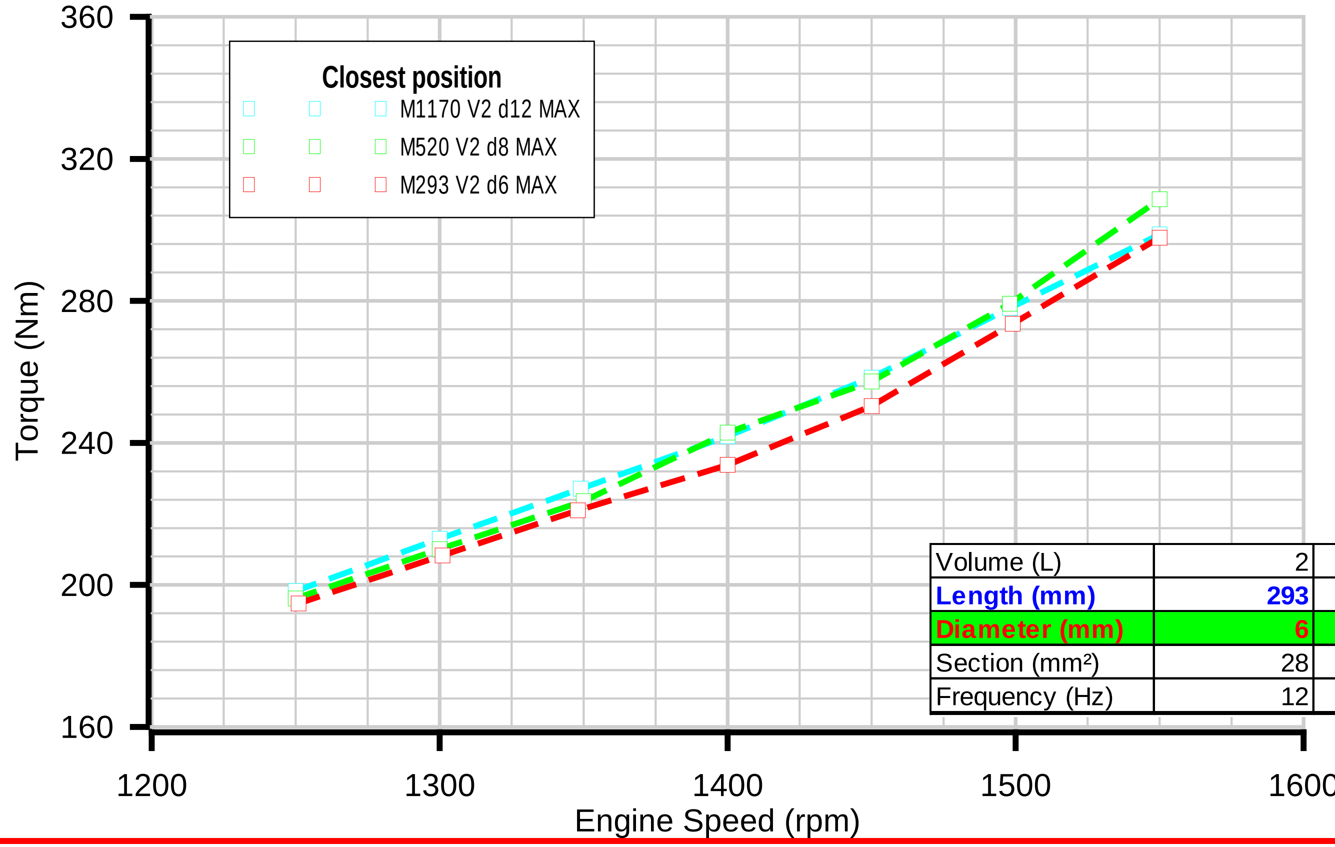


| | | | |
|---|---|---|---|
| Volume (L) | 2 | 2 | 2 |
| **Length (mm)** | **293** | **520** | **1170** |
| **Diameter (mm)** | **6** | **8** | **12** |
| Section (mm²) | 28 | 50 | 113 |
| Frequency (Hz) | 12 | 12 | 12 |

# LF resonator: volume effect

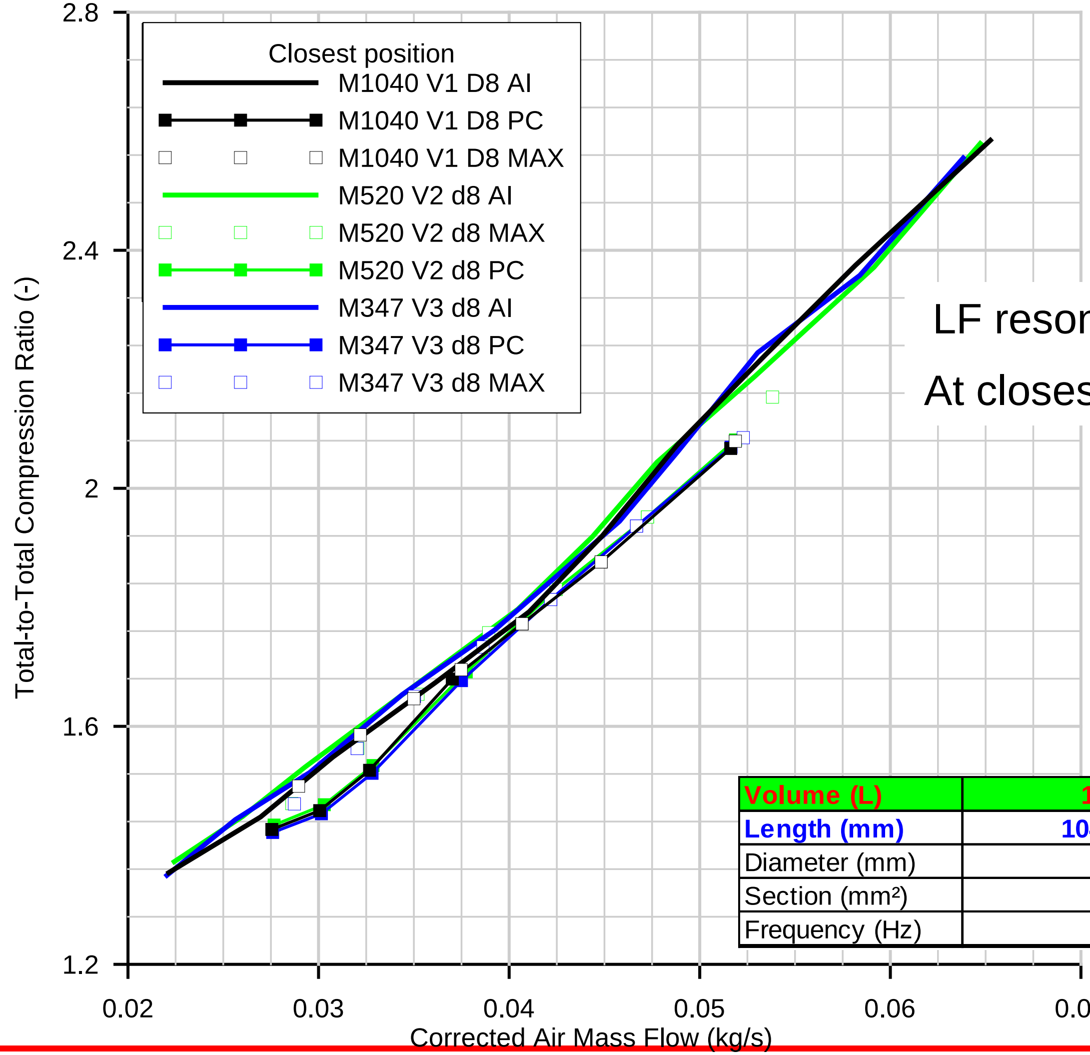


LF resonator d=8 mm

At closest position

| Volume (L) | 1.0 | 2.0 | 3.0 |
|---|---|---|---|
| Length (mm) | 1040 | 520 | 347 |
| Diameter (mm) | 8 | 8 | 8 |
| Section (mm²) | 50 | 50 | 50 |
| Frequency (Hz) | 12 | 12 | 12 |

# LF resonator: volume effect

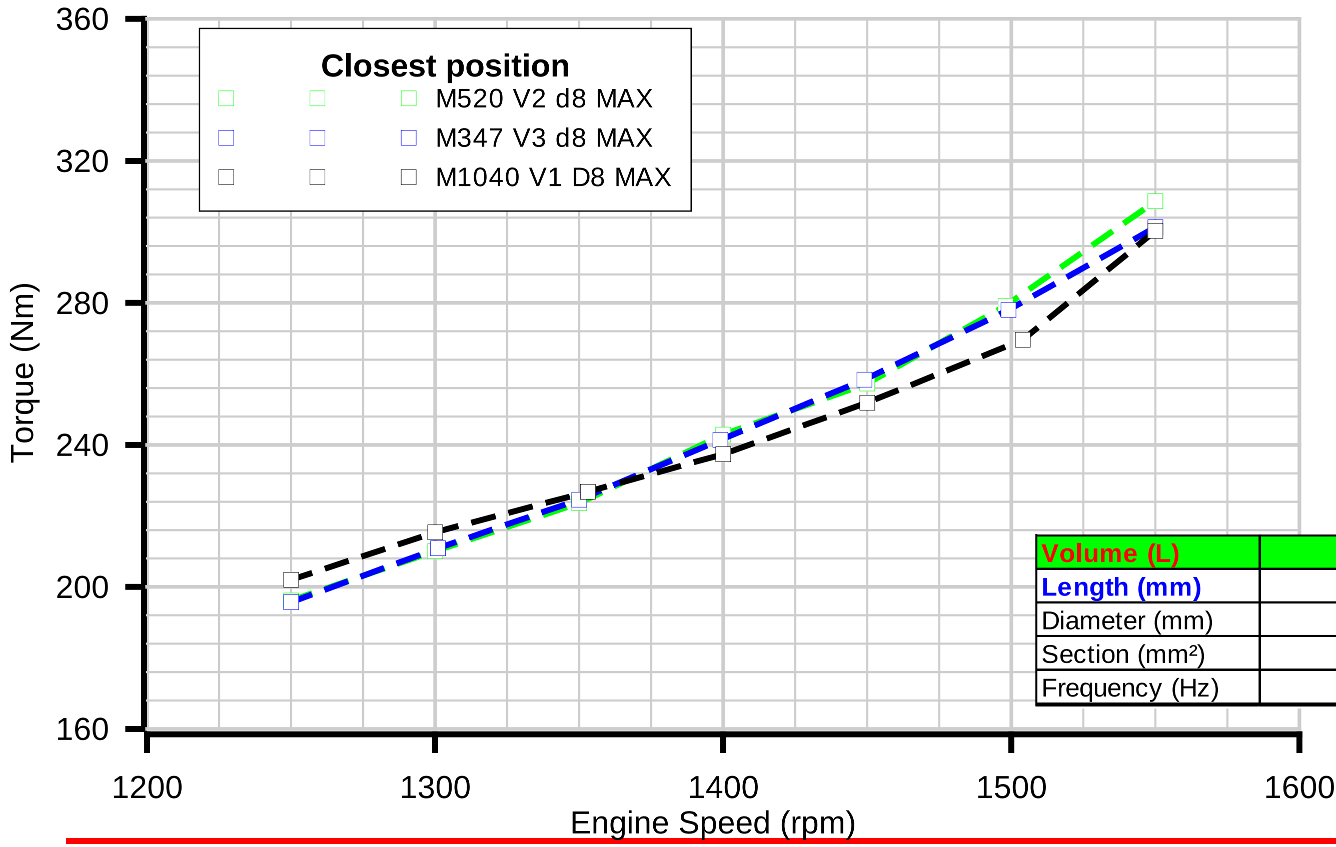


| Volume (L) | 1.0 | 2.0 | 3.0 |
|---|---|---|---|
| Length (mm) | 1040 | 520 | 347 |
| Diameter (mm) | 8 | 8 | 8 |
| Section (mm²) | 50 | 50 | 50 |
| Frequency (Hz) | 12 | 12 | 12 |

# LF resonator: length effect

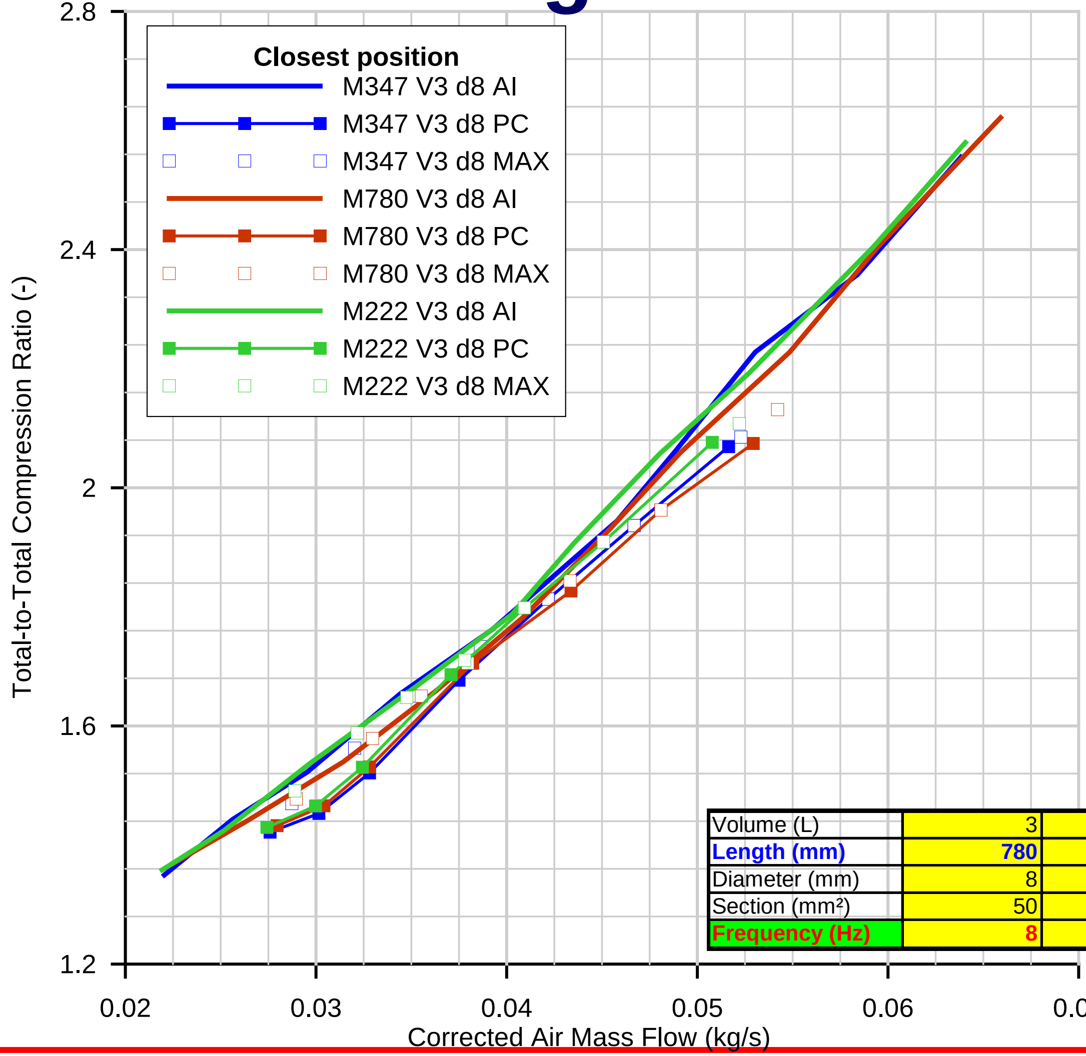


| | | | | |
|---|---|---|---|---|
| Volume (L) | 3 | 3 | 3 | 3 |
| **Length (mm)** | **780** | **499** | **347** | **222** |
| Diameter (mm) | 8 | 8 | 8 | 8 |
| Section (mm²) | 50 | 50 | 50 | 50 |
| **Frequency (Hz)** | **8** | **10** | **12** | **15** |

# LF resonator: length effect

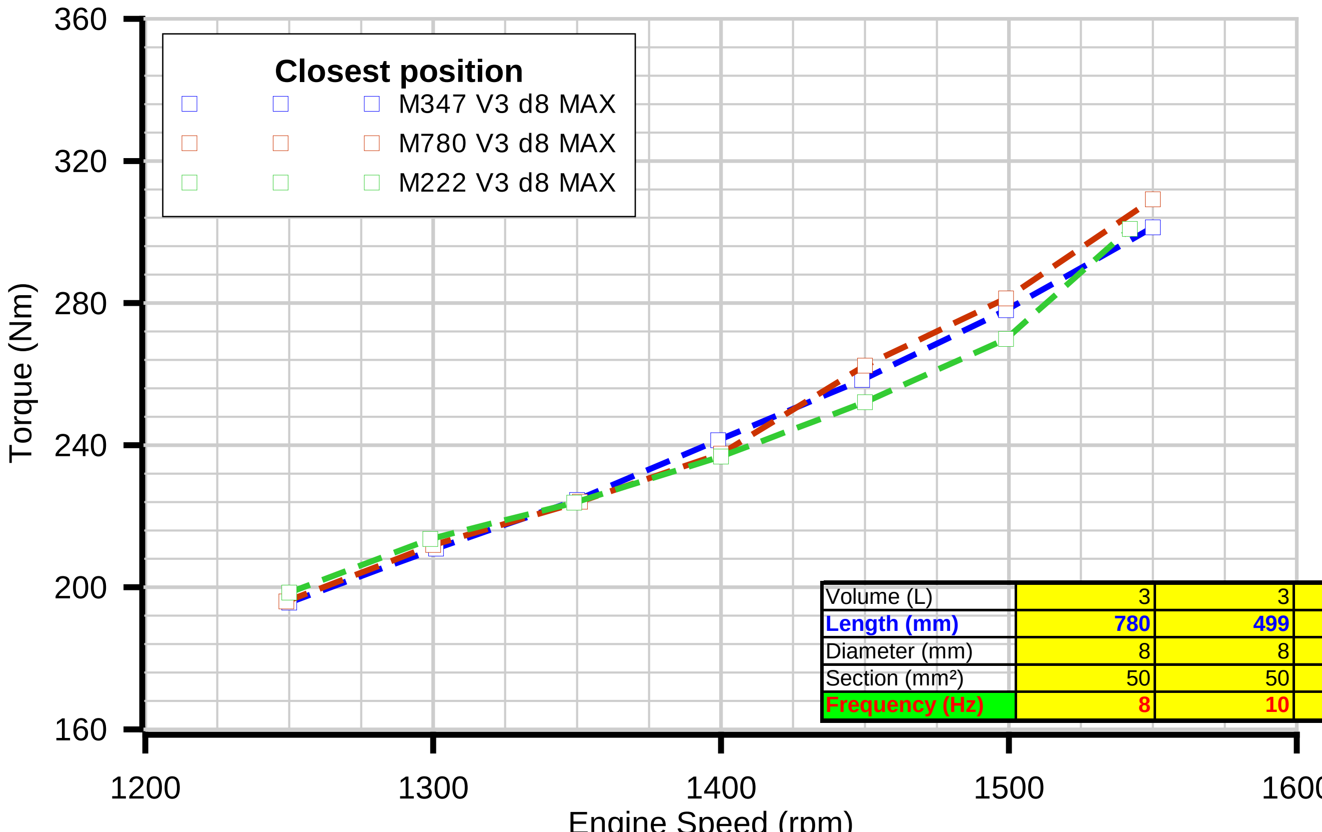


| | | | | |
|---|---|---|---|---|
| Volume (L) | 3 | 3 | 3 | 3 |
| **Length (mm)** | **780** | **499** | **347** | **222** |
| Diameter (mm) | 8 | 8 | 8 | 8 |
| Section (mm²) | 50 | 50 | 50 | 50 |
| **Frequency (Hz)** | **8** | **10** | **12** | **15** |

# ❑ Gas-Stand Tests: LF resonator Position effect

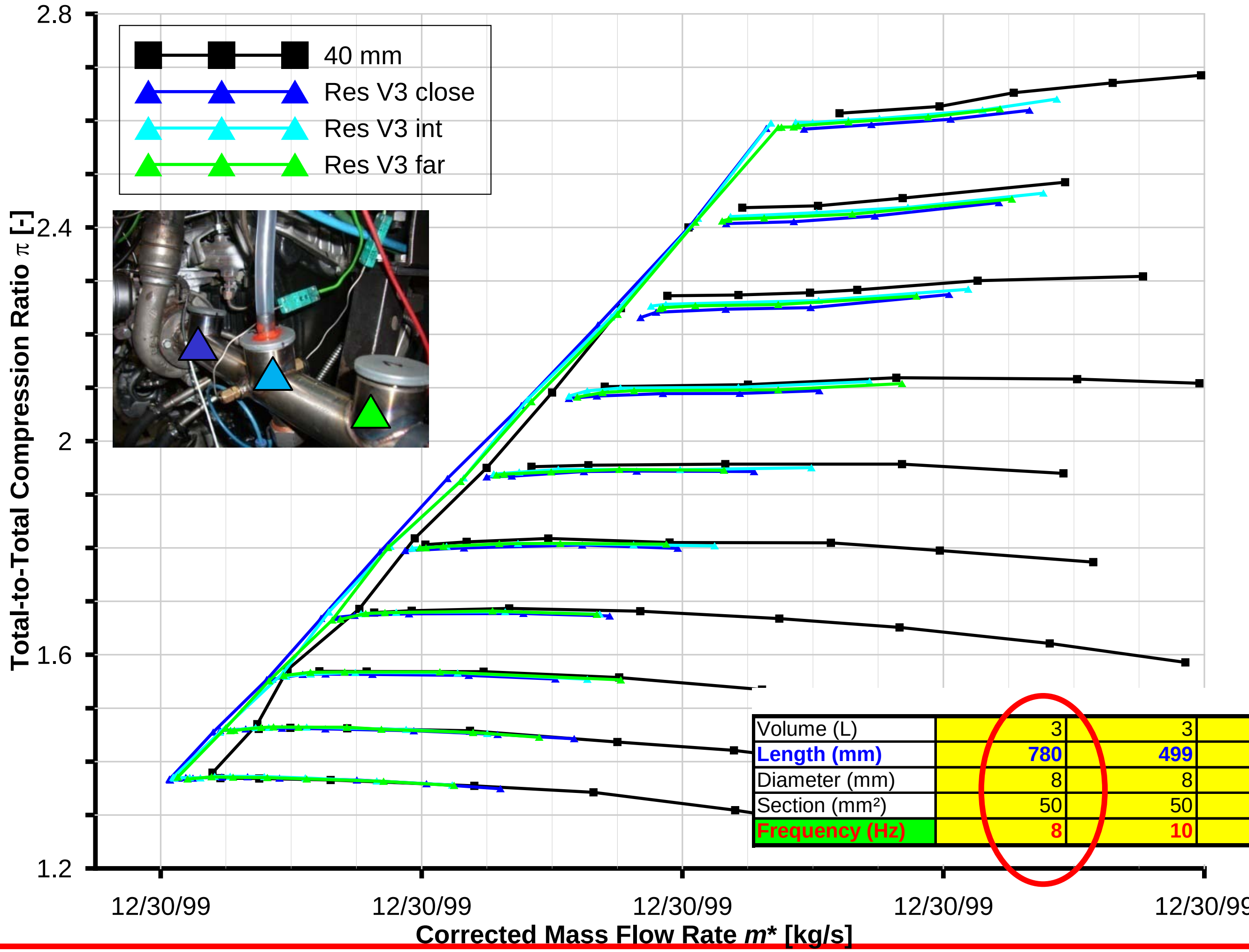


| | | | | |
|---|---|---|---|---|
| Volume (L) | 3 | 3 | 3 | 3 |
| **Length (mm)** | **780** | **499** | **347** | **222** |
| Diameter (mm) | 8 | 8 | 8 | 8 |
| Section (mm²) | 50 | 50 | 50 | 50 |
| **Frequency (Hz)** | **8** | **10** | **12** | **15** |

UNIVERSIDAD POLITECNICA DE VALENCIA

cmt motores térmicos

# ❑ Gas-Stand Tests: LF resonator Position effect

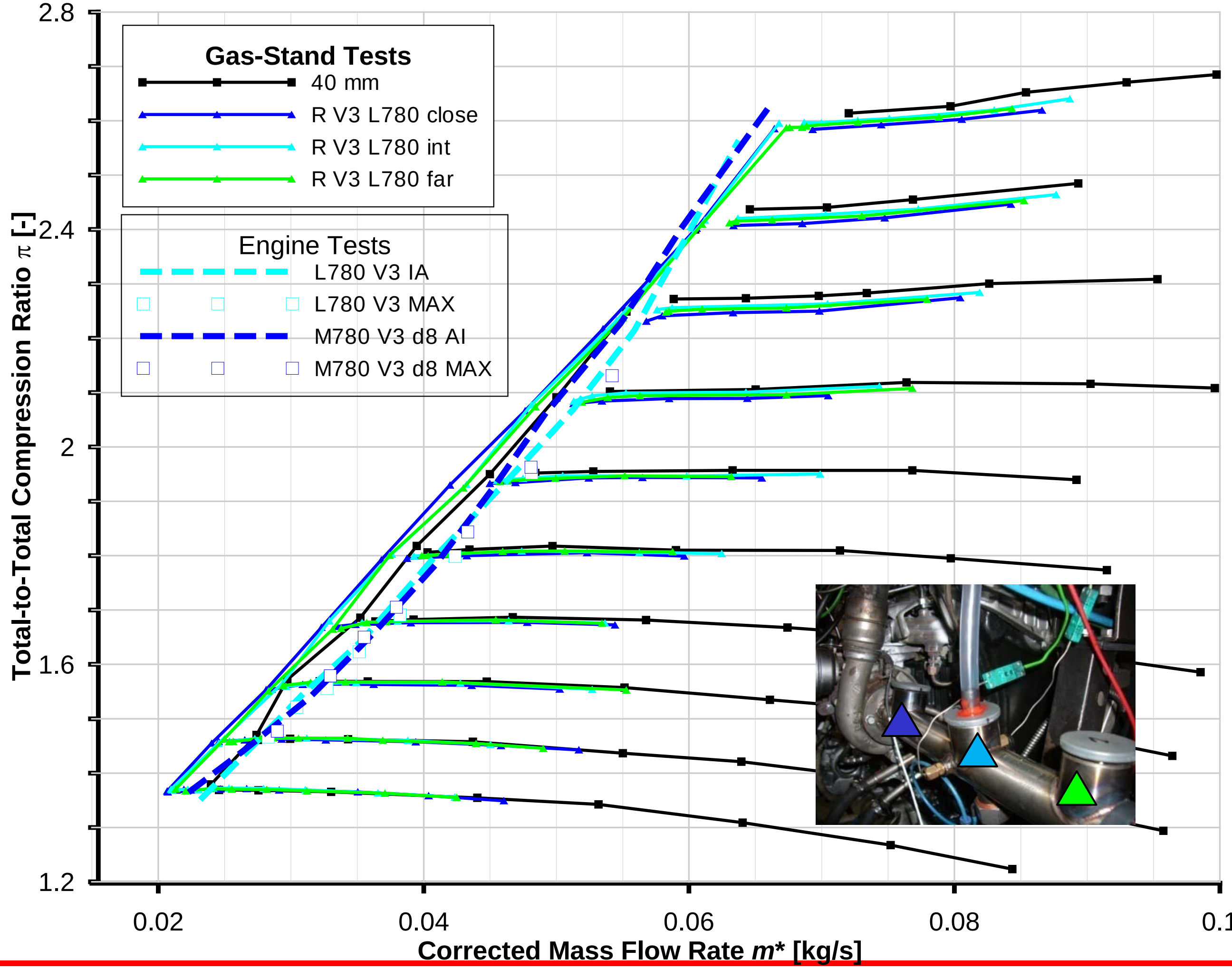

# ❑ Gas-Stand Tests: LF resonator Position effect

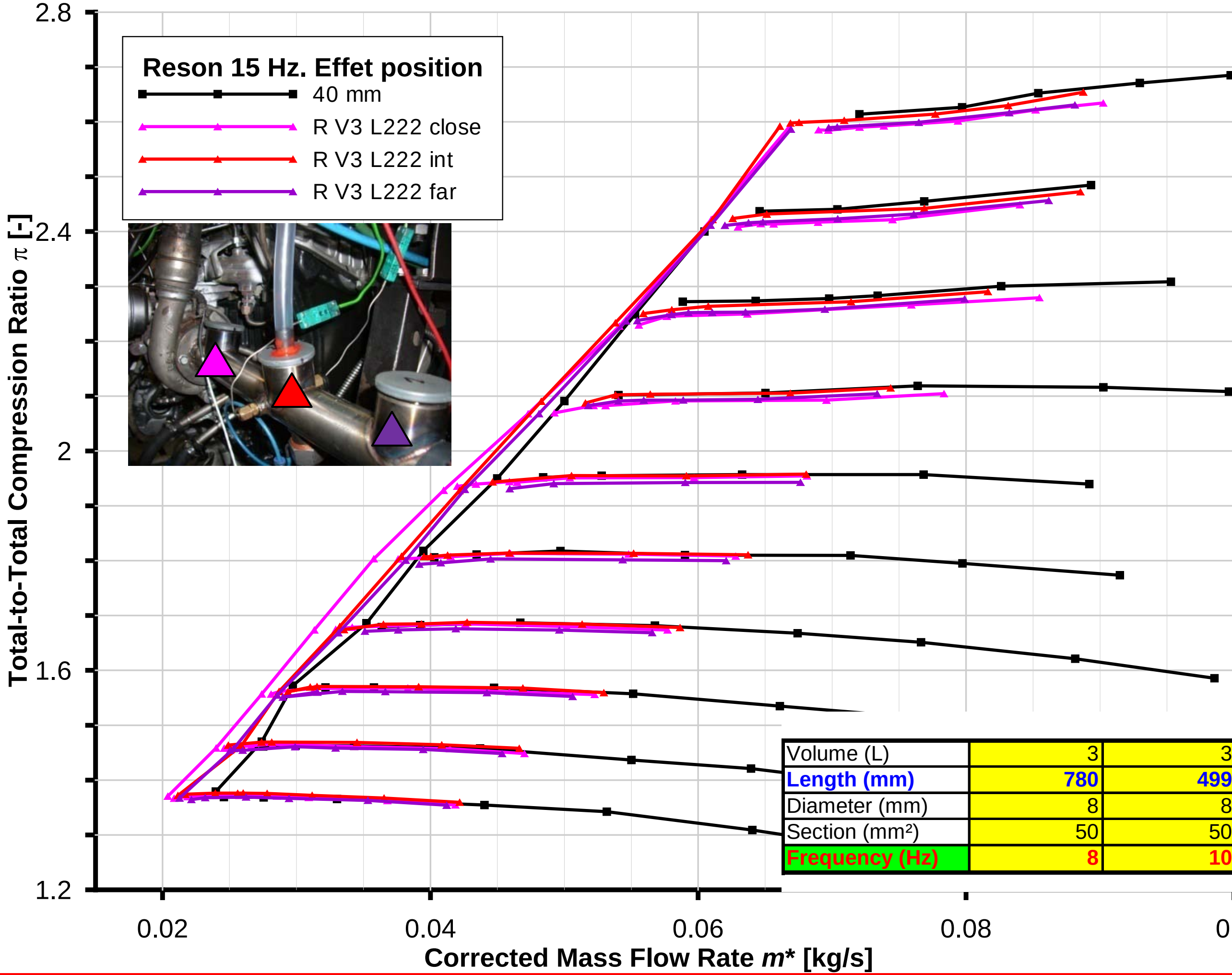


| | | | | |
|---|---|---|---|---|
| Volume (L) | 3 | 3 | 3 | 3 |
| **Length (mm)** | **780** | **499** | **347** | **222** |
| Diameter (mm) | 8 | 8 | 8 | 8 |
| Section (mm²) | 50 | 50 | 50 | 50 |
| **Frequency (Hz)** | **8** | **10** | **12** | **15** |

# Gas-Stand Tests: LF resonator Position effect

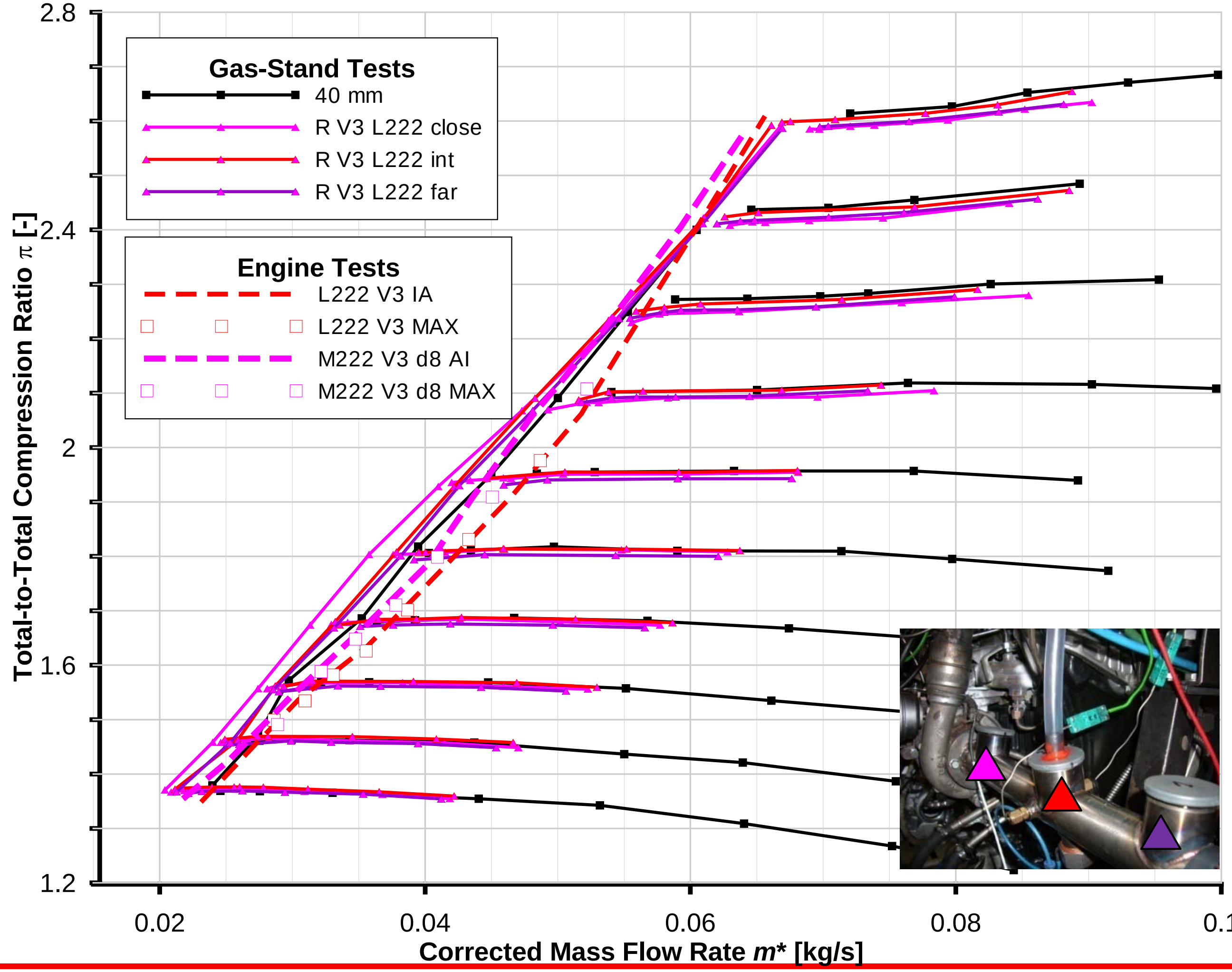

# Gas-Stand Tests:

| | | | | |
|---|---|---|---|---|
| Volume (L) | 3 | 3 | 3 | 3 |
| **Length (mm)** | **780** | **499** | **347** | **222** |
| Diameter (mm) | 8 | 8 | 8 | 8 |
| Section (mm²) | 50 | 50 | 50 | 50 |
| **Frequency (Hz)** | **8** | **10** | **12** | **15** |

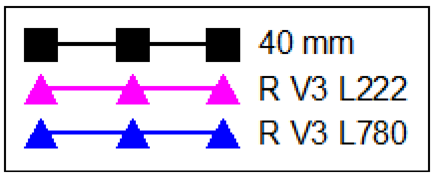


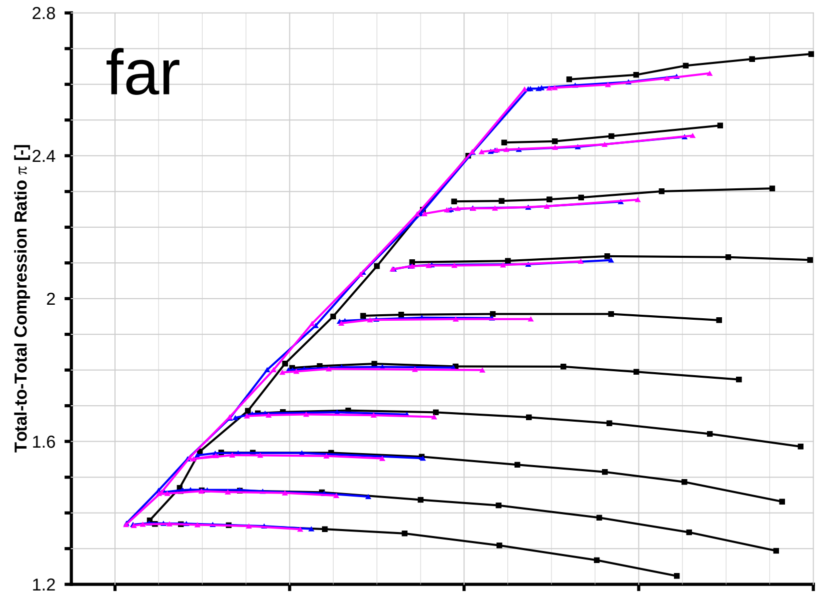


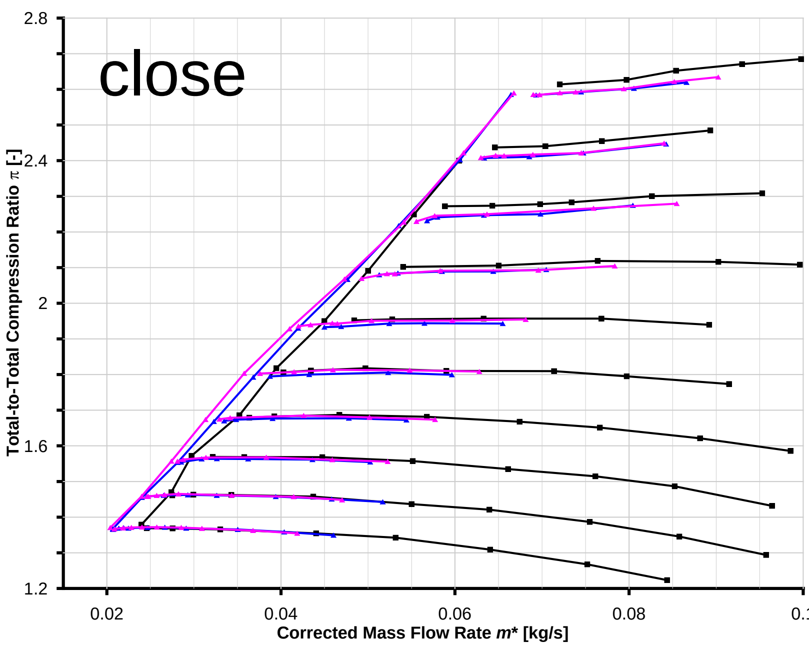


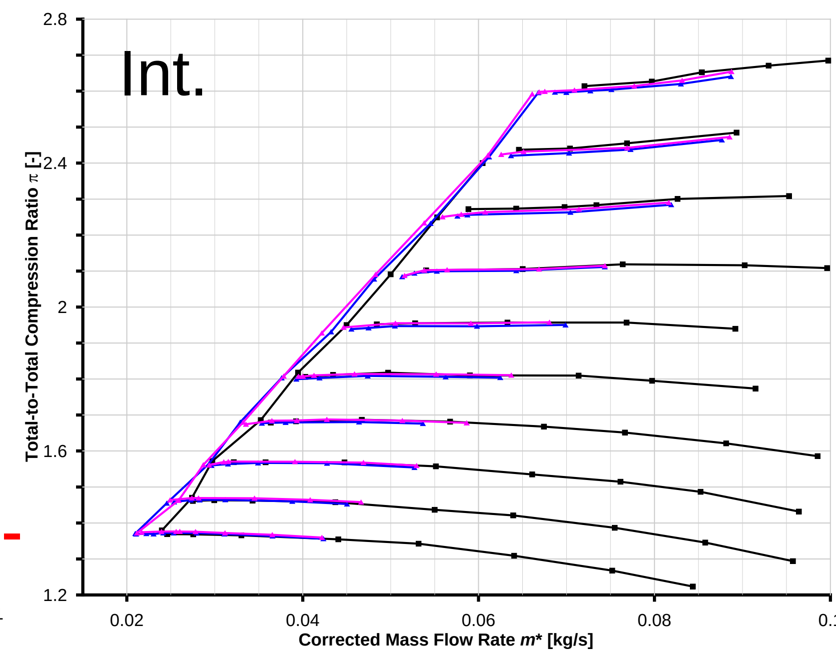

# ❑ Gas-Stand Tests: LF resonator, diameter effect

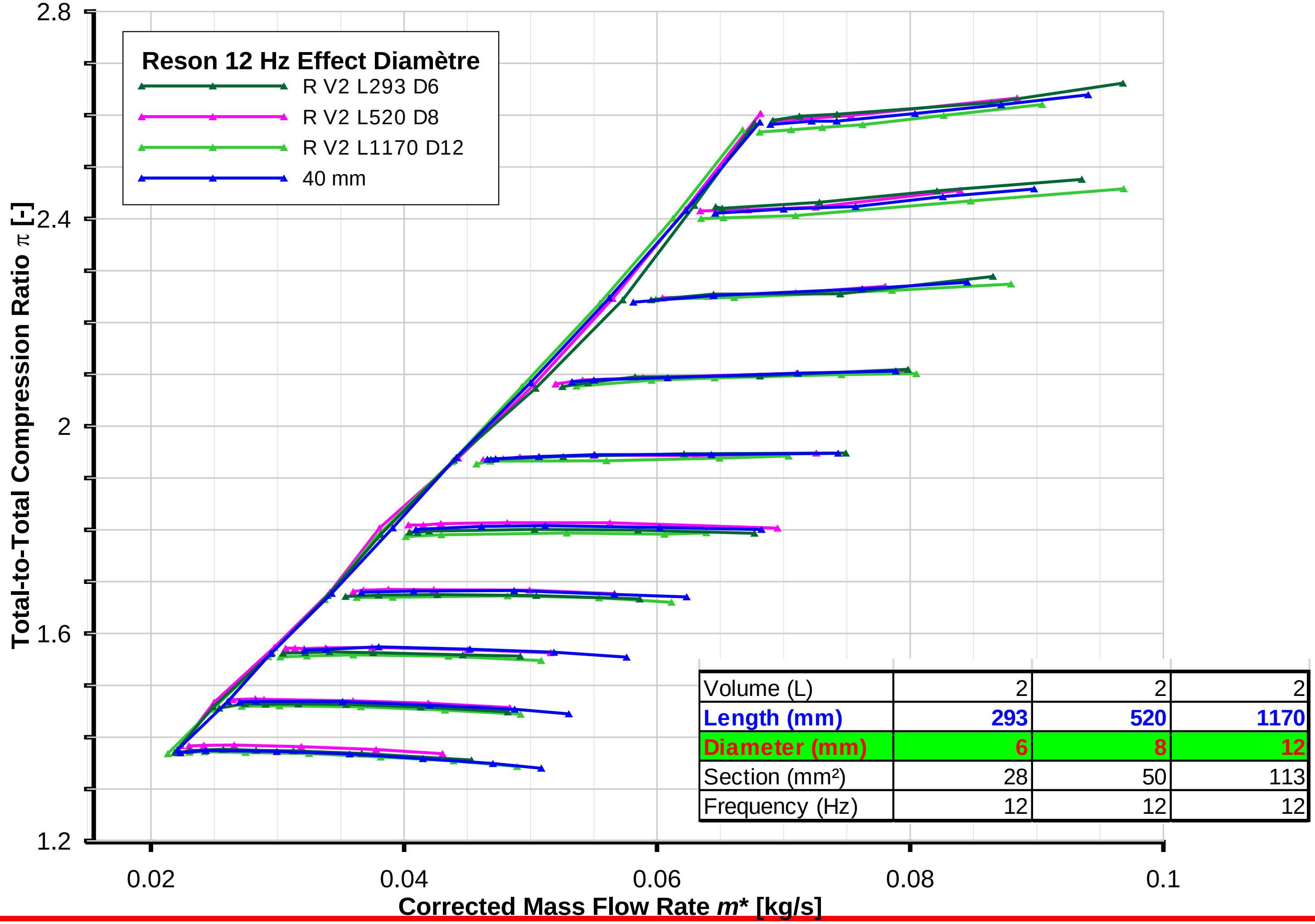


| | | | |
|---|---|---|---|
| Volume (L) | 2 | 2 | 2 |
| **Length (mm)** | **293** | **520** | **1170** |
| **Diameter (mm)** | **6** | **8** | **12** |
| Section (mm²) | 28 | 50 | 113 |
| Frequency (Hz) | 12 | 12 | 12 |

# ❑ Gas-Stand Tests: LF resonator, diameter effect

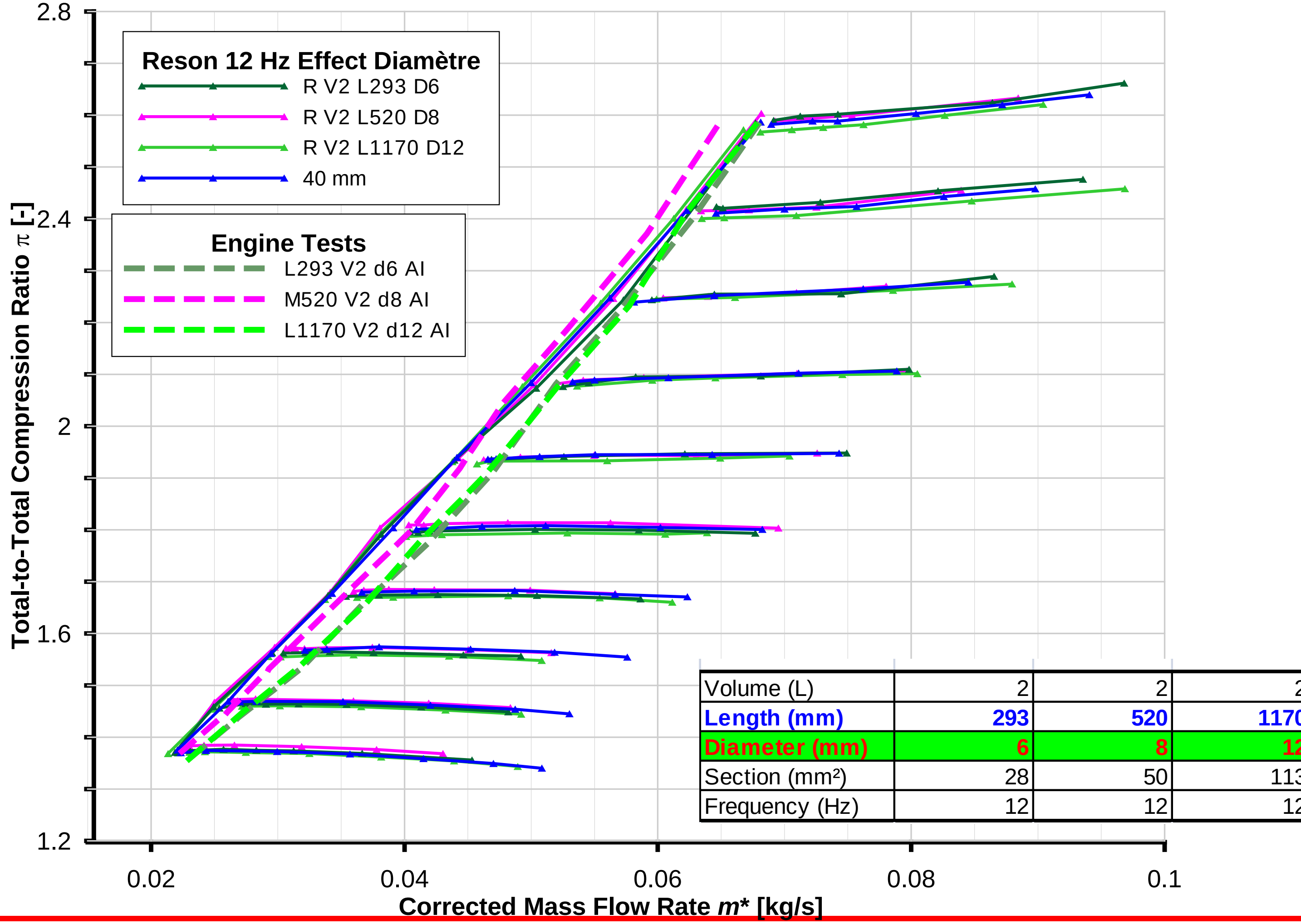


| | | | |
|---|---|---|---|
| Volume (L) | 2 | 2 | 2 |
| **Length (mm)** | **293** | **520** | **1170** |
| **Diameter (mm)** | **6** | **8** | **12** |
| Section (mm²) | 28 | 50 | 113 |
| Frequency (Hz) | 12 | 12 | 12 |

# Gas-Stand Tests: LF resonator, volume effect

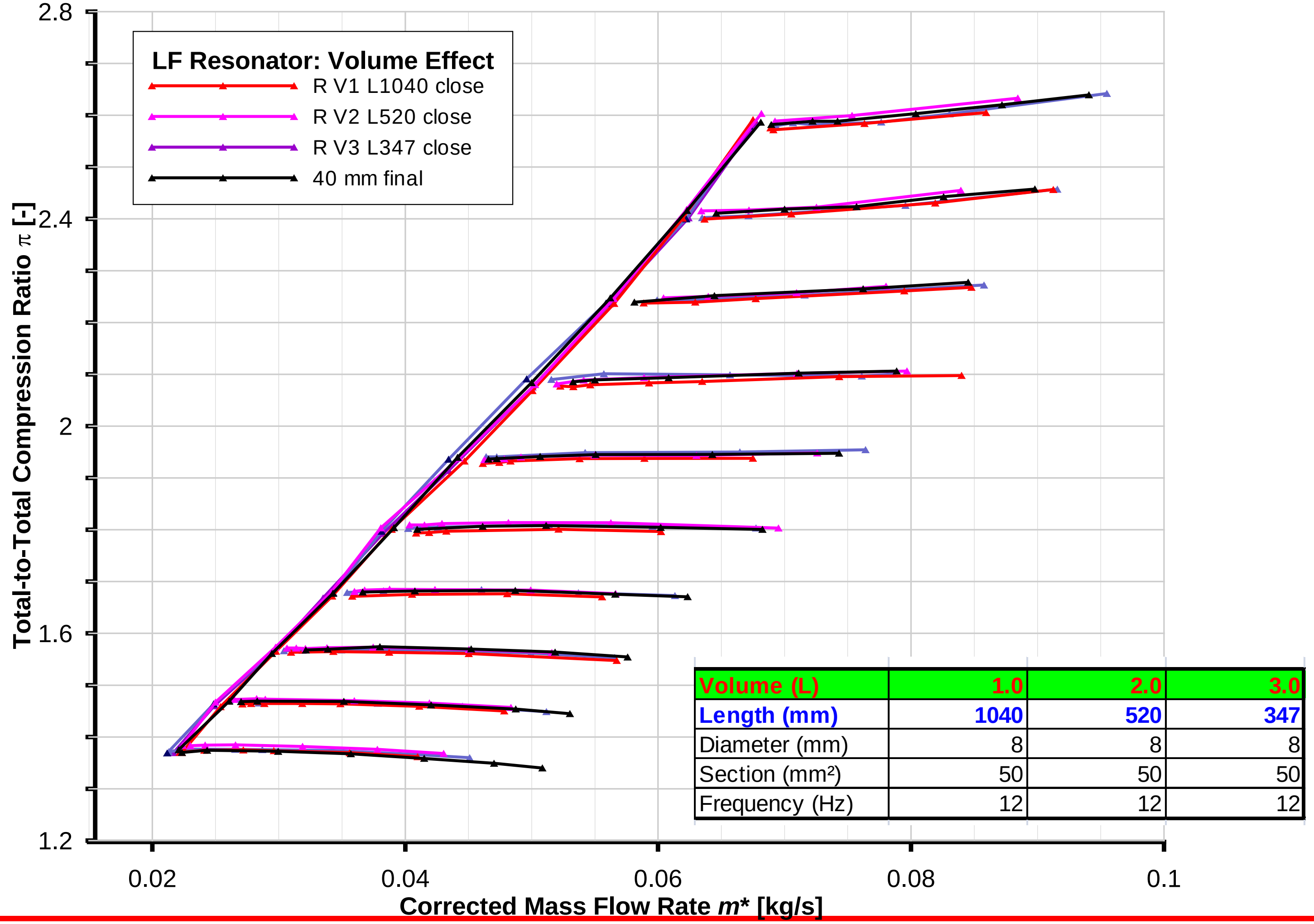


| Volume (L) | 1.0 | 2.0 | 3.0 |
|---|---|---|---|
| Length (mm) | 1040 | 520 | 347 |
| Diameter (mm) | 8 | 8 | 8 |
| Section (mm²) | 50 | 50 | 50 |
| Frequency (Hz) | 12 | 12 | 12 |

# Gas-Stand Tests: LF resonator, volume effect

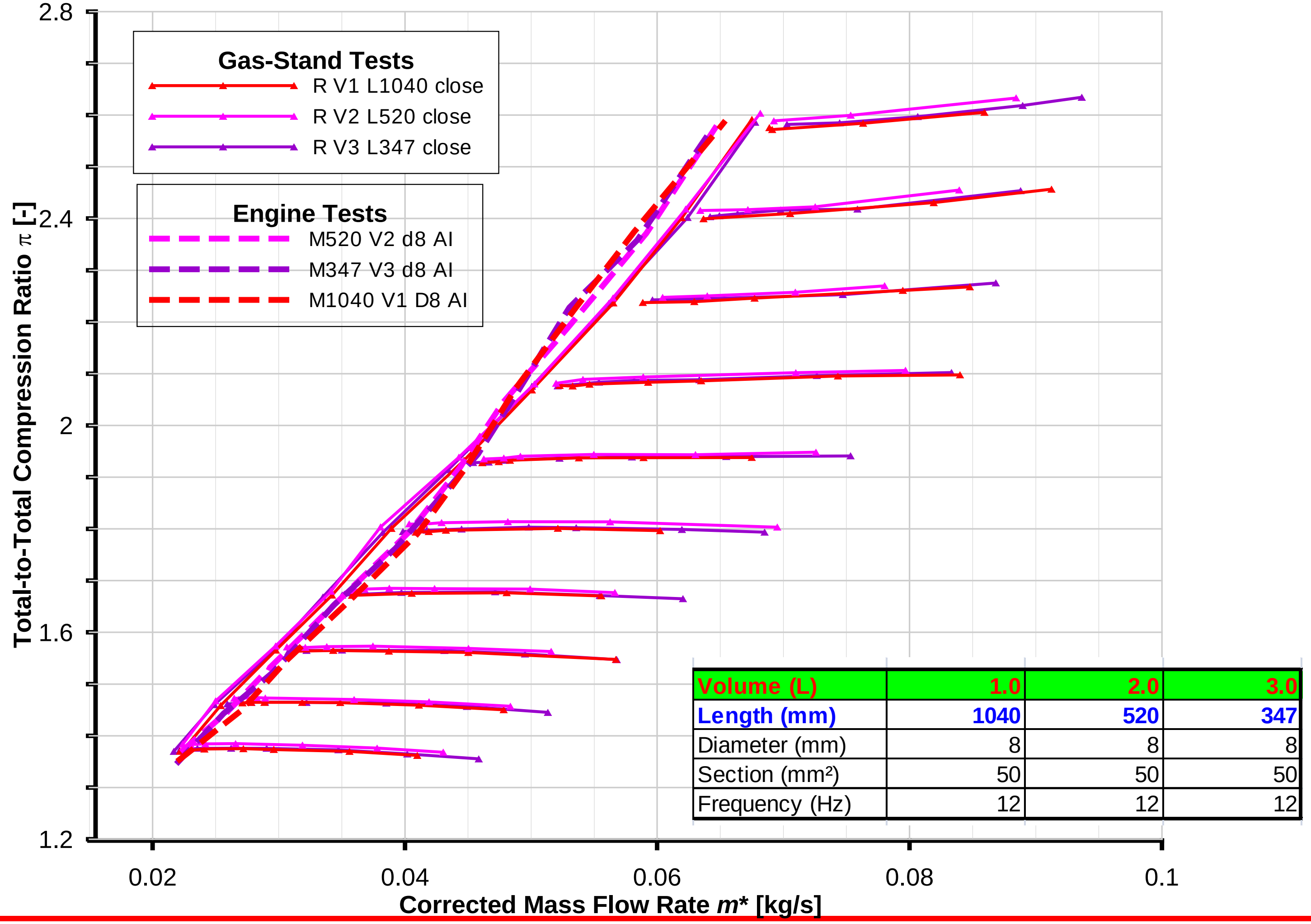


| Volume (L) | 1.0 | 2.0 | 3.0 |
|---|---|---|---|
| Length (mm) | 1040 | 520 | 347 |
| Diameter (mm) | 8 | 8 | 8 |
| Section (mm²) | 50 | 50 | 50 |
| Frequency (Hz) | 12 | 12 | 12 |

# Gas-Stand Tests: LF resonator, frequency effect

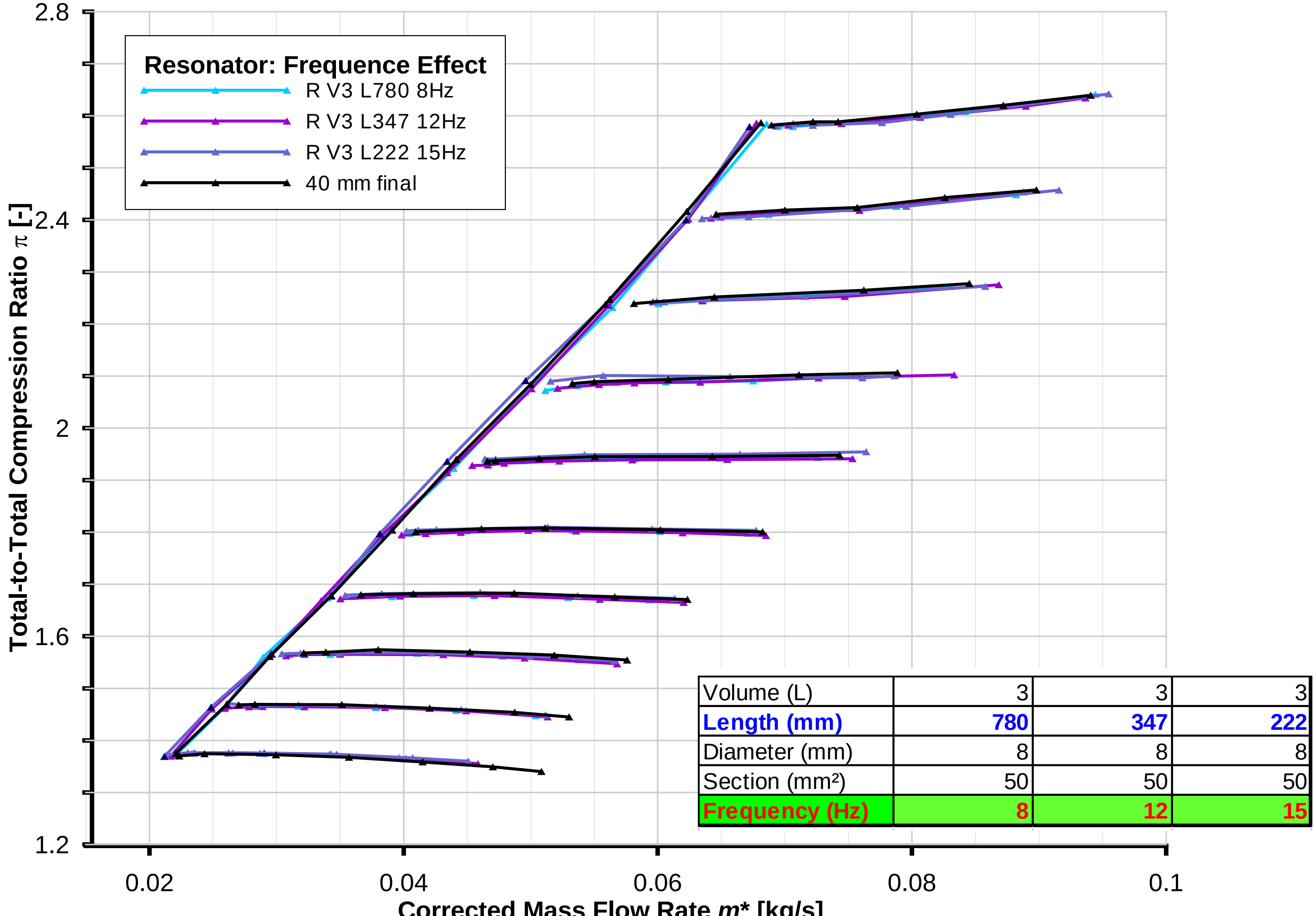


| Volume (L) | 3 | 3 | 3 |
|---|---|---|---|
| **Length (mm)** | **780** | **347** | **222** |
| Diameter (mm) | 8 | 8 | 8 |
| Section (mm²) | 50 | 50 | 50 |
| **Frequency (Hz)** | **8** | **12** | **15** |

# Gas-Stand Tests: LF resonator, frequency effect

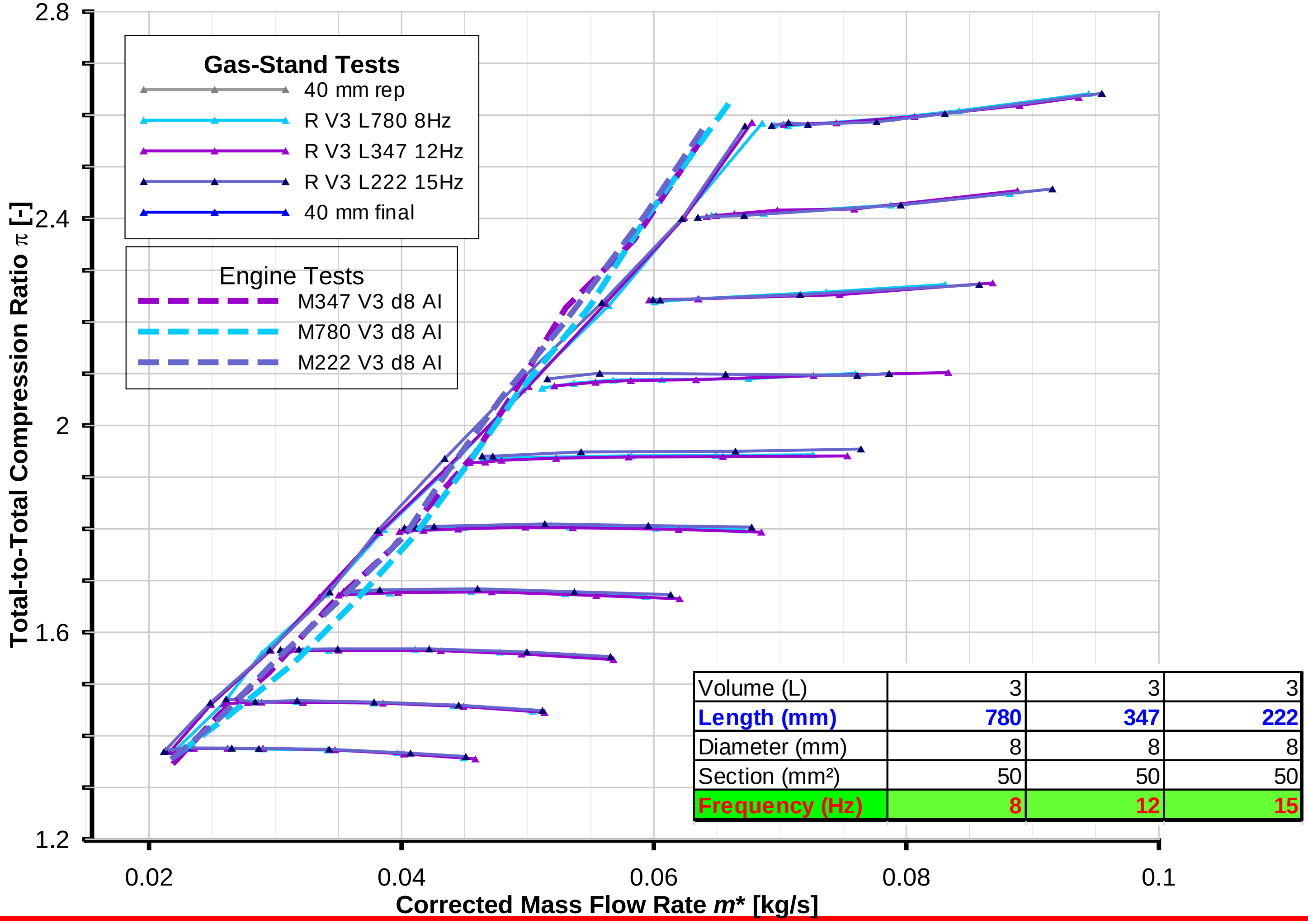


| | | | |
|---|---|---|---|
| Volume (L) | 3 | 3 | 3 |
| **Length (mm)** | **780** | **347** | **222** |
| Diameter (mm) | 8 | 8 | 8 |
| Section (mm²) | 50 | 50 | 50 |
| **Frequency (Hz)** | **8** | **12** | **15** |

# Conclusions LF resonator

**Engine tests**:

o The most influential parameter is the position close to the compressor

o At the closest position, most geometries lead to similar results. But little gain is obtained.

| | | | |
|---|---|---|---|
| Volume (L) | 3 | 3 | 3 |
| **Length (mm)** | **780** | **347** | **222** |
| Diameter (mm) | 8 | 8 | 8 |
| Section (mm²) | 50 | 50 | 50 |
| **Frequency (Hz)** | **8** | **12** | **15** |

| | | | |
|---|---|---|---|
| **Volume (L)** | **1.0** | **2.0** | **3.0** |
| **Length (mm)** | **1040** | **520** | **347** |
| Diameter (mm) | 8 | 8 | 8 |
| Section (mm²) | 50 | 50 | 50 |
| Frequency (Hz) | 12 | 12 | 12 |

| | | | |
|---|---|---|---|
| Volume (L) | 2 | 2 | 2 |
| **Length (mm)** | **293** | **520** | **1170** |
| **Diameter (mm)** | **6** | **8** | **12** |
| Section (mm²) | 28 | 50 | 113 |
| Frequency (Hz) | 12 | 12 | 12 |

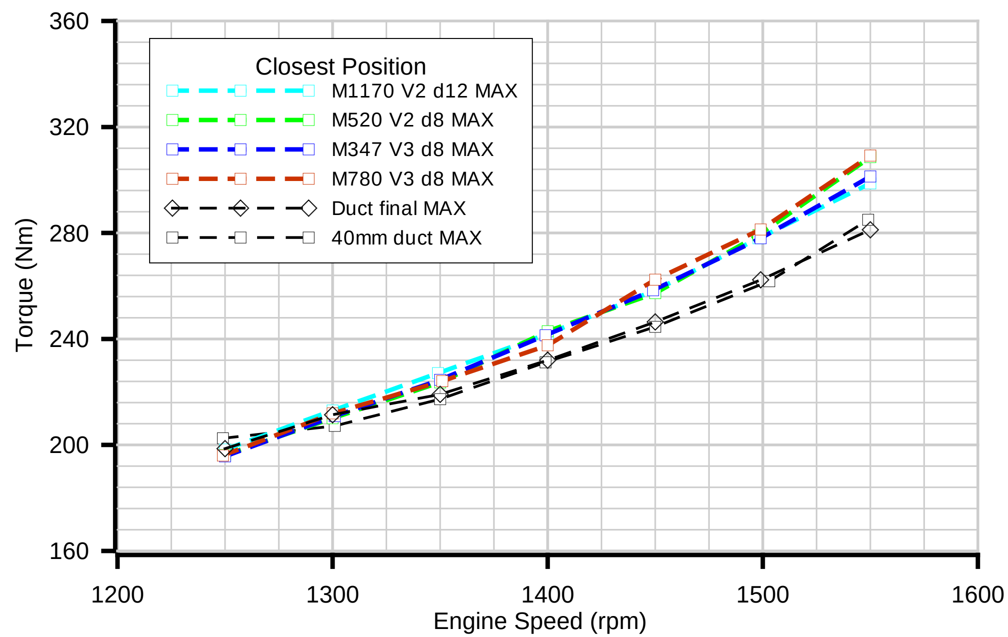

# Conclusions LF resonator

**Gas-Stand tests**:

o Gas-Stand results show little difference among the resonators (less than engine tests)

o The only parameter having an influence is the position close to the compressor

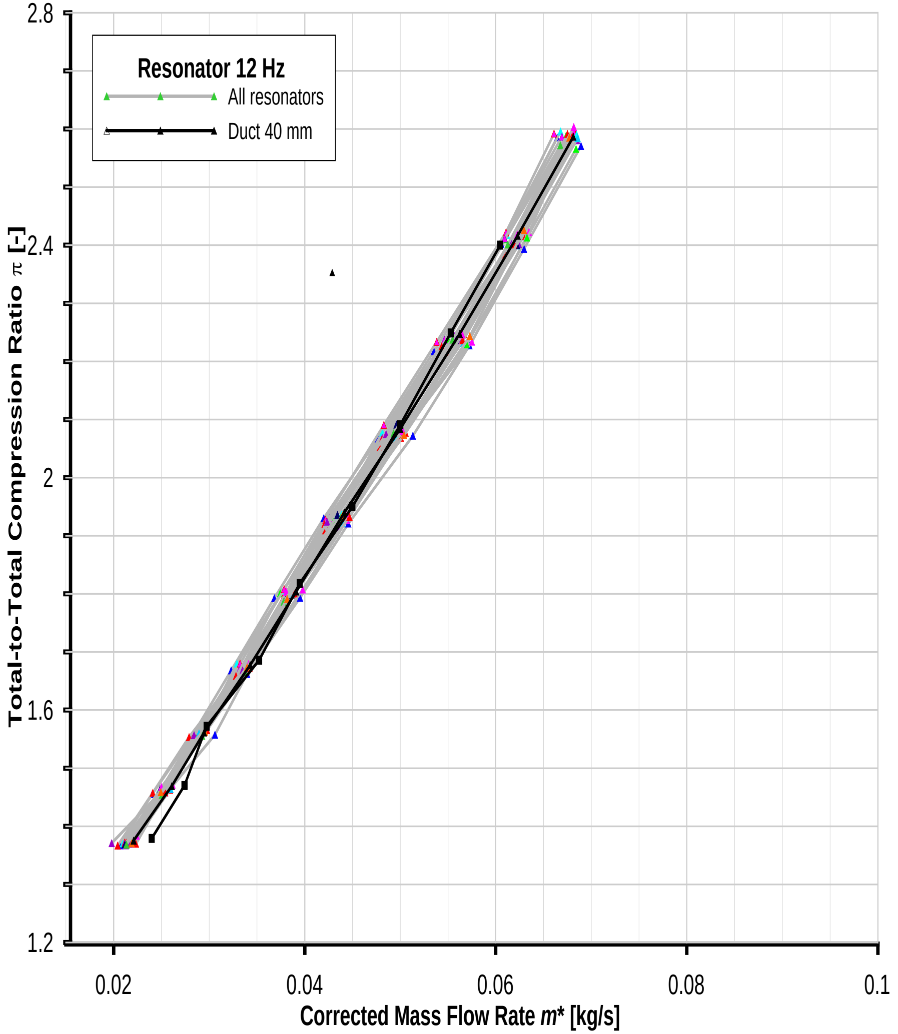

# Contents

- Introduction
  - Background, Objectives, Methodology
- Experimental procedure
- Volume before compressor
- Resonator before compressor
  - Low Frequency resonator (≈10 Hz)
  - High Frequency resonator (≈50 Hz)
- Discussion
- Conclusions

# ❑ High frequency resonator (≈50 Hz)

| VARIATION de la FREQUENCE @ iso-volume et iso-diamètre | | | | |
|---|---|---|---|---|
| Volume (L) | 1 | 1 | 1 | |
| Length (mm) | 462 | 374 | 309 | |
| Diameter (mm) | 20 | 20 | 20 | |
| Section (mm²) | 314 | 314 | 314 | |
| Frequency (Hz) | 45 | 50 | 55 | |
| | | | | |
| **VARIATION du VOLUME @ iso-fréquence et iso-diamètre** | | | | |
| **Volume (L)** | **1.0** | **2.0** | **3.0** | |
| **Length (mm)** | **374** | **187** | **125** | |
| Diameter (mm) | 20 | 20 | 20.0 | |
| Section (mm²) | 314 | 314 | 314 | |
| Frequency (Hz) | 50 | 50 | 50 | |
| | | | | |
| **VARIATION du DIAMETRE @ iso-fréquence et iso-volume** | | | | |
| Volume (L) | 3 | 3 | 3 | 3 |
| **Length (mm)** | **70** | **125** | **195** | **382** |
| **Diameter (mm)** | **15** | **20** | **25** | **35** |
| Section (mm²) | 177 | 314 | 491 | 962 |
| Frequency (Hz) | 50 | 50 | 50 | 50 |

# HF resonator: Length effect

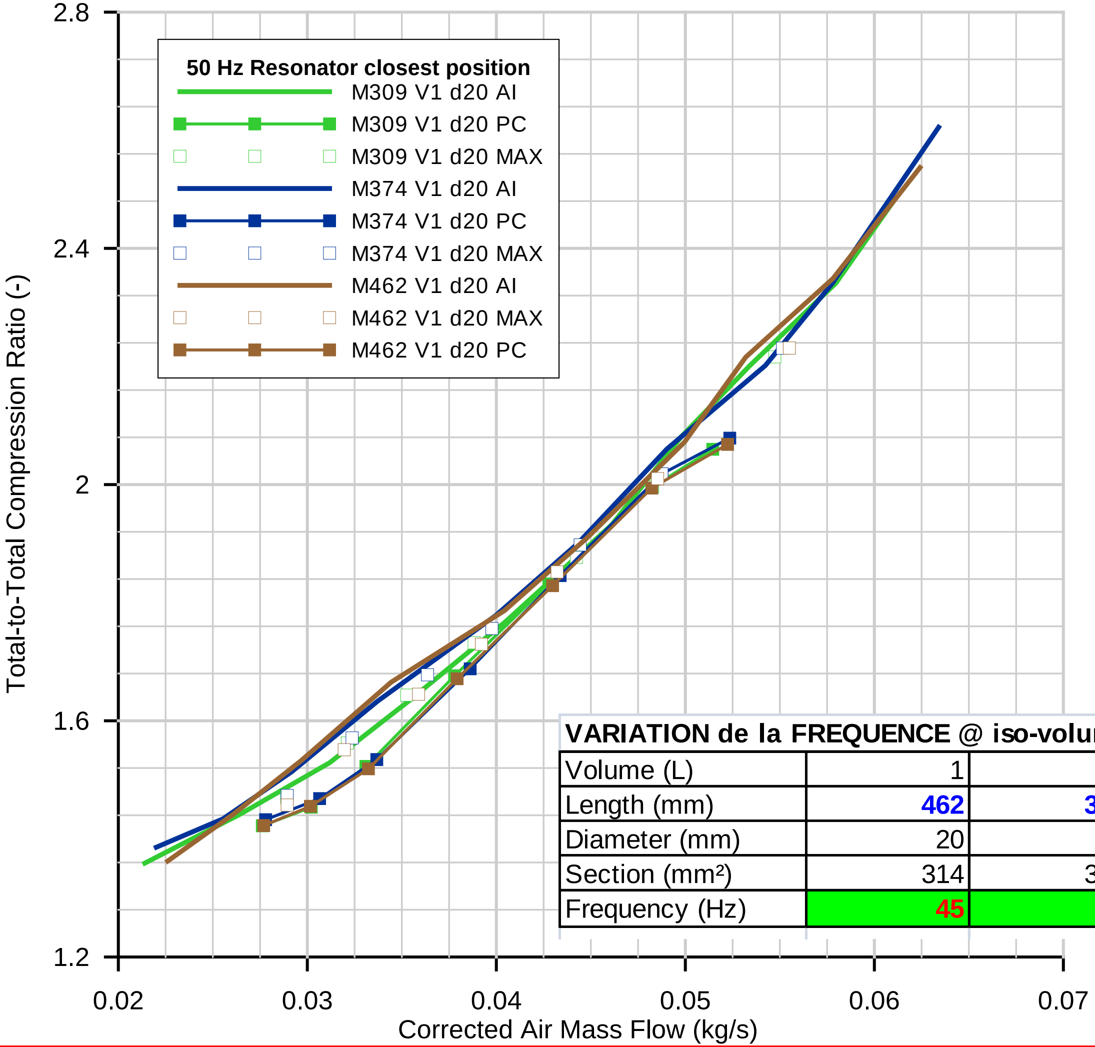


**VARIATION de la FREQUENCE @ iso-volume et iso-diamètre**

| | | | |
|---|---|---|---|
| Volume (L) | 1 | 1 | 1 |
| Length (mm) | **462** | **374** | **309** |
| Diameter (mm) | 20 | 20 | 20 |
| Section (mm²) | 314 | 314 | 314 |
| Frequency (Hz) | **45** | **50** | **55** |

# ❑ HF resonator: Length effect

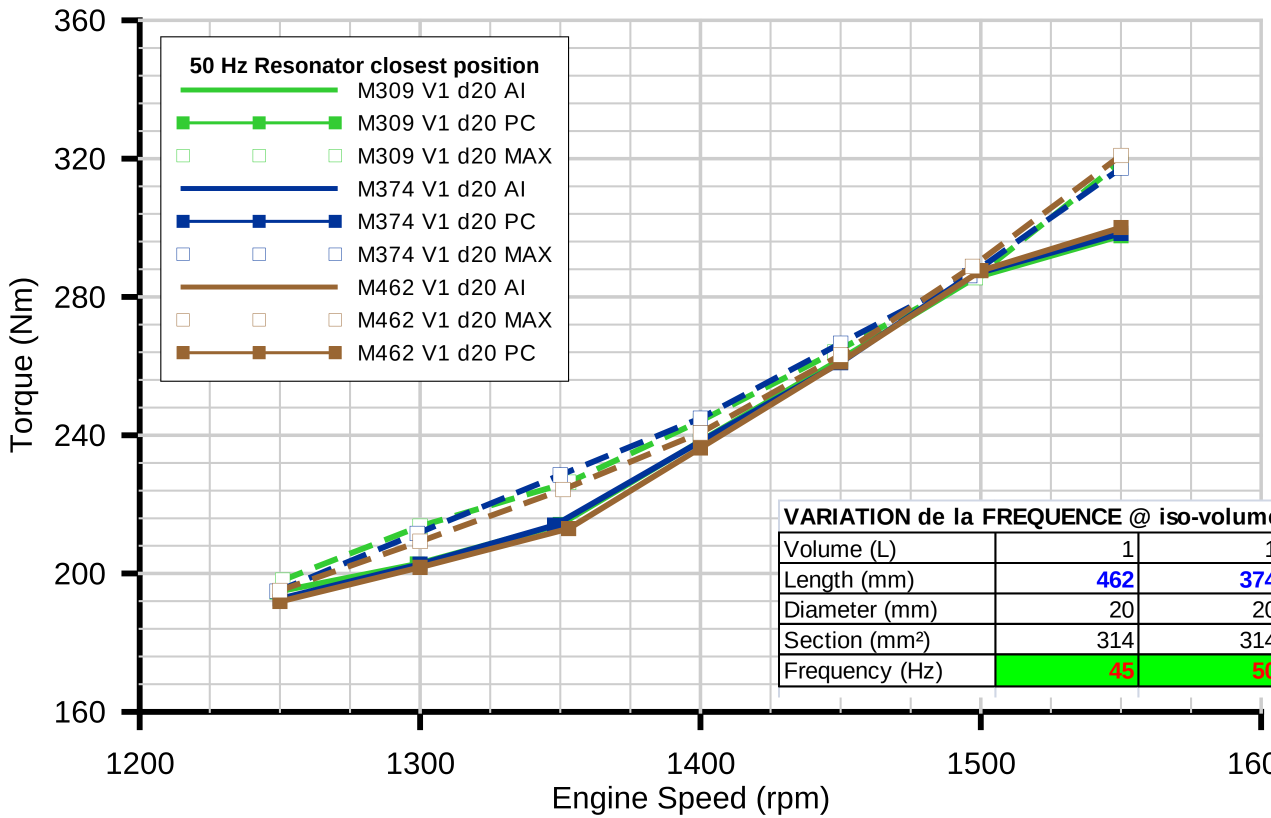


| VARIATION de la FREQUENCE @ iso-volume et iso-diamètre | | | |
|---|---|---|---|
| Volume (L) | 1 | 1 | 1 |
| Length (mm) | **462** | **374** | **309** |
| Diameter (mm) | 20 | 20 | 20 |
| Section (mm²) | 314 | 314 | 314 |
| Frequency (Hz) | **45** | **50** | **55** |

# HF resonator: Volume effect

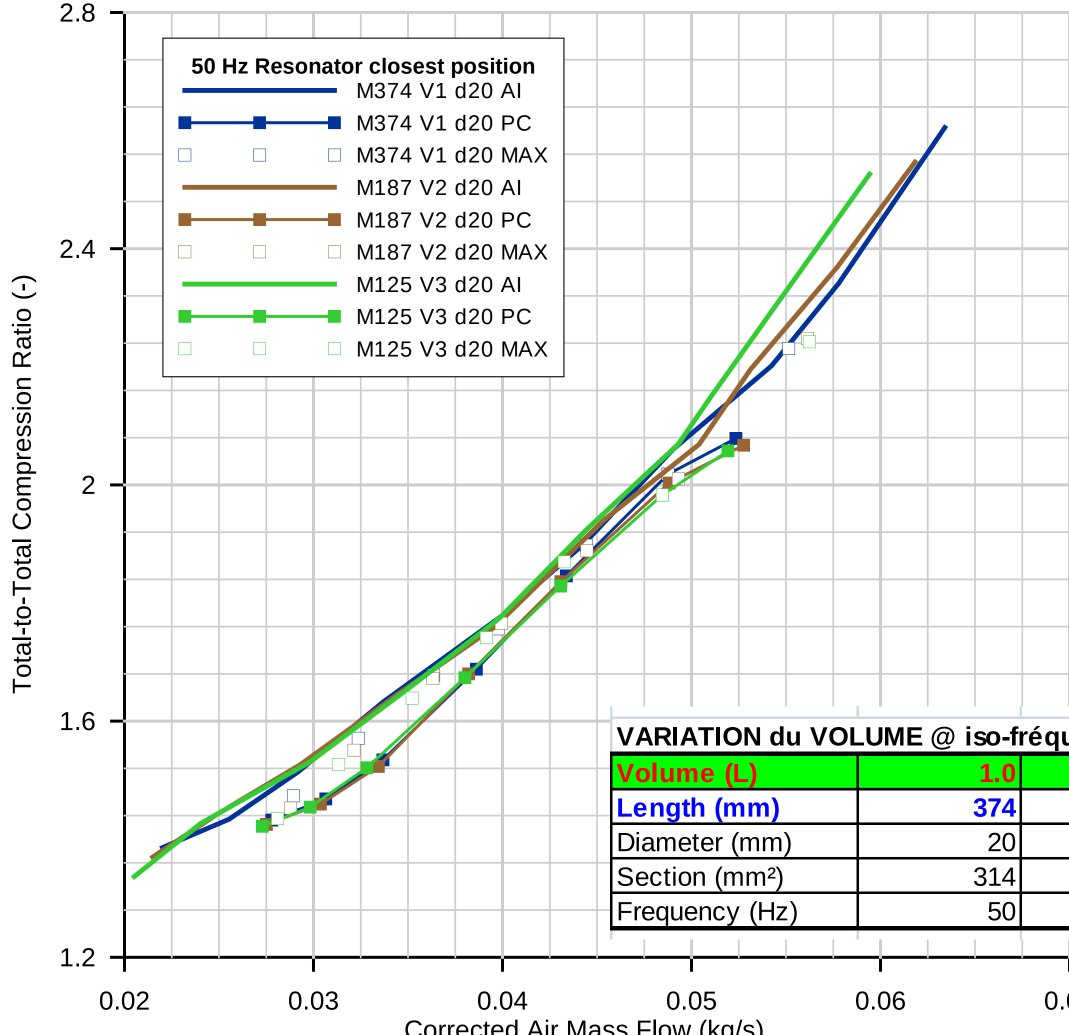


**VARIATION du VOLUME @ iso-fréquence et iso-diamètre**

| Volume (L) | 1.0 | 2.0 | 3.0 |
|---|---|---|---|
| Length (mm) | 374 | 187 | 125 |
| Diameter (mm) | 20 | 20 | 20.0 |
| Section (mm²) | 314 | 314 | 314 |
| Frequency (Hz) | 50 | 50 | 50 |

# HF resonator: Volume effect

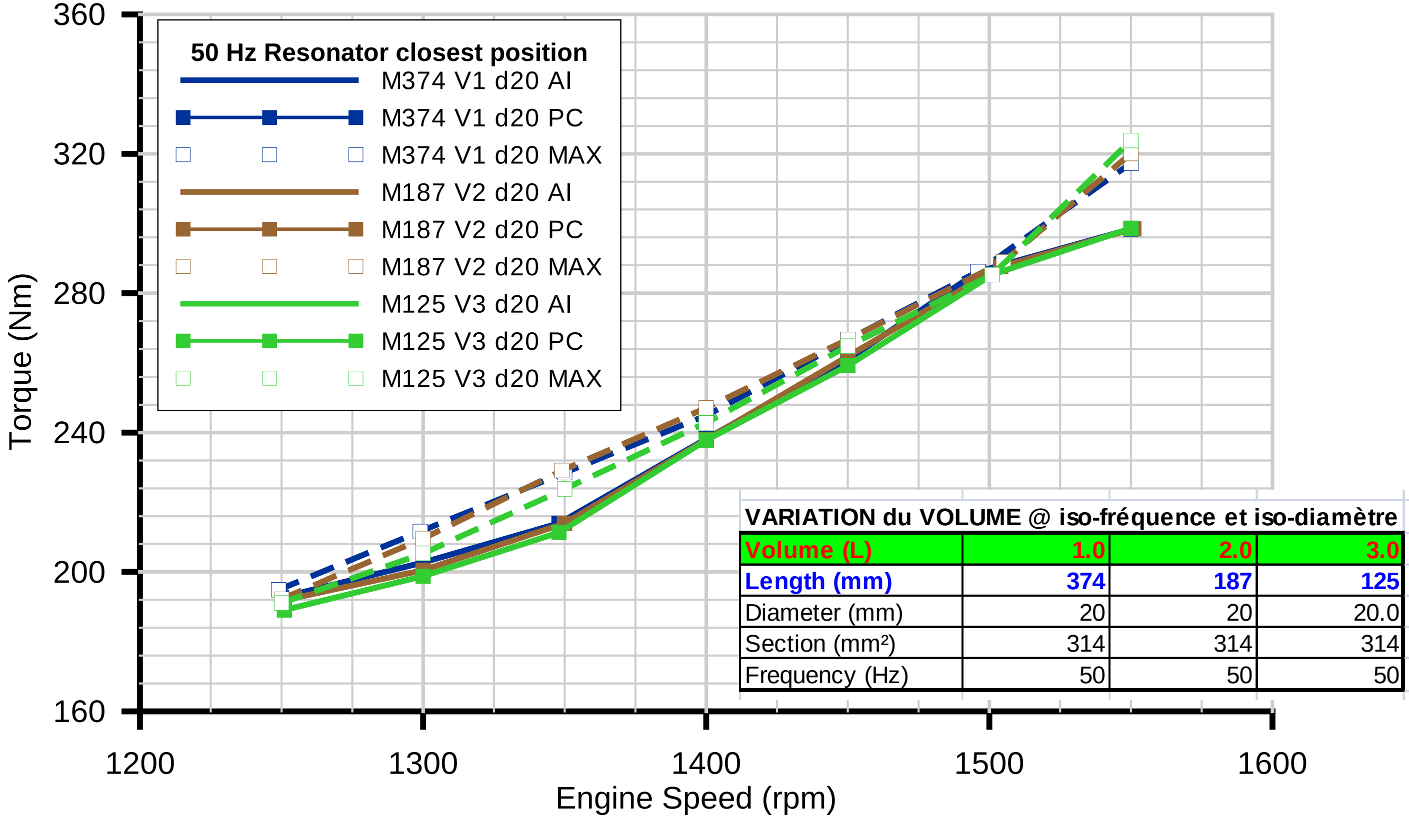


VARIATION du VOLUME @ iso-fréquence et iso-diamètre

| Volume (L) | 1.0 | 2.0 | 3.0 |
|---|---|---|---|
| Length (mm) | 374 | 187 | 125 |
| Diameter (mm) | 20 | 20 | 20.0 |
| Section (mm²) | 314 | 314 | 314 |
| Frequency (Hz) | 50 | 50 | 50 |

# ❑ HF resonator: Diameter effect

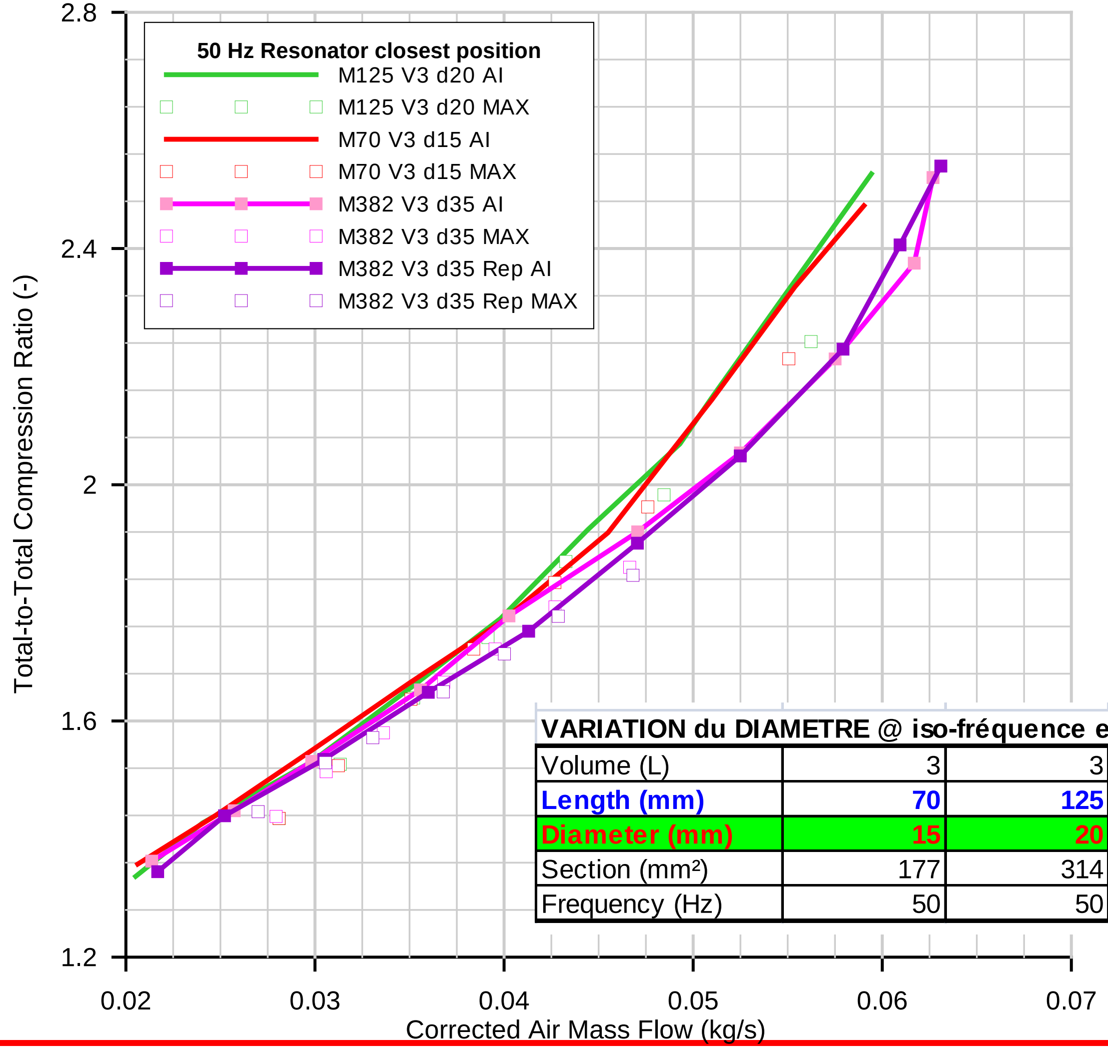


| VARIATION du DIAMETRE @ iso-fréquence et iso-volume | | | | |
|---|---|---|---|---|
| Volume (L) | 3 | 3 | 3 | 3 |
| **Length (mm)** | **70** | **125** | **195** | **382** |
| **Diameter (mm)** | **15** | **20** | **25** | **35** |
| Section (mm²) | 177 | 314 | 491 | 962 |
| Frequency (Hz) | 50 | 50 | 50 | 50 |

# HF resonator: Diameter effect

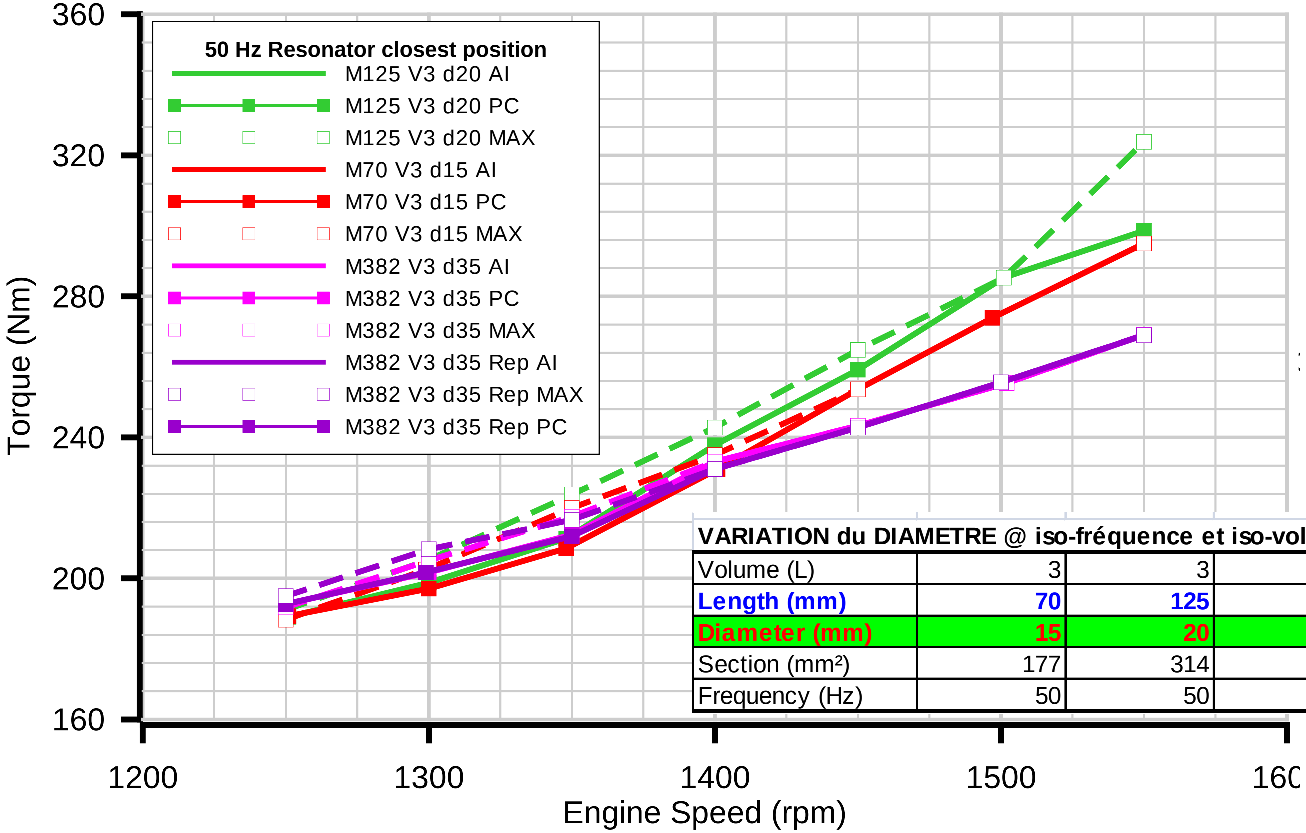


| VARIATION du DIAMETRE @ iso-fréquence et iso-volume | | | | |
|---|---|---|---|---|
| Volume (L) | 3 | 3 | 3 | 3 |
| **Length (mm)** | **70** | **125** | **195** | **382** |
| **Diameter (mm)** | **15** | **20** | **25** | **35** |
| Section (mm²) | 177 | 314 | 491 | 962 |
| Frequency (Hz) | 50 | 50 | 50 | 50 |

# Gas-Stand Tests: HF resonator, volume effect

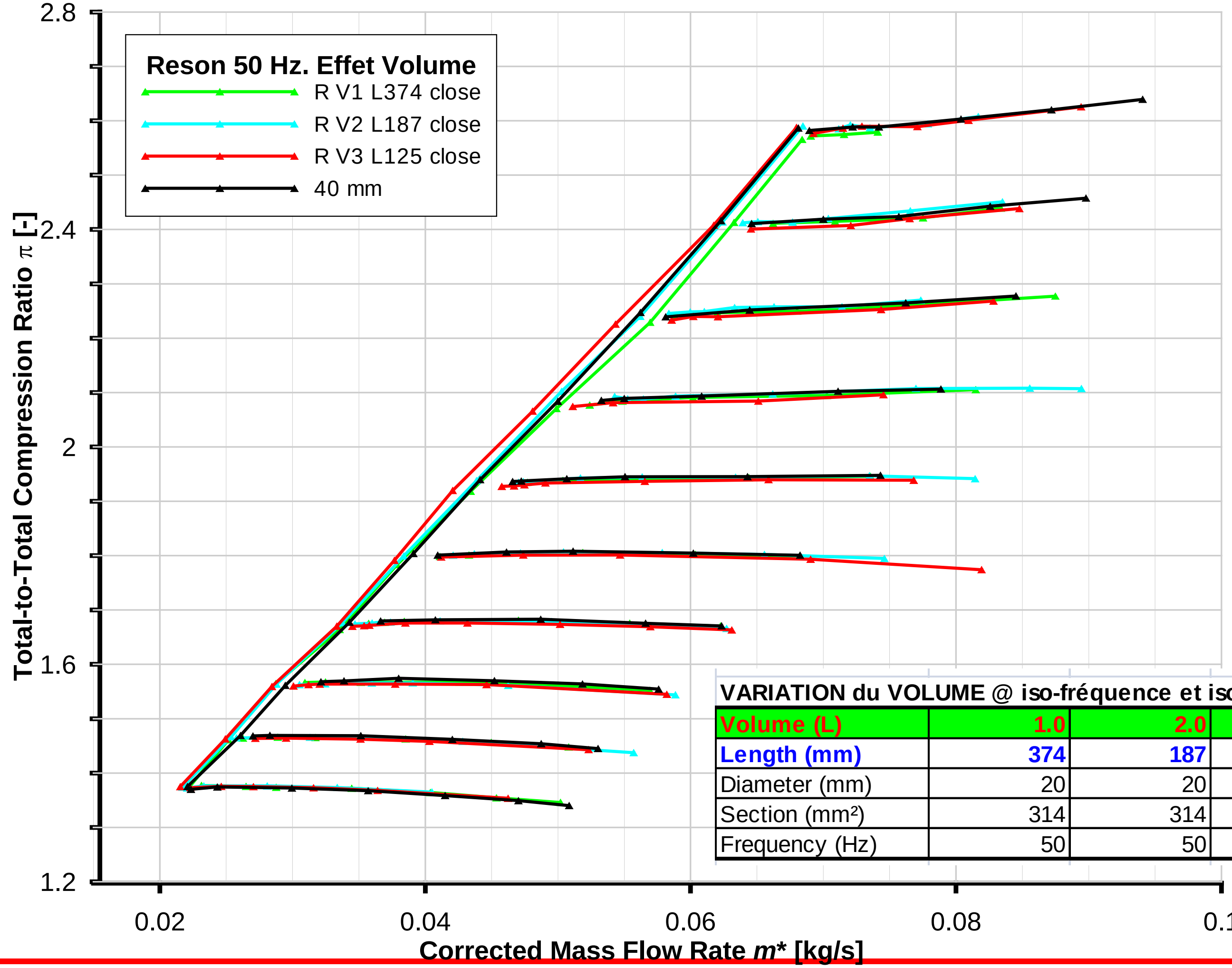


| VARIATION du VOLUME @ iso-fréquence et iso-diamètre | | | |
|---|---|---|---|
| Volume (L) | 1.0 | 2.0 | 3.0 |
| Length (mm) | 374 | 187 | 125 |
| Diameter (mm) | 20 | 20 | 20.0 |
| Section (mm²) | 314 | 314 | 314 |
| Frequency (Hz) | 50 | 50 | 50 |

# Gas-Stand Tests: HF resonator, length effect

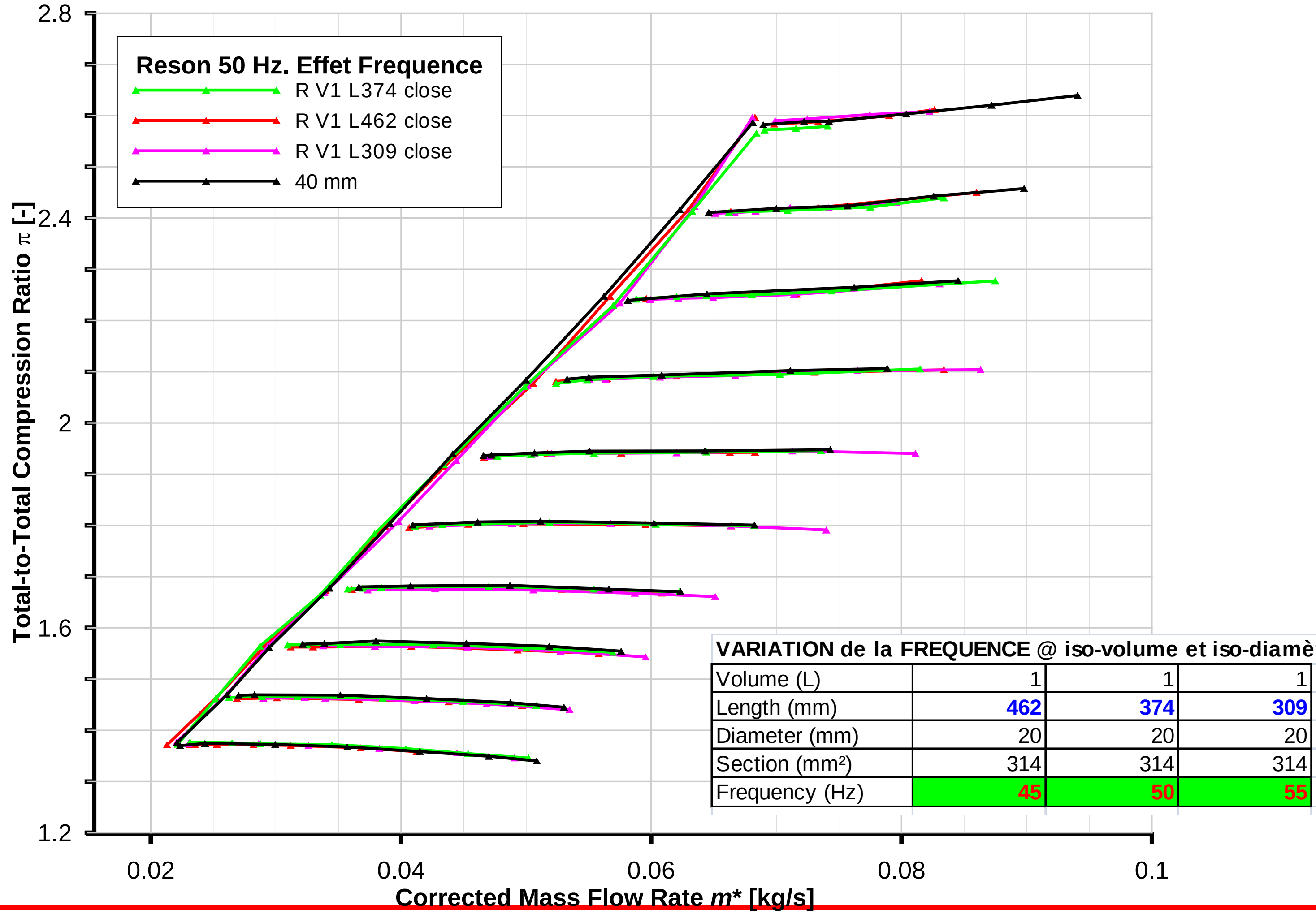


| VARIATION de la FREQUENCE @ iso-volume et iso-diamèt | | | |
|---|---|---|---|
| Volume (L) | 1 | 1 | 1 |
| Length (mm) | 462 | 374 | 309 |
| Diameter (mm) | 20 | 20 | 20 |
| Section (mm²) | 314 | 314 | 314 |
| Frequency (Hz) | 45 | 50 | 55 |

# ❑ Gas-Stand Tests: HF resonator, diameter effect

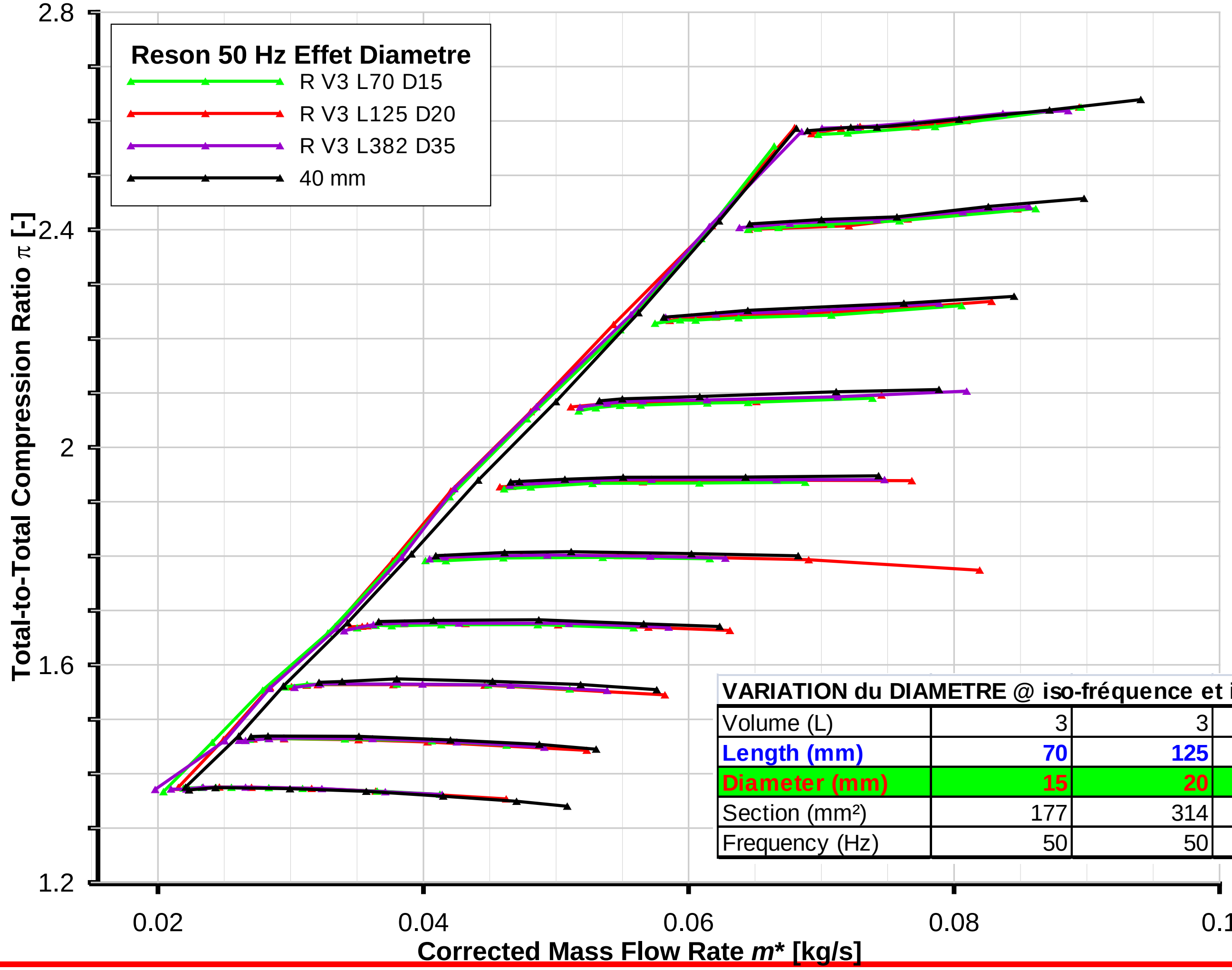


| VARIATION du DIAMETRE @ iso-fréquence et iso-volume | | | | |
|---|---|---|---|---|
| Volume (L) | 3 | 3 | 3 | 3 |
| Length (mm) | 70 | 125 | 195 | 382 |
| Diameter (mm) | 15 | 20 | 25 | 35 |
| Section (mm²) | 177 | 314 | 491 | 962 |
| Frequency (Hz) | 50 | 50 | 50 | 50 |

# Conclusions: HF Resonator

On engine tests:

oHF resonators may modify engine performance but they do not shift the surge line. The change in performance may be accounted to a change in the engine operating point (volumetric efficiency)

Gas-stand tests:

o HF resonators have not any influence on surge margin (tested close to the compressor)

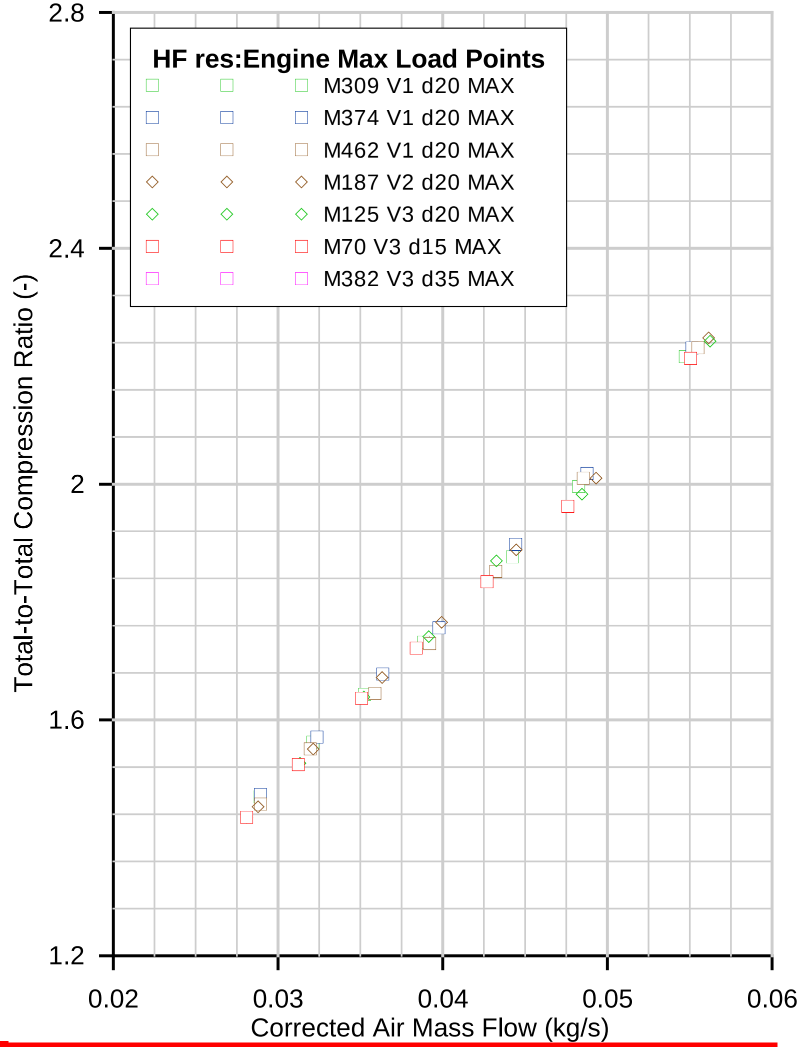

# Conclusions: HF Resonator

On engine tests:

o Almost all the resonator have the same torque

o Small improvement compared to the volumes

| VARIATION de la FREQUENCE @ iso-volume et iso-diamè | | | |
|---|---|---|---|
| Volume (L) | 1 | 1 | 1 |
| Length (mm) | 462 | 374 | 309 |
| Diameter (mm) | 20 | 20 | 20 |
| Section (mm²) | 314 | 314 | 314 |
| Frequency (Hz) | 45 | 50 | 55 |

| VARIATION du VOLUME @ iso-fréquence et iso-diamètre | | | |
|---|---|---|---|
| Volume (L) | 1.0 | 2.0 | 3.0 |
| Length (mm) | 374 | 187 | 125 |
| Diameter (mm) | 20 | 20 | 20.0 |
| Section (mm²) | 314 | 314 | 314 |
| Frequency (Hz) | 50 | 50 | 50 |

| VARIATION du DIAMETRE @ iso-fréquence et iso-volume | | | |
|---|---|---|---|
| Volume (L) | 3 | 3 | 3 |
| Length (mm) | 70 | 125 | 382 |
| Diameter (mm) | 15 | 20 | 35 |
| Section (mm²) | 177 | 314 | 962 |
| Frequency (Hz) | 50 | 50 | 50 |

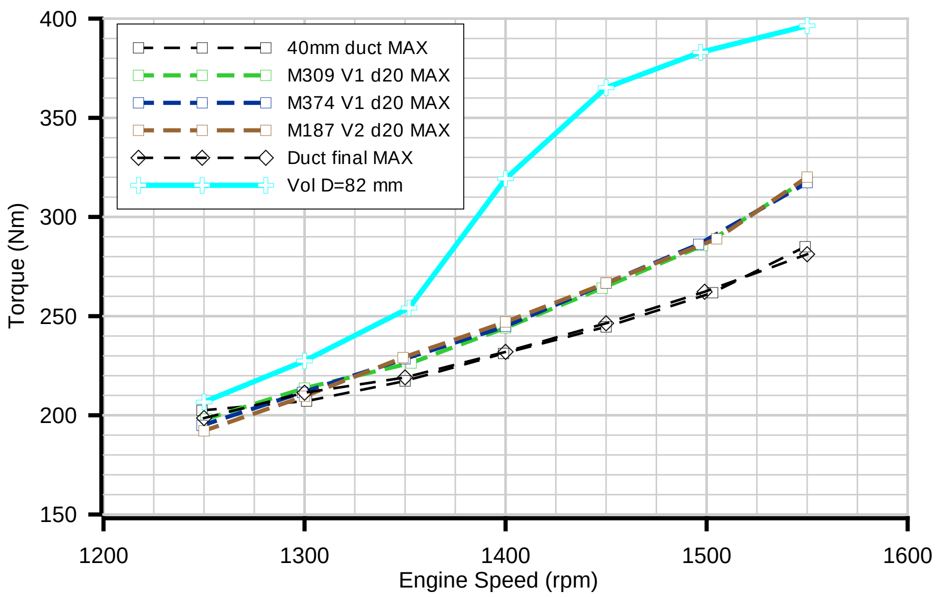

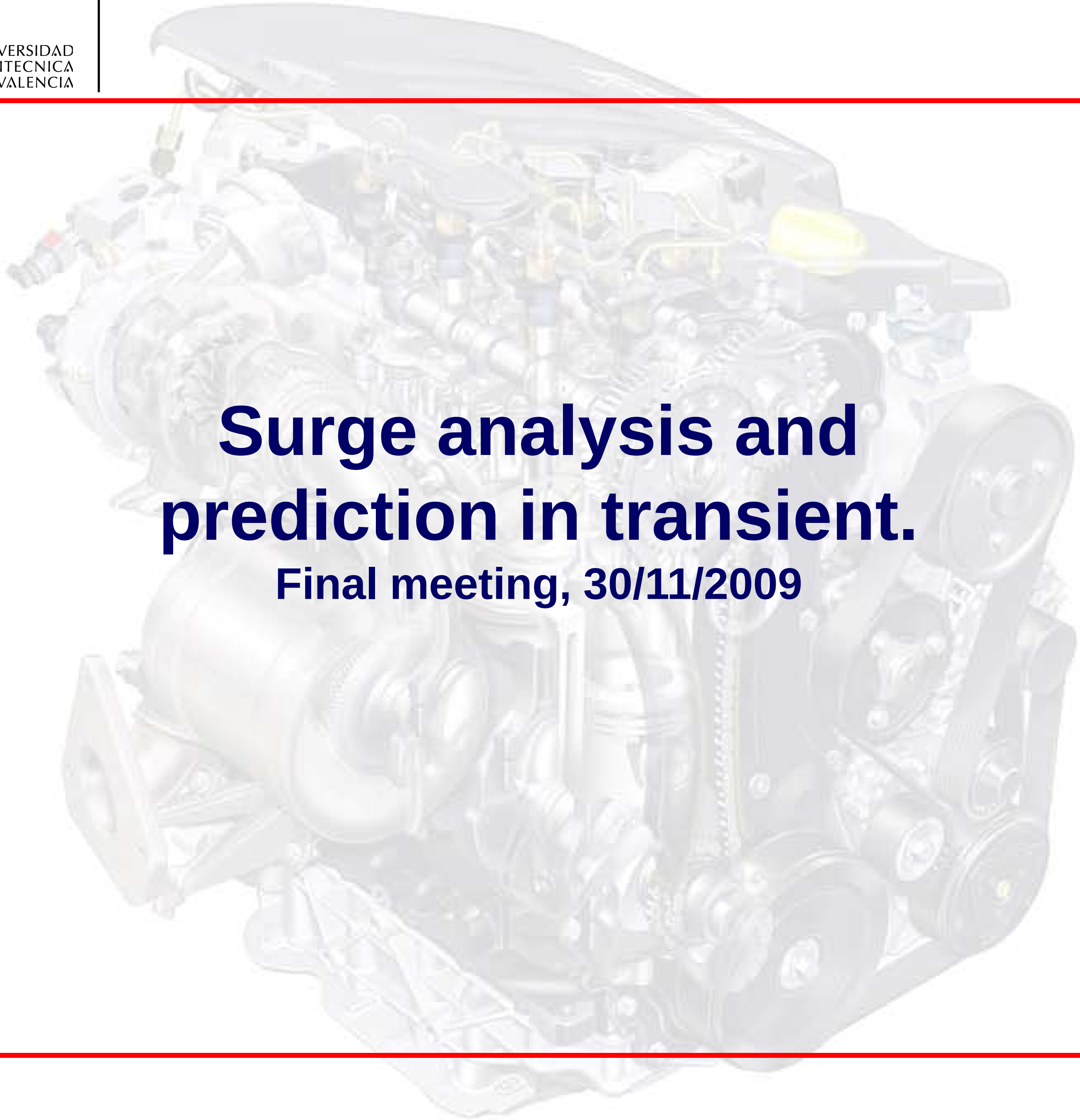

# Surge analysis and prediction in transient.

**Final meeting, 30/11/2009**

# Contents


- Introduction
  - Background and objectives
- Experimental procedure
  - Steady tests
  - Transient tests
- Experimental Results
- Modeling
- Discussion

# Introduction: Background

- In a previous project a non-steady compressor model was proposed able to predict surge under steady and pulsating conditions
- An experimental test study in a pulsating gas stand showed that pulsating flow may increase the steady surge margin

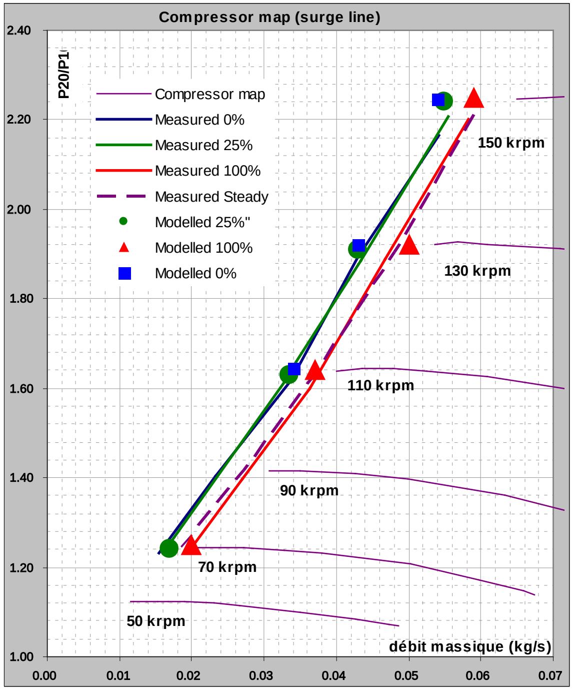


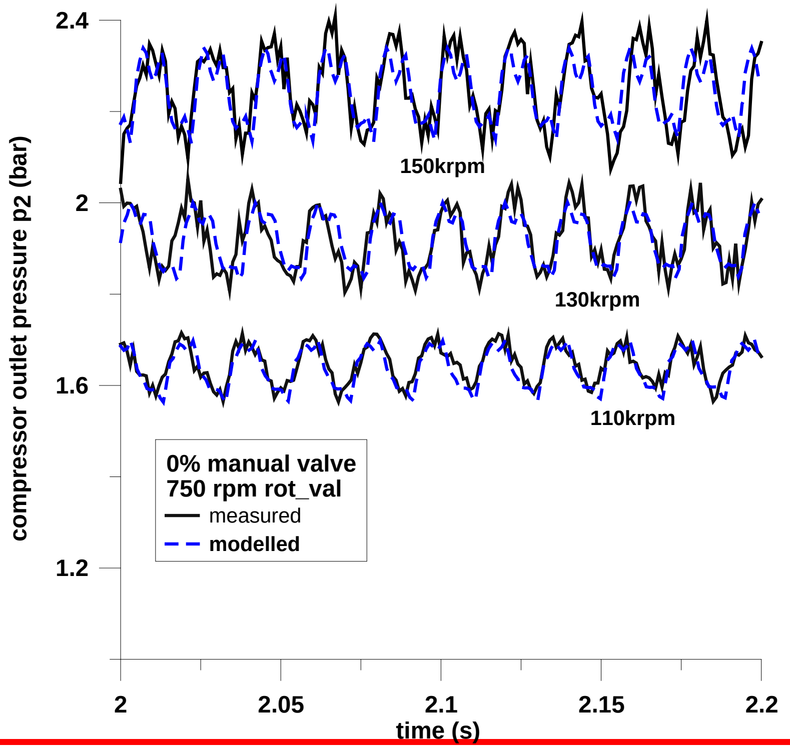

# Introduction: Objectives

- To analyze the physical phenomena which govern the surge during transient operating. Particularly, the reasons making the surge appear in transient even when the steady conditions are not favorable to surge.
- To determine whether a surge is possible in transient conditions without its installation and propagation.
- To model the surge phenomenon during engine accelerations or decelerations with 1D code with identifying the main variables of importance in the code.
- To find out strategies and technical solutions to avoid transient surge.
- To implement the model into GT-Power which is the 1D code used by (enterprise) for gas exchange simulations.

# Introduction: Work Plan

- Experimental
  - Characterization of components in **test flow rig**
  - Extended compressor maps measurement in **gas-stand**.
  - Develop **methodology** to detect/quantify surge
  - **Engine tests** with different upstream/downstream compressor geometries in **steady** and **transient**.
- Modelling
  - To calibrate the model
  - To use the user function to model the tests campaigns
  - To develop a User Function in GT with the compressor model
  - Transfer to (enterprise)

# Experimental Procedure

- Engine Test Bench
  - Steady Tests
    - Air Injection
    - Increase $p_{\text{boost}}$ at constant engine speed, AFR, $p_{\text{cyl max}}$, $T_{\text{intake}}$
  - Transient Tests
    - Acceleration/deceleration from 1250 to 2500 rpm at Full Load

- Gas-Stand
  - Steady Tests

# Experimental Procedure

- Air Injection Technique

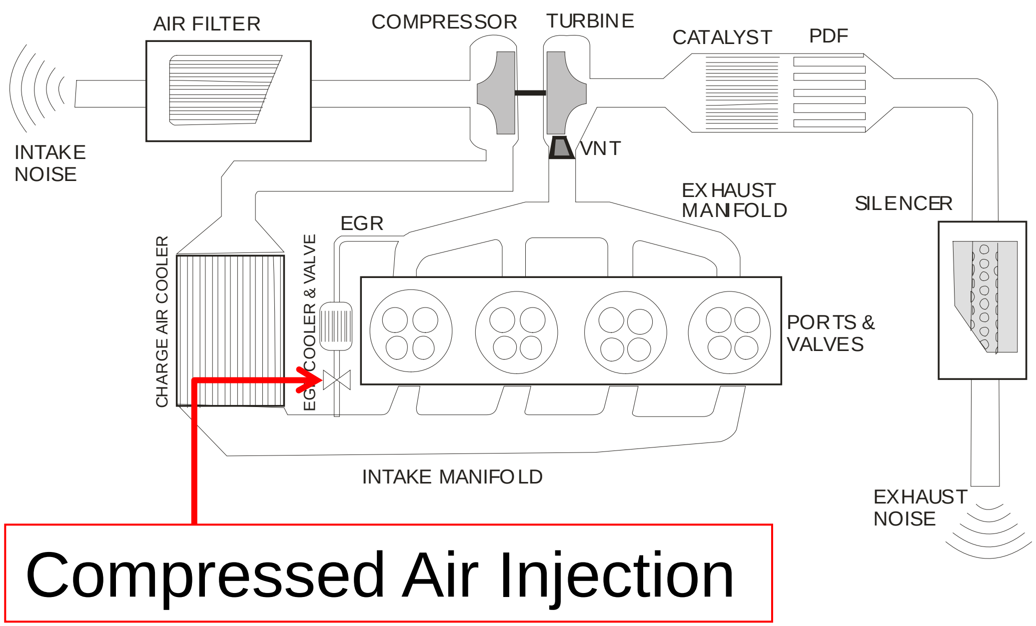


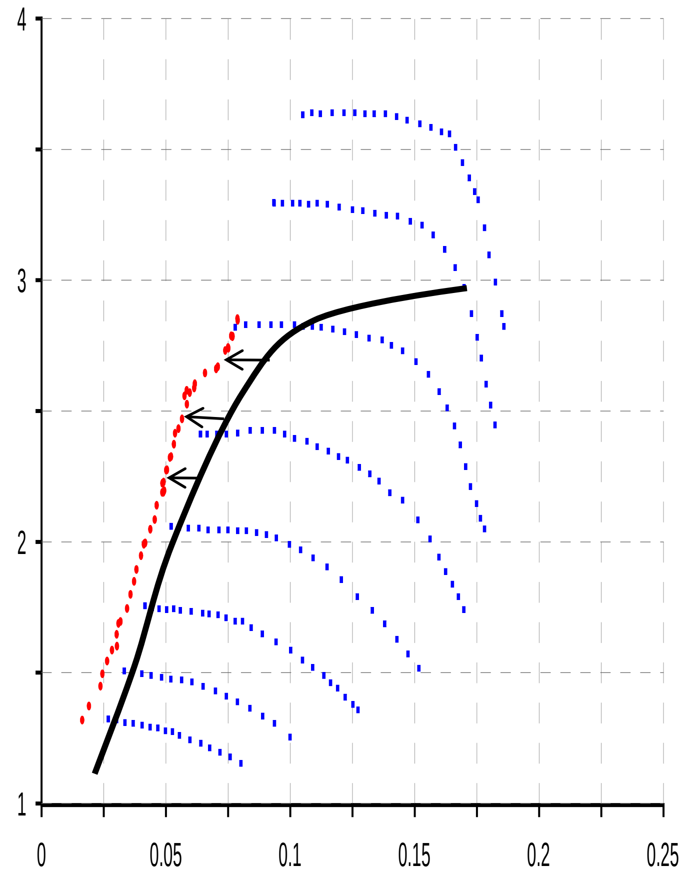

# ❑ Experimental Procedure: detection

- With air injection technique is possible to go to deep surge.
- Deep surge occurs suddenly.

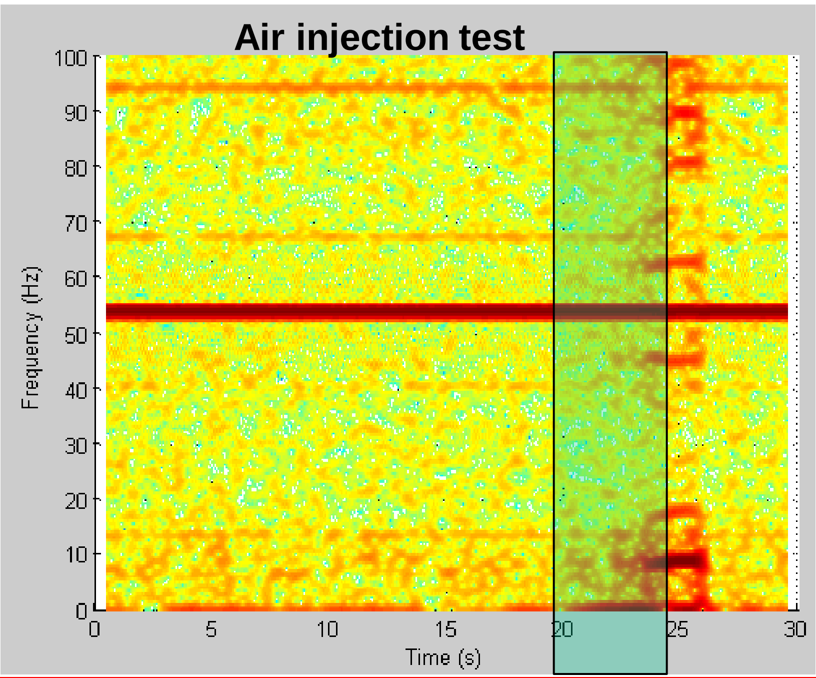


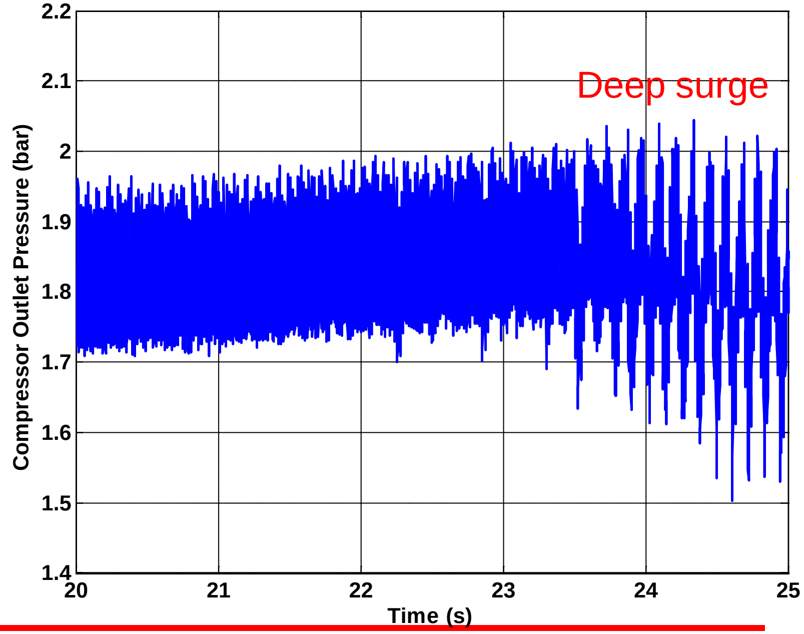

# ❑ Experimental Procedure: detection

- The Amplitude at low frequency (5-15 Hz) is used to choose a threshold for surge detection as a % of the peak value

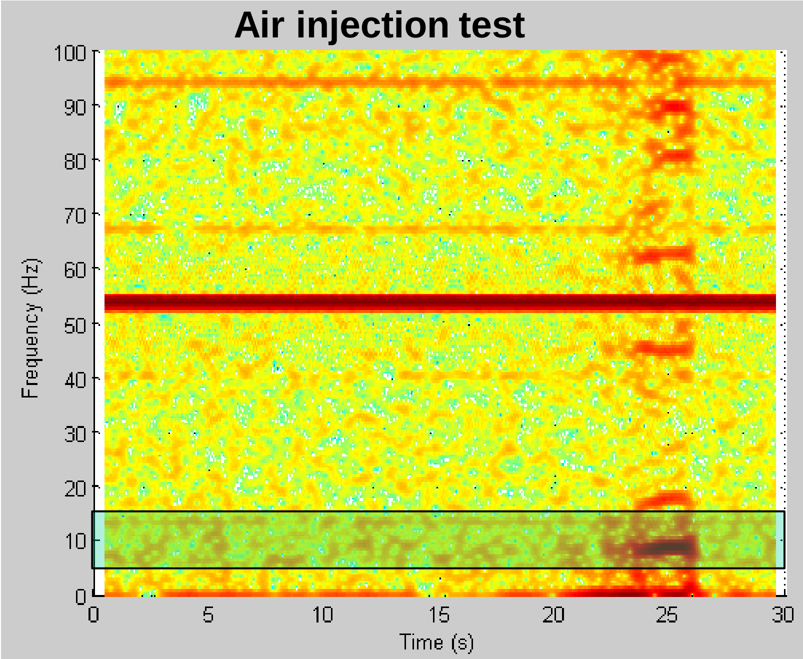


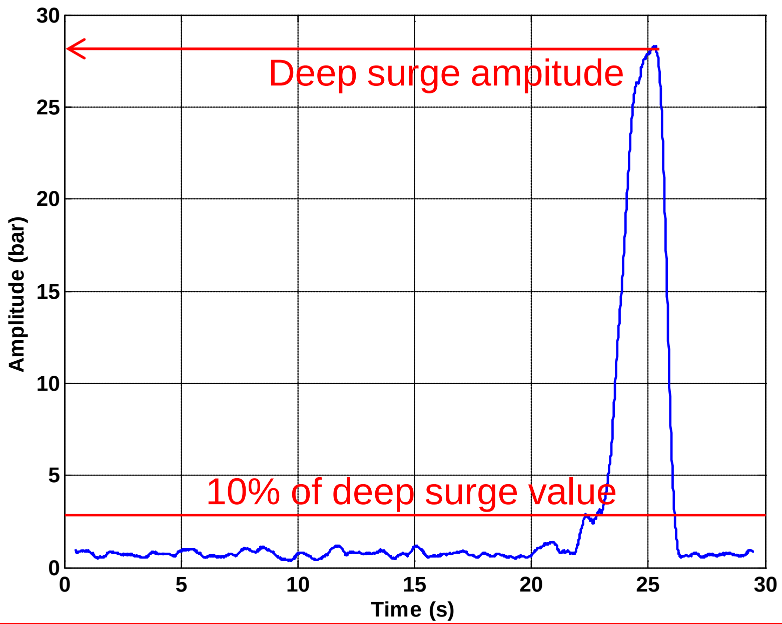

# Experimental Procedure: Detection

- This threshold is used in air injection tests to detect automatically the last stable point

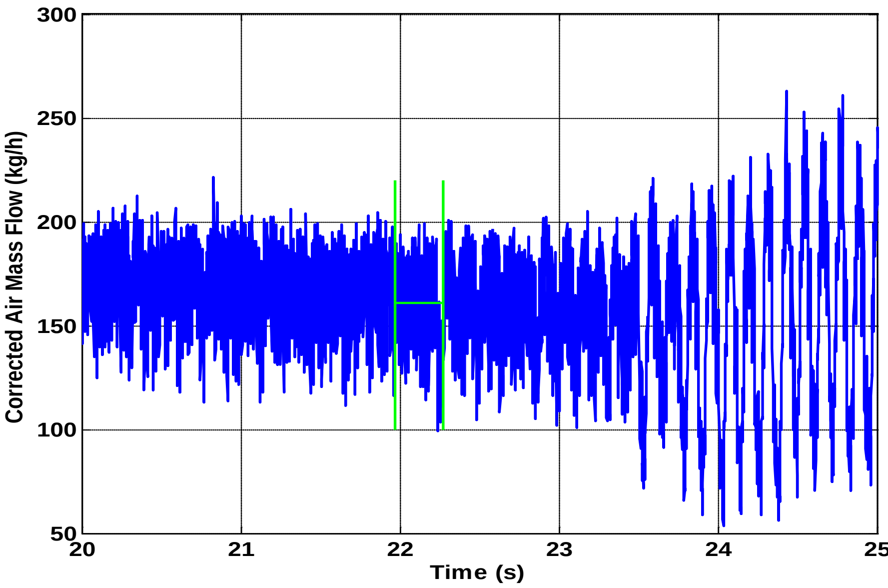


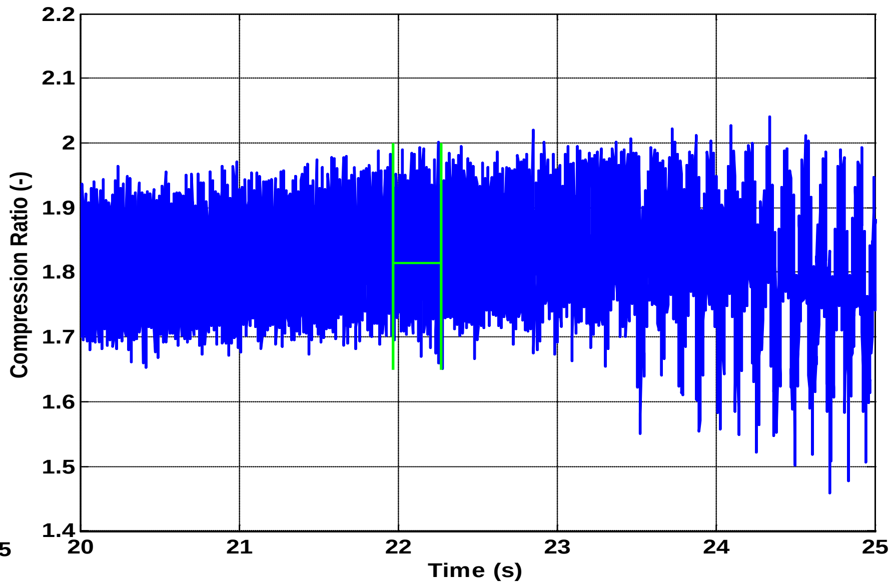

# Experimental Procedure: Detection

- Surge in engine tests is not so easy to detect
- The threshold is used to state if there is surge or not

**1300 rpm**

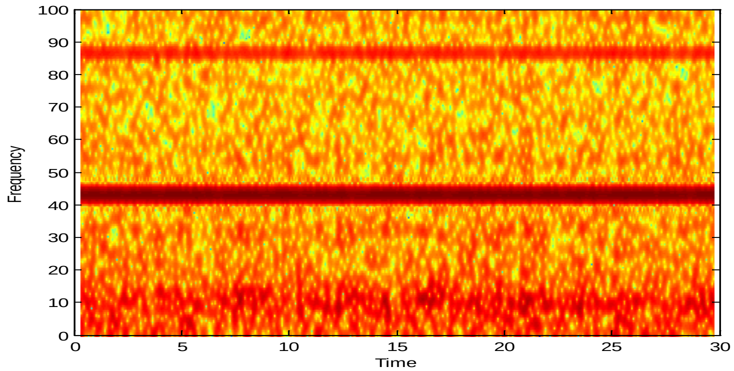


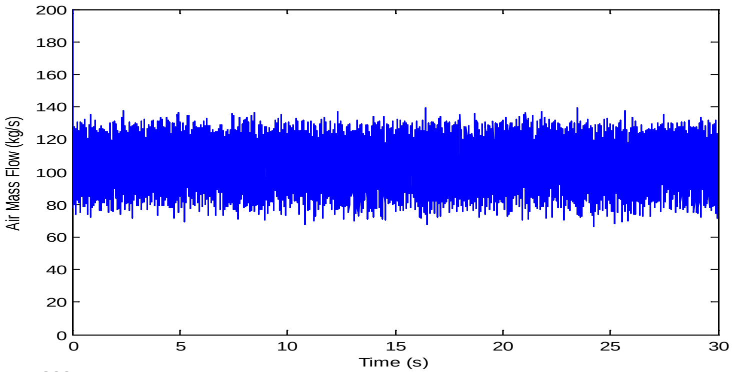


**1450 rpm**

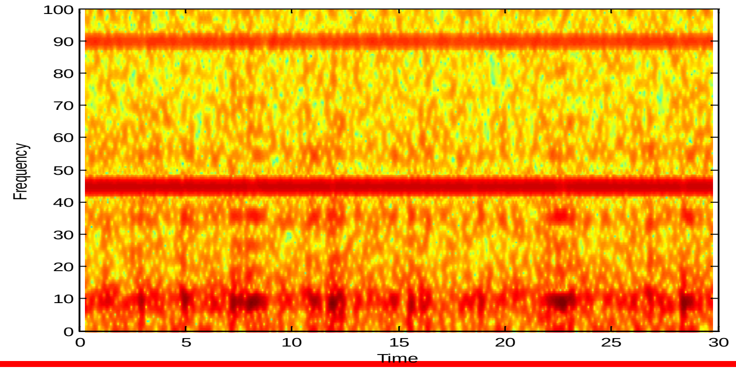


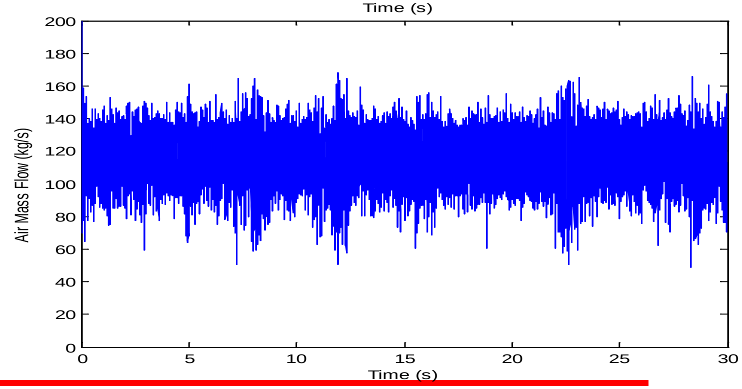

# Experimental Procedure

- Increasing boosting pressure drives the compressor to surge. Two values of amplitude in 5-15 Hz range are computed:
  - The maximum value during the 30 sec. recording time
  - The mean value during the recording time.

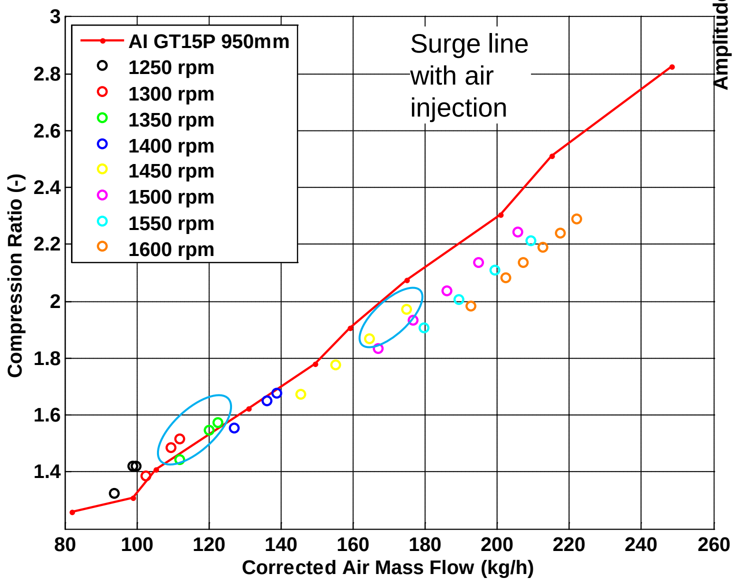


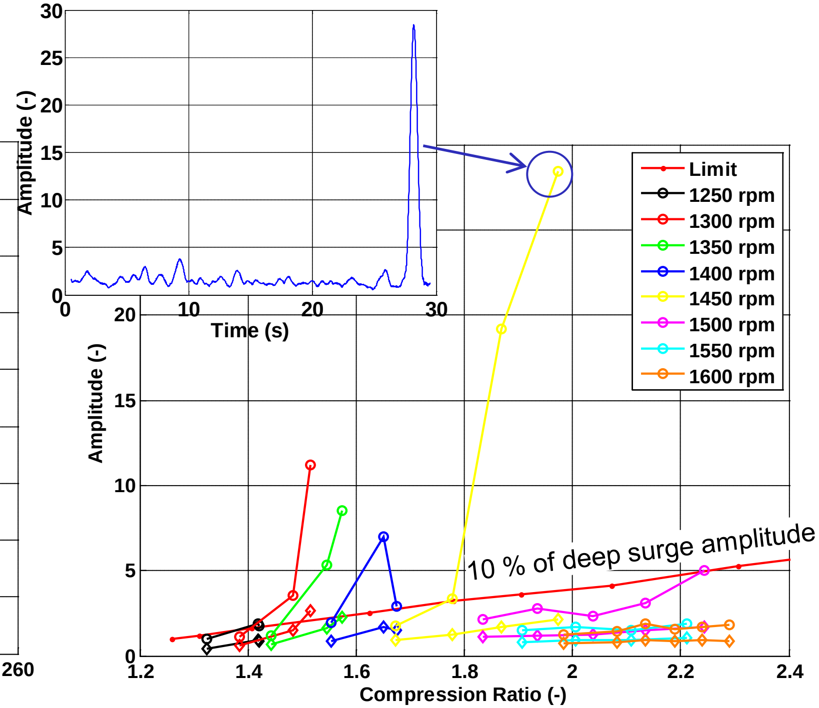

# Experimental procedure: transient

- Acceleration/deceleration at full load between 1250 and 2000 rpm

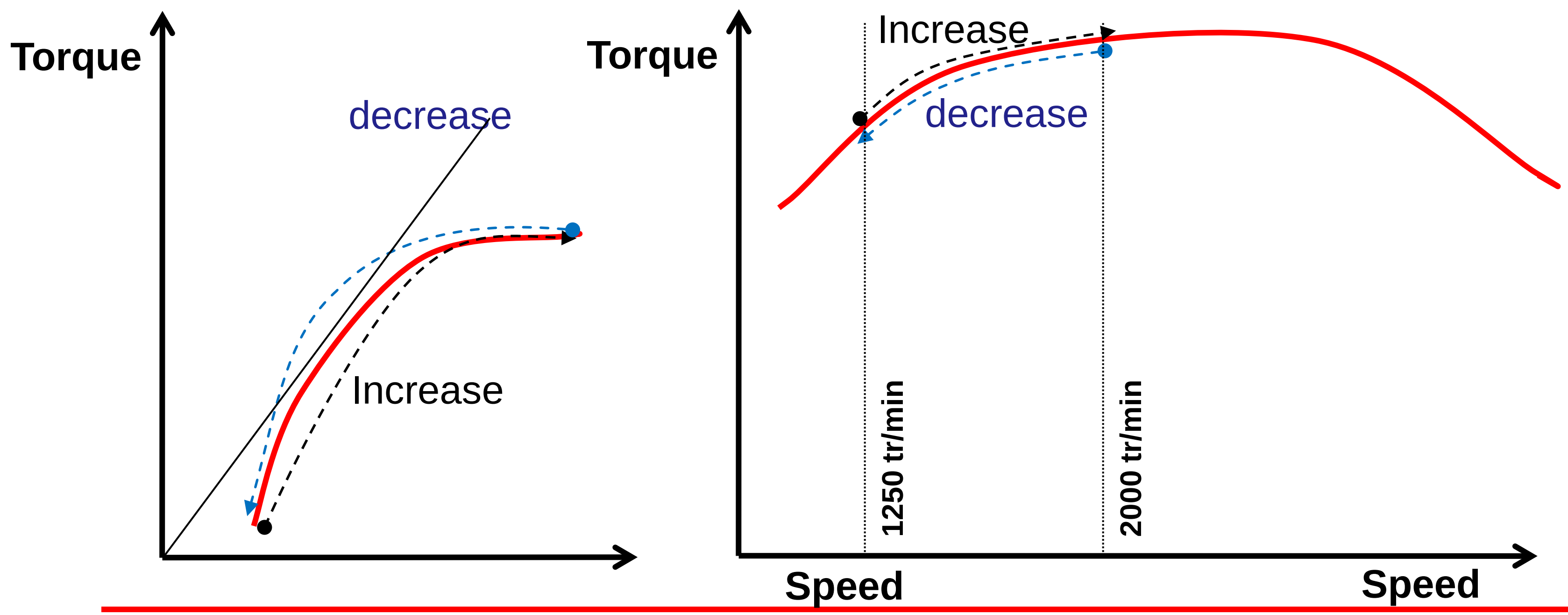

# Experimental procedure: transient

- Increasing speed tests:
  - Problems with the turbine controls
  - Increased boosting pressure settings

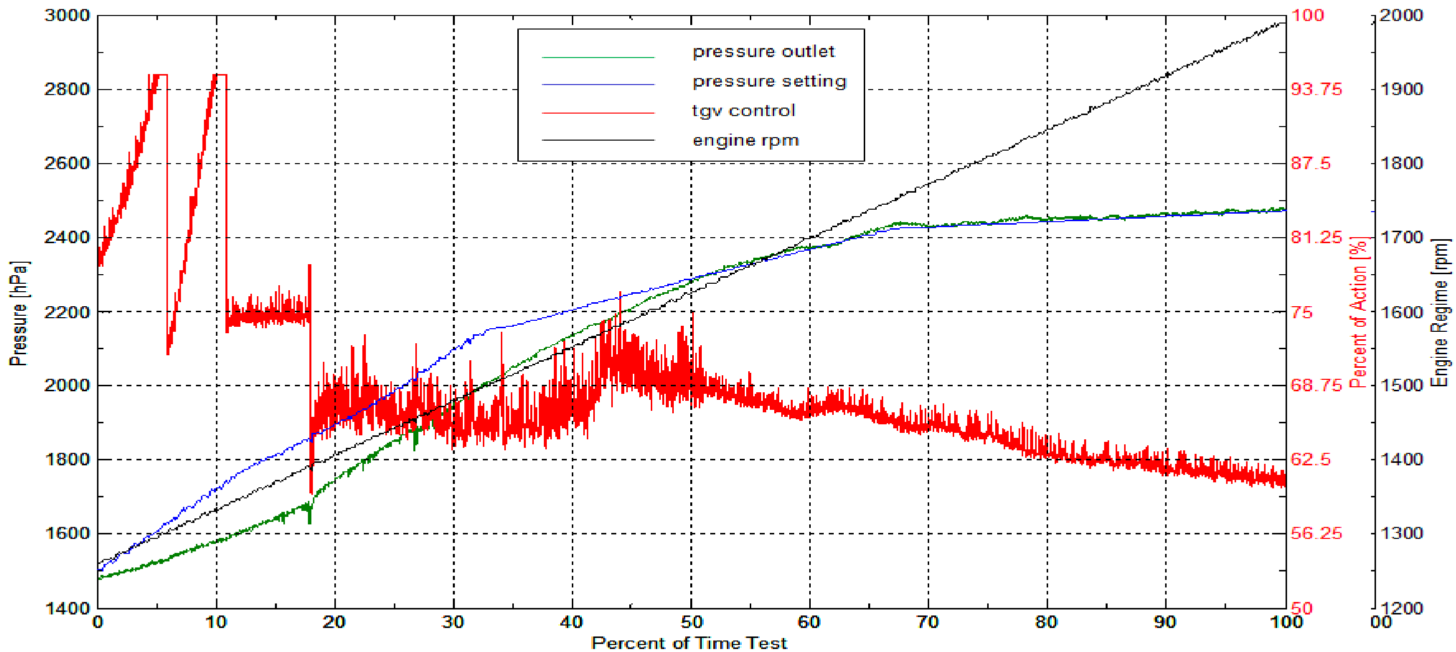

# Experimental procedure: transient

- Decreasing speed tests:
  - Increased boosting pressure settings

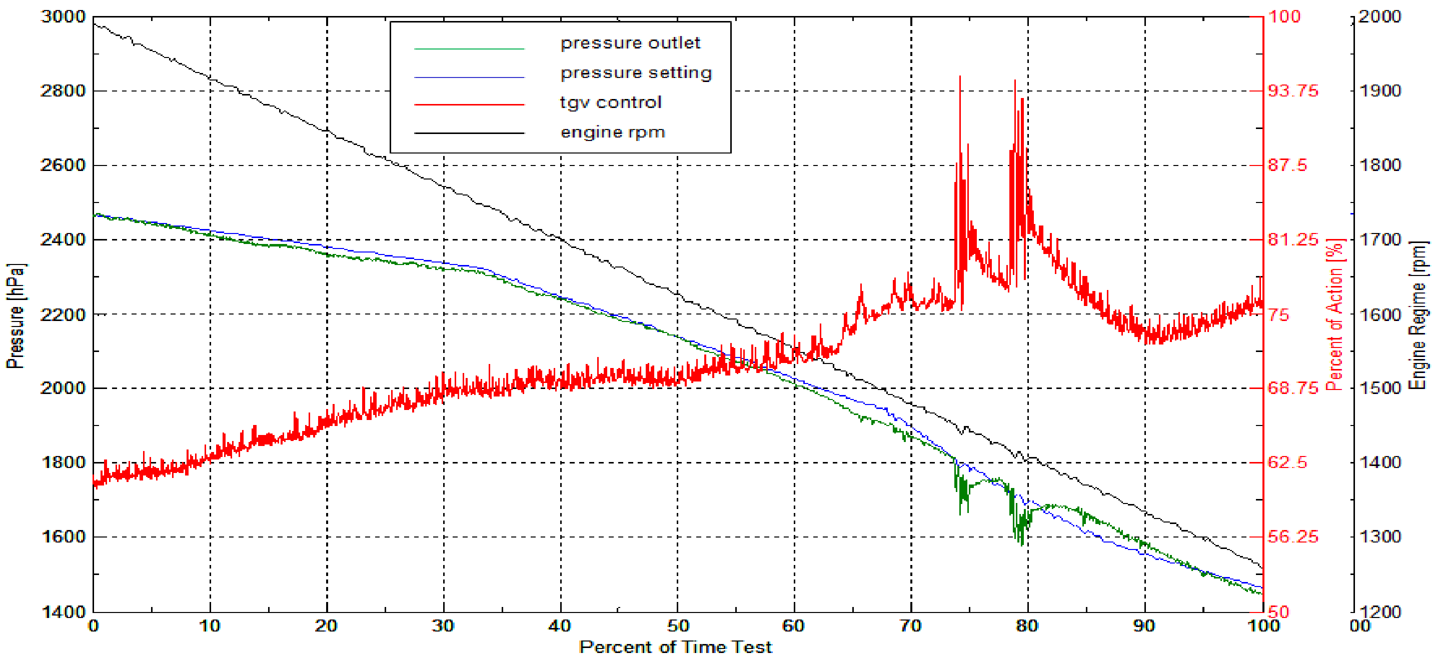

# Contents


- Introduction
- Experimental procedure
- Experimental Results
  - Gas-Stand
  - Steady tests
  - Transient tests
- Modeling
- Discussion

# Gas-Stand Tests

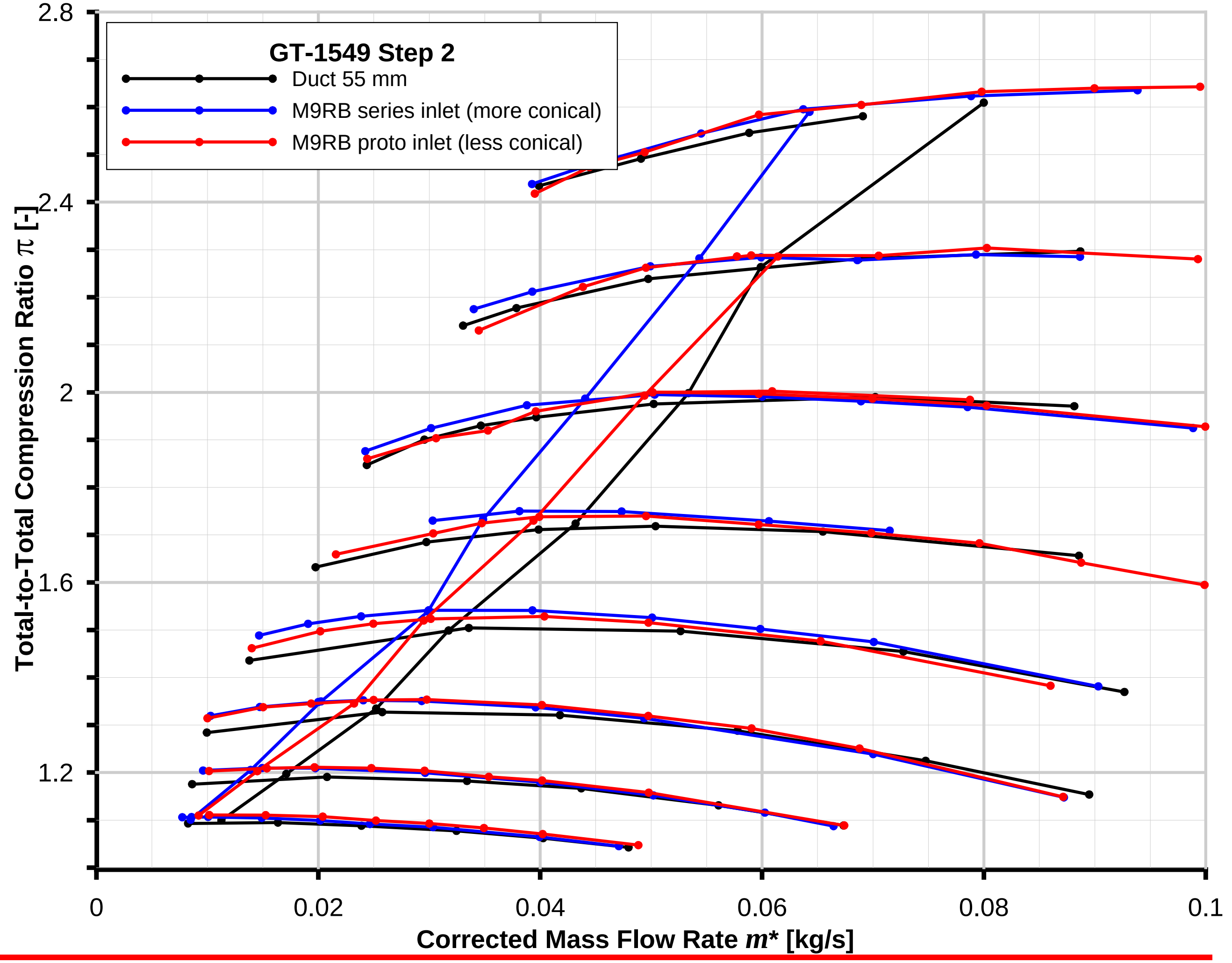

# Gas-Stand Tests

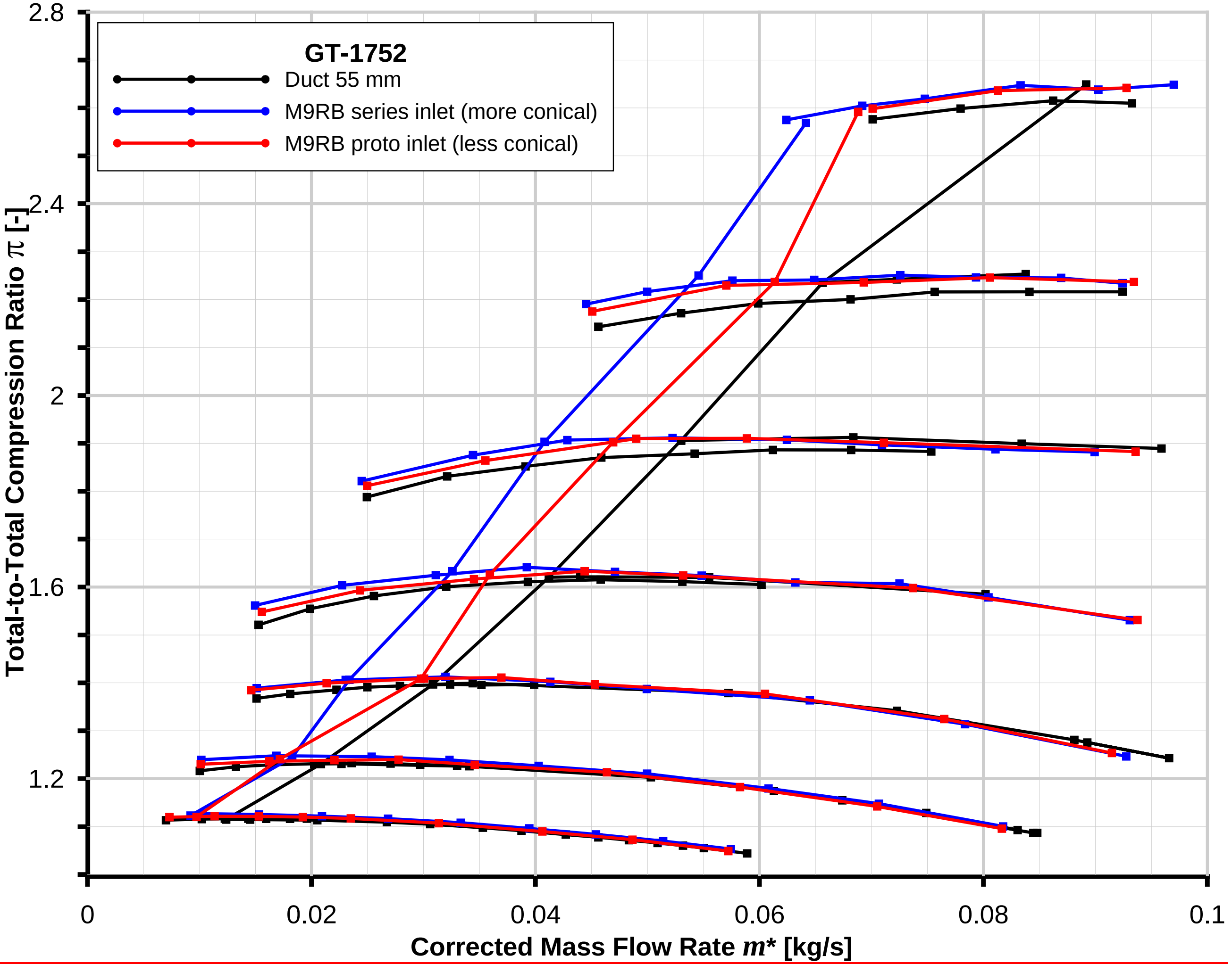

# Gas-Stand Tests

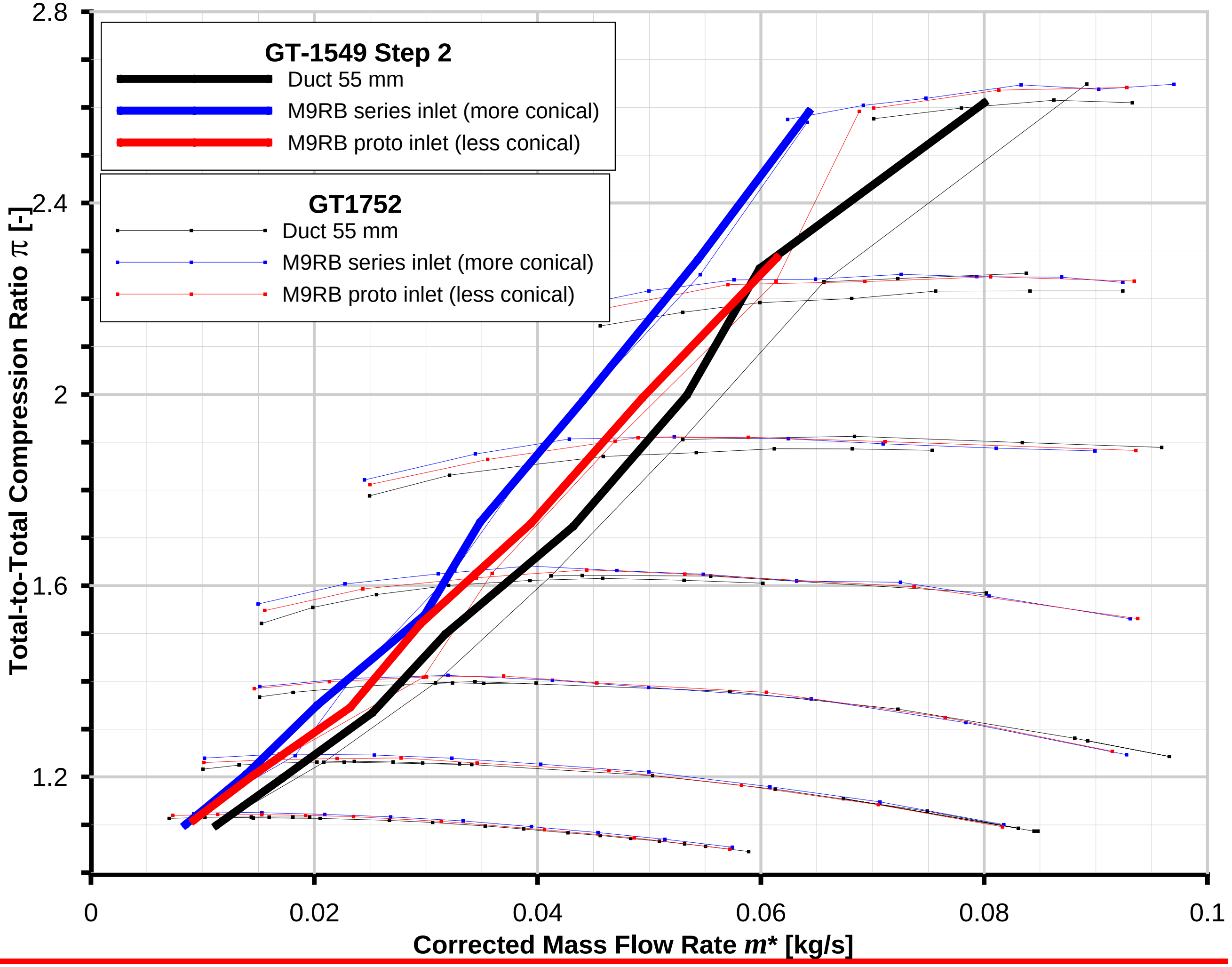

# Engine tests: Surge line

- Air injection surge lines

**From best …**

Conf8: Series inlet, Long duct, original filter
Conf6: Series inlet, Long duct, bigger filter
Conf7: Series inlet, Short duct, original filter
Conf2: Proto inlet, Long duct, original filter
Conf5: Series inlet, Short duct, bigger filter
Conf1: Proto inlet, Short duct, original filter
Conf3: Proto inlet, Short duct, bigger filter
Conf4: Proto inlet, Long duct, bigger filter

**… to worst**

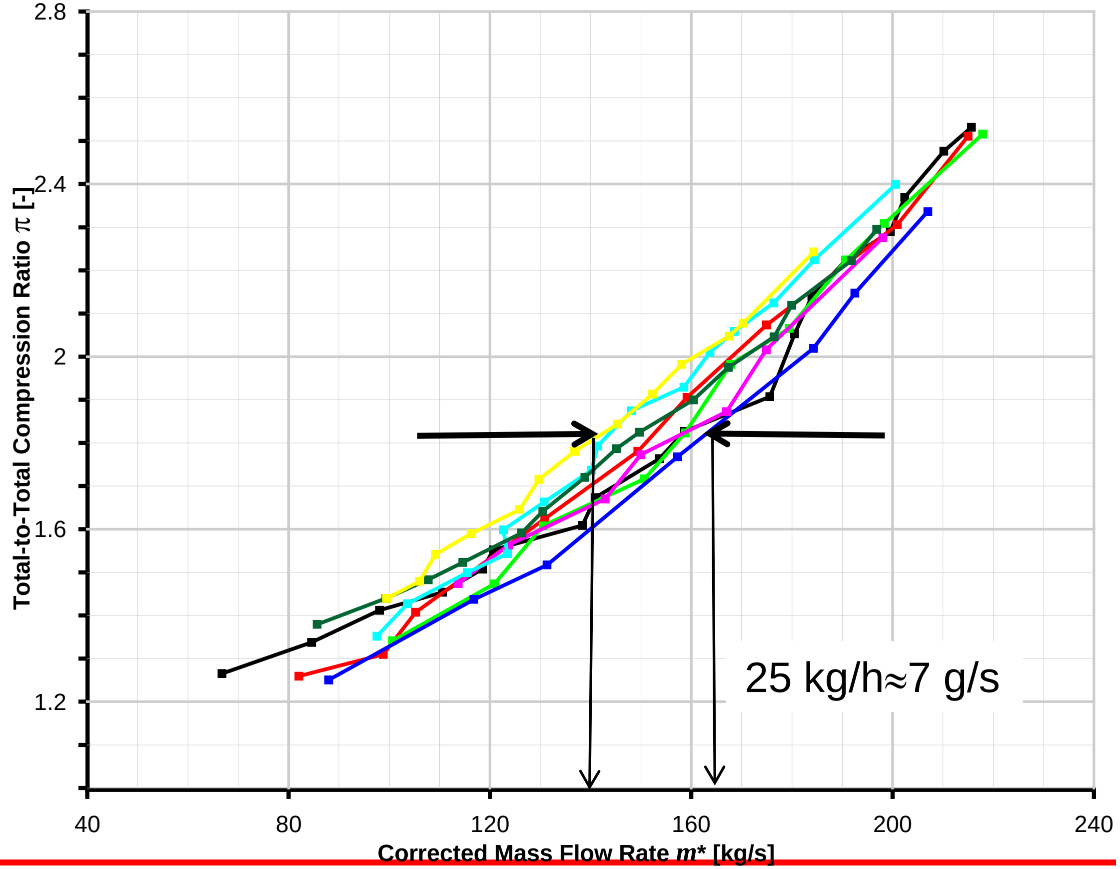

# Engine tests: Surge line

- The most influential parameter is the compressor inlet

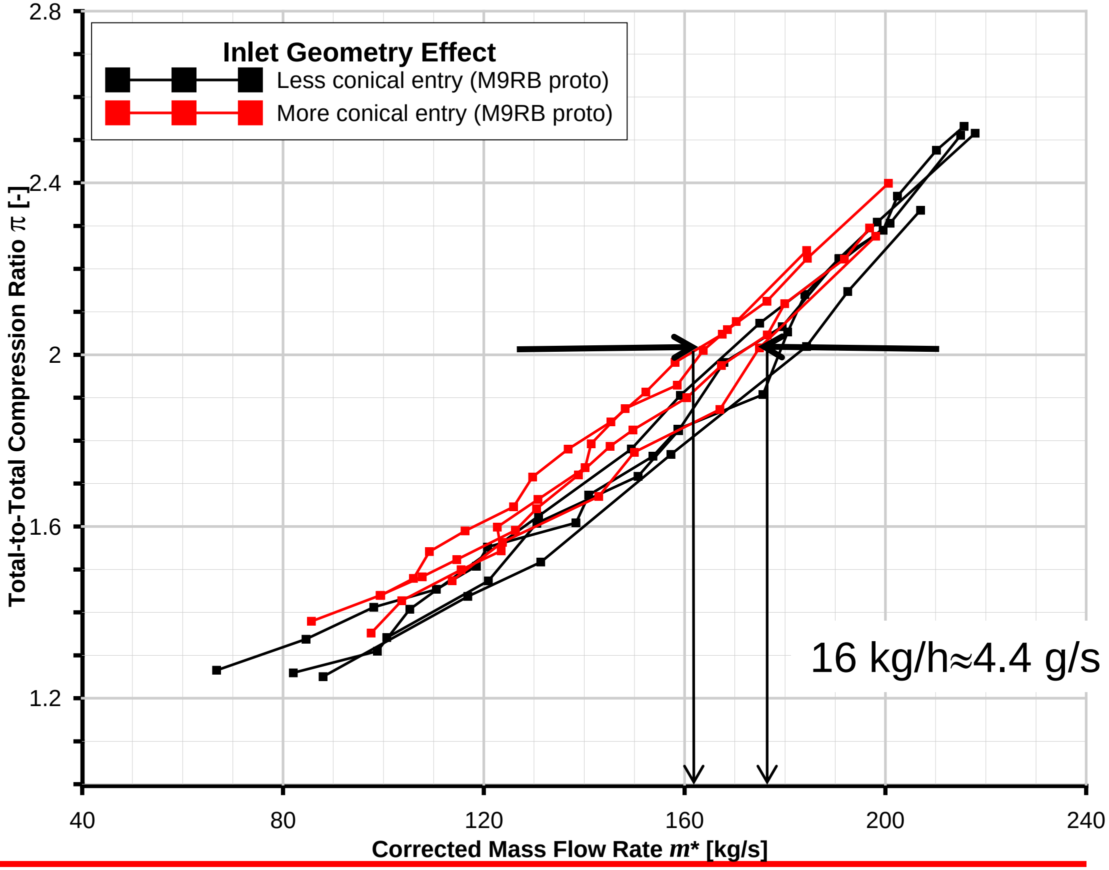

# Engine tests: Surge line

- Long duct downstream CAC is also good for surge

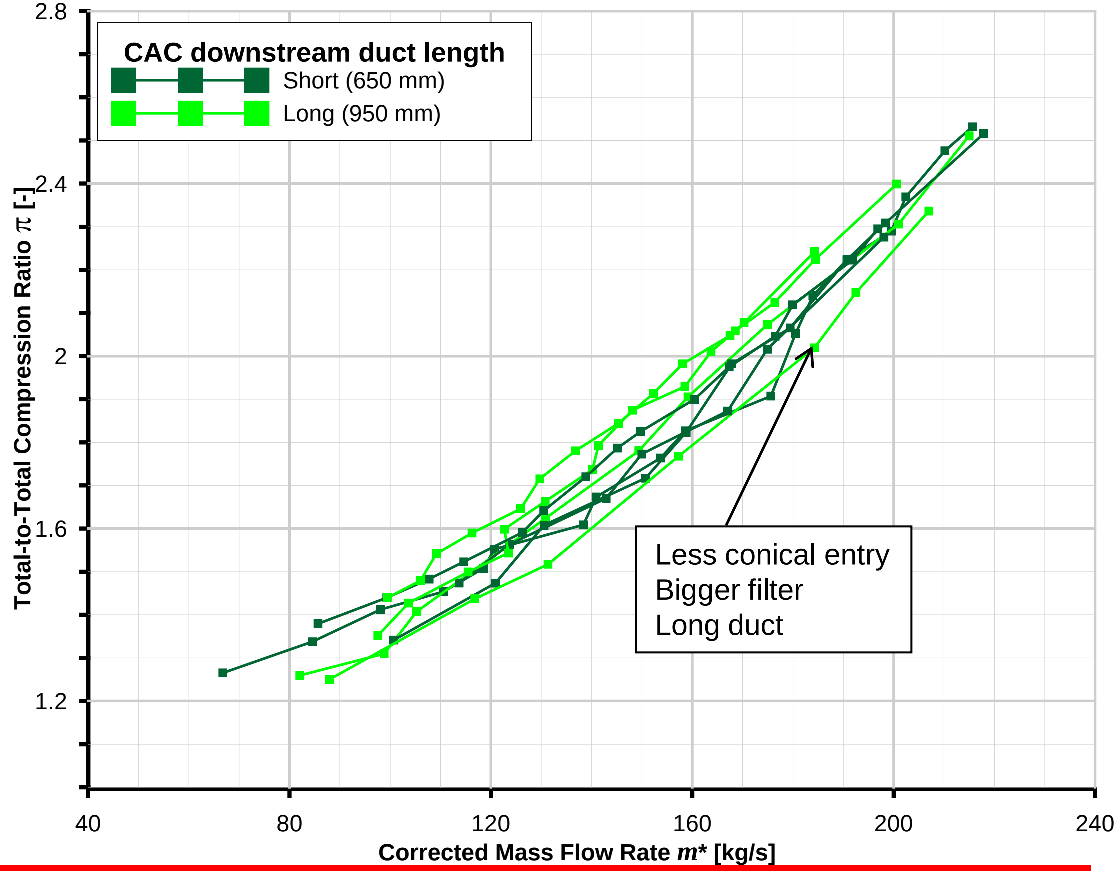

# Engine tests: Surge line

- Small filter volume is generally better

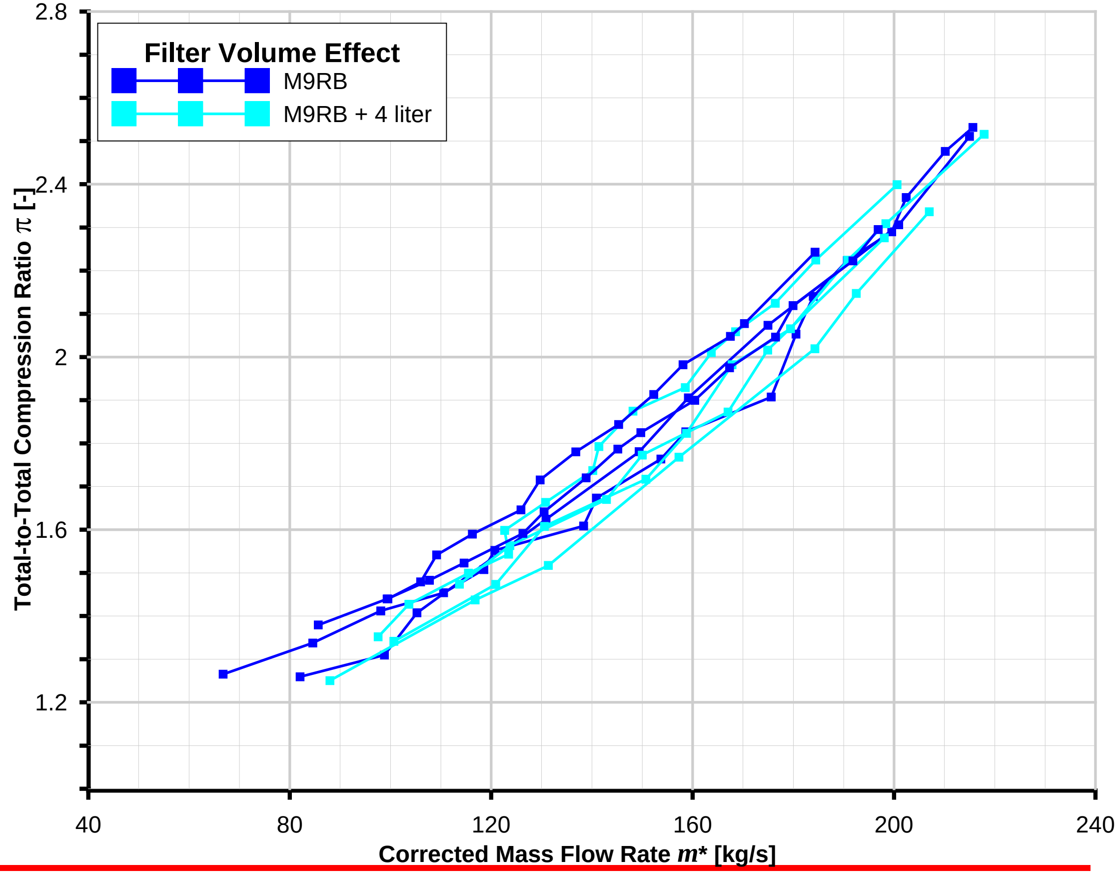

# Engine tests: Surge line

- Configuration 1:
  - Less conical inlet, Short duct, original filter

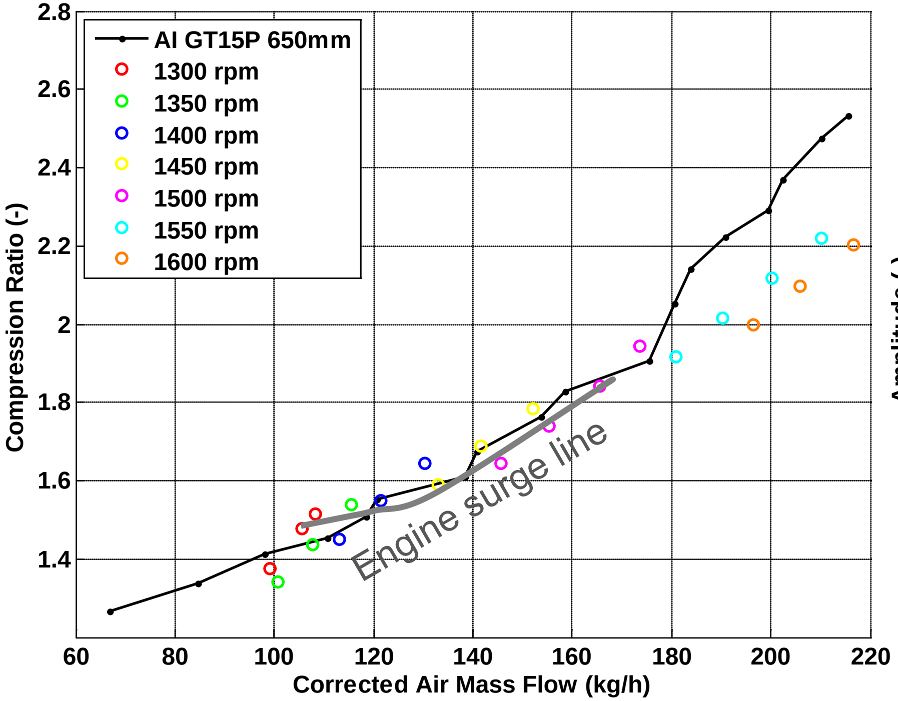


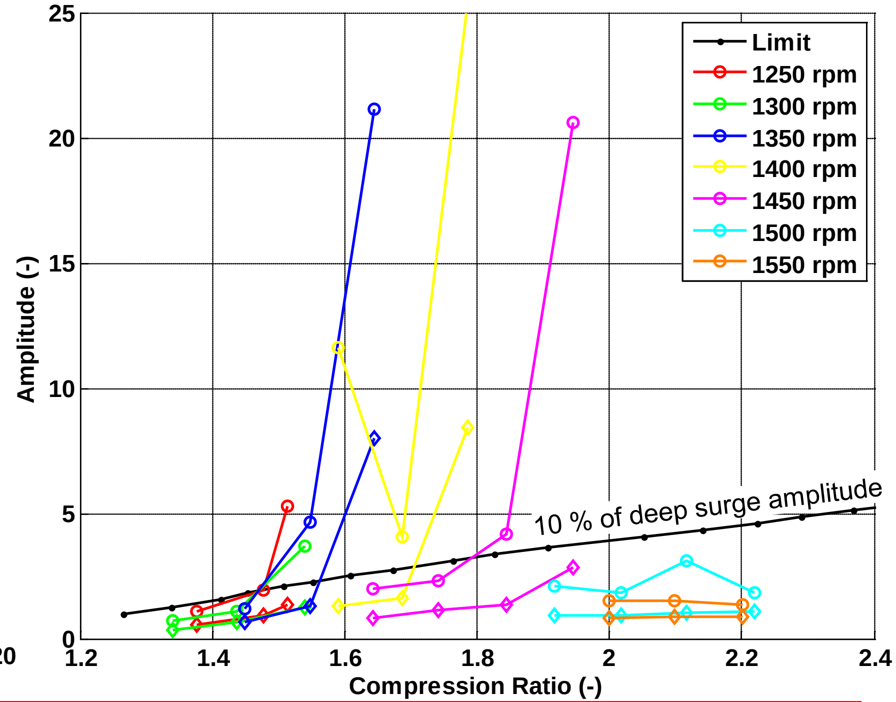

# Engine tests: Surge line

- Configuration 2:
  - Less conical inlet, Long duct, original filter

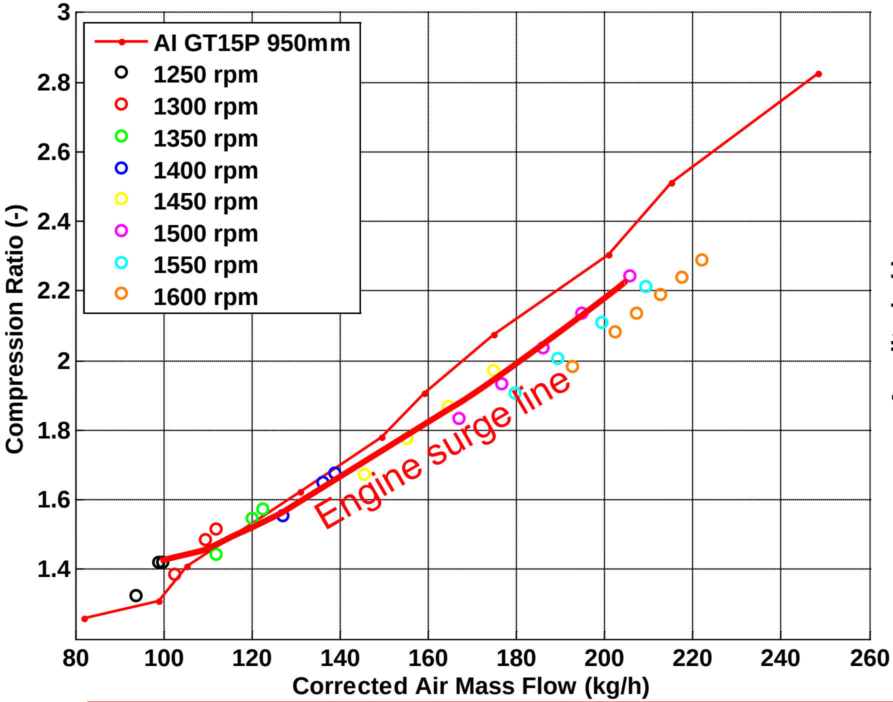


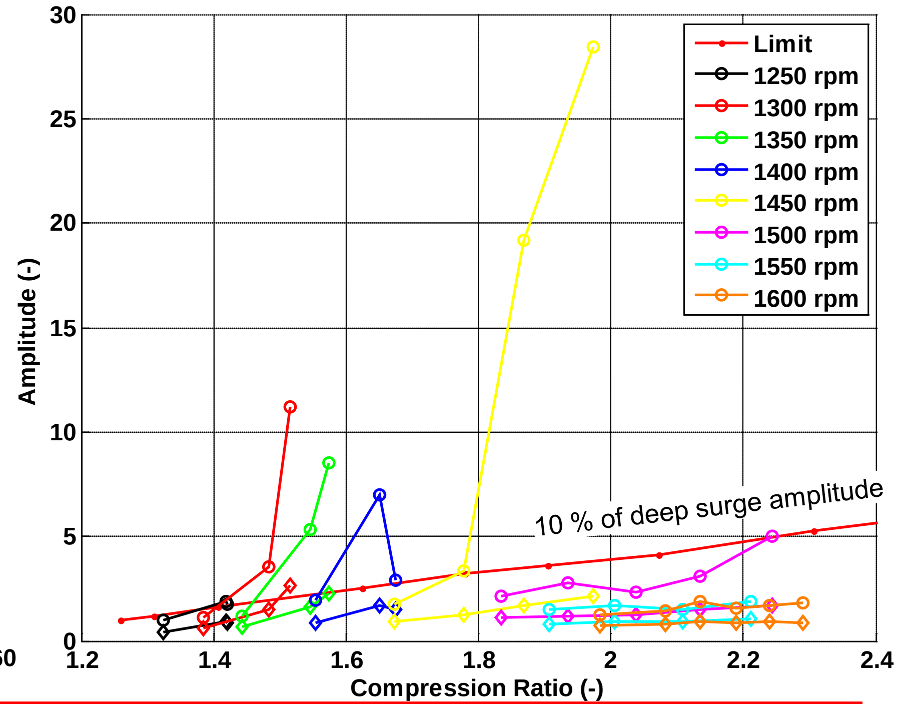

# ❑ Engine tests: Surge line

- Configuration 3:
  - Less conical inlet, Short duct, Bigger filter

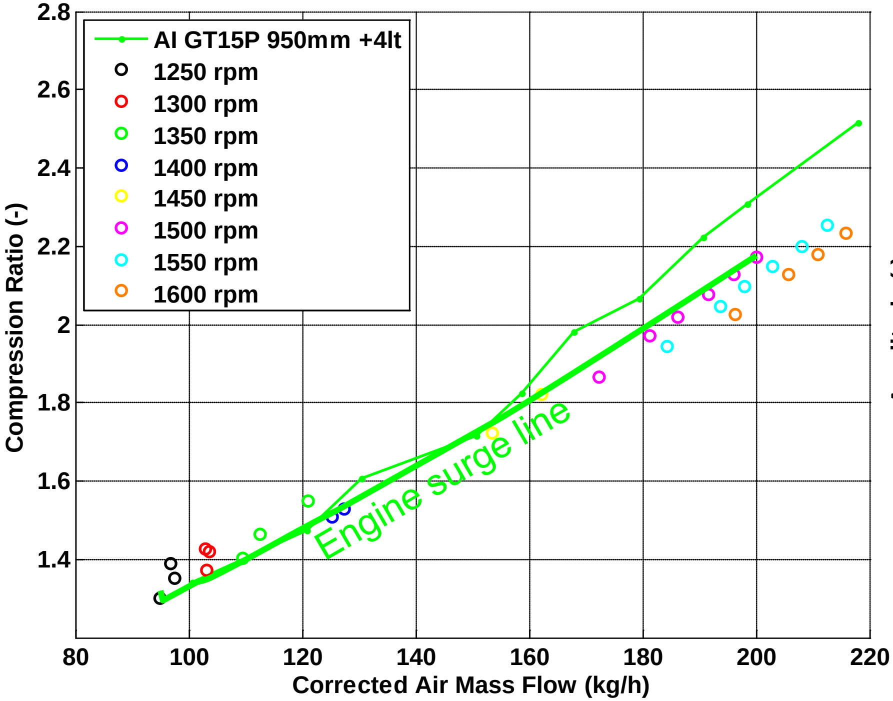


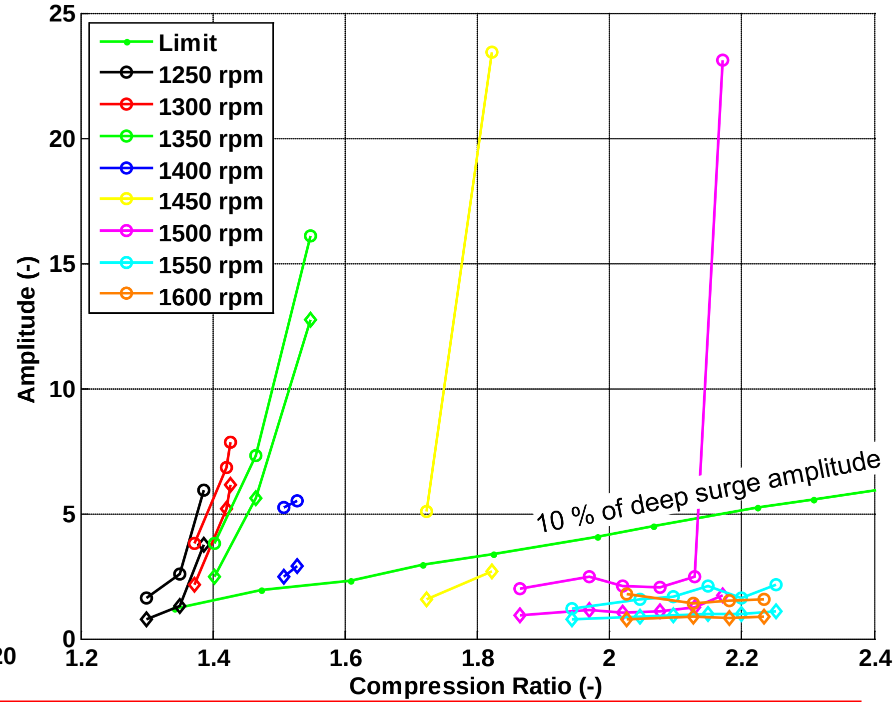

# Engine tests: Surge line

- Configuration 4:
  - Less conical inlet, Long duct, Bigger filter

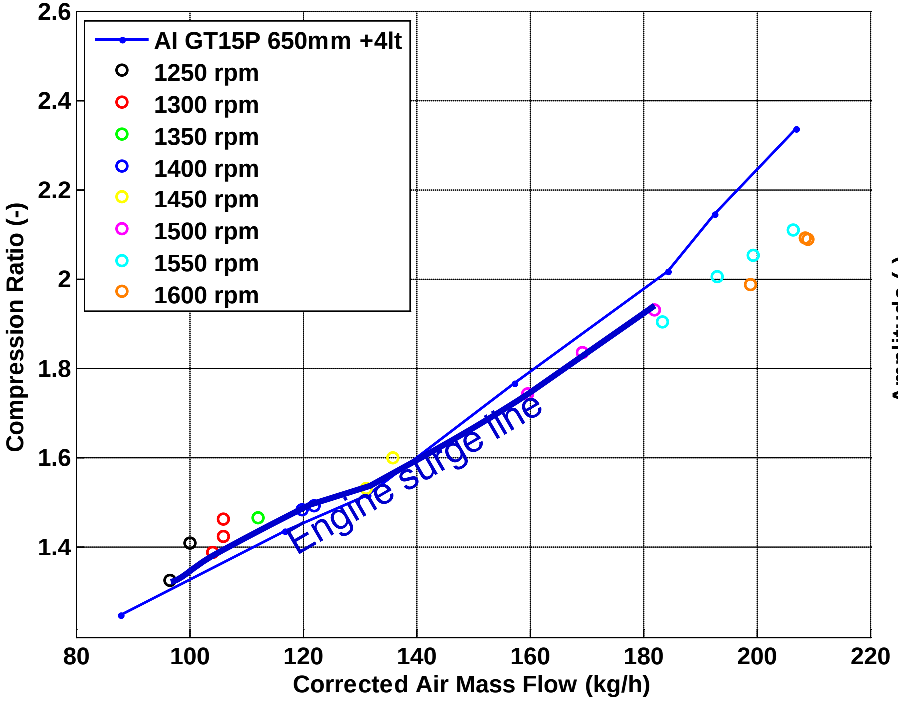


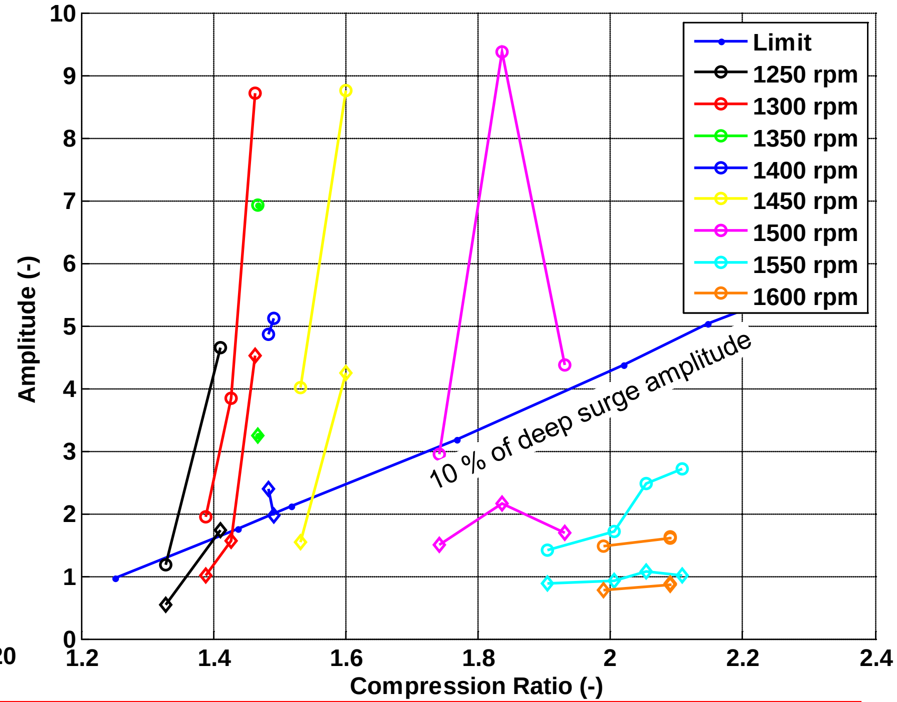

# ❑ Engine tests: Surge line

- o Configuration 5:
  - More conical inlet, Short duct, Bigger filter

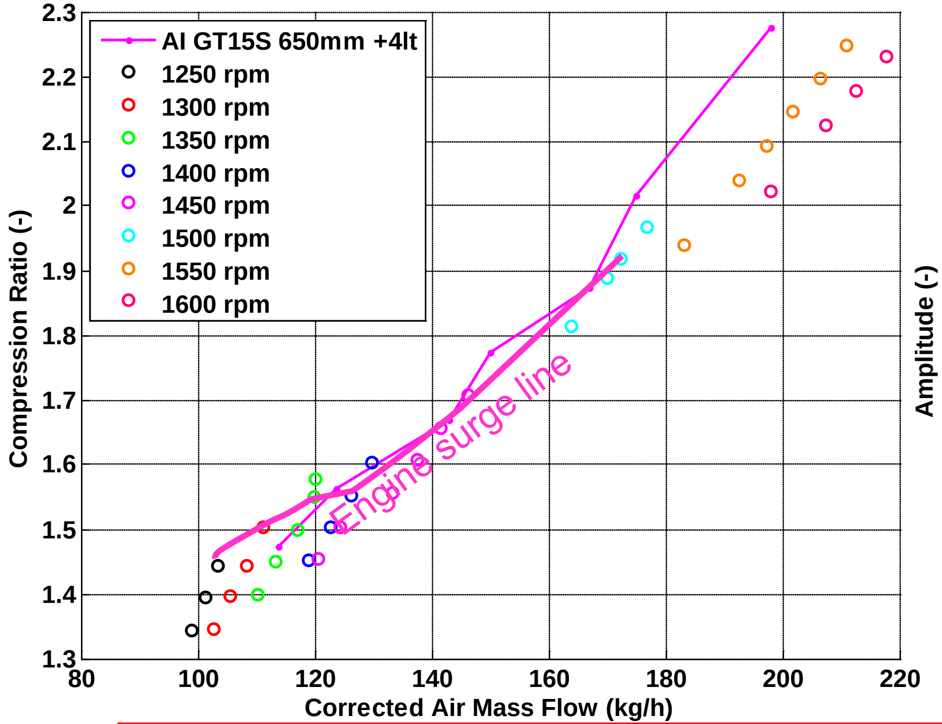


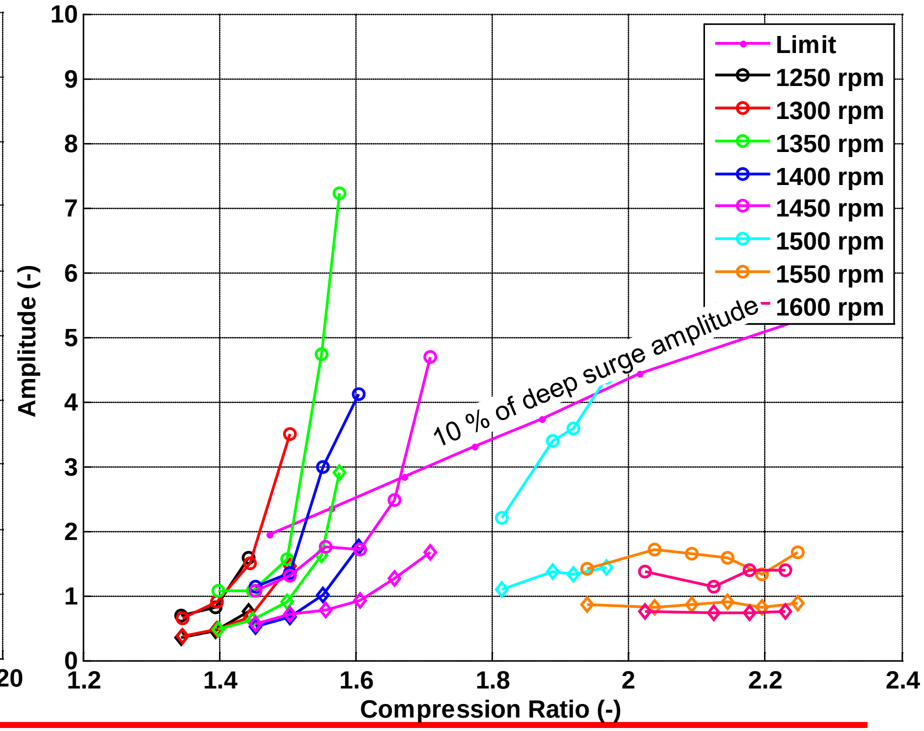

# Engine tests: Surge line

- Configuration 6:
  - More conical inlet, Long duct, Bigger filter

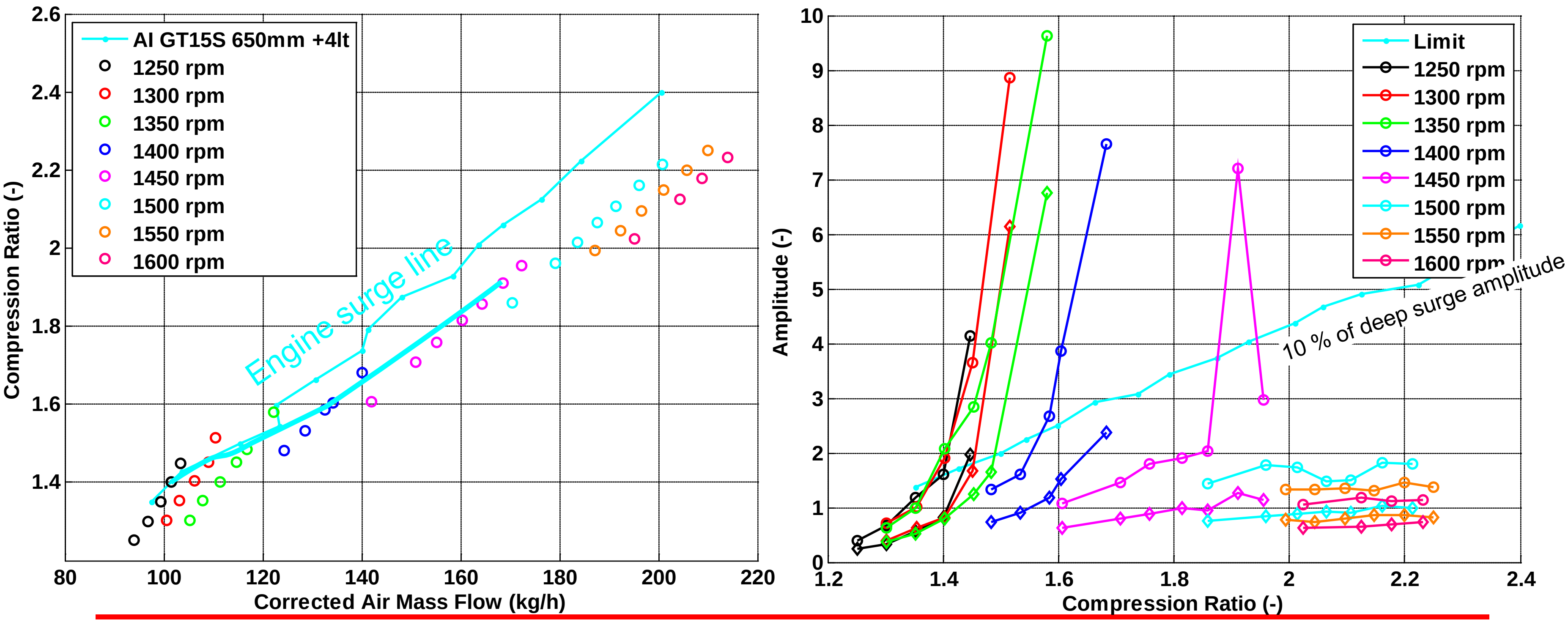

# Engine tests: Surge line

- Configuration 7:
  - More conical inlet, Short duct, Original filter

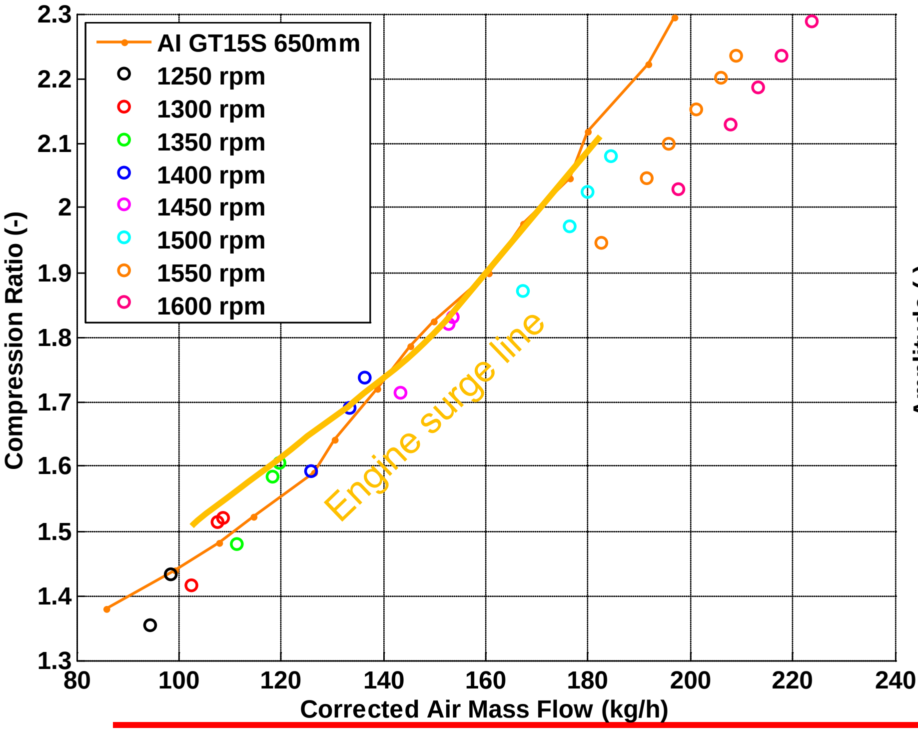


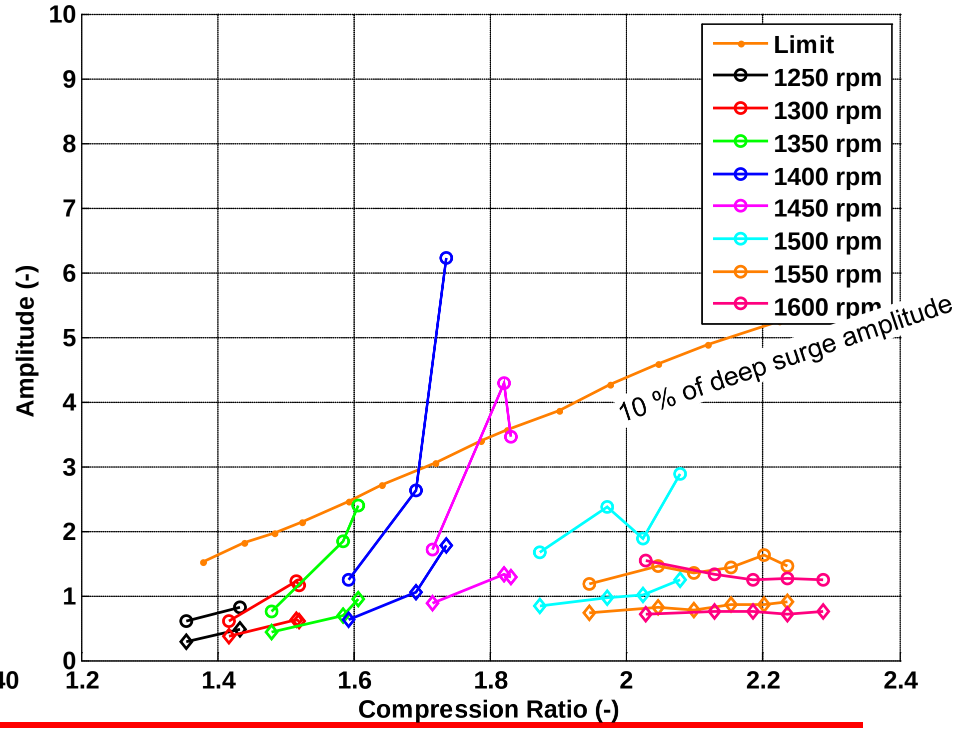

# Engine tests: Surge line

- Volumetric efficiency is as important as surge limit to get the maximum air mass flow at a given engine speed
- Best configs: 5, 6, 7 , 2, 3

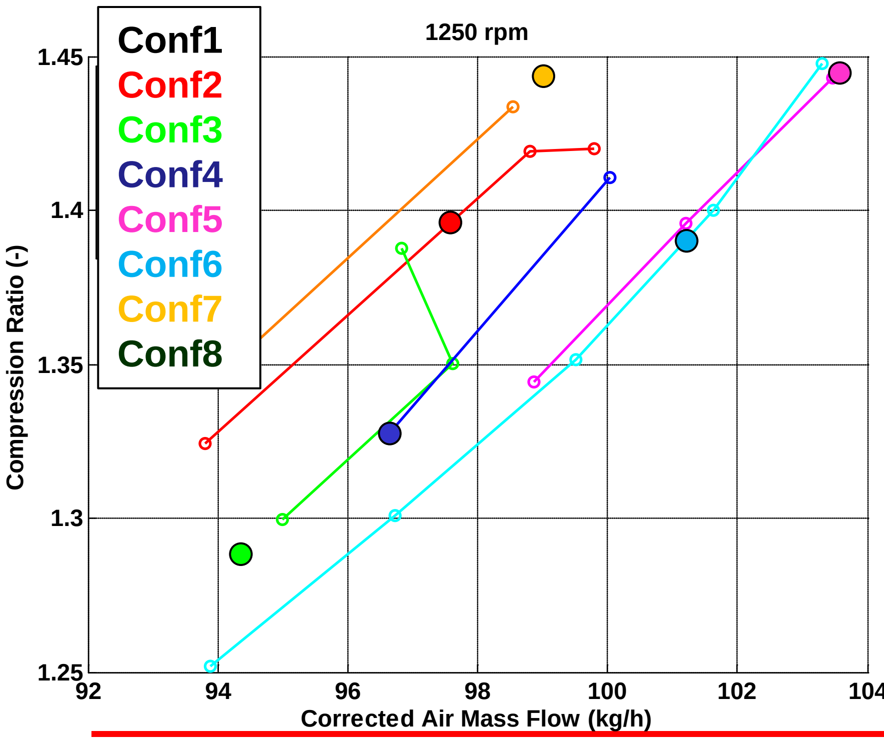


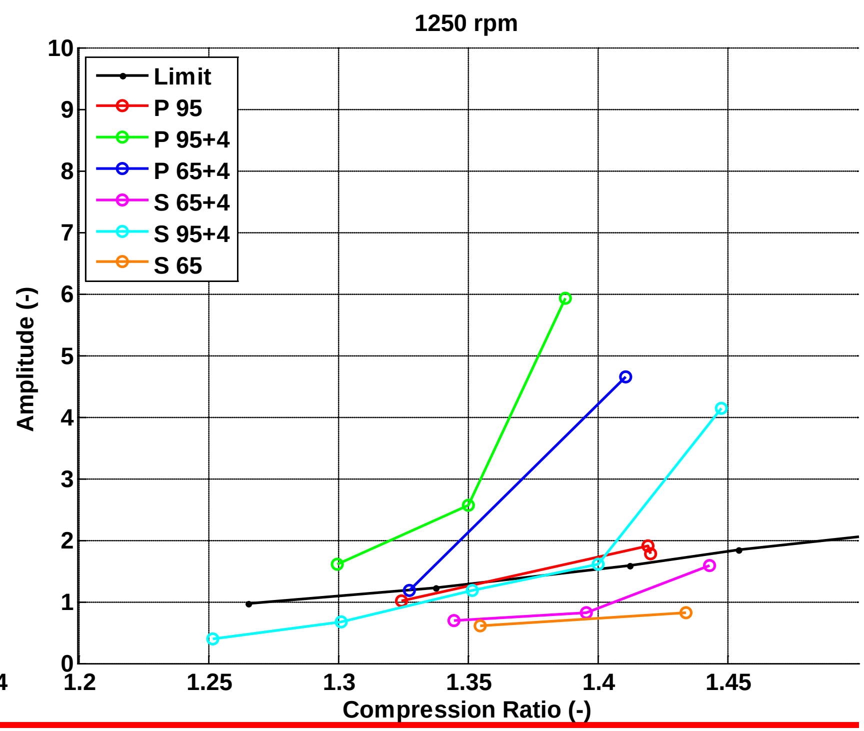

# Engine tests: Surge line

- At low speeds the bigger filter leads to higher volumetric eff.
- Best configs: 7, 5, 1, 6, 4, 2, 3

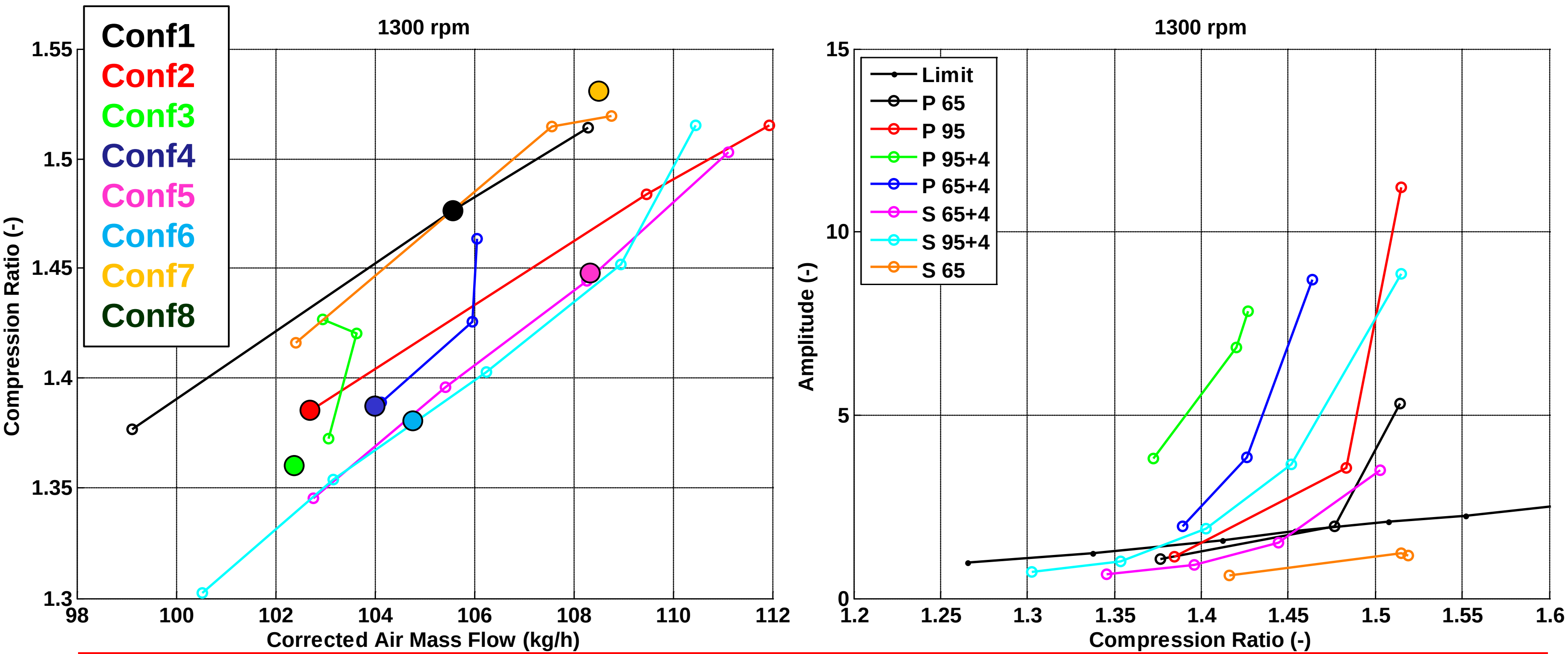

# Engine tests: Surge line

- Best configs: 7, 5, 1, 2, 6, 3, 4

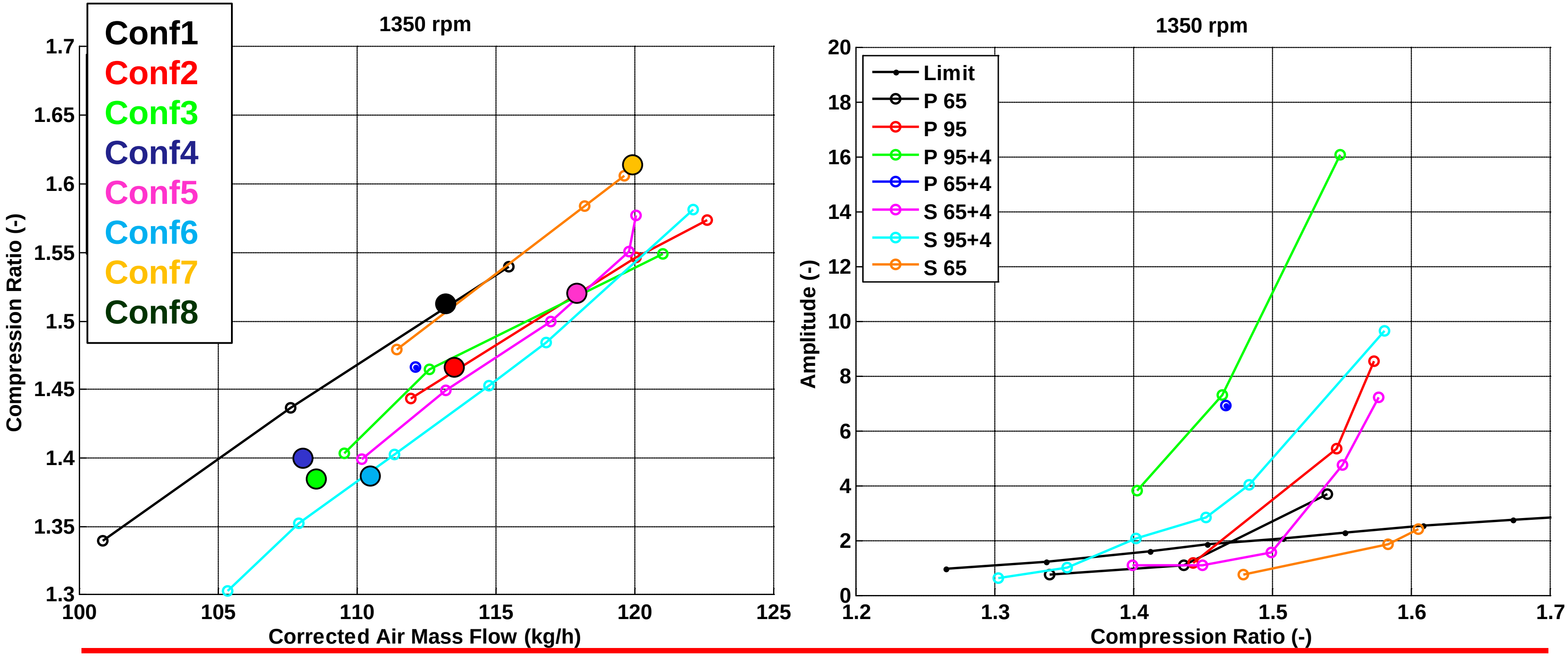

# Engine tests: Surge line

- Best configs: 7, 6, 2, 5, 3, 4, 1

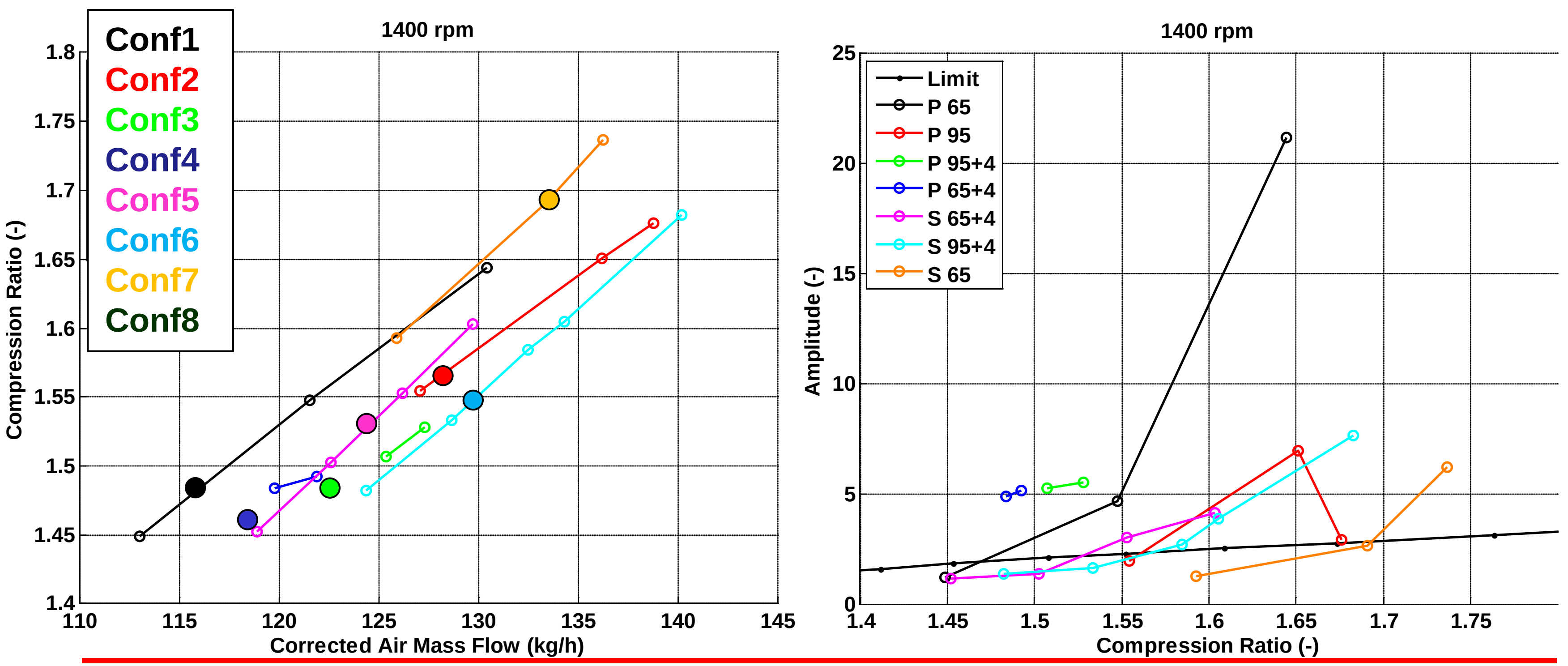

# ❑ Engine tests: Surge line

- Best configs: 6, 7, 2, 5, 3, 7, 1, 4

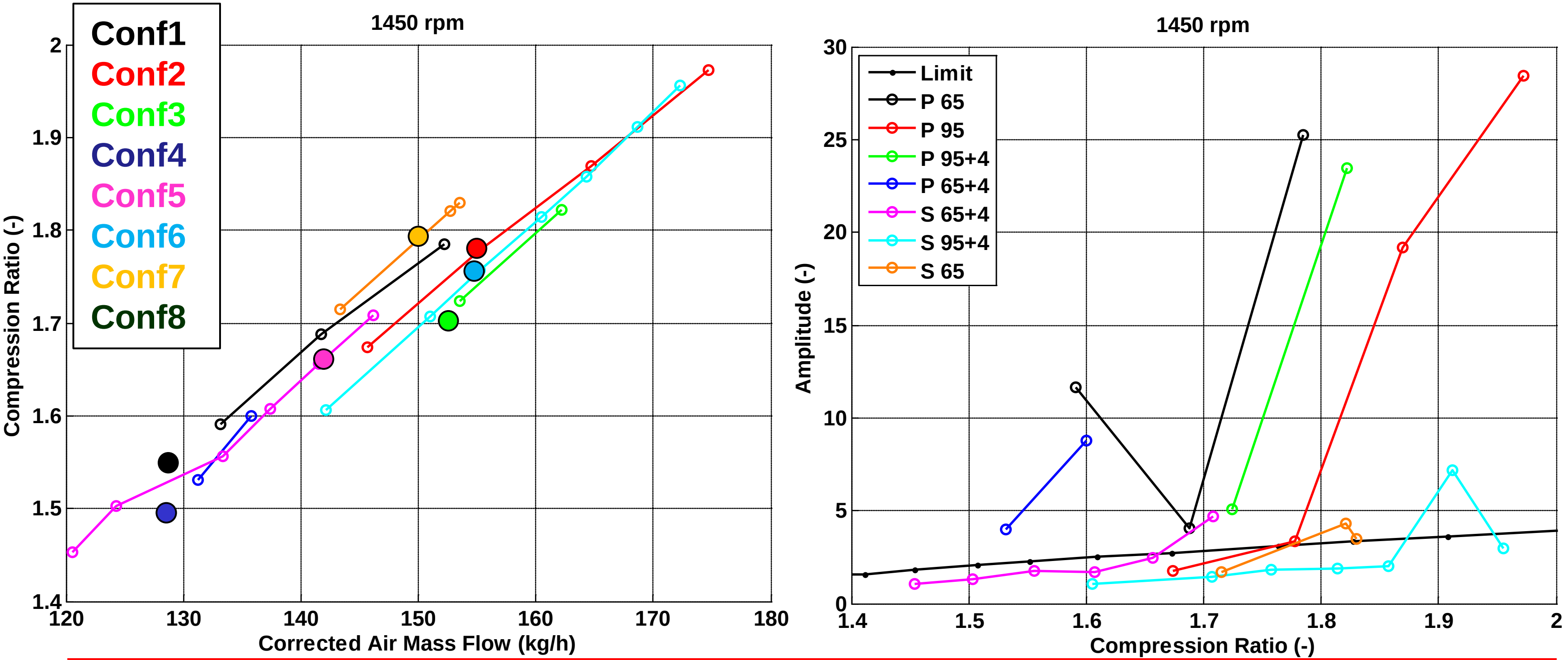

# Engine tests: Surge line

- Best configs: 6, 7, 2, 5, 4, 3, 1

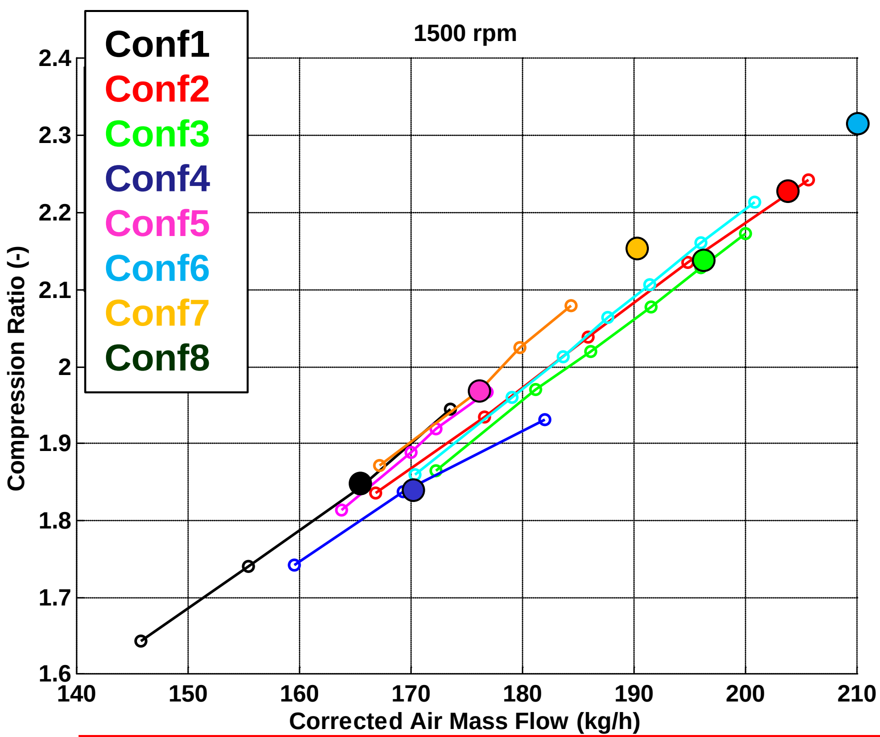


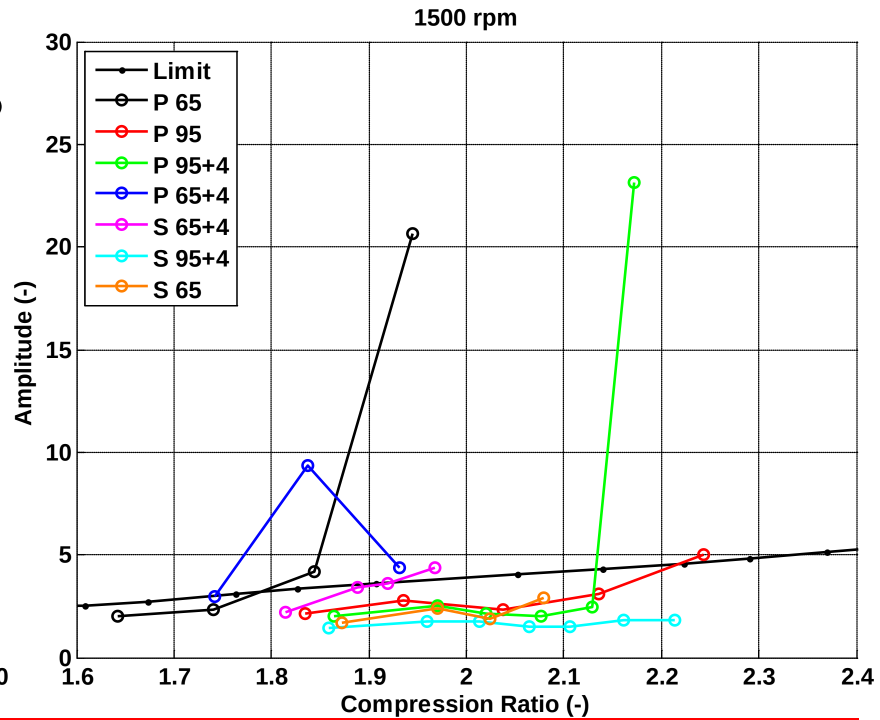

# Engine tests: Surge line

- Best configs: all

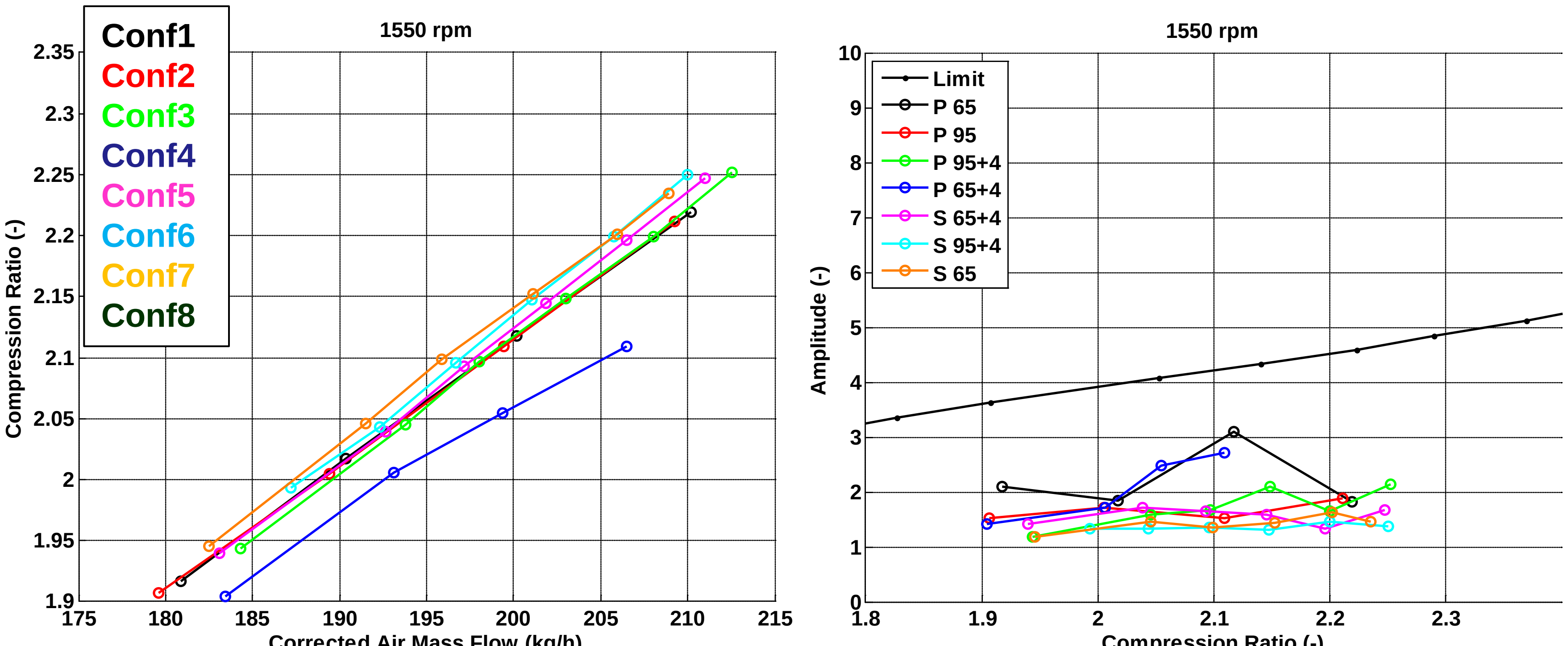

# Engine tests: Surge line

- Best configs: all

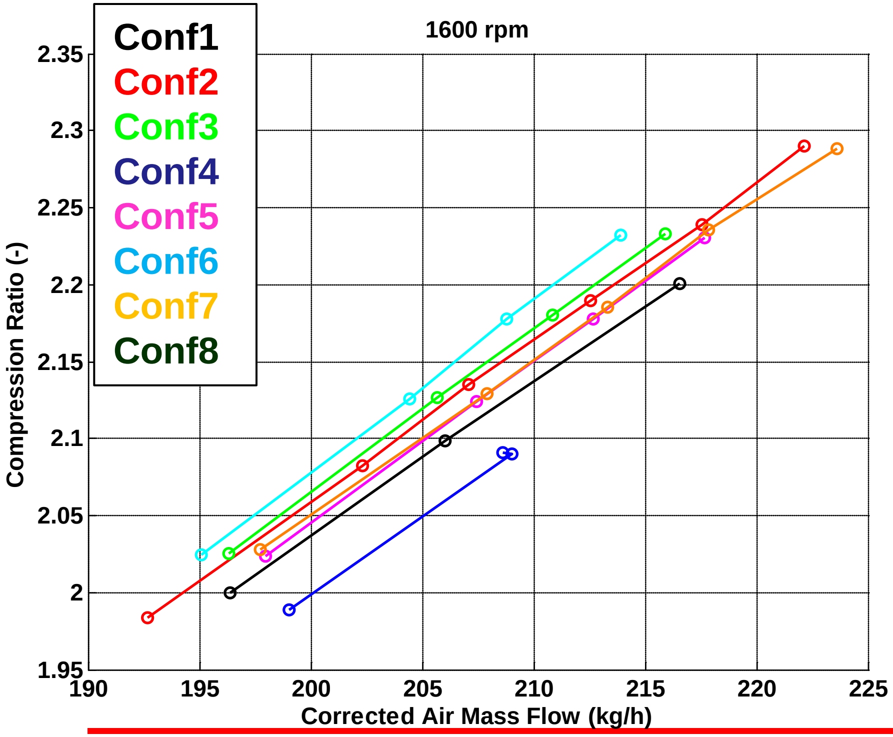


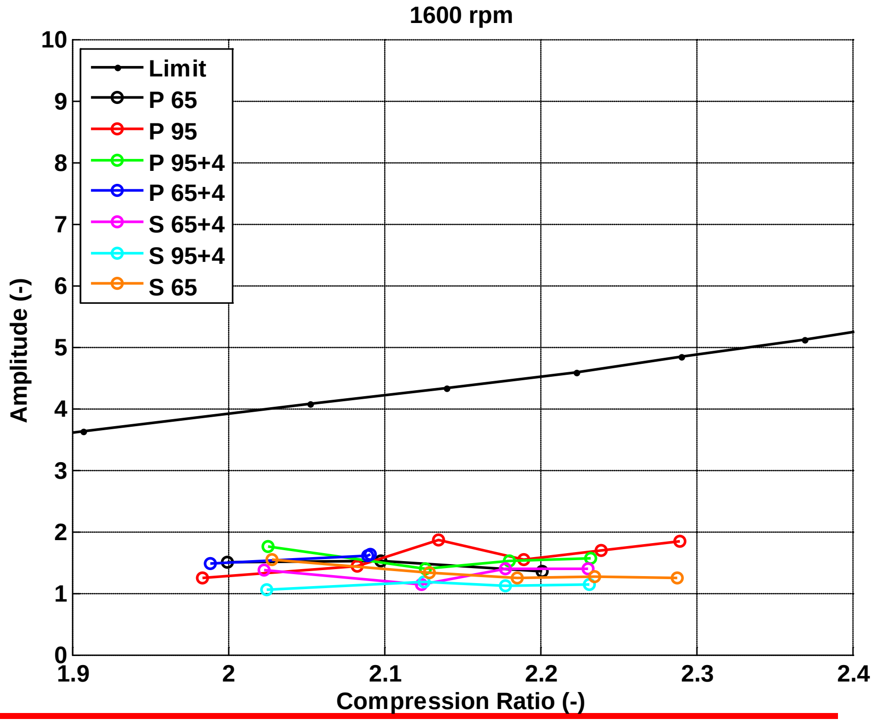

# Engine steady tests: Conclusions

- The most influential parameter in surge is to have or not the conical entry
- Moderate agreement between air injection and maximum boosting pressure tests. Surge is overestimated at low speed and underestimated at medium speed in air injection tests. But the trends are well predicted
- Amplitude at low frequency is a good parameter to compare surge in different configurations
- Volumetric efficiency is as important as surge margin to increase air mass flow at a given engine speed
- This is the reason why some geometries are better at low-medium speed than others. In any case the conical entry effect is bigger than that of the volumetric eff.

# Engine tests: Transient tests

- Acceleration tests at Full Load from 1250 to 2000 rpm
  - Tests duration from 10 to 100 ms
  - Increased boost pressure
  - Surge is more relevant for slow tests
  - Worst configs: **conf4**, conf1, conf3 and conf6

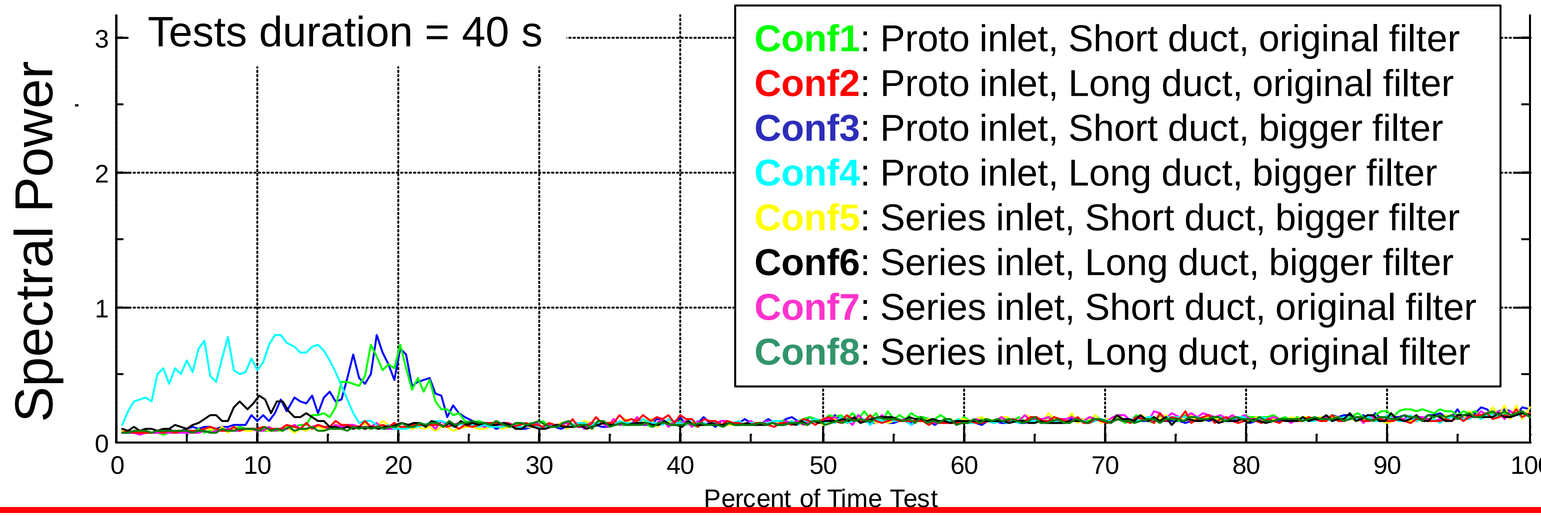

# ❑ Engine tests: Transient tests

- Acceleration tests at Full Load from 1250 to 2000 rpm
  - Tests duration from 100 to 10 ms
  - Increased boost pressure
  - Surge is more relevant for slow tests
  - Worst configs: **conf4**, conf1, conf3 and conf6

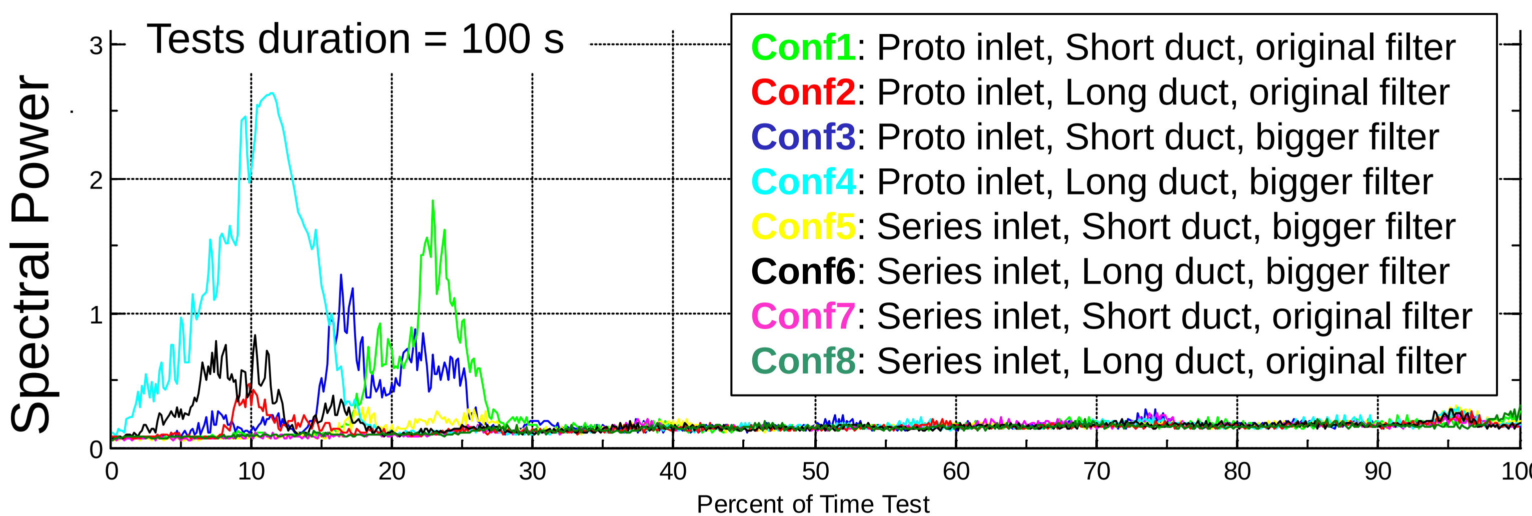

# Engine tests: Transient tests

- Deceleration tests at Full Load from 2000 to 1250 rpm
  - Surge does not depend on test duration
  - Worst configs: **conf3**, conf4, conf1 and conf5

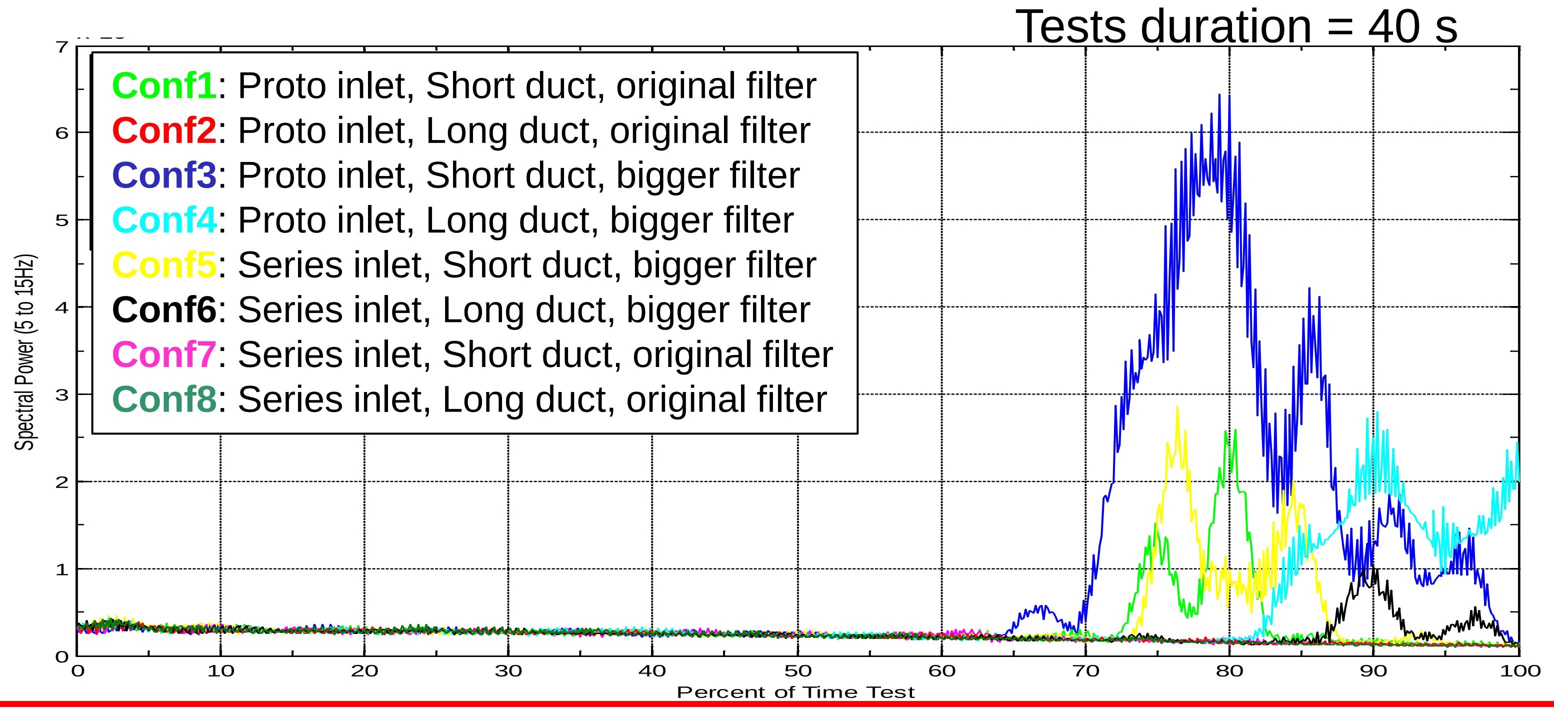

# Engine transient tests: Conclusions

- In decelerations surge is more likely to occur than in accelerations
- There is surge in acceleration only if boosting pressure settings are increased over steady surge limit during very slow transients
- In general, configurations that have lower surge limit in steady also have in transient

**STEADY**

From worst…

**Conf4**: Proto inlet, Long duct, bigger filter
**Conf3**: Proto inlet, Short duct, bigger filter
**Conf1**: Proto inlet, Short duct, original filter
**Conf5**: Series inlet, Short duct, bigger filter
**Conf2**: Proto inlet, Long duct, original filter
**Conf7**: Series inlet, Short duct, original filter
**Conf6**: Series inlet, Long duct, bigger filter
**Conf8**: Series inlet, Long duct, original filter

… to best

**TRANSIENT**

From worst …

**Conf3**: Proto inlet, Short duct, bigger filter
**Conf4**: Proto inlet, Long duct, bigger filter
**Conf1**: Proto inlet, Short duct, original filter
**Conf5**: Series inlet, Short duct, bigger filter
**Conf6**: Series inlet, Long duct, bigger filter
**Conf2**: Proto inlet, Long duct, original filter
**Conf7**: Series inlet, Short duct, original filter
**Conf8**: Series inlet, Long duct, original filter

… to best

# Contents

- o Introduction
- o Experimental procedure
- o Experimental Results
- o Modeling
  - 3. To calibrate the model
  - 4. To use the user function to model the tests campaigns
  - 1. To develop a User Function in GT with the compressor model
  - 2. Transfer to (enterprise)
- o Discussion

# Modeling work: integration in GT

- Flow diagram

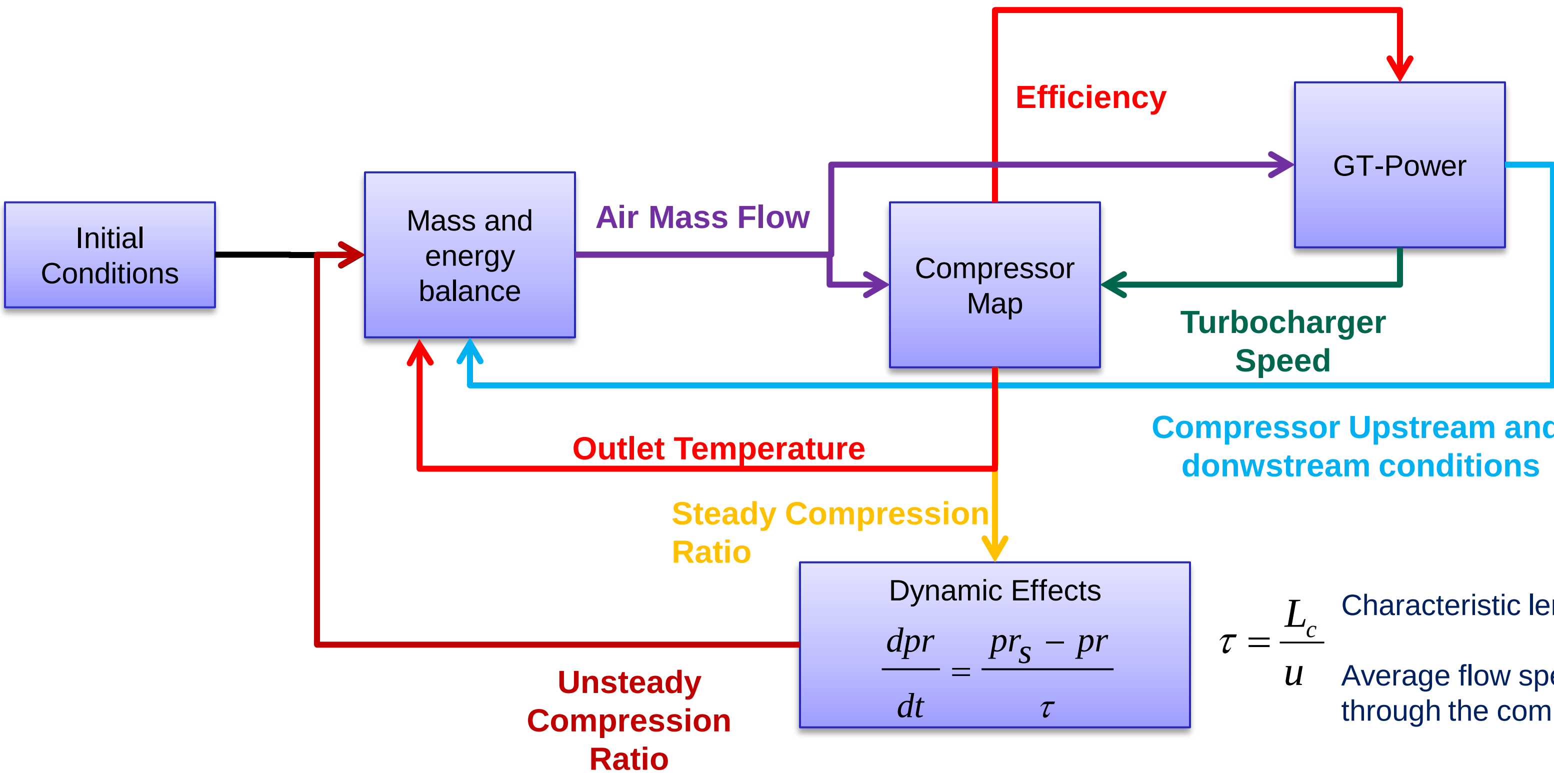


$$\tau = \frac{L_c}{u}$$

Characteristic length

Average flow speed through the compressor

# ❑ Modeling work: integration in GT

- o Flow diagram

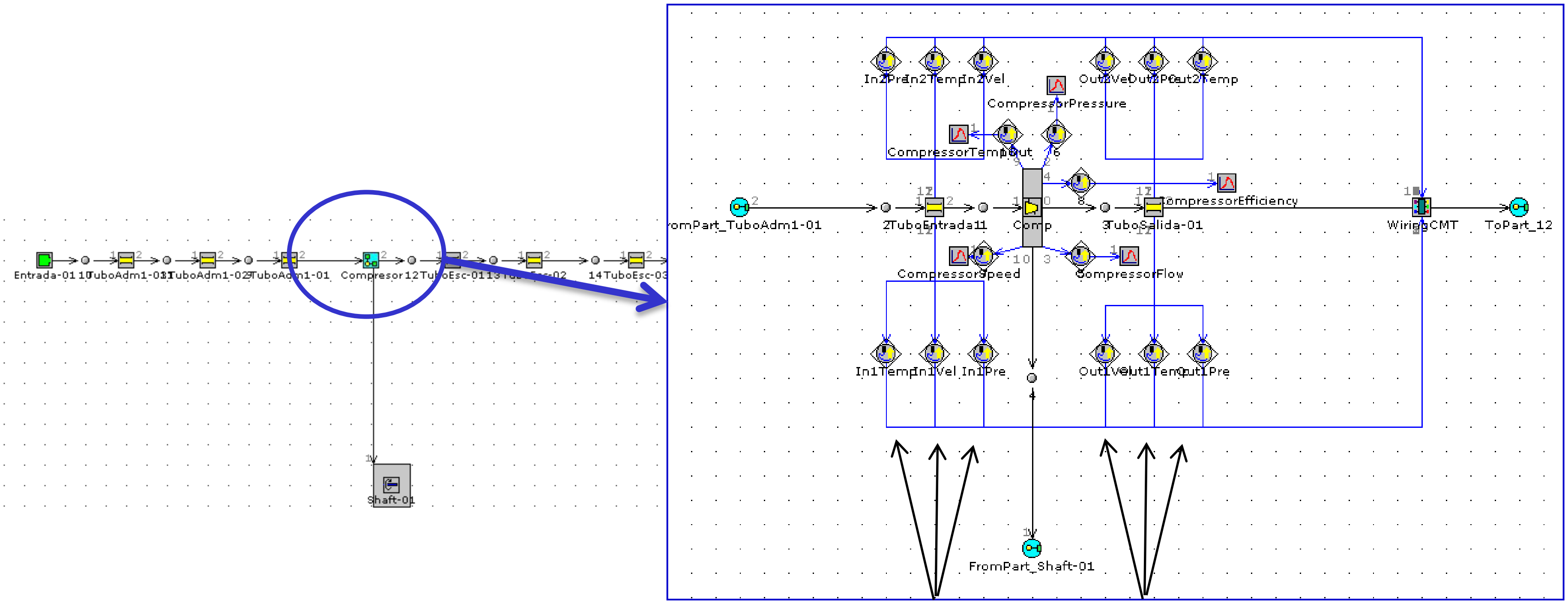


3 sensors up- and downstream to calculate incident characteristics

# ❑ Modeling work: integration in GT

## o Input data

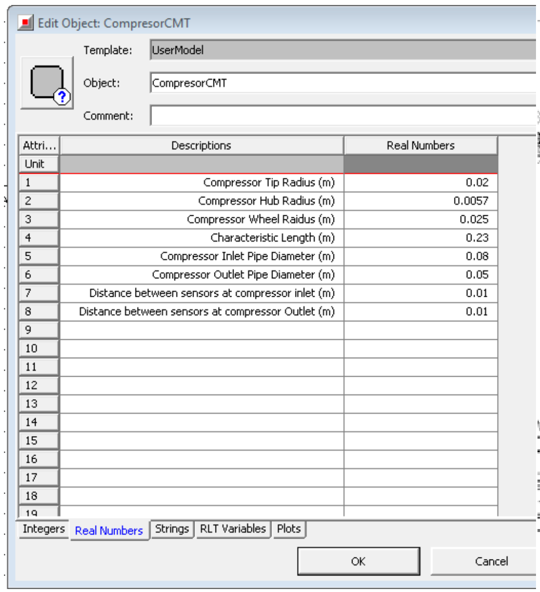



| Attri... | Descriptions | Real Numbers |
|---|---|---|
| Unit | | |
| 1 | Compressor Tip Radius (m) | 0.02 |
| 2 | Compressor Hub Radius (m) | 0.0057 |
| 3 | Compressor Wheel Raidus (m) | 0.025 |
| 4 | Characteristic Length (m) | 0.23 |
| 5 | Compressor Inlet Pipe Diameter (m) | 0.08 |
| 6 | Compressor Outlet Pipe Diameter (m) | 0.05 |
| 7 | Distance between sensors at compressor inlet (m) | 0.01 |
| 8 | Distance between sensors at compressor Outlet (m) | 0.01 |
| 9 | | |
| 10 | | |
| 11 | | |
| 12 | | |
| 13 | | |
| 14 | | |
| 15 | | |
| 16 | | |
| 17 | | |
| 18 | | |
| 19 | | |



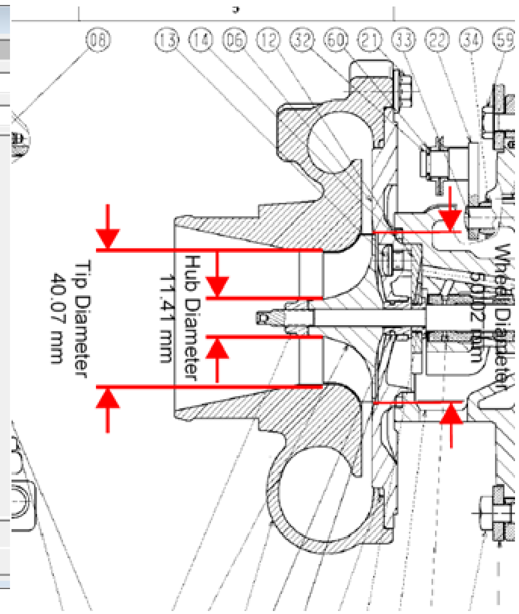



- Tip Radius (see figure).
- Hub Radius (see figure).
- Wheel Radius (see figure).
- Characteristic length. Distance that the flow cover through the compressor.
- Compressor Inlet Pipe Diameter. If the diameter of the pipe upstream of the compressor is modified, this parameter must be also modified.
- Compressor Outlet Pipe Diameter. The same as the inlet.

# ❑ Modeling work: integration in GT

o Input data: Compressor map

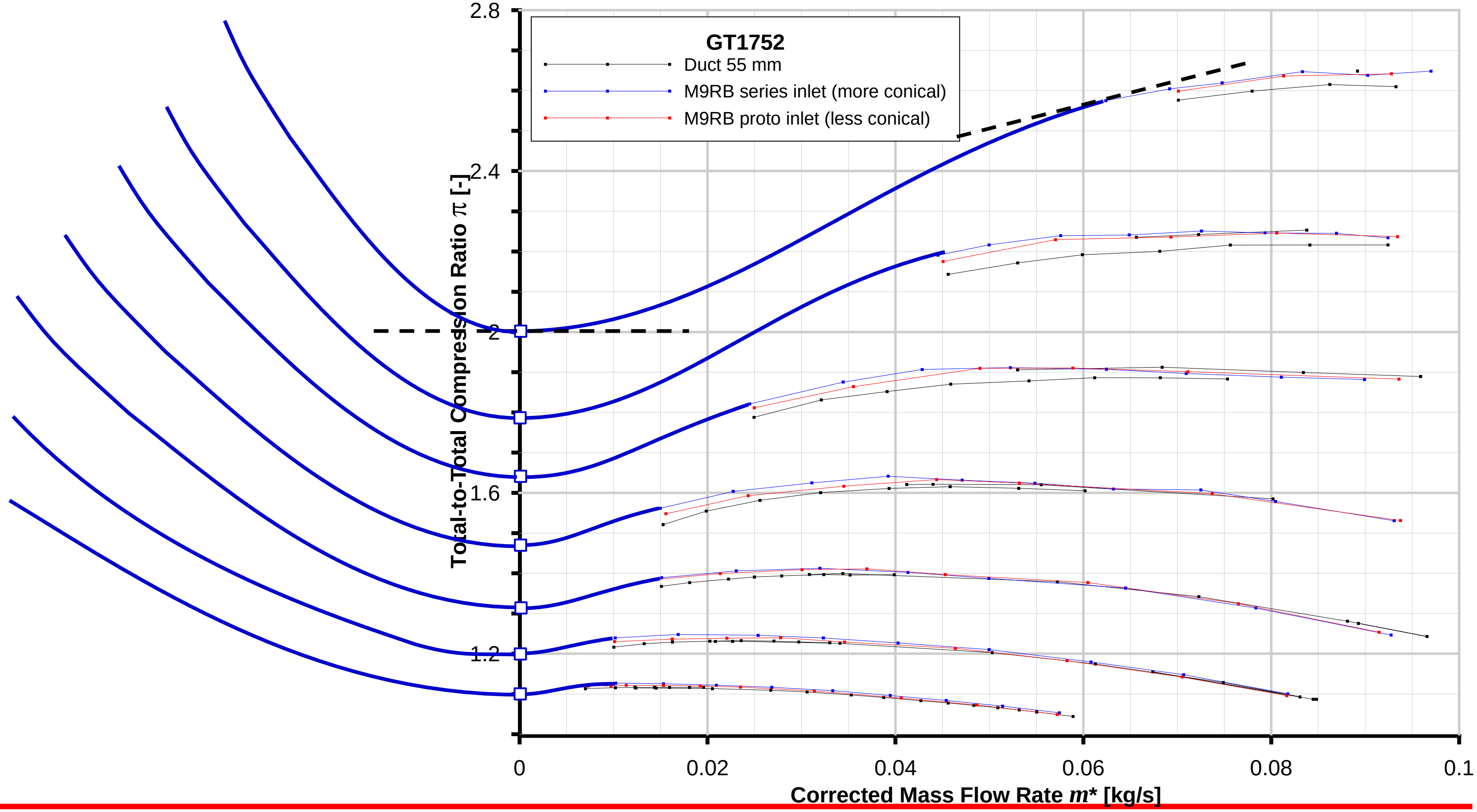

# Modeling work: calibration

- Gas-Stand tests
  - The model predicts quite well steady tests
  - But, small modifications in the measured map lead to big changes in surge prediction
  - Modeling gas-stand tests may be used to improve map quality around surge line
  - It won’t be possible to predict surge accurately!

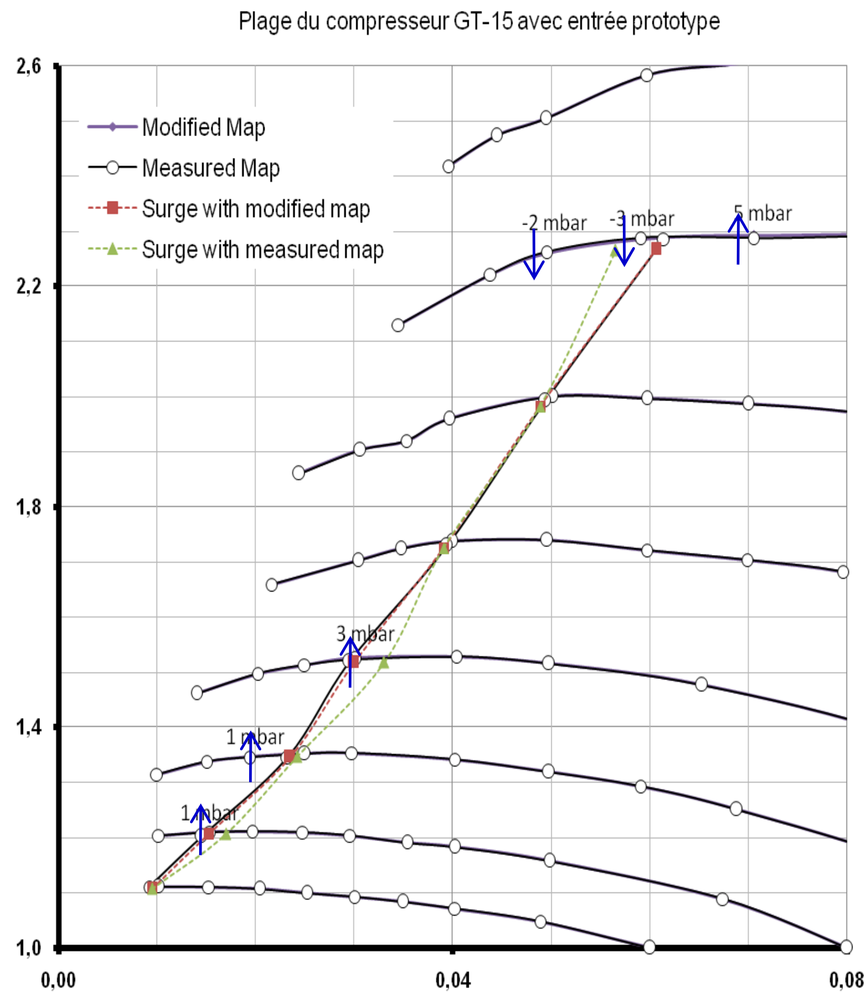

# Modeling work: calibration

- Gas-Stand tests
  - Modeling in between measured isospeed lines is not well predictive
  - We have changed the method of map interpolation using now polar coordinates

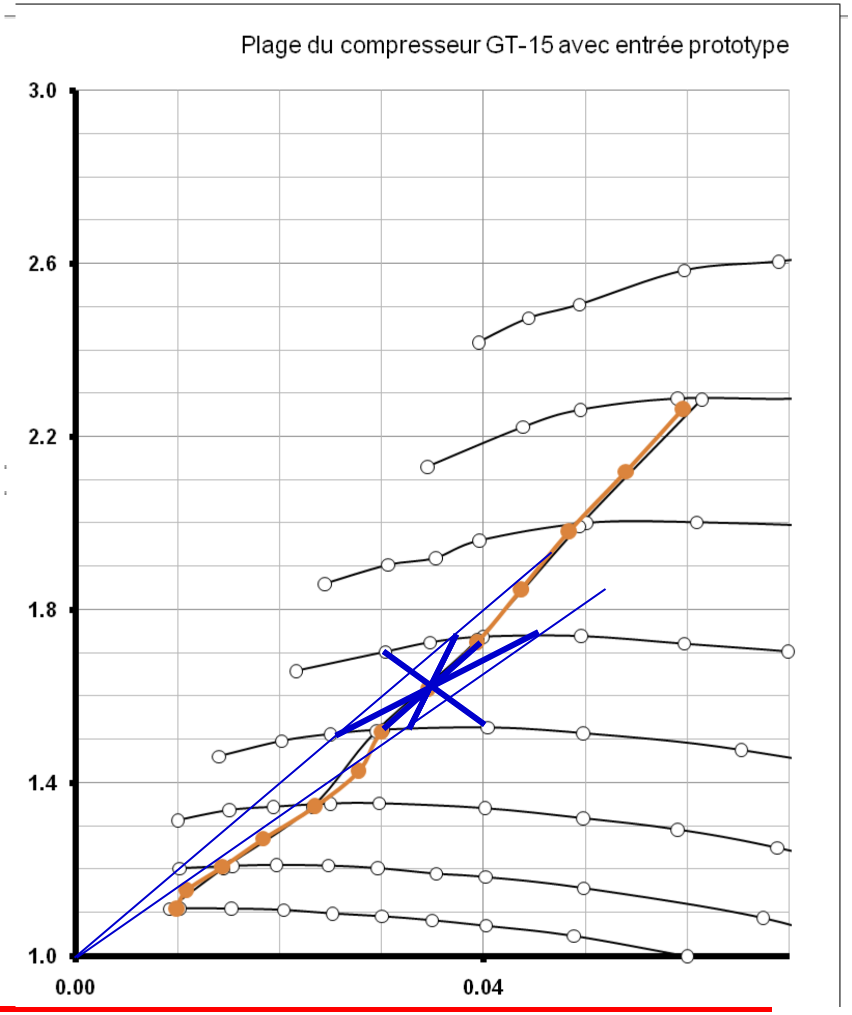

# Modeling work: calibration

- Engine tests
  - The initial model was not accurate for the acoustical calculation of compressor upstream system.
  - A test campaign using wave decomposition technique was carried out
  - A simplified version of the system was proposed to fit experimental results

Modeling work: calibration

- Engine tests
  - The model predicts reasonably acoustical behavior of compressor upstream system

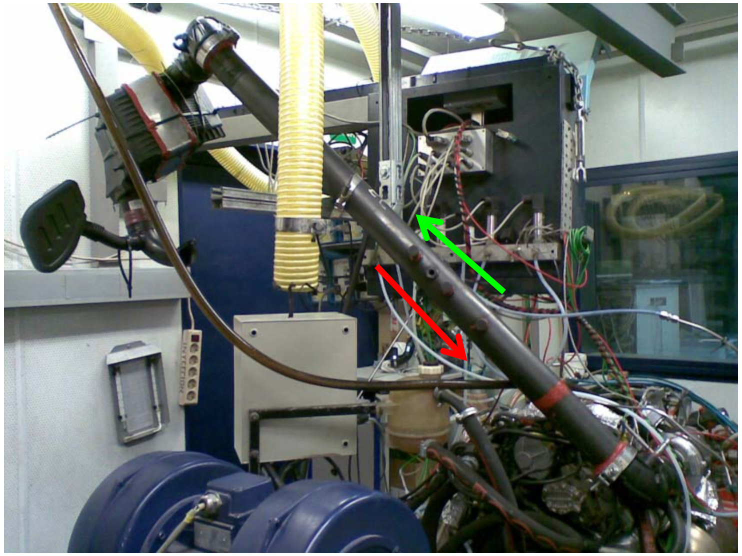

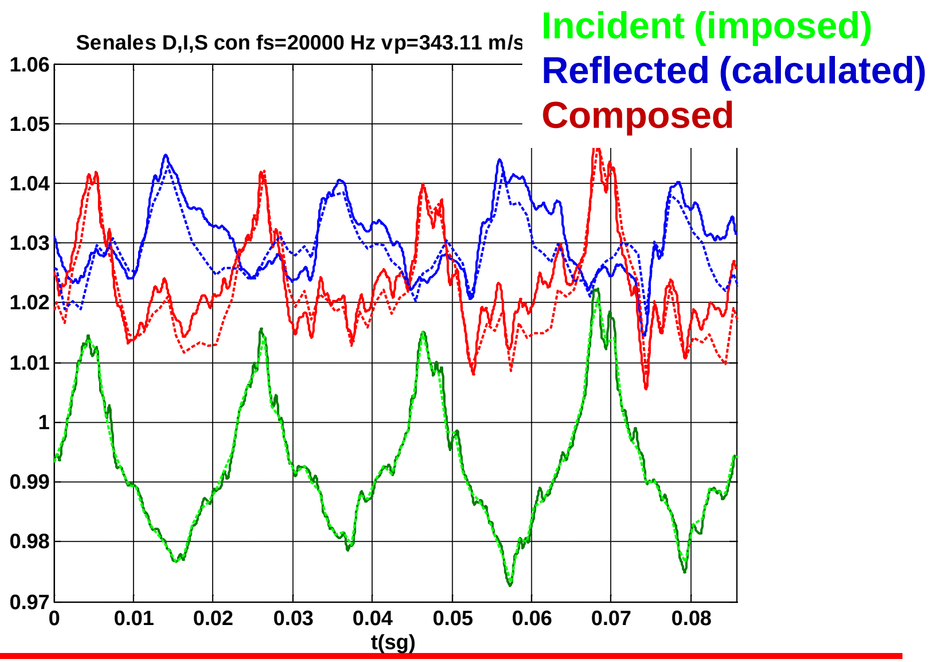

# ❑ Modeling work: calibration

- Engine tests mean values fitting

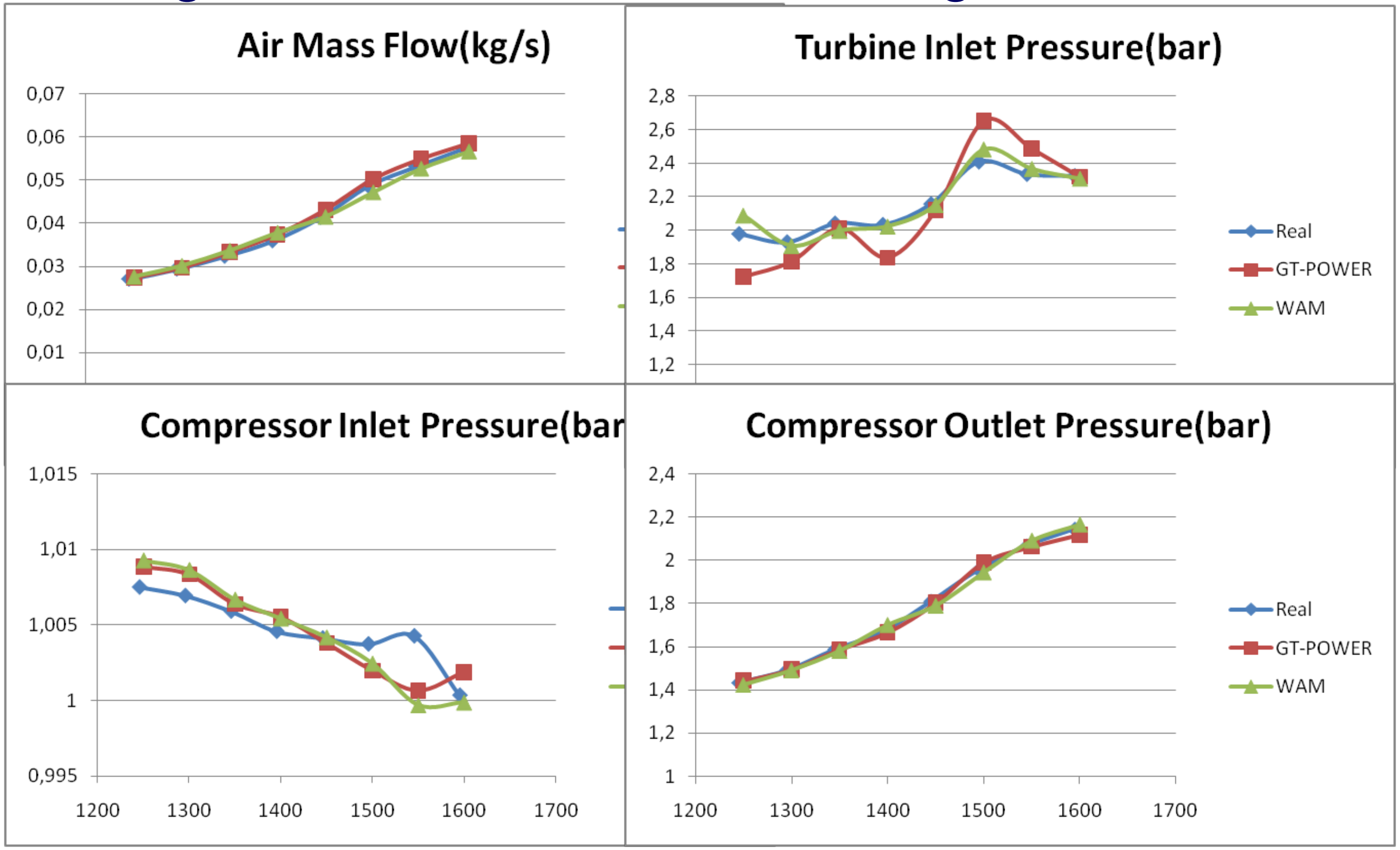

# ❑ Modeling work: calibration

o Engine tests mean values fitting

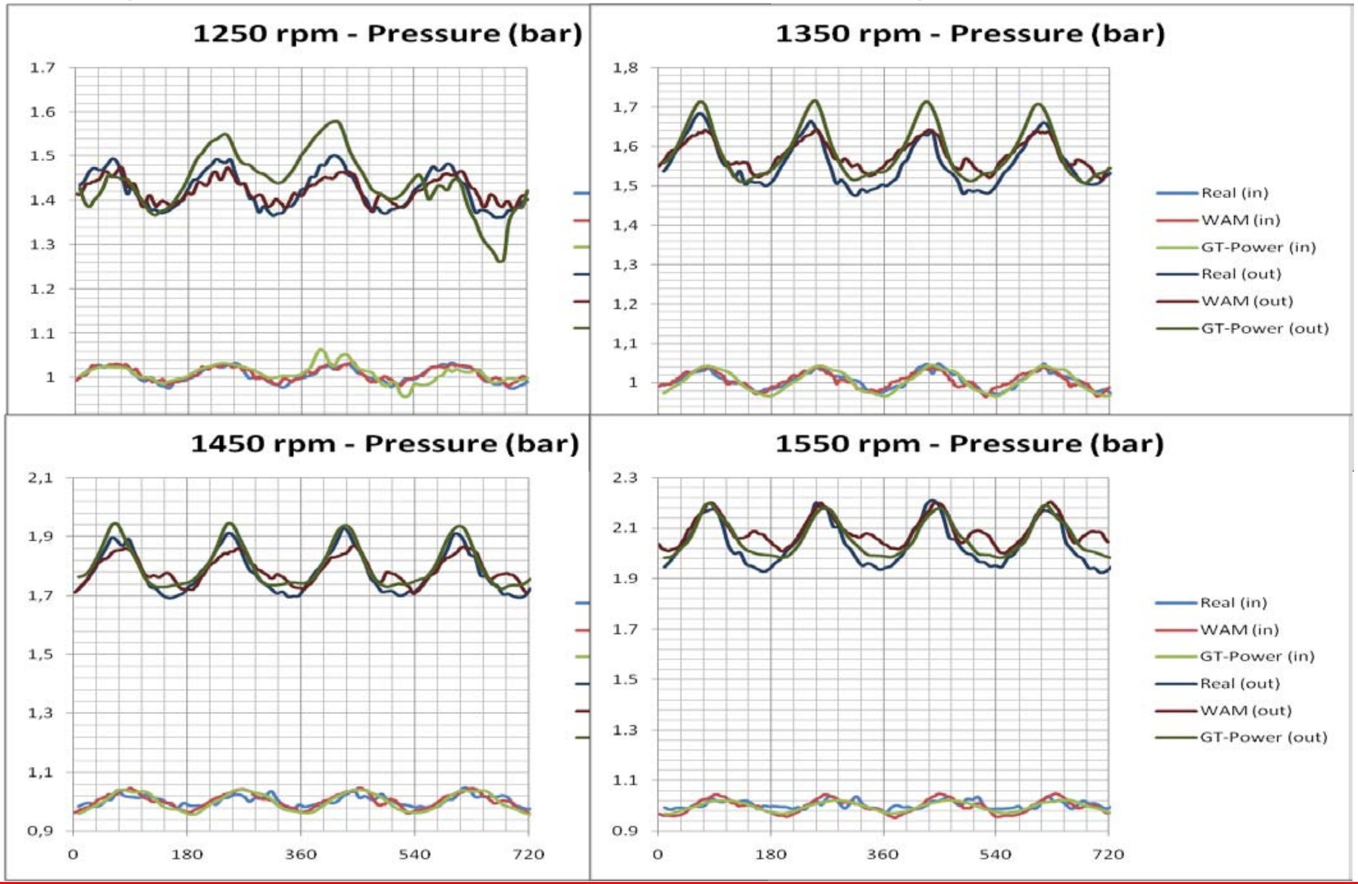

# Modeling work: prediction

- Air Injection Tests
  - Again, small modifications in the compressor map lead to different surge prediction

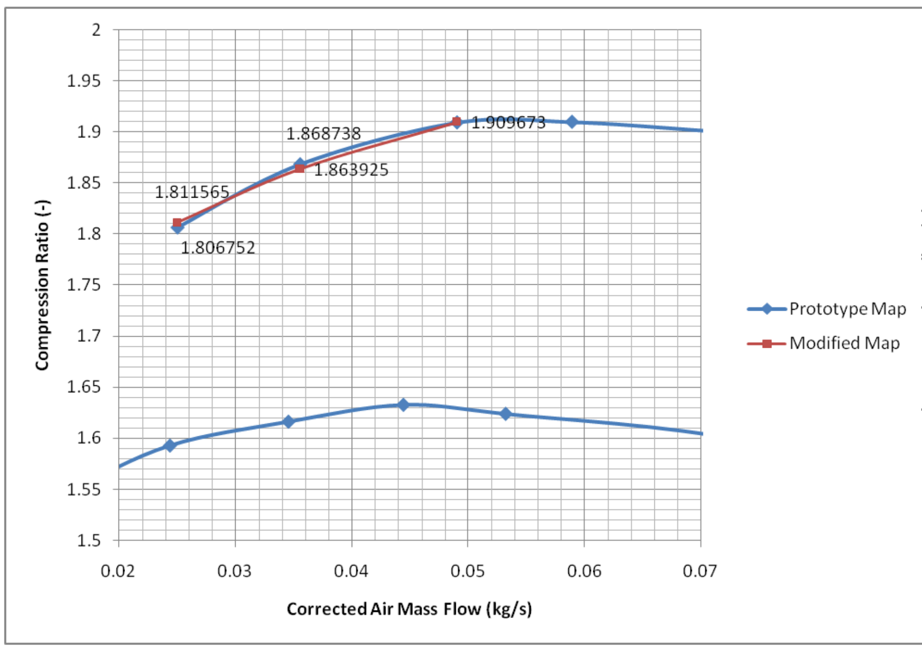


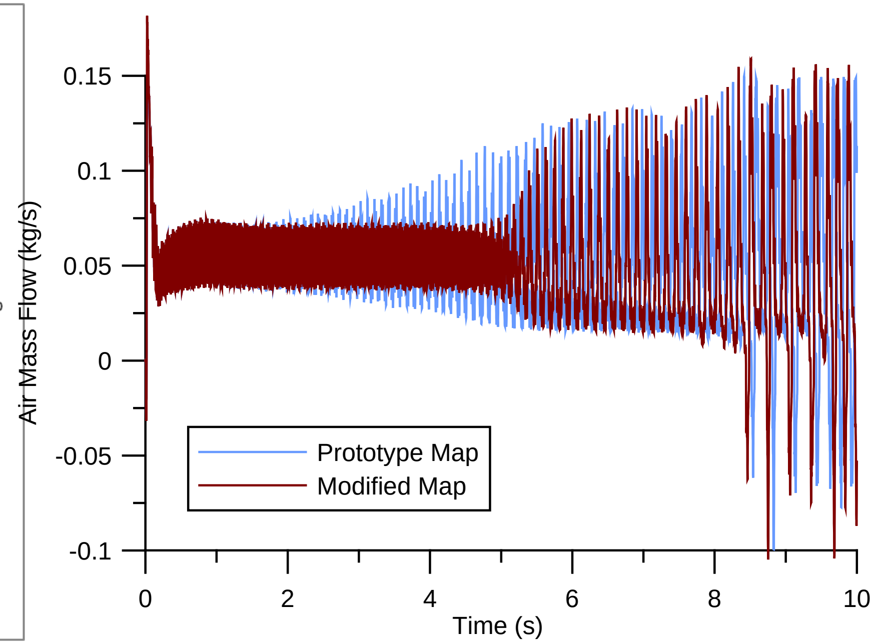

# Modeling work: prediction

- Air Injection Tests
  - Bad engine model calibration leads to bad surge prediction

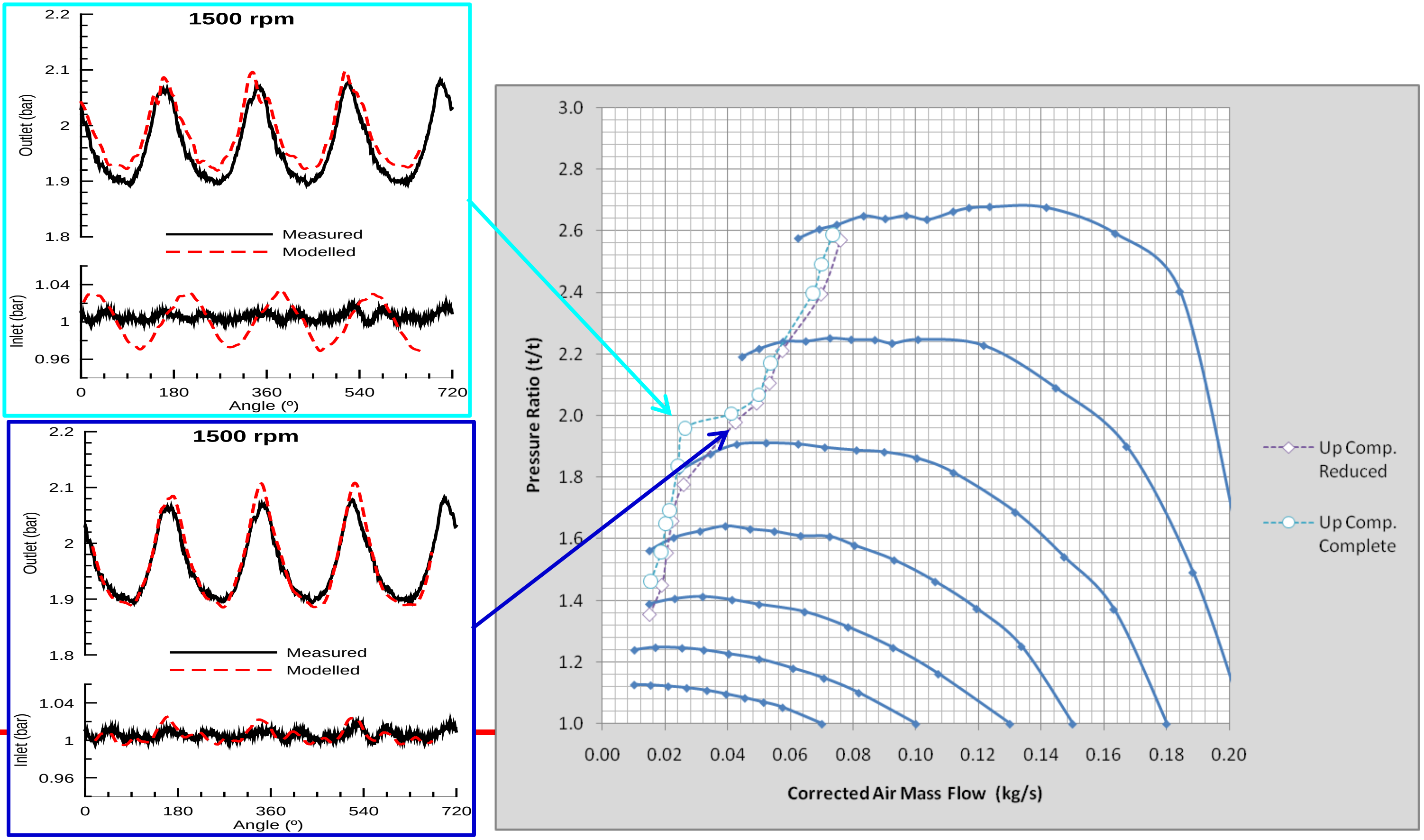

# Modeling work: prediction

- Air Injection Tests
  - We have used the characteristic length to fit the measurements

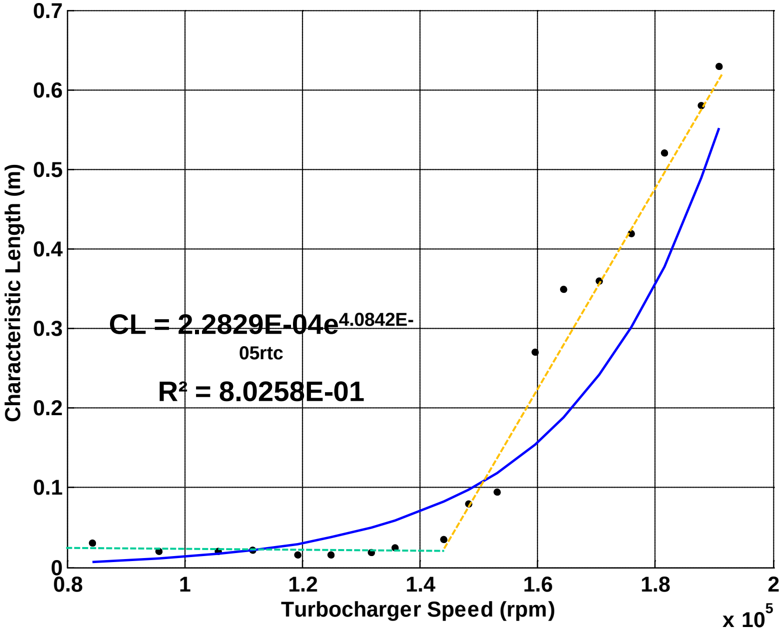


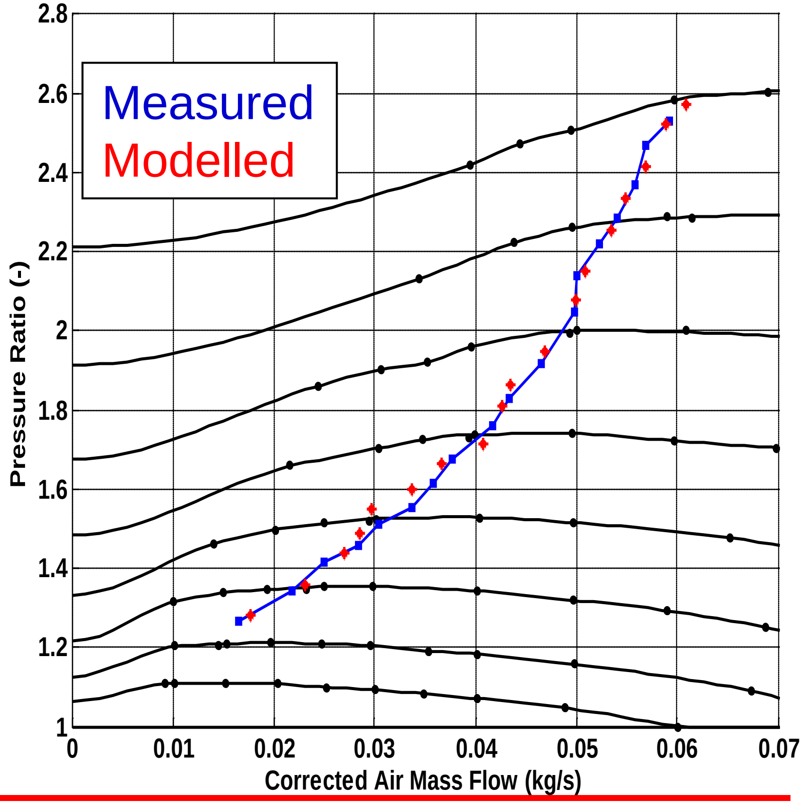

# Modeling work: prediction

- Air Injection Tests
  - We have used the characteristic length to fit the measurements

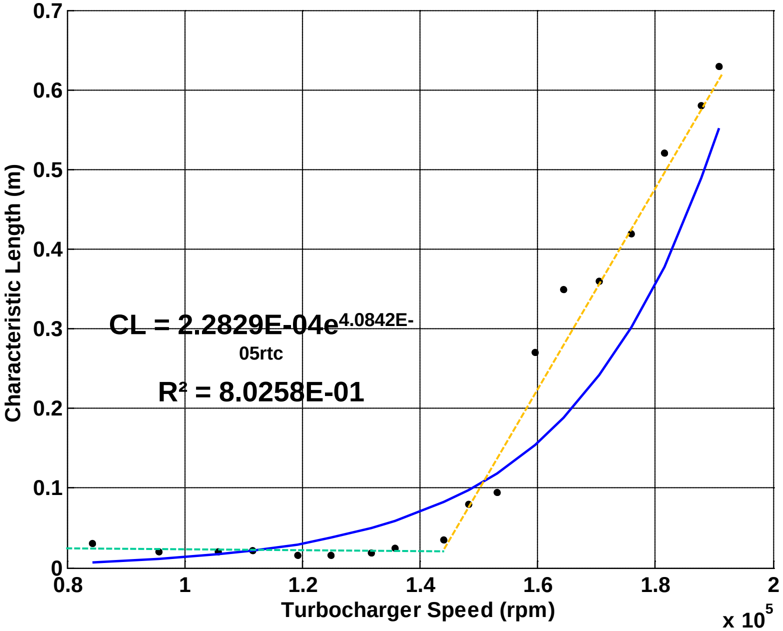


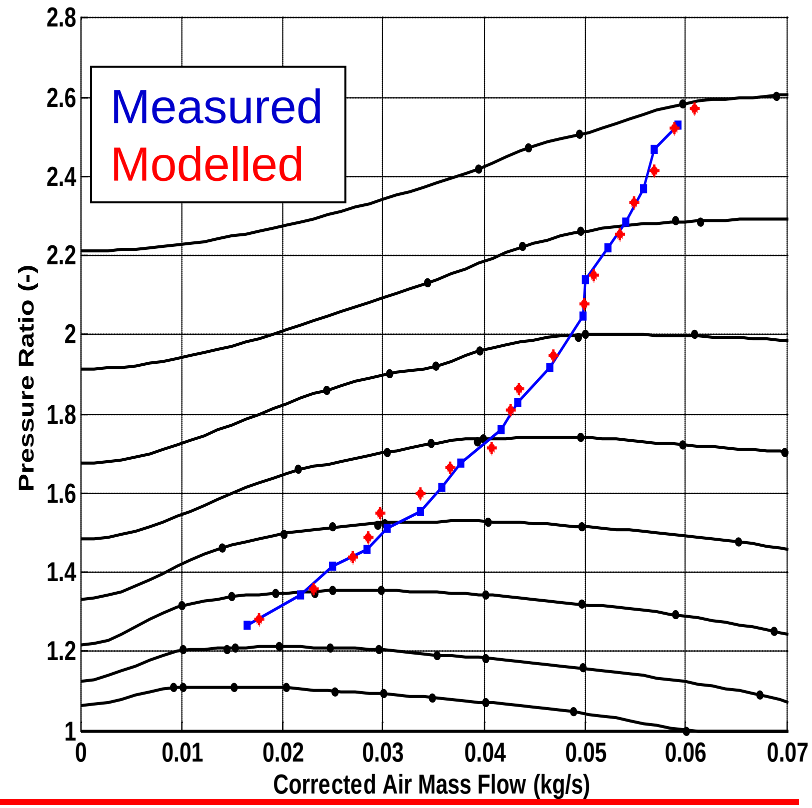

# Modeling work: prediction

- Air Injection Tests
  - Using the CL obtained with a formula

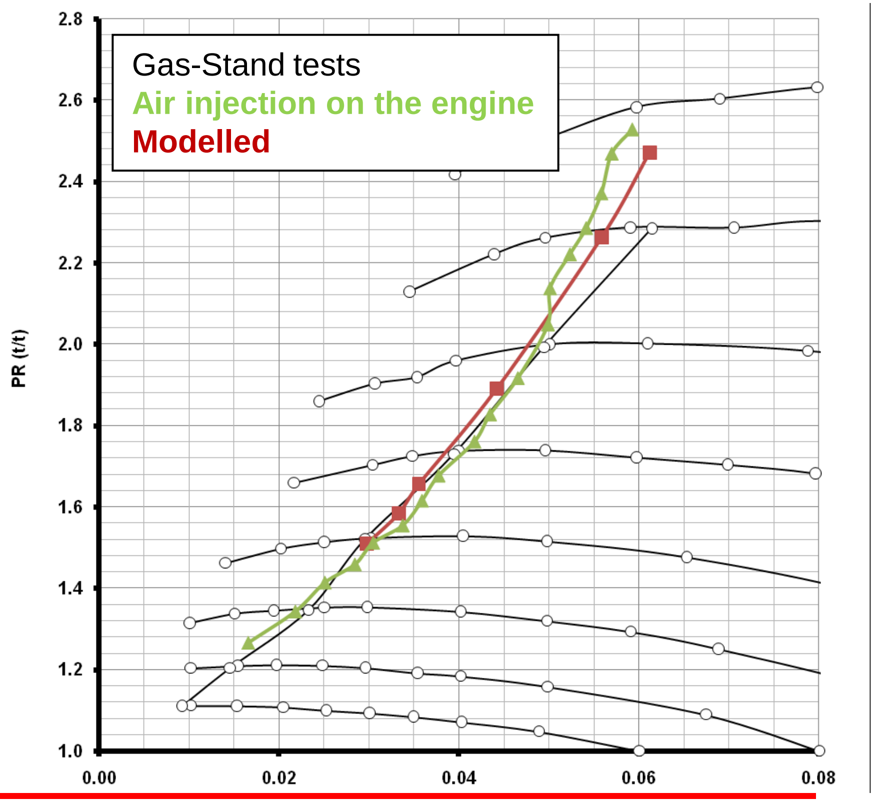

# Modeling work: prediction

o Air injection tests with different geometries

- The model is not able to predict the trend when the CAC duct is modified

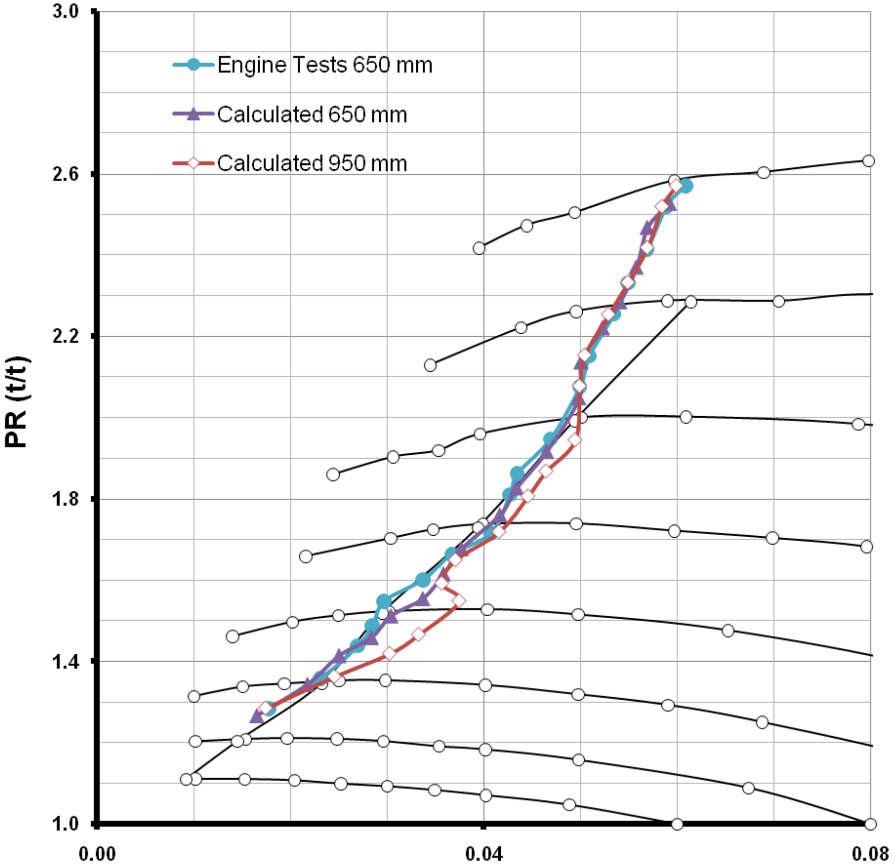

# Modeling work: proposed 2nd model

- **Idea**: to use the same strategy than GT map interpolation
  - There is a problem to interpolate mass flow from compression ratio
  - The Greitzer inertia equation is also used

$$m^k = m^{k-1} + \frac{{m_{MAP}}^k - m^{k-1}}{\tau}$$

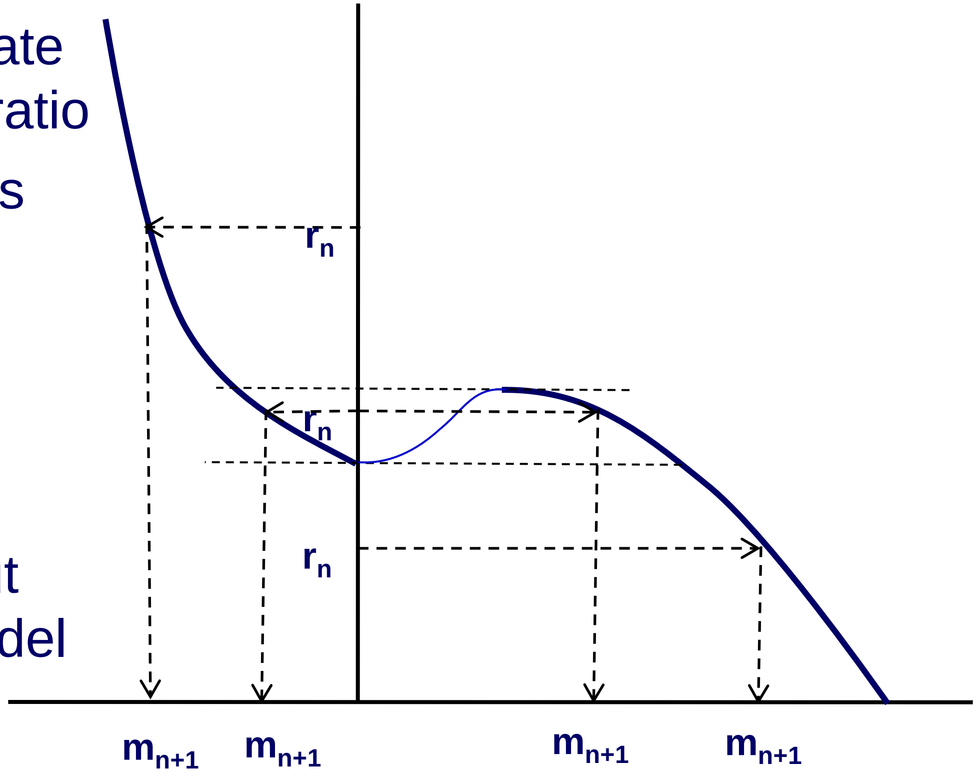


  - The results are not so bad, but worst than those of the 1st model

# ❑ Modeling work: model improvement

- The steady tests have been repeated using the wave decomposition technique.
- The objective is to use the decomposed waves as boundary conditions in the 1D model to skip the fitting of the intake line.

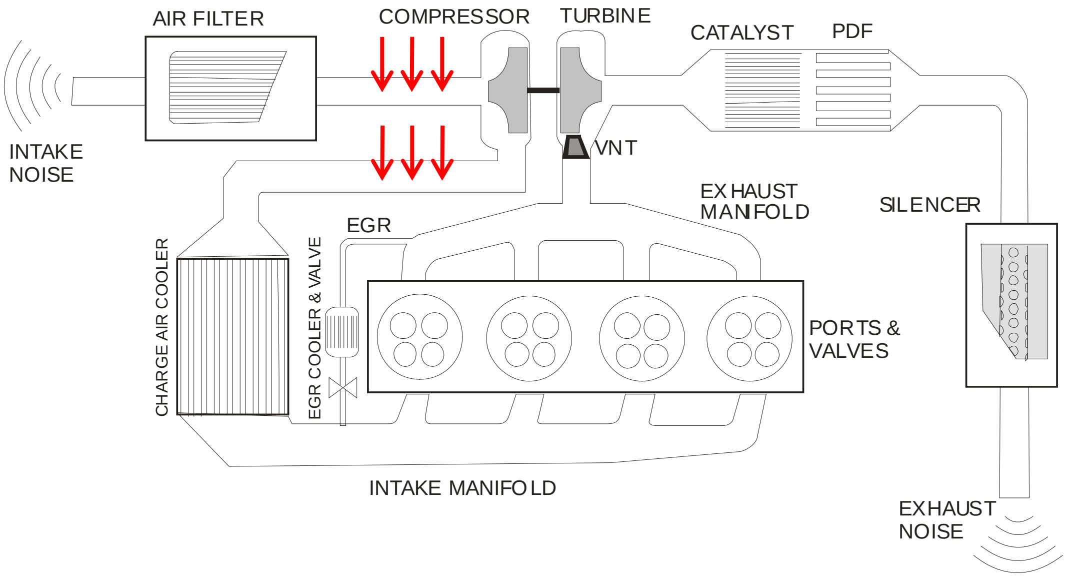

# Modeling work: model improvement

- We have tried to keep the same inlet geometry to have similar acoustic behavior

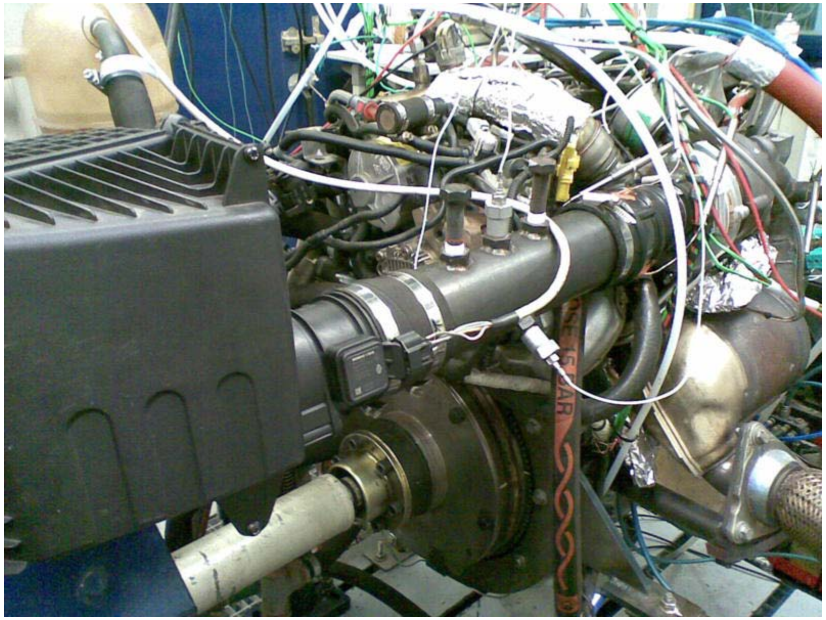

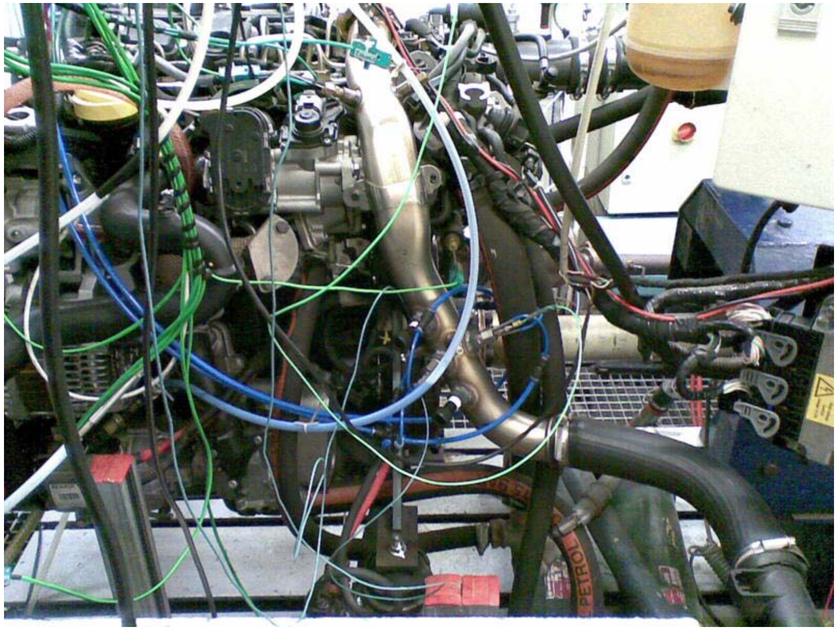

# Modeling work: model improvement

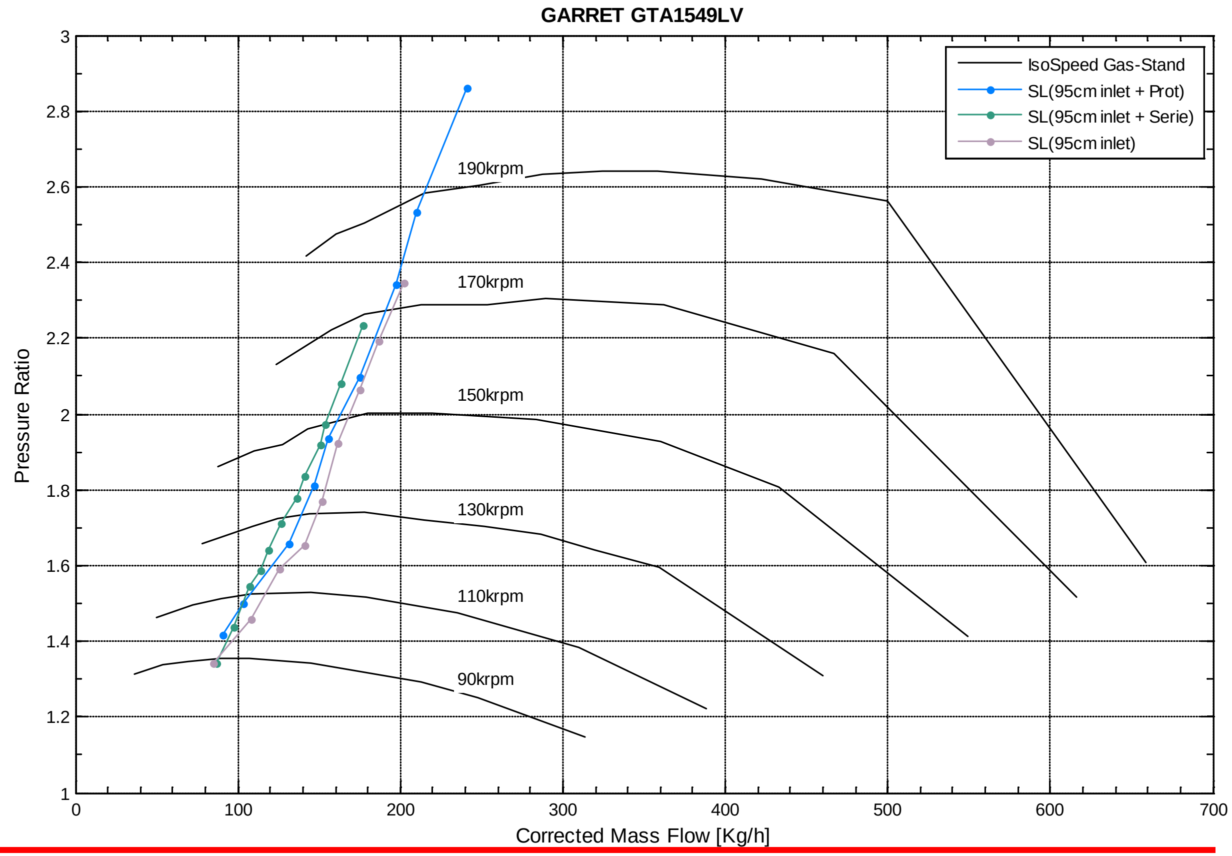

# ❑ Modeling work: model improvement

- Only the compressor is now modelled
  - Measured leftward pressure is imposed at the compressor outlet
  - Measured rightward pressure is imposed at the compressor inlet
  - The other pressure wave component is calculated and compared to the measured value

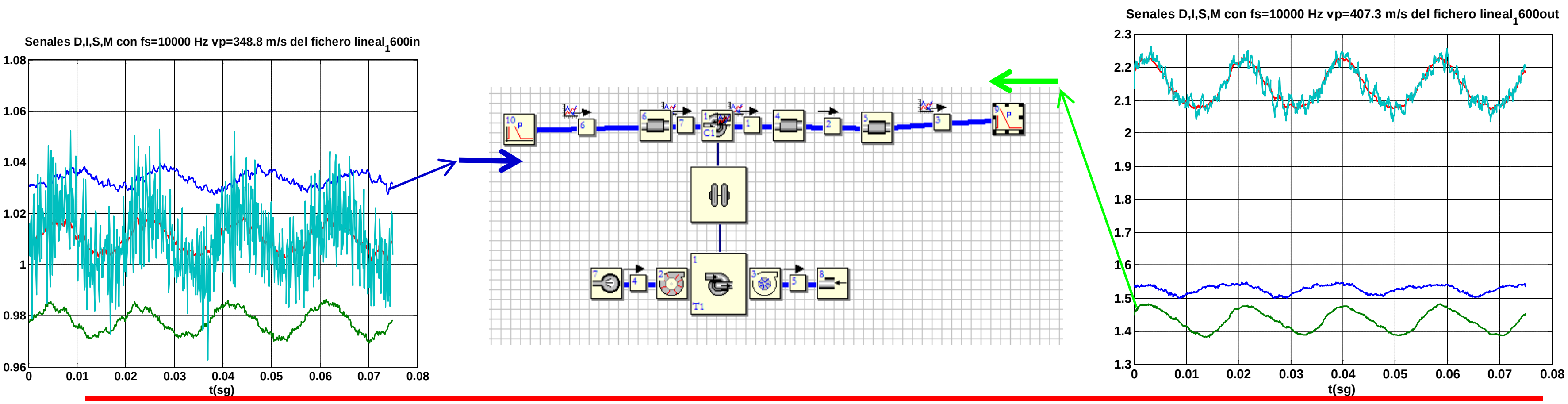

# Modeling work: model improvement

- Only the compressor is now modelled (1st model)

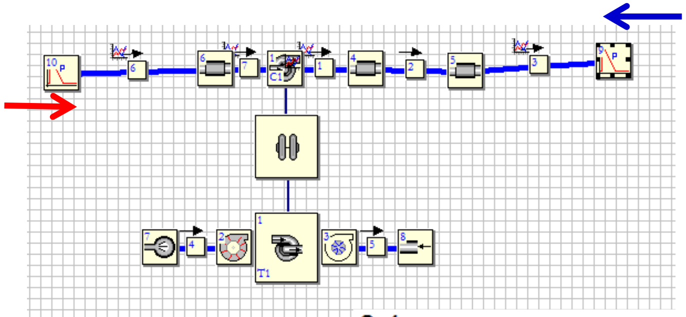


1600 rpm – full load

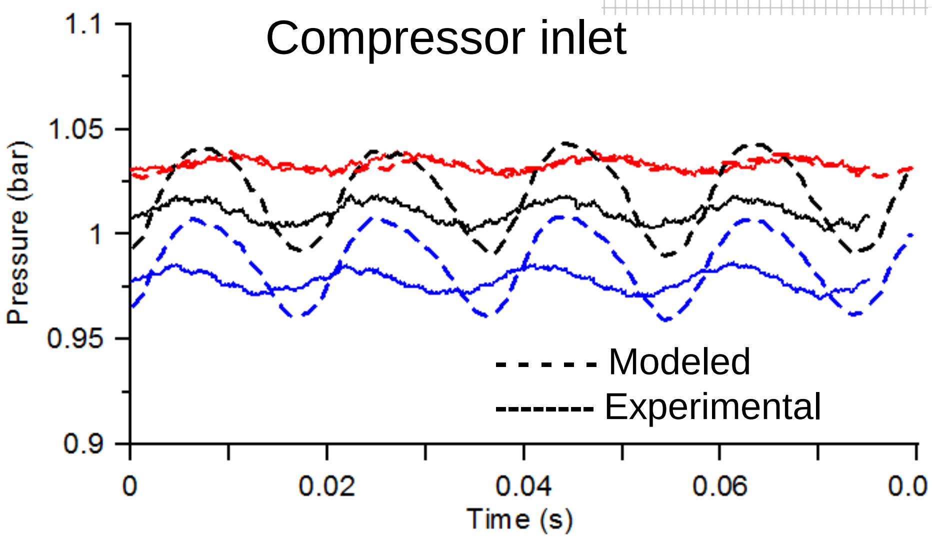


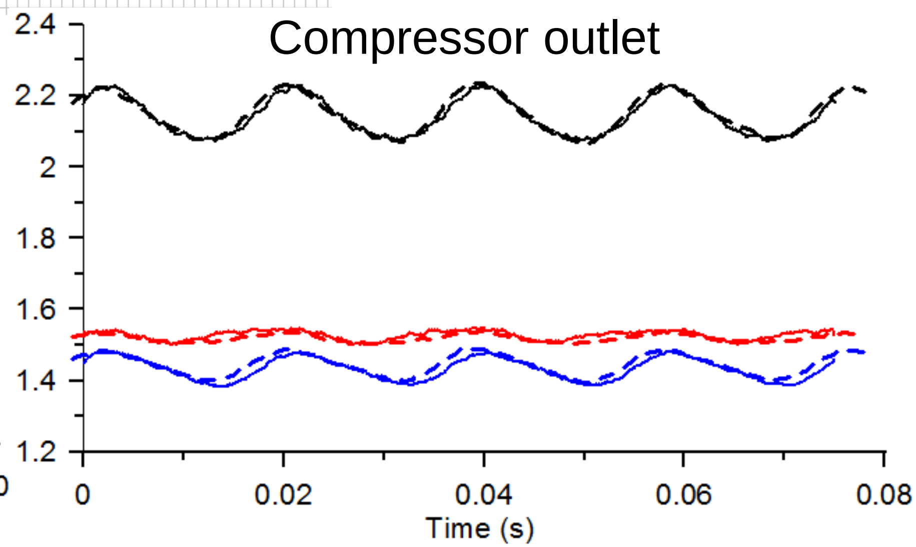

# ❑ Modeling work: model improvement

- The compressor model, as it is, can not predict properly wave transmission and reflection and therefore surge prediction.
- This is because the instantaneous mass flow rate is the same up- and downstream, so the pulsations have similar amplitude
- The solution is to go to a “volume based” model where there is a damping of pressure pulsations with different instantaneous mass flow rate

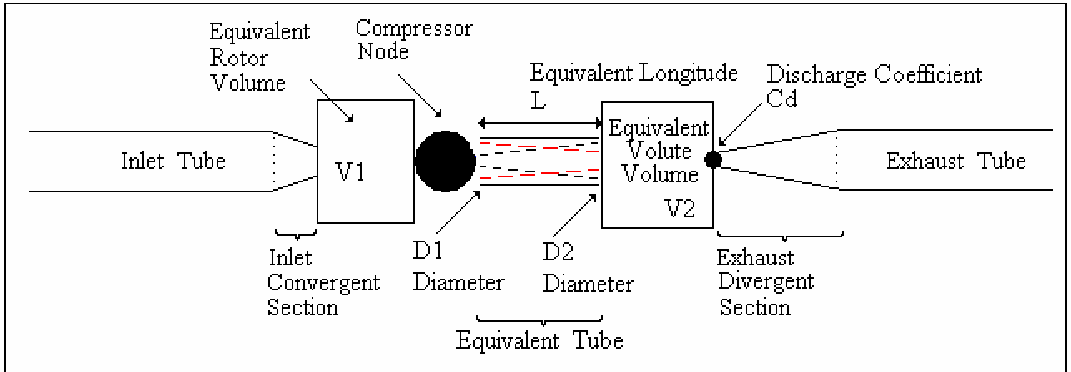


MODEL 4 COMPRESSOR SCHEME

# ❑ Modeling work: model improvement

- The problem of the two-volumes model are the pressure losses that have to be counterbalanced in a modified compressor map
- The modified map has different slopes than the original one, so surge prediction will be different

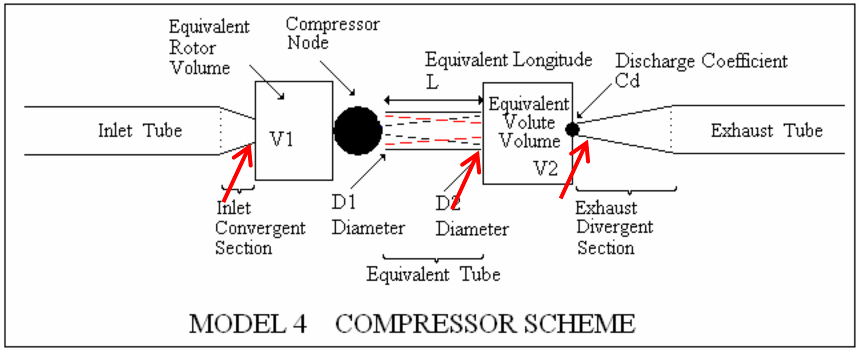


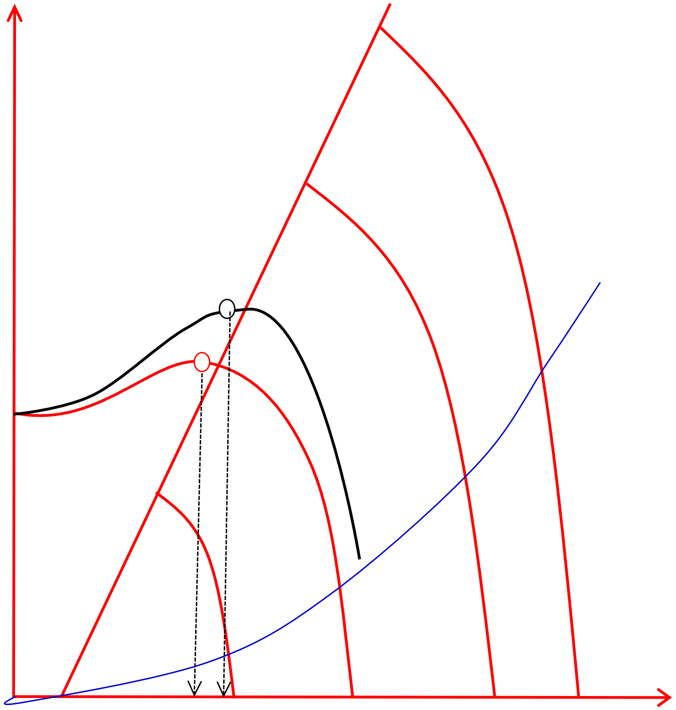

# Modeling work: New model proposal

- A model with a volume in the outlet side is proposed
- There are not pressure losses and therefore the original map can still be used
- The model has been implemented and it is being evaluated

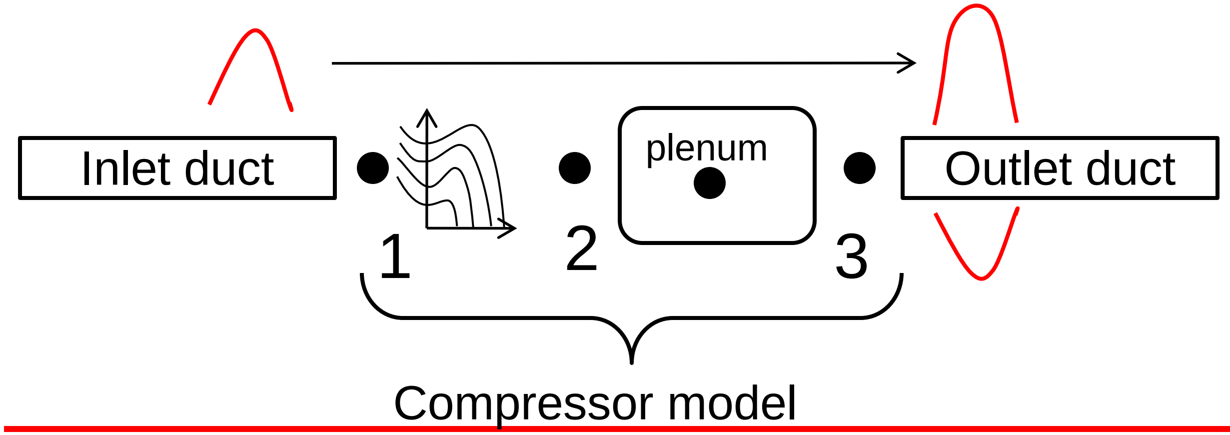


$$\dot{m}_1 = \dot{m}_2 \neq \dot{m}_3$$

$$T_2 = T_1 + w_c / c_p$$

$$p_{20} = p_{plenum} = p_{30}$$

# Modelling work: GT surge model

- CMT surge model implemented in GT v6.2

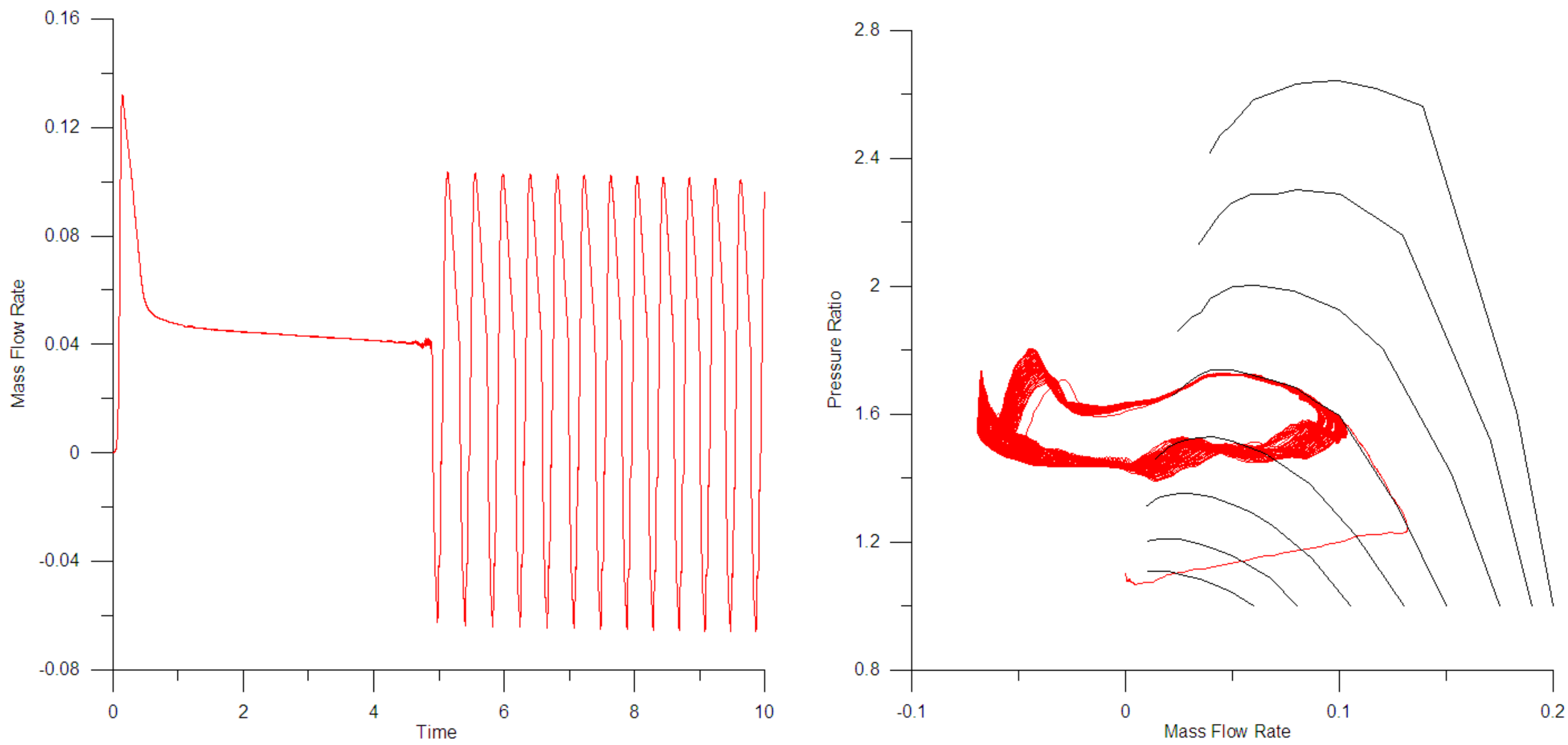

# Modelling work: GT surge model

- GT v7.0 surge model
  - The model goes into surge when flow is almost 0
  - Compression ratio is increased when the flow is reduced

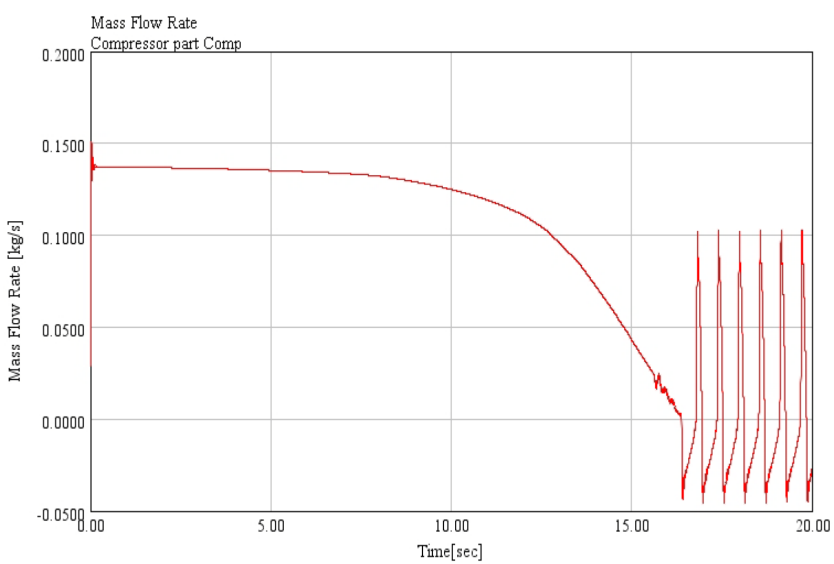


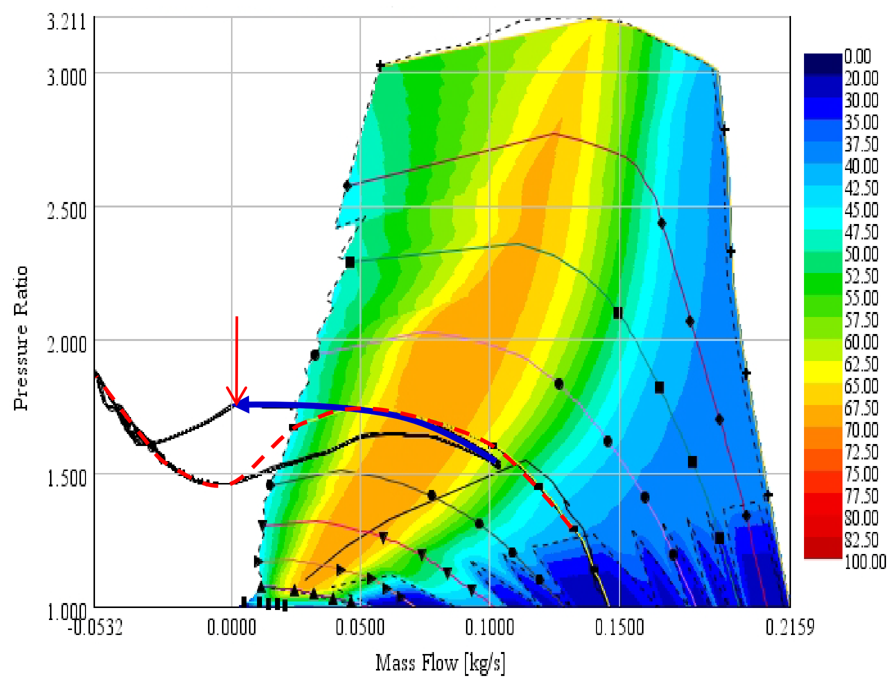

# Modelling work: GT surge model

- Comparison

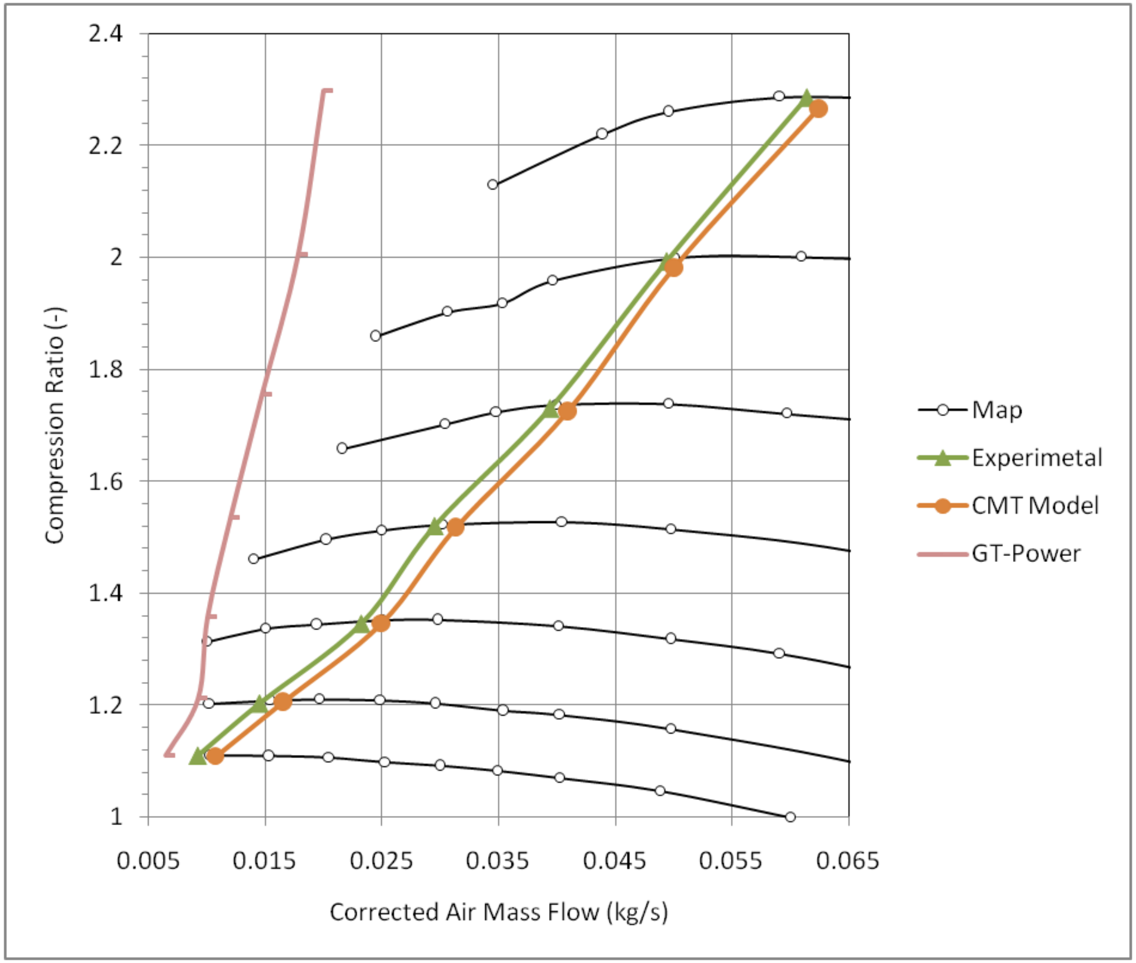

# Modeling work: Conclusions

- CMT compressor model has been implemented as an user function in GT
- The model predicts properly gas-stand steady tests. But small modifications in the measured map lead to a big shift of the surge line
- The model predicts moderately surge line with air injection, but the characteristic length has to be recalibrated
- The model is not able to predict surge line by increasing boosting pressure at constant speed
- The model is not able to predict surge line shift due to inlet system modifications